ORGANOCATALYTIC METHODOLOGIES TOWARDS ASYMMETRIC HETERO- & CARBOCYCLE SYNTHESIS

By

Xinliang Ding

A DISSERTATION

Submitted to
Michigan State University
in partial fulfillment of the requirements
for the degree of

Chemistry—Doctor of Philosophy

2018

ABSTRACT

ORGANOCATALYTIC METHODOLOGIES TOWARDS ASYMMETRIC HETERO- & CARBOCYCLE SYNTHESIS

By

Xinliang Ding

There are four chapters in this dissertation. In Chapter I, a brief review of organocatalytic Morita-Baylis-Hillman (MBH) reaction is discussed, which covers the mechanisms of N-based and P-based catalytic cycles, the asymmetric format of MBH reaction with different catalyst systems, the application of the MBH reaction and its products, and the deviation of the MBH reaction—the Lewis base catalyzed cyclization reactions. Based on the modified MBH reaction—the formal [4+2] cycloaddition reaction, in Chapter II, we demonstrate a fast assembly towards the synthesis of substituted hexahydro-2*H*-chromenes in high stereoselectivity, containing up to 5 contiguous stereocenters *via* consecutive [4+2]/[4+2] cycloaddition reactions. Inspired by two observations from the reactions in Chapter II, methods of a consecutive [4+2] cycloaddition/Brønsted acid catalyzed rearrangement and a consecutive [4+2] cycloaddition/base catalyzed rearrangement toward the synthesis of chiral cyclohex-2-ones and chiral 4*H*-pyrans, respectively, have been reported in Chapter III. Gaining the inspiration from both Chapter II and Chapter III, in Chapter IV, we describe amidine mediated the synthesis of pyran derivatives through formal [1,5]-H shift. Furthermore, a rearrangement of some of these pyrans to furnish phenolic derivatives under acidic conditions is also report. Lastly, incorporation of primary amines in the synthesis of carbocyclic β–amino ester from dihydropyran has been investigated as well

Dedicated to Lihui Jia and Joshua J. Ding

ACKNOWLEDGEMENTS

First of all, I would like to express my deepest gratitude to my research advisor, Professor Babak Borhan, for his kind and careful guidance, generous support and continuing encouragement. I am grateful to have the opportunity to work on wonderful projects in the group, and learn not only the knowledge of interdisciplinary fields but also the critical scientific thinking of how to solve problems that will definitely benefit for my whole career. Thanks for his mentoring, I feel enjoyable and fulfilling of doing research all the time. Obviously, he made my Ph. D program a precious experience in my whole life.

I am greatly thankful to my committee member, Professor Robert E. Maleczka, Professor Xuefei Huang, Professor James H. Geiger, for their constructive suggestions and firm support during my Ph. D. program.

I would like to thank all the former and current members of the Borhan lab for their invaluable support, intellectual inputs into my research, as well as their friendship in the past few years. Especially, I would like to thank Dr. Chrysoula Vasileiou for her kind help and support, and her effort on proofreading my dissertation. I immensely appreciate Dr. Kumar Ashtekar, Wei Sheng, Dr. Yi Yi, Dr. Nastaran Salehi Marzijarani and Dr. Hadi Gholami, Dr. Arvind Jaganathan for giving me the opportunities to collaborate with them and to learn from them. The former and current members, Dr. Carmin Burrell, Dr. Camille Watson, Dr. Calvin Grant, Dr. Tetyana Berbasova, Dr. Ipek Yapici, Dr. Elizabeth M. Santos, Dr. Setare T. Nick, Dr. Bardia Soltanzadeh, Dr. Jun Zhang, Aritra Sarkar, Saeedeh Torabi Kohlbouni, Rahele Esmatpour Salmani, Dan Steigerwald, Debarshi

Chakraborty, Soham Maity, Ankush Chakrabarty, Emily Dzurka, Mehdi Moemeni are acknowledged for their support, encouragement and help during my graduate studies. I would like to thank my talented undergraduate students, Neil T. Heberer, Michael S. Behrendt, Christopher Rahn for greatly helping me with my research projects.

I would like to extent my sincere gratitude to all my friends, faculty members and staffs for all their help in the chemistry department for their support and encouragement. I specially thank Professor Daniel A. Jones and Professor William D. Wulff for their encouragement and guidance on my job search and projects, respectively. I would like to thank Tayeb Kakeshpour for help me understand the calculation of the mechanistic study. I would like to thank Professor Kevin Walker and Professor David B. Collum for their help with my seminar. I would like to thank Dr. Daniel Holmes and Dr. Li Xie for the NMR help, and Dr. Lijun Chen and Dr. Tony Schilmiller for Mass help, and Dr. Richard J. Staples for X-ray crystallography help.

Last but not least, I want to deliver my deepest appreciation to my beloved wife Dr. Lihui Jia, who trusts and encourages me all the time. Her unconditional love and support is driving me to be better through all my life. During my Ph. D program, she is not only the best friend, but also a good listener and brain trust. She is always inspiring and encouraging me on my research. I appreciate her patience when I got lost and when I am upset. Also, I would like to thank my family, specially my parents, my parents in law and my son Joshua Ding for their endless love and support.

TABLE OF CONTENTS

LIST OF TABLES

LIST OF FIGURES

LIST OF SCHEMES

KEY TO SYMBOLS AND ABBREVIATIONS

Å	angstrom
Ac	acetyl
cm^{-1}	wavenumber
DABCO	1,4-diazabicyclo[2.2.2]octane
DBU	1,8-diazabicyclo[5.4.0]undec-7-ene
DBN	1,5-diazabicyclo[4.3.0]non-5-ene
DCM	dichloromethane
$(DHQ)_2AQN$	dihydroquinine (anthraquinone-1,4-diyl) diether
DHQD-PHN	dihydroquinidine-9-phenanthryl ether
DMAP	4-dimethylaminopyridine
DMF	*N,N*-dimethylformamide
DMSO	dimethylsulfoxide
ee	enantioselectivity
er	enantioselectivity ratio
ESI-MS	electrospray ionization-mass spectroscopy
Et	ethyl
EtOAc	ethyl acetate
$(Et)_3N$	triethylamine
$(Et)_2O$	diethyl ether
equiv	equivalent

h	hour
HRMS	high-resolution mass spectroscopy
IR	infrared
Me	methyl
Min	minutes
M	molar
MBH	Morita-Baylis-Hillman
mM	minimolar
mg	minigram
mmol	minimole
MTBD	7-methyl-1,5,7-triazabicyclo[4.4.0]dec-5-ene
m.p.	melting point
$MgSO_4$	magnesium sulfate
n-Bu	*n*-butyl
NHCs	*N*-heterocyclic carbenes
NMR	nuclear magnetic resonance
Na_2SO_4	sodium sulfate
NaOH	sodium hydroxide
Ph	phenyl
ppm	parts per million
QD	quinidine
QN	quinine

rt	room temperature
[α]	specific rotation
δ	chemical shift
TBD	triazabicyclodecene
THF	tetrahydrofuran
TLC	thin layer chromatography
TMG	1,1,3,3-tetramethyguanidine
TS	transition state
>	larger than
<	less than

Chapter I: A Brief Review of Organocatalytic Morita-Baylis-Hillman (MBH) Reaction

I-1. General introduction of organocatalysis

It was until early this century that organocatalysis was recognized as the third pillar of modern asymmetric catalysis after enzymatic and organometallic catalysis. In recent years, although a new field, organocatalysis has grown dramatically, becoming a thriving area that has been widely applied in asymmetric reactions, as illustrated by the citation statistics from the literature.[1] Organocatalysis could be viewed as a catalysis with small organic molecules, where an inorganic element is not part of the active principle. Most but not all organocatalysts can be broadly classified into four types, namely Lewis bases, Lewis acids, Brønsted bases and Brønsted acids (**Scheme I-1**).[2] The classification is based on the reaction mechanism (proposed) and the mode of activation of the catalyst

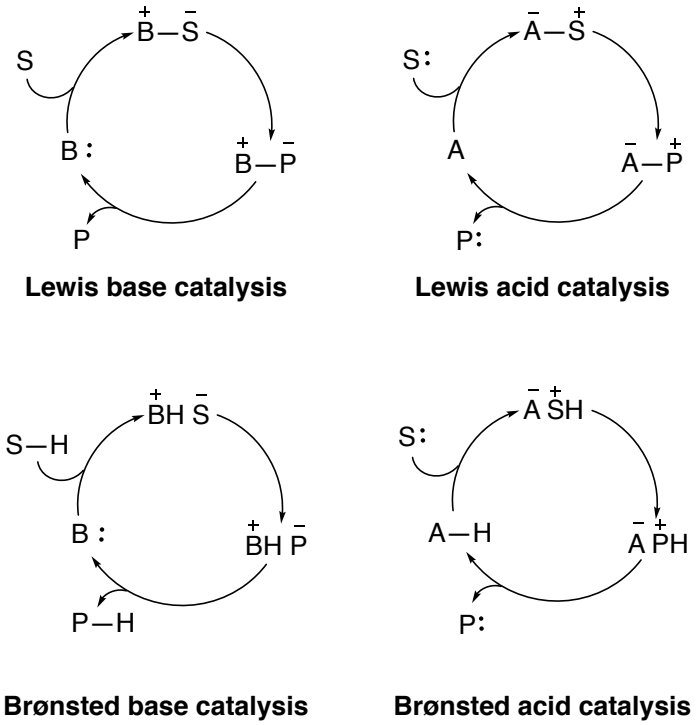

Lewis base catalysis **Lewis acid catalysis**

Brønsted base catalysis **Brønsted acid catalysis**

Scheme I-1. Simplified catalytic cycles of four types of organocatalysts.

in the catalytic cycle, either by providing or removing electrons or protons from a substrate or a transition state. For example, in a Lewis base (**B:**) catalytic cycle, a nucleophilic addition to the substrate (**S**) is followed by a reaction, the product (**P**) is released and the catalyst is recovered for further turnover. Although the exact mechanisms are not often available, and even more challenging is the fact that some of the organocatalysts are bifunctional, it is still helpful to organize this field with a somewhat logical structure.[2] Among these four, Lewis base catalysts dominate the field with several types of catalysts, such as amines, phosphines and carbenes. However, it is noteworthy that Brønsted acid catalysts have grown significantly recently and are expected to ultimately deliver extremely active catalysts, which are comparable the efficiency of enzymes, as well as that of the few super active chiral transition metal complexes, such as certain Suzuki reaction catalysts.[3]

Organocatalysts have advantages that are attractive to chemists. More specifically, most of them are stable in air and water, widely available from biological materials, generally inexpensive and easy to prepare, simple to use, both enantioseries are available, and typically they are non-toxic.[1] As a sequence, this field has quickly flooded with research groups, greatly accelerating the development of this area. As a result, it is not surprising that organocatalysts have been used as generic modes of activation and induction with many reaction variants, such as Hajos-Parrish-Eder-Sauer-Wiechert reaction, aldol reaction, Michael reaction, Mannich reaction, Strecker reaction, Morita-Baylis-Hillman reaction, to name a few. For each individual reaction, almost every aspect has been well developed, including substrate scope, innovative catalysts design and

synthesis, mechanistic studies, and new applications of the reaction itself and its products. Our journey will begin with one of the famous organocatalytic reactions—the Morita-Baylis-Hillman reaction, as the most important part of my work is based on the modified format of this reaction.

I-2. An introduction of Morita-Baylis-Hillman (MBH) reaction

The most fundamental reactions of organic chemistry are the C-C bond formation and the functional group transformations. Among these C-C bond formation reactions, the Morita-Baylis-Hillman (MBH) transformation is an important contributor leading to multifunctional scaffolds. The classical MBH reaction is commonly defined as the C-C bond formation between the α–position of conjugated carbonyl compounds and carbon electrophiles, such as aldehydes and imines, in the presence of a nucleophilic catalyst,

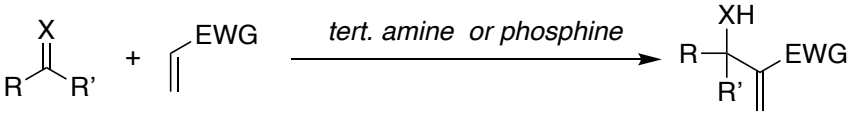

R = aryl, alkyl, heteroaryl, *etc.*; R' = H, CO_2R", alkyl, *etc.*
X = O, NCO_2R", NSO_2Ar, *etc.*
EWG = COR", CHO, CN, CO_2R", $PO(OEt)_2$, SO_2Ph, SO_3Ph, SOPh, *etc.*

Scheme I-2. General equation of the Morita-Baylis-Hillman (MBH) reaction.

particularly a tertiary amine or a phosphine (**Scheme I-2**).[4] The origin of this reaction dates back to 1968, when Morita reported this reaction catalyzed by a phosphine.[5,6] Four years later, Baylis and Hillman described a similar reaction, however, using an amine as the catalyst.[7] After a decade, several groups, including Drewes, Hoffmann, Perlmutter, and Basavaish reinvestigated and explored this reaction as evidenced by their numerous research papers.[8-13] During the past few decades, there has been remarkable progress made by several groups, such as Shi, Aggarwal, Miller and Zhu,[4,14-17] especially in the

area of organocatalytic asymmetric MBH reactions. Meanwhile, mechanistic studies by several groups, such as Hoffman, McQuade, Aggarwal, and Coelho have also been investigated.[9,15,18-20] Also, aza-Morita-Baylis-Hillman (aza-MBH) reaction, in which imines, instead of aldehydes, react as the secondary electrophiles, has been widely studied. The reasons for the dramatic growth of MBH/aza-MBH reaction can be attributed to several advantages of this reaction as follows: (i) the starting materials are usually commercially available; (ii) the reaction is easily scaled up to industrial scale; (iii) it is an atom-economic reaction; (iv) usually the reaction condition is mild; (v) it is often catalyzed by an organocatalysis, as a result, no contamination with heavy-metals; (vi) the scaffolds formed through this reaction contain multi-functionalities that could be easily modified to other synthetically useful products.

The MBH reaction has been studied for several decades. In the following paragraphs, the MBH reaction will be reviewed by looking at mechanistic studies, catalysts involved in the reaction, and the applications or transformations of the products of this reaction.

I-3. Mechanism

I-3.1. Amine-Catalyzed MBH Reaction

The elementary steps of the MBH reaction catalyzed by simple amine species have been described in detail in the early literature, which generally include three sequential steps: the Michael addition, aldol coupling reaction (involving proton migration) and followed by elimination of the catalyst. This was first proposed by Hoffman[9] and later confined by Hill and Isaacs,[21-23] as well as other groups,[24-26] through kinetic studies (**Scheme I-3**). Take acrylonitrile as an example, the 1st step of the catalytic cycle starts

with the Michael reaction of tertiary amine **I-1** to the activated alkene (acrylonitrile **I-2**), to produce the zwitterionic amine-acrylate **I-3**, which reacts as the secondary nucleophile to attack the aldehyde **I-4**, generating zwitterion **I-5**, followed by intramolecular proton transfer, leading to the formation of intermediate **I-6**. Subsequently, elimination of the catalyst **I-1** *via* E2 or E1cb mechanism produces the product **I-7** and recovers the catalyst **I-1**. The low kinetic isotopic effect (KIE = 1.03 ± 0.1, in **Scheme I-3**) indicates the conjugated addition step **II** is the MBH rate-determining process (RDS). Later, the isolation of one intermediate which was confirmed by X-ray crystallography and the use of electrospray ionization with mass and tandem mass spectrometry to trap all the key intermediates supported the proposed mechanism.[8,27]

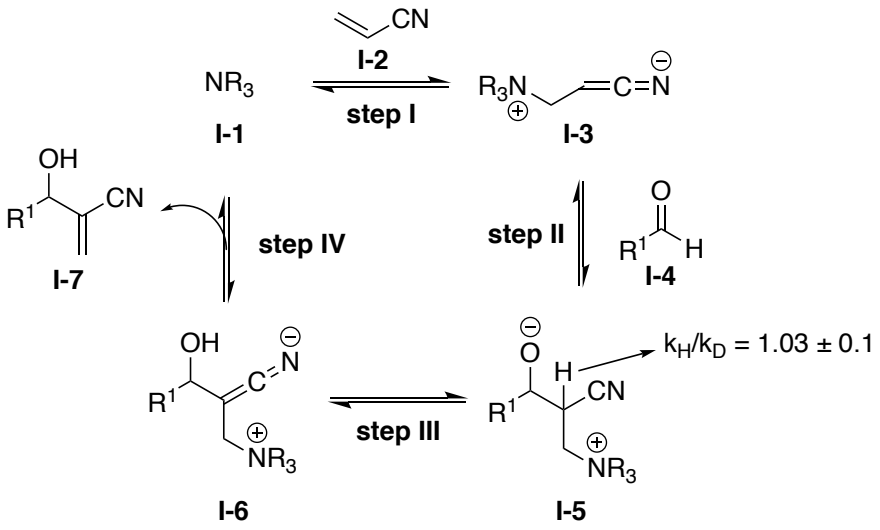

Scheme I-3. Hill-Isaacs proposed mechanism of MBH reaction between acrylonitrile and aldehyde catalyzed by tertiary amines.

However, when McQuade's[18,19] and Aggarwal's[15] groups re-investigated this reaction by using carbonyl activated alkenes (such as a ketone) through kinetics and theoretical studies, they observed a significant kinetic isotopic effect (KIE = 5.2 ± 0.6 in DMSO, in **Scheme I-4**), which suggests the relevant proton transfer **step III** is the rate-determining

step. It is also reported the MBH reaction could be accelerated by protic reagents, such as methanol and phenol, which provides another evidence for their plausible mechanism.[15] As a result, both groups proposed a six-membered intermediate formed during the proton-transfer step. (**Scheme I-4**) The difference between these two models is the partner participating in this six-membered ring formation. In McQuade's proposal, the 2nd molecule of the aldehyde electrophile **I-4** is used to form a hemiacetal intermediate **I-10a**. While in Aggarwal's proposal, the final product **I-12** plays the role of an intermolecular proton transfer agent through intermediate **I-10b**. As a result, the autocatalytic effect of the product observed in this type reaction can be explained by Aggarwal's model. Apart from kinetic studies, theoretical studies have also suggested that

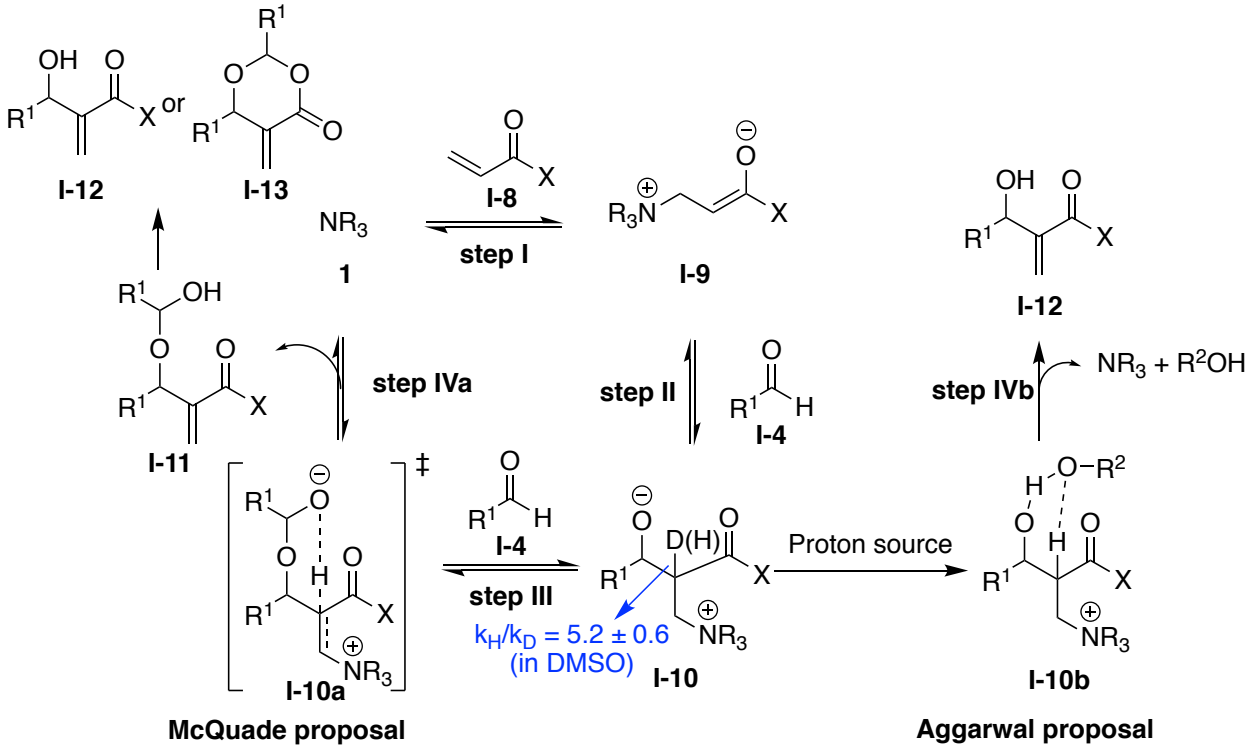

Scheme I-4. McQuade proposed MBH reaction mechanism: proton-transfer step *via* a six-membered TS formed with a 2nd molecule of aldehyde; Aggarwal proposed MBH reaction mechanism: proton-transfer step *via* a six-membered intermediate formed by autocatalysis.

these two pathways are competing mechanisms, with one more favored depending on the specific reaction conditions.[28,29]

The mechanism will be more complicated if a co-catalytic system and/or multi-/bifunctional catalyst is used. Furthermore, the mechanistic study of the asymmetric MBH reactions is even more challenging as several intermediates and transition states are involved in the reaction process.[30-33]

I-3.2. Phosphine-Catalyzed MBH Reaction

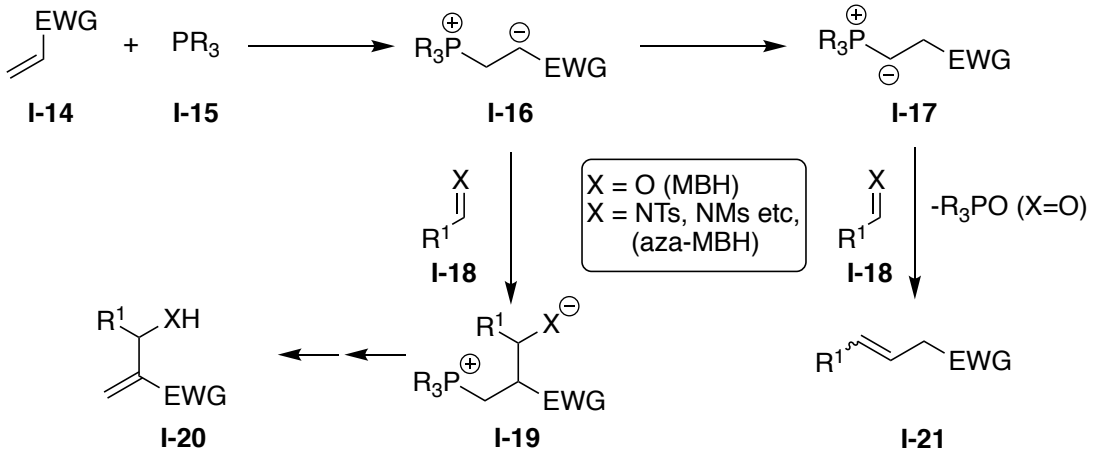

Scheme I-5. Proposed phosphine-catalyzed MBH reaction mechanism.

Almost identical to the amine-catalyzed MBH reaction, phosphine-catalyzed MBH also proceeds through three steps; the Michael addition, the aldol reaction and the elimination of the catalyst, with the exception for the formation of a potential phosphorus ylide, such as **I-17,** after the Michael addition step, delivering olefination product **I-21** (**Scheme I-5**).[4] The latter process is not observed under mild reaction conditions, requiring elevated temperatures.

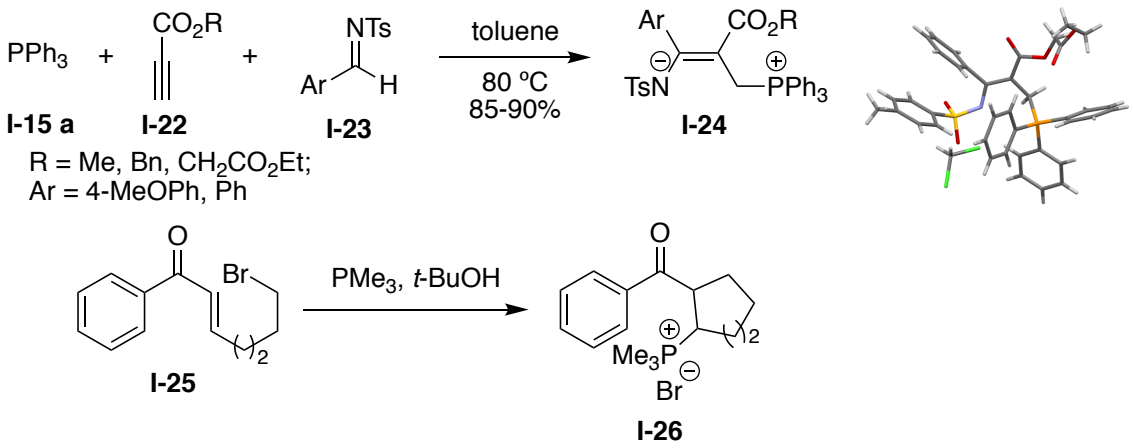

Scheme I-6. Isolated stable phosphonium zwitterions, which are key intermediates of the phosphine-catalyzed MBH reaction.

Recently, the postulated phosphine-catalyzed MBH reaction mechanism was experimentally supported by isolating stable phosphonium zwitterions **I-24** and **I-26**; the intermolecular example by Tong's group[34] and intramolecular example by Krafft's group[35], respectively (**Scheme I-6**). The X-ray crystal structure of the zwitterion **I-24** is shown in **Scheme I-6**, which is one of the key intermediates of the proposed aza-MBH reaction mechanism.

a. Chiral electrophiles

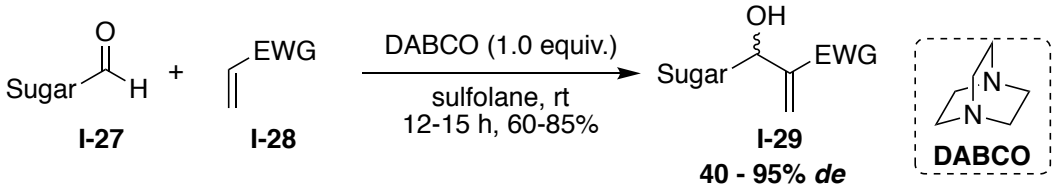

b. Chiral activated alkenes and alkynes

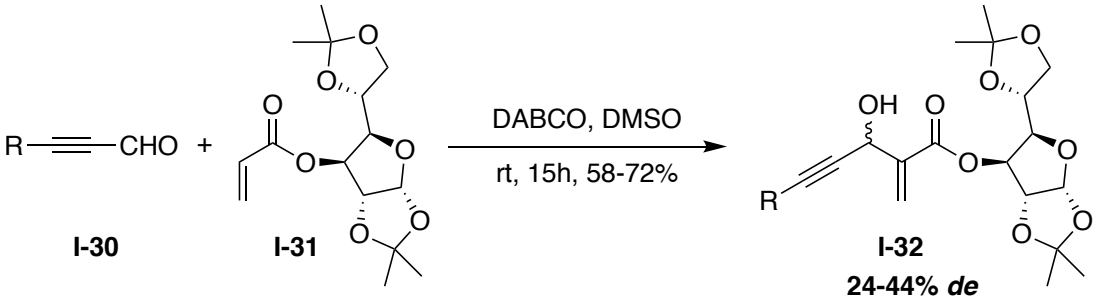

Scheme I-7. Representative examples of substrate-control MBH reactions.

I-4. Catalytic Asymmetric Induction of the MBH Reaction

The asymmetric version of the MBH reaction was developed several decades ago, including substrate-control (either through electrophiles or activated alkenes) and catalyst-control.[4,36] Representative examples are depicted in **Scheme I-7** for substrate-control MBH reactions, in which 1,4-diazabicyclo[2.2.2]octane (**DBACO**) was used as the catalyst for both of cases.[37,38] Also, as is described in **Scheme I-7**, embedding sugar analogues as the auxiliary in substrates, such as **I-27** and **I-31**, is a popular strategy for substrate-control asymmetric MBH reaction.[17,39-44] However, in recent years, with increasing options for catalysts and broader substrate scope, more focus has been placed on the organocatalytic asymmetric MBH/aza-MBH reactions, making it as a major objective and central theme. Based on the types of the catalysts used in the reaction, catalyst-control MBH reactions could be divided into three main categories. They are chiral Lewis base catalyzed MBH reactions,[17,42,45-47] chiral Lewis acid catalyzed MBH reactions,[43,48] and chiral Brønsted acid catalyzed MBH reactions.[44,49,50] Among them, the use of chiral Lewis bases is the most well-developed field, being systematically studied by many research groups globally.[4,36]

I-4.1. Chiral Lewis Base Catalyzed MBH Reactions

Either nitrogen-based, or phosphine-based, or the hybridization of both, these Lewis base catalysts have been widely designed and synthesized, for the purpose of applying them to MBH reactions. As a classic example, *β*-isocupreidine (*β*-ICD) is one of the most successful chiral tertiary amine catalysts and has been intensively investigated. It was firstly reported by Hetakeyama and co-workers in 1999, studying the asymmetric MBH

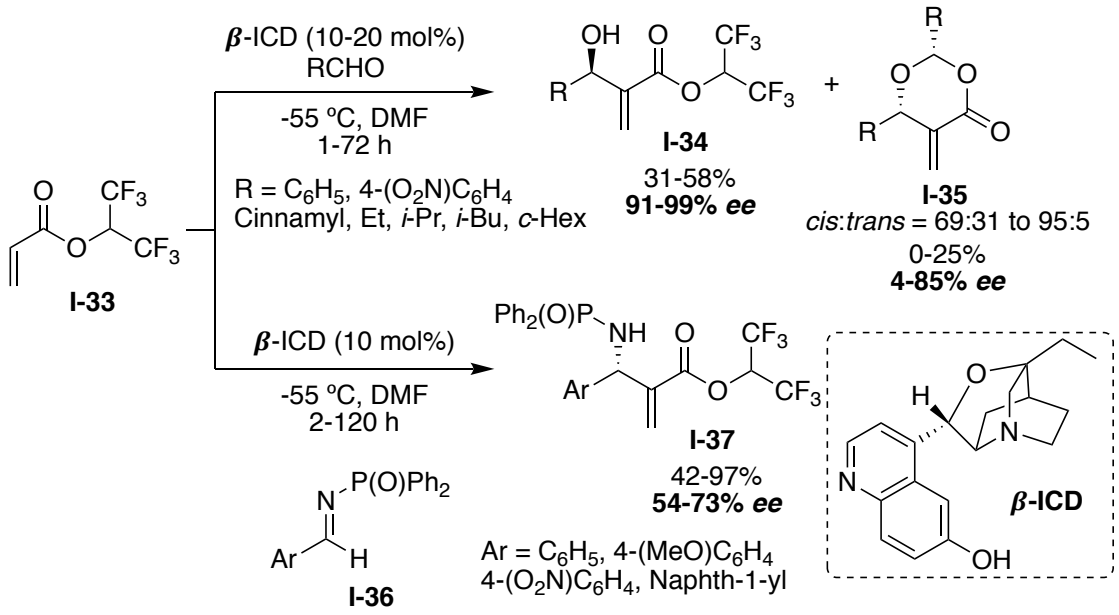

Scheme I-8. *β*-ICD initiated asymmetric MBH/ aza-MBH reactions.

reaction of 1,1,1,3,3,3-hexafluoroisopropyl acrylate (HFIPA) **I-33** and aldehydes, delivering MBH adduct with excellent enantioselectivity, as shown in **Scheme I-8**.[31] Subsequently, they were also able to extend this strategy to aza-MBH reaction, by using phosphonate protected imine **I-36,**[51] with moderate to good enantioselectivity.

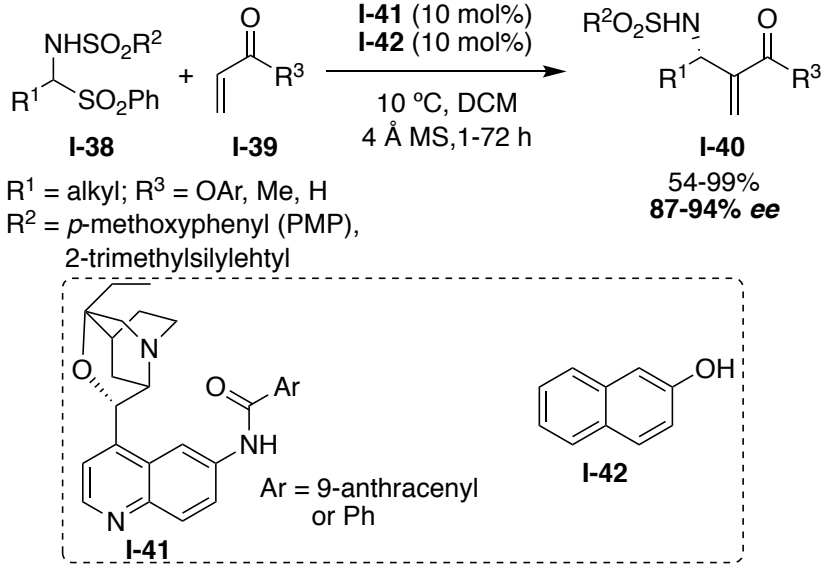

Scheme I-9. *β*-ICD-amide served as both Brønsted base and Lewis base in aza-MBH reaction.

Later, the *β*-ICD catalyst has been modified and applied to even a broader substrate scope for the MBH/aza-MBH reactions by several other groups, delivering excellent yields, as well as enantioselectivities. For example, Zhu's group reported a *β*-ICD-amide **I-41** catalyzed aza-MBH reaction between a readily available ***α***–amidosulfones and different types of Michael acceptors (***α,β***-unsaturated ester, ketone and aldehyde, see **Scheme I-9**).[52] During this cascade process, the catalyst *β*-ICD-amide **I-41** serves as a trifunctional catalyst, triggering the generation of the *N*-sulfonylimine *in situ* as a Brønsted base, which initiates the aza-MBH reaction as a Lewis base. In addition, the amide residue plays a role as H-bonding donor to assist the high enantioselectivity. It was also discovered that the additive *β*–naphthol can enhance the enantioselectivity of this reaction through H-bonding. Several groups have applied the *β*-ICD catalyst in other MBH reactions when isatin derivatives reacted as activated ketones. The obtained adducts could be further transformed to 3-aryl-3-hydroxypyrrolidin-2-ones, as precursors for promising drug candidates for treatment of HIV-1 infection.[53] (see **Scheme I-10**)

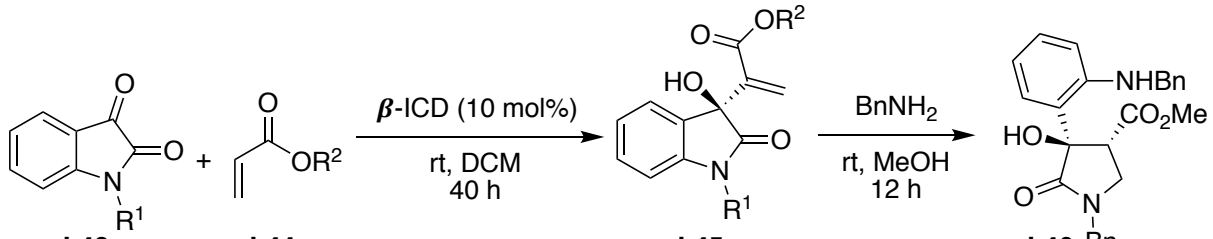

I-43 **I-44** **I-45** **I-46**

R^1 = Bn, allyl, 9-anthracenylmethyl, Me, Tf
R^2 = 2- or 1-naphthyl, Ph

up to 99% yield, **96% *ee***

87% yield, **91% *ee***

Scheme I-10. *β*-ICD catalyzed MBH reaction to modify isatin derivatives.

Not only cinchona alkaloid derived catalysts, but also other chiral amine catalysts have been used for the MBH/aza-MBH reactions. These include Fu's planar chiral DMAP **I-47**,[47] isothiourea **I-48**,[47] proline derived diamine **I-49**,[42] a dual catalytic system

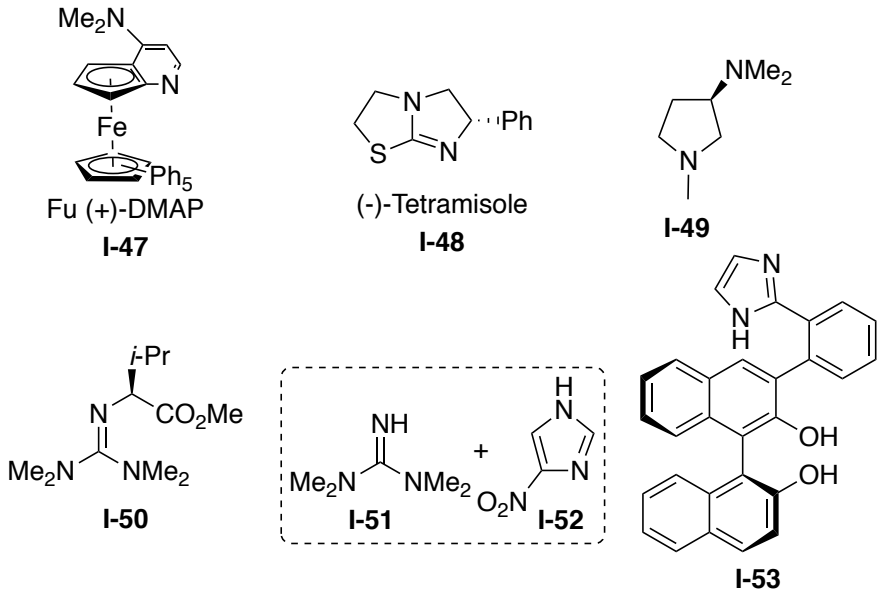

Figure I-1. Other chiral tertiary amine catalysts/ co-catalyst systems involved in MBH/ aza-MBH reactions.

composed of chiral α-guanidininoester **I-50** and PPh_3,[54] a guanidine **I-51**/azole **I-52** co-catalytic system,[46] an acid—base bifunctional catalyst **I-53**,[45] to name a few (see **Figure I-1**).

Chiral phosphine catalysts have also been developed and applied efficiently in MBH/aza-MBH reactions. Furthermore, multifunctional catalysts have been designed and synthesized, namely, the combination of Lewis basic and Brønsted basic/acidic moieties within one chiral backbone. Many of these novel catalysts are efficient in MBH/aza-MBH or its related reactions.[16,55]

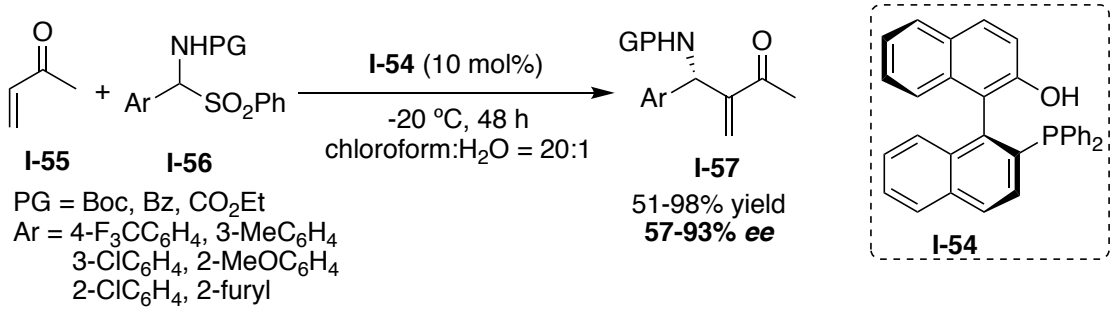

Scheme I-11. Bifunctional chiral phosphine catalyzed aza-MBH reaction.

Based on 1,1'-bi-2,2'-naphthol (BINOL) backbone, Shi's group first reported chiral bifunctional phosphine **I-54** could be used in the asymmetric aza-MBH reaction of *N*-tosyl imines with several vinyl ketones (see **Scheme I-11**).[56] Similarly, using the same backbone, Liu's group further developed several trifunctional chiral phosphine catalysts, containing a Lewis base, a Brønsted base and a Brønsted acid moiety. An example of

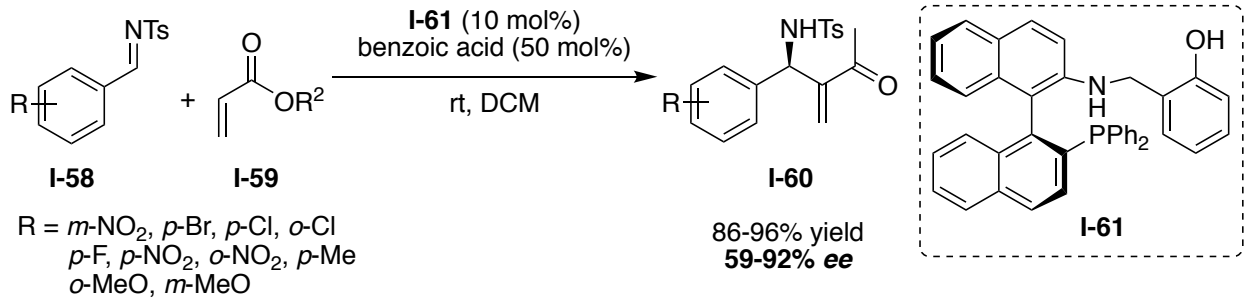

Scheme I-12. Trifunctional chiral phosphine catalyzed aza-MBH reaction.

the latter trifunctional catalyst is compound **I-61** described in **Scheme I-12**.[57] In this example, the phosphine moiety reacts as a Lewis base, secondary amine reacts as a Brønsted base and the phenol moiety plays the role of the Brønsted acid. Also, in this reaction, catalytic amount of benzoic acid was used to increase both the reaction rate and enantioselectivity. It is hypothesized that the favored transition state involves the

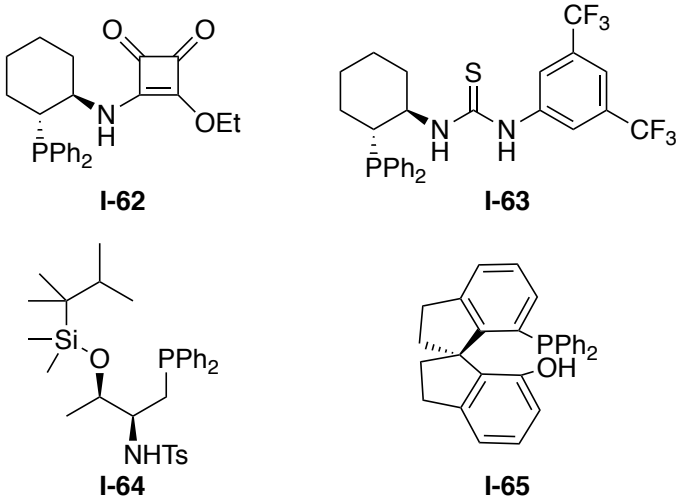

Figure I-2. Representative examples of other multifunctional catalysts.

formation of hydrogen bonding and chiral ion pair between the catalyst and the benzoic acid after protonation.[58] Several multifunctional chiral phosphine catalysts with different backbones and/or hybridized Brønsted acid moieties are also reported with applications in the MBH/aza-MBH and related reactions. Representative examples are shown in **Figure I-2**.[4]

I-4.2. Chiral Lewis Acid Catalyzed MBH Reactions

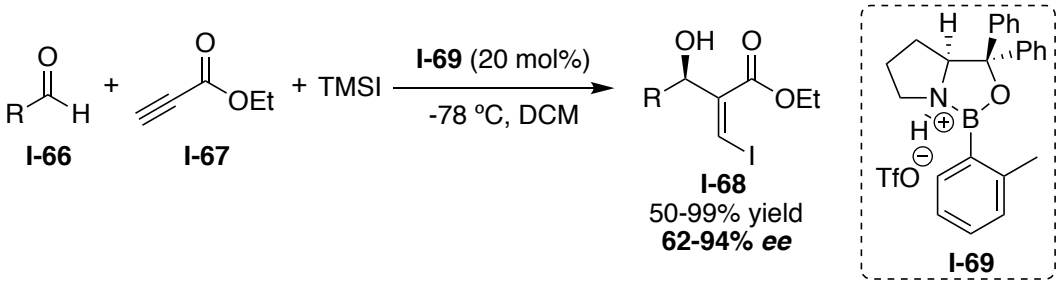

Scheme I-13. Chiral oxazaborolidinium catalyzed three-component MBH reaction.

Not as popular as chiral Lewis bases, there are interesting reports about using chiral Lewis acids as effective catalysts for MBH reactions. The chiral cationic oxazaborolidinium catalyst **I-69** as an example, Ryu's group reported a highly enantioselective and *Z*-controlled three-component coupling reactions with acetylenic esters, aldehydes and trimethylsilyl iodide (TMSI) (see **Scheme I-13**).[43] Both enantiomers were obtained for this three-component coupling reaction by using an *S*- or *R*-oxazaborolidinium salt. Apart from boron reagents, other metal containing Lewis acids (such as Ti, La and Ba), combined with chiral ligands and/or achiral Lewis bases, also have been utilized for asymmetric MBH reactions.

I-4.3. Chiral Brønsted Acid Catalyzed MBH Reactions

Typically, the role of a chiral Brønsted acid in an asymmetric MBH/aza-MBH reaction is to provide a local chiral environment through H-bonding in the transition state of the

reaction. As a result, several important H-bonding scaffolds, including chiral thioureas, chiral proline derivatives and chiral thiols, have been applied for the asymmetric MBH/aza-MBH reactions. Successful examples are reported when these scaffolds are used either as a moiety of a chiral bifunctional catalyst, or as a component in a co-catalytic system.

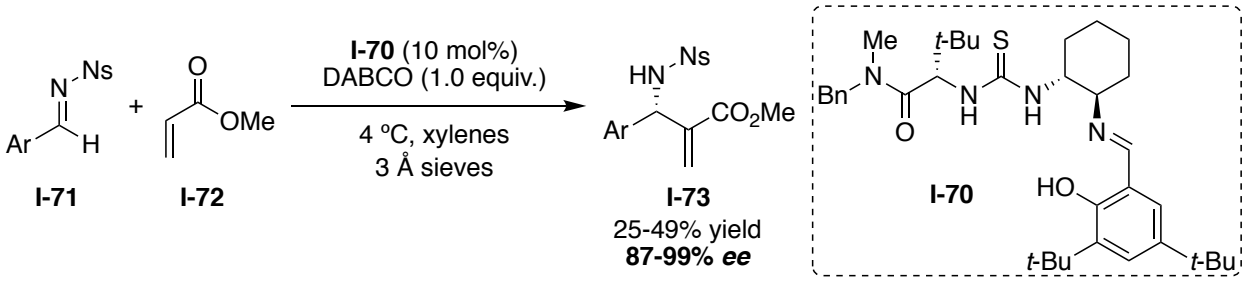

Scheme I-14. Chiral thiourea catalyzed aza-MBH reaction.

For example, in 2005, Jacobsen's and co-workers described a chiral thiourea catalyst **I-70** for the highly enantioselective aza-MBH reaction between methyl acrylate and arylimines (**Scheme I-14**).[59] Later, Ito described an efficient chiral biaryl-based bis(thiourea) organocatalyst **I-74** for MBH reactions of cyclohexenones and aldehydes (**Scheme I-15**).[60] In both reactions, the thiourea agents function as co-catalysts for the

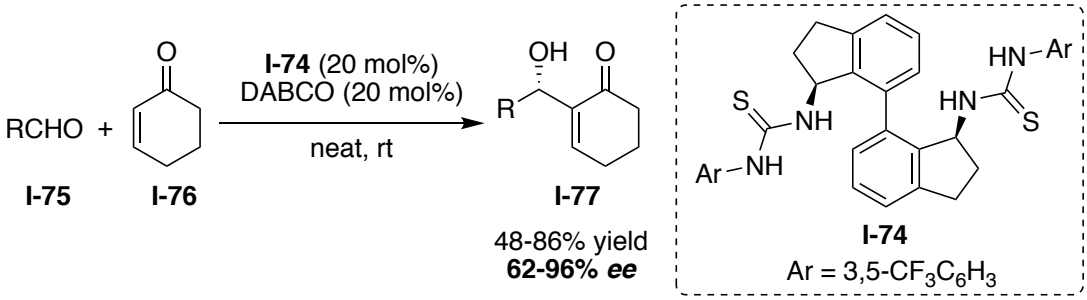

Scheme I-15. Chiral thiourea catalyzed MBH reaction of cyclohexanone and aldehydes.

purpose of forming a local chiral environment. Meanwhile, researchers also developed a series of chiral bifunctional organocatalysts by taking advantage of the naturally existing

chiral backbones, such as amino acids. Lu's group[61] first synthesized an effective L-threonine-derived bifunctional phosphine-thiourea catalyst **I-78** for the asymmetric MBH reactions of acrylates with aromatic aldehydes (**Scheme I-16 a**). Also, they revealed the importance of H-bonding interactions for achieving high enantioselectivity by investigating the influences of several achiral protic additives, such as MeOH, PhOH and PhCOOH.

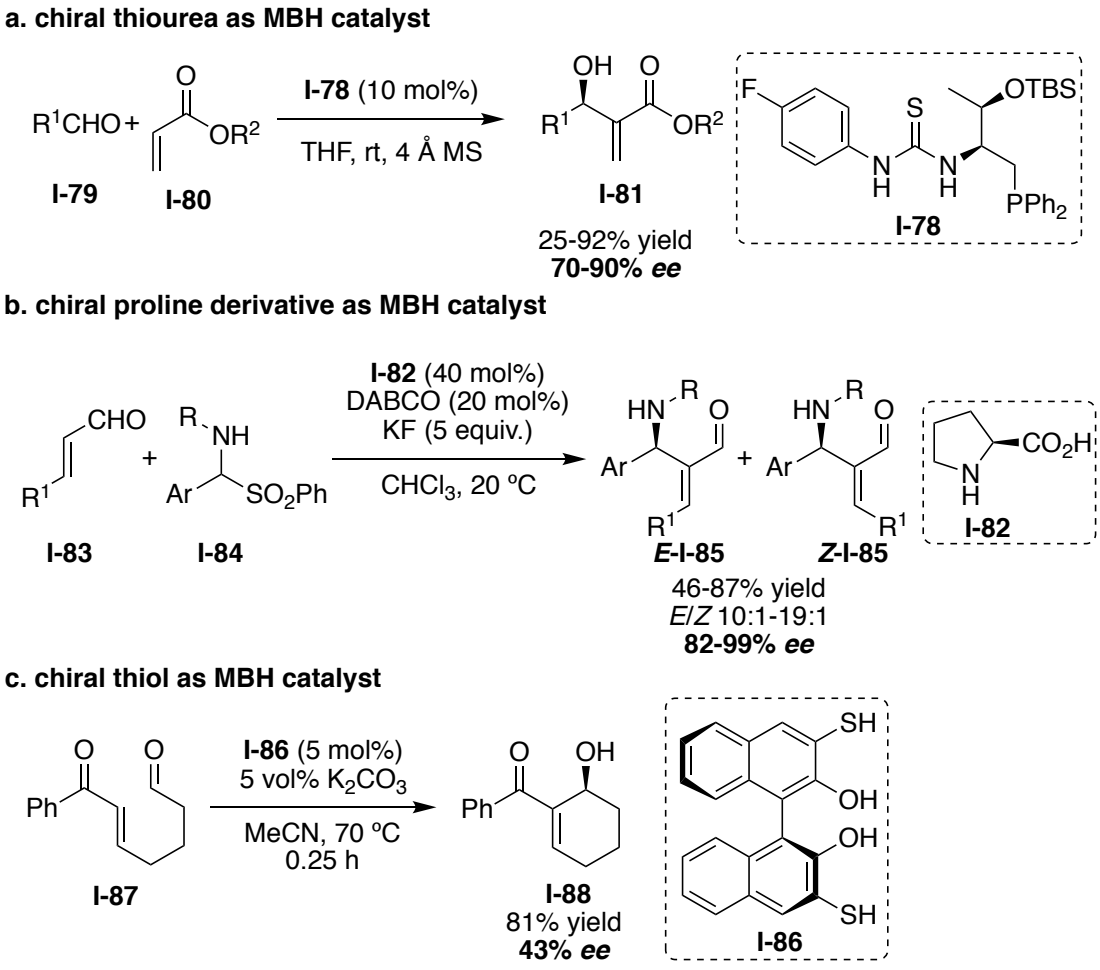

Scheme I-16. Three types of chiral Brønsted acid catalyzed MBH reactions.

Proline carboxylic or alcoholic derivatives are reported as robust Brønsted acid catalysts for MBH /aza-MBH reactions as well. In contrast to thiourea catalysts, some proline derivatives could catalyze MBH reactions individually since they carry a secondary amine as the Lewis base moiety. But proline derived co-catalytic systems are also well

established. **Scheme I-16 b** provides an example reported by Veselý's group,[49] in which (*S*)-proline **I-82** was identified as the best Brønsted acid catalyst, together with DABCO as the Lewis base co-catalyst. In addition, an excess amount of KF was used as an additive to enhance the diastereoselectivity of this reaction. Recently, Miller's group[50] uncovered that *ortho*-mercaptobenzoic acid, *ortho*-mercaptophenols and their analogues as efficient thiol catalysts for both the MBH and the Rauhut-Currier reactions (see example in **Scheme I-16 c**).

I-5. Application of MBH Products

Beside the development of MBH reaction, the transformation of MBH products have also attracted a great deal of attention from organic chemists.[62,63] As multi-functionalized scaffolds (including at least three functional groups in close proximity—hydroxyl/amino, alkene and electron-withdrawing groups), these products could be facilely and flexibly converted into other synthons based on different strategies. As a result, many investigators have focused efforts on modifying these functionalities either individually or collectively. In fact, some of these methodologies have been successfully employed in the synthesis of a variety of biologically active molecules and natural products.[64]

I-5.1. Transformations of MBH Products Catalyzed by Organocatalysts

More recently, both Basavaiah[36] and Shi[4] have reviewed the transformations of MBH products from different aspects. From a systematic viewpoint, Basavaiah summarized most of the reactions in pictorial forms, covering the synthetic transformations of MBH alcohols, acetates and bromides, where these MBH products have been employed as substrates in a number of named and unnamed reactions, such as Heck reaction, Friedel-

Crafts reaction, isomerization and hydrogenation.[36,65] **Figure 3** illustrates some representative transformations of MBH alcohols.[36] Also, efforts have been made to convert these MBH products into various tri-substituted alkenes with defined stereochemistry. More importantly, the MBH adducts and their derivatives have been used to construct biologically important carbo- and heterocyclic molecules.[64,65]

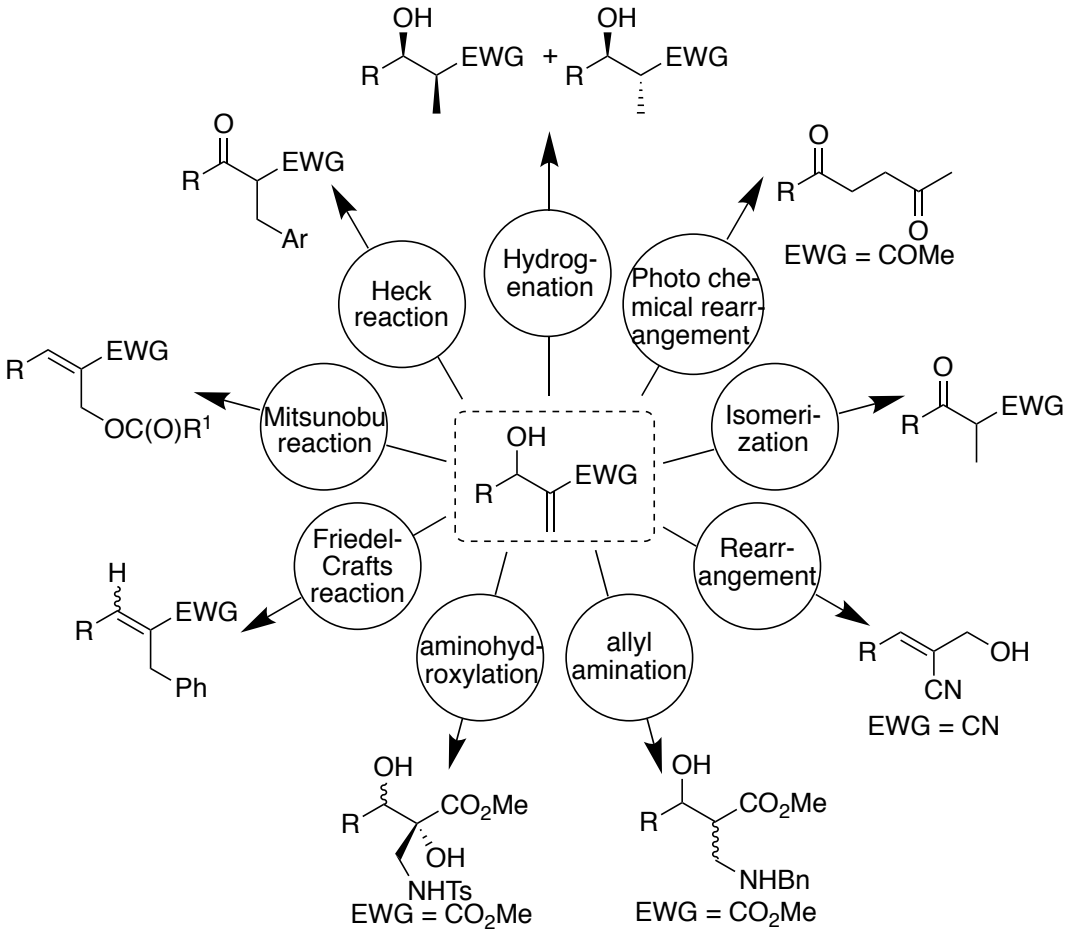

Figure I-3. Representative transformations of MBH alcohols.

Shi has described allylic substitution reactions of MBH acetates and carbonates, and annulation of MBH acetates and carbonates with electron-deficient olefins.[4] After a quinidine-catalyzed S_N2' reaction to produce chiral MBH propargylic ethers reported by Basavaiah,[65] asymmetric transformations of MBH products *via* substitution of MBH

acetates/carbonates by different types of nucleophiles have become widely investigated and intensively reported.[66-71] The general equation of the allylic substitution reactions of

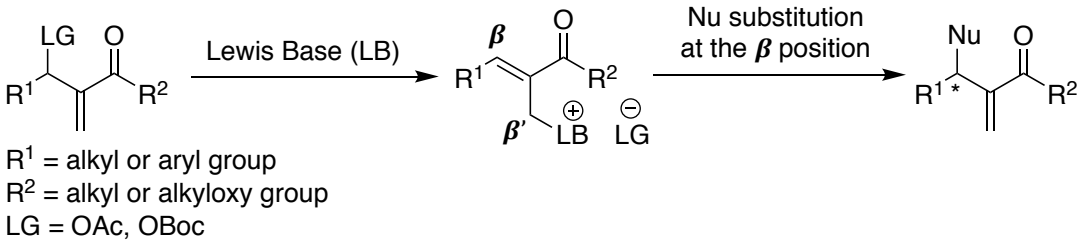

Scheme I-17. General scheme of the allylic substitution reactions of MBH acetates and carbonates.

MBH acetates and carbonates is illustrated in **Scheme I-17**.[4] In 2004, Krische's group[72,73] reported intermolecular allylic substitution reactions of MBH products using phosphine catalysts to form C-C and C-hetero atom bonds. In these reactions, N- and C-nucleophiles, such as 4,5-dichlorophthalimides and 2-trimethylsilyloxyfuran (TMSOF) were employed to furnish allylic amines and γ–butenolides in high regio- and diastereoselectivity and in good yields, respectively. Later, several other groups developed chiral Lewis base catalyzed allylic substitution reactions of MBH products, achieving excellent enantioselectivities with good yields. Overall, 1,1'-bi-2-naphthol (BINOL) and cinchona alkaloid derived Lewis bases are commonly used for this transformation. More recently, Wang's group[74,75] reported quinidine catalyzed allylic substitution reaction of MBH carbonates with phosphine oxides to directly approach

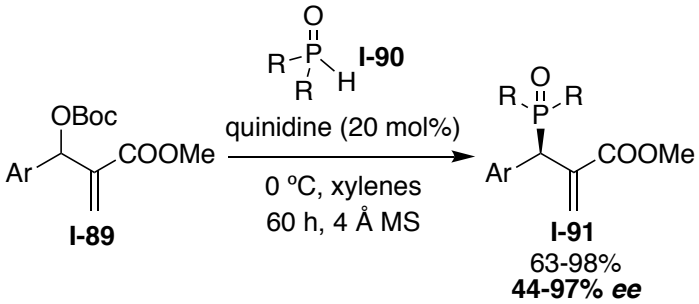

Scheme I-18. Chiral allylic phosphine oxides synthesis through asymmetric allylic substitution of MBH adduct derivatives.

optically active allylic phosphine oxides in an easy and efficient way with satisfactory enantioselectivities and yields (**Scheme I-18**). MBH acetates and carbonates can undergo annulation reactions with electron-deficient olefins to construct multifunctional carbo- and hetero-cyclic compounds.[76-79] During the annulation reaction, in the presence

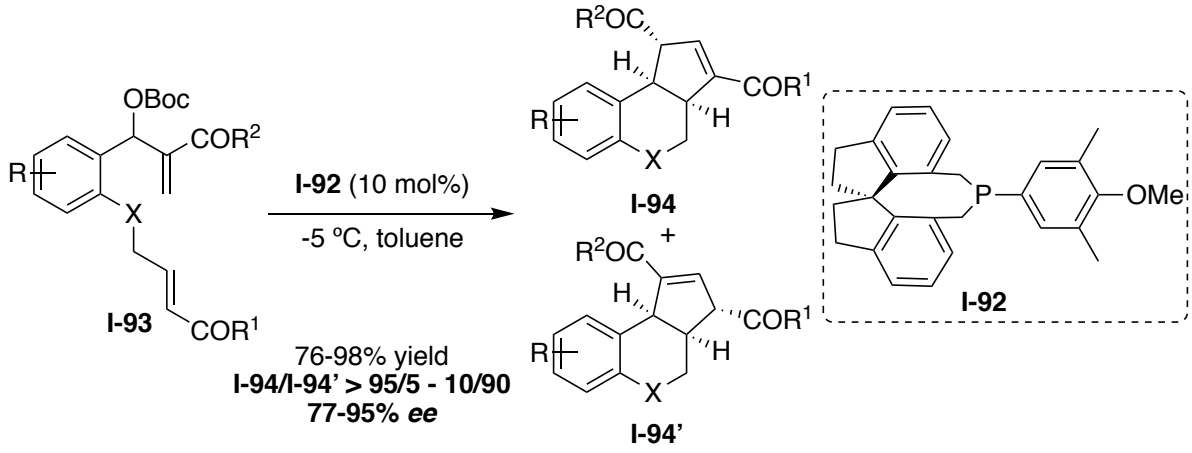

Scheme I-19. Chiral phosphine mediated asymmetric intramolecular [3+2] annulation of MBH carbonates.

of tertiary phosphines, the *in situ* generated phosphorus ylides derived from MBH acetates and carbonates, are very reactive 1,3-dipoles intermediates. Both intermolecular and intramolecular [3+2] cycloaddition reactions have been reported.[80,81] An example from Tang's group[82] is illustrated in **Scheme I-19**, in which a spirobiindane-based chiral phosphine **I-92** was used as the catalyst. Interestingly, Zhang,[76] Huang[78] and He's[83] groups have simultaneously reported [4+1] annulations recently, utilizing MBH acetates

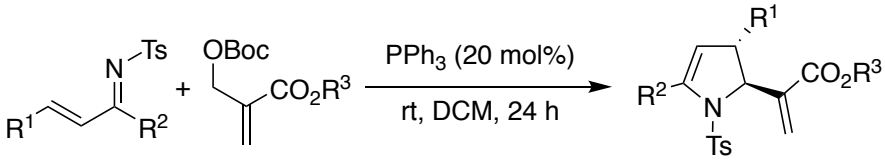

I-95 **I-96**

I-97
80-99% yield,
***dr* >20:1**

Scheme I-20. Phosphine mediated intermolecular [4+1] cycloaddition reaction of MBH carbonates.

and carbonates, as shown in **Scheme I-20**. In this reaction, MBH carbonate was reacted as a C1 synthon.

I-5.2. Applications of the MBH Reaction toward Natural Products and Drug Molecules Synthesis

One of the major goals in organic synthetic chemistry is the synthesis of complex natural products from common, simple and commercially available starting materials. Toward this objective, organic chemists have devoted a great deal of effort into constructing simple scaffolds decorated with densely functionalized groups, which present opportunities not only directed to the target compounds, but also to construct a library of analogues. Morita-Baylis-Hillman (MBH) reaction meets this requirement by providing diversely functionalized scaffolds, such as alkene-hydroxyl-carbonyl and alkene-amino-carbonyl functional groups, which are important synthons of medicinally bioactive compounds and natural products. As a result, it is not surprising that this reaction has been utilized in the synthesis of a range of molecules, obtained from

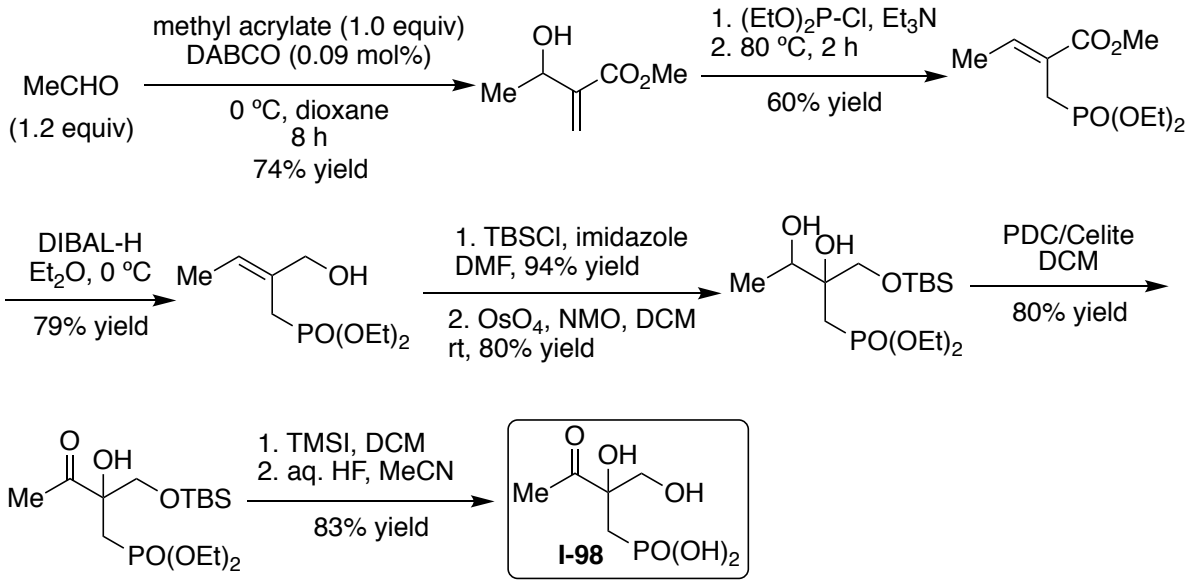

Scheme I-21. Total synthesis of Phosphonothrixin **I-98**.

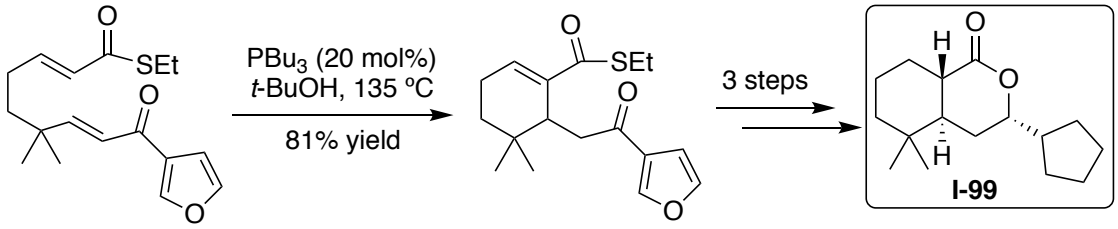

Scheme I-22. Total synthesis of (±)–Ricciocarpine A **I-99**.

microbial, animal, moss, terrestrial and marine origins. Also, some of the MBH products are precursors to several drug molecules or their intermediates. Recently, a number of reviews describing the applications of the MBH reaction towards the synthesis of natural products and drug molecules or their intermediates have been discussed systematically and extensively.[36,62,64,84-89] Based on the origins of the natural products, representative examples (in simplified sequences) of each origin have been selected to demonstrate the applications of the MBH reaction in total synthesis. Phosphonothrixin **I-98** in **Scheme I-21** is a phosphorous containing herbicidal natural product of microbial origin, isolated from *Saccharothrix* sp. ST-888 and the synthesis was reported by Fields's group.[90] (±)–Ricciocarpine A **I-99** in **Scheme I-22**, a furanosesquiterpene from moss, isolated from the liverwort *Ricciocarpos natans*, exhibits its good molluscicidal activity against the water snail *Biomphalaria glabrata*, with synthesis reported from Krische's group.[91] Grandisine alkaloid **I-100**, isolated from the leaves of the Australian rainforest tree *Elaeocarpus grandis*, are of terrestrial origin, exhibiting affinity for the human ***δ***–opioid receptor and the synthesis was performed by Tamura and co-workers (**Scheme I-23**).[92]

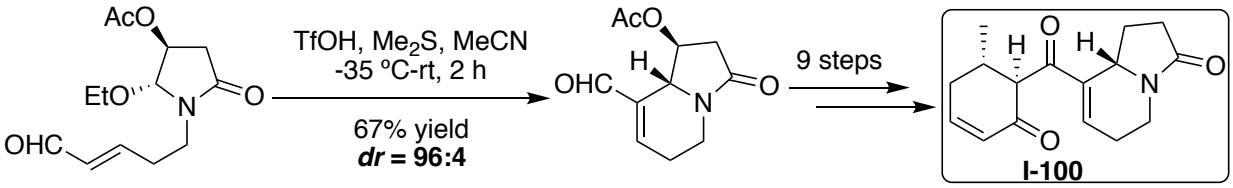

Scheme I-23. Total synthesis of Gradisine alkaloid **I-100**.

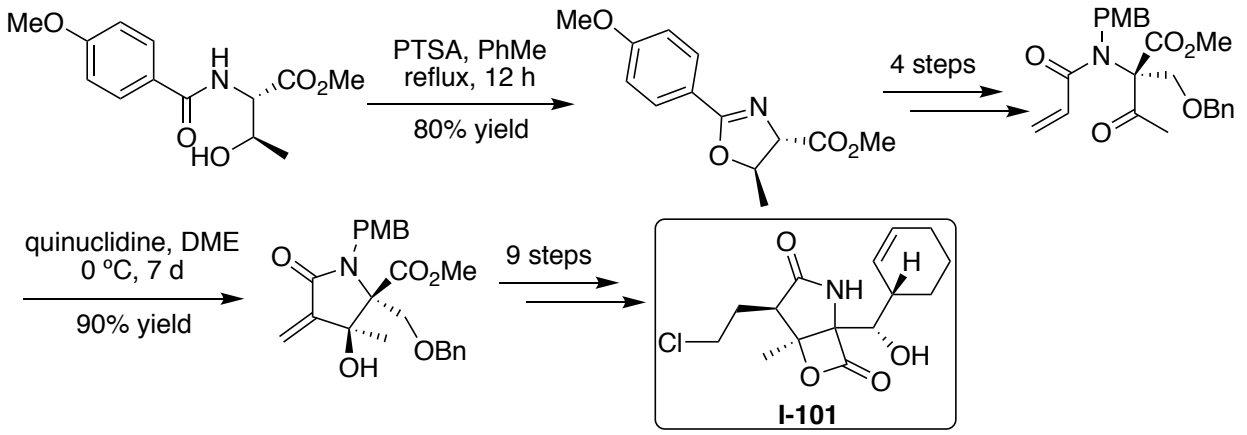

Scheme I-24. Total synthesis of Salinosporamide **I-101**.

Salinosporamide A **I-101** is a bioactive natural product of a marine organism with effective proteasome inhibition property, widely distributed in ocean sediments. Corey's group[93] utilized an intramolecular MBH reaction to achieve the synthesis of this molecule, as shown in **Scheme I-24**. Basavaiah's group[94] developed the synthesis of the biologically active himanimide A **I-102**, which is a natural product with animal origin, in 11.38% overall yield (**Scheme I-25**).

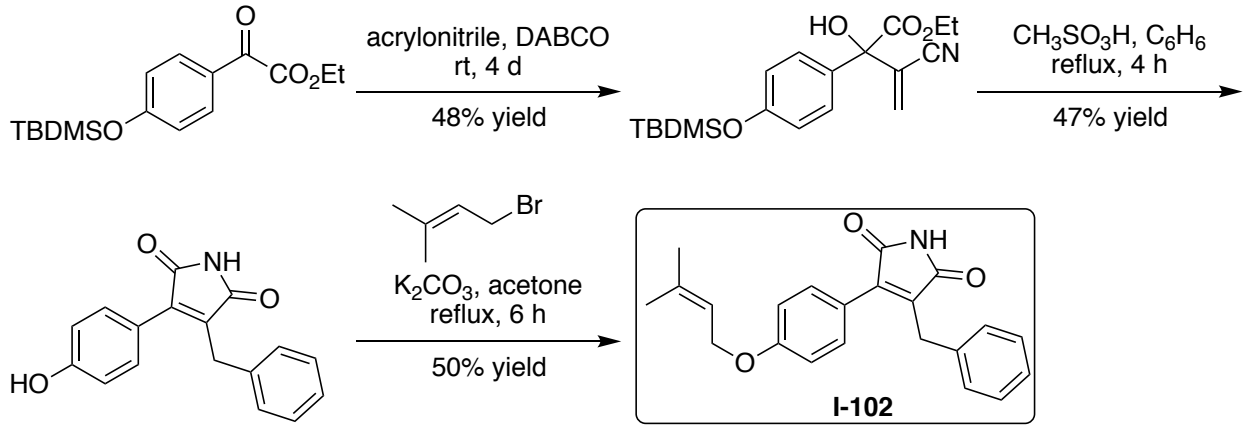

Scheme I-25. Total synthesis of himanimide A **I-102**.

As can be seen, the MBH reaction has made tremendous contributions to the realms of synthetic chemistry and continues to offer more opportunities for future applications.

Hence, there is no doubt that further studies of this reaction will be also important for the synthetic chemistry field.

I-6. Deviations from the MBH reaction—the Lewis base catalyzed cyclization reactions

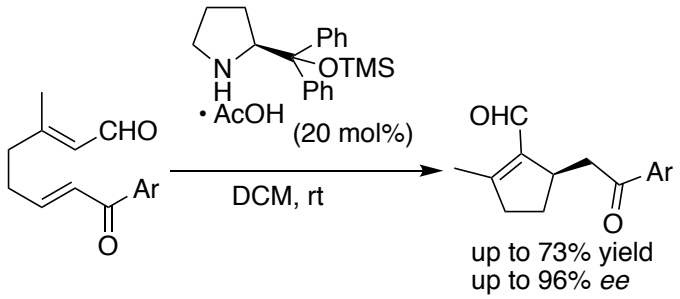

Scheme I-26. An example of intramolecular Rauhut-Currier reaction.

The most relevant to the Morita-Baylis-Hillman (MBH) reaction is the Rauhut-Currier (RC) reaction, also known as vinylogous Morita-Baylis-Hillman reaction. In general, it is a reaction that involves any coupling of one active/latent enolate to a second Michael acceptor, creating a new C-C bond between the α–position of one activated alkene and the β–position of a second alkene under the influence of a nucleophilic catalyst.[95] An intramolecular RC type of reaction developed by Christamn's group[96] is as an example given in **Scheme I-26**. Mechanistically, the RC reaction is essentially a variant of the MBH reaction.

Interestingly, nucleophilic organocatalysts, such as tertiary amines, phosphines and *N*-heterocyclic carbenes (NHCs) catalyzed cycloaddition reactions are becoming more popular as these reactions are efficient methods for carbo- and heterocycles synthesis. Generally, these organocatalytic cycloaddition reactions proceed *via* a zwitterion-oriented strategy depicted in **Scheme I-27**, in which the addition of a nucleophilic organocatalyst

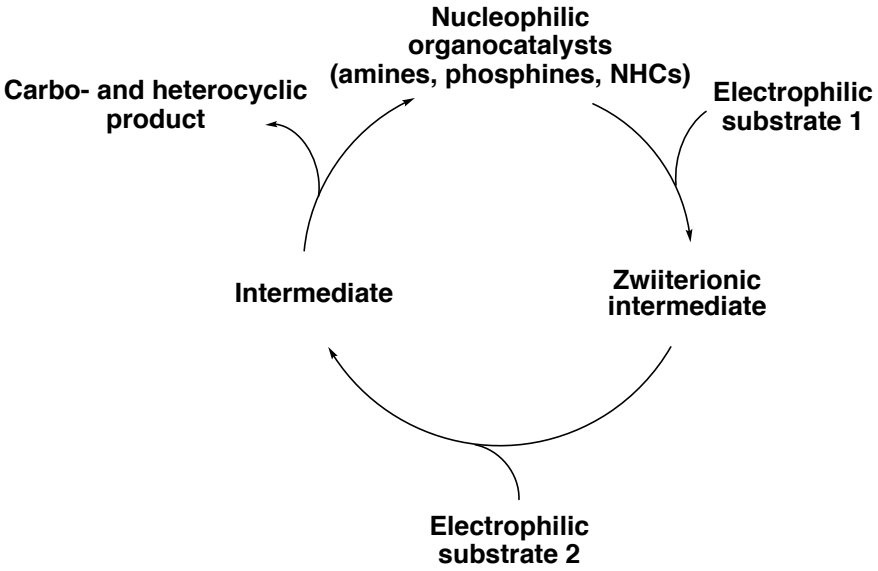

Scheme I-27. General mechanism of organocatalytic cycloaddition reaction.

to the electrophilic substrate generates the zwitterion intermediate. The intermediate then undergoes the addition with the second electrophilic substrate, followed by cyclization and release of the catalyst to provide carbo- and heterocyclic products.[97] From a mechanistic viewpoint, it is reasonable to attribute these organocatalytic cycloaddition reactions as deviations of the Morita-Baylis-Hillman reaction in general.

As a zwitterion-oriented synthetic strategy, these reactions are more tunable with subtle changes of the catalysts, substrates or reaction conditions, which provides a divergent synthetic route to produce a diverse set of carbo- and heterocycles.[97] The influence of catalysts on the mode of the cycloaddition reaction provides a good example to illustrate this conclusion. In organocatalytic reactions of allenoates and activated alkenes, generally, phosphine catalysts will deliver [3+2] cycloaddition reaction products, while amine catalysts will furnish [4+2] cycloaddition products or *via* an intermediate of Rauhut-Currier reaction to provide [4+2] cycloaddition products (see **Scheme I-28**). Yu's group[98] employed DFT calculations to investigate the different behaviors of these

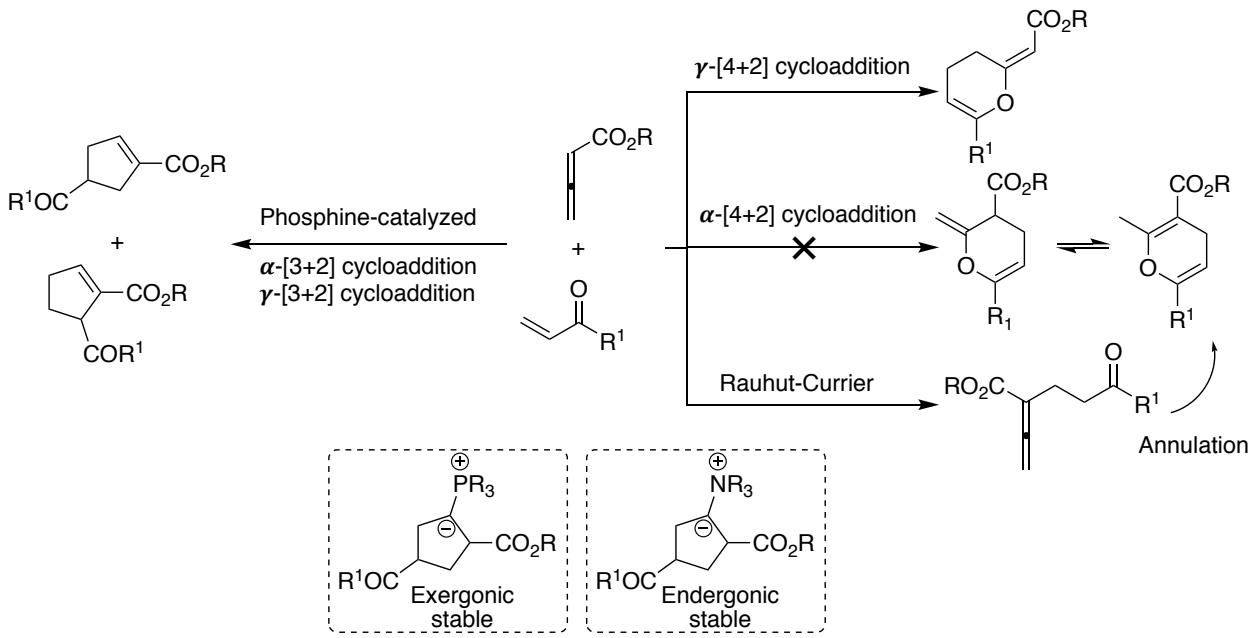

Scheme I-28. General mechanism of organocatalytic cycloaddition reaction between α,β–unsaturated compounds and allenoate.

catalysts. They show that the formation of the [3+2] phosphorus ylide is exergonic, which

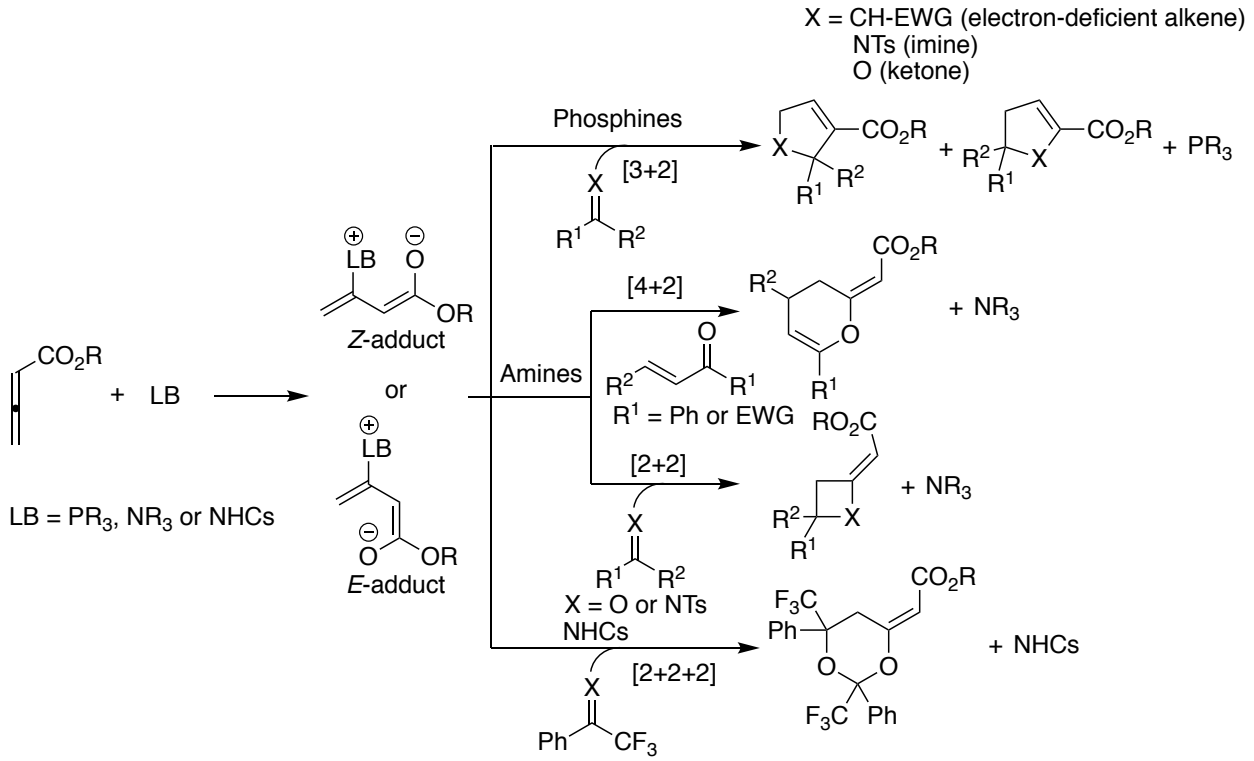

Scheme I-29. The cycloaddition reaction modes affected by different LB catalysts.

leads to the kinetically more favored [3+2] cycloaddition, as compared to the [4+2]

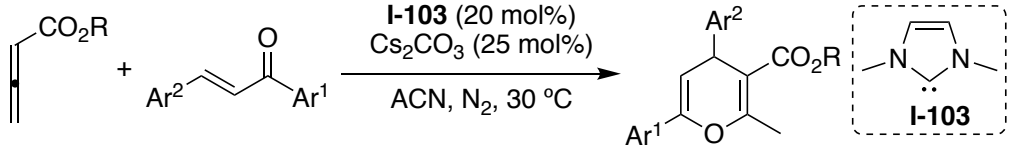

Scheme I-30. NHC-catalyzed [4+2] cycloaddition reaction of allenoate and chalcones.

cycloaddition. However, the formation of [3+2] ammonium ylide is endergonic, which enables the [4+2] cycloaddition reaction. More interestingly, further DFT calculation from the same group showed NHC-allenoate intermediates are the most exergonic.[99] These adducts are even more stable than the expected [2+2] cycloaddition product, instead, the thermodynamically controlled [2+2+2] annulation occurs when NHCs react as the catalyst. A summary of these three types of Lewis bases catalyzed cycloaddition reactions is shown in **Scheme I-29**. However, examples of [4+2] cycloaddition catalyzed by phosphines[100] or NHCs[101] have also been reported. **Scheme I-30** shows an example of NHC-mediated [4+2] cycloaddition reaction. Also, even though both DMAP and DABCO are N-based catalysts, they deliver (*Z*) and (*E*) stereoisomers, respectively.[102] More investigations are necessary to further understand the underpinnings of the Lewis base catalyzed cycloaddition reactions.

REFERENCES

REFERENCES

(1) MacMillan, D. W. C. The advent and development of organocatalysis. *Nature* **2008,** *455* (7211), 304.

(2) Seayad, J.; List, B. Asymmetric organocatalysis. *Organic & Biomolecular Chemistry* **2005,** *3* (5), 719.

(3) List, B. Introduction: Organocatalysis. *Chemical Reviews* **2007,** *107* (12), 5413.

(4) Wei, Y.; Shi, M. Recent Advances in Organocatalytic Asymmetric Morita-Baylis-Hillman/aza-Morita-Baylis-Hillman Reactions. *Chemical Reviews* **2013,** *113* (8), 6659.

(5) Morita, K. In *Japan Patent*, 1968.

(6) Morita, K.; Suzuki, Z.; Hirose, H. A TERTIARY PHOSPHINE-CATALYZED REACTION OF ACRYLIC COMPOUNDS WITH ALDEHYDES. *Bulletin of the Chemical Society of Japan* **1968,** *41* (11), 2815.

(7) Baylis, A. B. H., M. E. D. In *German Patent*, 1972.

(8) Drewes, S. E.; Emslie, N. D. NECIC ACID SYNTHONS .1. TOTAL SYNTHESIS OF INTEGERRINECIC ACID. *Journal of the Chemical Society-Perkin Transactions 1* **1982**, 2079.

(9) Hoffmann, H. M. R.; Rabe, J. DABCO-CATALYZED COUPLING OF ALDEHYDES WITH ACTIVATED DOUBLE-BONDS .1. PREPARATION OF 2-(1-HYDROXYALKYL)ACRYLIC ESTERS - SIMPLE 3-STEP SYNTHESIS OF MIKANECIC ACID. *Angewandte Chemie-International Edition in English* **1983,** *22* (10), 795.

(10) Basavaiah, D.; Gowriswari, V. V. L. A SIMPLE SYNTHESIS OF ALPHA-METHYLENE-BETA-HYDROXYALKANONES. *Tetrahedron Letters* **1986,** *27* (18), 2031.

(11) Perlmutter, P.; Teo, C. C. A SIMPLE SYNTHESIS OF 2-METHYLIDENE-3-AMINOPROPANOATES. *Tetrahedron Letters* **1984,** *25* (51), 5951.

(12) Hoffmann, H. M. R.; Rabe, J. 1,4-DIAZOBICYCLO 2.2.2 OCTANE-CATALYZED COUPLING OF ALDEHYDES AND ACTIVATED DOUBLE-BONDS .3. A SHORT AND PRACTICAL SYNTHESIS OF MIKANECIC ACID (4-VINYL-1-CYCLOHEXENE-1,4-DICARBOXYLIC ACID). *Helvetica Chimica Acta* **1984,** *67* (2), 413.

(13) Hoffmann, H. M. R.; Rabe, J. DABCO-CATALYZED COUPLING OF ALDEHYDES WITH ACTIVATED DOUBLE-BONDS .4. STEREOSELECTIVE SYNTHESIS OF TRISUBSTITUTED

OLEFINS AND TERPENOID BUILDING-BLOCKS VIA 2-(HYDROXYALKYL)-2-PROPENOIC ESTERS. *Journal of Organic Chemistry* **1985,** *50* (20), 3849.

(14) Wei, Y.; Shi, M. Multifunctional Chiral Phosphine Organocatalysts in Catalytic Asymmetric Morita-Baylis-Hillman and Related Reactions. *Accounts of Chemical Research* **2010,** *43* (7), 1005.

(15) Aggarwal, V. K.; Fulford, S. Y.; Lloyd-Jones, G. C. Reevaluation of the mechanism of the Baylis-Hillman reaction: Implications for asymmetric catalysis. *Angewandte Chemie-International Edition* **2005,** *44* (11), 1706.

(16) Cowen, B. J.; Miller, S. J. Enantioselective catalysis and complexity generation from allenoates. *Chemical Society Reviews* **2009,** *38* (11), 3102.

(17) Masson, G.; Housseman, C.; Zhu, J. P. The enantioselective morita-baylis-hiliman reaction and its aza counterpart. *Angewandte Chemie-International Edition* **2007,** *46* (25), 4614.

(18) Price, K. E.; Broadwater, S. J.; Jung, H. M.; McQuade, D. T. Baylis-Hillman mechanism: A new interpretation in aprotic solvents. *Organic Letters* **2005,** *7* (1), 147.

(19) Price, K. E.; Broadwater, S. J.; Walker, B. J.; McQuade, D. T. A new interpretation of the Baylis-Hillman mechanism. *Journal of Organic Chemistry* **2005,** *70* (10), 3980.

(20) Regiani, T.; Santos, V. G.; Godoi, M. N.; Vaz, B. G.; Eberlin, M. N.; Coelho, F. On the mechanism of the aza-Morita-Baylis-Hillman reaction: ESI-MS interception of a unique new intermediate. *Chemical Communications* **2011,** *47* (23), 6593.

(21) Hill, J. S.; Isaacs, N. S. FUNCTIONALIZATION OF THE ALPHA-POSITION OF ACRYLATE SYSTEMS BY THE ADDITION OF CARBONYL-COMPOUNDS - HIGHLY PRESSURE-DEPENDENT REACTIONS. *Tetrahedron Letters* **1986,** *27* (41), 5007.

(22) Hill, J. S.; Isaacs, N. S. MECHANISM OF ALPHA-SUBSTITUTION REACTIONS OF ACRYLIC DERIVATIVES. *Journal of Physical Organic Chemistry* **1990,** *3* (5), 285.

(23) Hill, J. S. I., N. S. *J. Chem. Res.* **1988**, 330.

(24) Bode, M. L.; Kaye, P. T. A KINETIC AND MECHANISTIC STUDY OF THE BAYLIS-HILLMAN REACTION. *Tetrahedron Letters* **1991,** *32* (40), 5611.

(25) Fort, Y.; Berthe, M. C.; Caubere, P. THE BAYLIS-HILLMAN REACTION-MECHANISM AND APPLICATIONS REVISITED. *Tetrahedron* **1992,** *48* (31), 6371.

(26) Vanrozendaal, E. L. M.; Voss, B. M. W.; Scheeren, H. W. EFFECT OF SOLVENT, PRESSURE AND CATALYST ON THE E/Z-SELECTIVITY IN THE BAYLIS-HILLMAN REACTION BETWEEN CROTONONITRILE AND BENZALDEHYDE. *Tetrahedron* **1993,** *49* (31), 6931.

(27) Santos, L. S.; Pavam, C. H.; Almeida, W. P.; Coelho, F.; Eberlin, M. N. Probing the mechanism of the Baylis-Hillman reaction by electrospray ionization mass and tandem mass spectrometry. *Angewandte Chemie-International Edition* **2004,** *43* (33), 4330.

(28) Xu, J. H. Probing the mechanism of Morita-Baylis-Hillman reaction in dichloromethane by density functional theory. *Journal of Molecular Structure-Theochem* **2006,** *767* (1-3), 61.

(29) Roy, D.; Sunoj, R. B. Ab initio and density functional theory evidence on the rate-limiting step in the Morita-Baylis-Hiliman reaction. *Organic Letters* **2007,** *9* (23), 4873.

(30) Amarante, G. W.; Benassi, M.; Milagre, H. M. S.; Braga, A. A. C.; Maseras, F.; Eberlin, M. N.; Coelho, F. Bronsted Acid Catalyzed Morita-Baylis-Hillman Reaction: A New Mechanistic View for Thioureas Revealed by ESI-MS(/MS) Monitoring and DFT Calculations. *Chemistry-a European Journal* **2009,** *15* (45), 12460.

(31) Iwabuchi, Y.; Nakatani, M.; Yokoyama, N.; Hatakeyama, S. Chiral amine-catalyzed asymmetric Baylis-Hillman reaction: A reliable route to highly enantiomerically enriched (alpha-methylene-beta-hydroxy)esters. *Journal of the American Chemical Society* **1999,** *121* (43), 10219.

(32) Anstiss, C.; Garnier, J. M.; Liu, F. Mechanistic investigations of multidentate organocatalyst-promoted counterion catalysis for fast and enantioselective aza-Morita-Baylis-Hillman reactions at ambient temperature. *Organic & Biomolecular Chemistry* **2010,** *8* (19), 4400.

(33) Duarte, F. J. S.; Cabrita, E. J.; Frenking, G.; Santos, A. G. Density Functional Study of Proline-Catalyzed Intramolecular Baylis-Hillman Reactions. *Chemistry-a European Journal* **2009,** *15* (7), 1734.

(34) Liu, H. M.; Zhang, Q. M.; Wang, L. M.; Tong, X. F. PPh_3-Catalyzed Reactions of Alkyl Propiolates with N-Tosylimines: A Facile Synthesis of Alkyl 2- aryl(tosylimino)methyl acrylate and an Insight into the Reaction Mechanism. *Chemistry-a European Journal* **2010,** *16* (6), 1968.

(35) Krafft, M. E.; Haxell, T. F. N.; Seibert, K. A.; Abboud, K. A. Mechanistic implications in the Morita-Baylis-Hillman alkylation: Isolation and characterization of an intermediate. *Journal of the American Chemical Society* **2006,** *128* (13), 4174.

(36) Basavaiah, D.; Reddy, B. S.; Badsara, S. S. Recent Contributions from the Baylis-Hillman Reaction to Organic Chemistry. *Chemical Reviews* **2010,** *110* (9), 5447.

(37) Krishna, P. R.; Kannan, V.; Sharma, G. V. M.; Rao, M. Diastereoselective Baylis-Hillman reaction: Use of sugar derived aldehydes as chiral electrophiles. *Synlett* **2003**, 888.

(38) Krishna, P. R.; Sekhar, E. R.; Kannan, V. The use of acetylenic aldehydes in Baylis-Hillman reactions: synthesis of versatile allyl propargyl alcohols. *Tetrahedron Letters* **2003,** *44* (27), 4973.

(39) Krishna, P. R.; Manjuvani, A.; Narsingam, M.; Raju, G. Stereodefined Access to 3-Deoxy Sugars Through a Tandem Baylis-Hillman and Lewis Acid Catalyzed Reaction Sequence. *European Journal of Organic Chemistry* **2010**, 813.

(40) Santos, B. S.; Cardoso, A. L.; Beja, A. M.; Silva, M. R.; Paixao, J. A.; Palacios, F.; Melo, T. Diastereoselective Aza-Baylis-Hillman Reactions: Synthesis of Chiral alpha-Allenylamines and 2-Azetines from Allenic Esters. *European Journal of Organic Chemistry* **2010**, 3249.

(41) Dermenci, A.; Selig, P. S.; Domaoal, R. A.; Spasov, K. A.; Anderson, K. S.; Miller, S. J. Quasi-biomimetic ring contraction promoted by a cysteine-based nucleophile: Total synthesis of Sch-642305, some analogs and their putative anti-HIV activities. *Chemical Science* **2011,** *2* (8), 1568.

(42) Pouliquen, M.; Blanchet, J.; De Paolis, M.; Devi, B. R.; Rouden, J.; Lasne, M. C.; Maddaluno, J. Chiral 3-aminopyrrolidines as a rigid diamino scaffold for organocatalysis and organometallic chemistry. *Tetrahedron-Asymmetry* **2010,** *21* (11-12), 1511.

(43) Senapati, B. K.; Hwang, G. S.; Lee, S.; Ryu, D. H. Enantioselective Synthesis of beta-Iodo Morita-Baylis-Hillman Esters by a Catalytic Asymmetric Three-Component Coupling Reaction. *Angewandte Chemie-International Edition* **2009,** *48* (24), 4398.

(44) Sohtome, Y.; Tanatani, A.; Hashimoto, Y.; Nagasawa, K. Development of bis-thiourea-type organocatalyst for asymmetric Baylis-Hillman reaction. *Tetrahedron Letters* **2004,** *45* (29), 5589.

(45) Takizawa, S.; Horii, A.; Sasai, H. Acid-base organocatalysts for the aza-Morita-Baylis-Hillman reaction of nitroalkenes. *Tetrahedron-Asymmetry* **2010,** *21* (8), 891.

(46) Terada, M.; Fukuchi, S.; Amagai, K.; Nakano, M.; Ube, H. Guanidine/Azole Binary System as an Efficient Catalyst for Morita-Baylis-Hillman Reaction. *Chemcatchem* **2012,** *4* (7), 963.

(47) Bugarin, A.; Connell, B. T. MgI_2-accelerated enantioselective Morita-Baylis-Hillman reactions of cyclopentenone utilizing a chiral DMAP catalyst. *Chemical Communications* **2010,** *46* (15), 2644.

(48) Yukawa, T.; Seelig, B.; Xu, Y. J.; Morimoto, H.; Matsunaga, S.; Berkessel, A.; Shibasaki, M. Catalytic Asymmetric Aza-Morita-Baylis-Hillman Reaction of Methyl Acrylate: Role of a

Bifunctional La(O-iPr)$_3$/Linked-BINOL Complex. *Journal of the American Chemical Society* **2010,** *132* (34), 11988.

(49) Cihalova, S.; Dziedzic, P.; Cordova, A.; Vesely, J. Asymmetric Aza-Morita-Baylis-Hillman-Type Reactions: The Highly Enantioselective Reaction between Unmodified alpha,beta-Unsaturated Aldehydes and N-Acylimines by Organo-co-catalysis. *Advanced Synthesis & Catalysis* **2011,** *353* (7), 1096.

(50) Selig, P. S.; Miller, S. J. ortho-Acidic aromatic thiols as efficient catalysts of intramolecular Morita-Baylis-Hillman and Rauhut-Currier reactions. *Tetrahedron Letters* **2011,** *52* (17), 2148.

(51) Kawahara, S.; Nakano, A.; Esumi, T.; Iwabuchi, Y.; Hatakeyama, S. beta-isocupreidine-catalyzed asymmetric Baylis-Hillman reaction of imines. *Organic Letters* **2003,** *5* (17), 3103.

(52) Abermil, N.; Masson, G.; Zhu, J. P. Enantioselective Aza-Morita-Baylis-Hillman Reaction Using Aliphatic alpha-Amidosulfones as Imine Surrogates. *Advanced Synthesis & Catalysis* **2010,** *352* (4), 656.

(53) Guan, X. Y.; Wei, Y.; Shi, M. Construction of Chiral Quaternary Carbon through Morita-Baylis-Hillman Reaction: An Enantioselective Approach to 3-Substituted 3-Hydroxyoxindole Derivatives. *Chemistry-a European Journal* **2010,** *16* (46), 13617.

(54) Shah, J.; Yacob, Z.; Bunge, A.; Liebscher, J. A New Dual Catalytic System for Asymmetric Morita-Baylis-Hillman Reaction. *Synlett* **2010**, 2079.

(55) Marinetti, A.; Voituriez, A. Enantioselective Phosphine Organocatalysis. *Synlett* **2010**, 174.

(56) Shi, M.; Chen, L. H. Chiral phosphine Lewis base catalyzed asymmetric aza-Baylis-Hillman reaction of N-sulfonated imines with methyl vinyl ketone and phenyl acrylate. *Chemical Communications* **2003**, 1310.

(57) Garnier, J. M.; Anstiss, C.; Liu, F. Enantioselective Trifunctional Organocatalysts for Rate-Enhanced Aza-Morita-Baylis-Hillman Reactions at Room Temperature. *Advanced Synthesis & Catalysis* **2009,** *351* (3), 331.

(58) Garnier, J. M.; Liu, F. Trifunctional organocatalyst-promoted counterion catalysis for fast and enantioselective aza-Morita-Baylis-Hillman reactions at ambient temperature. *Organic & Biomolecular Chemistry* **2009,** *7* (7), 1272.

(59) Raheem, I. T.; Jacobsen, E. N. Highly enantioselective aza-Baylis-Hillman reactions catalyzed by chiral thiourea derivatives. *Advanced Synthesis & Catalysis* **2005,** *347* (11-13), 1701.

(60) Nakayama, Y.; Gotanda, T.; Ito, K. Asymmetric Morita-Baylis-Hillman reactions of 2-cyclohexen-1-one catalyzed by chiral biaryl-based bis(thiourea) organocatalysts. *Tetrahedron Letters* **2011,** *52* (47), 6234.

(61) Han, X. Y.; Wang, Y. Q.; Zhong, F. R.; Lu, Y. X. Enantioselective Morita-Baylis-Hillman reaction promoted by L-threonine-derived phosphine-thiourea catalysts. *Organic & Biomolecular Chemistry* **2011,** *9* (19), 6734.

(62) Liu, T. Y.; Xie, M.; Chen, Y. C. Organocatalytic asymmetric transformations of modified Morita-Baylis-Hillman adducts. *Chemical Society Reviews* **2012,** *41* (11), 4101.

(63) Rios, R. Organocatalytic enantioselective methodologies using Morita-Baylis-Hillman carbonates and acetates. *Catalysis Science & Technology* **2012,** *2* (2), 267.

(64) Bhowmik, S.; Batra, S. Applications of Morita-Baylis-Hillman Reaction to the Synthesis of Natural Products and Drug Molecules. *Current Organic Chemistry* **2014,** *18* (24), 3078.

(65) Basavaiah, D.; Kumaragurubaran, N.; Sharada, D. S.; Reddy, R. M. Applications of Baylis-Hillman chemistry: enantioselective synthesis of (-)-methyl 3-aryl-2-methylene-3-(prop-2-yn-1-yloxy)propanoates via chiral leaving group strategy. *Tetrahedron* **2001,** *57* (38), 8167.

(66) Cui, H. L.; Feng, X.; Peng, J.; Lei, J.; Jiang, K.; Chen, Y. C. Chemoselective Asymmetric N-Allylic Alkylation of Indoles with Morita-Baylis-Hillman Carbonates. *Angewandte Chemie-International Edition* **2009,** *48* (31), 5737.

(67) Cui, H. L.; Huang, J. R.; Lei, J.; Wang, Z. F.; Chen, S.; Wu, L.; Chen, Y. C. Direct Asymmetric Allylic Alkylation of Butenolides with Morita-Baylis-Hillman Carbonates. *Organic Letters* **2010,** *12* (4), 720.

(68) Deng, H. P.; Wei, Y.; Shi, M. Chiral Bifunctional Thiourea-Phosphane Organocatalysts in Asymmetric Allylic Amination of Morita-Baylis-Hillman Acetates. *European Journal of Organic Chemistry* **2011**, 1956.

(69) Pei, C. K.; Zhang, X. C.; Shi, M. Novel Quinidine-Derived Organocatalysts for the Asymmetric Substitutions of O-Boc-Protected Morita-Baylis-Hillman Adducts. *European Journal of Organic Chemistry* **2011**, 4479.

(70) Peng, J.; Huang, X.; Cui, H. L.; Chen, Y. C. Organocatalytic and Electrophilic Approach to Oxindoles with C3-Quaternary Stereocenters. *Organic Letters* **2010,** *12* (19), 4260.

(71) Yang, Y. L.; Pei, C. K.; Shi, M. Multifunctional chiral phosphines-catalyzed highly diastereoselective and enantioselective substitution of Morita-Baylis-Hillman adducts with oxazolones. *Organic & Biomolecular Chemistry* **2011,** *9* (9), 3349.

(72) Cho, C. W.; Kong, J. R.; Krische, M. J. Phosphine-catalyzed regiospecific allylic amination and dynamic kinetic resolution of Morita-Baylis-Hillman acetates. *Organic Letters* **2004,** *6* (8), 1337.

(73) Cho, C. W.; Krische, M. J. Regio- and stereoselective construction of gamma-butenolides through phosphine-catalyzed substitution of Morita-Baylis-Hillman acetates: An organocatalytic allylic alkylation. *Angewandte Chemie-International Edition* **2004,** *43* (48), 6689.

(74) Hong, L.; Sun, W. S.; Liu, C. X.; Zhao, D. P.; Wang, R. Enantioselective construction of allylic phosphine oxides through substitution of Morita-Baylis-Hillman carbonates with phosphine oxides. *Chemical Communications* **2010,** *46* (16), 2856.

(75) Sun, W. S.; Hong, L. A.; Liu, C. X.; Wang, R. Base-Accelerated Enantioselective Substitution of Morita-Baylis-Hillman Carbonates with Dialkyl Phosphine Oxides. *Organic Letters* **2010,** *12* (17), 3914.

(76) Chen, Z. L.; Zhang, J. L. An Unexpected Phosphine-Catalyzed Regio- and Diastereoselective 4+1 Annulation Reaction of Modified Allylic Compounds with Activated Enones. *Chemistry-an Asian Journal* **2010,** *5* (7), 1542.

(77) Tan, B.; Candeias, N. R.; Barbas, C. F. Core-Structure-Motivated Design of a Phosphine-Catalyzed 3+2 Cycloaddition Reaction: Enantioselective Syntheses of Spirocyclopenteneoxindoles. *Journal of the American Chemical Society* **2011,** *133* (13), 4672.

(78) Xie, P. Z.; Huang, Y.; Chen, R. Y. Phosphine-Catalyzed Domino Reaction: Highly Stereoselective Synthesis of trans-2,3-Dihydrobenzofurans from Salicyl N-Thiophosphinyl Imines and Allylic Carbonates. *Organic Letters* **2010,** *12* (17), 3768.

(79) Zhong, F. R.; Han, X. Y.; Wang, Y. Q.; Lu, Y. X. Highly Enantioselective 3+2 Annulation of Morita-Baylis-Hillman Adducts Mediated by L-Threonine-Derived Phosphines: Synthesis of 3-Spirocyclopentene-2-oxindoles having Two Contiguous Quaternary Centers. *Angewandte Chemie-International Edition* **2011,** *50* (34), 7837.

(80) Deng, H. P.; Wang, D.; Wei, Y.; Shi, M. Chiral multifunctional thiourea-phosphine catalyzed asymmetric 3+2 annulation of Morita-Baylis-Hillman carbonates with maleimides. *Beilstein Journal of Organic Chemistry* **2012,** *8*, 1098.

(81) Zhong, F. R.; Chen, G. Y.; Han, X. Y.; Yao, W. J.; Lu, Y. X. Asymmetric Construction of Functionalized Bicyclic Imides via 3+2 Annulation of MBH Carbonates Catalyzed by Dipeptide-Based Phosphines. *Organic Letters* **2012,** *14* (14), 3764.

(82) Wang, Q. G.; Zhu, S. F.; Ye, L. W.; Zhou, C. Y.; Sun, X. L.; Tang, Y.; Zhou, Q. L. Catalytic Asymmetric Intramolecular Cascade Reaction for the Construction of Functionalized Benzobicyclo 4.3.0 Skeletons. Remote Control of Enantioselectivity. *Advanced Synthesis & Catalysis* **2010,** *352* (11-12), 1914.

(83) Tian, J. J.; Zhou, R.; Sun, H. Y.; Song, H. B.; He, Z. J. Phosphine-Catalyzed 4+1 Annuiation between alpha,beta-Unsaturated Imines and Allylic Carbonates: Synthesis of 2-Pyrroilines. *Journal of Organic Chemistry* **2011,** *76* (7), 2374.

(84) Basavaiah, D.; Rao, A. J.; Satyanarayana, T. Recent advances in the Baylis-Hillman reaction and applications. *Chemical Reviews* **2003,** *103* (3), 811.

(85) Basavaiah, D.; Sahu, B. C. Conceptual Influence of the Baylis-Hillman Reaction on Recent Trends in Organic Synthesis. *Chimia* **2013,** *67* (1-2), 8.

(86) Basavaiah, D.; Veeraraghavaiah, G. The Baylis-Hillman reaction: a novel concept for creativity in chemistry. *Chemical Society Reviews* **2012,** *41* (1), 68.

(87) Declerck, V.; Martinez, J.; Lamaty, F. aza-Baylis-Hillman Reaction. *Chemical Reviews* **2009,** *109* (1), 1.

(88) Gowrisankar, S.; Lee, H. S.; Kim, S. H.; Lee, K. Y.; Kim, J. N. Recent advances in the Pd-catalyzed chemical transformations of Baylis-Hillman adducts. *Tetrahedron* **2009,** *65* (43), 8769.

(89) Lima, C. G.; Vasconcellos, M. Morita-Baylis-Hillman adducts: Biological activities and potentialities to the discovery of new cheaper drugs. *Bioorganic & Medicinal Chemistry* **2012,** *20* (13), 3954.

(90) Fields, S. C. Total synthesis of (+/-)-phosphonothrixin. *Tetrahedron Letters* **1998,** *39* (37), 6621.

(91) Agapiou, K.; Krische, M. J. Catalytic crossed Michael cycloisomerization of thioenoates: Total synthesis of (+/-)-ricciocarpin A. *Organic Letters* **2003,** *5* (10), 1737.

(92) Kurasaki, H.; Okamoto, I.; Morita, N.; Tamura, O. Total Synthesis of Grandisine D. *Organic Letters* **2009,** *11* (5), 1179.

(93) Reddy, L. R.; Saravanan, P.; Corey, E. J. A simple stereocontrolled synthesis of salinosporamide A. *Journal of the American Chemical Society* **2004,** *126* (20), 6230.

(94) Basavaiah, D.; Devendar, B.; Aravindu, K.; Veerendhar, A. A Facile One-Pot Transformation of Baylis-Hillman Adducts into Unsymmetrical Disubstituted Maleimide and Maleic Anhydride Frameworks: A Facile Synthesis of Himanimide A. *Chemistry-a European Journal* **2010,** *16* (7), 2031.

(95) Aroyan, C. E.; Dermenci, A.; Miller, S. J. The Rauhut-Currier reaction: a history and its synthetic application. *Tetrahedron* **2009,** *65* (21), 4069.

(96) Marques-Lopez, E.; Herrera, R. P.; Marks, T.; Jacobs, W. C.; Konning, D.; de Figueiredo, R. M.; Christmann, M. Crossed Intramolecular Rauhut-Currier-Type Reactions via Dienamine Activation. *Organic Letters* **2009,** *11* (18), 4116.

(97) Shi, M. W., Y.; Zhao, M. X.; Zhang, J *Organocatalytic cycloadditions for synthesis of carbo- and heterocycles*; Wiley-VCH, 2018.

(98) Huang, G. T.; Lankau, T.; Yu, C. H. A Computational Study: Reactivity Difference between Phosphine- and Amine-Catalyzed Cycloadditions of Allenoates and Enones. *Journal of Organic Chemistry* **2014,** *79* (4), 1700.

(99) Huang, G. T.; Lankau, T.; Yu, C. H. A computational study of the activation of allenoates by Lewis bases and the reactivity of intermediate adducts. *Organic & Biomolecular Chemistry* **2014,** *12* (37), 7297.

(100) Yao, W. J.; Dou, X. W.; Lu, Y. X. Highly Enantioselective Synthesis of 3,4-Dihydropyrans through a Phosphine-Catalyzed 4+2 Annulation of Allenones and beta,gamma-Unsaturated alpha-Keto Esters. *Journal of the American Chemical Society* **2015,** *137* (1), 54.

(101) Hu, Y.; Li, S.; Wang, Z. L.; Yao, Y. B.; Li, T. J.; Yu, C. X.; Yao, C. S. NHC-Catalyzed Hetero-Diels-Alder Reaction of Allenoate with Chalcone: Synthesis of Polysubstituted Pyranyl Carboxylate. *Journal of Organic Chemistry* **2018,** *83* (6), 3361.

(102) Liu, Y. F.; Du, Y. L.; Yu, A. M.; Qin, D. B.; Meng, X. T. Diverse synthesis of pyrano 2,3-b indol and dihydropyrano 2,3-b indol via tunable Lewis bases catalyzed domino reactions. *Tetrahedron* **2015,** *71* (40), 7706.

Chapter II: Mechanistically Inspired Route toward Hexahydro-2*H*-chromenes *via* Consecutive [4+2]/[4+2] Cycloaddition Reactions

II-1. Introduction

Hexahydro-2*H*-chromene is an important heterocyclic scaffold both in natural products and biologically active compounds, and has attracted a great deal of synthetic interest.[1-4] Not surprisingly, the synthesis of hexahydro-2*H*-chromenes **II-4** can be achieved through a number of strategic disconnections.[5-9] However, we sought to explore a rapid assembly by combining two robust C-C bond-forming reactions—the modified Morita-Baylis-Hillman reaction and the Diels-Alder reaction, as depicted retro synthetically in **Scheme II-2**. The enantioenriched precursor diene **II-3**, which is required for the concomitant Diels-Alder reaction, would be obtained by a cinchona based chiral amine catalyzed modified Morita-Baylis-Hillman reaction between allenoate **II-2** and chalcone **I-1** that precedes a formal [4+2] cycloaddition reaction. This reported strategy provides an expedient route toward the synthesis of substituted hexahydro-2*H*-chromenes with high stereoselectivity, containing up to 5 contiguous stereocenters *via* two consecutive [4+2] cycloaddition reactions.

The approach described above requires a facile strategy for the synthesis of dihydropyrans, which could react as Danishefsky type diene, but with the general structure depicted in **Scheme II-3** with high enantioselectivity. Recently, our group, as well as others, have reported a chiral Lewis base catalyzed formal [4+2] cycloaddition reaction of enones with allenoate to provide the dihydropyrans in high stereoselectivity, which are ready for the Diels-Alder reaction (see examples in **Scheme II-1**).[10-15] Our

endeavor in this field commenced with the early discovery for the mechanistically guided

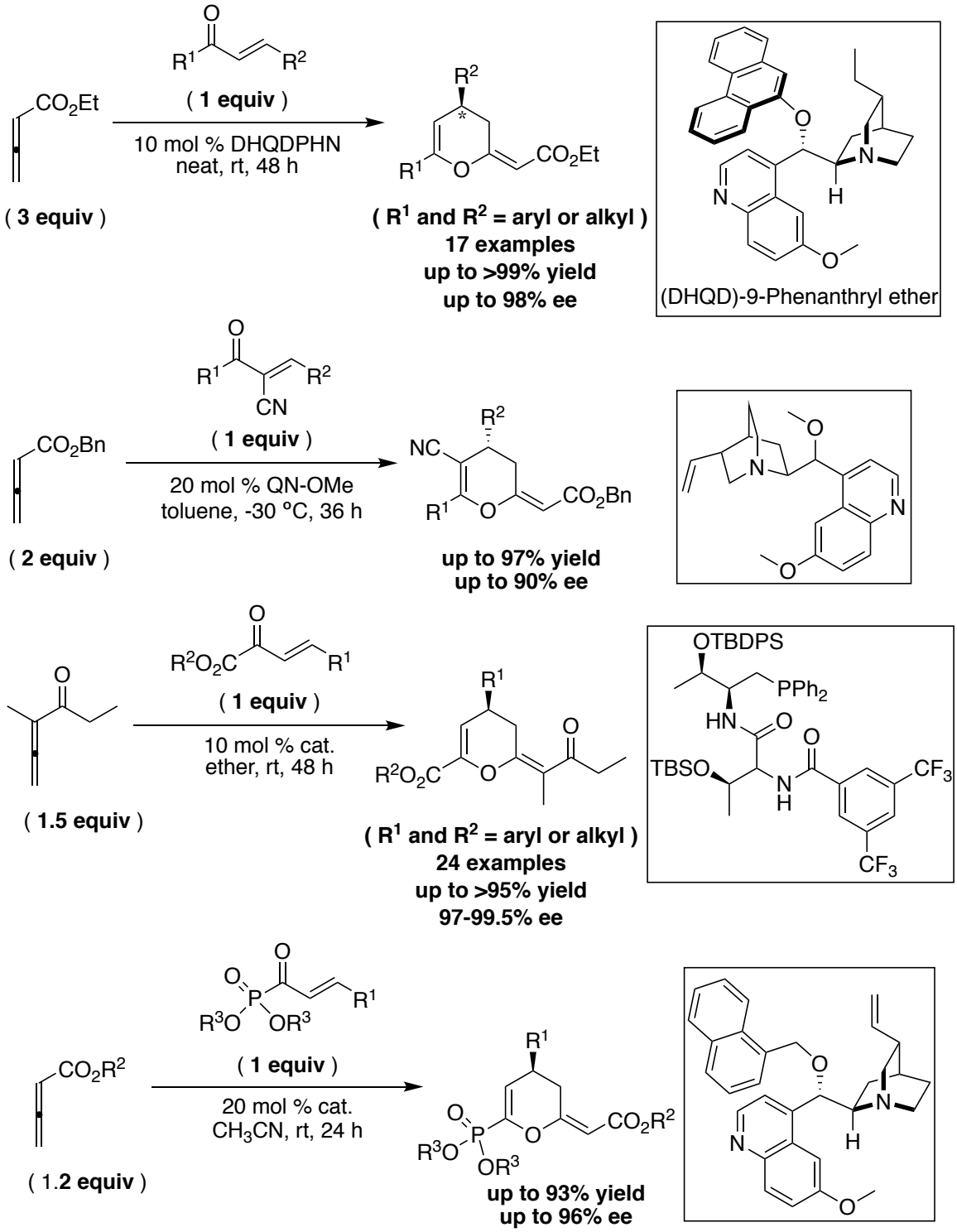

Scheme II-1. Examples of recently reported chiral Lewis base catalyzed formal [4+2] cycloaddition reaction to assemble dihydropyrans with high stereoselectivity.

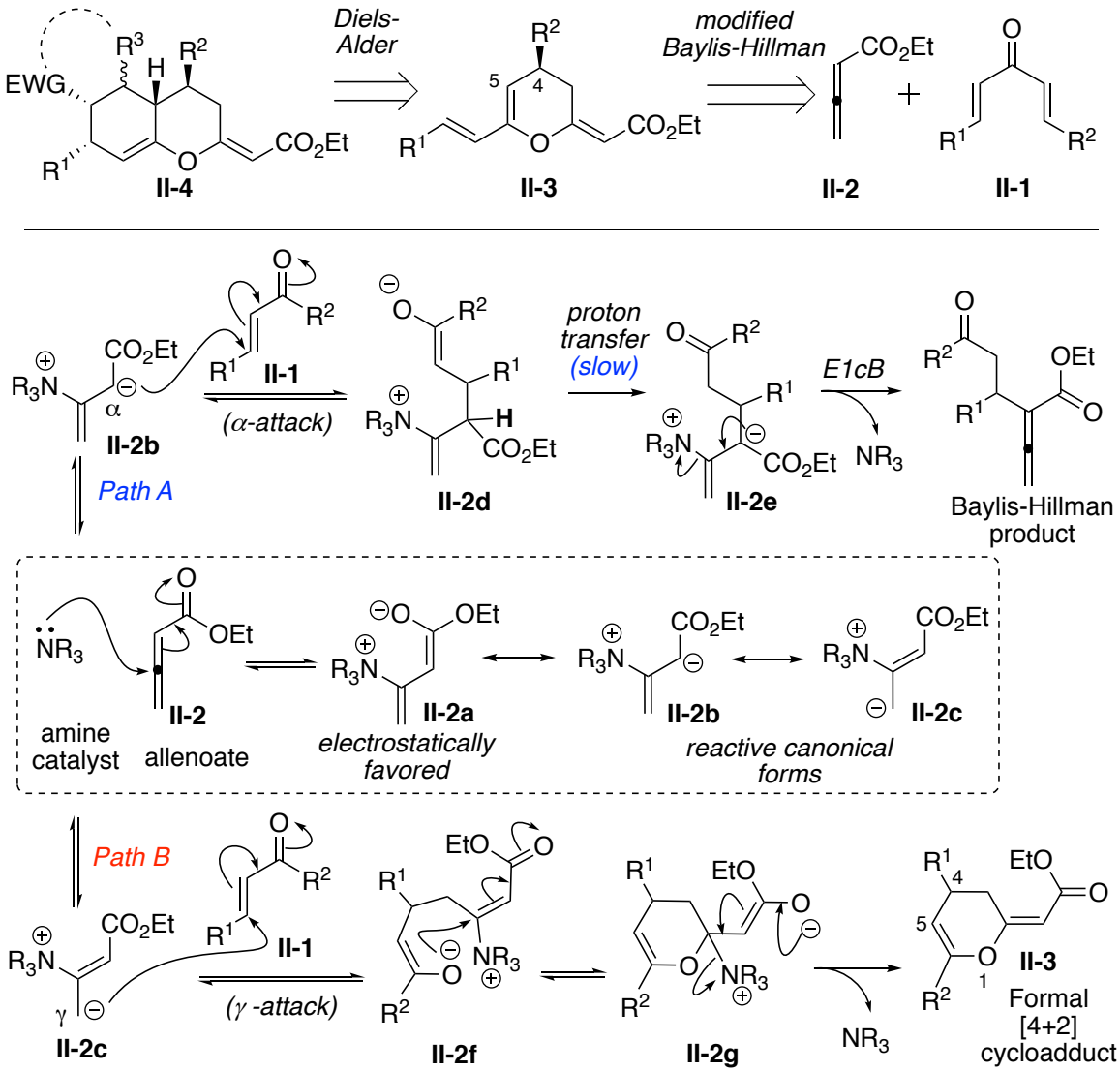

Scheme II-2. Top: Retrosynthetic strategy for the synthesis of hexahydro-2*H*-chromenes. Bottom: Path A and B represent a simplified mechanistic picture of the canonical *vs*. the modified Morita-Baylis-Hillman pathway. Possible resonance structures of the amine-allenoate adduct are shown in dashed box with **II-2a** being the major contributor.

synthesis of substituted dihydropyrans.[14] As shown in **Scheme II-2**, when allenoate **II-2** was utilized as the primary electrophile, two possible zwitterions could be formed in an equilibrium. These intermediates could follow two paths to yield different products—the Rauhut Currier product and the formal [4+2] cycloadduct. As reported, proton transfer is the rate determining step associated with the Baylis-Hillman reaction (path A, **II-2d** → **II-**

2e).[16,17] We planned to circumvent path A by utilizing acyclic enones/dienones **II-1** as secondary electrophiles, as well as using aprotic solvent or neat reaction conditions. Under these conditions, the relatively fast intramolecular trapping of the oxyanion **II-2f**, siphons the reaction towards formation of the corresponding dihydropyran **II-3** in high yields and enantioselectivity, *via* path B (the modified Morita-Baylis-Hillman route). The sequence of events highlighted in path B is akin to the Morita-Baylis-Hillman reaction (thus referred to as the modified MBH) that has been interrupted with an intramolecular cyclization, prior to the elimination of the amine catalyst, which regenerates the olefin. To generate the required diene **II-3** for the 2nd cycloaddition—Diels-Alder reaction, we designed a similar transformation initiated with a symmetric dienone (such as **II-1** in **Scheme II-2**). Furthermore, we surmised that the enantioenriched C4 substituent in **II-3**, would serve as a stereo-chemical driver of the subsequent [4+2] cycloaddition reaction. The conjugated diene motif in **II-3** displays a unique integration of two key features: a) the extended cross-conjugation of the pyranyl oxygen atom (O1) results in an electronic bias that may allow regioselective trapping of an unsymmetrically substituted dienophile; b) the nucleophilic carbon (C5) and the stereo-chemical driver (C4 substituent), both being part of a conformationally rigid cyclic framework, may allow an easy access to the diastereoselective [4+2] cycloaddition reaction.

II-2. Preliminary results from model reactions

The aforementioned hypotheses were readily examined by simply subjecting a model dienone, dibenzalacetone **II-1a**, to the organocatalytic asymmetric formal [4+2] cycloaddition reaction under already optimized set of conditions (see **Scheme II-3**). In the

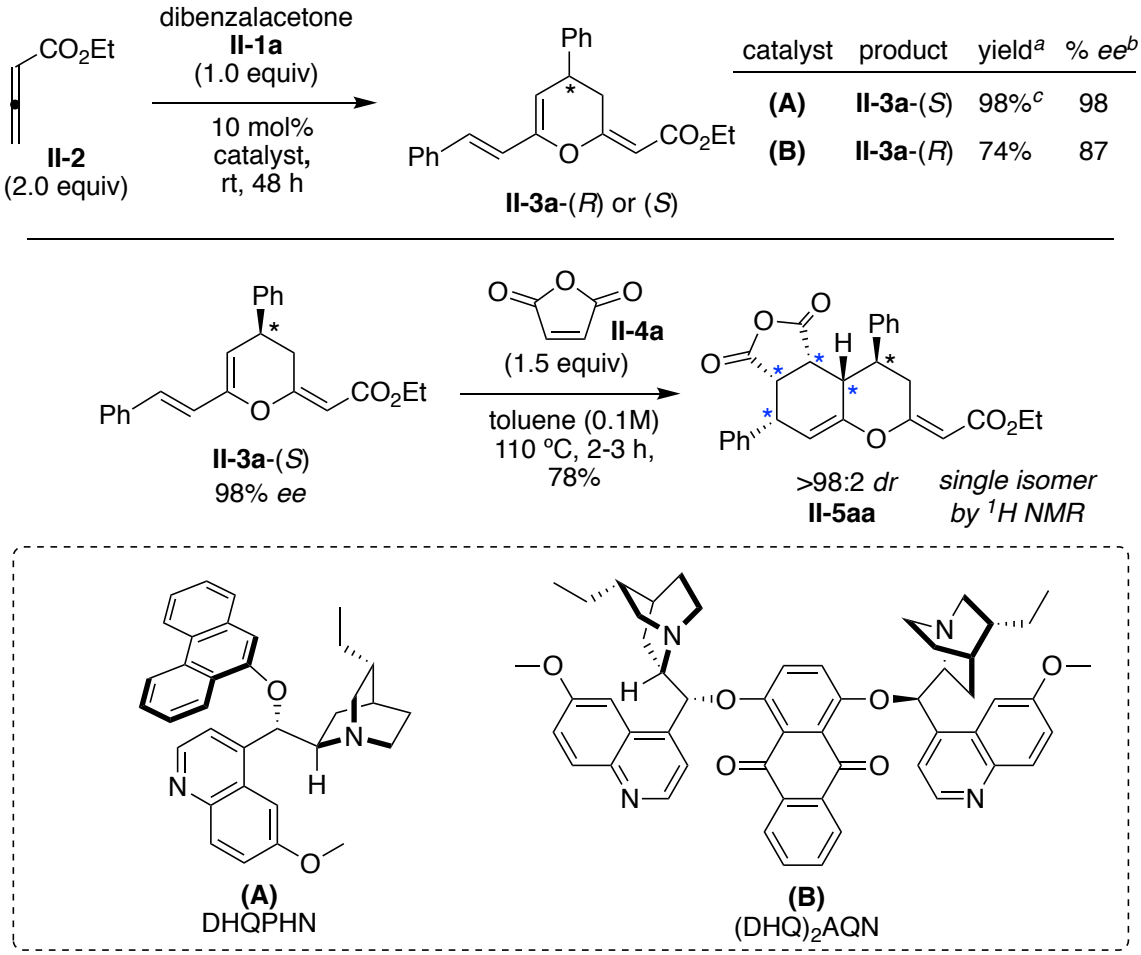

Scheme II-3. Preliminary results for consecutive [4+2] cycloaddition reactions under optimized conditions using dibenzalacetone (**II-1a**) as a model substrate. [a]Isolated yields. [b]Ratios were determined by HPLC analysis. [c]Reaction was performed using 1 g (4.3 mmol) of **II-1a**.

previous report, we demonstrated that catalysts **A** and **B** were the optimum for the formal [4+2] cycloaddition, delivering both enantiomers. In the model reaction, catalysts **A** and **B** delivered oxa-triene **II-3a**-(*S*) and **II-3a**-(*R*), respectively. Using catalyst **A** under neat reaction conditions, oxa-triene **II-3a**-(*S*) was obtained in 98% yield and 98% *ee*. A consequent treatment of this oxa-triene with maleic anhydride **II-4a** furnished the stereo-pentad **II-5aa** as a single diastereomer in 78% yield. This offers an alternative approach, compared to previous methodologies,[18-26] directed towards controlling stereoselectivity in cycloaddition reactions of dienes bearing an allylic chiral center.[27-29]

II-3. Results and discussion.

Encouraged by the preliminary results, we planned to explore this consecutive [4+2] cycloaddition further. However, intrigued by the levels of stereoinduction, we decided to employ quantum chemical computational analysis of the transition states (TS) at the B3LYP/6-31G*/SM8 (toluene) level of theory to probe the origins of stereoselectivity, especially in the substrate-controlled Diels-Alder reaction step.[30-34] To reduce the computational expense, we used hydroquinidine (QD) instead of catalyst **A** for our calculation. In agreement with the earlier discoveries,[14] the diastereomeric transition state of the formal [4+2] cycloaddition: TS-1 (**Figure II-1a**) that leads to the formation of product **II-3a-**(*S*), was favored by 2.7 kcal/mol (corresponding to *er* = 99:1) over TS-2. The steric congestion (gauche interactions as highlighted by bonds in red color) and the diminished electrostatic stabilization (as determined by the distance of $C{=}O^{\delta-\cdots\delta+}NR_4$) in TS-2, make it energetically less favorable than TS-1. The computational analysis corroborates the experimental results in the initial formal [4+2] cycloaddition (98% *ee* using the catalyst **A**, see **II-4. experimental** for details).

Next, we examined the stereoinduction associated with the Diels-Alder reaction of the model reaction between substrate **II-3a-**(*S*) with maleic anhydride **II-4a**. In line with the experimentally observed endo-selectivity,[22,35] TS-3_{endo} was found to be more favored than TS-4_{exo} by 2.8 kcal/mol (**Figure II-1b**). TS-4_{exo} also suffers from the electrostatic repulsion between the electron density on the proximal carbonyl of **II-4a** and the π–cloud of the C4 phenyl substituent in **II-3a-**(*S*) (see **II-4. Experimental** for details). Furthermore,

the corresponding TS-5$_{endo}$ involved in the approach of dienophile **II-4a** from the sterically

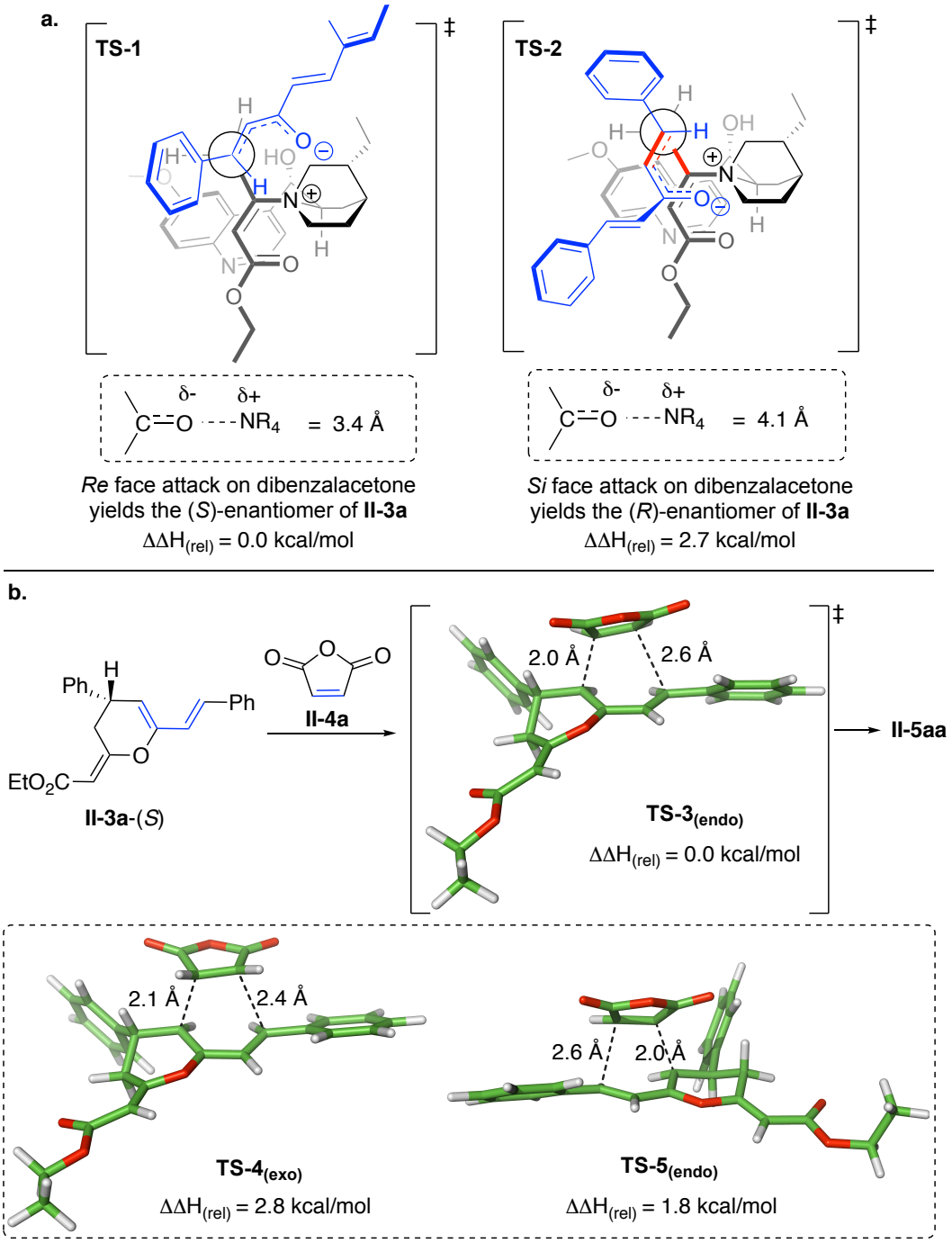

Figure II-1. a. Two diastereomeric transition states TS-1 and TS-2 calculated at the B2LYP/6-31G*/SM8 (toluene) level of theory. The bonds highlighted in red color depict the unfavorable gauche interactions in TS-2. b. Three possible transition states associated with the [4+2] cycloaddition of **II-3a-**(*S*) and **II-4a**. TS-3$_{(endo)}$ is favored by 2.8 kcal/mol over TS-4$_{(exo)}$ and by 1.8 kcal/mol over TS-5$_{(endo)}$. The fourth possible TS involving an exo approach of **II-4a** from the same face as the C4-Ph substituent cannot be calculated due to severe steric clash between the approach dienophile and the aromatic ring.

hindered face of the diene is disfavored by 1.8 kcal/mol over TS-3_{endo} (check dashed box in **Figure II-1b**). Although the B3LYP/6-31G* level of the theory underestimates the energetics of secondary interactions in the Diels-Alder reaction,[36,37] it clearly depicts the correct energetic trend as observed experimentally. An exhaustive analysis at the MP2 level of theory can be attempted (requires longer time and higher computational expense) to capture the precise energetics in the Diels-Alder reaction, however, our approach utilizes the B3LYP/6-31G* analysis to map the reaction pathway and compares the relative energies of the transition states involved at a relatively low computational expense. Overall, the stereochemical driver of the C4 substituent, obtained from the initial formal [4+2] cycloaddition, perfectly governs the stereospecificity in the concomitant Diels-Alder reaction.

To explore the scope of this consecutive [4+2]/[4+2] cycloaddition reaction, we decided to focus on each step separately. For the scope of the 1st formal [4+2] cycloaddition reaction, a series of substituted dienones (**II-1a** – **II-1p**) were screened with allenoate **II-2** under the optimized reaction condition (see **Table II-1**). To access both enantiomers of the corresponding dihydropyrans **II-3a** – **II-3p**, both catalyst **A** and **B** (see **Scheme II-2**) were employed in this reaction. Similar to previous observations,[14] catalyst **A** displayed better results than catalyst **B** with regards to both efficiency and stereoinduction. Regardless of the electronic properties of the attached substituents on the aryl substrate, electron donating groups (entries **II-2** – **II-6** and **II-13**), electron withdrawing groups (entries **II-7** – **II-12**), and even aliphatic substituents (entries **II-14** –

II-16) showed excellent enantioinductions by using catalyst **A** for the reaction. The X-ray crystal structures of derivatives of **II-3b-**(*S*) and **II-3j-**(*S*) provided unequivocal evidence

Table II-1. Substrate scope for the enantioselective synthesis of substituted oxa-trienes

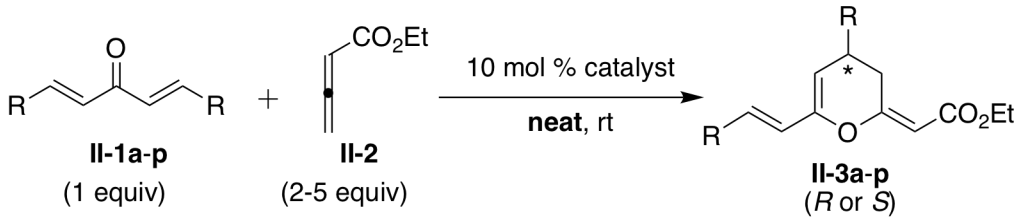

II-1a-p (1 equiv) + **II-2** (2-5 equiv) → **II-3a-p** (*R* or *S*)

entry	R	cat.	product	time (h)	%yield[a]	%*ee*[b]
1	Ph	**A**	**II-3a-***S*	40	98[c]	98
		B	**II-3a-***R*	8	74	87
2	*o*-OMe-C_6H_4	**A**	**II-3b-***S*	60	60[d]	90
		B	**II-3b-***R*	60	65[d]	82
3	*m*-OMe-C_6H_4	**A**	**II-3c-***S*	12	98	96
		B	**II-3c-***R*	12	87	88
4	*p*-OMe-C_6H_4	**A**	**II-3d-***S*	60	25[d]	94
		B	**II-3d-***R*	60	20[d]	76
5	*o*-Me-C_6H_4	**A**	**II-3e-***S*	40	75	88
		B	**II-3e-***R*	10	68	82
6	*p*-Me-C_6H_4	**A**	**II-3f-***S*	60	43[d]	94
		B	**II-3f-***R*	60	57[d]	72
7	*o*-F-C_6H_4	**A**	**II-3g-***S*	48	78	92
		B	**II-3g-***R*	48	71	88

Table II-1. (cont'd)

entry	R	cat.	product	time (h)	%yield[a]	%*ee*[b]
8	*o*-Br-C_6H_4	**A**	**II-3h-***S*	30	95	88
		B	**II-3h-***R*	30	95	78
9	*p*-Br-C_6H_4	**A**	**II-3i-***S*	40	66	94
		B	**II-3i-***R*	40	32	72
10	*o*-Cl-C_6H_4	**A**	**II-3j-***S*	25	99[e]	90
		B	**II-3j-***R*	25	89	84
11	*p*-Cl-C_6H_4	**A**	**II-3k-***S*	48	58	91
		B	**II-3k-***R*	48	36	88
12	2-furyl	**A**	**II-3l-***S*	48	27	95
		B	**II-3l-***R*	48	32	78
13	1-naphthyl	**A**	**II-3m-***S*	40	76	92
		B	**II-3m-***R*	40	69	72
14	*n*-propyl	**A**	**II-3n-***S*	72	28 (52)[d,f]	90
		B	**II-3n-***R*	72	24 (50)[d,f]	67
15	isopropyl	**A**	**II-3o-***S*	72	29 (87)[d,f]	94
		B	**II-3o-***R*	72	23 (80)[d,f]	58
16	Me	**A**	**II-3p-***S*	36	48	90
		B	**II-3p-***R*	36	26	72

[a] Isolated yields. [b] Ratios were determined by HPLC analysis using chiral stationary phase columns. [c] Reactions was performed on a 1 g scale of **II-1a**. [d] Longer reaction times led to degradation of allenoate **II-2** and incomplete conversion of dienones was observed. [e] Reaction was performed on a 0.5 g scale of **II-1j**. [f] Numbers in parentheses refer to yield based on recovered starting material.

Table II-2. Substrate scope for the formal [4+2] cycloaddition of allenoate with asymmetric cross-conjugated oxa-trienes

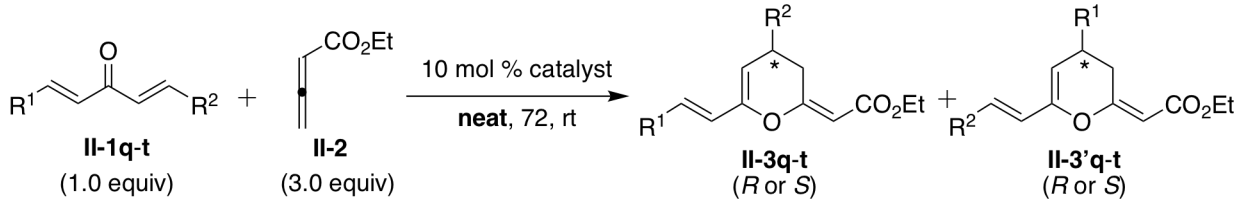

entry	R^1	R^2	cat.	%yield[a]	II-3 / II-3'[b]
1	*p*-Br-C_6H_4	*p*-OMe-C_6H_4	**A**	48	2:3
			B	19	2:3
2	*p*-Cl-C_6H_4	*p*-OMe-C_6H_4	**A**	19	2:3
			B	nd	2:3
3	Ph	Cy	**A**	54	3:5
			B	46	3:5
4	Ph	*t*-Bu	**A**	50	1:10
			B	31	1:10

[a] Isolated yields. [b] Ratios were determined by ^{1}H NMR after purified by column. nd = not determined.

for the absolute stereochemistry of the products obtained using catalyst **A** (see **Scheme II-4**, dashed box). These results also further confirmed the quantum chemical computational analysis (see **Figure II-1a**) that revealed both the absence of gauche interaction (steric) and the stronger electrostatic stabilization in TS-1 is responsible for favoring the (*S*)-enantiomer.

We have also explored the formal [4+2] cycloaddition reaction with unsymmetrically substituted dienones. **Table II-2** summarizes the results of all four substrates with both catalysts. Although the resulting products were obtained with modest regioselectivity of

2:3 (entries 1 and 2) to good regioselectivity 1:10 (entry 4), they were inseparable by

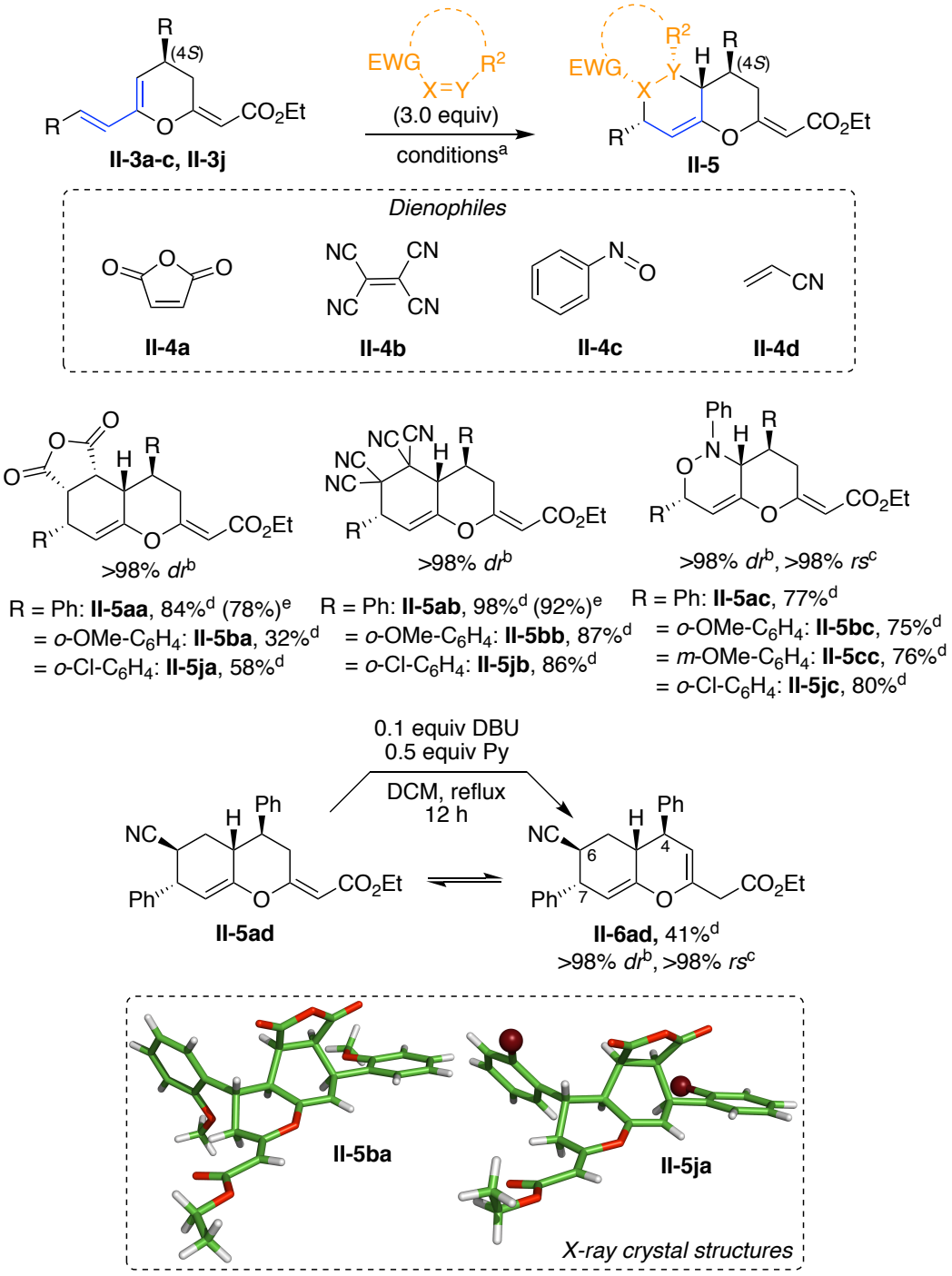

Scheme II-4. Diels-Alder reaction of substituted oxa-trienes (**II-3a-c**, **II-3j**) with illustrative dienophiles (**II-4a-d**). [a] Diels-Alder reaction conditions for each dienophile is as follows: dienophile **II-4a**: 0.1 M in toluene, reflux, 2-16 h. Dienophile **II-4b**: 0.1 M in toluene, reflux, 2 h. Dienophile **II-4c**: 0.1 M in EtOH/DCM (1:1), 0 ºC→rt, 12 h. Dienophile **II-4d**: 0.1 M in toluene, reflux, 12 h. [b] Diastereomeric ratios (*dr*) were determined by ^{1}H NMR analysis of the crude reaction mixture. [c] Regioselectivity (*rs*) and relative stereochemistry was determined *via* NMR analysis of the purified product. [d] Isolated yields. [e] Isolated yield for 'one pot' consecutive transformations from **II-1a** as a starting material.

analytical techniques to evaluate the stereoinduction. As shown in **Table II-2**, both electronic properties of the substitution on the aryl substrates and the steric congestion of the substitutions play a role in guiding the selectivity. In general, a. the products are formed in favor of the electron-withdrawing substitution side; b. the formal [4+2] cycloaddition reaction prefers the less bulky substituents.

As a proof-of-principle, we next explored the ability of these dihydropyrans to control the facial-, regio- and stereoinduction of the Diels-Alder reaction. A summary of the results of 11 cycloaddition reactions between either **II-3a-**(*S*), **II-3b-**(*S*), **II-3c-**(*S*) or **II-3j-**(*S*) and an illustrative set of dienophiles **II-4a – II-4d** is shown in **Scheme II-4**. Dienophiles **II-4a** and **II-4b** displayed exclusive diastereoselective addition, while dienophiles **II-4c** and **II-4d** not only displayed this good diastereoselectivity, but also exhibited excellent regioselection. Furthermore, these sequential transformations (the formal [4+2] cycloaddition reaction followed by the concomitant Diels-Alder reaction) were also performed efficiently as a 'one pot' Domino reaction (see **Scheme II-4**, products **II-5aa** and **II-5ab**). As anticipated, the cross-conjugation of the endocyclic oxygen (O1) not only enhances the HOMO energy of the diene motif in **II-3**, but also generates an electronic bias that allows regio-specific trapping of the dienophiles **II-4c** and **II-4d**, thus validating the initial hypothesis. One interesting observation is the reaction between **II-3a** and **II-4d**, which furnish the formation of an isomeric mixture of products **II-5ad** and **II-6ad** in nearly equimolar ratios. Fortuitously, upon treatment with DBU in refluxing DCM, the mixture was cleanly converted to yield the endocyclic product **II-6ad** in high regio- and diastereoselectivity. Unlike the other Diels-Alder reaction products depicted in **Scheme**

II-4, the adduct **II-6ad** (and for that matter **II-5ad**) is the result of an *exo* [4+2] cycloaddition reaction (see **II-4. experimental** for details of the stereochemical assignment based on NMR studies). Although we see no evidence of the *endo* product during the course of

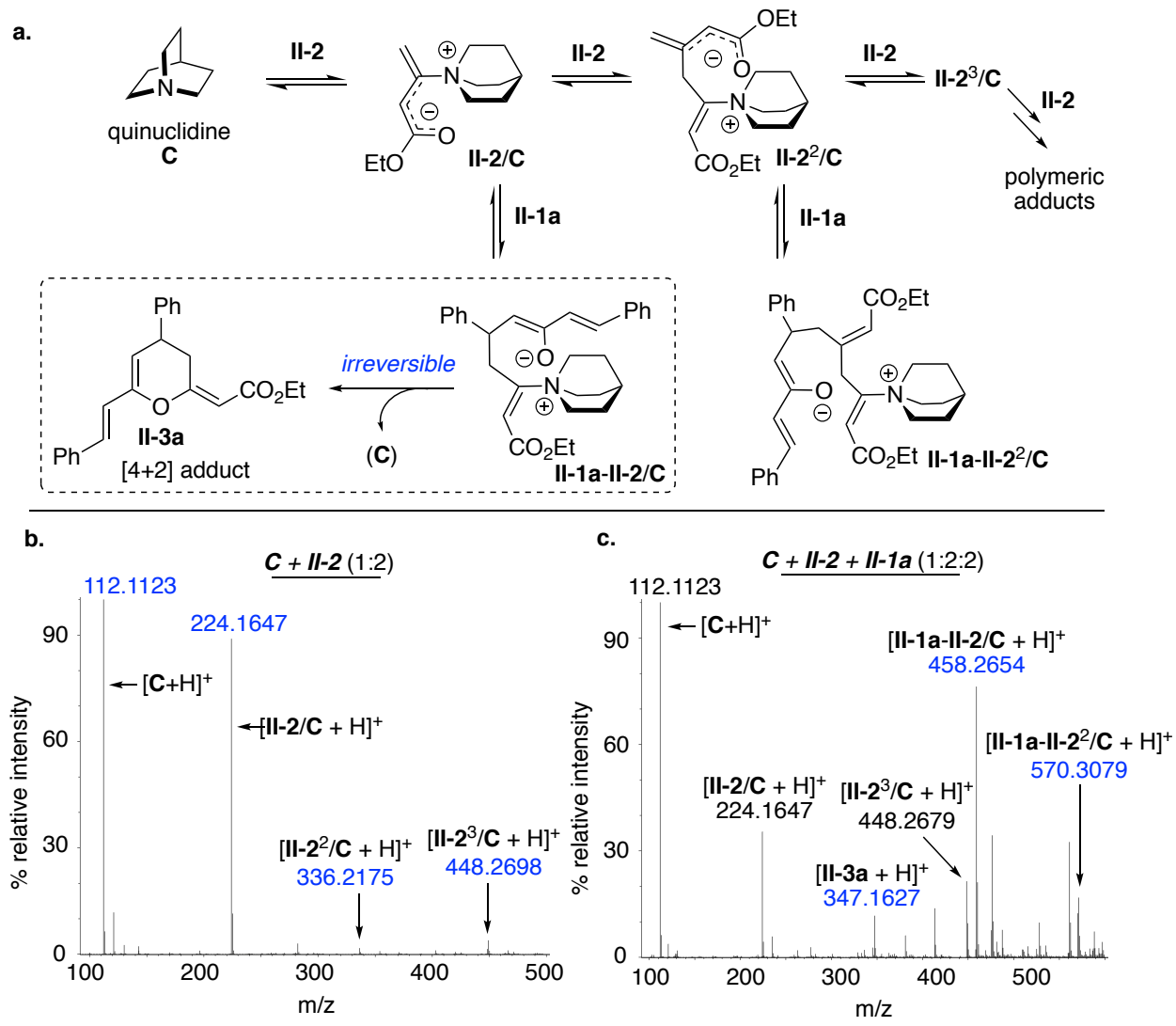

Figure II-2. a. An equilibrium mixture of putative intermediates in the Morita-Baylis-Hillman reaction of **II-1a** and **II-2**. For simplicity, intermediates arising only from the γ–attack of the enolate are shown. b. ESI-MS spectrum of a reaction mixture (pre-incubated for 30 min) constituting of a 1:2 ratio of quinuclidine (**C**) and allenoate **II-2**. c. ESI-MS spectrum obtained after 1 h upon addition of **II-1a** to the mixture of (**C**) and **II-2.**

the reaction, we cannot exclude the possibility of either epimerization at C6 or a reversible Diels-Alder process that ultimately settles for the thermodynamic product.

The mechanistic nuances underpinning the formal [4+2] cycloaddition reaction of allenoate (the primary electrophile) with dibenzalacetone (the secondary electrophile) are more complex than the simplified picture depicted in **Scheme II-2**, leading to the following central question. Despite the possibility for the formation of several theoretical adducts (based on the relative reactivity of the primary and the secondary electrophile), which factor governs the formation of **II-3** as the predominant product? To address this question, ESI-MS was utilized to investigate the identity of stable intermediates that arise during the reaction between **II-1a** and **II-2** with the catalyst of quinuclidine **C** (an achiral surrogate of catalysts **A** and **B**) (see **Figure II-2**). Upon the nucleophilic attack of the Lewis base **C** on allenoate **II-2**, the zwitterionic intermediate **II-2/C** will be generated. The resulting enolate can attack another allenoate **II-2** to furnish the intermediate **II-2^2/C**. Sequential additions of **II-2** will yield the trimeric adduct **II-2^3/C** and high oligomers that constitute several polymeric adducts in equilibrium. These key intermediates were directly intercepted by ESI-MS spectrometry analysis of a pre-incubated mixture of **C** and **II-2** (see **Figure II-2b**). When this mixture was treated with the secondary electrophile **II-1a**, intermediates **1a-2/C** *en route* to product **II-3a** and higher order adduct **1a-2^2/C** were observed (see **Figure II-2c**). The final ESI-MS spectrum displayed the same peaks regardless of the order of addition of **II-1a**, **II-2** and **C**. MS spectra obtained at longer time points depict the anticipated difference in relative intensities of the intermediates as the reaction progress to yield more product. Furthermore, for simplicity, **Figure II-2** depicts adducts that arise only from γ–attack of the allenoate whereas, the actual mixture may comprise equilibrating intermediates formed via γ and α attack. This study suggests that

the reaction of **II-1a**, **II-2** and **C** directly furnished a mixture of several adducts in equilibrium. However, the irreversibility associated with the ring closure step (see dashed box, **Figure II-2a**), adventitiously siphons the equilibrium mixture to the desired cycloadduct **II-3a**.

In summary, a two-step process is developed for the efficiency synthesis of hexahydro-2*H*-chromenes in high stereoselectivity. The asymmetric formal [4+2] cycloaddition reaction provides the dihydropyrans in high stereoselectivity, which will react as a diene in the concomitant Diels-Alder reaction. The ensuing Diels-Alder reaction is also under strict regio- and stereochemcial control. The C4 stereocenter of the dihydropyran, established during the initial [4+2] cycloaddition, is the stereochemical driver, whereas the cross-conjugation of pyranyl oxygen (O1) aids to generate an electronic bias for the observed regioselectivity in the Diels-Alder reaction. This methodology provides a complementary approach to control the stereochemistry in Diels-Alder reactions of chiral dienes,[19,23,25,26] unlocking opportunities towards expanding the repertoire of regio- and stereoselective reactions of chiral dienes.

II-4. Experimental.

II-4.1. General remarks:

All reactions were carried out in flame dried or oven dried glassware under inert gas atmosphere or in a desiccator. Unless specified, the reagents were purchased from commercial sources. THF and diethyl ether were distilled from sodium benzophenone ketyl. Methylene chloride, toluene and triethylamine were dried over CaH_2 and freshly distilled prior to use. Ethyl-2,3-butadienoate was synthesized as reported[38] and stored at -20 ºC.

Column chromatography was performed using Silicycle 60 Å, 35-75 µm silica gel. Thin layer chromatography was performed using 0.2 mm thickness silica gel 60 F254 plates and visualized using UV light, iodine, potassium permanganate stain, p-anisaldehyde stain or phosphomolybdic acid in EtOH stain.

^{1}H NMR and ^{13}C NMR, as well as all the 2D NMR spectra, were obtained using a 500 MHz Varian NMR spectrometer and referenced using the residual ^{1}H peak from the deuterated solvent. For HRMS (ESI) analysis, a Waters 2795 (Alliance HT) instrument was used and referenced against Polyethylene Glycol (PEG-400-600). Infrared spectra were reported on a Nicolet IR/42 spectrometer FT-IR (thin film, NaCl cells). Optical rotations were obtained on a Jasco P-2000 polarimeter at 20 °C and 589 nm. The specific rotations were calculated according to the equation $[\alpha]^{20}_D = (100\alpha)/(l \times c)$, where l is the path length in decimeters and c is the concentration in g/100mL.

II-4.2. General procedure for formal [4+2] cycloaddition of ethyl-2,3-butadienoate with substituted dienones:

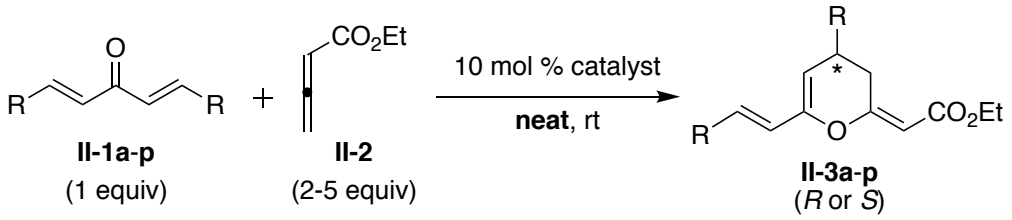

II-1a-p (1 equiv) + **II-2** (2-5 equiv) → **II-3a-p** (*R* or *S*)

A mixture of ethyl-2,3-butadienoate (2.0 equiv) and the corresponding dienone (1.0 equiv) with 10 mol% chiral amine catalysts (**A** or **B**) was charged in a 1 dram vial and stirred at room temperature. (Note: The order of addition did not make any difference to the selectivity or the yield.) Most importantly, the efficiency of stirring this neat reaction is highly crucial for optimum yields.

The progress of the reaction was monitored by TLC. When the dienone was consumed completely, usually around 8-72 h, the reaction mixture was diluted with 100-200 μL of DCM or ethyl acetate and directly purified by silica gel column chromatography using ethyl acetate and hexanes as eluents.

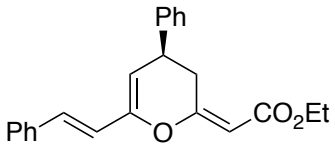

II-3a-*S*

II-3a-*S*: Ethyl (*E*)-2-((*S*)-4-phenyl-6-((*E*)-styryl)-3,4-dihydro-2*H*-pyran-2-ylidene) acetate: Using 10 mol % catalyst **A**, **II-2** (956.0 mg, 8.5 mmol) and **II-1a** (1.0 g, 4.3 mmol), 1.45 g (98% yield) of the pure product was isolated as a white solid, m.p 85 °C; ^{1}H NMR (500 MHz, $CDCl_3$) δ 7.43-7.47 (2H, m), 7.30-7.38 (4H, m), 7.22-7.29 (4H, m), 6.98 (1H,

d, *J* = 16.0 Hz), 6.53 (1H, d, *J* = 16.0 Hz), 5.71 (1H, s), 5,36 (1H, d, *J* = 4.0 Hz), 4.07-4.18 (2H, m), 3.68-3.75 (2H, m), 3.08-3.16 (1H, m), 1.25 (3H, t, *J* = 7.5 Hz) ppm; ^{13}C NMR (125 MHz, $CDCl_3$) δ 167.3, 166.1, 148.6, 143.0, 136.4, 128.7, 128.7, 128.6, 128.0, 127.3, 127.0, 126.7, 121.4, 108.5, 99.4, 59.6, 36.2, 31.0, 14.3 ppm; IR (film) 3028, 2980, 1708 (s), 1657 (s), 1278, 1118 (s), 691 cm^{-1}. HRMS (ESI) Calculated Mass for $C_{23}H_{23}O_3$: 347.1647 ($[M+H]^+$), Found 347.1640 ($[M+H]^+$). The enantiomeric excess was determined by HPLC analysis, using DAICEL CHIRALPAK OJ-H column (5% isopropanol in *n*-hexanes at 1.0 mL/min), R_t = 48.9 min (minor) and 54.3 min (major), **II-3a**-*S* (98% *ee*): $[\alpha]^{20}_D$= -137 (*c* = 2.00, $CDCl_3$).

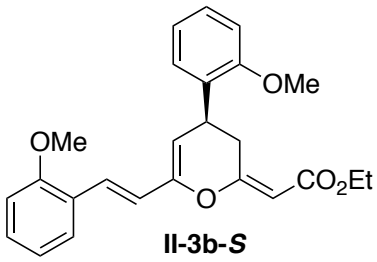

II-3b-*S*

II-3b-*S*: Ethyl (*E*)-2-((*S*)-4-(2-methoxyphenyl)-6-((*E*)-2-methoxystyryl)-3,4-dihydro-2*H*-pyran-2-ylidene) acetate: Using 10 mol % catalyst **A**, **II-2** (20.0 mg, 0.18 mmol) and **II-1b** (26.5 mg, 0.09 mmol), 21.9 mg (60% yield) of the pure product was isolated as a pale yellow oil; ^{1}H NMR (500 MHz, $CDCl_3$) δ 7.47 (1H, dd, *J* = 9.0 Hz, 2.0 Hz), 7.15-7.30 (4H, m), 6.85-6.98 (4H, m), 6.60 (1H, d, *J* = 16.0 Hz), 5.70 (1H, s), 5.31 (1H, d, *J* = 4.5 Hz), 4.06-4.16 (3H, m), 3.89 (3H, s), 3.86 (3H, s), 3.51 (1H, dd, *J* = 16.0 Hz, 6.5 Hz), 3.27 (1H, dd, *J* = 15.0 Hz, 7.0 Hz), 1.24 (3H, t, *J* = 7.0 Hz) ppm; ^{13}C NMR (125 MHz, $CDCl_3$) δ 167.4, 167.0, 157.1, 156.8, 149.2, 130.9, 129.0, 127.9, 127.7, 127.0, 125.6, 123.2, 122.3, 120.7, 120.6, 110.9, 110.4, 108.1, 99.1, 59.5, 55.4, 29.7, 29.3, 14.3 ppm; IR (film) 3078,

2933, 2838, 1708 (s), 1656 (s), 1598, 1498 (s), 1244 (s), 1118 (s), 752 cm^{-1}. HRMS (ESI) Calculated Mass for $C_{25}H_{27}O_5$: 407.1858 ($[M+H]^+$), Found 407.1850 ($[M+H]^+$). The enantiomeric excess was determined by HPLC analysis, using DAICEL CHIRALPAK OJ-H column (20% isopropanol in *n*-hexanes at 1.0 mL/min), R_t = 19.5 min (minor) and 40.2 min (major), **II-3b**-*S* (90% *ee*): $[\alpha]^{20}_D$= -52 (*c* = 1.92, $CDCl_3$).

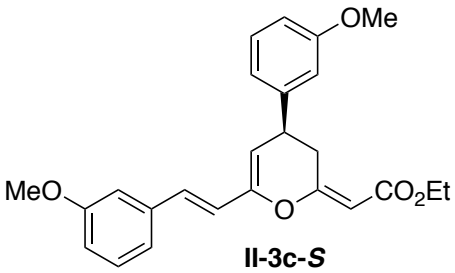

II-3c-*S*

II-3c-*S*: Ethyl (*E*)-2-((*S*)-4-(3-methoxyphenyl)-6-((*E*)-3-methoxystyryl)-3,4-dihydro-2*H*-pyran-2-ylidene) acetate: Using 10 mol % catalyst **A**, **II-2** (20.0 mg, 0.18 mmol) and **II-1c** (26.5 mg, 0.09 mmol), 35.9 mg (98% yield) of the pure product was isolated as a colorless oil; ^{1}H NMR (500 MHz, $CDCl_3$) δ 7.19-7.25 (2H, m), 7.01-7.06 (1H, m), 6.90-6.97 (2H, m), 6.75-6.85 (4H, m), 6.49 (1H, d, *J* = 15.5 Hz), 5.69 (1H, s), 5,33 (1H, d, *J* = 3.5 Hz), 4.07-4.15 (2H, m), 3.82 (3H, s), 3.78 (3H, s), 3.63-3.72 (2H, m), 3.06-3.14 (1H, m), 1.24 (3H, t, *J* = 7.5 Hz) ppm; ^{13}C NMR (125 MHz, $CDCl_3$) δ 167.3, 166.1, 159.8, 159.8, 148.5, 144.6, 137.9, 129.7, 129.6, 128.6, 121.7, 119.7, 119.3, 113.7, 113.0, 112.2, 111.9, 108.6, 99.4, 59.6, 55.2, 55.2, 36.2, 30.8, 14.3 ppm; IR (film) 3052, 2937, 2837, 1707 (s), 1656 (s), 1600 (s), 1488 (s), 1272 (s), 1120 (s), 1048 (s) cm^{-1}. HRMS (ESI) Calculated Mass for $C_{25}H_{27}O_5$: 407.1858 ($[M+H]^+$), Found 407.1855 ($[M+H]^+$). The enantiomeric excess was determined by HPLC analysis, using DAICEL CHIRALPAK OJ-H column

(25% isopropanol in *n*-hexanes at 1.0 mL/min), R_t = 43.4 min (minor) and 55.9 min (major), **II-3c**-*S* (96% *ee*): $[\alpha]^{20}_D$= -118 (*c* = 3.59, $CDCl_3$).

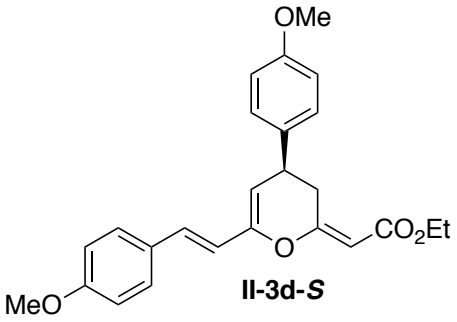

II-3d-*S*

II-3d-*S*: Ethyl (*E*)-2-((*S*)-4-(4-methoxyphenyl)-6-((*E*)-4-methoxystyryl)-3,4-dihydro-2*H*-pyran-2-ylidene) acetate: Using 10 mol % catalyst **A**, **II-2** (20.0 mg, 0.18 mmol) and **II-1d** (26.5 mg, 0.09 mmol), 9.1 mg (25% yield) of the pure product was isolated as a pale yellow oil; ^{1}H NMR (500 MHz, $CDCl_3$) δ 7.37-7.40 (2H, m), 7.14-7.18 (2H, m), 6.92 (1H, d, *J* = 16.0 Hz), 6.83-6.90 (4H, m), 6.39 (1H, d, *J* = 16.0 Hz), 5.68 (1H, s), 5,28 (1H, d, *J* = 4.5 Hz), 4.08-4.16 (2H, m), 3.83 (3H, s), 3.79 (3H, s), 3.60-3.68 (2H, m), 3.08-3.15 (1H, m), 1.25 (3H, t, *J* = 7.5 Hz) ppm; ^{13}C NMR (125 MHz, $CDCl_3$) δ 167.4, 166.4, 159.6, 158.4, 148.6, 135.2, 129.2, 128.3, 128.1, 128.0, 119.3, 114.1, 114.0, 107.8, 99.2, 59.6, 55.3, 55.3, 35.3, 31.2, 14.3 ppm; IR (film) 2930, 2837, 1708 (s), 1656 (s), 1663 (s), 1512 (s), 1251 (s), 1176 (s), 1118 (s), 1037 (s) cm^{-1}. HRMS (ESI) Calculated Mass for $C_{25}H_{27}O_5$: 407.1858 ($[M+H]^+$), Found 407.1847 ($[M+H]^+$). The enantiomeric excess was determined by HPLC analysis, using DAICEL CHIRALPAK AD-H column (1% isopropanol in *n*-hexanes at 1.2 mL/min), R_t = 58.0 min (minor) and 68.7 min (major), **II-3d**-*S* (94% *ee*): $[\alpha]^{20}_D$= -113 (*c* = 0.90, $CDCl_3$).

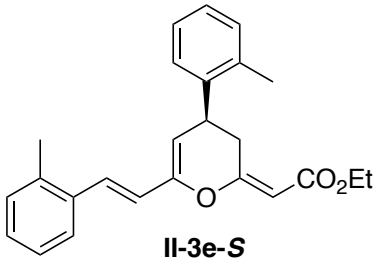

II-3e-*S*

II-3e-*S*: Ethyl (*E*)-2-((*S*)-6-((*E*)-2-methylstyryl)-4-(*o*-tolyl)-3,4-dihydro-2*H*-pyran-2-ylidene) acetate: Using 10 mol % catalyst **A**, **II-2** (20.0 mg, 0.18 mmol) and **II-1e** (23.6 mg, 0.09 mmol), 25.3 mg (75% yield) of the pure product was isolated as a colorless oil; ^{1}H NMR (500 MHz, $CDCl_3$) δ 7.48-7.54 (1H, m), 7.13-7.24 (8H, m), 6.46 (1H, d, *J* = 16.0 Hz), 5.72 (1H, s), 5.32 (1H, d, *J* = 4.0 Hz), 4.09-4.16 (2H, m), 3.91-3.96 (1H, m), 3.78 (1H, dd, *J* = 15.0 Hz, 6.5 Hz), 2.98 (1H, dd, *J* = 15.0 Hz, 8.5 Hz), 2.42 (3H, s), 2.41 (3H, s), 1.25 (3H, t, *J* = 7.5 Hz) ppm; ^{13}C NMR (125 MHz, $CDCl_3$) δ 167.3,166.3, 149.2, 140.9, 136.2, 135.5, 135.4, 130.6, 130.5, 127.9, 126.8, 126.6, 126.4, 126.2, 126.0, 125.2, 122.5, 108.7, 99.3, 59.6, 32.4, 29.7, 19.8, 19.3, 14.3 ppm; IR (film) 3020, 2927, 1709 (s), 1656 (s), 1461, 1254, 1118 (s), 1049 (s) 802, 753 cm^{-1}. HRMS (ESI) Calculated Mass for $C_{25}H_{27}O_3$: 375.1960 ($[M+H]^+$), Found 375.1966 ($[M+H]^+$). The enantiomeric excess was determined by HPLC analysis, using DAICEL CHIRALPAK OJ-H column (5% isopropanol in *n*-hexanes at 1.0 mL/min), R_t = 16.7 min (minor) and 33.0 min (major), **II-3e**-*S* (88% *ee*): $[\alpha]^{20}_D$= -78 (*c* = 0.81, $CDCl_3$).

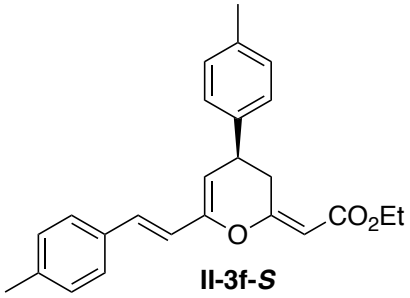

II-3f-*S*

II-3f-*S:* **Ethyl (*E*)-2-((*S*)-6-((*E*)-4-methylstyryl)-4-(*p*-tolyl)-3,4-dihydro-2*H*-pyran-2-ylidene) acetate:** Using 10 mol% catalyst **A**, **II-2** (20.0 mg, 0.18 mmol) and **II-1f** (23.6 mg, 0.09 mmol), 14.5 mg (43% yield) of the pure product was isolated as a colorless oil; ^{1}H NMR (500 MHz, $CDCl_3$) δ 7.32-7.37 (2H, m), 7.12-7.17 (6H, m), 6.94 (1H, d, *J* = 16.5 Hz), 6.47 (1H, d, *J* = 16.0 Hz), 5.69 (1H, s), 5,34 (1H, d, *J* = 3.0 Hz), 4.08-4.16 (2H, m), 3.64-3.72 (2H, m), 3.04-3.13 (1H, m), 2.35 (3H, s), 2.33 (3H, s), 1.25 (3H, t, *J* = 7.5 Hz) ppm; ^{13}C NMR (125 MHz, $CDCl_3$) δ 167.4, 166.4, 148.6, 140.0, 138.0, 136.4, 133.7, 129.4, 129.3, 128.5, 127.2, 126.6, 120.5, 108.3, 99.2, 59.6, 35.8, 31.1, 21.3, 14.3 ppm; IR (film) 3022, 2923, 2856, 1708 (s), 1656 (s), 1636 (s), 1513, 1276, 1117 (s), 1048, 810 cm^{-1}. HRMS (ESI) Calculated Mass for $C_{25}H_{27}O_3$: 375.1960 ([M+H]$^+$), Found 375.1951 ([M+H]$^+$). The enantiomeric excess was determined by HPLC analysis, using DAICEL CHIRALPAK OJ-H column (8% isopropanol in *n*-hexanes at 0.3 mL/min), R_t = 97.8 min (minor) and 166.4 min (major), **II-3e**-*S* (88% *ee*): $[\alpha]^{20}_D$= -138 (*c* = 0.71, $CDCl_3$).

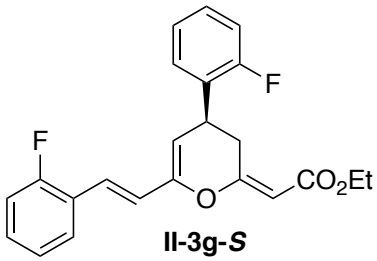

II-3g-*S*

II-3g-*S*: Ethyl (*E*)-2-((*S*)-4-(2-fluorophenyl)-6-((*E*)-2-fluorostyryl)-3,4-dihydro-2*H*-pyran-2-ylidene) acetate: Using 10 mol% catalyst **A**, **II-2** (20.0 mg, 0.18 mmol) and **II-1g** (24.3 mg, 0.09 mmol), 26.8 mg (78% yield) of the pure product was isolated as a pale yellow oil; ^{1}H NMR (500 MHz, $CDCl_3$) δ 7.45-7.52 (1H, m), 7.19-7.25 (3H, m), 7.02-7.15 (5H, m), 6.63 (1H, d, J = 16.0 Hz), 5.73 (1H, s), 5,35 (1H, d, J = 4.0 Hz), 4.05-4.17 (3H, m), 3.56 (1H, dd, J = 15.5 Hz, 6.5 Hz), 3.34 (1H, dd, J = 15.5 Hz, 7.5 Hz), 1.25 (3H, t, J = 7.5 Hz) ppm; ^{13}C NMR (125 MHz, $CDCl_3$) δ 167.1, 165.5, 160.6 (d, $^{1}J_{C,F}$ = 260.75 Hz), 160.5 (d, $^{1}J_{C,F}$ = 233.6 Hz), 149.0, 129.4 (d, $^{2}J_{C,F}$ = 13.6 Hz), 129.3 (d, $^{3}J_{C,F}$ = 8.8 Hz), 128.5 (d, $^{3}J_{C,F}$ = 5.8 Hz), 128.5, 127.7 (d, $^{3}J_{C,F}$ = 3.9 Hz), 124.3, 124.2 (d, $^{3}J_{C,F}$ = 8.8 Hz), 124.2, 123.7 (d, $^{3}J_{C,F}$ = 5.9 Hz), 121.4 (d, $^{3}J_{C,F}$ = 3.9 Hz), 115.9 (d, $^{2}J_{C,F}$ = 22.4 Hz), 115.4 (d, $^{2}J_{C,F}$ = 22.4 Hz), 107.7, 99.9, 59.7, 29.2, 29.1, 14.2 ppm; ^{19}F NMR (470 MHz, $CDCl_3$) δ -116.8—-117.9 (1F, m.), -118.6—-118.8 (1F, m.) ppm; IR (film) 3066, 2928, 2863, 1708 (s), 1657 (s), 1583, 1488 (s), 1456, 1269.0, 1231, 1124 (s), 1047, 755 cm^{-1}. HRMS (ESI) Calculated Mass for $C_{23}H_{21}F_2O_3$: 383.1459 ($[M+H]^+$), Found 383.1473 ($[M+H]^+$). The enantiomeric excess was determined by HPLC analysis, using DAICEL CHIRALPAK OJ-H column (5% isopropanol in *n*-hexanes at 1.0 mL/min), R_t = 15.8 min (minor) and 19.9 min (major), **II-3g**-*S* (92% *ee*): $[\alpha]^{20}_{D}$= -130 (*c* = 1.14, $CDCl_3$).

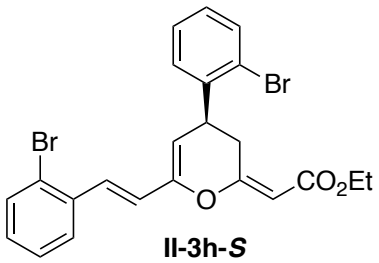

II-3h-*S*

II-3h-*S*: Ethyl (*E*)-2-((*S*)-4-(2-bromophenyl)-6-((*E*)-2-bromostyryl)-3,4-dihydro-2*H*-pyran-2-ylidene) acetate: Using 10 mol % catalyst **A**, **II-2** (20.0 mg, 0.18 mmol) and **II-1h** (35.3 mg, 0.09 mmol), 43.1 mg (95% yield) of the pure product was isolated as a pale yellow oil; ^{1}H NMR (500 MHz, $CDCl_3$) δ 7.54-7.61 (3H, m), 7.35 (1H, d, *J* = 16.0 Hz), 7.26-7.31 (2H, m), 7.21-7.25 (1H, m), 7.08-7.15 (2H, m), 6.48 (1H, d, *J* = 16.0 Hz), 5.75 (1H, s), 5,37 (1H, d, *J* = 4.5 Hz), 4.17-4.23 (1H, m), 4.06-4.17 (2H, m), 3.58 (1H, dd, *J* = 15.5 Hz, 6.5 Hz), 3.30 (1H, dd, *J* = 15.0 Hz, 6.5 Hz), 1.24 (3H, t, *J* = 7.0 Hz) ppm; ^{13}C NMR (125 MHz, $CDCl_3$) δ 167.0, 165.1, 149.1, 141.3, 136.2, 133.2, 133.0, 129.2, 128.5, 128.5, 127.8, 127.6, 127.6, 126.6, 124.4, 124.1, 123.8, 108.0, 100.3, 59.7, 35.5, 29.0, 14.3 ppm; IR (film) 3061, 2979, 2937, 1708 (s), 1658 (s), 1565, 1467, 1438, 1294, 1275, 1164, 1119 (s), 1047, 1024, 752 cm^{-1}. HRMS (ESI) Calculated Mass for $C_{23}H_{21}Br_2O_3$: 502.9857 ($[M+H]^+$), Found 502.9856 ($[M+H]^+$). The enantiomeric excess was determined by HPLC analysis, using DAICEL CHIRALPAK OJ-H column (5% isopropanol in *n*-hexanes at 1.0 mL/min), R_t = 20.8 min (minor) and 41.3 min (major), **II-3h-*S*** (88% *ee*): $[\alpha]^{20}_D$= -71 (*c* = 2.57, $CDCl_3$).

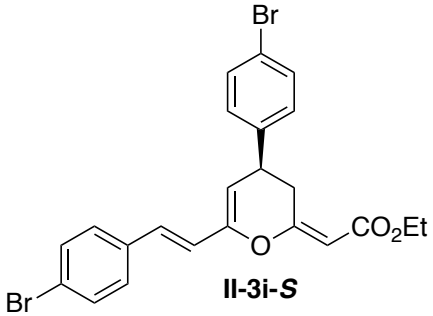

II-3i-*S*

II-3i-*S*: Ethyl (*E*)-2-((*S*)-4-(4-bromophenyl)-6-((*E*)-4-bromostyryl)-3,4-dihydro-2*H*-pyran-2-ylidene) acetate: Using 10 mol % catalyst **A**, **II-2** (20.0 mg, 0.18 mmol) and **II-**

1i (35.3 mg, 0.09 mmol), 30.0 mg (66% yield) of the pure product was isolated as a pale yellow oil; ^{1}H NMR (500 MHz, $CDCl_3$) δ 7.40-7.49 (4H, m), 7.28-7.33 (2H, m), 7.07-7.13 (2H, m), 6.91 (1H, d, *J* = 16.0 Hz), 6.49 (1H, d, *J* = 16.5 Hz), 5.70 (1H, s), 5.31 (1H, d, *J* = 4.5 Hz), 4.07-4.17 (2H, m), 3.63-3.71 (1H, m), 3.59 (1H, dd, *J* = 15.0 Hz, 6.0 Hz), 3.19 (1H, dd, *J* = 15.0 Hz, 8.0 Hz), 1.25 (3H, t, *J* = 7.0 Hz) ppm; ^{13}C NMR (125 MHz, $CDCl_3$) δ 167.1, 165.3, 148.7, 141.8, 135.3, 131.8, 131.7, 129.0, 128.2, 127.7, 121.9, 121.8, 120.8, 108.1, 99.9, 59.8, 35.7, 30.6, 14.3 ppm; IR (film) 3024, 2928, 2854, 1706 (s), 1655 (s), 1587, 1489(s), 1288, 1275, 1273, 1118 (s), 1073, 1010, 814 cm^{-1}. HRMS (ESI) Calculated Mass for $C_{23}H_{21}Br_2O_3$: 502.9857 ($[M+H]^+$), Found 502.9842 ($[M+H]^+$). The enantiomeric excess was determined by HPLC analysis, using DAICEL CHIRALPAK OD-H column (2% isopropanol in *n*-hexanes at 1.2 mL/min), R_t = 13.0 min (minor) and 15.7 min (major), **II-3i**-*S* (94% *ee*): $[\alpha]^{20}_D$= -107 (*c* = 0.61, $CDCl_3$).

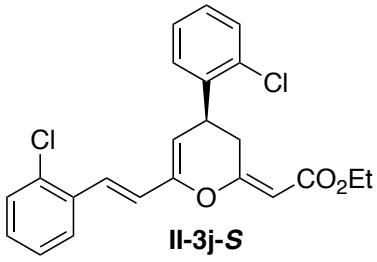

II-3j-*S*

II-3j-*S*: Ethyl (*E*)-2-((*S*)-4-(2-chlorophenyl)-6-((*E*)-2-chlorostyryl)-3,4-dihydro-2*H*-pyran-2-ylidene) acetate: Using 10 mol % catalyst **A**, **II-2** (369.4 mg, 3.3 mmol) and **II-1j** (500.0 mg, 1.6 mmol), 0.34 g (quantitative yield) of the pure product was isolated as a pale yellow oil (0.25 gram scale reaction); ^{1}H NMR (500 MHz, $CDCl_3$) δ 7.55-7.60 (1H, m), 7.35-7.41 (3H, m), 7.16-7.26 (5H, m), 6.52 (1H, d, *J* = 16.0 Hz), 5.75 (1H, s), 5.37 (1H, d, *J* = 5.0 Hz), 4.19-4.27 (1H, m), 4.06-4.17 (2H, m), 3.56 (1H, dd, *J* = 16.0 Hz, 6.5

Hz), 3.34 (1H, dd, *J* = 16.0 Hz, 7.5 Hz), 1.24 (3H, t, *J* = 6.5 Hz) ppm; ^{13}C NMR (125 MHz, $CDCl_3$) δ 167.0, 165.2, 149.2, 139.7, 134.5, 133.7, 133.5, 129.9, 129.7, 128.9, 128.4, 128.2, 127.1, 126.9, 126.5, 124.9, 123.7, 107.9, 100.2, 59.7, 32.8, 28.9, 14.2 ppm; IR (film) 3065, 2980, 2928, 2854, 1708 (s), 1658 (s), 1471, 1442, 1374, 1348, 1295, 1276, 1118 (s), 1049 (s), 755 cm^{-1}. HRMS (ESI) Calculated Mass for $C_{23}H_{21}Cl_2O_3$: 415.0868 ($[M+H]^+$), Found 415.0863 ($[M+H]^+$). The enantiomeric excess was determined by HPLC analysis, using DAICEL CHIRALPAK AD-H column (1% isopropanol in *n*-hexanes at 0.3 mL/min), R_t = 50.9 min (minor) and 55.1 min (major), **II-3j**-*S* (90% *ee*): $[\alpha]^{20}_D$= -115 (*c* = 3.25, $CDCl_3$).

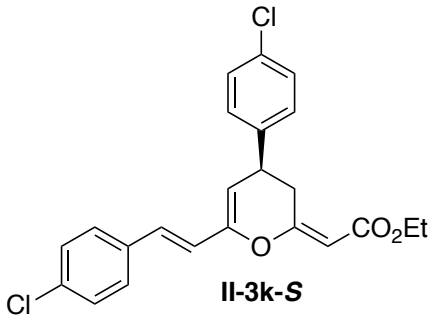

II-3k-*S*

II-3k-*S:* **Ethyl (*E*)-2-((*S*)-4-(4-chlorophenyl)-6-((*E*)-4-chlorostyryl)-3,4-dihydro-2*H*-pyran-2-ylidene) acetate:** Using 10 mol % catalyst **A**, **II-2** (20.0 mg, 0.18 mmol) and **II-1k** (27.3 mg, 0.09 mmol), 21.7 mg (58% yield) of the pure product was isolated as a pale yellow oil; ^{1}H NMR (500 MHz, $CDCl_3$) δ 7.34-7.40 (2H, m), 7.27-7.33 (4H, m), 7.14-7.19 (2H, m), 6.93 (1H, d, *J* = 15.5 Hz), 6.48 (1H, d, *J* = 16.0 Hz), 5.70 (1H, s), 5.31 (1H, d, *J* = 4.5 Hz), 4.06-4.17 (2H, m), 3.65-3.73 (1H, m), 3.59 (1H, dd, *J* = 15.0 Hz, 6.5 Hz), 3.18 (1H, dd, *J* = 15.0 Hz, 8.0 Hz), 1.25 (3H, t, *J* = 6.5 Hz) ppm; ^{13}C NMR (125 MHz, $CDCl_3$) δ 167.2, 165.4, 148.7, 141.3, 134.8, 133.7, 132.7, 128.9, 128.8, 128.7, 127.9, 127.7, 121.7,

108.1, 99.9, 59.8, 35.6, 30.7, 14.3 ppm; IR (film) 3051, 2980, 2927, 2854, 1707 (s), 1657 (s), 1491 (s), 1344, 1288, 1274, 1119 (s), 1092, 818 cm^{-1}. HRMS (ESI) Calculated Mass for $C_{23}H_{21}Cl_2O_3$: 415.0868 ($[M+H]^+$), Found 415.0862 ($[M+H]^+$). The enantiomeric excess was determined by HPLC analysis, using DAICEL CHIRALPAK OD-H column (1% isopropanol in *n*-hexanes at 1.0 mL/min), R_t = 16.8 min (minor) and 24.2 min (major), **II-3k**-*S* (91% *ee*): $[\alpha]^{20}_D$= -139 (*c* = 1.33, $CDCl_3$).

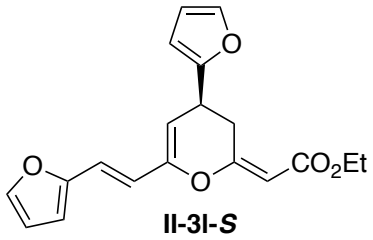

II-3l-*S*

II-3l-*S:* **Ethyl (*E*)-2-((*S*)-4-(furan-2-yl)-6-((*E*)-2-(furan-2-yl) vinyl)-3,4-dihydro-2*H*-pyran-2-ylidene) acetate:** Using 10 mol % catalyst **A**, **II-2** (20.0 mg, 0.18 mmol) and **II-1l** (19.3 mg, 0.09 mmol), 7.9 mg (27% yield) of the pure product was isolated as a pale yellow oil; ^{1}H NMR (500 MHz, $CDCl_3$) δ 7.32-7.40 (2H, m), 6.74 (1H, d, *J* = 15.5 Hz), 6.38-6.45 (2H, m), 6.33-6.38 (1H, m), 6.27-6.30 (1H, m), 6.07-6.11 (1H, m), 5.76 (1H, s), 5.36 (1H, d, *J* = 4.5 Hz), 4.11-4.21 (2H, m), 3.75-3.81 (1H, m), 3.55 (1H, dd, *J* = 15.0 Hz, 6.0 Hz), 3.39 (1H, dd, *J* = 15.5 Hz, 7.5 Hz), 1.28 (3H, t, *J* = 7.0 Hz) ppm; ^{13}C NMR (125 MHz, $CDCl_3$) δ 167.3, 165.5, 155.1, 152.4, 148.4, 142.7, 141.8, 119.5, 116.7, 111.8, 110.2, 109.9, 105.2, 105.1, 99.7, 59.7, 29.9, 27.5, 14.3 ppm; IR (film) 2960, 2927, 2858, 1708 (s), 1657 (s), 1284, 1119 (s), 734 cm^{-1}. HRMS (ESI) Calculated Mass for $C_{19}H_{19}O_5$: 327.1232 ($[M+H]^+$), Found 327.1241 ($[M+H]^+$). The enantiomeric excess was determined by HPLC analysis, using DAICEL CHIRALPAK OJ-H column (15% isopropanol in *n*-

hexanes at 1.0 mL/min), R_t = 13.6 min (minor) and 21.9 min (major), **II-3l**-*S* (95% *ee*): $[\alpha]^{20}_D$= -90 (*c* = 0.73, $CDCl_3$).

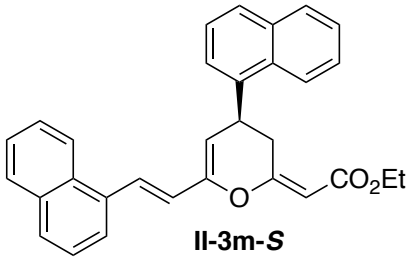

II-3m-*S*

II-3m-*S:* **Ethyl (*E*)-2-((*S*)-4-(naphthalen-1-yl)-6-((*E*)-2-(naphthalen-1-yl)vinyl)-3,4-dihydro-2*H*-pyran-2-ylidene)acetate:** Using 10 mol % catalyst **A**, **II-2** (20.0 mg, 0.18 mmol) and **II-1m** (30.1 mg, 0.09 mmol), 30.5 mg (76% yield) of the pure product was isolated as a pale yellow oil; ^{1}H NMR (500 MHz, $CDCl_3$) δ 8.24 (1H, d, *J* = 8.5 Hz), 8.15 (1H, d, *J* = 8.5 Hz), 7.76-7.93 (5H, m), 7.70 (1H, d, *J* = 7.0 Hz), 7.42-7.62 (7H, m), 6.65 (1H, d, *J* = 15.5 Hz), 5.83 (1H, s), 5.52 (1H, d, *J* = 4.0 Hz), 4.54-4.61 (1H, m), 4.06-4.12 (2H, m), 3.93 (1H, dd, *J* = 15.0 Hz, 5.5 Hz), 3.37 (1H, dd, *J* = 15.5 Hz, 8.5 Hz), 1.20 (3H, t, *J* = 7.0 Hz) ppm; ^{13}C NMR (125 MHz, $CDCl_3$) δ 167.2, 166.1, 149.1, 138.2, 134.0, 134.0, 133.7, 131.3, 131.0, 129.1, 128.6, 128.4, 127.6, 126.4, 126.2, 125.9, 125.7, 125.6, 125.5, 125.5 124.3, 124.1, 123.7, 123.5, 122.8, 108.9, 99.8, 59.7, 32.0, 29.9, 14.2 ppm; IR (film) 3058, 2926, 2854, 1706 (s), 1654 (s), 1509, 1284, 1259, 1118 (s), 1049, 798, 777 cm^{-1}. HRMS (ESI) Calculated Mass for $C_{31}H_{27}O_5$: 447.1960 ($[M+H]^+$), Found 447.1954 ($[M+H]^+$). The enantiomeric excess was determined by HPLC analysis, using DAICEL CHIRALPAK AD-H column (10% isopropanol in *n*-hexanes at 1.0 mL/min), R_t = 10.5 min (minor) and 8.8 min (major), **II-3m**-*S* (82% *ee*): $[\alpha]^{20}_D$= -84 (*c* = 1.03, $CDCl_3$).

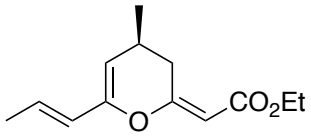

II-3p-*S*

II-3p-*S:* **Ethyl (*E*)-2-((*S*)-4-methyl-6-((*E*)-prop-1-en-1-yl)-3,4-dihydro-2*H*-pyran-2-ylidene)acetate:** Using 10 mol % catalyst **A**, **II-2** (20.0 mg, 0.18 mmol) and **II-1p** (9.9 mg, 0.09 mmol), 9.6 mg (48% yield) of the pure product was isolated as a colorless oil; ^{1}H NMR (500 MHz, $CDCl_3$) δ 6.00-6.08 (1H, m), 5.73-5.79 (1H, m), 5.56 (1H, s), 4.85-4.89 (1H, m), 4.15 (2H, dd, *J* = 14.5 Hz, 7.0 Hz), 3.45 (1H, dd, *J* = 15.0 Hz, 5.5 Hz), 2.60 (1H, dd, *J* = 15.5 Hz, 9.0 Hz), 2.38-2.48 (1H, m), 1.78 (3H, d, *J* = 6.5 Hz), 1.28 (3H, t, *J* = 7.0 Hz), 1.06 (3H, d, *J* = 6.5 Hz) ppm; ^{13}C NMR (125 MHz, $CDCl_3$) δ 167.7, 176.6, 147.3, 125.6, 124.4, 108.2, 98.4, 59.5, 30.4, 24.6, 20.7, 17.9, 14.3 ppm; IR (film) 3045, 2934, 2929, 2863, 1710(s), 1674, 1648 (s), 1375, 1117 (s), 1052,974 cm^{-1}. HRMS (ESI) Calculated Mass for $C_{13}H_{19}O_3$: 223.1334 ($[M+H]^+$), Found 223.1342 ($[M+H]^+$). The enantiomeric excess was determined by HPLC analysis, using DAICEL CHIRALPAK AI column (*n*-hexanes at 1.0 mL/min), R_t = 18.9 min (minor) and 21.5 min (major), **II-3p**-*S* (90% *ee*): $[\alpha]^{20}_D$= -88 (*c* = 1.29, $CDCl_3$).

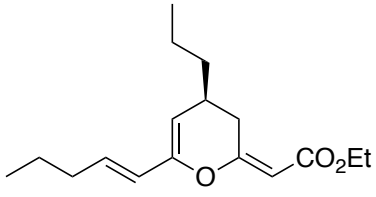

II-3n-*S*

II-3n-*S:* **Ethyl (E)-2-((S)-6-((E)-pent-1-en-1-yl)-4-propyl-3,4-dihydro-2H-pyran-2-ylidene)acetate:** Using 10 mol % catalyst **A**, **II-2** (20.0 mg, 0.18 mmol) and **II-1n** (15.0

mg, 0.09 mmol), 7.0 mg (28% yield) of the pure product was isolated as a colorless oil; ^{1}H NMR (500 MHz, $CDCl_3$) δ 6.03 (1H, dt, *J* = 15.5 Hz, 7.0 Hz), 5.75 (1H, d, *J* = 15.5 Hz), 5.57 (1H, s), 4.93-4.96 (1H, m), 4.15 (2H, q, *J* = 7.0 Hz), 3.32 (1H, dd, *J* = 15.0 Hz, 6.0 Hz), 2.81 (1H, dd, *J* = 15.0 Hz, 8.5 Hz), 2.28-2.36 (1H, m), 2.04-2.12 (2H, m), 1.31-1.48 (6H, m), 1.27 (3H, t, *J* = 7.0 Hz), 0.87-0.95 (6H, m) ppm; ^{13}C NMR (125 MHz, $CDCl_3$) δ 167.8, 147.4, 130.7, 123.3, 107.1, 98.4, 59.5, 37.4, 34.5, 29.4, 28.4, 22.3, 19.8, 14.3, 14.0, 13.7 ppm; IR (film) 2959, 2930, 2873, 1711 (s), 1648 (s), 1464, 1376, 1286, 1118 (s), 1051, 962, 846 cm^{-1}. HRMS (ESI) Calculated Mass for $C_{17}H_{27}O_3$: 279.1960 ($[M+H]^+$), Found 279.1969 ($[M+H]^+$). The enantiomeric excess was determined by HPLC analysis, using DAICEL CHIRALPAK AI column (*n*-hexanes at 0.5 mL/min), R_t = 19.3 min (minor) and 22.4 min (major), **II-3n**-*S* (90% *ee*): $[\alpha]^{20}_D$= -108 (*c* = 0.55, $CDCl_3$).

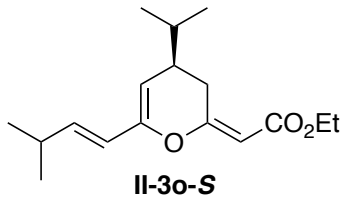

II-3o-*S*

II-3o-*S:* **Ethyl (E)-2-((R)-4-isopropyl-6-((E)-3-methylbut-1-en-1-yl)-3,4-dihydro-2H-pyran-2-ylidene)acetate:** Using 10 mol % catalyst **A**, **II-2** (20.0 mg, 0.18 mmol) and **II-1o** (15.0 mg, 0.09 mmol), 7.3 mg (29% yield) of the pure product was isolated as a colorless oil; ^{1}H NMR (500 MHz, $CDCl_3$) δ 6.01 (1H, dd, *J* = 15.5 Hz, 7.0 Hz), 5.74 (1H, dd, *J* = 15.5 Hz, 1.0 Hz), 5.56 (1H, s), 4.97-5.00 (1H, m), 4.15 (2H, q, *J* = 6.5 Hz), 3.22 (1H, dd, *J* = 15.0 Hz, 6.0 Hz), 2.99 (1H, dd, *J* = 15.0 Hz, 7.5 Hz), 2.32-2.41 (1H, m), 2.08-2.15 (1H, m), 1.58-1.65 (1H, m), 1.27 (3H, t, *J* = 6.5 Hz), 1.03 (6H, d, *J* = 7.0 Hz), 0.90-

0.96 (6H, m) ppm; ^{13}C NMR (125 MHz, $CDCl_3$) δ 168.3, 167.8, 147.9, 137.4, 120.5, 105.8, 98.2, 59.5, 36.2, 32.1, 30.9, 25.9, 22.2, 22.2, 19.9, 19.5, 14.3 ppm; IR (film) 3043, 2961 (s), 2933, 2872, 1710 (s), 1670, 1647 (s), 1465, 1374, 1281, 1174, 1118 (s), 966, 844 cm^{-1}. HRMS (ESI) Calculated Mass for $C_{17}H_{27}O_3$: 279.1960 ($[M+H]^+$), Found 279.1973 ($[M+H]^+$). The enantiomeric excess was determined by HPLC analysis, using DAICEL CHIRALPAK AI column (*n*-hexanes at 0.1 mL/min), R_t = 96.5 min (minor) and 101.3 min (major), **II-3o**-*S* (94% *ee*): $[\alpha]^{20}_D$= -96 (*c* = 1.46, $CDCl_3$).

II-4.3. General procedure for synthesis of aromatic dienones:

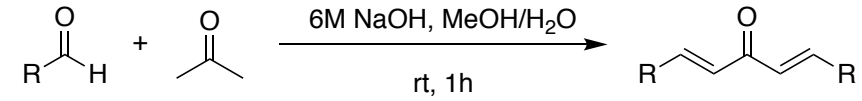

(2.0 equiv) (1.0 equiv) **II-1a-m**

To a solution of the corresponding aryl aldehyde (2.0 equiv) and acetone (1.0 equiv) in the mixed solvent of methanol/H_2O (v/v = 1:1), 6M NaOH (6.0 equiv) was added dropwise (approximately 2 drops/sec to avoid formation of side products). The reaction mixture warmed up rapidly forming a cloudy suspension. The mixture was allowed to stir at room temperature for another hour. The reaction was neutralized with the addition of HCl (concentrated), followed by extraction with dichlormethane. The combined organic extracts were washed with brine, dried over sodium sulfate, filtrated through celite, concentrated under rotavapor, and finally subjected to purification by silica gel flash column chromatography or by recrystallization.

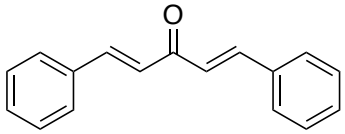

I-1a

II-1a: (1*E*, 4*E*)-1,5-diphenylpenta-1,4-dien-3-one (Dibenzalacetone): Using benzaldehyde (573.0 mg, 5.4 mmol) and acetone (156.8 mg, 2.7 mmol), 322.6 mg (51% yield) of the pure product was isolated as yellow needle shaped crystals, mp 111 °C (lit.[39] 112 °C). ^{1}H NMR (500 MHz, $CDCl_3$) δ 7.73 (2H, d, *J* = 15.6 Hz), 7.61-7.60 (4H, m), 7.41-7.60 (6H, m), 7.07 (2H, d, *J* = 16.2 Hz) ppm; ^{13}C NMR (125 MHz, $CDCl_3$) δ 188.9, 143.3, 134.8, 130.5, 129.0, 128.4, 125.4 ppm.

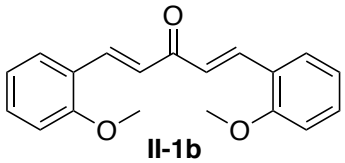

II-1b

II-1b: (1E, 4E)-1,5-bis(2-methoxyphenyl)penta-1,4-dien-3-one): Using 2-anisaldehyde (735.2 mg, 5.4 mmol) and acetone (156.8 mg, 2.7 mmol), 762.9 mg (96% yield) of the pure product was isolated as a yellow solid, mp 110 °C (lit.[40] 118-120 °C). ^{1}H NMR (500 MHz, $CDCl_3$) δ 8.07 (2H, d, *J* = 16.0 Hz), 7.63 (2H, dd, *J* = 7.5 Hz, *J* = 1.5 Hz), 7.63 (2H, td, *J* = 7.5 Hz, *J* = 1.5 Hz), 7.18 (2H, d, *J* = 16.0 Hz), 6.99 (2H, t, *J* = 7.0 Hz), 6.94 (2H, d, *J* = 8.5 Hz), 3.92 (6H, s) ppm; ^{13}C NMR (125 MHz, $CDCl_3$) δ 190.0, 158.5, 138.2, 131.5, 128.7, 126.2, 124.0, 120.7, 111.1, 55.5 ppm.

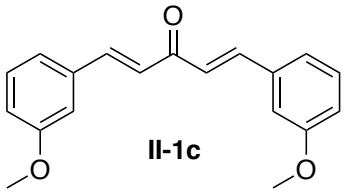

II-1c

II-1c: (1*E*,4*E*)-1,5-bis(3-methoxyphenyl)penta-1,4-dien-3-one: Using 3-anisaldehyde (735.2 mg, 5.4 mmol) and acetone (156.8 mg, 2.7 mmol), 437.1 mg (55% yield) of the pure product was isolated as a yellow oil (lit.[41] yellow solid 64-65 °C). ^{1}H NMR (500 MHz, $CDCl_3$) δ 7.71 (2H, d, *J* = 16.0 Hz), 7.34 (2H, t, *J* = 8.0 Hz), 7.20-7.24 (2H, *m*), 7.12-7.16 (2H, m), 7.07 (2H, d, *J* = 15.5 Hz), 6.97 (2H, dd, *J* = 8.0 Hz, 2.5 Hz), 3.86 (6H, s) ppm; ^{13}C NMR (125 MHz, $CDCl_3$) δ 188.9, 159.9, 143.3, 136.2, 130.0, 125.7, 121.1, 116.4, 113.2, 55.4 ppm.

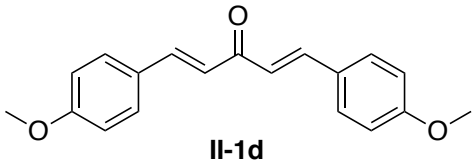

II-1d

II-1d: (1*E*,4*E*)-1,5-bis(4-methoxyphenyl)penta-1,4-dien-3-one: Using 4-anisaldehyde (735.2 mg, 5.4 mmol) and acetone (156.8 mg, 2.7 mmol), 492.7 mg (62% yield) of the pure product was isolated as a yellow solid 120 °C (lit.[41] 128-130 °C). ^{1}H NMR (500 MHz, $CDCl_3$) δ 7.70 (2H, d, *J* = 15.5 Hz), 7.54-7.60 (4H, m), 6.91-6.98 (6H, m), 3.85 (6H, s) ppm; ^{13}C NMR (125 MHz, $CDCl_3$) δ 188.8, 161.5, 142.6, 130.1, 127.6, 123.5, 114.4, 55.4 ppm.

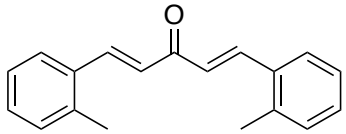

II-1e

II-1e: (1*E*,4*E*)-1,5-di-*o*-tolylpenta-1,4-dien-3-one: Using *o*-tolualdehyde (648.8 mg, 5.4 mmol) and acetone (156.8 mg, 2.7 mmol), 587.9 mg (83% yield) of the pure product was isolated as a yellow solid, mp 70 °C (lit.[41] 98-100 °C). ^{1}H NMR (500 MHz, $CDCl_3$) δ 8.05 (2H, d, *J* = 16.0 Hz), 7.64-7.68 (2H, m), 7.29-7.34 (2H, m), 7.22-7.27 (2H, m), 7.00 (2H, d, *J* = 15.5 Hz), 2.49 (6H, s) ppm; ^{13}C NMR (125 MHz, $CDCl_3$) δ 188.9, 140.9, 138.2, 133.8, 130.9, 130.2, 126.7, 126.4, 126.4, 19.9 ppm.

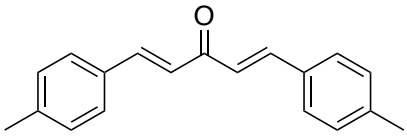

II-1f

II-1f: (1*E*,4*E*)-1,5-di-*p*-tolylpenta-1,4-dien-3-one: Using *p*-tolualdehyde (648.8 mg, 5.4 mmol) and acetone (156.8 mg, 2.7 mmol), 517.1 mg (73% yield) of the pure product was isolated as a yellow solid, mp 166 °C (lit.[42] 177.0-177.5 °C). ^{1}H NMR (500 MHz, $CDCl_3$) δ 7.72 (2H, d, *J* = 16.0 Hz), 7.52 (4H, d, *J* = 8.5 Hz), 7.22 (4H, d, *J* = 8.5 Hz), 7.05 (2H, d, *J* = 15.5 Hz) 2.39 (6H, s) ppm; ^{13}C NMR (125 MHz, $CDCl_3$) δ 189.1, 143.2, 141.0, 132.1, 129.7, 128.4, 124.6, 21.5 ppm.

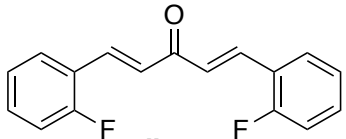

II-1g

II-1g: (1*E*,4*E*)-1,5-bis(2-fluorophenyl)penta-1,4-dien-3-one: Using 2-fluoraldehyde (670.2 mg, 5.4 mmol) and acetone (156.8 mg, 2.7 mmol), 357.6 mg (49% yield) of the pure product was isolated as a dark brown solid, mp 52 °C (lit.[43] 68-70 °C). ^{1}H NMR (500 MHz, $CDCl_3$) δ 7.87 (2H, d, J = 16.0 Hz), 7.61-7.67 (2H, m), 7.35-7.42 (2H, m), 7.10-7.23 (6H, m), ppm; ^{13}C NMR (125 MHz, $CDCl_3$) 189.0, 162.6 (d, $^{1}J_{C,F}$ = 252.4 Hz), 136.1 (d, $^{4}J_{C,F}$ = 2.9 Hz), 131.9 (d, $^{3}J_{C,F}$ = 8.5 Hz), 129.3 (d, $^{4}J_{C,F}$ = 2.8 Hz), 127.6 (d, $^{3}J_{C,F}$ = 6.6 Hz), 124.5 (d, $^{3}J_{C,F}$ = 3.9 Hz), 122.8 (d, $^{2}J_{C,F}$ = 11.4 Hz), 116.3 (d, $^{2}J_{C,F}$ = 21.9 Hz).

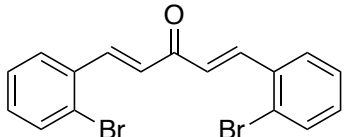

II-1h

II-1h: (1*E*,4*E*)-1,5-bis(2-bromophenyl)penta-1,4-dien-3-one: Using 2-bromobenzaldehyde (999.1 mg, 5.4 mmol) and acetone (156.8 mg, 2.7 mmol), 328.2 mg (31% yield) of the pure product was isolated as an orange solid, mp 94 °C (lit.[44] 97 °C). ^{1}H NMR (500 MHz, $CDCl_3$) δ 8.09 (2H, d, J = 16.0 Hz), 7.62-7.74 (4H, m), 7.34-7.40 (2H, m), 7.24-7.29 (2H, m), 7.03 (2H, d, J = 16.0 Hz) ppm; ^{13}C NMR (125 MHz, $CDCl_3$) δ 188.7, 142.0, 134.8, 133.5, 131.4, 127.8, 127.8, 127.7, 125.9 ppm.

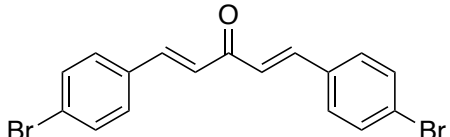

II-1i

II-1i: (1*E*,4*E*)-1,5-bis(4-bromophenyl)penta-1,4-dien-3-one: Using 4-bromobenzaldehyde (999.1 mg, 5.4 mmol) and acetone (156.8 mg, 2.7 mmol), 1.03 g

(97% yield) of the pure product was isolated as an orange solid, mp 205 °C (lit.[42] 212.2-212.9 °C). ^{1}H NMR (500 MHz, $CDCl_3$) δ 7.67 (2H, d, *J* = 15.5 Hz), 7.55 (4H, d, *J* = 8.0 Hz), 7.47 (4H, d, *J* = 8.0 Hz), 7.05 (2H, d, *J* = 16.0 Hz) ppm; ^{13}C NMR (125 MHz, $CDCl_3$) δ 188.3, 142.2, 133.6, 132.2, 129.7, 125.7, 124.9 ppm.

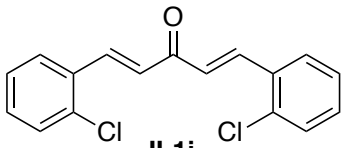

II-1j

II-1j. (1*E*,4*E*)-1,5-bis(2-chlorophenyl)penta-1,4-dien-3-one: Using 2-chlorobenzaldehyde (759.1 mg, 5.4 mmol) and acetone (156.8 mg, 2.7 mmol), 409.3 mg (50% yield) of the pure product was isolated as an orange solid, mp 108 °C (lit.[42] 112.5-113.0 °C). ^{1}H NMR (500 MHz, $CDCl_3$) δ 8.14 (2H, d, *J* = 16.0 Hz), 7.70-7.76 (4H, m), 7.42-7.48 (2H, m), 7.30-7.38 (2H, m), 7.08 (2H, d, *J* = 16.5 Hz) ppm; ^{13}C NMR (125 MHz, $CDCl_3$) δ 189.0, 139.4, 135.4, 133.0, 131.3, 130.3, 127.7, 127.5, 127.1 ppm.

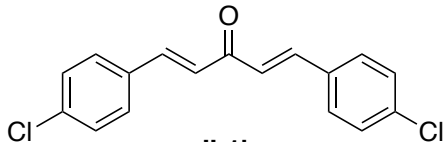

II-1k

II-1k: (1*E*,4*E*)-1,5-bis(4-chlorophenyl)penta-1,4-dien-3-one: Using 4-chlorobenzaldehyde (759.1 mg, 5.4 mmol) and acetone (156.8 mg, 2.7 mmol), 802.2 mg (98% yield) of the pure product was isolated as a yellow solid, mp 170 °C (lit.[42] 184-186 °C). ^{1}H NMR (500 MHz, $CDCl_3$) δ 7.73 (2H, d, *J* = 16.0 Hz), 7.61 (4H, d, *J* = 8.5 Hz), 7.45

(4H, d, *J* = 9.0 Hz), 7.09 (2H, d, *J* = 15.5 Hz) ppm; ^{13}C NMR (125 MHz, $CDCl_3$) δ 188.3, 142.1, 136.5, 133.2, 129.5, 129.3, 129.2, 125.7 ppm.

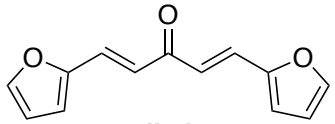

II-1l

II-1l: (1*E*,4*E*)-1,5-di(furan-2-yl)penta-1,4-dien-3-one: Using 2-furaldehyde (518.9 mg, 5.4 mmol) and acetone (156.8 mg, 2.7 mmol), 341.3 mg (59% yield) of the pure product was isolated as a black oil (lit.[45] Solid 59-60 °C). ^{1}H NMR (500 MHz, $CDCl_3$) δ 7.52 (2H, d, *J* = 1.0 Hz), 7.48 (2H, d, *J* = 16.0 Hz), 6.92 (2H, d, *J* = 15.5 Hz), 6.69 (2H, d, *J* = 3.5 Hz), 6.50 (2H, dd, *J* = 3.5 Hz, *J* = 1.5 Hz) ppm; ^{13}C NMR (125 MHz, $CDCl_3$) δ 188.1, 151.5, 144.9, 129.2, 123.2, 115.9, 112.6 ppm.

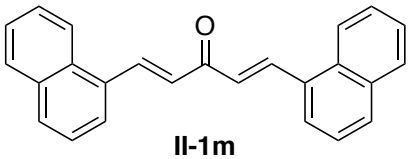

II-1m

II-1m: (1*E*,4*E*)-1,5-di(naphthalen-1-yl)penta-1,4-dien-3-one: Using 1-naphthaldehyde (843.4 mg, 5.4 mmol) and acetone (156.8 mg, 2.7 mmol), 243.8 mg (27% yield) of the pure product was isolated as a yellow solid, mp 113 °C (lit.[46] 134-135 °C). ^{1}H NMR (500 MHz, $CDCl_3$) δ 8.66 (2H, d, *J* = 16.0 Hz), 8.29 (2H, d, *J* = 9.0 Hz), 7.87-7.98 (6H, m), 7.51-7.65 (6H, m), 7.25 (2H, d, *J* = 14.5 Hz) ppm; ^{13}C NMR (125 MHz, $CDCl_3$) δ 188.6, 140.4, 133.7, 132.2, 131.7, 130.8, 128.8, 128.1, 127.0, 126.3, 125.5, 125.2, 123.4 ppm.

II-4.4. Synthesis of alkyl substituted dienones II-1n – II-1p:[42,47]

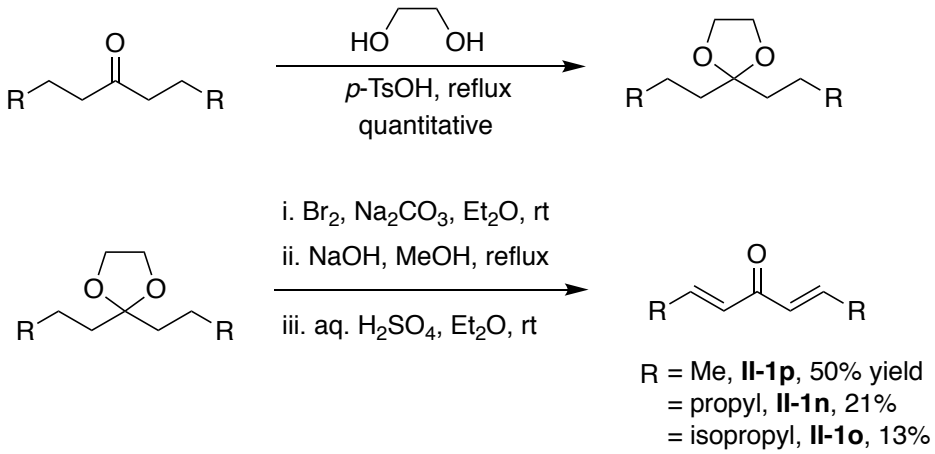

A solution of ketone (1.0 equiv), ethylene glycol (7.1 equiv) and 4 mol % of *p*-TsOH in benzene was refluxed for 24 h, with azotropic removal of water (Dean-Stark apparatus). The reaction mixture was then cooled to room temperature and quenched with water and the separated aqueous layer was extracted with ether. The combined organic layers were washed with dilute base 10% (wt) NaOH solution, and dried with Na_2SO_4. After filtration, the solution was concentrated under the reduced pressure to furnish the 2,2-dipropyl-1,3-dioxolane (quantitative yield) as a pale-yellow oil, which was used for the next step without further purification.

To the above ketal (1.0 equiv) in Et_2O was added bromine (2.02 equiv) at room temperature. After the addition was complete, Na_2CO_3 (4.4 equiv) was added in one portion and the resulting mixture was stirred overnight at room temperature. After this time, the reaction mixture was filtered through cotton and concentrated to dryness. The obtained dibromo species was dissolved in methanol, and NaOH (8.7 equiv) was added at room temperature. The mixture was refluxed for two days. Once the mixture was cooled

down to room temperature again, it was diluted with water and extracted with n-pentane. The organic phase was dried over $MgSO_4$. After removal of the solvent the desired material was obtained. The crude diene ketal was placed without further purification in a flask, containing Et_2O and sulfuric acid (3%). The mixture was stirred for 3 h, the organic phase was separated, the water phase was extracted with Et_2O, and the combined organic phase was dried over Na_2SO_4 and concentrated under reduced pressure. The residue was purified by silica gel column chromatography (0-5% EtOAc in hexane) to furnish the desired product.

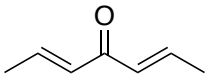

II-1o

II-1o: (2E,5E)-hepta-2,5-dien-4-one: Using 4-heptanone (3.0 g, 26.3 mmol), 520.0 mg (50% yield) of the pure product was isolated as a pale-yellow oil. ^{1}H NMR (500 MHz, $CDCl_3$) δ 6.91 (2H, qd, *J* = 15.5 Hz, 7.0 Hz), 6.34 (2H, dd, *J* = 15.5 Hz, 1.5 Hz), 1.91 (6H, d, *J* = 6.5 Hz) ppm; ^{13}C NMR (125 MHz, $CDCl_3$) δ 189.3, 142.9, 130.2, 18.4 ppm.

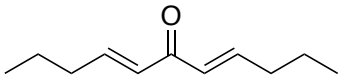

II-1n

II-1n: (4E,7E)-undeca-4,7-dien-6-one: Using undecan-6-one (3.0 g, 17.6 mmol), 615.2 mg (21% yield) of the pure product was isolated as a pale-yellow liquid. ^{1}H NMR (500 MHz, $CDCl_3$) δ 6.90 (2H, dt, *J* = 16.0 Hz, 7.0 Hz), 6.33 (2H, dt, *J* = 16.0 Hz, 1.5 Hz), 2.22

(4H, qd, *J* = 7.0 Hz, 1.5 Hz), 1.47-1.55 (4H, m), 0.95 (6H, t, *J* = 7.5 Hz) ppm; ^{13}C NMR (125 MHz, $CDCl_3$) δ 189.7, 147.7, 128.8, 34.7, 21.4, 13.7 ppm.

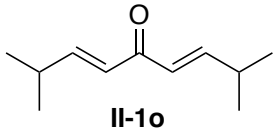

II-1o

II-1o: (3E,6E)-2,8-dimethylnona-3,6-dien-5-one: Using 2,8-dimethylnonan-5-one (3.0 g, 17.6 mmol), 380.7 mg (13% yield) of the pure product was isolated as a pale yellow liquid. ^{1}H NMR (500 MHz, $CDCl_3$) δ 6.87 (2H, dd, *J* = 16.0 Hz, 7.0 Hz), 6.33 (2H, dd, *J* = 16.0 Hz, 1.5 Hz), 2.44-2.54 (2H, m), 1.09 (12H, d, *J* = 7.0 Hz) ppm; ^{13}C NMR (125 MHz, $CDCl_3$) δ 190.3, 153.9, 125.9, 31.3, 21.4 ppm.

II-4.5. Synthesis of formal [4+2] cycloadditions of unsymmetrically substituted dineones:[48]

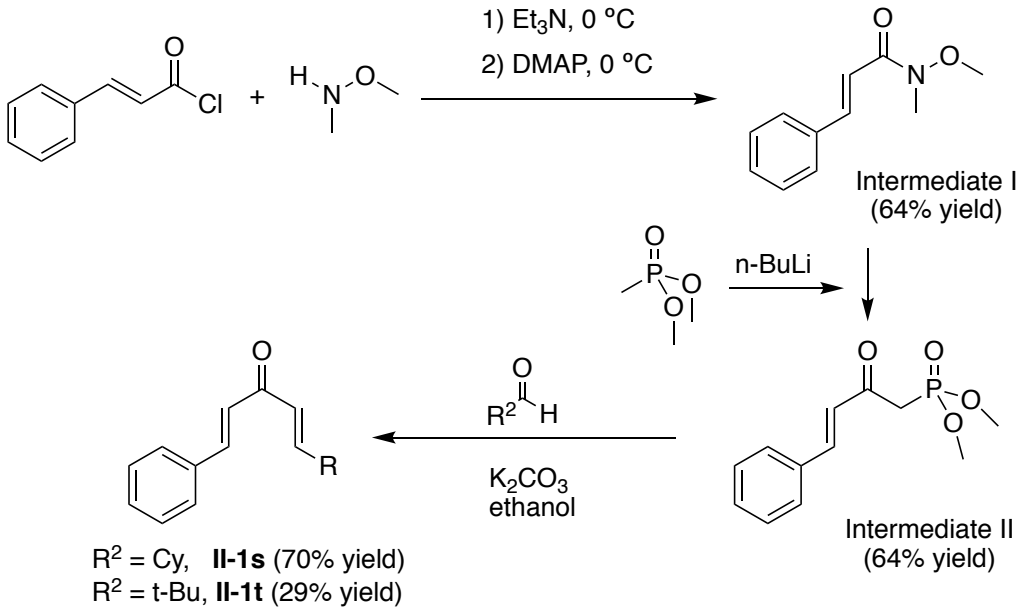

The intermediates *N*-methoxy-*N*-methylcinnamamide (intermediate I) and (*E*)-dimethyl 2-oxo-4-phenylbut-3-enylphosphonate (intermediate II), as well as compound **II-1s** were prepared by previously reported procedures.[48] **II-1s:** ^{1}H NMR (500 MHz, $CDCl_3$) δ 7.65 (1H, d, *J* = 16.0 Hz), 7.54-7.61 (2H, m), 7.37-7.42 (3H, m), 6.99 (1H, d, *J* = 16.5 Hz), 6.95 (1H, dd, *J* = 15.5 Hz, 6.5 Hz), 6.38 (1H, dd, *J* = 15.5 Hz, 1.0 Hz) 2.17-2.27 (1H, m), 1.74-1.87 (4H, m), 1.27-1.37 (2H, m), 1.15-1.27 (4H, m) ppm; ^{13}C NMR (125 MHz, $CDCl_3$) δ 189.7, 153.2, 142.9, 134.9, 130.3, 128.9, 128.3, 128.2, 126.8, 124.8, 40.9, 31.8, 25.9, 25.7 ppm.

II-1t was synthesized in a similar fashion as described below: To a solution of phosphonate (200.0 mg, 0.79 mmol) in ethanol (4.0 mL) was added K_2CO_3 (100.0 mg, 0.72 mmol) and allowed to stir for 0.5 h. After cooling the reaction mixture to 0 °C, a solution of aldehyde (61.6, 78 μL, 0.72 mmol) in ethanol (1.0 mL) was added dropwise and stirred overnight. The reaction was quenched with 1 M HCl (aq) (15.0 mL), extracted with dichloromethane (3×15mL), and the organic layers combined. The extract was dried with Na_2SO_4, filtrated and concentrated under reduced pressure. The crude material was purified by flash silica column chromatography with EtOAc in hexane (1.5%-20%) to furnish **II-1t** (49.6 mg, 29% yield) as a yellow oil. ^{1}H NMR (500 MHz, $CDCl_3$) δ 7.66 (1H, d, *J* = 16.0 Hz), 7.56-7.62 (2H, m), 7.38-7.42 (3H, m), 7.00 (1H, d, *J* = 16.0 Hz), 7.00 (1H, d, *J* = 16.0 Hz), 1.14 (9H, s) ppm; ^{13}C NMR (125 MHz, $CDCl_3$) δ 189.8, 157.9, 142.9, 130.3, 128.9, 128.3, 124.9, 124.5, 28.8 ppm.

II-4.6. Procedures for Diels-Alder reaction of chiral dihydropyrans (II-3) with dienophiles II-4a – II-4d:

General procedure for Diels-Alder reaction using dienophiles II-4a and II-4b:

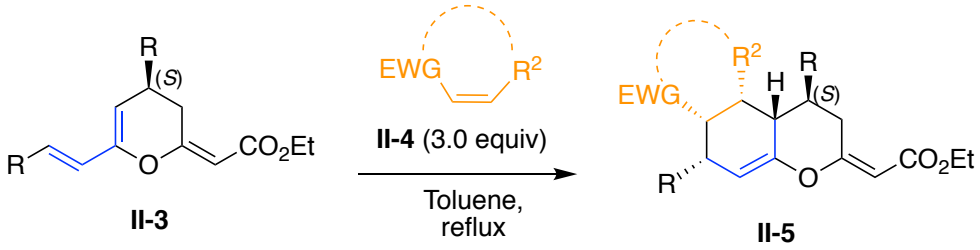

A solution of diene (0.05 mmol) and dienophile (0.15 mmol) in anhydrous toluene (0.5 mL) was refluxed in an oil bath. The reaction was monitored by TLC, which was completed in as early 2 h and up to 3 days. The solvent was removed under nitrogen flow and the residue was directly purified by silica gel column chromatography using ethyl acetate/hexane with different percentage as eluents, typically (1.5% to 20% gradient).

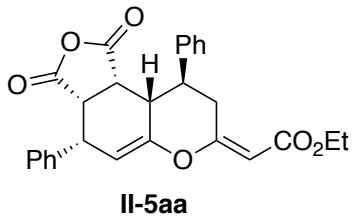

II-5aa

II-5aa: Ethyl (*E*)-2-((3a*S*,4*S*,9*S*,9a*S*,9b*R*)-1,3-dioxo-4,9-diphenyl-1,3,3a,4,8,9,9a,9b-octahydro-7*H*-furo[3,4-*f*]chromen-7-ylidene) acetate: Using **II-3a** (17.3 mg, 0.05 mmol) and **II-4a** (14.7 mg, 0.15 mmol), 18.7 mg (84% yield) of the pure product was isolated as a crystalline white solid, mp 184-188 °C. ^{1}H NMR (500 MHz, $CDCl_3$) δ 7.43-7.44 (4H, m), 7.40-7.42 (2H, m), 7.28-7.34 (2H, m), 7.22-7.23 (2H, m), 5.73 (1H, dd, *J* = 3.5 Hz, 3.0 Hz), 5.54 (1H, d, *J* = 2.0 Hz), 4.33 (1H, dd, *J* = 16.0 Hz, 3.0 Hz), 4.16 (2H,

ddd, *J* = 15.0 Hz, 7.0 Hz, 1.0 Hz), 3.95 (1H, dddd, *J* = 15.0 Hz, 13.5 Hz, 12.0 Hz, 3.0 Hz), 3.77-3.80 (1H, m), 3.46 (1H, t, *J* = 9.5 Hz), 3.33 (1H, dd, *J* = 9.0 Hz, 5.0 Hz), 2.89 (1H, dddd, *J* = 10.0 Hz, 7.0 Hz, 5.0 Hz, 3.0 Hz), 2.58 (1H, dddd, *J* = 16.0 Hz, 16.0 Hz, 13.5 Hz, 2.0 Hz), 1.26 (3H, t, *J* = 7.5 Hz) ppm; ^{13}C NMR (125 MHz, $CDCl_3$) δ 170.7, 168.7, 167.3, 166.9, 151.5, 140.2, 137.5, 133.0, 129.7, 129.2, 128.7, 128.5, 128.3, 128.0, 127.9, 127.5, 104.7, 98.0, 69.2, 64.0, 59.8, 47.8, 42.9, 42.8, 41.3, 35.1, 31.5, 14.3 ppm; IR (film) 3062, 2928, 2854, 1779 (s), 1701, 1629 (s), 1337, 1170, 1135 (s), 939, 703 cm^{-1}. HRMS (ESI) Calculated Mass for $C_{27}H_{25}O_6$: 445.1651 ($[M+H]^+$), Found 445.1653 ($[M+H]^+$). The enantiomeric excess was determined by HPLC analysis, using DAICEL CHIRALPAK AD-H column, R_t = 24.7 min (minor) and 31.3 min (major), **II-5aa** (96% *ee*). $[\alpha]^{20}_D$= +75 (*c* = 1.00, CH_2Cl_2). The relative stereochemistry is assigned based on NOESY experiments.

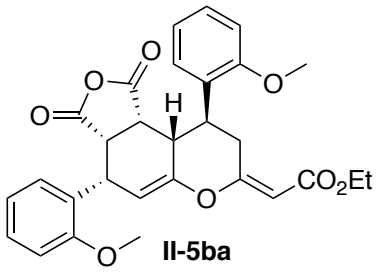

II-5ba

II-5ba: Ethyl (*E*)-2-((3a*S*,4*S*,9*S*,9a*S*,9b*R*)-4,9-bis(2-methoxyphenyl)-1,3-dioxo-1,3,3a,4,8,9,9a,9b-octahydro-7*H*-furo[3,4-*f*]chromen-7-ylidene) acetate: Using **II-3b** (20.3 mg, 0.05 mmol) and **II-4a** (14.7 mg, 0.15 mmol), 8.1 mg (32% yield) of the pure product was isolated as a crystalline colorless solid, mp 166 °C. ^{1}H NMR (500 MHz, $CDCl_3$) δ 7.35 (1H, dd, *J* = 7.5 Hz, 1.5 Hz), 7.28-7.33 (2H, m), 7.15 (1H, dd, *J* = 8.0 Hz, 1.5 Hz), 6.89-7.01 (4H, m), 5.56-5.65 (1H, m), 5.47 (1H, d, *J* = 1.5 Hz), 4.15-4.22 (2H,

m), 4.12 (2H, q, *J* = 7.0 Hz), 4.04-4.09 (1H, m), 3.79-3.91 (7H, m), 3.56 (1H, t, *J* = 9.0 Hz), 3.31 (1H, dd, *J* = 9.0 Hz, 5.0 Hz), 3.22-3.28 (1H, m), 1.26 (3H, t, *J* = 7.0 Hz) ppm; ^{13}C NMR (125 MHz, $CDCl_3$) δ 171.2, 169.5, 168.1, 167.6, 158.1, 156.9, 151.5, 129.7, 129.2, 129.0, 128.9, 128.1, 125.7, 121.1, 120.8, 111.3, 110.3, 104.2, 97.2, 61.0, 59.6, 55.7, 55.4, 55.2, 45.5, 44.1, 35.6, 29.7, 14.4 ppm; IR (film) 3068, 2927, 2851, 1855, 1780(s), 1703, 1628(s), 1494, 1463, 1245(s), 1135(s), 1027, 930, 755 cm^{-1}. HRMS (ESI) Calculated Mass for $C_{29}H_{29}O_8$: 505.1862 ($[M+H]^+$), Found 505.1865 ($[M+H]^+$). The enantiomeric excess was determined by HPLC analysis, using DAICEL CHIRALPAK AD-H column, R_t = 24.5 min (minor) and 71.2 min (major), **II-5ba** (96% *ee*): $[\alpha]^{20}_D$= +33 (*c* = 0.52, $CDCl_3$).

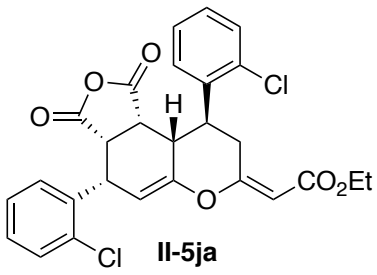

II-5ja

II-5ja: Ethyl (*E*)-2-((3a*S*,4*S*,9*S*,9a*S*,9b*R*)-4,9-bis(2-chlorophenyl)-1,3-dioxo-1,3,3a,4,8,9,9a,9b-octahydro-7*H*-furo[3,4-*f*]chromen-7-ylidene) acetate: Using **II-3j** (20.8 mg, 0.05 mmol) and **II-4a** (14.7 mg, 0.15 mmol), 14.9 mg (58% yield) of the pure product was isolated as a crystalline colorless solid, mp 173 °C. ^{1}H NMR (500 MHz, $CDCl_3$) δ 7.41-7.48 (3H, m), 7.27-7.36 (4H, m), 7.22-7.25 (1H, m), 5.65-5.68 (1H, m), 5.52-5.54 (1H, m), 4.43-4.53 (1H, br, m), 4.17-4.31 (3H, m), 4.14 (2H, q, *J* = 7.0 Hz), 3.68-3.78 (2H, m), 3.38-3.46 (1H, br, m), 1.27 (3H, t, *J* = 7.0 Hz) ppm; ^{13}C NMR (125 MHz,

$CDCl_3$) δ 168.6, 167.2, 151.9, 135.1, 133.6, 130.1, 129.6, 129.2, 129.1, 128.3, 127.6, 127.4, 103.8, 98.2, 59.9, 45.1, 43.6, 37.7, 31.6, 22.7, 14.3, 14.2 ppm; IR (film) 3067, 2973, 2932, 2888, 1851, 1781(s), 1702, 1630(s), 1476, 1377, 1339, 1257, 1165, 1141(s), 1038, 953, 756 cm^{-1}. HRMS (ESI) Calculated Mass for $C_{27}H_{23}O_6Cl_2$: 513.0872 ($[M+H]^+$), Found 513.0875 ($[M+H]^+$). The enantiomeric excess was determined by HPLC analysis, using DAICEL CHIRALPAK AD-H column, R_t = 14.3 min (minor) and 40.1 min (major), **II-5ja** (91% *ee*): $[\alpha]^{20}_D$= +62 (*c* = 1.11, $CDCl_3$).

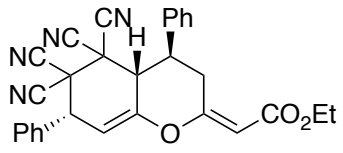

II-5ab

II-5ab: Ethyl 2-((4*S*,4a*S*,7*R*,*E*)-5,5,6,6-tetracyano-4,7-diphenyl-3,4,4a,5,6,7-hexahydro-2*H*-chromen-2-ylidene) acetate: Using **II-3a** (17.3 mg, 0.05 mmol) and **II-4b** (19.2 mg, 0.15 mmol), 23.3 mg (98% yield) of the pure product was isolated as an off white solid, decomposes above 160 °C. ^{1}H NMR (500 MHz, $CDCl_3$) δ 7.46-7.51 (5H, m), 7.37-7.42 (5H, m), 5.75 (1H, dd, *J* = 3.0 Hz, 2.0 Hz), 5.67 (1H, br, s), 4.45 (1H, t, *J* = 3.0 Hz), 4.05-4.09 (2H, m), 3.58-3.66 (3H, m), 3.54 (1H, ddd, *J* = 15.0 Hz, 7.0 Hz, 0.5 Hz), 1.18 (3H, t, *J* = 5.5 Hz) ppm; ^{13}C NMR (125 MHz, $CDCl_3$) δ 166.3, 164.4, 146.2, 137.7, 132.1, 130.5, 130.5, 129.6, 129.4, 129.0, 127.9, 111.0, 109.9, 109.3, 108.3, 105.6, 101.1, 60.1, 46.3, 44.9, 44.7, 41.5, 40.5, 32.7, 14.2 ppm; IR (film) 3066, 3035, 2984, 2936, 2906, 2255, 1730(s), 1706(s), 1643(s), 1456, 1331, 1249, 1201(s), 1175(s), 1148(s), 1127(s), 1044, 848, 762, 703 cm^{-1}. HRMS (ESI) Calculated Mass for $C_{29}H_{23}N_4O_3$: 475.1770

([M+H]$^+$), Found 475.1776 ([M+H]$^+$). The enantiomeric excess was determined by HPLC analysis, using DAICEL CHIRALPAK AD-H column (10% isopropanol in *n*-hexanes at 1.0 mL/min), R_t = 10.8 min (minor) and 16.4 min (major), **II-5ab** (96% *ee*): $[\alpha]^{20}_D$= +106 (*c* = 2.63, $CDCl_3$).

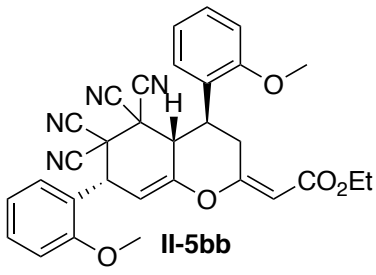

II-5bb

II-5bb: Ethyl 2-((4*S*,4a*S*,7*S*,*E*)-5,5,6,6-tetracyano-4,7-bis(2-methoxyphenyl)-3,4,4a,5,6,7-hexahydro-2*H*-chromen-2-ylidene) acetate: Using **II-3b** (20.3 mg, 0.05 mmol) and **II-4b** (19.2 mg, 0.15 mmol), 23.3 mg (87% yield) of the pure product was isolated as a crystalline pale yellow solid, m.p. 64-66 °C. ^{1}H NMR (500 MHz, $CDCl_3$) δ 7.36-7.46 (3H, m), 7.25 (1H, dd, *J* = 8.0 Hz, 2.0 Hz), 6.91-7.04 (4H, m), 5.55-5.60 (2H, m), 5.01-5.05 (1H, m), 4.34 (1H, dt, *J* = 11.0 Hz, 2.5 Hz), 4.13 (2H, q, *J* = 7.0 Hz), 3.97 (1H, dd, *J* = 17.5 Hz, 3.5 Hz), 3.94 (3H, s), 3.92 (3H, s), 3.58 (1H, ddd, *J* = 18.0 Hz, 12.5 Hz, 2.5 Hz), 3.42 (1H, td, *J* = 12.0 Hz, 4.0 Hz), 1.26 (3H, t, *J* = 7.0 Hz) ppm; ^{13}C NMR (125 MHz, $CDCl_3$) δ 167.0, 165.0, 158.9, 157.4, 145.9, 131.8, 131.8, 131.5, 131.0, 122.9, 121.5, 121.1, 120.4, 111.9, 111.6, 110.7, 110.2, 110.1, 108.4, 103.3, 99.3, 60.0, 55.3, 55.2, 44.2, 41.9, 39.8, 39.7, 38.9, 30.5, 14.3 ppm;. IR (film) 3072, 2975, 2927, 2845, 2255, 1707(s), 1705(s), 1603, 1589, 1493, 1465, 1341, 1288, 1249(s), 1182(s), 1127(s), 1027, 910, 772, 734 cm^{-1}. HRMS (ESI) Calculated Mass for $C_{31}H_{27}N_4O_5$: 535.1981 ([M+H]$^+$),

Found 535.1984 ([M+H]$^+$). The enantiomeric excess was determined by HPLC analysis, using DAICEL CHIRALPAK AD-H column (10% isopropanol in *n*-hexanes at 1.0 mL/min), R_t = 8.8 min (minor) and 12.6 min (major), **II-5bb** (88% *ee*): $[\alpha]^{20}_D$= +128 (*c* = 0.98, $CDCl_3$).

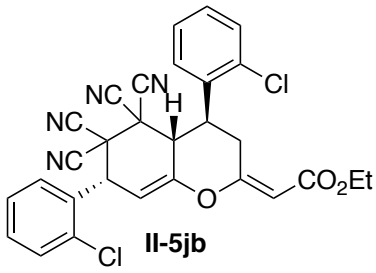

II-5jb

II-5jb: Ethyl 2-((4*S*,4a*S*,7*S*,*E*)-4,7-bis(2-chlorophenyl)-5,5,6,6-tetracyano-3,4,4a,5,6,7-hexahydro-2*H*-chromen-2-ylidene) acetate: Using **II-3a** (20.8 mg, 0.05 mmol) and **II-4a** (14.7 mg, 0.15 mmol), 23.4 mg (86% yield) of the pure product was isolated as a crystalline light brown solid, m.p. 68-70 °C. ^{1}H NMR (500 MHz, $CDCl_3$) δ 7.53-7.59 (2H, m), 7.46-7.51 (1H, m), 7.38-7.46 (2H, m), 7.34-7.38 (3H, m), 5.65-5.69 (1H, m), 5.63-5.65 (1H, s), 5.15-5.19 (1H, m), 4.07-4.14 (3H, m), 3.98-4.04 (1H, m), 3.82 (1H, dd, *J* = 17.0 Hz, 4.5 Hz), 3.52 (1H, dd, *J* = 17.0 Hz, 9.5 Hz), 1.22 (3H, t, *J* = 7.5 Hz) ppm; ^{13}C NMR (125 MHz, $CDCl_3$) δ 166.3, 163.4, 145.7, 135.7, 134.3, 132.0, 131.8, 131.2, 131.0, 130.5, 130.2, 127.9, 127.5, 110.9, 109.3, 109.0, 108.5, 105.0, 100.8, 60.2, 43.0, 31.1, 14.2 ppm. IR (film) 3069, 2983, 2929, 2873, 2257, 1706(s), 1644(s), 1477, 1379, 1336, 1278, 1203, 1180(s), 1151(s), 1129(s), 1041, 759, 734 cm^{-1}. HRMS (ESI) Calculated Mass for $C_{29}H_{21}N_4O_3Cl_2$: 543.0991 ([M+H]$^+$), Found 543.1000 ([M+H]$^+$). The enantiomeric excess was determined by HPLC analysis, using DAICEL CHIRALPAK AD-

H column (10% isopropanol in *n*-hexanes at 1.0 mL/min), R_t = 9.1 min (minor) and 16.9 min (major), **II-5jb** (86% *ee*): $[\alpha]^{20}_D$= +94 (*c* = 0.97, $CDCl_3$).

Specific procedure for synthesizing compound II-6ad:

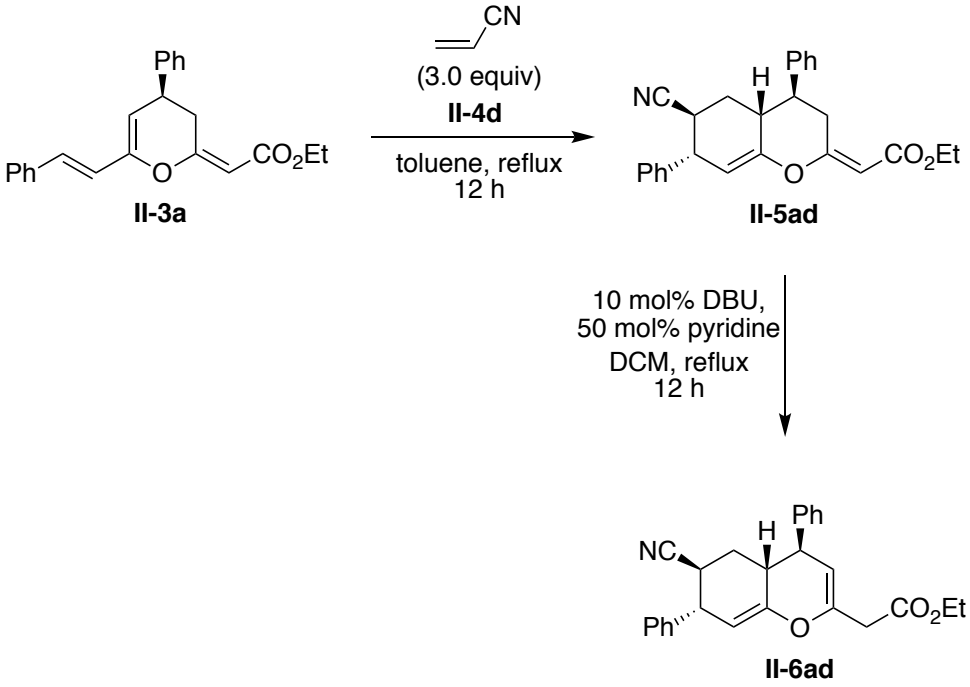

A solution of **II-3a** (0.05 mmol) and **II-4d** (0.15 mmol) in anhydrous toluene (0.5 mL) was refluxed in an oil bath. The reaction was monitored by TLC, which was completed in 24 h. The solvent was removed under nitrogen flow and the residue was directly purified by silica gel column chromatography using ethyl acetate/hexane (0-1:4) as eluents to provide **II-5ad** (8.2 mg, 41% yield) as yellow oil.

To a solution of **II-5ad** (43.3 mg, 0.1 mmol) in dichloromethane (1 mL), DBU (1.5 mg, 1.5 µL) and pyridine (4.0 mg, 4.0 µL) were added at room temperature. Then the reaction mixture was heated to reflux for 12 h. The mixture was cooled, concentrated and purified

by silica gel chromatography column using ethyl acetate/hexane (0-1:5) as eluents to give **II-6ad** (43.0 mg) in quantitative yield as a light-yellow oil.

II-6ad: Ethyl 2-((4*S*,4a*R*,6*S*,7*R*)-6-cyano-4,7-diphenyl-4a,5,6,7-tetrahydro-4*H*-chromen-2-yl) acetate: ^{1}H NMR (500 MHz, $CDCl_3$) δ 7.36-7.40 (2H, m), 7.27-7.34 (6H, m), 7.17-7.21 (2H, m), 5.36 (1H, dd, *J* = 5.0 Hz, 2.0 Hz), 4.87 (1H, d, *J* = 1.5 Hz), 4.23 (2H, q, *J* = 7.0 Hz), 3.92 (1H, br, s), 3.20-3.27 (3H, m), 2.79-2.83 (1H, m), 2.69-2.76 (1H, m), 1.74 (1H, ddd, *J* = 8.5 Hz, 2.0 Hz), 1.58 (1H, ddd, *J* = 14.5 Hz, 9.5 Hz, 3.5 Hz), 1.31 (3H, t, *J* = 7.5 Hz) ppm; ^{13}C NMR (125 MHz, $CDCl_3$) δ 169.6, 152.1, 146.0, 142.0, 141.2, 128.8, 128.3, 127.9, 127.6, 127.3, 121.1, 104.4, 102.9, 61.1, 44.0, 43.2, 39.4, 35.8, 32.2, 25.5, 14.2 ppm; IR (film) 3029, 2926, 2854, 2241, 1737 (s), 1691 (s), 1631, 1602, 1452, 1339, 1256 (s), 1169 (s), 1031 (s), 758, 702 cm^{-1}. HRMS (ESI) Calculated Mass for $C_{26}H_{26}NO_3$: 400.1913 ($[M+H]^+$), Found 400.1926 ($[M+H]^+$). The relative stereochemistry is assigned based on NOESY experiments.

<u>General procedure for Diels-Alder reaction using dienophiles II-4c:</u>

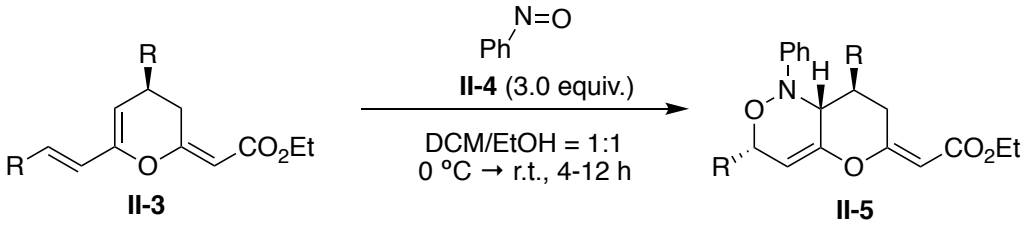

II-3 **II-5**

To a solution of nitrosobenzene (3.0 equiv) in EtOH/DCM (0.1 mL/0.1 mL), **II-3** (1.0 equiv) was added at 0 °C. The solution was gradually warmed up to room temperature. The reactions monitored by TLC required between 4 h to 12 h to complete. The reaction was quenched by H_2O (1 mL) and extracted by DCM (1 mL) twice. The combined organic

layers were dried with anhydrous Na_2SO_4 and concentrated under reduced pressure. The residue was purified by silica gel column chromatography using ethyl acetate-hexanes as eluents.

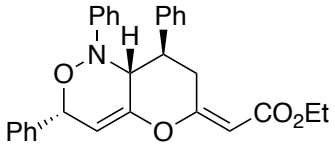

II-5ac

II-5ac: Ethyl (*E*)-2-((3*R*,8*R*,8a*R*)-1,3,8-triphenyl-3,7,8,8a-tetrahydro-1*H*,6*H*-pyrano[3,2-*c*][1,2]oxazin-6-ylidene) acetate: Using **II-3a** (20.0 mg, 0.058 mmol) and **II-4c** (18.6 mg, 0.174 mmol), 20.3 mg (77% yield) of the pure product was isolated as a yellow oil. ^{1}H NMR (500 MHz, $CDCl_3$) δ 7.40-7.50 (5H, m), 7.06-7.16 (7H, m), 6.85-6.89 (1H, m), 6.77-6.81 (2H, m), 5.71-5.74 (1H, m), 5.66-5.68 (1H, m), 5.47-5.50 (1H, m), 4.39 (1H, ddd, *J* = 8.0 Hz, 2.0 Hz, 2.0 Hz), 4.07-4.15 (2H, m), 3.98 (1H, dd, *J* = 16.0 Hz, 3.5 Hz), 3.53 (1H, ddd, *J* = 9.0 Hz, 9.0 Hz, 3.5 Hz), 3.13 (1H, ddd, *J* = 16.0 Hz, 8.5 Hz, 8.0 Hz), 1.21 (3H, t, *J* = 6.5 Hz) ppm; ^{13}C NMR (125 MHz, $CDCl_3$) δ 168.8, 167.0, 148.7, 146.8, 142.8, 138.2, 128.9, 128.7, 128.6, 128.4, 128.3, 127.2, 126.6, 122.8, 117.7, 108.0, 99.5, 75.3, 62.3, 59.7, 41.2, 31.8, 14.3 ppm; IR (film) 3062, 3031, 2979, 2925, 2854, 1708(s), 1641(s), 1493, 1454, 1304, 1153(s), 1132(s), 1040, 758, 697 cm^{-1}. HRMS (ESI) Calculated Mass for $C_{29}H_{28}NO_4$: 454.2018 ($[M+H]^+$), Found 454.2030 ($[M+H]^+$). The enantiomeric excess was determined by HPLC analysis, using DAICEL CHIRALPAK AD-H column (2% isopropanol in *n*-hexanes at 0.8 mL/min), R_t = 13.2 min (major) and 15.0 min (minor), **II-5ac** (96% *ee*): $[\alpha]^{20}_D$= -64 (*c* = 1.06, $CDCl_3$).

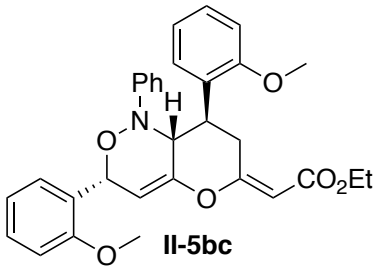

II-5bc

II-5bc: Ethyl (*E*)-2-((3*R*,8*R*,8a*R*)-3,8-bis(2-methoxyphenyl)-1-phenyl-3,7,8,8a-tetrahydro-1*H*,6*H*-pyrano[3,2-*c*][1,2]oxazin-6-ylidene) acetate: Using **II-3b** (23.6 mg, 0.058 mmol) and **II-4c** (18.6 mg, 0.174 mmol), 22.3 mg (75% yield) of the pure product was isolated as a light brown solid, amorphous. ^{1}H NMR (500 MHz, $CDCl_3$) δ 7.56 (1H, dd, *J* = 8.0 Hz, 2.0 Hz), 7.35 (1H, ddd, *J* = 7.5 Hz, 7.5 Hz, 1.5 Hz), 7.00-7.10 (5H, m), 7.92-7.95 (1H, m), 6.83-6.86 (2H, m), 6.76-6.81 (1H, m), 6.68-6.74 (2H, m), 5.95-5.98 (1H, m), 5.63-5.65 (1H, s), 5.56-5.58 (1H, m), 4.80 (1H, ddd, *J* = 9.0 Hz, 2.0 Hz, 2.0 Hz), 4.05-4.11 (2H, m), 3.86-3.90 (1H, m), 3.85 (3H, s), 3.74-3.80 (1H, m), 3.67 (3H, s), 3.14 (1H, ddd, *J* = 16.5 Hz, 9.0 Hz, 1.5 Hz), 1.21 (3H, t, *J* = 7.5 Hz) ppm. ^{13}C NMR (125 MHz, $CDCl_3$) δ 170.1, 167.3, 157.2, 157.1, 156.8, 148.9, 147.4, 130.1, 129.9, 129.7, 128.7, 128.4, 128.3, 127.9, 126.6, 121.6, 120.6, 120.4, 116.5, 110.6, 110.4, 107.4, 97.8, 69.2, 61.0, 59.5, 59.1, 55.4, 54.7, 31.3, 14.3 ppm; IR (film) 3058, 2988, 2930, 2906, 2839, 1735, 1707(s), 1637(s), 1599(s), 1494(s), 1463, 1248(s), 1153(s), 1120(s), 1030, 753, 693 cm^{-1}. HRMS (ESI) Calculated Mass for $C_{31}H_{32}NO_6$: 514.2230 ($[M+H]^+$), Found 514.2236 ($[M+H]^+$). The enantiomeric excess was determined by HPLC analysis, using DAICEL CHIRALPAK AD-H column (10% isopropanol in *n*-hexanes at 0.6 mL/min), R_t = 9.4 min (major) and 12.9 min (minor), **II-5bc** (84% *ee*): $[\alpha]^{20}_D$= -51 (*c* = 1.69, $CDCl_3$).

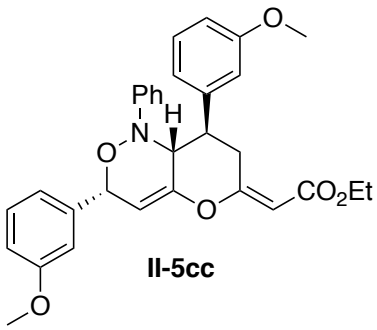

II-5cc

II-5cc: Ethyl (*E*)-2-((3*R*,8*R*,8a*R*)-3,8-bis(3-methoxyphenyl)-1-phenyl-3,7,8,8a-tetrahydro-1*H*,6*H*-pyrano[3,2-*c*][1,2]oxazin-6-ylidene) acetate: Using **II-3c** (23.6 mg, 0.058 mmol) and **II-4c** (18.6 mg, 0.174 mmol), 22.6 mg (76% yield) of the pure product was isolated as a yellow oil. ^{1}H NMR (500 MHz, $CDCl_3$) δ 7.35 (1H, t, *J* = 8.0 Hz), 7.00-7.11 (5H, m), 6.94 (1H, dd, *J* = 3.0 Hz, 1.0 Hz), 6.88 (1H, t, *J* = 7.5 Hz), 6.80-6.84 (2H, m), 6.64-6.69 (2H, m), 6.57-6.60 (1H, m), 6.70-6.72 (1H, m), 5.65-5.68 (1H, m), 5.44-5.46 (1H, m), 4.37 (1H, dt, *J* = 8.5 Hz, 2.0 Hz), 4.08-4.15 (2H, m), 4.00 (1H, dd, *J* = 16.0 Hz, 3.5 Hz), 3.85 (3H, s), 3.66 (3H, s), 3.51 (1H, ddd, *J* = 9.0 Hz, 9.0 Hz, 3.0 Hz), 3.06 (1H, ddd, *J* = 15.5 Hz, 8.5 Hz, 1.0 Hz),1.22 (3H, t, *J* = 7.5 Hz) ppm; ^{13}C NMR (125 MHz, $CDCl_3$) δ 168.9, 166.9, 159.7, 159.4, 148.5, 146.9, 144.5, 139.7, 129.7, 129.4, 128.7, 122.8, 120.5, 119.5, 114.0, 114.0, 112.6, 112.5, 108.0, 99.4, 75.3, 62.5, 59.7, 55.3, 55.0, 41.2, 31.6, 14.3 ppm; IR (film) 3060, 2927, 2836, 1707 (s), 1641 (s), 1600 (s), 1491 (s), 1464, 1263 (s), 1139 (s), 1130 (s), 1045 (s), 689 cm^{-1}. HRMS (ESI) Calculated Mass for $C_{31}H_{32}NO_6$: 514.2230 ($[M+H]^+$), Found 514.2236 ($[M+H]^+$).

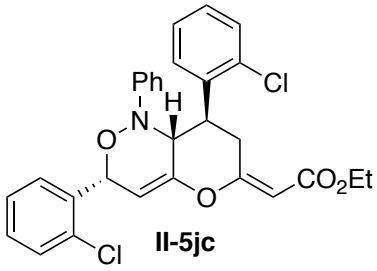

II-5jc

II-5jc: Ethyl (*E*)-2-((3*R*,8*R*,8a*R*)-3,8-bis(2-chlorophenyl)-1-phenyl-3,7,8,8a-tetrahydro-1*H*,6*H*-pyrano[3,2-*c*][1,2]oxazin-6-ylidene) acetate: Using **II-3j** (24.1 mg, 0.058 mmol) and **II-4c** (18.6 mg, 0.174 mmol), 24.2 mg (80% yield) of the pure product was isolated as a yellow oil. ^{1}H NMR (500 MHz, $CDCl_3$) δ 7.68 (1H, dd, *J* = 8.0 Hz, 2.0 Hz), 7.43 (1H, dd, *J* = 7.0 Hz, 1.5 Hz), 7.30-7.38 (2H, m), 7.22-7.25 (1H, m), 7.11-7.18 (2H, m), 7.03-7.08 (3H, m), 6.87 (1H, t, *J* = 7.5 Hz), 6.80-6.84 (2H, m), 5.91-5.93 (1H, m), 5.73-5.75 (1H, m), 5.60-5.62 (1H, m), 4.60-4.66 (1H, m), 4.00-4.12 (3H, m), 3.72 (1H, dd, *J* = 16.0 Hz, 4.0 Hz), 3.15 (1H, ddd, *J* = 16.5 Hz, 8.5 Hz, 1.5 Hz), 1.17 (3H, t, *J* = 7.0 Hz) ppm; ^{13}C NMR (125 MHz, $CDCl_3$) δ 167.9, 166.8, 160.1, 148.9, 146.4, 139.4, 136.0, 133.7, 129.8, 129.7, 129.6, 129.6, 128.6, 127.9, 127.0, 123.5, 118.7, 107.8, 99.6, 72.8, 59.7, 31.5, 29.7, 22.7, 14.2 ppm. IR (film) 3064, 2981, 2931, 2905, 2871, 1737, 1708(s), 1642(s), 1493, 1478, 1243, 1196(s), 1157(s), 1039, 754 cm^{-1}. HRMS (ESI) Calculated Mass for $C_{29}H_{26}NO_4Cl_2$: 522.1239 ($[M+H]^+$), Found 522.1252 ($[M+H]^+$). The enantiomeric excess was determined by HPLC analysis, using DAICEL CHIRALPAK AD-H column (2% isopropanol in *n*-hexanes at 0.8 mL/min), R_t = 14.8 min (minor) and 17.3 min (major), **II-5jc** (83% *ee*): $[\alpha]^{20}_D$= -25 (*c* = 0.32, $CDCl_3$).

II-4.7 Quantum chemical computational analysis:

General Considerations:

Full optimizations for all conformations of the model systems were performed in simulated toluene at the B3LYP/6-31G*/SM8 level using the Spartan-14 software running on Macintosh and Linux platform. To verify convergence and consistency of the optimizations, a number of examples were re-optimized from multiple starting points; energetic variations of 0.02 kcal/mol or less were found among these calculated structures. To confirm that each structure was a true minimum, vibrational analyses were performed. Since analytical second derivatives are not available in SM8 solvated wavefunctions, these analyses relied on finite difference calculations. Similar to total energy calculations, their consistency was checked in multiple runs, and showed negligible variation. For comparison, the relative enthalpies ($\Delta H°_{rel}$) calculated by including zero-point and thermal corrections to 298.15 K are given in kcal/mol. It is these latter values that appear in the manuscript. Importantly, differences between relative E and relative H° values are generally small enough that either set of data could be used to arrive at the conclusions. All Transition State (TS) structures were validated as first-order stationary points (i.e. a single imaginary frequency) by vibrational analysis. Single-point solvation energies in simulated toluene were calculated at the B3LYP/6-31G*/SM8 level of theory. All values are in kcal/mol, eV or hartrees.

A. Cartesian Coordinates for Transition State-1 (TS-1):

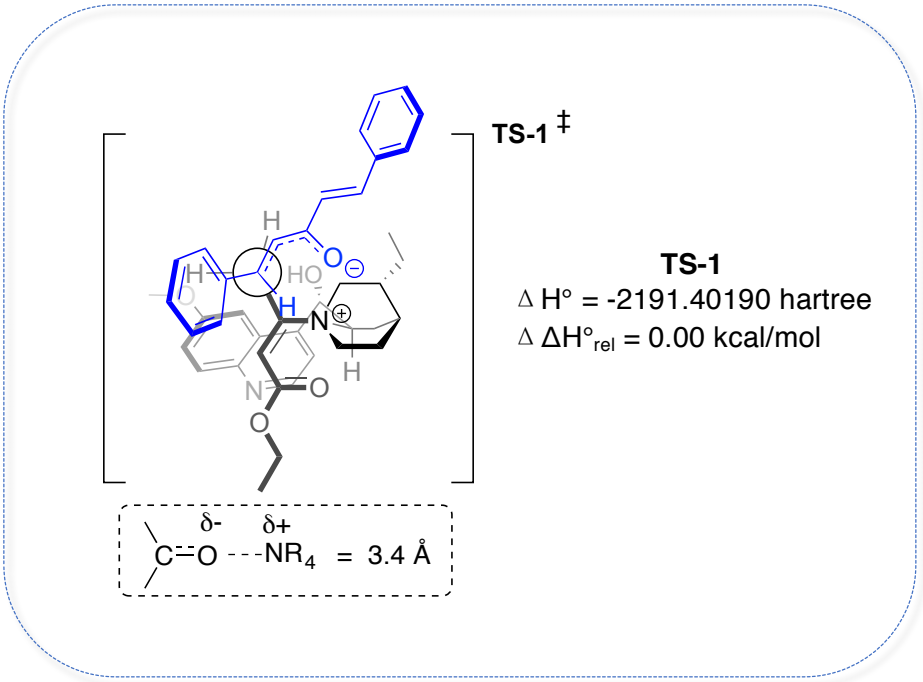

	Atom		X	Y	Z
1	C	C7	-0.0739432	-3.8932465	1.2778687
2	C	C1	-1.1534715	-3.6455902	0.2130982
3	H	H3	-0.8390065	-4.0483414	-0.7524698
4	H	H5	-2.0785155	-4.1586585	0.4986699
5	C	C2	-1.4525411	-2.1298323	0.0849976
6	H	H7	-2.3406172	-1.8619704	0.6563140
7	C	C3	-0.4913839	-3.1443495	2.5529348
8	H	H2	-1.5279600	-3.3807464	2.8187947
9	C	C4	-0.3462612	-1.6320497	2.3118344
10	H	H9	-1.1698308	-1.0806059	2.7490995
11	H	H10	0.6068365	-1.2467411	2.6787461
12	C	C5	1.2718369	-3.3010522	0.8121051
13	H	H13	1.9297445	-3.2412008	1.6904701
14	C	C6	1.0278899	-1.8598001	0.3045865
15	H	H14	0.9800600	-1.8287455	-0.7819368
16	N	N2	-0.3222020	-1.3312929	0.8024095
17	H	H18	0.1403438	-3.4307591	3.4010952
18	H	H19	0.0147179	-4.9659502	1.4763947
19	C	C8	2.0341569	-4.1026985	-0.2586010
20	H	H1	2.8990292	-3.4979320	-0.5615713
21	H	H4	1.4111659	-4.2158104	-1.1558113
22	C	C9	2.5271278	-5.4735796	0.2155143
23	H	H8	3.1274012	-5.9588252	-0.5620165
24	H	H11	1.6990054	-6.1502708	0.4572040
25	H	H12	3.1554624	-5.3816153	1.1097223

26	C	C10	-1.6823950	-1.6853987	-1.3715557
27	H	H16	-1.6458579	-0.5931087	-1.4214667
28	C	C11	-3.0764821	-2.1682363	-1.8710116
29	H	H17	-3.0023789	-2.2631101	-2.9611594
30	H	H21	-3.2666308	-3.1790631	-1.4949899
31	O	O1	-0.6529741	-2.2438686	-2.1974355
32	H	H20	-5.0472360	-2.5349139	-0.0036559
33	C	C13	-5.1452665	-1.6003347	-0.5490087
34	C	C14	-4.2327415	-1.2596737	-1.5229441
35	N	N1	-6.4258420	0.4259503	-0.8329588
36	C	C16	-4.4273252	-0.0125292	-2.2061199
37	C	C17	-6.2220412	-0.7318983	-0.2416610
38	C	C18	-5.5445278	0.7944258	-1.8095252
39	C	C19	-3.5872231	0.4547205	-3.2426193
40	H	H24	-6.9375388	-1.0187576	0.5282409
41	H	H25	-6.6062027	2.6282794	-2.1414601
42	C	C20	-3.8183021	1.6728145	-3.8602497
43	H	H27	-2.7409571	-0.1280633	-3.5892348
44	C	C21	-4.9172649	2.4748970	-3.4604555
45	C	C22	-5.7555390	2.0344302	-2.4605710
46	H	H29	-5.1066345	3.4297979	-3.9369273
47	O	O2	-2.9405075	2.0213025	-4.8441743
48	C	C15	0.5717084	0.8945919	0.0359336
49	C	C23	-0.5180681	0.1608913	0.5910907
50	C	C24	-1.6755436	0.8023580	1.0101232
51	H	H32	-1.6863673	1.8579896	0.7643023
52	C	C28	-2.8576976	0.3904042	1.7352280
53	H	H28	0.2711035	1.8407531	-0.4033492
54	O	O3	-3.6913952	1.4550977	1.8925201
55	C	C26	-4.8877046	1.2349616	2.6634395
56	H	H30	-5.3251984	0.2735583	2.3845641
57	H	H34	-4.6132683	1.1803814	3.7246486
58	C	C27	-5.8330111	2.3895437	2.3852061
59	H	H33	-6.1420473	2.3866052	1.3353997
60	O	O4	-3.1517620	-0.7249154	2.1858131
61	H	H36	-6.7293560	2.2930075	3.0085831
62	H	H15	1.8226276	-1.2003243	0.6615926
63	H	H35	-5.3569840	3.3490906	2.6125758
64	H	H37	-0.6659843	-1.7762532	-3.0466097
65	C	C12	-3.1218149	3.2592969	-5.5170217
66	H	H6	-3.0461315	4.1098510	-4.8274852
67	H	H22	-4.0870634	3.2992573	-6.0381629
68	H	H23	-2.3152167	3.3187963	-6.2497564
69	C	C25	3.9645687	0.7049255	0.6979760
70	O	O5	3.6581415	-0.4880667	0.9873651
71	C	C29	5.3172707	1.0144425	0.1662698
72	C	C30	6.2377050	0.0507800	-0.0303995
73	H	H26	5.5310957	2.0583566	-0.0576557
74	H	H38	5.9228431	-0.9625234	0.2167759
75	C	C31	3.0795622	1.8047042	0.8539981
76	C	C32	1.7964817	1.6181395	1.4349137
77	H	H39	3.3806004	2.7848881	0.4956708
78	C	C33	7.6030002	0.1979545	-0.5371628
79	C	C34	10.2502614	0.3657448	-1.5159795
80	C	C35	8.1958512	1.4445404	-0.8220811

81	C	C36	8.3775141	-0.9577426	-0.7535877
82	C	C37	9.6821450	-0.8780513	-1.2370466
83	C	C38	9.4984033	1.5259311	-1.3038112
84	H	H41	7.6311988	2.3576468	-0.6570322
85	H	H42	7.9399429	-1.9296863	-0.5367550
86	H	H43	10.2557266	-1.7881956	-1.3944128
87	H	H44	9.9333749	2.5002036	-1.5131383
88	H	H45	11.2680509	0.4334250	-1.8911376
89	C	C39	1.0395008	2.7851525	1.9686733
90	C	C40	-0.3963129	4.9745918	3.0263536
91	C	C41	0.3782439	2.6906600	3.2028502
92	C	C42	0.9569021	4.0026119	1.2699084
93	C	C43	0.2500175	5.0834255	1.7912098
94	C	C44	-0.3280973	3.7732784	3.7303025
95	H	H46	0.4335837	1.7609152	3.7637021
96	H	H47	1.4502102	4.0995276	0.3058988
97	H	H48	0.2019154	6.0150284	1.2326829
98	H	H49	-0.8262277	3.6742379	4.6914814
99	H	H50	-0.9480487	5.8183612	3.4322070
100	H	H31	1.2987233	0.3658025	-0.5631743
101	H	H40	1.7578489	0.7480506	2.0879904

B. Cartesian Coordinates for Transition State-2 (TS-2):

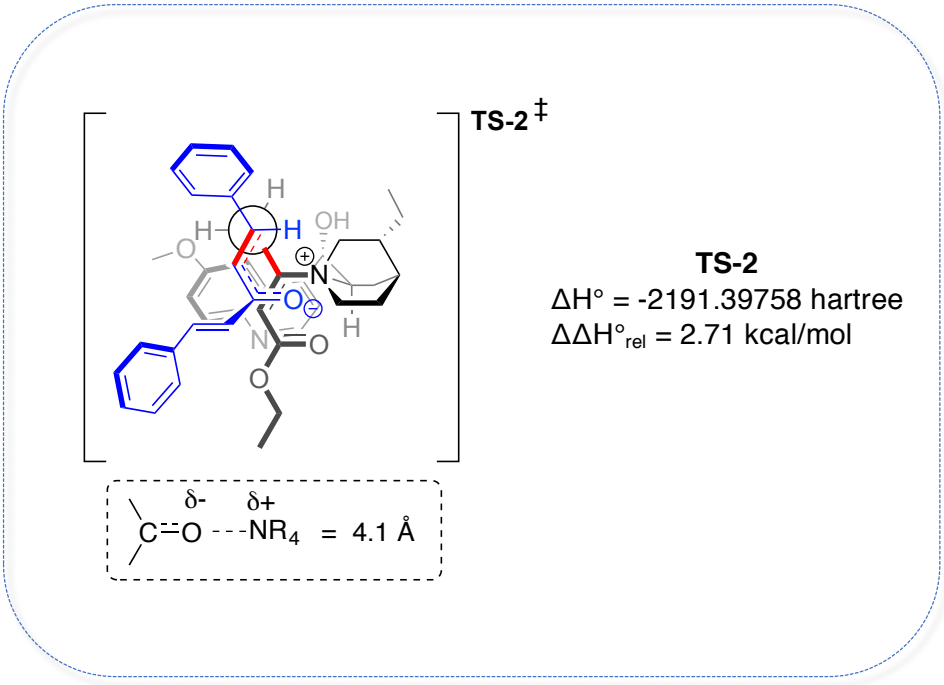

	Atom		X	Y	Z
1	C	C7	0.4057419	-4.0002737	1.2168415
2	C	C1	-0.4092211	-3.9157327	-0.0826647
3	H	H3	0.0515952	-4.5170973	-0.8706842
4	H	H5	-1.4158237	-4.3151287	0.0860535

5	C	C2	-0.5372507	-2.4438512	-0.5445837
6	H	H7	-1.4721537	-2.0014531	-0.1960490
7	C	C3	-0.1699925	-2.9724546	2.1996894
8	H	H2	-1.2541245	-3.1048220	2.2966900
9	C	C4	0.1592526	-1.5547908	1.7015179
10	H	H9	-0.6959877	-0.9015331	1.8061093
11	H	H10	1.0315718	-1.1061230	2.1821079
12	C	C5	1.8739729	-3.6122144	0.9492475
13	H	H13	2.3430766	-3.4247720	1.9246338
14	C	C6	1.8907891	-2.2855568	0.1478401
15	H	H14	2.1048476	-2.4746234	-0.9008302
16	N	N2	0.5317337	-1.5894253	0.1996414
17	H	H18	0.2638140	-3.1029793	3.1975119
18	H	H19	0.3411708	-5.0112251	1.6318426
19	C	C8	2.7249756	-4.6740190	0.2276745
20	H	H1	3.6930440	-4.2184597	-0.0237637
21	H	H4	2.2591442	-4.9330046	-0.7322111
22	C	C9	2.9769640	-5.9419563	1.0504081
23	H	H8	3.6354003	-6.6310171	0.5101979
24	H	H11	2.0489270	-6.4818750	1.2705627
25	H	H12	3.4577597	-5.7038269	2.0071059
26	C	C10	-0.4988560	-2.2853299	-2.0698433
27	H	H16	-0.4142652	-1.2207677	-2.3072862
28	C	C11	-1.7947306	-2.8384557	-2.7248389
29	H	H17	-1.6049390	-2.8915776	-3.8050088
30	H	H21	-1.9510464	-3.8701755	-2.3925129
31	O	O1	0.6414586	-2.9886460	-2.5775235
32	H	H20	-3.8898478	-3.3992585	-1.0672630
33	C	C13	-3.9945944	-2.4416800	-1.5712722
34	C	C14	-3.0332266	-2.0131824	-2.4598875
35	N	N1	-5.3422734	-0.4599308	-1.8421756
36	C	C16	-3.2445705	-0.7492467	-3.1047122
37	C	C17	-5.1228405	-1.6329592	-1.2889631
38	C	C18	-4.4240947	-0.0137689	-2.7500905
39	C	C19	-2.3656266	-0.2000180	-4.0662117
40	H	H24	-5.8643728	-1.9797531	-0.5702778
41	H	H25	-5.5586535	1.7749235	-3.0854802
42	C	C20	-2.6224421	1.0271878	-4.6544628
43	H	H27	-1.4689405	-0.7246701	-4.3761501
44	C	C21	-3.7851287	1.7571274	-4.2991590
45	C	C22	-4.6587098	1.2384926	-3.3692358
46	H	H29	-3.9947123	2.7172055	-4.7564436
47	O	O2	-1.7056253	1.4558787	-5.5691567
48	C	C15	1.7126881	0.1779852	-1.1784993
49	C	C23	0.5892952	-0.1931058	-0.3890807
50	C	C24	-0.3870112	0.7564787	-0.1293520
51	H	H32	-0.1561041	1.7281657	-0.5505215
52	C	C28	-1.7334844	0.6870803	0.4022335
53	H	H28	1.4790903	0.9388079	-1.9150594
54	O	O3	-2.3011636	1.9239671	0.3955396
55	C	C26	-3.6655609	1.9951254	0.8546222
56	H	H30	-4.2834140	1.3177237	0.2566735
57	H	H34	-3.7109788	1.6546784	1.8950279
58	C	C27	-4.1124543	3.4392887	0.7149271
59	H	H33	-4.0630861	3.7614884	-0.3303963

60	O	O4	-2.3654199	-0.3010736	0.7896736
61	H	H36	-5.1471168	3.5436870	1.0599268
62	H	H15	2.5977981	-1.5740991	0.5744628
63	H	H35	-3.4800869	4.1052712	1.3112186
64	H	H37	0.7790263	-2.7077330	-3.4950557
65	C	C12	-1.8999280	2.7164799	-6.1936903
66	H	H6	-1.9114156	3.5338460	-5.4610073
67	H	H22	-2.8290552	2.7402562	-6.7779944
68	H	H23	-1.0498346	2.8483703	-6.8652828
69	C	C25	2.2766133	1.3486482	2.1240631
70	O	O5	2.5891766	0.1300419	2.2773458
71	C	C29	1.6842660	2.1160935	3.2468140
72	C	C30	1.5212465	1.5746164	4.4696522
73	H	H26	1.3923342	3.1437432	3.0387644
74	H	H38	1.8568737	0.5444194	4.5831460
75	C	C31	2.4772726	2.0369434	0.8969223
76	C	C32	3.0798527	1.3472455	-0.1755851
77	H	H39	2.1657598	3.0729560	0.8055755
78	C	C33	0.9527486	2.2027307	5.6634607
79	C	C34	-0.1367489	3.3156271	8.0223909
80	C	C35	0.4538772	3.5207561	5.6831309
81	C	C36	0.8884751	1.4619769	6.8588378
82	C	C37	0.3520301	2.0084712	8.0231861
83	C	C38	-0.0816312	4.0677685	6.8445248
84	H	H41	0.4847381	4.1198018	4.7776802
85	H	H42	1.2681034	0.4426007	6.8648579
86	H	H43	0.3157959	1.4128066	8.9319484
87	H	H44	-0.4599346	5.0870793	6.8330563
88	H	H45	-0.5563601	3.7456304	8.9280320
89	C	C39	3.6888789	2.0646344	-1.3277908
90	C	C40	4.8862212	3.3504428	-3.5398676
91	C	C41	4.8291309	1.5306237	-1.9494701
92	C	C42	3.1570803	3.2583300	-1.8464957
93	C	C43	3.7488503	3.8935879	-2.9367535
94	C	C44	5.4251174	2.1646781	-3.0393604
95	H	H46	5.2578106	0.6092095	-1.5611011
96	H	H47	2.2699386	3.6927628	-1.3926224
97	H	H48	3.3202819	4.8174391	-3.3178522
98	H	H49	6.3121964	1.7325694	-3.4961514
99	H	H50	5.3464843	3.8472226	-4.3900222
100	H	H31	2.3735585	-0.5837343	-1.5706167
101	H	H40	3.6569891	0.4864086	0.1550001

C. Cartesian Coordinates for Transition State-3 (TS-3):

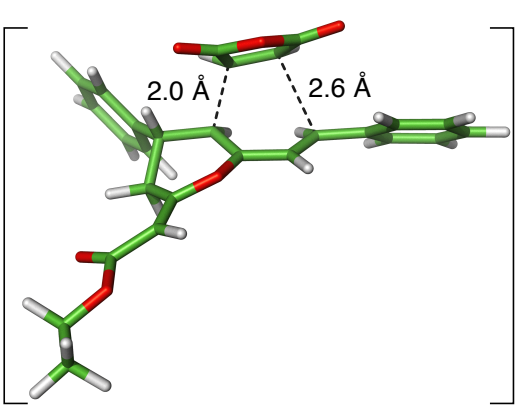

$TS\text{-}3^{\ddagger}_{(endo)}$

TS-3
$\Delta H° = -1494.13590$ hartree
$\Delta\Delta H°_{rel} = 0.00$ kcal/mol

	Atom		X	Y	Z
1	C	C1	0.8609413	-0.6213862	-1.4622941
2	C	C3	-0.1214979	0.3349001	0.6197591
3	C	C4	-0.3358583	-2.0058724	0.2473504
4	O	O1	-0.1401574	-0.9480645	1.1117391
5	C	C6	-0.2128968	-1.7117673	-1.2201091
6	C	C25	0.4810300	0.5996585	-0.6323544
7	H	H11	-1.1845350	-1.3679335	-1.6039467
8	H	H2	1.8068919	-1.0107097	-1.0676956
9	H	H12	0.0177369	-2.6379998	-1.7472858
10	C	C5	-0.6333198	-3.1790976	0.8388777
11	H	H4	-0.7033349	-3.2111872	1.9202898
12	C	C7	-0.9480849	-4.4147057	0.1104858
13	O	O2	-0.9152825	-4.5939012	-1.0968605
14	O	O3	-1.3339495	-5.3765223	0.9855187
15	C	C8	-1.7689675	-6.6235958	0.4018068
16	H	H6	-0.9282780	-7.0814931	-0.1307006
17	H	H7	-2.5509107	-6.4146552	-0.3359579
18	C	C9	-2.2736922	-7.5011268	1.5323946
19	H	H8	-1.4772285	-7.7062169	2.2550018
20	H	H9	-2.6325761	-8.4560909	1.1319269
21	H	H10	-3.1015162	-7.0160364	2.0605908
22	C	C10	1.0568327	-0.3118607	-2.9353945
23	C	C11	1.4422109	0.2188359	-5.6726712
24	C	C12	0.0329422	0.2579918	-3.7065100
25	C	C13	2.2764658	-0.6077009	-3.5581101
26	C	C14	2.4693060	-0.3456696	-4.9160718
27	C	C15	0.2225235	0.5212362	-5.0629469
28	H	H1	-0.9259333	0.4906058	-3.2476529
29	H	H13	3.0801222	-1.0464673	-2.9712006
30	H	H14	3.4227451	-0.5835682	-5.3801299
31	H	H15	-0.5836431	0.9600871	-5.6450251

32	H	H16	1.5890323	0.4221644	-6.7299712
33	C	C16	-0.5295210	1.3182271	1.5237564
34	H	H17	-0.7660406	0.9906283	2.5324941
35	C	C24	-0.5633517	2.6659889	1.2037551
36	C	C18	-0.9302586	3.7222625	2.1422133
37	C	C19	-1.8086151	5.7246784	3.9054352
38	C	C20	-0.6429962	3.6391487	3.5184458
39	C	C21	-1.6348059	4.8453016	1.6640764
40	C	C22	-2.0837037	5.8295505	2.5389700
41	C	C23	-1.0773974	4.6354271	4.3885374
42	H	H5	-0.0513109	2.8113265	3.8964504
43	H	H19	-1.8550035	4.9229848	0.6014666
44	H	H20	-2.6505143	6.6757202	2.1584094
45	H	H21	-0.8390705	4.5651591	5.4461535
46	H	H22	-2.1549526	6.4948428	4.5895281
47	H	H23	-0.6031739	2.9451972	0.1553829
48	H	H25	0.0566285	1.4331372	-1.1859028
49	O	O4	2.8464826	1.3140396	1.9569881
50	C	C2	2.3751606	2.6610736	1.8436844
51	C	C17	1.9216492	2.8418467	0.4776435
52	C	C26	2.1468622	1.6524358	-0.2396700
53	C	C27	2.8757383	0.7437521	0.7091525
54	H	H26	1.7077216	3.8229125	0.0777766
55	H	H27	2.4472006	1.6342442	-1.2833918
56	O	O5	3.3993931	-0.3207610	0.4919843
57	O	O6	2.4267609	3.3990249	2.7938080

D. Cartesian Coordinates for Transition State-4 (TS-4):

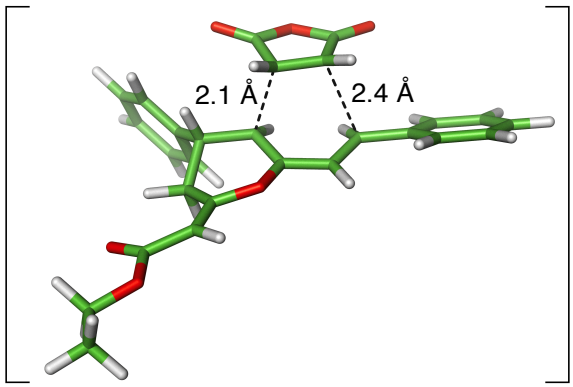

$TS\text{-}4^{\ddagger}_{(exo)}$

TS-4

$\Delta H° = -1494.13138$ hartree

$\Delta\Delta H°_{rel} = 2.84$ kcal/mol

Atom			X	Y	Z
1	C	C1	1.3529596	-0.8480866	-0.6481265
2	C	C3	-0.6149020	0.3851006	0.3294388
3	C	C4	-0.5092905	-1.9853883	0.6386729

4	O	O1	-0.9314114	-0.7445835	1.0530671
5	C	C6	0.3414423	-2.0239968	-0.5918822
6	C	C29	0.6031812	0.4617746	-0.3835385
7	H	H11	-0.3190341	-1.9610197	-1.4687688
8	H	H2	2.0875289	-1.0015283	0.1521533
9	H	H12	0.8441130	-2.9895164	-0.6492338
10	C	C5	-0.9580850	-3.0187990	1.3800552
11	H	H4	-1.6051881	-2.8051352	2.2234882
12	C	C7	-0.6895625	-4.4326152	1.0898376
13	O	O2	0.0188370	-4.8904528	0.2074056
14	O	O3	-1.3787017	-5.2158617	1.9576026
15	C	C8	-1.2603182	-6.6394878	1.7501498
16	H	H6	-0.2048214	-6.9229348	1.8152408
17	H	H7	-1.6020921	-6.8778677	0.7371436
18	C	C9	-2.1034559	-7.3251691	2.8092053
19	H	H8	-1.7488143	-7.0754865	3.8145043
20	H	H9	-2.0471515	-8.4119987	2.6830346
21	H	H10	-3.1528927	-7.0229818	2.7294786
22	C	C10	2.0964289	-0.8816115	-1.9777059
23	C	C11	3.4499487	-1.0696478	-4.4362634
24	C	C12	1.4201005	-0.6656794	-3.1866635
25	C	C13	3.4599346	-1.1928796	-2.0206757
26	C	C14	4.1328625	-1.2847779	-3.2389442
27	C	C15	2.0897353	-0.7577325	-4.4071045
28	H	H1	0.3577990	-0.4297768	-3.1806294
29	H	H13	4.0025436	-1.3416402	-1.0921101
30	H	H14	5.1940016	-1.5186214	-3.2499475
31	H	H15	1.5475959	-0.5895429	-5.3340107
32	H	H16	3.9739869	-1.1424784	-5.3854304
33	C	C16	-1.4374917	1.4752955	0.6035458
34	H	H17	-2.2236404	1.3121392	1.3358137
35	C	C28	-1.1833966	2.7591099	0.1325998
36	C	C18	-1.9308131	3.9446049	0.5564207
37	C	C19	-3.3747255	6.2405716	1.3000909
38	C	C20	-2.5862310	4.0111384	1.8022614
39	C	C21	-1.9917170	5.0638127	-0.2938387
40	C	C22	-2.7163738	6.1962092	0.0699950
41	C	C23	-3.3005718	5.1466543	2.1684880
42	H	H5	-2.5166270	3.1763164	2.4942848
43	H	H19	-1.4679021	5.0376955	-1.2448427
44	H	H20	-2.7621049	7.0464876	-0.6042265
45	H	H21	-3.7945950	5.1844204	3.1357829
46	H	H22	-3.9345556	7.1261664	1.5878684
47	O	O4	2.6401692	3.2994098	-0.5567025
48	C	C24	2.8436114	2.0271833	-0.0557758
49	C	C25	1.6938132	1.6886289	0.8471346
50	C	C26	1.0469011	2.9159888	1.0954363
51	C	C27	1.6178570	3.9249831	0.2053396
52	H	H24	1.8709370	0.9400227	1.6115766
53	H	H25	0.5137011	3.2043304	1.9878685
54	O	O5	1.3561103	5.0875225	0.0380212
55	O	O6	3.8092344	1.3687130	-0.3348211
56	H	H28	-0.6292714	2.8741055	-0.7932937
57	H	H30	0.6104043	1.1689129	-1.2084704

E. Cartesian Coordinates for Transition State-5 (TS-5):

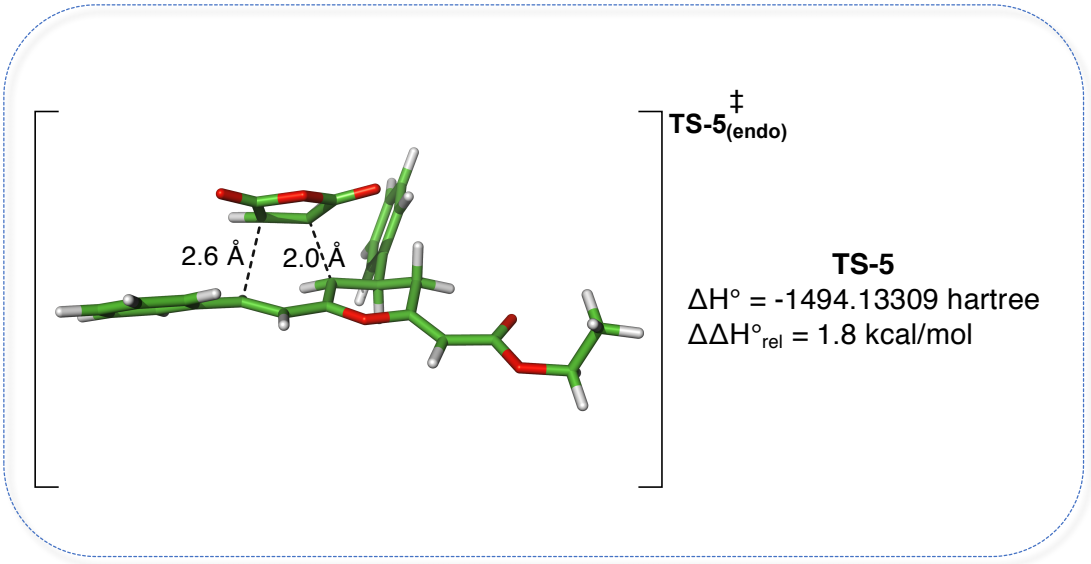

	Atom		X	Y	Z
1	C	C1	1.2099891	-0.3471042	-1.2800966
2	C	C3	0.2734533	0.4472441	0.9054393
3	C	C4	0.7973839	-1.8951960	0.6561338
4	O	O1	0.3694607	-0.8230627	1.4099870
5	C	C6	0.7550584	-1.7495885	-0.8344474
6	C	C25	0.4811677	0.7262971	-0.4665002
7	H	H11	-0.2819923	-1.9167358	-1.1448726
8	H	H2	2.2673951	-0.2408241	-0.9892722
9	H	H12	1.3667268	-2.5317808	-1.2835679
10	C	C7	1.5912905	-4.2576008	0.8089053
11	O	O2	1.7957316	-4.5165365	-0.3666533
12	O	O3	1.7729394	-5.1592587	1.8086631
13	C	C8	2.2069066	-6.4801433	1.4150166
14	H	H6	2.6820114	-6.8835522	2.3130711
15	H	H7	2.9525666	-6.3873576	0.6210412
16	C	C9	1.0358452	-7.3445767	0.9697317
17	H	H8	0.2689351	-7.3923471	1.7500195
18	H	H9	1.3828268	-8.3639438	0.7644093
19	H	H10	0.5878308	-6.9429787	0.0568042
20	C	C10	1.1668548	-0.1284825	-2.7885856
21	C	C11	1.1538459	0.3529657	-5.5649571
22	C	C12	2.1809780	0.6267717	-3.3946327
23	C	C13	0.1443219	-0.6436374	-3.5997932
24	C	C14	0.1402725	-0.4040312	-4.9754608
25	C	C15	2.1761479	0.8702510	-4.7683740
26	H	H1	2.9901157	1.0224863	-2.7835894
27	H	H13	-0.6638268	-1.2188678	-3.1593251
28	H	H14	-0.6603367	-0.8133706	-5.5859152
29	H	H15	2.9751546	1.4560282	-5.2156076
30	H	H16	1.1486091	0.5351967	-6.6361722
31	C	C16	-0.2082550	1.3871035	1.8226156

32	H	H17	-0.5406519	1.0037565	2.7829210
33	C	C24	-0.3691868	2.7274526	1.5073844
34	C	C18	-0.9826042	3.7284035	2.3719023
35	C	C19	-2.0919751	5.7220064	4.0142521
36	C	C20	-1.9059339	3.3948018	3.3817145
37	C	C21	-0.6474764	5.0845689	2.1892436
38	C	C22	-1.1898776	6.0712053	3.0057048
39	C	C23	-2.4490860	4.3837527	4.1959135
40	H	H5	-2.2183532	2.3638275	3.5108206
41	H	H19	0.0552628	5.3564683	1.4043900
42	H	H20	-0.9130820	7.1110553	2.8560713
43	H	H21	-3.1654391	4.1116971	4.9657839
44	H	H22	-2.5228204	6.4911146	4.6494097
45	H	H23	0.2078272	3.1322538	0.6826189
46	H	H25	0.8346269	1.7325675	-0.6736259
47	O	O4	-3.1060526	0.5688202	0.2196682
48	C	C2	-2.2679826	0.1088159	-0.7577732
49	C	C17	-1.3474266	1.2275106	-1.1658063
50	C	C26	-1.8725443	2.3774922	-0.5408898
51	C	C27	-2.9873292	1.9972776	0.3008425
52	H	H26	-0.9941825	1.2255563	-2.1916098
53	H	H27	-1.7021314	3.4084872	-0.8167359
54	O	O5	-3.7616493	2.6239252	0.9762221
55	O	O6	-2.3232885	-1.0258272	-1.1684288
56	C	C5	1.1397717	-2.9816431	1.3779094
57	H	H4	1.0621748	-2.9287144	2.4580821

APPENDIX

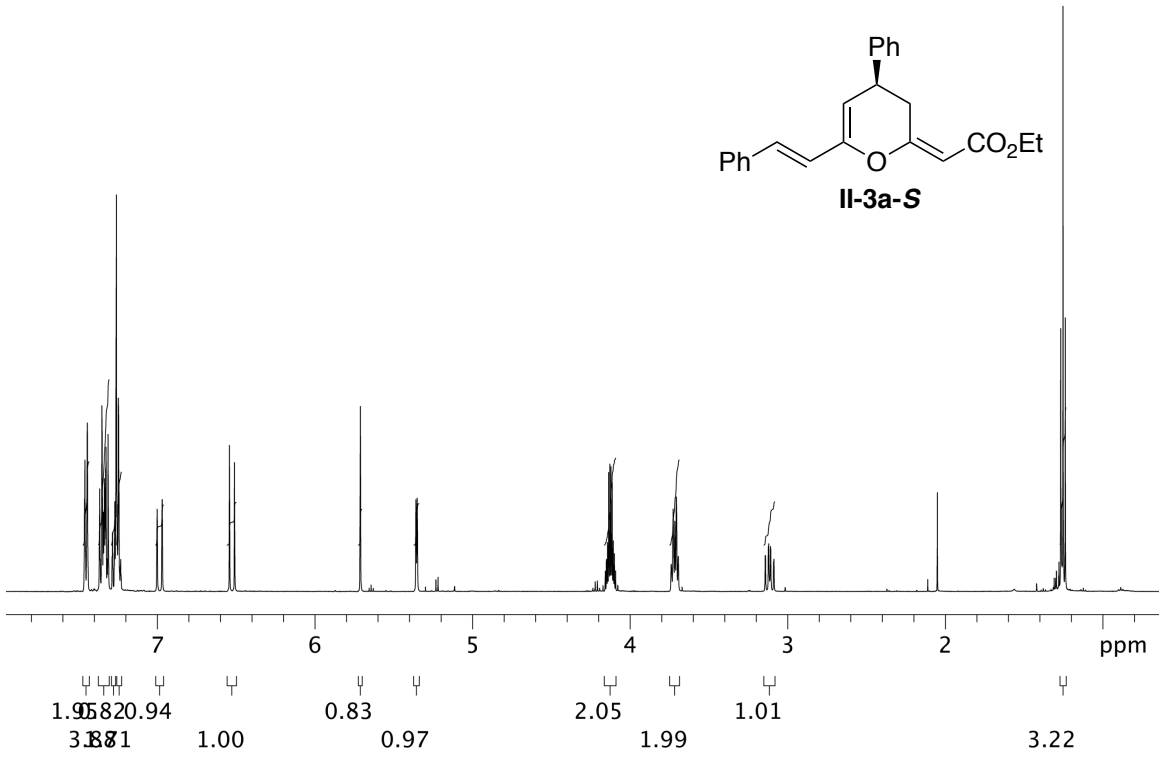
Ph
Ph
O
CO2Et
II-3a-S
7
6
5
4
3
2
ppm
1.00
0.83
0.97
2.05
1.99
1.01
3.22

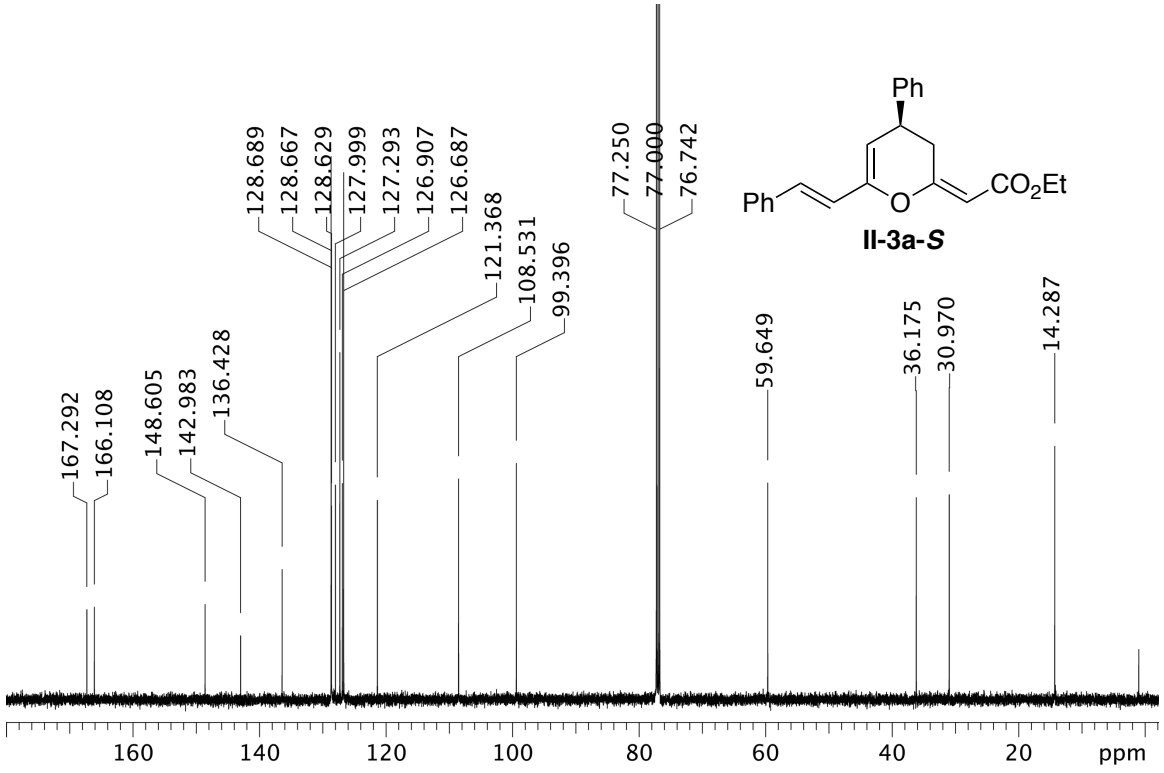
Ph
Ph
O
CO2Et
II-3a-S
128.689
128.667
128.629
127.999
127.293
126.907
126.687
121.368
108.531
99.396
77.250
77.000
76.742
167.292
166.108
148.605
142.983
136.428
59.649
36.175
30.970
14.287
160
140
120
100
80
60
40
20
ppm

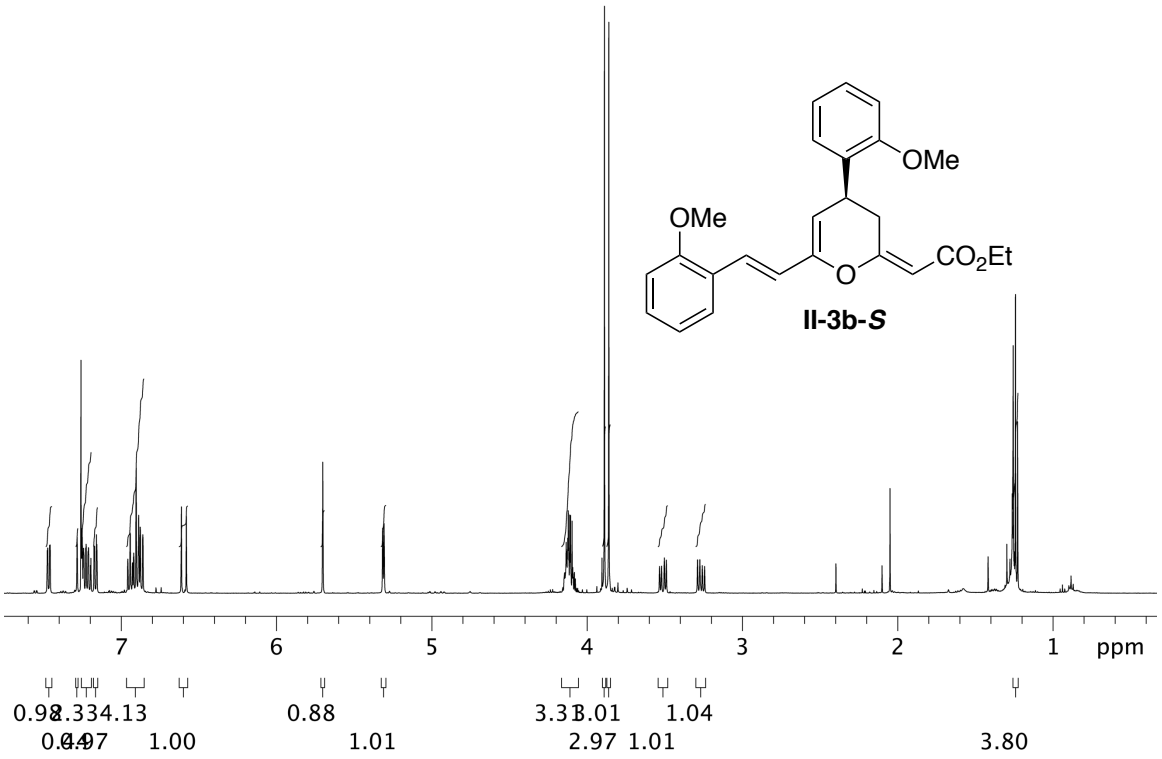
OMe
OMe
CO2Et
O
II-3b-S
7
6
5
4
3
2
1
ppm
0.98
2.33
4.13
0.88
3.31
3.01
1.04
0.44
0.97
1.00
1.01
2.97
1.01
3.80

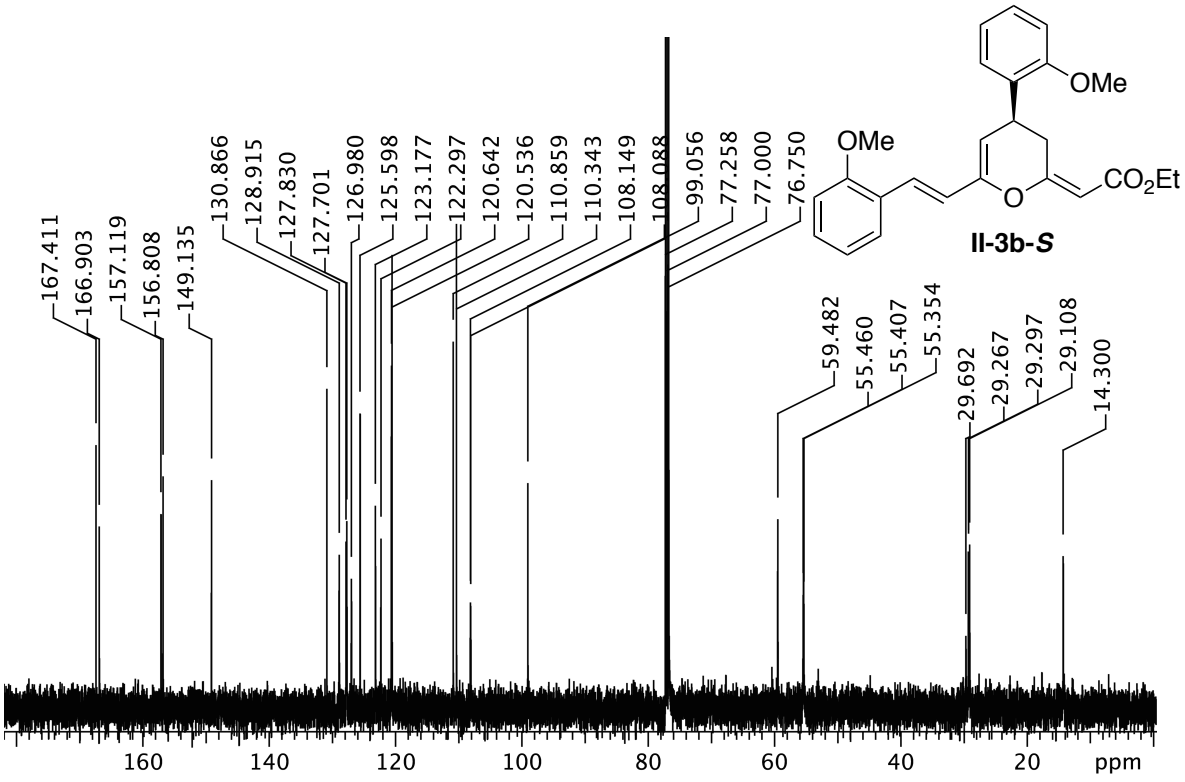
OMe
OMe
CO2Et
O
II-3b-S
167.411
166.903
157.119
156.808
149.135
130.866
128.915
127.830
127.701
126.980
125.598
123.177
122.297
120.642
120.536
110.859
110.343
108.149
108.088
99.056
77.258
77.000
76.750
59.482
55.460
55.407
55.354
29.692
29.267
29.297
29.108
14.300
160
140
120
100
80
60
40
20
ppm

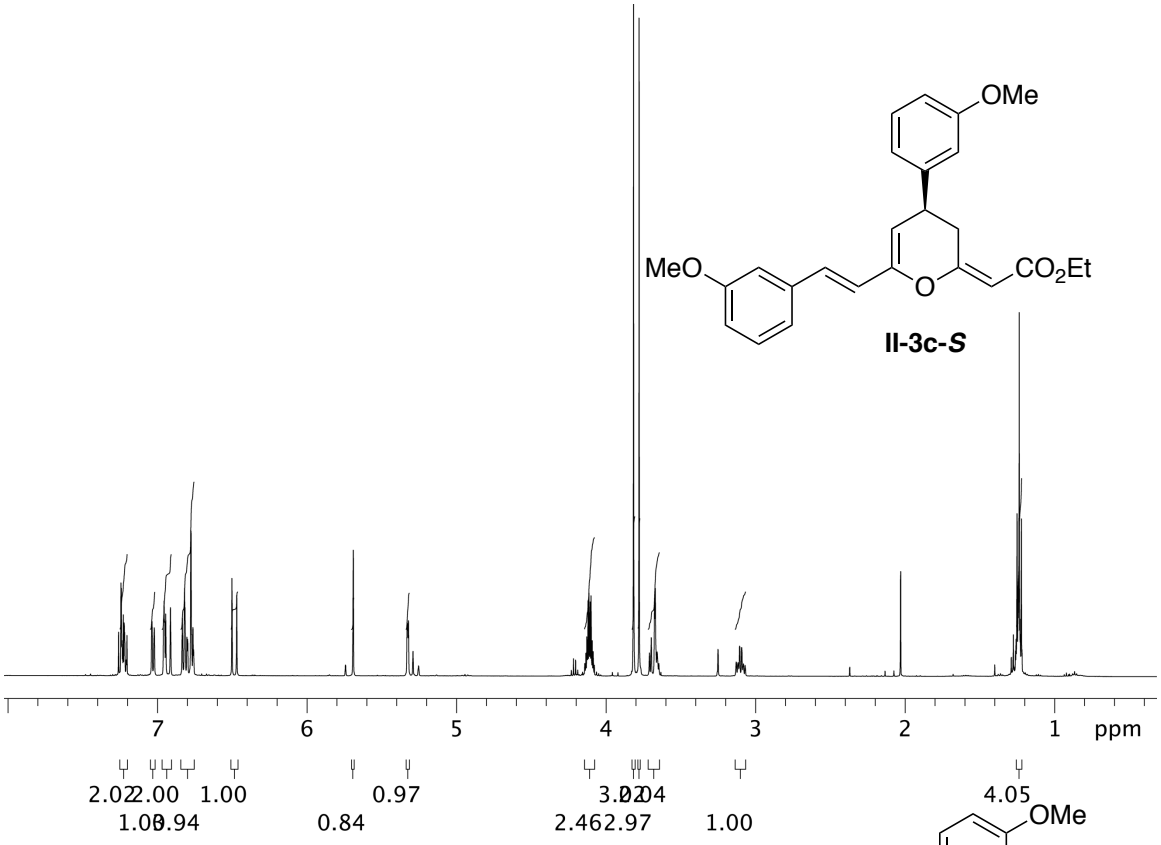
OMe
MeO
CO2Et
O
II-3c-S
7
6
5
4
3
2
1
ppm
2.02
2.00
1.00
0.97
1.08
0.94
0.84
2.46
2.97
1.00
4.05

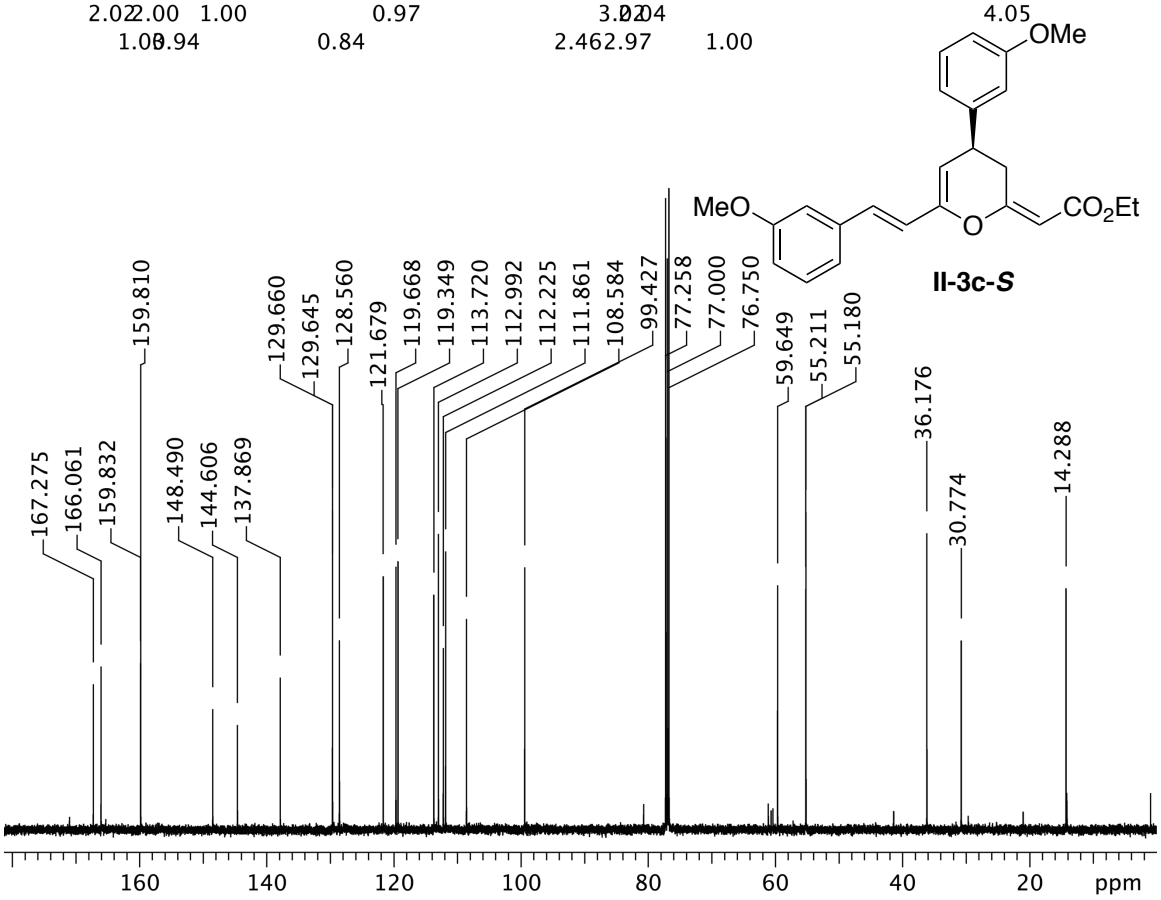
OMe
MeO
CO2Et
O
II-3c-S
167.275
166.061
159.832
159.810
148.490
144.606
137.869
129.660
129.645
128.560
121.679
119.668
119.349
113.720
112.992
112.225
111.861
108.584
99.427
77.258
77.000
76.750
59.649
55.211
55.180
36.176
30.774
14.288
160
140
120
100
80
60
40
20
ppm

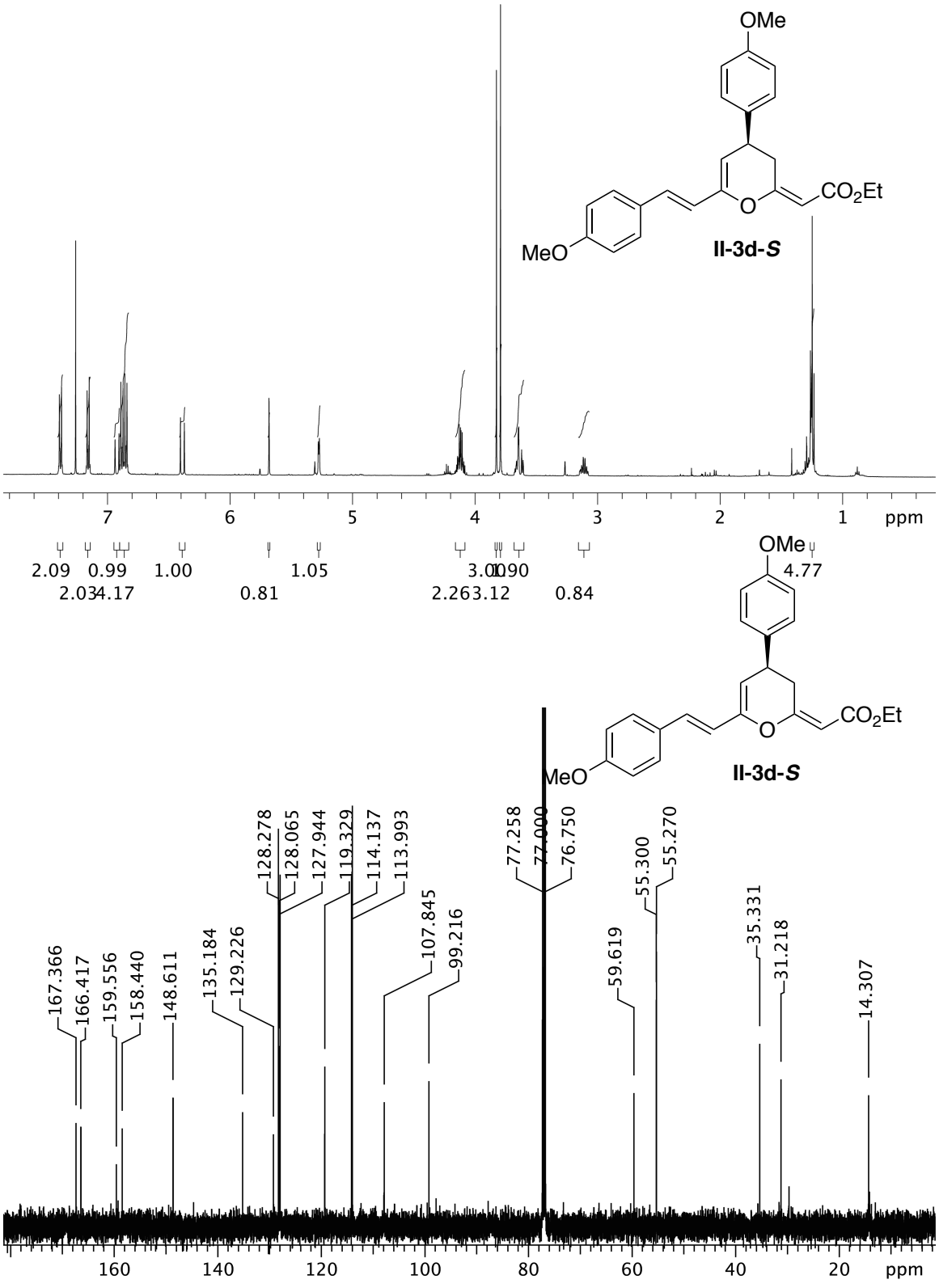
OMe
CO2Et
O
MeO
II-3d-S
7
6
5
4
3
2
1
ppm
2.09
0.99
1.00
1.05
3.01
0.90
2.03
4.17
0.81
2.26
3.12
0.84
4.77
167.366
166.417
159.556
158.440
148.611
135.184
129.226
128.278
128.065
127.944
119.329
114.137
113.993
107.845
99.216
77.258
77.000
76.750
59.619
55.300
55.270
35.331
31.218
14.307
160
140
120
100
80
60
40
20
ppm

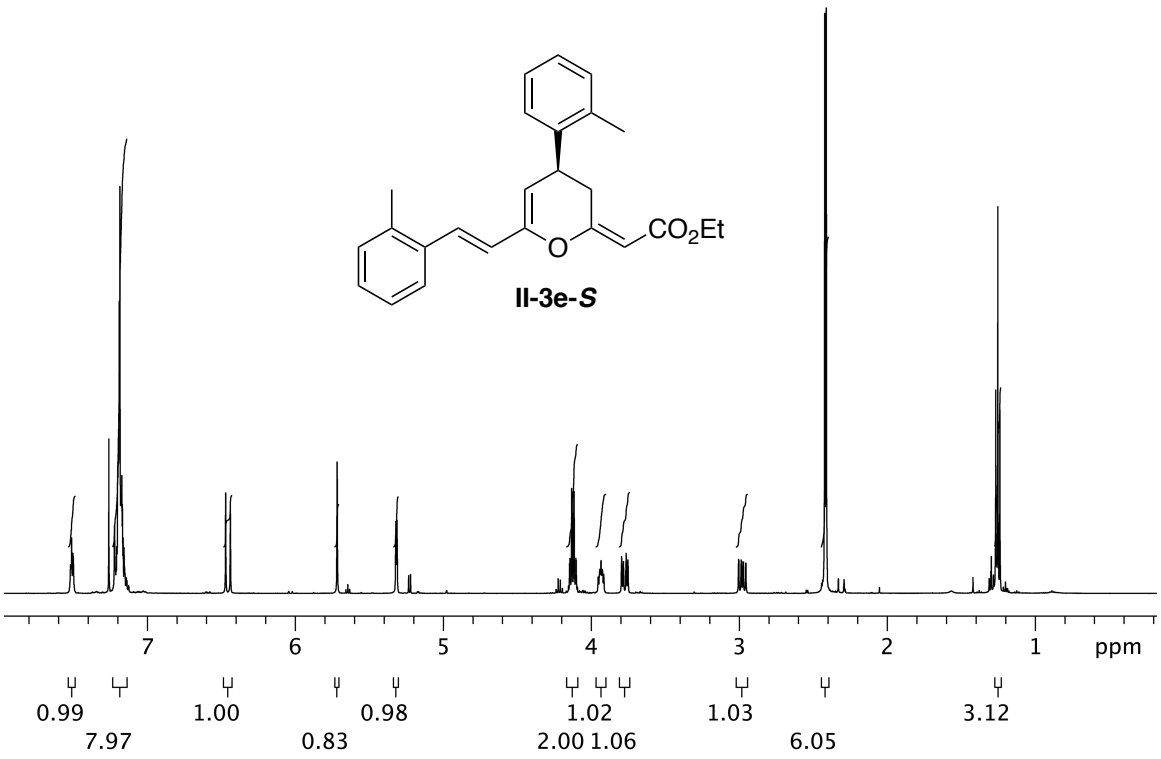
CO2Et
O
II-3e-S
7
6
5
4
3
2
1
ppm
0.99
1.00
0.98
1.02
1.03
3.12
7.97
0.83
2.00 1.06
6.05

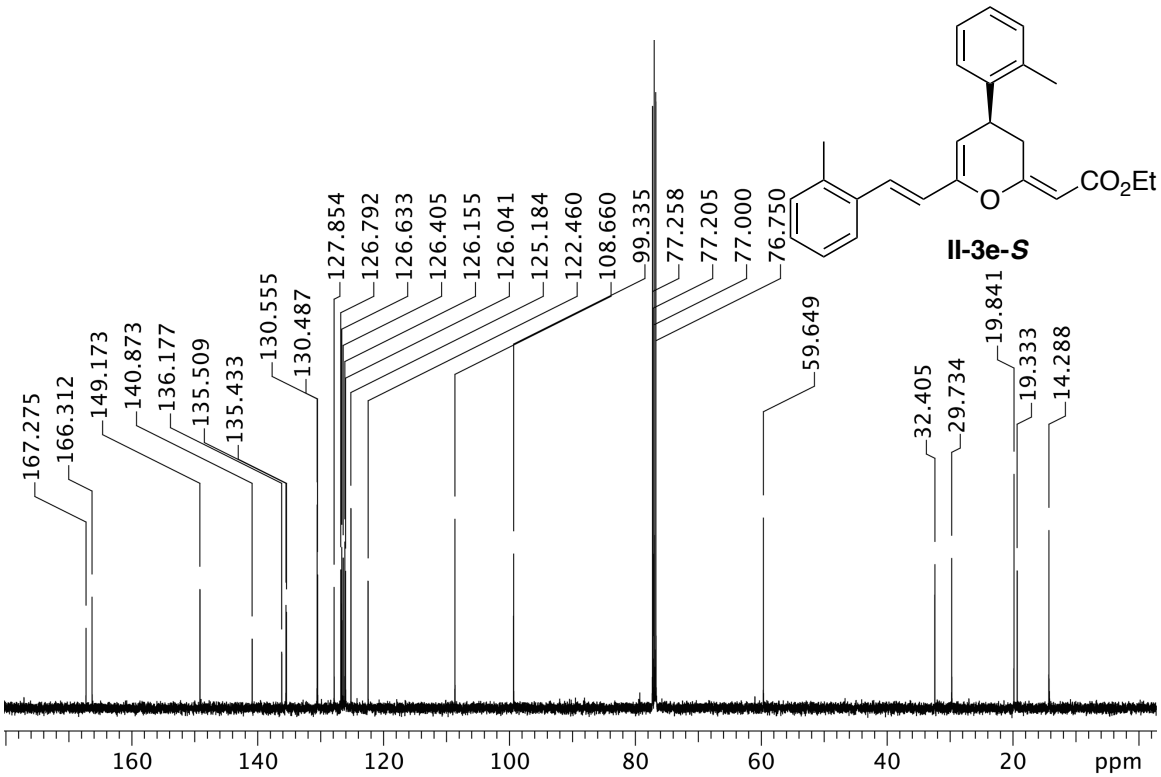
CO2Et
O
II-3e-S
167.275
166.312
149.173
140.873
136.177
135.509
135.433
130.555
130.487
127.854
126.792
126.633
126.405
126.155
126.041
125.184
122.460
108.660
99.335
77.258
77.205
77.000
76.750
59.649
32.405
29.734
19.841
19.333
14.288
160
140
120
100
80
60
40
20
ppm

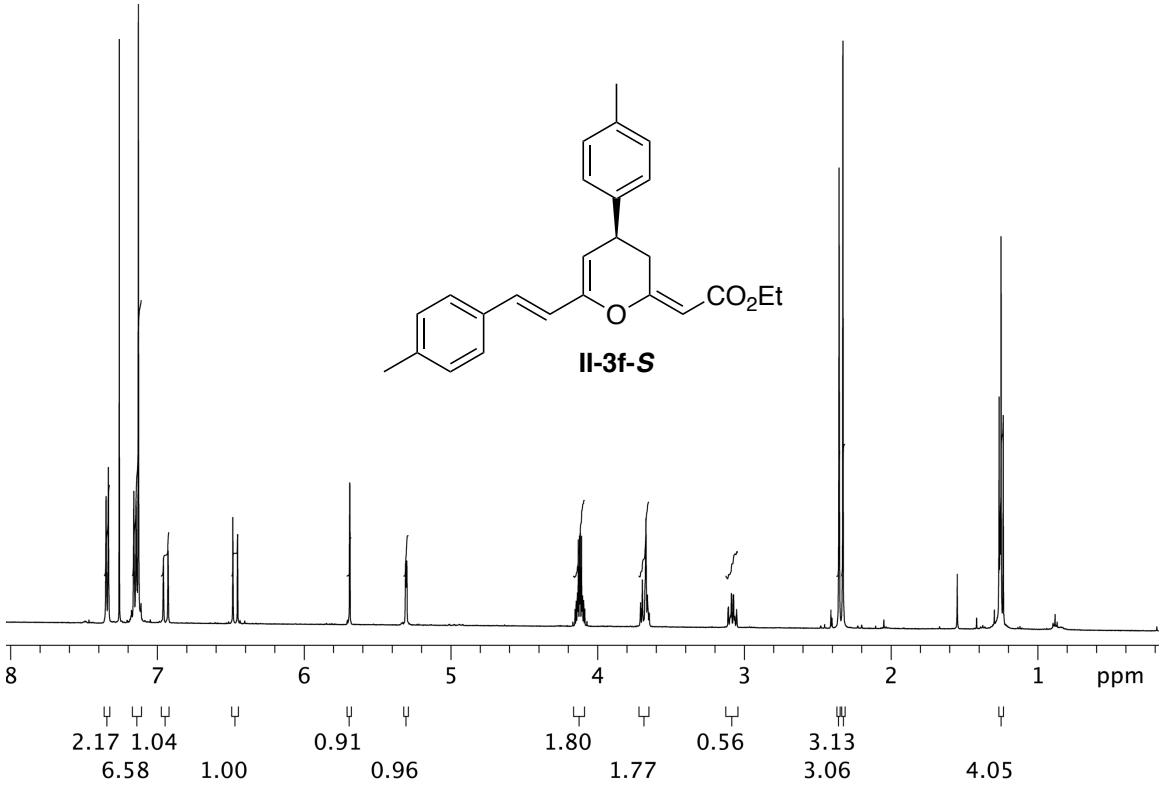
CO2Et
O
II-3f-S
8
7
6
5
4
3
2
1
ppm
2.17
1.04
1.00
0.91
0.96
1.80
1.77
0.56
3.13
3.06
4.05
6.58

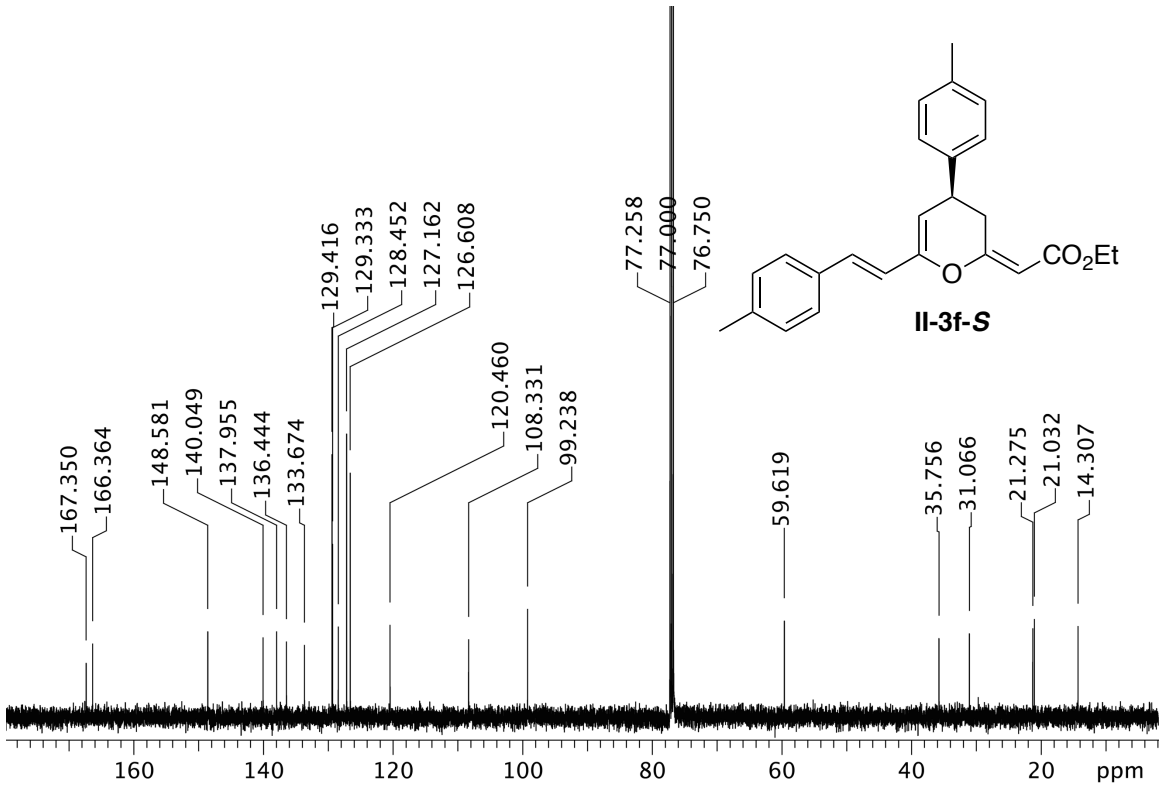
CO2Et
O
II-3f-S
167.350
166.364
148.581
140.049
137.955
136.444
133.674
129.416
129.333
128.452
127.162
126.608
120.460
108.331
99.238
77.258
77.000
76.750
59.619
35.756
31.066
21.275
21.032
14.307
160
140
120
100
80
60
40
20
ppm

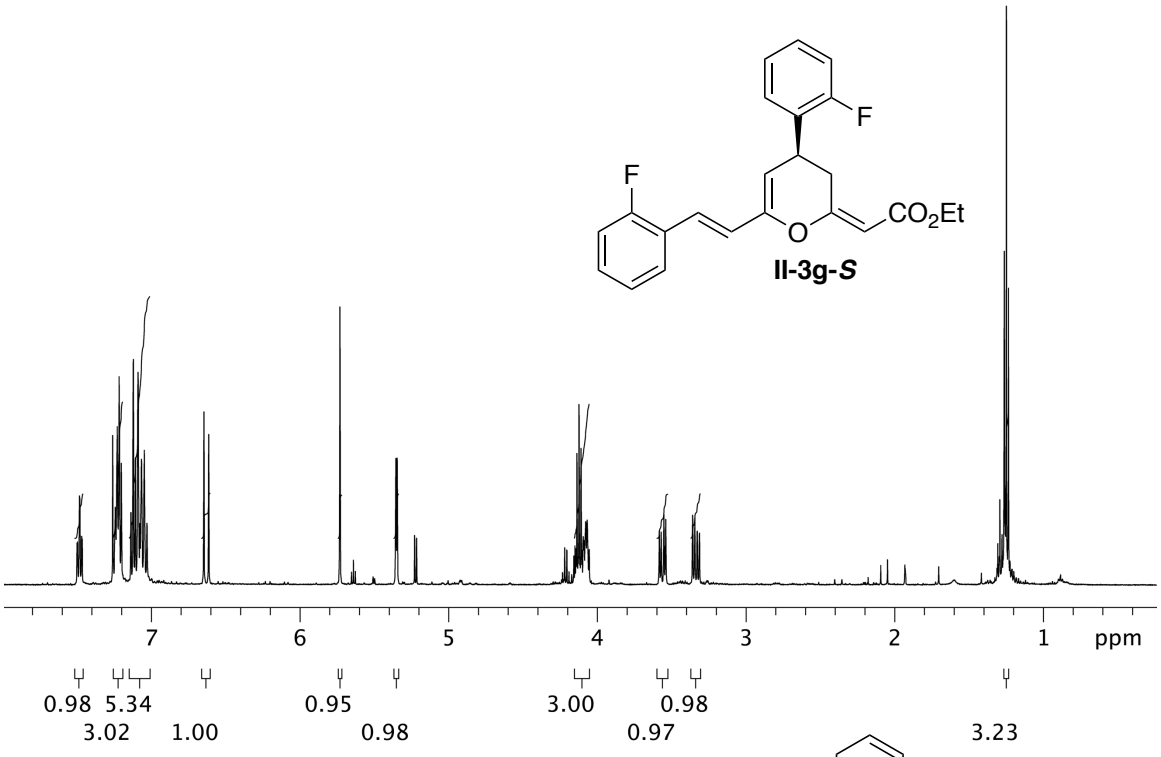
F
F
O
CO2Et
II-3g-S
7
6
5
4
3
2
1
ppm
0.98
5.34
3.02
1.00
0.95
0.98
3.00
0.97
0.98
3.23

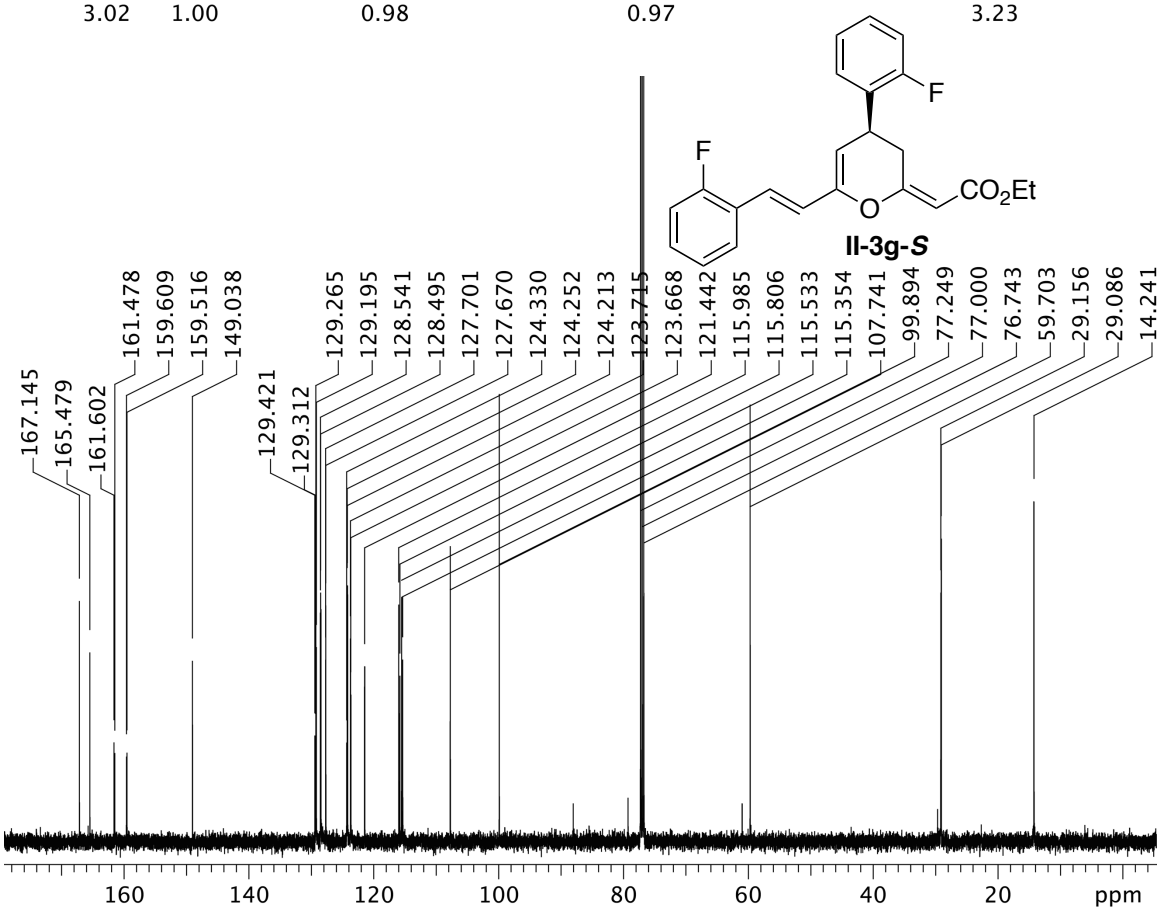
F
F
O
CO2Et
II-3g-S
167.145
165.479
161.602
161.478
159.609
159.516
149.038
129.421
129.312
129.265
129.195
128.541
128.495
127.701
127.670
124.330
124.252
124.213
123.715
123.668
121.442
115.985
115.806
115.533
115.354
107.741
99.894
77.249
77.000
76.743
59.703
29.156
29.086
14.241
160
140
120
100
80
60
40
20
ppm

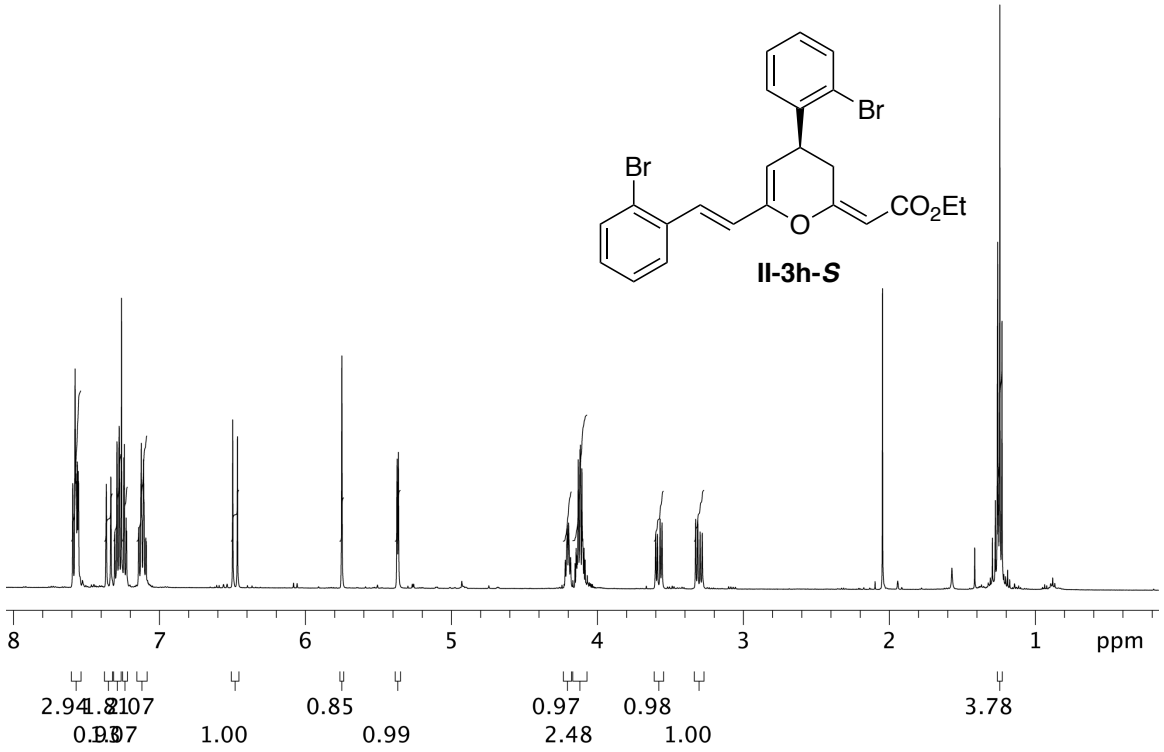
Br
Br
O
CO2Et
II-3h-S
8
7
6
5
4
3
2
1
ppm
2.94
1.82
2.07
0.85
0.97
0.98
3.78
0.97
1.00
0.99
2.48
1.00

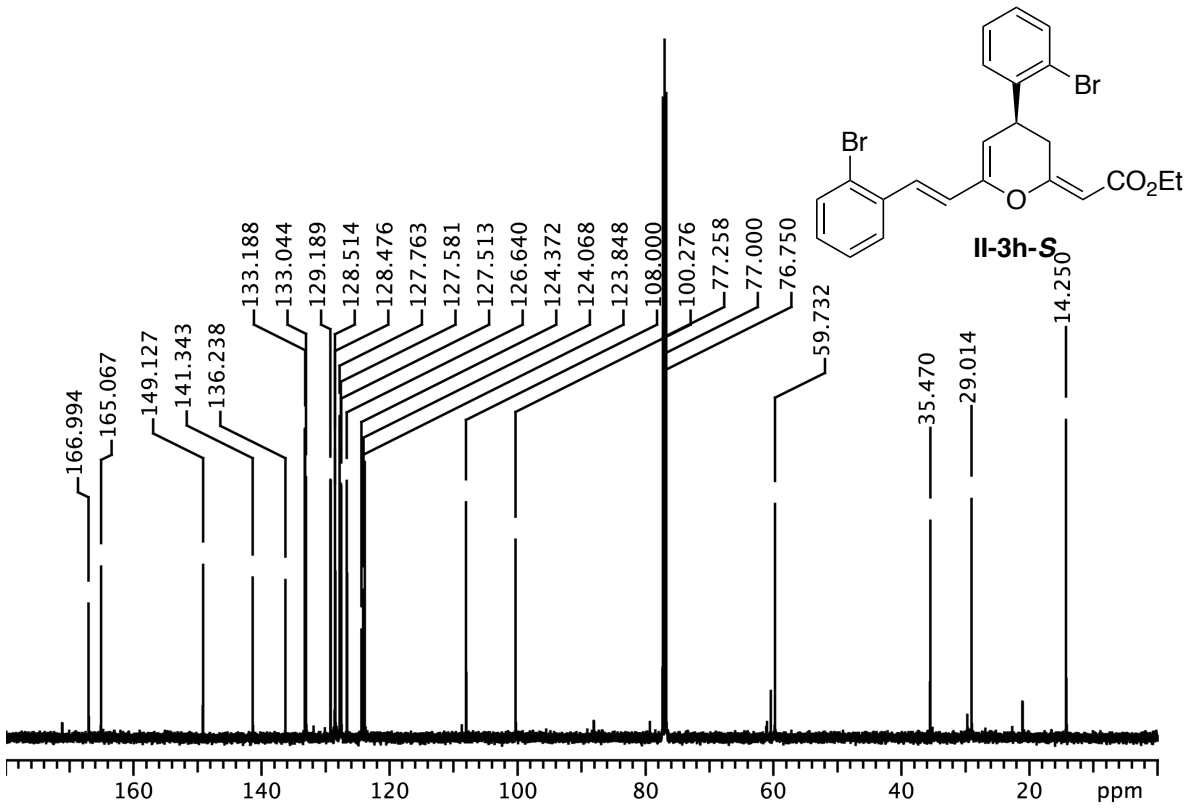
Br
Br
O
CO2Et
II-3h-S
166.994
165.067
149.127
141.343
136.238
133.188
133.044
129.189
128.514
128.476
127.763
127.581
127.513
126.640
124.372
124.068
123.848
108.000
100.276
77.258
77.000
76.750
59.732
35.470
29.014
14.250
160
140
120
100
80
60
40
20
ppm

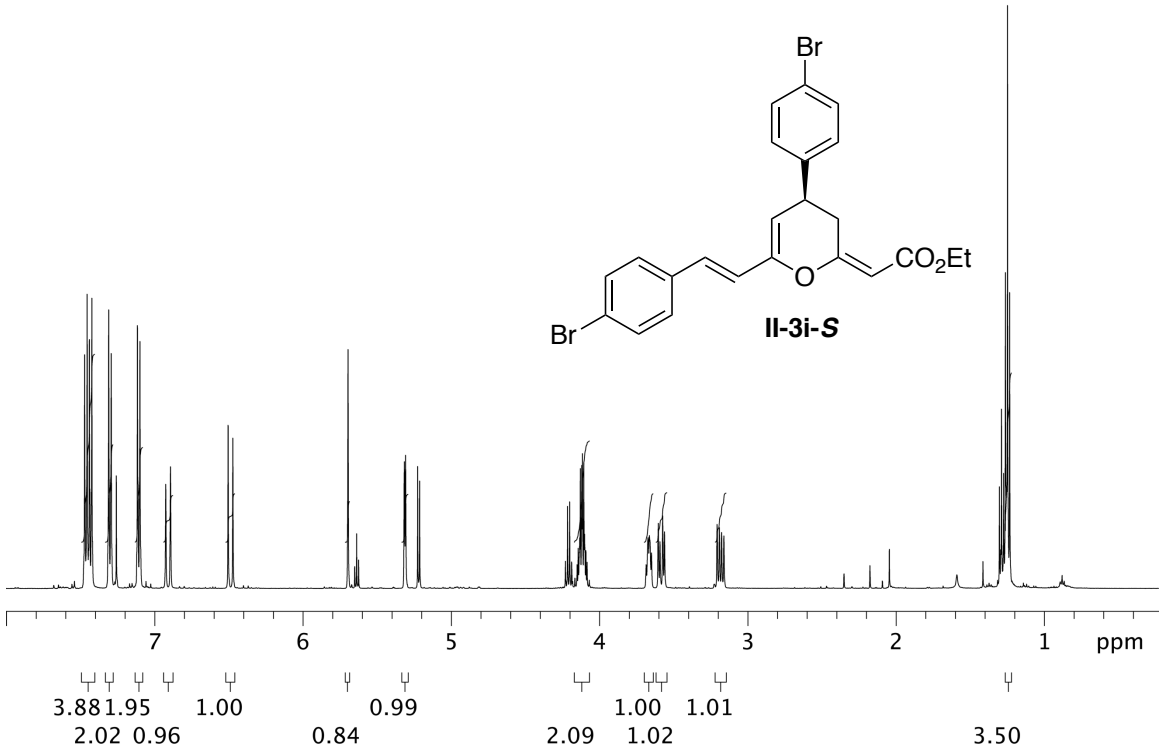
Br
CO2Et
O
Br
II-3i-S
7
6
5
4
3
2
1
ppm
3.88 1.95 1.00 0.99 1.00 1.01
2.02 0.96 0.84 2.09 1.02 3.50

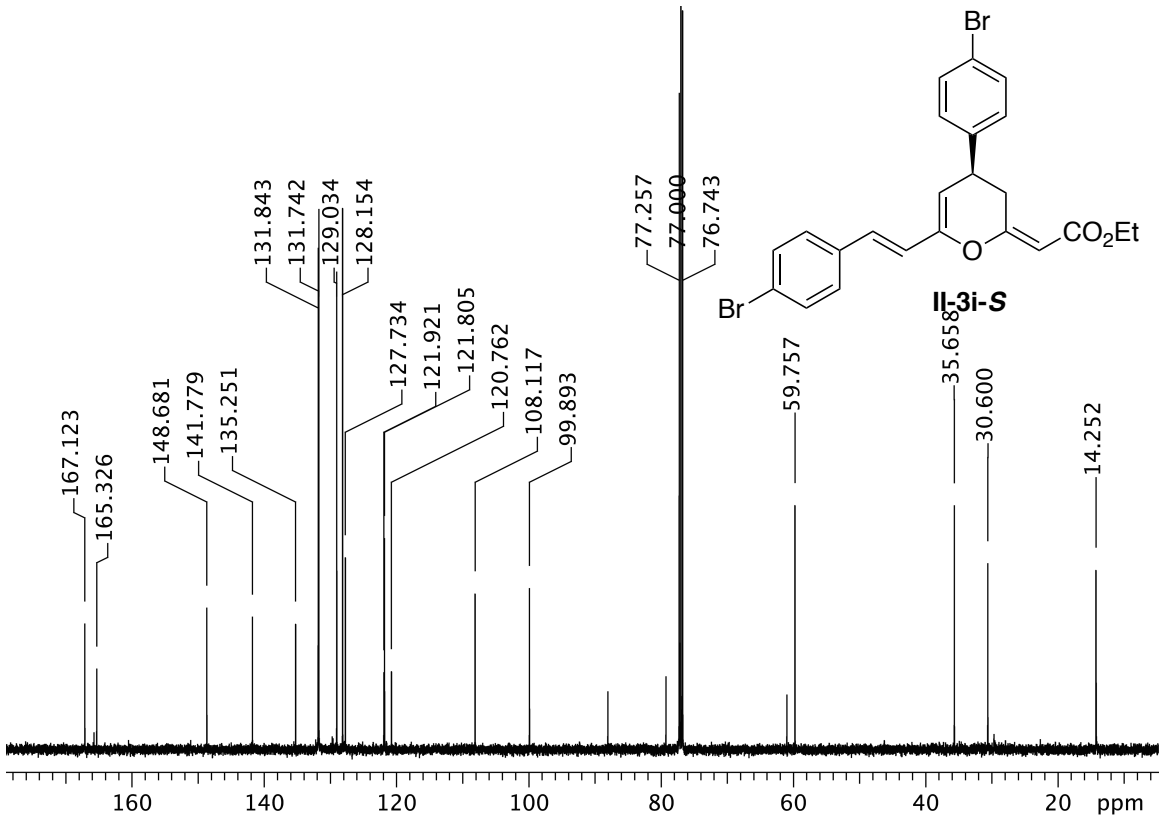
Br
CO2Et
O
Br
II-3i-S
167.123
165.326
148.681
141.779
135.251
131.843
131.742
129.034
128.154
127.734
121.921
121.805
120.762
108.117
99.893
77.257
77.000
76.743
59.757
35.658
30.600
14.252
160
140
120
100
80
60
40
20
ppm

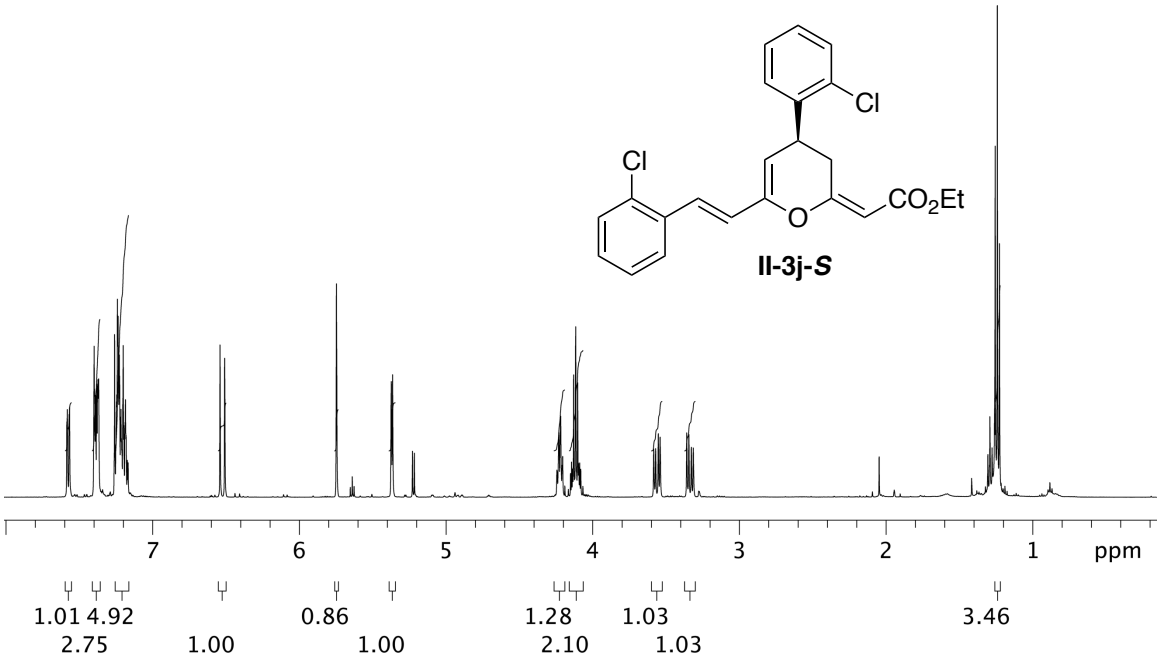
Cl
Cl
O
CO2Et
II-3j-S
7
6
5
4
3
2
1
ppm
1.01
4.92
2.75
1.00
0.86
1.00
1.28
2.10
1.03
1.03
3.46

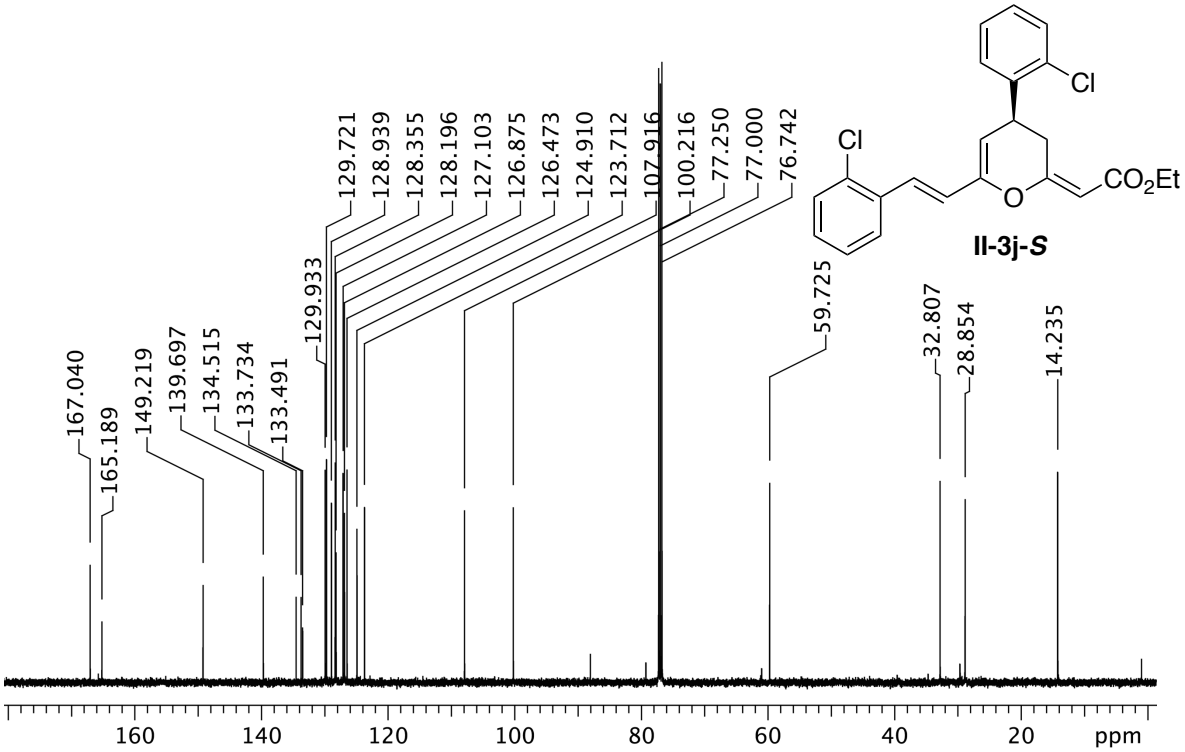
Cl
Cl
O
CO2Et
II-3j-S
167.040
165.189
149.219
139.697
134.515
133.734
133.491
129.933
129.721
128.939
128.355
128.196
127.103
126.875
126.473
124.910
123.712
107.916
100.216
77.250
77.000
76.742
59.725
32.807
28.854
14.235
160
140
120
100
80
60
40
20
ppm

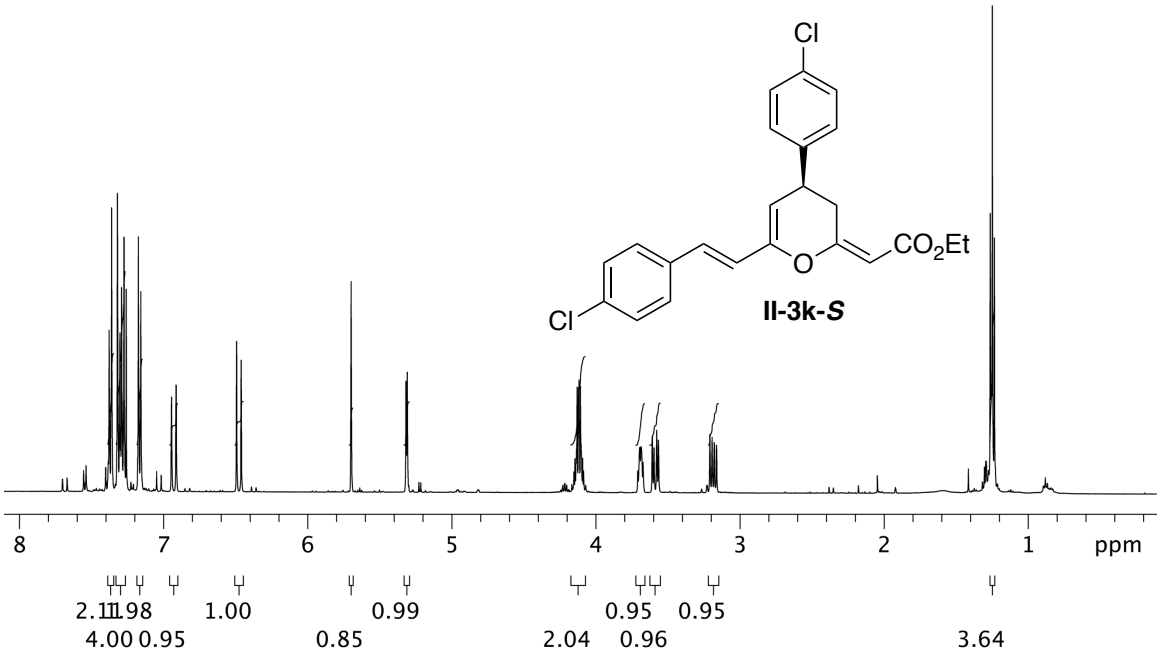
Cl
CO2Et
O
Cl
II-3k-S
8
7
6
5
4
3
2
1
ppm
2.11
1.98
1.00
0.99
0.95
0.95
4.00
0.95
0.85
2.04
0.96
3.64

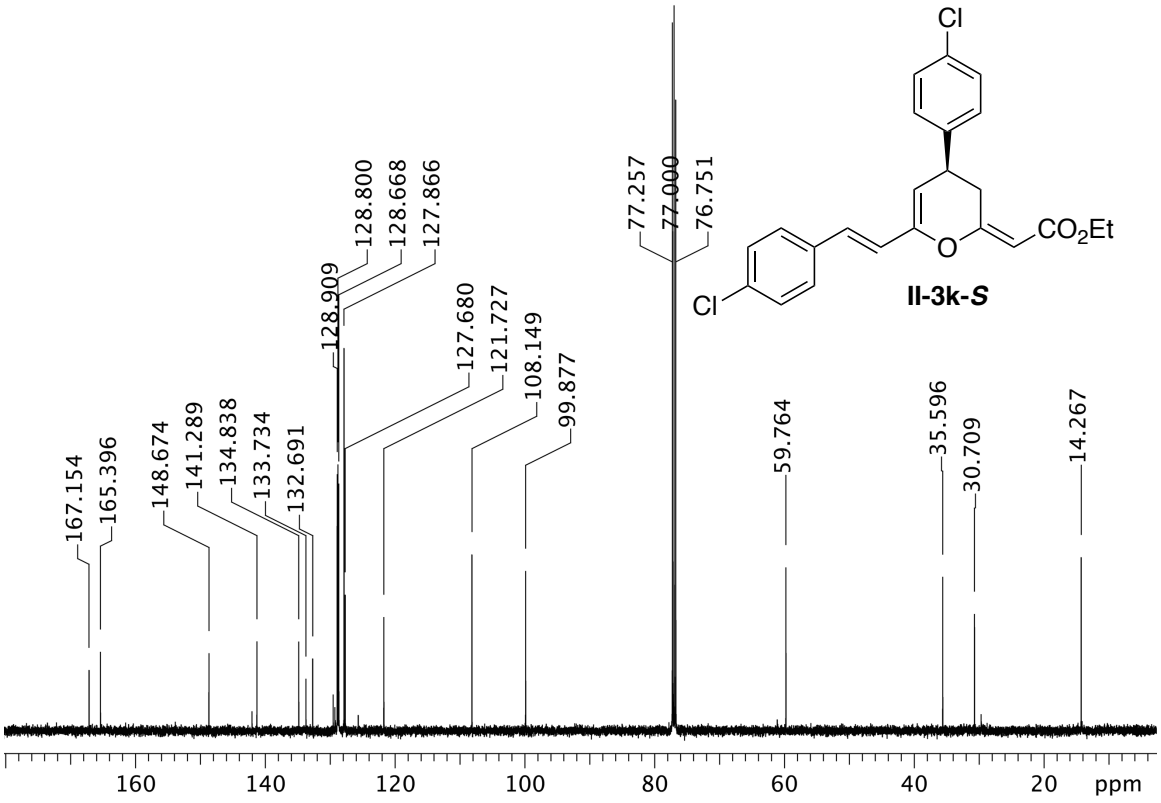
Cl
CO2Et
O
Cl
II-3k-S
77.257
77.000
76.751
128.800
128.668
127.866
128.909
127.680
121.727
108.149
99.877
167.154
165.396
148.674
141.289
134.838
133.734
132.691
59.764
35.596
30.709
14.267
160
140
120
100
80
60
40
20
ppm

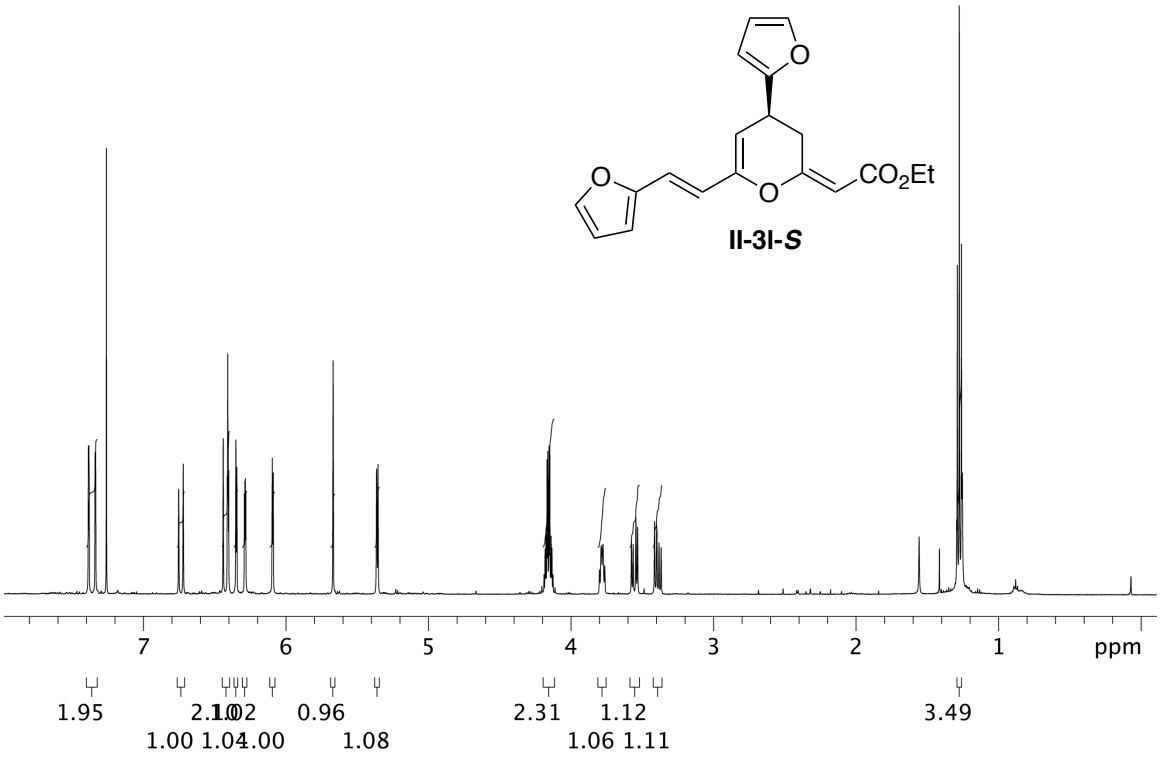
O
O
O
CO2Et
II-3l-S
7
6
5
4
3
2
1
ppm
1.95
2.10
1.02
0.96
2.31
1.12
3.49
1.00
1.04
4.00
1.08
1.06
1.11

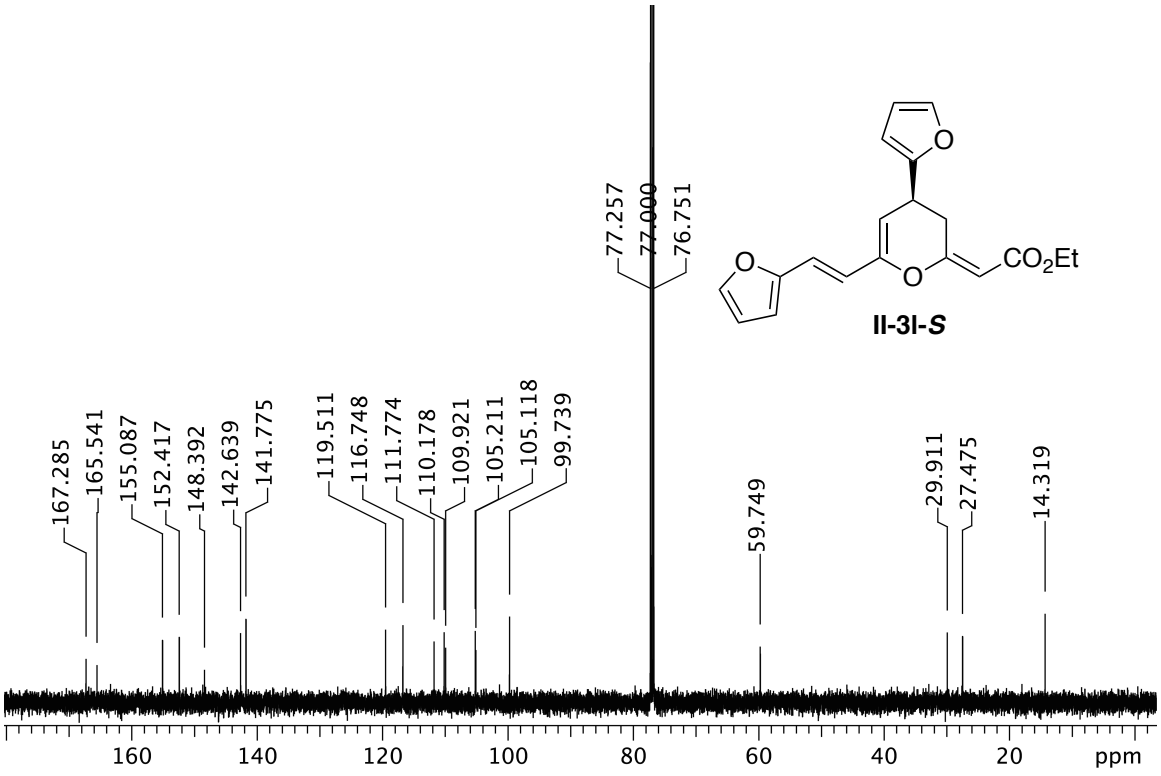
77.257
77.000
76.751
O
O
O
CO2Et
II-3l-S
167.285
165.541
155.087
152.417
148.392
142.639
141.775
119.511
116.748
111.774
110.178
109.921
105.211
105.118
99.739
59.749
29.911
27.475
14.319
160
140
120
100
80
60
40
20
ppm

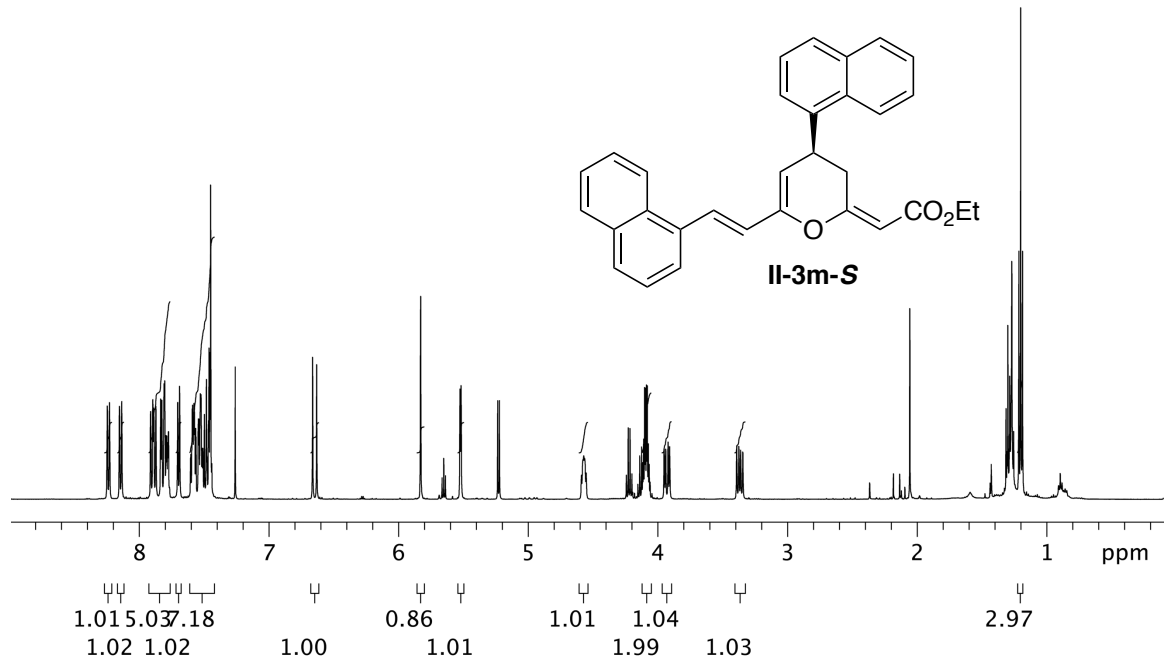
CO2Et
O
II-3m-S
8
7
6
5
4
3
2
1
ppm
1.01 5.03 7.18 0.86 1.01 1.04 2.97
1.02 1.02 1.00 1.01 1.99 1.03

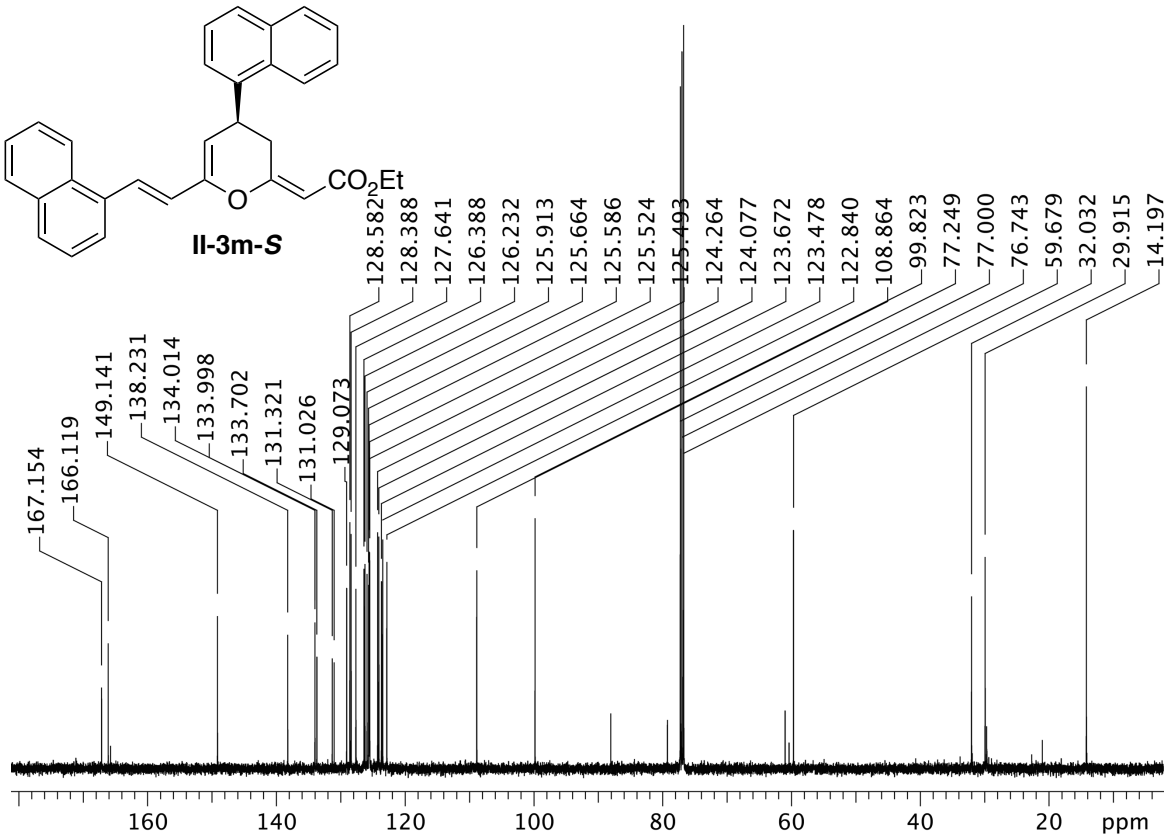
CO2Et
O
II-3m-S
128.582
128.388
127.641
126.388
126.232
125.913
125.664
125.586
125.524
125.493
124.264
124.077
123.672
123.478
122.840
108.864
99.823
77.249
77.000
76.743
59.679
32.032
29.915
14.197
167.154
166.119
149.141
138.231
134.014
133.998
133.702
131.321
131.026
129.073
160
140
120
100
80
60
40
20
ppm

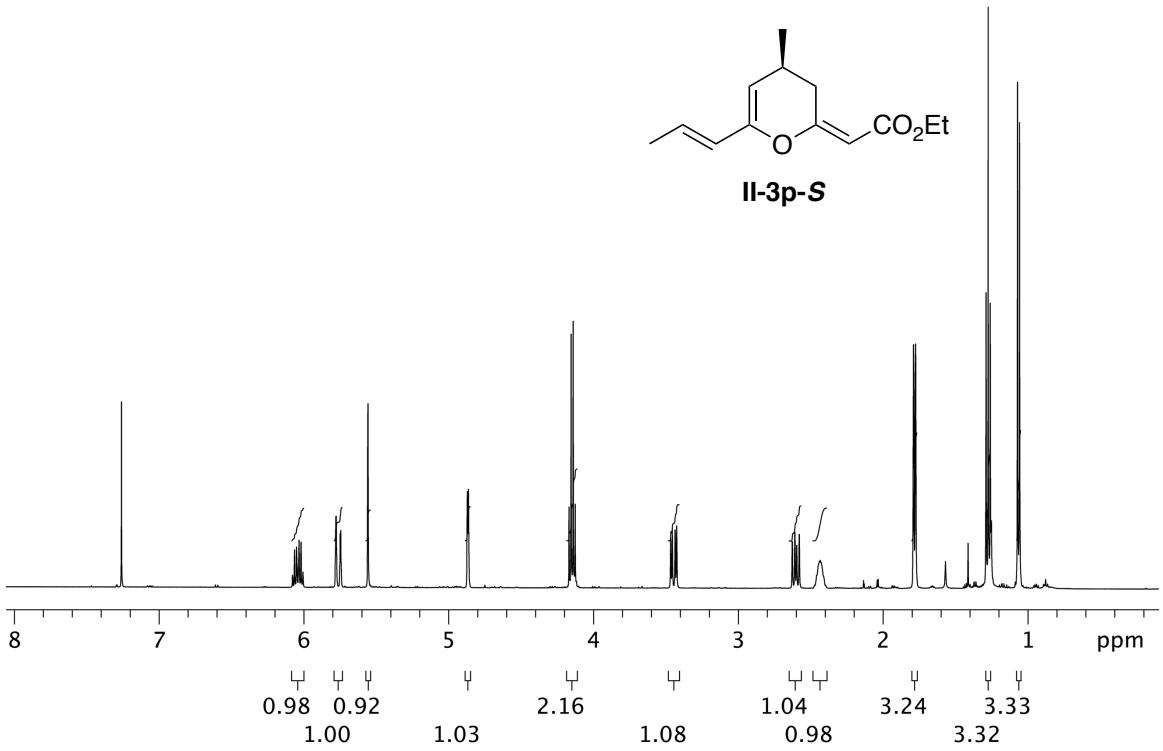
CO2Et
O
II-3p-S
8
7
6
5
4
3
2
1
ppm
0.98
0.92
2.16
1.04
3.24
3.33
1.00
1.03
1.08
0.98
3.32

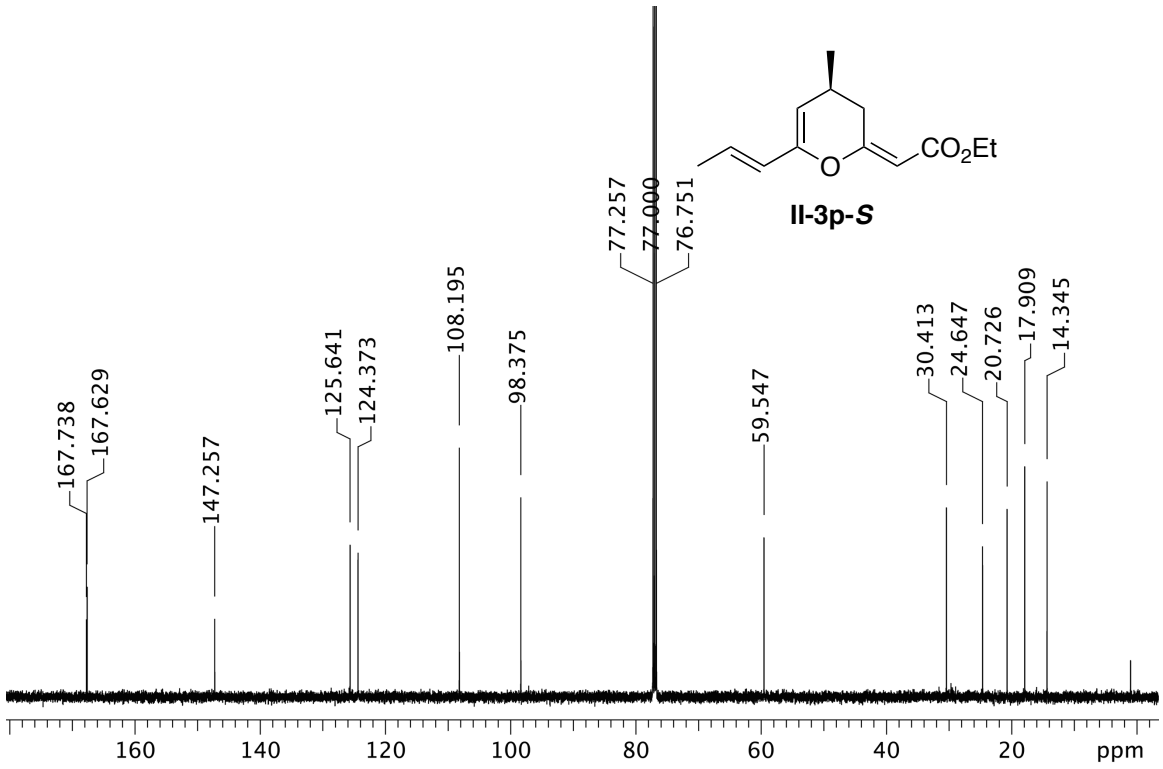
CO2Et
O
II-3p-S
77.257
77.000
76.751
167.738
167.629
147.257
125.641
124.373
108.195
98.375
59.547
30.413
24.647
20.726
17.909
14.345
160
140
120
100
80
60
40
20
ppm

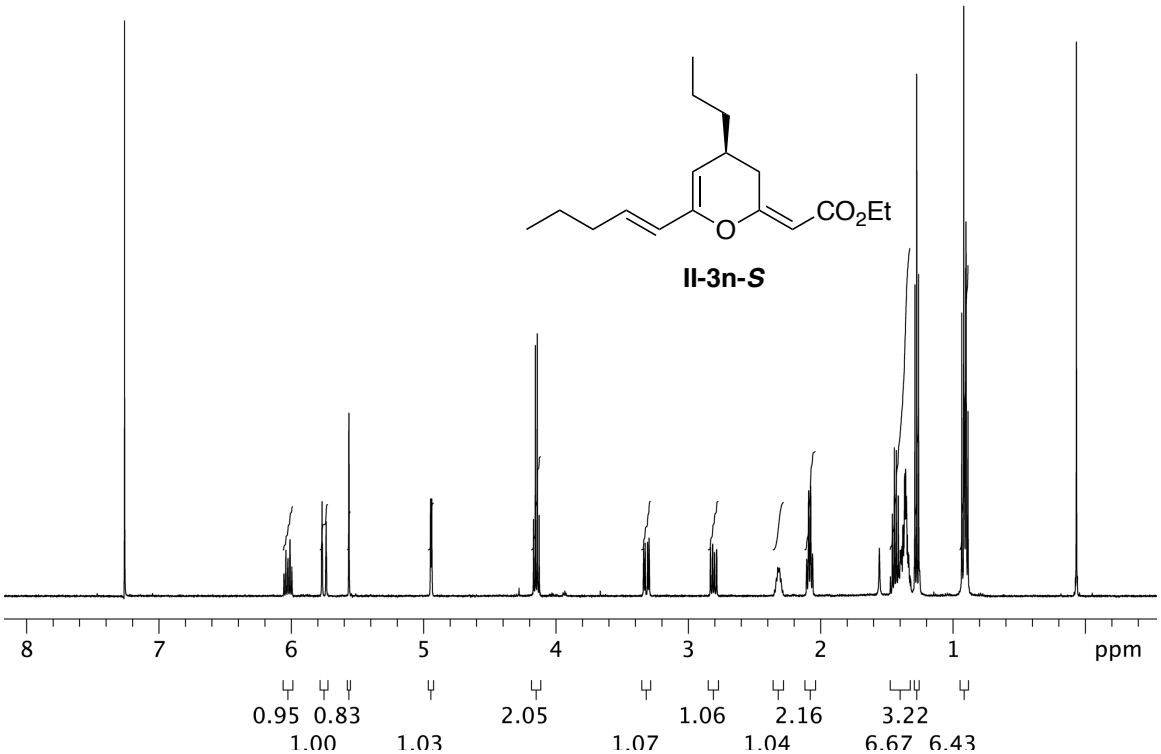
CO2Et
O
II-3n-S
8
7
6
5
4
3
2
1
ppm
0.95
0.83
2.05
1.06
2.16
3.22
1.00
1.03
1.07
1.04
6.67
6.43

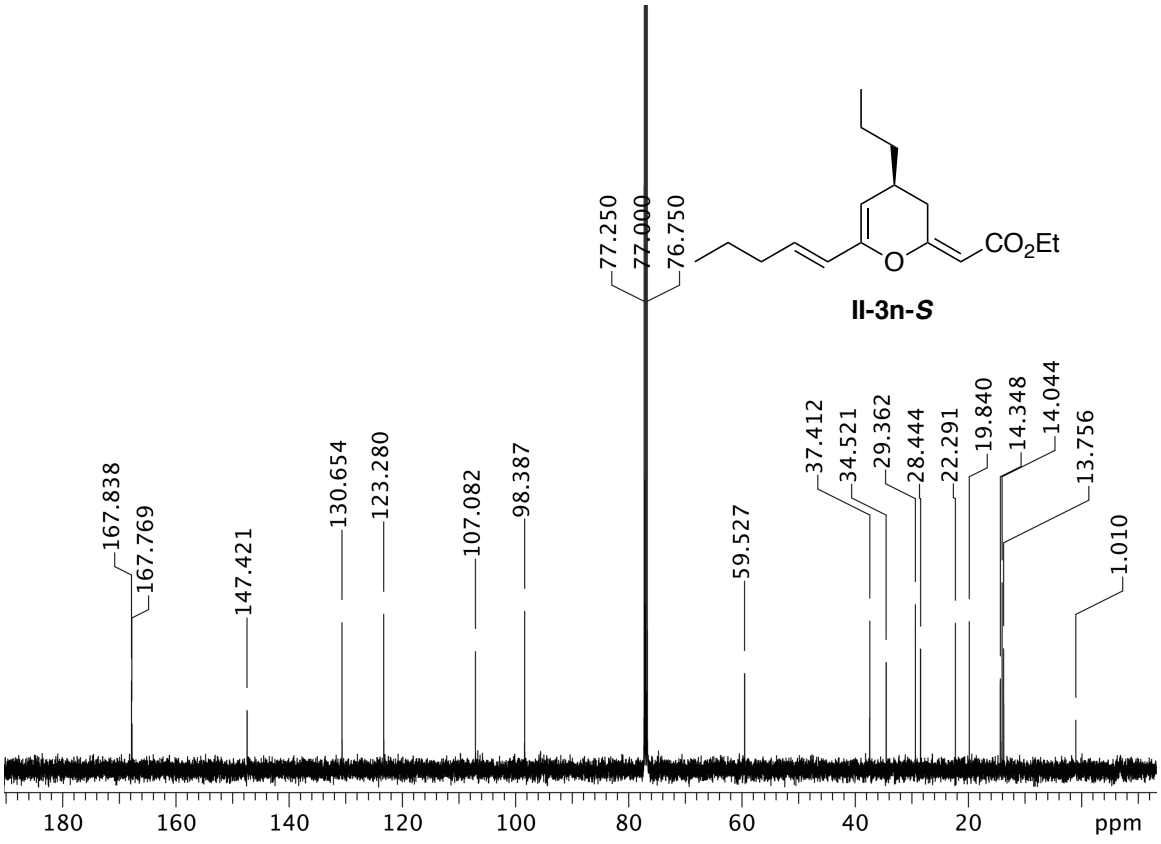
77.250
77.000
76.750
CO2Et
O
II-3n-S
167.838
167.769
147.421
130.654
123.280
107.082
98.387
59.527
37.412
34.521
29.362
28.444
22.291
19.840
14.348
14.044
13.756
1.010
180
160
140
120
100
80
60
40
20
ppm

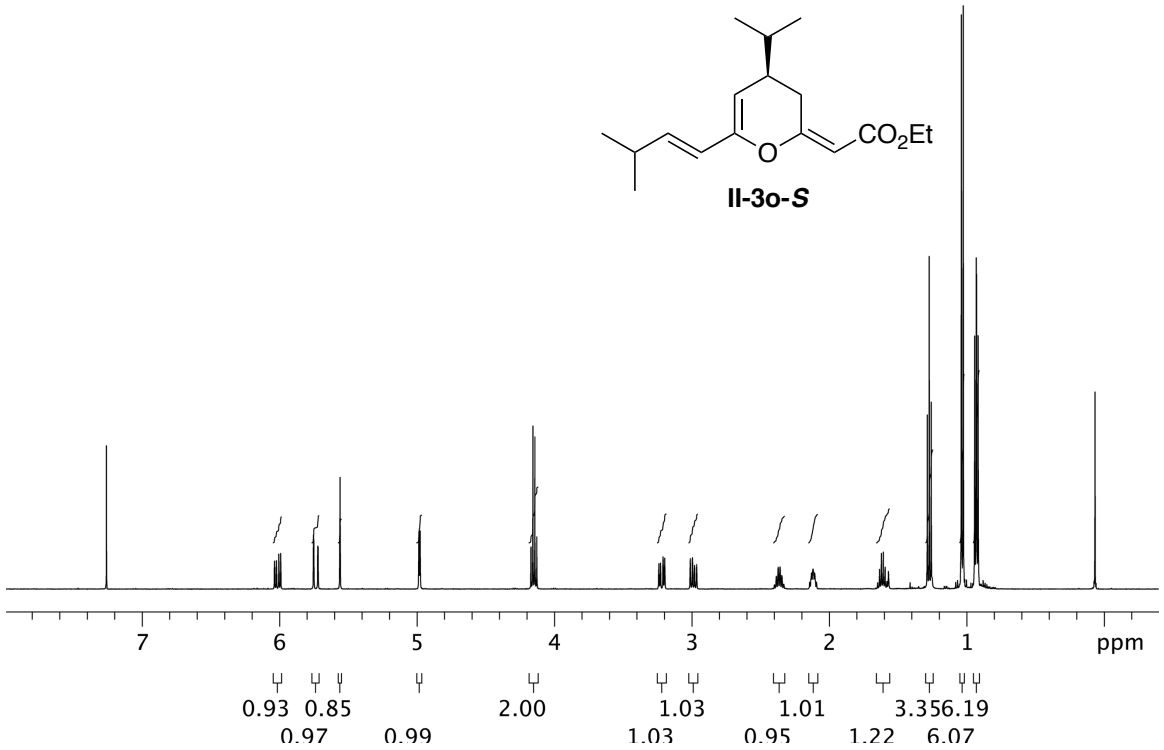
CO2Et
O
II-3o-S
7
6
5
4
3
2
1
ppm
0.93
0.85
0.97
0.99
2.00
1.03
1.03
1.01
0.95
3.35
1.22
6.19
6.07

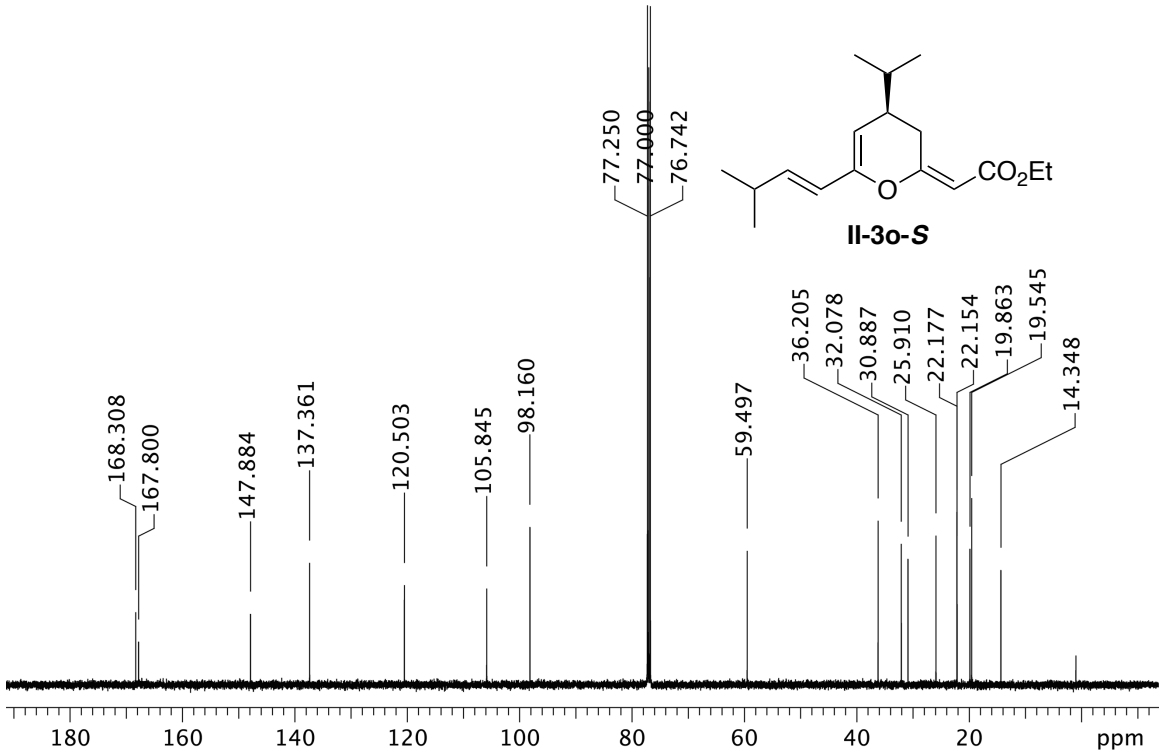
77.250
77.000
76.742
CO2Et
O
II-3o-S
168.308
167.800
147.884
137.361
120.503
105.845
98.160
59.497
36.205
32.078
30.887
25.910
22.177
22.154
19.863
19.545
14.348
180
160
140
120
100
80
60
40
20
ppm

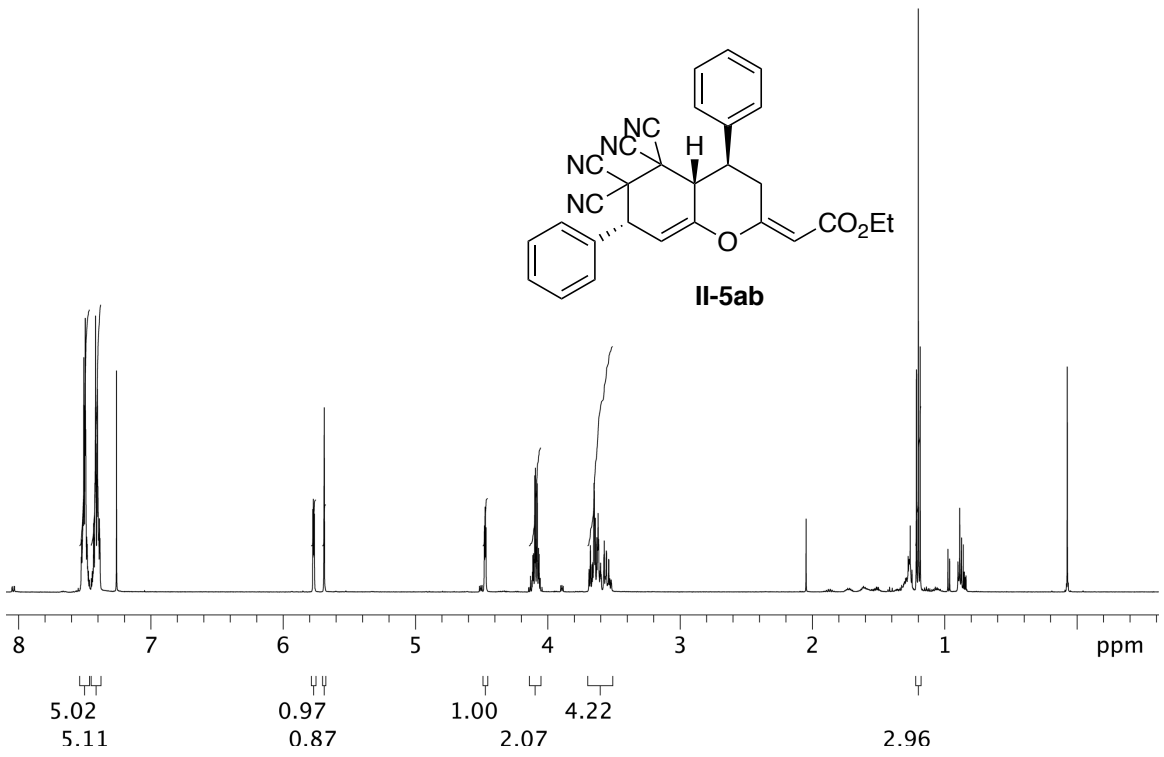
NC
NC
NC
NC
H
O
CO2Et
II-5ab
8
7
6
5
4
3
2
1
ppm
5.02
5.11
0.97
0.87
1.00
2.07
4.22
2.96

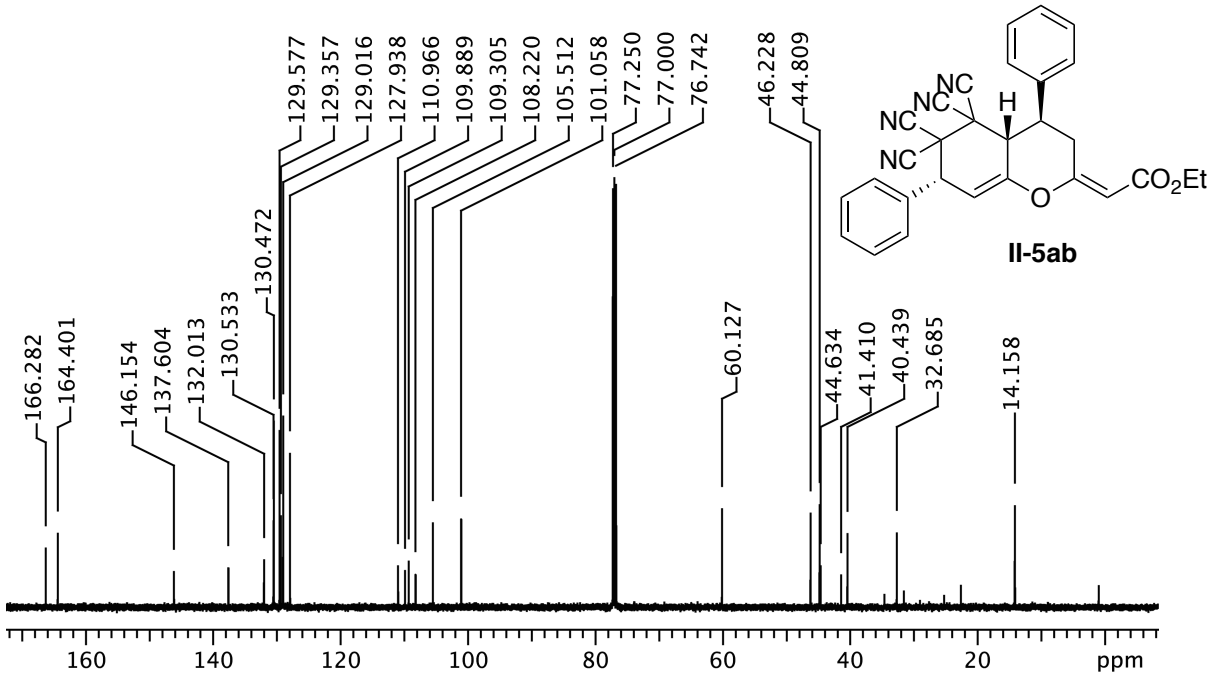
166.282
164.401
146.154
137.604
132.013
130.533
130.472
129.577
129.357
129.016
127.938
110.966
109.889
109.305
108.220
105.512
101.058
77.250
77.000
76.742
60.127
46.228
44.809
44.634
41.410
40.439
32.685
14.158
NC
NC
NC
NC
H
O
CO2Et
II-5ab
160
140
120
100
80
60
40
20
ppm

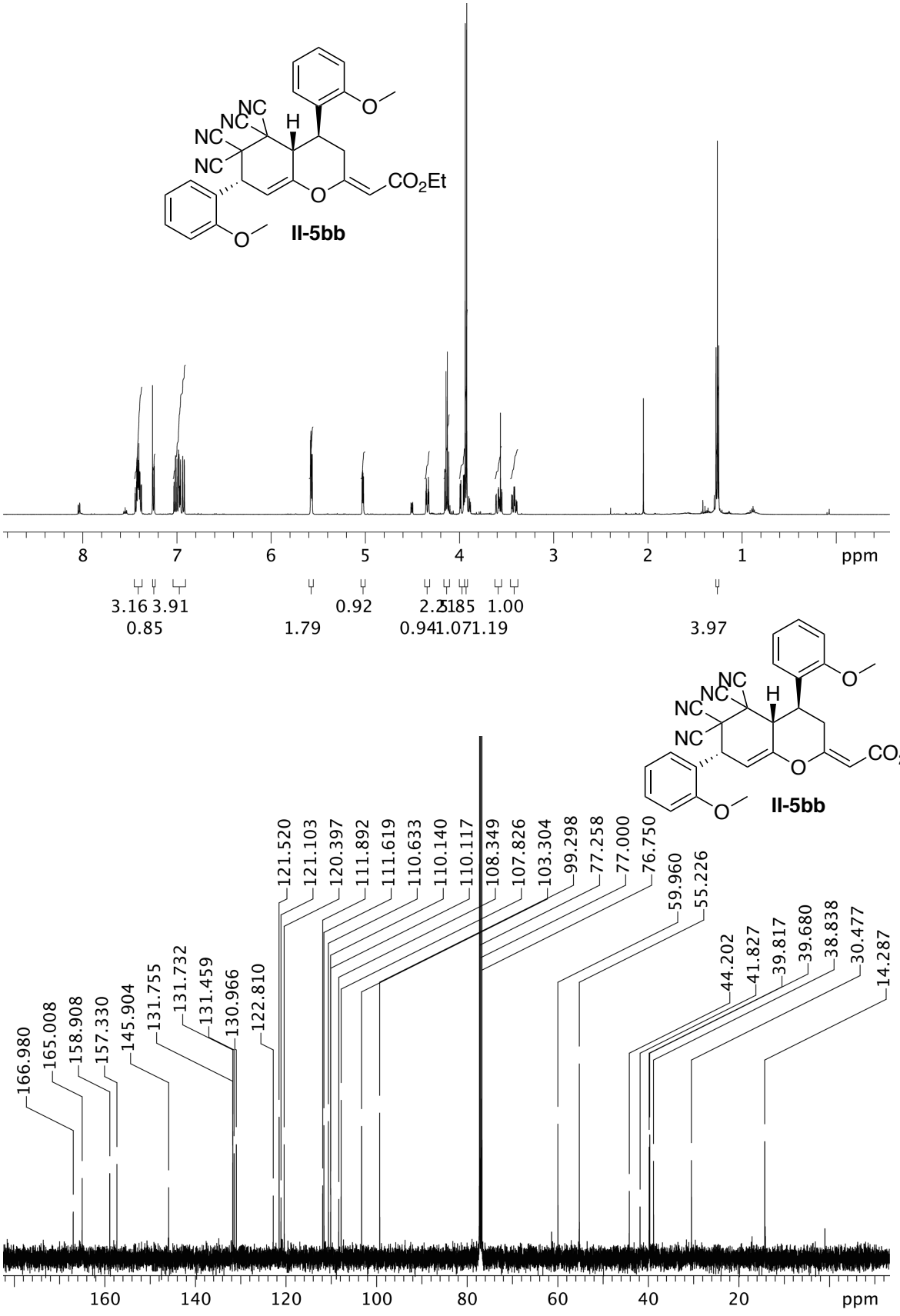
NC
NC
NC
NC
H
O
CO2Et
O
O
II-5bb
8
7
6
5
4
3
2
1
ppm
3.16
3.91
0.92
1.00
3.97
0.85
1.79
0.94
1.07
1.19
166.980
165.008
158.908
157.330
145.904
131.755
131.732
131.459
130.966
122.810
121.520
121.103
120.397
111.892
111.619
110.633
110.140
110.117
108.349
107.826
103.304
99.298
77.258
77.000
76.750
59.960
55.226
44.202
41.827
39.817
39.680
38.838
30.477
14.287
160
140
120
100
80
60
40
20
ppm

DXL-2-81-3A1_PROTON_01

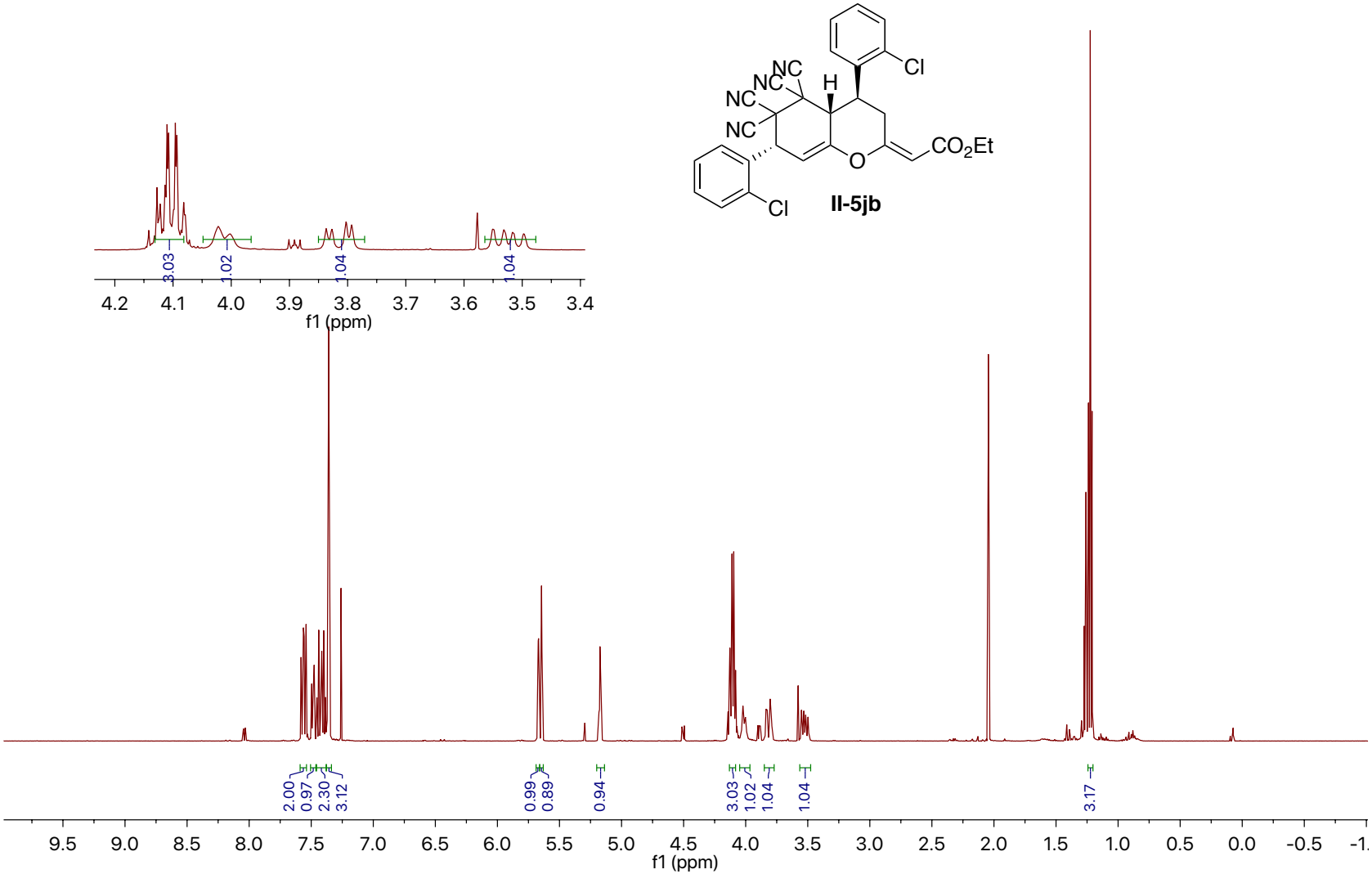

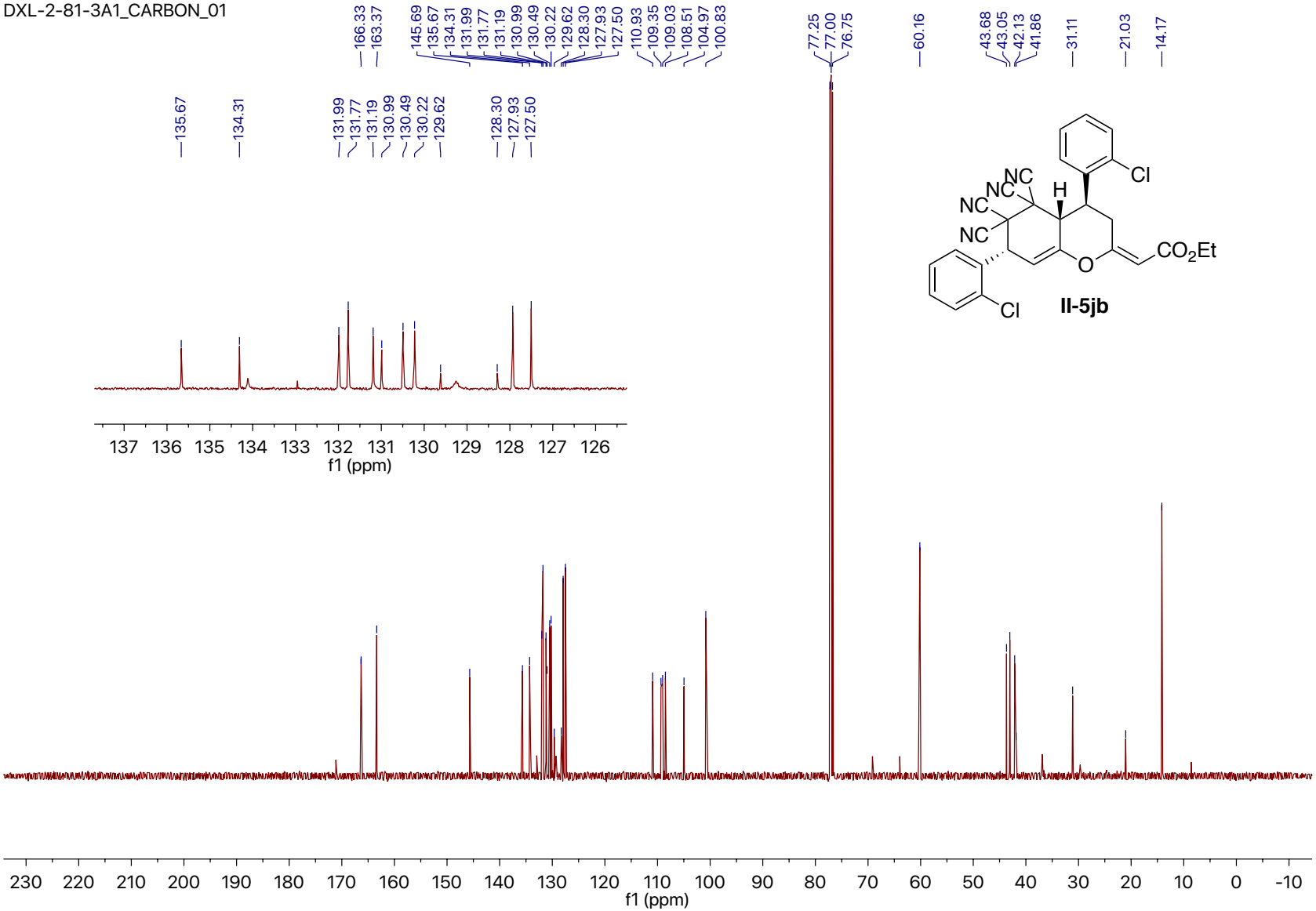
DXL-2-81-3A1_CARBON_01
166.33
163.37
145.69
135.67
134.31
131.99
131.77
131.19
130.99
130.49
130.22
129.62
128.30
127.93
127.50
110.93
109.35
109.03
108.51
104.97
100.83
77.25
77.00
76.75
60.16
43.68
43.05
42.13
41.86
31.11
21.03
14.17
NC
NC
NC
NC
H
Cl
Cl
O
CO2Et
II-5jb
f1 (ppm)
f1 (ppm)

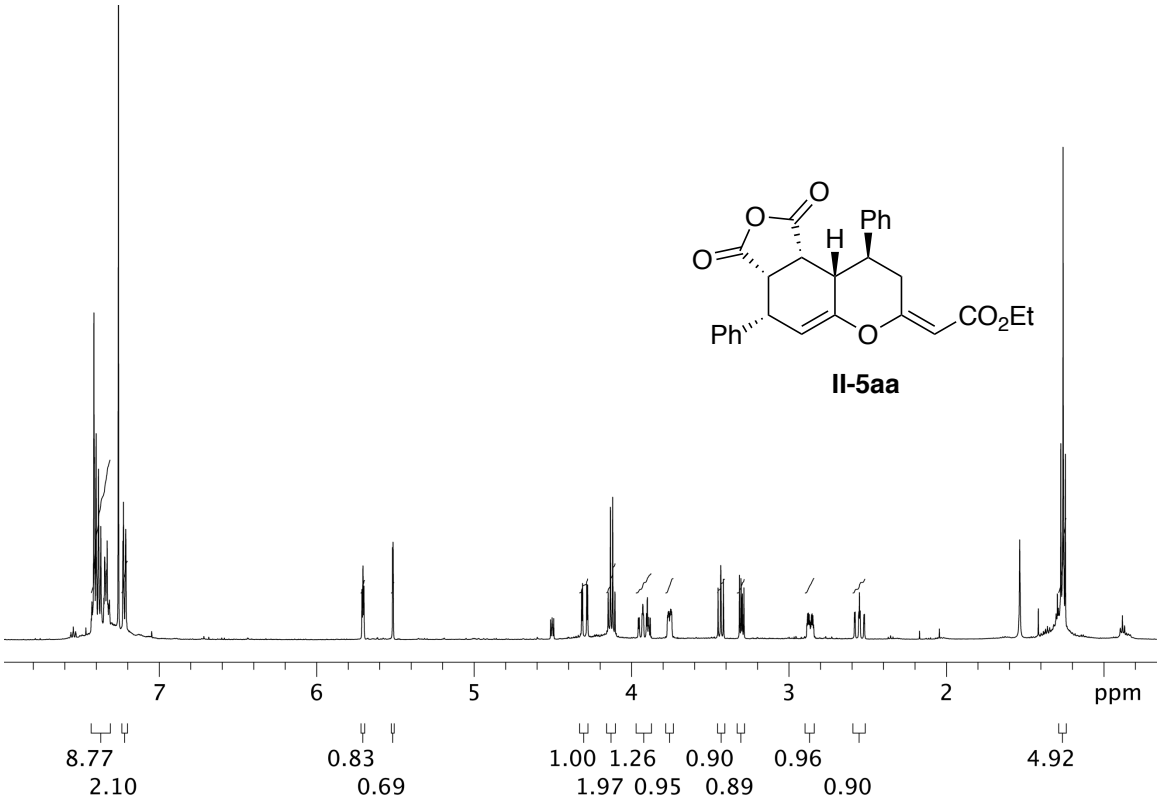
O
O
O
Ph
H
Ph
O
CO2Et
7
6
5
4
3
2
ppm
8.77
2.10
0.83
0.69
1.00
1.26
0.90
0.96
4.92
1.97
0.95
0.89
0.90

II-5aa

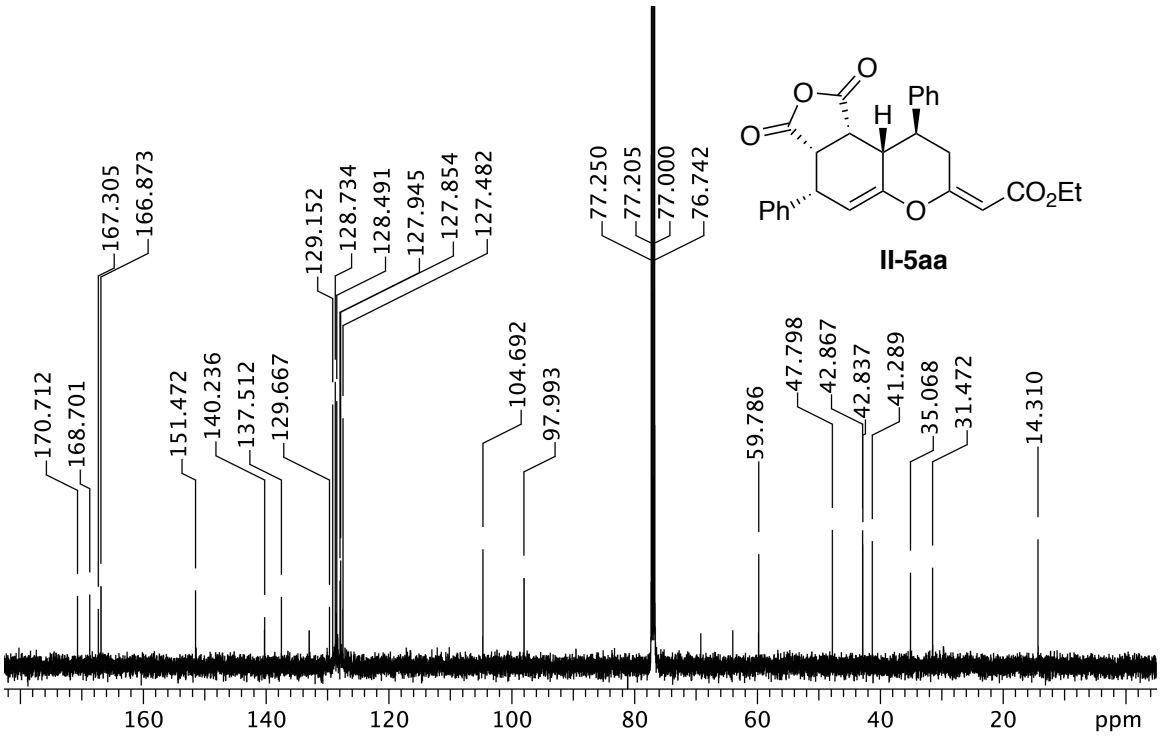
O
O
O
Ph
H
Ph
O
CO2Et
170.712
168.701
167.305
166.873
151.472
140.236
137.512
129.667
129.152
128.734
128.491
127.945
127.854
127.482
104.692
97.993
77.250
77.205
77.000
76.742
59.786
47.798
42.867
42.837
41.289
35.068
31.472
14.310
160
140
120
100
80
60
40
20
ppm

II-5aa

DXL-2-85-3A1_PROTON_01

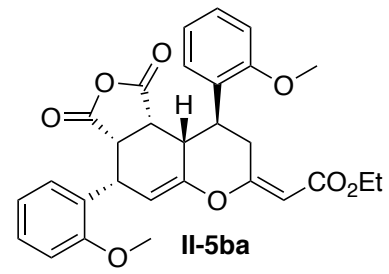

II-5ba

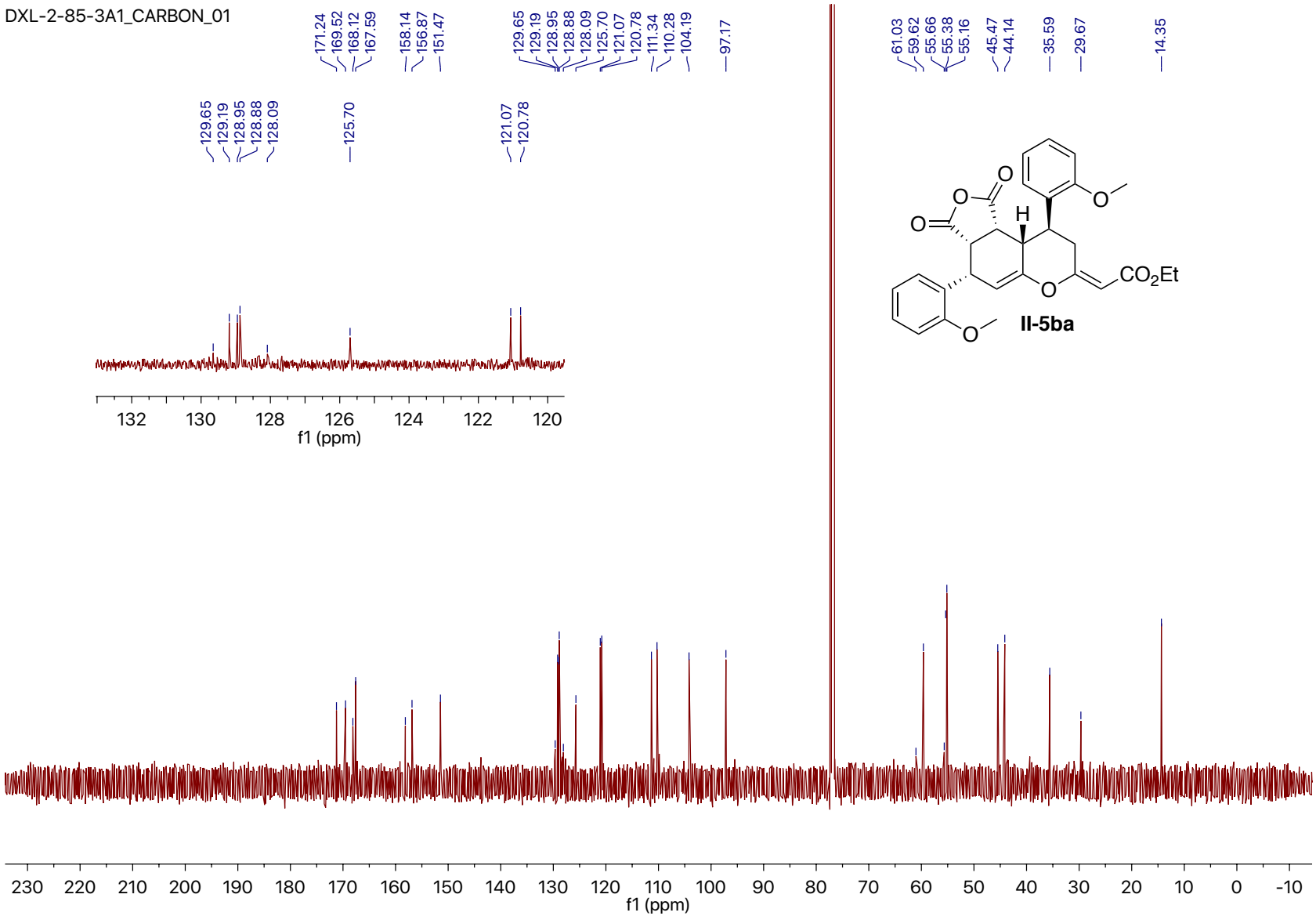
DXL-2-85-3A1_CARBON_01
171.24
169.52
168.12
167.59
158.14
156.87
151.47
129.65
129.19
128.95
128.88
128.09
125.70
121.07
120.78
111.34
110.28
104.19
97.17
61.03
59.62
55.66
55.38
55.16
45.47
44.14
35.59
29.67
14.35
CO2Et
II-5ba
f1 (ppm)
f1 (ppm)

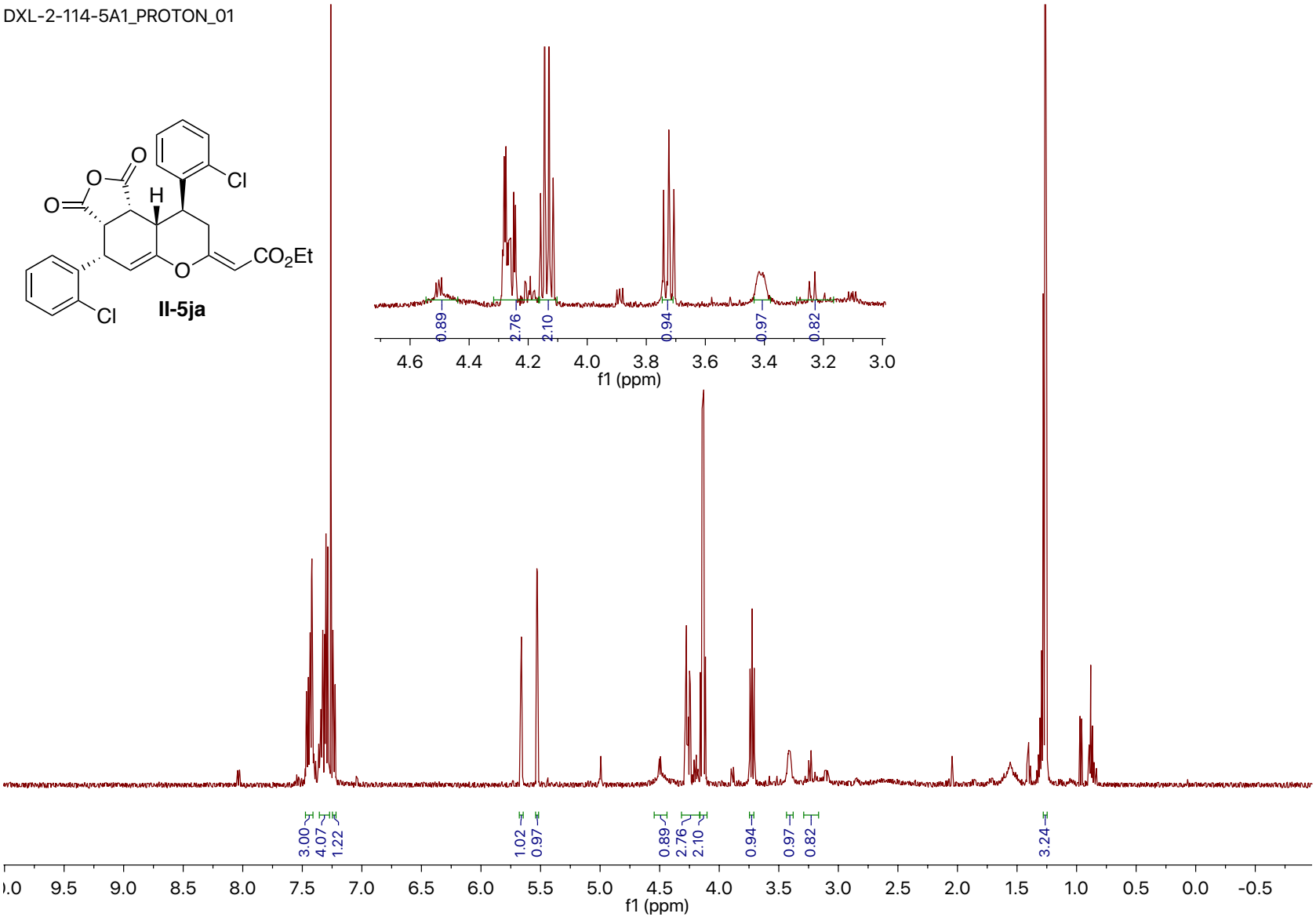
DXL-2-114-5A1_PROTON_01
O
O
O
H
Cl
CO2Et
O
Cl
II-5ja
0.89
2.76
2.10
0.94
0.97
0.82
4.6
4.4
4.2
4.0
3.8
3.6
3.4
3.2
3.0
f1 (ppm)
3.00
4.07
1.22
1.02
0.97
0.89
2.76
2.10
0.94
0.97
0.82
3.24
9.5
9.0
8.5
8.0
7.5
7.0
6.5
6.0
5.5
5.0
4.5
4.0
3.5
3.0
2.5
2.0
1.5
1.0
0.5
0.0
-0.5
f1 (ppm)

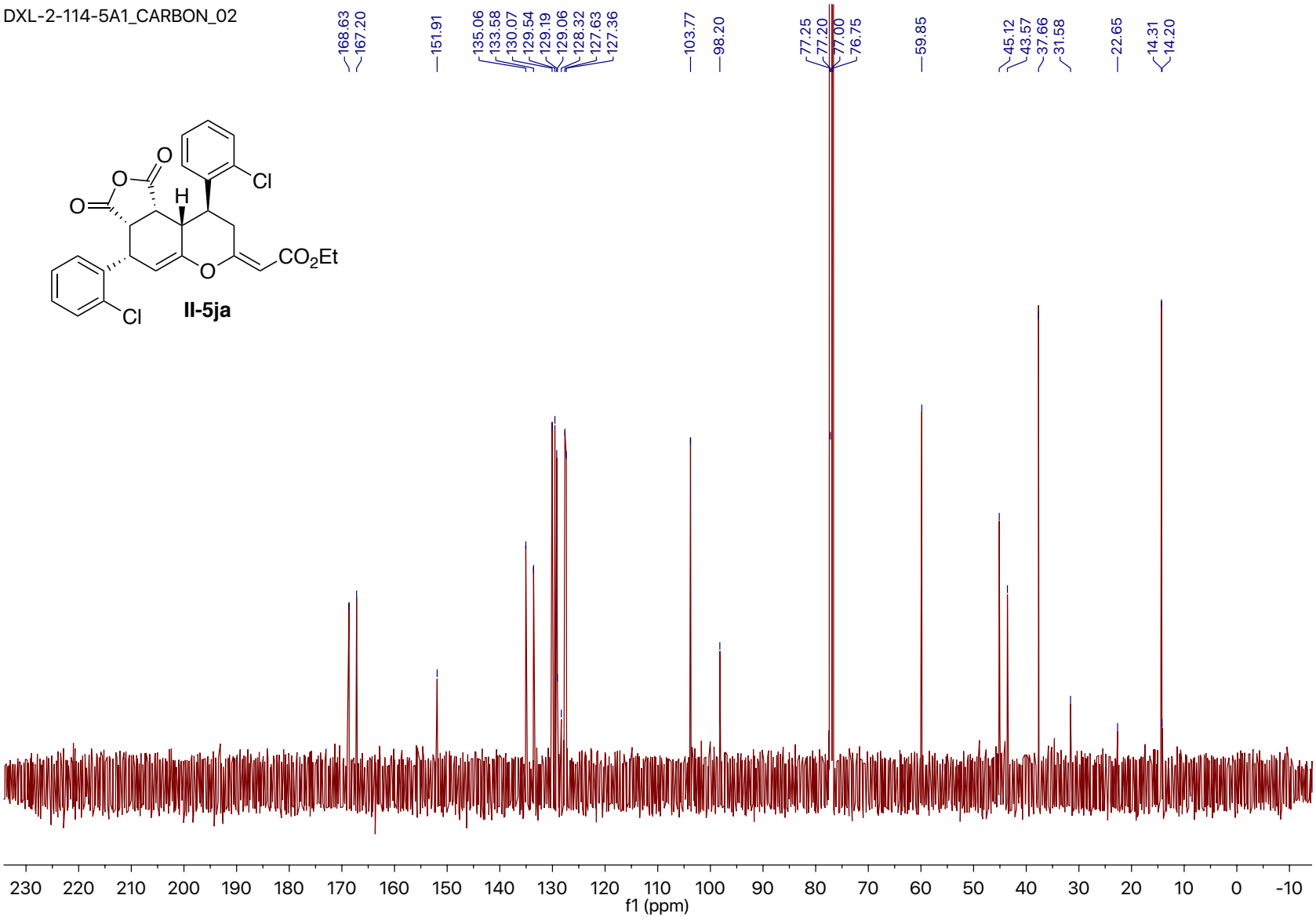
DXL-2-114-5A1_CARBON_02
168.63
167.20
151.91
135.06
133.58
130.07
129.54
129.19
129.06
128.32
127.63
127.36
103.77
98.20
77.25
77.20
77.00
76.75
59.85
45.12
43.57
37.66
31.58
22.65
14.31
14.20
O
O
O
H
Cl
CO2Et
O
Cl
II-5ja
230 220 210 200 190 180 170 160 150 140 130 120 110 100 90 80 70 60 50 40 30 20 10 0 -10
f1 (ppm)

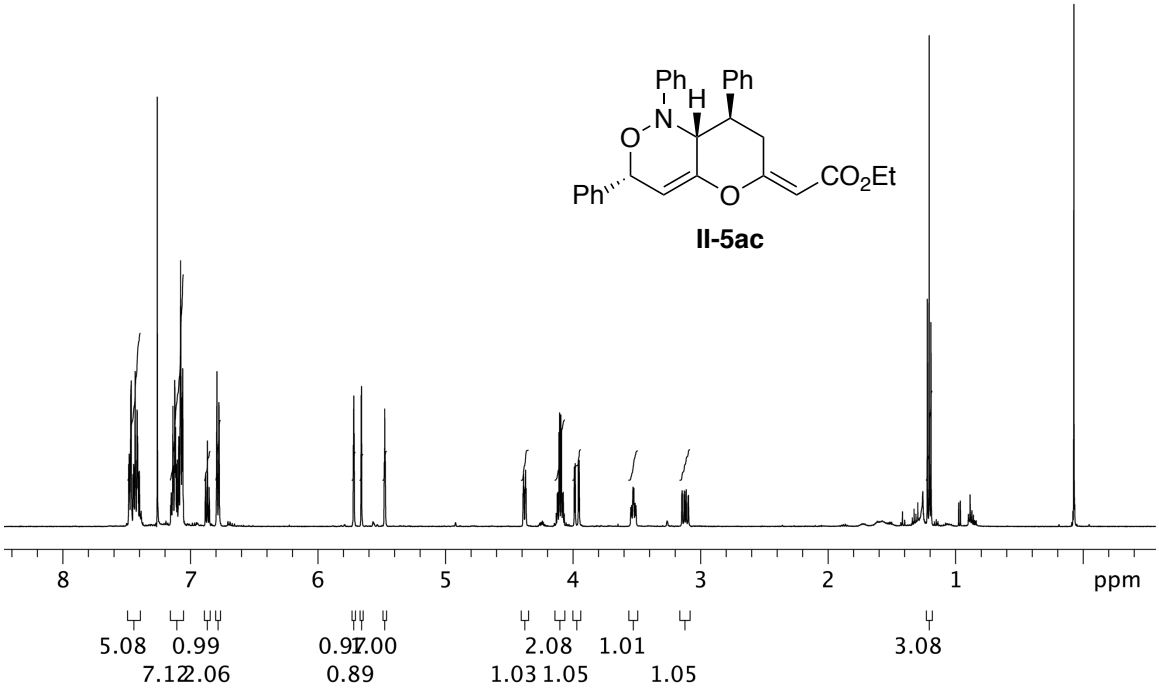
Ph
Ph
H
N
O
O
Ph
O
CO2Et
II-5ac
8
7
6
5
4
3
2
1
ppm
5.08
0.99
7.12
2.06
0.97
0.89
1.00
2.08
1.03
1.05
1.01
1.05
3.08

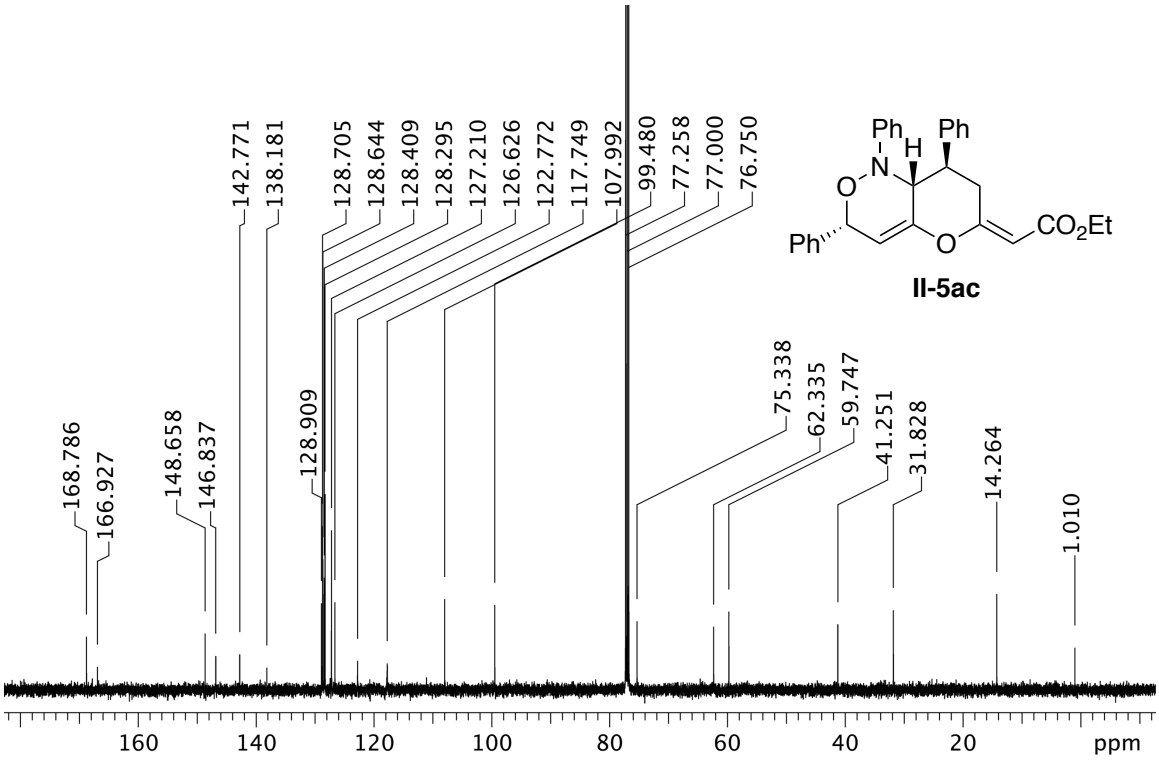
142.771
138.181
128.705
128.644
128.409
128.295
127.210
126.626
122.772
117.749
107.992
99.480
77.258
77.000
76.750
168.786
166.927
148.658
146.837
128.909
75.338
62.335
59.747
41.251
31.828
14.264
1.010
Ph
Ph
H
N
O
O
Ph
O
CO2Et
II-5ac
160
140
120
100
80
60
40
20
ppm

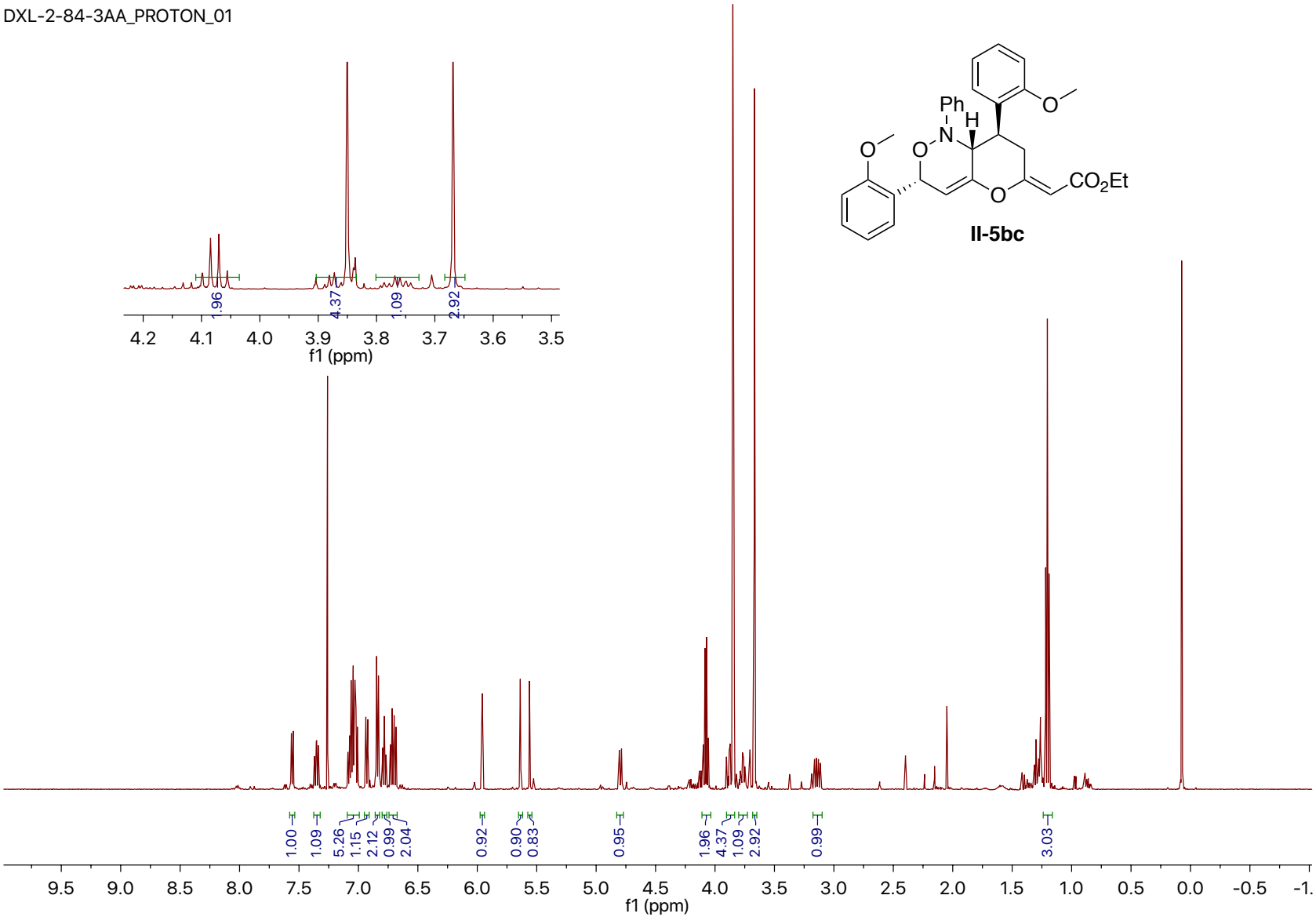
DXL-2-84-3AA_PROTON_01
Ph
N
H
O
O
O
O
O
CO_2Et
II-5bc
1.96
4.37
1.09
2.92
4.2 4.1 4.0 3.9 3.8 3.7 3.6 3.5
f1 (ppm)
1.00 1.09 5.26 1.15 2.12 0.99 2.04 0.92 0.90 0.83 0.95 1.96 4.37 1.09 2.92 0.99 3.03
9.5 9.0 8.5 8.0 7.5 7.0 6.5 6.0 5.5 5.0 4.5 4.0 3.5 3.0 2.5 2.0 1.5 1.0 0.5 0.0 -0.5 -1.
f1 (ppm)

DXL-2-84-3AA_CARBON_01

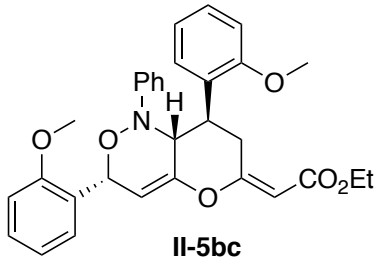

II-5bc

DXL-2-65-3A1_PROTON_01

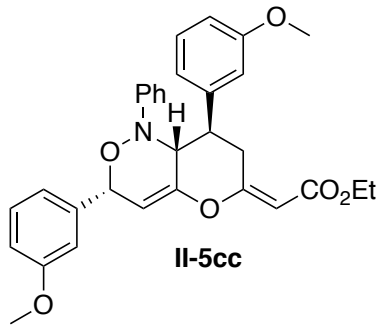

II-5cc

DXL-2-65-3A1_CARBON_01

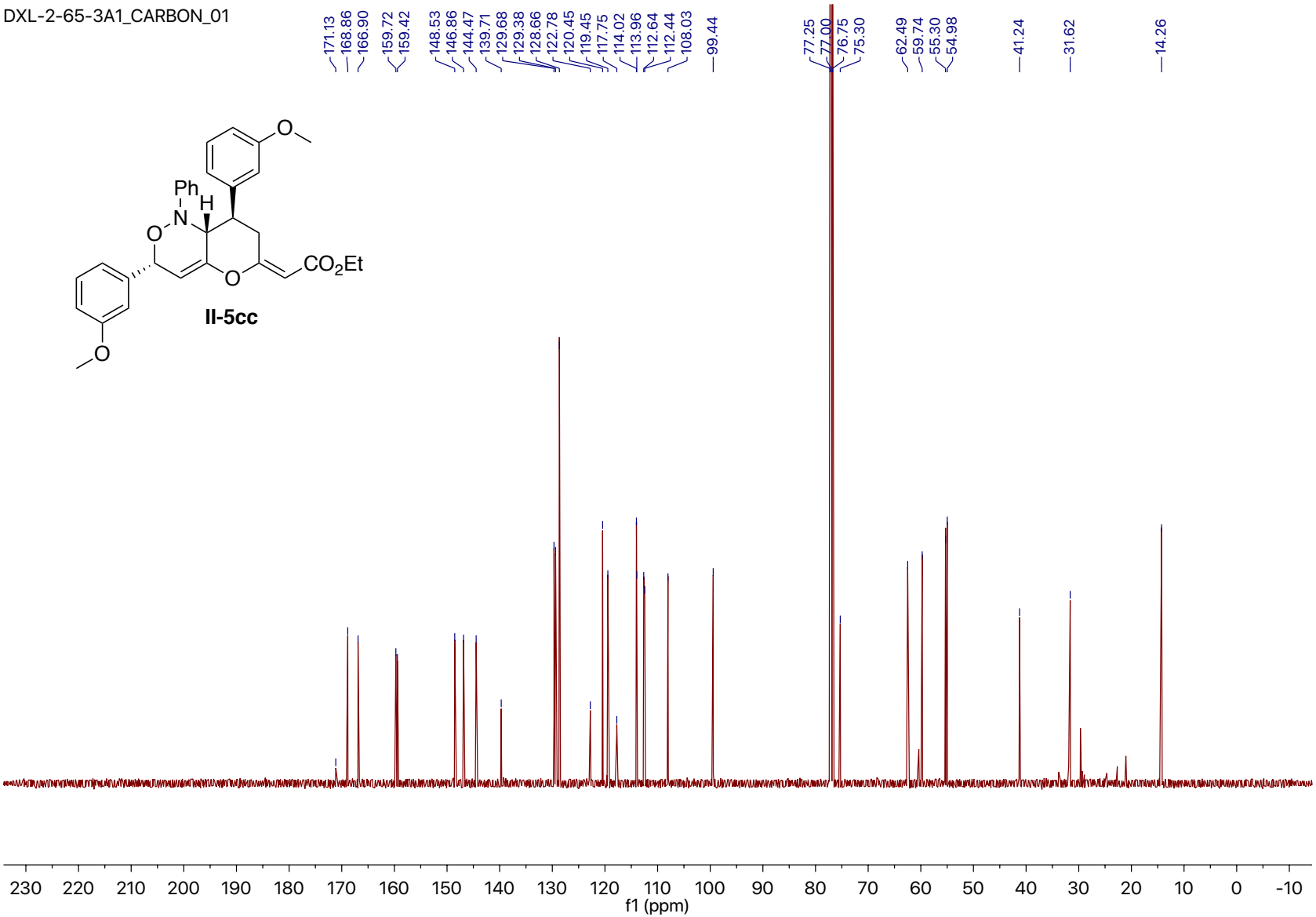

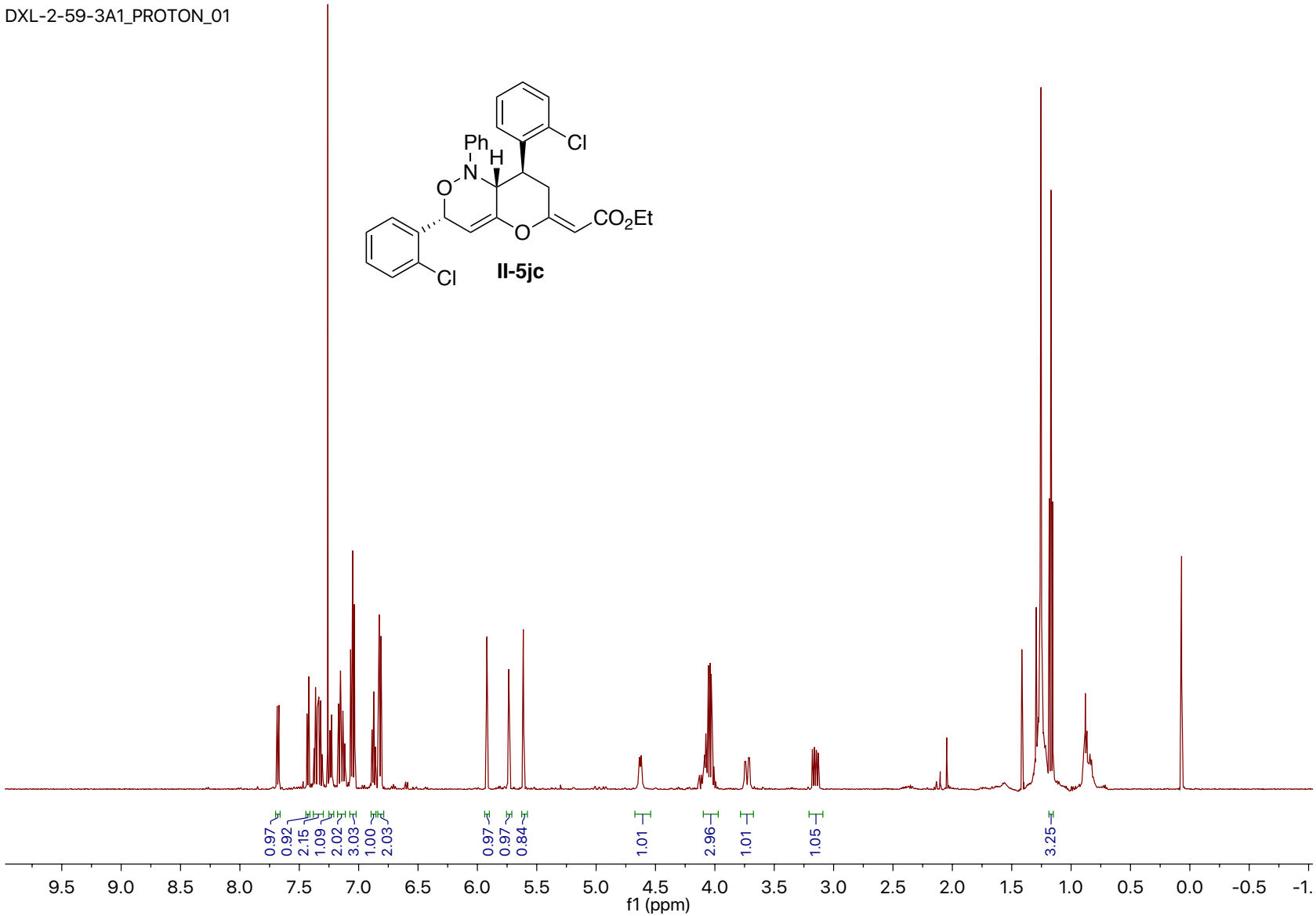
DXL-2-59-3A1_PROTON_01
Ph
N
H
O
Cl
O
CO2Et
Cl
II-5jc
0.97
0.92
2.15
1.09
2.02
3.03
1.00
2.03
0.97
0.97
0.84
1.01
2.96
1.01
1.05
3.25
9.5
9.0
8.5
8.0
7.5
7.0
6.5
6.0
5.5
5.0
4.5
4.0
3.5
3.0
2.5
2.0
1.5
1.0
0.5
0.0
-0.5
-1.
f1 (ppm)

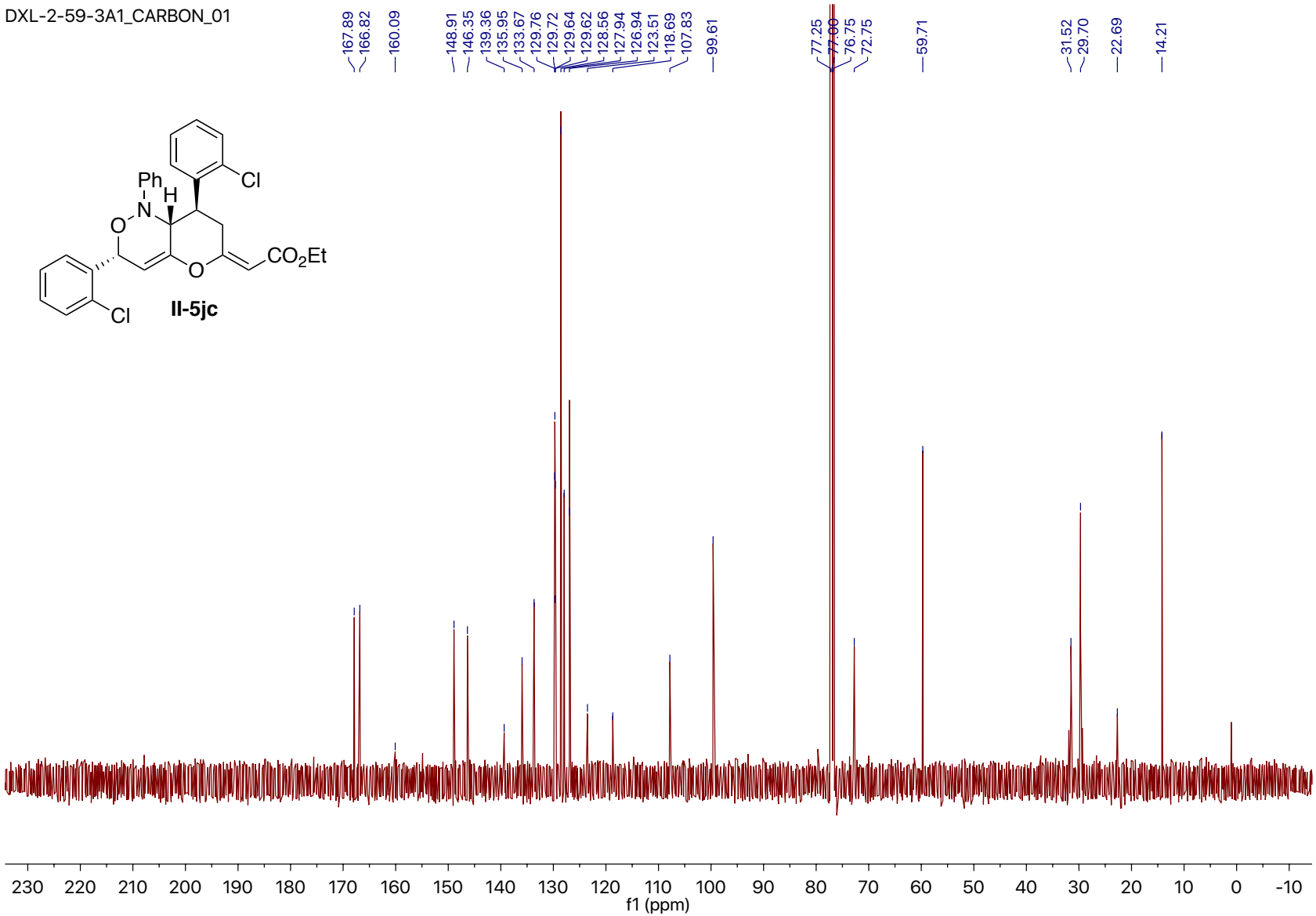
DXL-2-59-3A1_CARBON_01
167.89
166.82
160.09
148.91
146.35
139.36
135.95
133.67
129.76
129.72
129.64
129.62
128.56
127.94
126.94
123.51
118.69
107.83
99.61
77.25
77.00
76.75
72.75
59.71
31.52
29.70
22.69
14.21
Ph
H
N
O
Cl
O
O
CO2Et
Cl
II-5jc
230 220 210 200 190 180 170 160 150 140 130 120 110 100 90 80 70 60 50 40 30 20 10 0 -10
f1 (ppm)

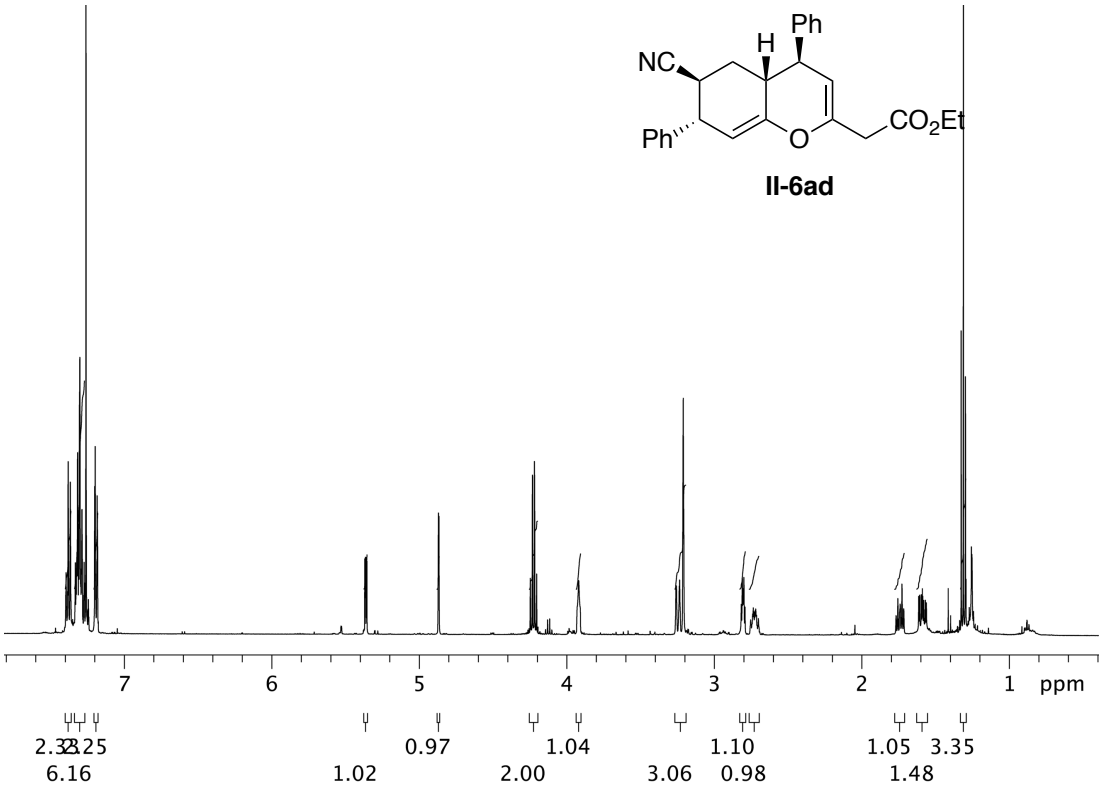
NC
H
Ph
Ph
O
CO2Et
II-6ad
7
6
5
4
3
2
1
ppm
2.32
3.25
6.16
1.02
0.97
2.00
1.04
3.06
1.10
0.98
1.05
3.35
1.48

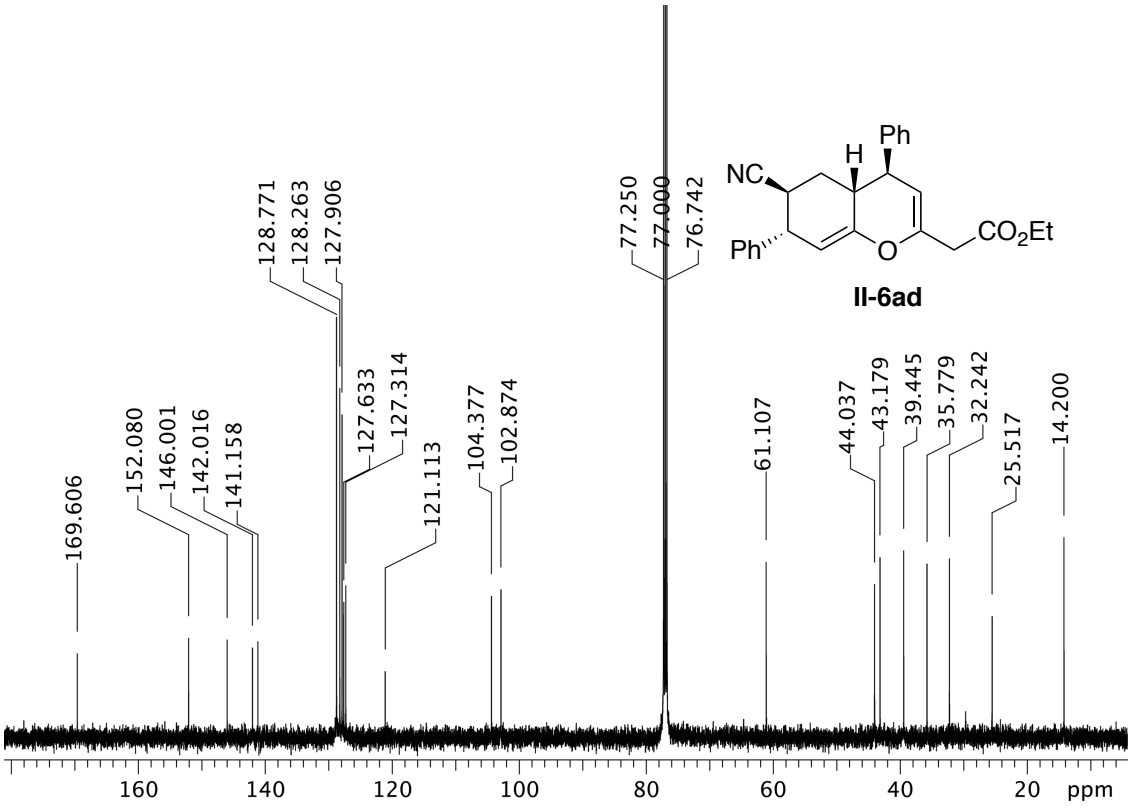
NC
H
Ph
Ph
O
CO2Et
II-6ad
169.606
152.080
146.001
142.016
141.158
128.771
128.263
127.906
127.633
127.314
121.113
104.377
102.874
77.250
77.000
76.742
61.107
44.037
43.179
39.445
35.779
32.242
25.517
14.200
160
140
120
100
80
60
40
20
ppm

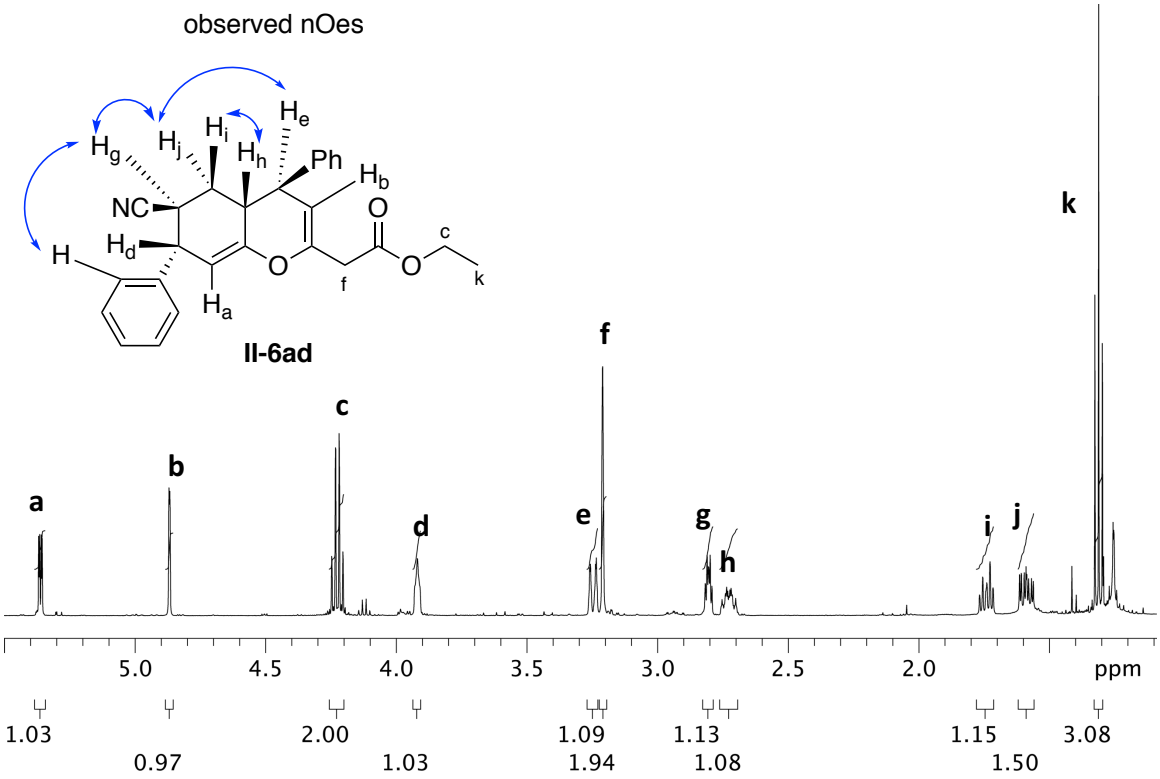
observed nOes
II-6ad
a
b
c
d
e
f
g
h
i
j
k
5.0
4.5
4.0
3.5
3.0
2.5
2.0
ppm
1.03
0.97
2.00
1.03
1.09
1.94
1.13
1.08
1.15
1.50
3.08

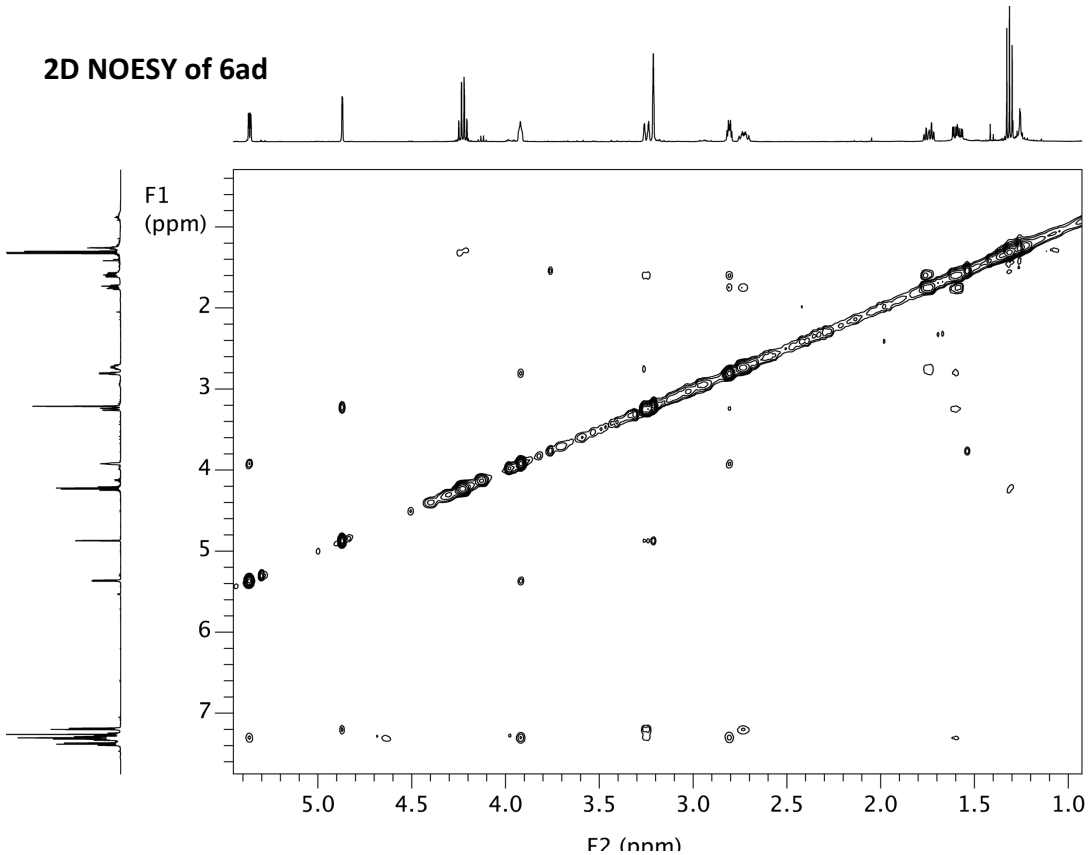
2D NOESY of 6ad
F1
(ppm)
2
3
4
5
6
7
5.0
4.5
4.0
3.5
3.0
2.5
2.0
1.5
1.0
F2 (ppm)

Crystal Structure:

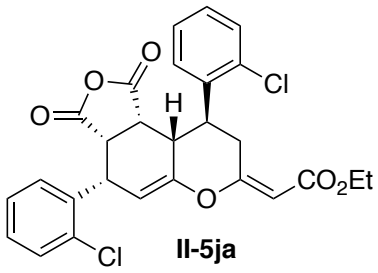

II-5ja

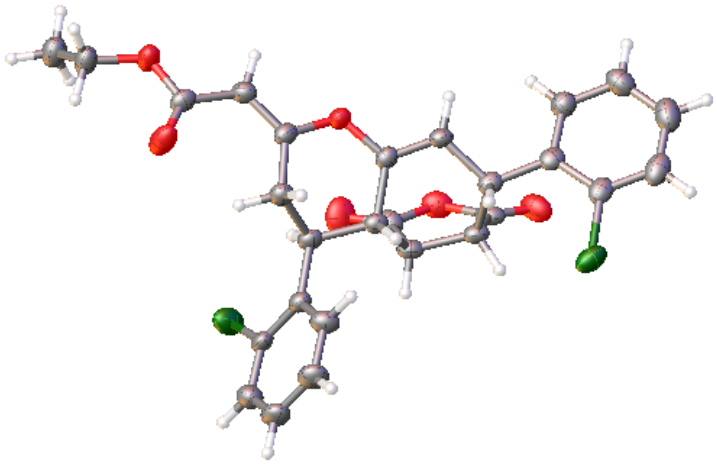

Table 1: Fractional Atomic Coordinates (×10⁴) and Equivalent Isotropic Displacement Parameters (Å²×10³) for **BB315a**. U_{eq} is defined as 1/3 of the trace of the orthogonalised U_{ij}.

Atom	x	y	z	U_{eq}
Cl1	7945.3(18)	5989.4(15)	5572.8(4)	52.7(4)
Cl2	1800.9(18)	7783.2(13)	7817.9(5)	46.4(4)
O1	8918(4)	9836(3)	6731.9(10)	34.7(8)
O2	8746(5)	5987(3)	7324.1(11)	41.3(9)
O3	7152(5)	5791(3)	7918.1(11)	46.5(9)
O4	9596(6)	6286(4)	6666.8(13)	57.7(11)
O5	12500(5)	11451(4)	5692.5(10)	43.1(9)
O6	9648(5)	11053(4)	5463.1(11)	54.3(11)
C1	8940(6)	10098(4)	6314.1(15)	30.1(11)
C2	7336(7)	9605(5)	6073.8(15)	33.9(12)
C3	6894(6)	8181(4)	6195.8(14)	30.4(11)
C4	6356(6)	8201(4)	6655.3(14)	26.8(11)
C5	6437(7)	6865(4)	6880.7(15)	30.1(11)
C6	8408(8)	6371(5)	6919.3(16)	38.9(13)
C7	7193(7)	6187(5)	7572.7(17)	35.5(12)
C8	5782(7)	6943(4)	7331.8(14)	29.8(11)
C9	5641(7)	8404(4)	7487.6(14)	29.4(11)
C10	7216(6)	9201(4)	7311.9(14)	29.2(11)
C11	7485(6)	9140(4)	6908.7(14)	27.9(11)
C12	10421(7)	10746(5)	6180.4(15)	32.9(11)
C13	10739(7)	11091(5)	5747.9(16)	32.2(11)
C14	13115(7)	11751(6)	5276.8(15)	41.6(13)
C15	14862(7)	11045(6)	5198.3(16)	47.7(15)
C16	5410(7)	7622(5)	5916.4(14)	30.5(12)
C17	5758(7)	6668(5)	5618.9(15)	33.8(12)
C18	4417(8)	6238(6)	5346.5(16)	44.4(14)
C19	2662(8)	6741(6)	5369.7(17)	46.3(14)
C20	2274(8)	7688(6)	5663.2(17)	45.4(14)
C21	3617(7)	8111(5)	5927.9(16)	38.9(13)
C22	5371(7)	8507(4)	7951.0(15)	31.3(11)
C23	3652(7)	8242(5)	8130.2(16)	35.8(12)
C24	3371(9)	8329(5)	8551.4(18)	47.0(15)
C25	4788(9)	8702(5)	8809.6(18)	52.6(16)
C26	6494(8)	8978(5)	8642.5(16)	46.4(14)
C27	6769(7)	8876(5)	8218.8(15)	36.6(12)

Table 2: Anisotropic Displacement Parameters (×10⁴) **BB315a**. The anisotropic displacement factor exponent takes the form: $-2\pi^2[h^2a^{*2} \times U_{11} + \ldots + 2hka^* \times b^* \times U_{12}]$

Atom	U_{11}	U_{22}	U_{33}	U_{23}	U_{13}	U_{12}
Cl1	35.3(8)	64.7(9)	58.0(9)	-24.0(7)	5.8(7)	0.6(7)
Cl2	31.5(7)	39.2(7)	68.6(10)	1.2(7)	6.7(7)	-4.5(6)
O1	30.2(19)	43(2)	30.8(19)	-2.1(16)	2.3(15)	-11.6(17)
O2	36(2)	38(2)	50(2)	-1.1(17)	-9.5(17)	9.4(17)
O3	59(2)	41(2)	39(2)	2.8(17)	-14.8(19)	1.9(19)
O4	46(2)	67(3)	60(3)	6(2)	10(2)	25(2)
O5	30.3(19)	66(2)	33.3(19)	3.5(17)	1.0(16)	-11.3(17)
O6	35(2)	81(3)	47(2)	21(2)	-7.6(19)	-16(2)

Atom	U_{11}	U_{22}	U_{33}	U_{23}	U_{13}	U_{12}
C1	27(3)	27(3)	36(3)	-2(2)	3(2)	-1(2)
C2	28(3)	39(3)	34(3)	0(2)	-4(2)	-4(2)
C3	21(2)	32(3)	38(3)	-2(2)	-2(2)	-3(2)
C4	21(2)	25(2)	34(3)	-3(2)	-1(2)	1(2)
C5	28(3)	24(3)	39(3)	-4(2)	-7(2)	0(2)
C6	45(3)	31(3)	40(3)	2(2)	-5(3)	4(3)
C7	38(3)	25(3)	44(3)	-4(2)	-13(3)	-2(2)
C8	27(3)	25(3)	38(3)	-4(2)	-3(2)	-3(2)
C9	27(3)	24(3)	38(3)	3(2)	0(2)	2(2)
C10	26(3)	27(3)	34(3)	-3(2)	-2(2)	-5(2)
C11	23(2)	27(3)	33(3)	2(2)	1(2)	1(2)
C12	32(3)	33(3)	34(3)	-1(2)	-6(2)	-3(2)
C13	22(3)	32(3)	43(3)	1(2)	0(2)	1(2)
C14	31(3)	59(4)	35(3)	8(2)	2(2)	-3(3)
C15	38(3)	65(4)	40(3)	5(3)	3(3)	-2(3)
C16	27(3)	32(3)	32(3)	1(2)	0(2)	-7(2)
C17	28(3)	40(3)	32(3)	0(2)	3(2)	-12(2)
C18	47(3)	49(3)	37(3)	-6(3)	-2(3)	-11(3)
C19	38(3)	58(4)	43(3)	0(3)	-12(3)	-14(3)
C20	32(3)	55(3)	49(3)	0(3)	-13(3)	-4(3)
C21	34(3)	38(3)	45(3)	-4(2)	-9(3)	-1(2)
C22	32(3)	21(2)	41(3)	-1(2)	2(2)	1(2)
C23	38(3)	24(3)	45(3)	1(2)	8(3)	3(2)
C24	52(4)	33(3)	56(4)	7(3)	18(3)	5(3)
C25	70(4)	46(4)	42(3)	2(3)	11(3)	7(3)
C26	56(4)	43(3)	40(3)	-5(2)	-8(3)	3(3)
C27	36(3)	36(3)	38(3)	3(2)	0(2)	1(3)

Table 3: Bond Lengths in Å for **BB315a**.

Atom	Atom	Length/Å
Cl1	C17	1.741(5)
Cl2	C23	1.745(6)
O1	C1	1.373(5)
O1	C11	1.383(5)
O2	C6	1.385(6)
O2	C7	1.400(6)
O3	C7	1.185(6)
O4	C6	1.190(6)
O5	C13	1.344(6)
O5	C14	1.446(6)
O6	C13	1.214(6)
C1	C2	1.488(6)
C1	C12	1.334(6)
C2	C3	1.535(7)
C3	C4	1.532(6)
C3	C16	1.517(6)
C4	C5	1.542(6)
C4	C11	1.501(6)
C5	C6	1.524(8)
C5	C8	1.533(7)
C7	C8	1.499(7)
C8	C9	1.573(6)
C9	C10	1.513(6)
C9	C22	1.510(7)
C10	C11	1.316(6)
C12	C13	1.457(7)
C14	C15	1.482(7)
C16	C17	1.388(7)
C16	C21	1.396(7)
C17	C18	1.384(7)
C18	C19	1.377(8)
C19	C20	1.380(8)
C20	C21	1.367(7)
C22	C23	1.404(7)
C22	C27	1.386(7)
C23	C24	1.376(7)
C24	C25	1.378(8)
C25	C26	1.381(8)
C26	C27	1.385(7)

Table 4: Bond Angles in ° for **BB315a**.

Atom	Atom	Atom	Angle/°
C1	O1	C11	120.8(4)
C6	O2	C7	110.8(4)
C13	O5	C14	118.4(4)
O1	C1	C2	115.8(4)
C12	C1	O1	115.0(4)
C12	C1	C2	129.2(4)
C1	C2	C3	110.4(4)
C4	C3	C2	106.8(4)
C16	C3	C2	110.5(4)
C16	C3	C4	113.4(4)
C3	C4	C5	115.7(4)
C11	C4	C3	113.2(4)
C11	C4	C5	106.4(4)
C6	C5	C4	111.4(4)
C6	C5	C8	103.4(4)
C8	C5	C4	113.0(4)
O2	C6	C5	109.7(4)
O4	C6	O2	119.7(5)
O4	C6	C5	130.6(5)
O2	C7	C8	109.3(4)
O3	C7	O2	120.6(5)
O3	C7	C8	130.1(5)
C5	C8	C9	111.8(4)
C7	C8	C5	104.6(4)
C7	C8	C9	111.3(4)
C10	C9	C8	109.7(4)
C22	C9	C8	112.9(4)
C22	C9	C10	115.6(4)
C11	C10	C9	117.2(4)
O1	C11	C4	120.9(4)
C10	C11	O1	119.7(4)
C10	C11	C4	119.1(4)
C1	C12	C13	123.8(5)
O5	C13	C12	110.1(4)
O6	C13	O5	122.1(4)
O6	C13	C12	127.8(5)
O5	C14	C15	108.7(4)
C17	C16	C3	122.9(4)
C17	C16	C21	116.0(5)
C21	C16	C3	121.0(4)
C16	C17	Cl1	120.2(4)
C18	C17	Cl1	117.7(4)
C18	C17	C16	122.1(5)
C19	C18	C17	120.1(5)
C18	C19	C20	119.1(5)
C21	C20	C19	120.1(5)
C20	C21	C16	122.6(5)
C23	C22	C9	120.7(4)
C27	C22	C9	122.6(4)
C27	C22	C23	116.7(4)
C22	C23	Cl2	120.1(4)
C24	C23	Cl2	118.2(4)
C24	C23	C22	121.7(5)
C23	C24	C25	120.2(6)
C24	C25	C26	119.5(5)
C25	C26	C27	120.0(5)
C26	C27	C22	121.9(5)

Table 5: Hydrogen Fractional Atomic Coordinates ($\times 10^4$) and Equivalent Isotropic Displacement Parameters ($Å^2 \times 10^3$) for **BB315a**. U_{eq} is defined as 1/3 of the trace of the orthogonalised U_{ij}.

Atom	x	y	z	U_{eq}
H2A	7612	9648	5773	41
H2B	6254	10169	6129	41
H3	8032	7639	6163	36
H4	5053	8511	6670	32
H5	5682	6206	6726	36
H8	4557	6504	7359	36
H9	4499	8770	7360	35
H10	7978	9723	7485	35
H12	11320	10996	6379	39
H14A	13306	12710	5247	50
H14B	12174	11473	5073	50
H15A	15830	11408	5376	72
H15B	15212	11151	4907	72
H15C	14700	10109	5260	72
H18	4707	5594	5143	53
H19	1732	6440	5186	56

Atom	x	y	z	U_{eq}
H20	1071	8047	5681	55
H21	3319	8764	6128	47
H24	2198	8131	8665	56
H25	4594	8768	9100	63
H26	7477	9238	8818	56
H27	7951	9064	8108	44

Crystal Structure:

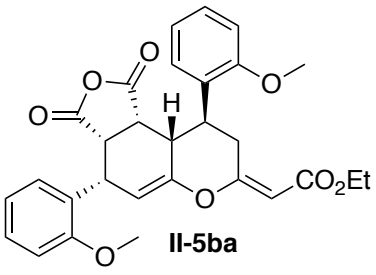

II-5ba

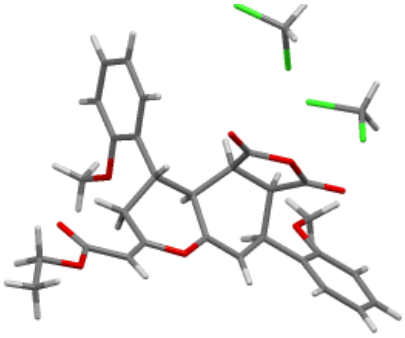

Table 1 Crystal data and structure refinement for BB715a.

Identification code	BB715a
Empirical formula	$C_{31}H_{32}Cl_4O_8$
Formula weight	674.36
Temperature/K	173.0
Crystal system	orthorhombic
Space group	$P2_12_12_1$
a/Å	10.9256(4)
b/Å	14.7077(4)
c/Å	19.6645(8)
α/°	90
β/°	90
γ/°	90
Volume/Å^3	3159.90(19)
Z	4
ρ_{calc}g/cm^3	1.418
μ/mm^{-1}	3.823
F(000)	1400.0
Crystal size/mm^3	0.256 × 0.044 × 0.043
Radiation	CuKα (λ = 1.54178)
2Θ range for data collection/°	7.506 to 143.998
Index ranges	-12 ≤ h ≤ 13, -18 ≤ k ≤ 15, -24 ≤ l ≤ 23
Reflections collected	15359
Independent reflections	5984 [R_{int} = 0.0820, R_{sigma} = 0.0958]
Data/restraints/parameters	5984/0/391
Goodness-of-fit on F^2	1.011
Final R indexes [I>=2σ (I)]	R_1 = 0.0631, wR_2 = 0.1459
Final R indexes [all data]	R_1 = 0.0953, wR_2 = 0.1646
Largest diff. peak/hole / e Å^{-3}	0.31/-0.34
Flack parameter	0.028(18)

Table 2 Fractional Atomic Coordinates (×10^4) and Equivalent Isotropic Displacement Parameters (Å^2×10^3) for BB715a. U_{eq} is defined as 1/3 of of the trace of the orthogonalised U_{IJ} tensor.

Atom	***x***	***y***	***z***	**U(eq)**
O1	947(4)	5039(3)	5329(3)	50.6(13)

O2	2464(4)	5923(3)	5678(2)	37.9(10)
O3	4236(5)	6601(3)	5876(3)	54.6(14)
O4	2652(4)	3070(3)	6452.2(19)	30.3(9)
O5	6982(4)	5112(3)	4977(2)	36(1)
O6	-1(4)	975(3)	6031(2)	41.9(11)
O7	-395(4)	1148(3)	7140(2)	40.2(11)
O8	3187(4)	1987(3)	4167(2)	38.7(10)
C1	2019(6)	5161(4)	5344(3)	33.2(13)
C2	3729(6)	5962(4)	5641(4)	35.5(14)
C3	4222(5)	5141(4)	5274(3)	28.1(12)
C4	3052(5)	4628(4)	5045(3)	27.6(12)
C5	3041(6)	3611(4)	5249(3)	26.7(12)
C6	3383(5)	3561(4)	6003(3)	27.6(12)
C7	4306(5)	4020(4)	6248(3)	27.1(12)
C8	5069(5)	4559(4)	5746(3)	27.0(12)
C9	6093(6)	5107(4)	6058(3)	30.2(13)
C10	6148(6)	5351(5)	6735(3)	40.9(16)
C11	7134(7)	5833(6)	6997(3)	54(2)
C12	8081(7)	6092(5)	6574(4)	50.1(19)
C13	8047(7)	5882(5)	5894(4)	41.8(15)
C14	7067(6)	5387(4)	5631(3)	30.7(13)
C15	7961(7)	5344(6)	4527(3)	47.9(17)
C16	1871(6)	3094(4)	5099(3)	30.5(13)
C17	1952(6)	2185(4)	5481(3)	32.3(13)
C18	1896(6)	2394(4)	6229(3)	29.3(12)
C19	1160(6)	2036(4)	6698(3)	30.0(13)
C20	232(6)	1338(4)	6562(3)	30.6(13)
C21	-1335(7)	457(5)	7070(4)	45.8(17)
C22	-1762(10)	201(7)	7752(4)	83(4)
C23	1566(6)	3021(4)	4338(3)	33.3(14)
C24	2224(6)	2469(4)	3889(3)	34.2(14)
C25	1902(7)	2426(5)	3205(3)	41.9(16)
C26	932(8)	2933(5)	2970(3)	48.1(18)
C27	276(7)	3490(6)	3395(4)	50.9(19)
C28	599(6)	3514(5)	4077(3)	39.4(15)
C29	3809(7)	1373(5)	3731(3)	42.9(16)
Cl3S	2579(3)	6516.5(19)	3847.6(16)	91.3(9)
Cl4S	128(3)	6145(2)	3323.0(14)	94.8(10)
C2S	1095(12)	6869(9)	3708(11)	158(9)
Cl1S	6040(3)	6352(2)	3172.1(13)	107.8(13)

Cl2S	5652(2)	7243.6(16)	4477.3(14)	73.9(7)
C1S	6322(9)	7341(7)	3651(5)	72(3)

Table 3 Anisotropic Displacement Parameters ($Å^2×10^3$) for BB715a. The Anisotropic displacement factor exponent takes the form: $-2π^2[h^2a^{*2}U_{11}+2hka^*b^*U_{12}+…]$.

Atom	U_{11}	U_{22}	U_{33}	U_{23}	U_{13}	U_{12}
O1	23(3)	47(3)	82(3)	-9(3)	1(2)	4(2)
O2	29(2)	34(2)	51(2)	-8(2)	7(2)	3.7(19)
O3	43(3)	33(2)	88(4)	-17(3)	-3(3)	-3(2)
O4	30(2)	31(2)	29.9(18)	2.7(17)	-1.3(16)	-10.6(18)
O5	27(2)	44(2)	37(2)	-1.8(19)	5.3(18)	-3(2)
O6	42(3)	45(3)	39(2)	-2(2)	-1(2)	-15(2)
O7	38(3)	45(3)	37(2)	6(2)	-0.8(19)	-19(2)
O8	35(3)	45(3)	36(2)	-8(2)	-4.2(18)	6(2)
C1	29(4)	33(3)	37(3)	4(3)	-2(3)	3(3)
C2	28(3)	29(3)	50(3)	1(3)	-3(3)	1(3)
C3	21(3)	31(3)	32(3)	-4(2)	2(2)	-2(2)
C4	24(3)	30(3)	29(2)	1(2)	-3(2)	-1(3)
C5	25(3)	23(3)	32(3)	-1(2)	0(2)	-1(2)
C6	27(3)	24(3)	32(3)	-5(2)	3(2)	2(2)
C7	26(3)	31(3)	25(2)	-3(2)	1(2)	-1(3)
C8	22(3)	27(3)	32(3)	-6(2)	-1(2)	-1(2)
C9	28(3)	25(3)	37(3)	-8(3)	2(2)	-1(3)
C10	31(4)	49(4)	43(3)	-12(3)	6(3)	-11(3)
C11	44(5)	76(5)	42(4)	-21(4)	3(3)	-26(4)
C12	33(4)	60(5)	57(4)	-20(4)	-4(3)	-19(4)
C13	29(4)	43(4)	54(4)	-5(3)	9(3)	-2(3)
C14	22(3)	30(3)	39(3)	-4(3)	0(2)	0(3)
C15	37(4)	65(5)	42(3)	-4(3)	10(3)	-3(4)
C16	21(3)	37(3)	33(3)	0(2)	1(2)	-4(3)
C17	31(3)	29(3)	37(3)	-4(2)	3(3)	-9(3)
C18	25(3)	26(3)	37(3)	1(2)	-6(2)	-1(3)
C19	32(3)	33(3)	26(3)	4(2)	-4(2)	1(3)
C20	28(3)	31(3)	32(3)	8(3)	-3(2)	0(3)
C21	41(4)	43(4)	53(4)	7(3)	8(3)	-11(3)
C22	102(8)	99(8)	48(4)	6(5)	6(5)	-64(7)

C23	28(3)	34(3)	38(3)	-3(3)	-3(2)	-7(3)
C24	32(4)	32(3)	39(3)	1(3)	0(3)	-9(3)
C25	44(4)	44(4)	38(3)	2(3)	0(3)	-10(3)
C26	57(5)	56(4)	31(3)	-2(3)	-16(3)	-8(4)
C27	47(5)	52(4)	54(4)	4(4)	-17(3)	2(4)
C28	35(4)	37(3)	47(3)	-1(3)	-9(3)	-2(3)
C29	40(4)	43(4)	45(4)	-11(3)	3(3)	-2(3)
Cl3S	83.8(19)	78.9(17)	111(2)	12.6(16)	8.7(16)	39.1(15)
Cl4S	120(2)	89(2)	75.3(15)	-3.9(14)	20.0(15)	-40.5(18)
C2S	83(9)	80(9)	310(30)	-70(12)	-82(12)	47(7)
Cl1S	145(3)	118(2)	60.8(13)	1.9(15)	-9.0(15)	-77(2)
Cl2S	73.3(16)	60.3(12)	88.1(16)	8.5(12)	11.5(12)	-12.9(12)
C1S	72(7)	68(6)	76(6)	27(5)	-6(5)	-19(5)

Table 4 Bond Lengths for BB715a.

Atom	**Length/Å**	**Atom**	**Length/Å**
O1-C1	1.184(8)	C9-C10	1.380(9)
O2-C1	1.387(7)	C9-C14	1.416(8)
O2-C2	1.385(8)	C10-C11	1.389(10)
O3-C2	1.184(8)	C11-C12	1.380(10)
O4-C6	1.393(7)	C12-C13	1.374(10)
O4-C18	1.365(7)	C13-C14	1.395(9)
O5-C14	1.351(7)	C16-C17	1.535(8)
O5-C15	1.430(8)	C16-C23	1.538(8)
O6-C20	1.200(8)	C17-C18	1.504(8)
O7-C20	1.357(7)	C18-C19	1.332(9)
O7-C21	1.451(8)	C19-C20	1.467(9)
O8-C24	1.381(8)	C21-C22	1.470(10)
O8-C29	1.419(8)	C23-C24	1.398(9)
C1-C4	1.495(8)	C23-C28	1.380(9)
C2-C3	1.507(9)	C24-C25	1.393(9)
C3-C4	1.551(8)	C25-C26	1.376(11)
C3-C8	1.564(8)	C26-C27	1.373(11)
C4-C5	1.548(7)	C27-C28	1.387(10)
C5-C6	1.529(7)	Cl3S-C2S	1.724(12)
C5-C16	1.516(8)	Cl4S-C2S	1.680(13)
C6-C7	1.306(8)	Cl1S-C1S	1.759(11)
C7-C8	1.516(8)	Cl2S-C1S	1.787(10)

C8-C9 1.509(8)

Table 5 Bond Angles for BB715a.

Atom	Angle/˚	Atom	Angle/˚
C2-O2-C1	111.1(5)	C12-C11-C10	119.9(6)
C18-O4-C6	121.3(4)	C13-C12-C11	120.3(7)
C14-O5-C15	117.8(5)	C12-C13-C14	119.9(7)
C20-O7-C21	114.9(5)	O5-C14-C9	115.1(5)
C24-O8-C29	116.9(5)	O5-C14-C13	124.2(6)
O1-C1-O2	118.7(6)	C13-C14-C9	120.6(6)
O1-C1-C4	131.1(6)	C5-C16-C17	107.1(5)
O2-C1-C4	110.2(5)	C5-C16-C23	114.0(5)
O2-C2-C3	110.4(5)	C17-C16-C23	115.3(5)
O3-C2-O2	118.7(6)	C18-C17-C16	107.3(5)
O3-C2-C3	130.9(6)	O4-C18-C17	116.0(5)
C2-C3-C4	103.5(5)	C19-C18-O4	115.5(5)
C2-C3-C8	111.5(5)	C19-C18-C17	128.3(6)
C4-C3-C8	113.2(5)	C18-C19-C20	124.6(5)
C1-C4-C3	104.7(5)	O6-C20-O7	122.0(6)
C1-C4-C5	113.4(5)	O6-C20-C19	128.0(6)
C5-C4-C3	113.6(5)	O7-C20-C19	109.9(5)
C6-C5-C4	107.3(4)	O7-C21-C22	108.4(6)
C16-C5-C4	116.2(5)	C24-C23-C16	122.9(6)
C16-C5-C6	111.7(5)	C28-C23-C16	119.4(6)
O4-C6-C5	120.0(5)	C28-C23-C24	117.6(6)
C7-C6-O4	118.4(5)	O8-C24-C23	116.1(5)
C7-C6-C5	121.4(5)	O8-C24-C25	123.5(6)
C6-C7-C8	117.1(5)	C25-C24-C23	120.5(6)
C7-C8-C3	110.3(5)	C26-C25-C24	119.6(7)
C9-C8-C3	112.8(5)	C27-C26-C25	121.5(6)
C9-C8-C7	115.0(5)	C26-C27-C28	118.1(7)
C10-C9-C8	124.3(6)	C23-C28-C27	122.7(7)
C10-C9-C14	117.6(6)	Cl4S-C2S-Cl3S	118.2(7)
C14-C9-C8	118.1(5)	Cl1S-C1S-Cl2S	110.4(5)
C9-C10-C11	121.7(6)		

Table 6 Torsion Angles for BB715a.

A	B	C	D	Angle/˚	A	B	C	D	Angle/˚
O1	C1	C4	C3	-178.2(7)	C8	C3	C4	C1	116.7(5)
O1	C1	C4	C5	-53.8(9)	C8	C3	C4	C5	-7.6(6)
O2	C1	C4	C3	3.0(6)	C8	C9	C10	C11	178.0(7)
O2	C1	C4	C5	127.4(5)	C8	C9	C14	O5	-1.2(8)
O2	C2	C3	C4	4.1(6)	C8	C9	C14	C13	-179.0(6)
O2	C2	C3	C8	-117.9(6)	C9	C10	C11	C12	1.1(13)
O3	C2	C3	C4	-174.5(7)	C10	C9	C14	O5	178.5(6)
O3	C2	C3	C8	63.5(9)	C10	C9	C14	C13	0.7(9)
O4	C6	C7	C8	-179.0(5)	C10	C11	C12	C13	0.6(13)
O4	C18	C19	C20	176.6(5)	C11	C12	C13	C14	-1.5(12)
O8	C24	C25	C26	-179.6(6)	C12	C13	C14	O5	-176.7(7)
C1	O2	C2	O3	176.4(6)	C12	C13	C14	C9	0.9(10)
C1	O2	C2	C3	-2.3(7)	C14	C9	C10	C11	-1.7(11)
C1	C4	C5	C6	-70.7(6)	C15	O5	C14	C9	-177.7(6)
C1	C4	C5	C16	55.0(6)	C15	O5	C14	C13	0.0(9)
C2	O2	C1	O1	-179.5(6)	C16	C5	C6	O4	0.7(7)
C2	O2	C1	C4	-0.5(7)	C16	C5	C6	C7	-174.6(6)
C2	C3	C4	C1	-4.1(6)	C16	C17	C18	O4	-48.1(7)
C2	C3	C4	C5	-128.4(5)	C16	C17	C18	C19	128.2(7)
C2	C3	C8	C7	75.7(6)	C16	C23	C24	O8	-0.5(9)
C2	C3	C8	C9	-54.4(6)	C16	C23	C24	C25	179.6(6)
C3	C4	C5	C6	48.7(6)	C16	C23	C28	C27	179.4(6)
C3	C4	C5	C16	174.4(5)	C17	C16	C23	C24	-52.7(8)
C3	C8	C9	C10	108.1(7)	C17	C16	C23	C28	126.9(7)
C3	C8	C9	C14	-72.2(7)	C17	C18	C19	C20	0.2(11)
C4	C3	C8	C7	-40.5(6)	C18	O4	C6	C5	22.4(8)
C4	C3	C8	C9	-170.7(5)	C18	O4	C6	C7	-162.1(6)
C4	C5	C6	O4	129.1(5)	C18	C19	C20	O6	1.2(11)
C4	C5	C6	C7	-46.2(7)	C18	C19	C20	O7	-177.4(6)
C4	C5	C16	C17	-167.5(5)	C20	O7	C21	C22	169.2(7)
C4	C5	C16	C23	63.7(7)	C21	O7	C20	O6	1.8(9)
C5	C6	C7	C8	-3.6(8)	C21	O7	C20	C19	-179.4(5)
C5	C16	C17	C18	67.7(6)	C23	C16	C17	C18	-164.2(5)
C5	C16	C23	C24	71.8(8)	C23	C24	C25	C26	0.2(10)
C5	C16	C23	C28	-108.6(7)	C24	C23	C28	C27	-1.0(10)
C6	O4	C18	C17	3.0(8)	C24	C25	C26	C27	0.6(12)
C6	O4	C18	C19	-173.8(5)	C25	C26	C27	C28	-1.5(12)
C6	C5	C16	C17	-44.0(6)	C26	C27	C28	C23	1.7(12)

C6	C5	C16	C23	-172.9(5)	C28	C23	C24	O8	179.9(6)
C6	C7	C8	C3	48.7(7)	C28	C23	C24	C25	0.0(9)
C6	C7	C8	C9	177.7(5)	C29	O8	C24	C23	175.5(6)
C7	C8	C9	C10	-19.6(9)	C29	O8	C24	C25	-4.6(9)
C7	C8	C9	C14	160.1(5)					

Table 7 Hydrogen Atom Coordinates (Å×10^4) and Isotropic Displacement Parameters (Å^2×10^3) for BB715a.

Atom	***x***	***y***	***z***	**U(eq)**
H3	4693	5341	4865	34
H4	2994	4667	4538	33
H5	3713	3307	4990	32
H7	4491	4016	6720	33
H8	5471	4101	5444	32
H10	5495	5186	7028	49
H11	7158	5984	7467	65
H12	8758	6416	6755	60
H13	8691	6075	5603	50
H15A	8738	5131	4719	72
H15B	7990	6005	4469	72
H15C	7827	5053	4085	72
H16	1190	3445	5314	37
H17A	1263	1785	5350	39
H17B	2729	1872	5370	39
H19	1242	2247	7152	36
H21A	-997	-82	6833	55
H21B	-2026	697	6798	55
H22A	-1070	-23	8021	125
H22B	-2383	-277	7714	125
H22C	-2119	734	7977	125
H25	2350	2048	2901	50
H26	711	2897	2504	58
H27	-380	3850	3227	61
H28	136	3885	4377	47
H29A	4396	1016	3997	64
H29B	4245	1715	3379	64
H29C	3215	964	3517	64
H2SA	737	7034	4153	189

H2SB	1128	7432	3432	189
H1SA	5973	7875	3414	86
H1SB	7216	7434	3696	86

Experimental

Single crystals of $C_{31}H_{32}Cl_4O_8$ [BB715a] were used as received. A suitable crystal was selected and mounted using a small amount of paratone oil on a nylon loop on a 'Bruker APEX-II CCD' diffractometer. The crystal was kept at 173(2) K during data collection. Using Olex2 [1], the structure was solved with the olex2.solve [2] structure solution program using Charge Flipping and refined with the XL [3] refinement package using Least Squares minimization.

1. Dolomanov, O.V., Bourhis, L.J., Gildea, R.J, Howard, J.A.K. & Puschmann, H. (2009), J. Appl. Cryst. 42, 339-341.
2. Bourhis, L.J., Dolomanov, O.V., Gildea, R.J., Howard, J.A.K., Puschmann, H. (2015). Acta Cryst. A71, 59-75.
3. Sheldrick, G.M. (2008). Acta Cryst. A64, 112-122.

Crystal structure determination of [BB715a]

Crystal Data for $C_{31}H_{32}Cl_4O_8$ (M =674.36 g/mol): orthorhombic, space group $P2_12_12_1$ (no. 19), a = 10.9256(4) Å, b = 14.7077(4) Å, c = 19.6645(8) Å, V = 3159.90(19) Å^3, Z = 4, T = 173.0 K, μ(CuKα) = 3.823 mm^{-1}, *Dcalc* = 1.418 g/cm^3, 15359 reflections measured (7.506° ≤ 2Θ ≤ 143.998°), 5984 unique (R_{int} = 0.0820, R_{sigma} = 0.0958) which were used in all calculations. The final R_1 was 0.0631 (I > 2σ(I)) and wR_2 was 0.1646 (all data).

Refinement model description

Number of restraints - 0, number of constraints - unknown.
Details:
1. Fixed Uiso
 At 1.2 times of:
  All C(H) groups, All C(H,H) groups
 At 1.5 times of:
  All C(H,H,H) groups
2.a Ternary CH refined with riding coordinates:
 C3(H3), C4(H4), C5(H5), C8(H8), C16(H16)
2.b Secondary CH2 refined with riding coordinates:
 C17(H17A,H17B), C21(H21A,H21B), C2S(H2SA,H2SB), C1S(H1SA,H1SB)
2.c Aromatic/amide H refined with riding coordinates:
 C7(H7), C10(H10), C11(H11), C12(H12), C13(H13), C19(H19), C25(H25), C26(H26), C27(H27), C28(H28)
2.d Idealised Me refined as rotating group:
 C15(H15A,H15B,H15C), C22(H22A,H22B,H22C), C29(H29A,H29B,H29C)

This report has been created with Olex2, compiled on 2015.01.26 svn.r3150 for OlexSys. Please let us know if there are any errors or if you would like to have additional features.

REFERENCES

REFERENCES

(1) Mikhalchenko, O. S.; Korchagina, D. V.; Volcho, K. P.; Salakhutdinov, N. F. A practical way to synthesize chiral fluoro-containing polyhydro-2*H*-chromenes from monoterpenoids. *Beilstein Journal of Organic Chemistry* **2016,** *12*, 648.

(2) Patrusheva, O. S.; Zarubaev, V. V.; Shtro, A. A.; Orshanskaya, Y. R.; Boldyrev, S. A.; Ilyina, I. V.; Kurbakova, S. Y.; Korchagina, D. V.; Volcho, K. P.; Salakhutdinov, N. F. Anti-influenza activity of monoterpene-derived substituted hexahydro-2H-chromenes. *Bioorganic & Medicinal Chemistry* **2016,** *24* (21), 5158.

(3) Pavlova, A.; Mikhalchenko, O.; Rogachev, A.; Il'ina, I.; Korchagina, D.; Gatilov, Y.; Tolstikova, T.; Volcho, K.; Salakhutdinov, N. Synthesis and analgesic activity of stereoisomers of 2-(3(4)-hydroxy-4(3)-methoxyphenyl)-4,7-dimethyl-3,4,4a,5,8,8a-hexahydro -2H-chromene-4,8-diols. *Medicinal Chemistry Research* **2015,** *24* (11), 3821.

(4) Pavlova, A.; Patrusheva, O.; Il'ina, I.; Volcho, K.; Tolstikova, T.; Salakhutdinov, N. The Decisive Role of Mutual Arrangement of Hydroxy and Methoxy Groups in (3(4)-hydroxy-4(3)-methoxyphenyl)-4,7-dimethyl-3,4,4a,5,8,8a-hexahydro-2 H-chromene-4,8-diols in their Biological Activity. *Letters in Drug Design & Discovery* **2017,** *14* (5), 508.

(5) De Benneville, P. L.; Connor, R. The hydrogenation of coumarin and related compounds. *Journal of the American Chemical Society* **1940,** *62*, 283.

(6) Griffiths, D. V.; Wilcox, G. SYNTHETIC AND STEREOCHEMICAL STUDIES OF THE OCTAHYDRO-1-BENZOPYRAN SYSTEM. *Journal of the Chemical Society-Perkin Transactions 2* **1988**, 431.

(7) Hanaki, N.; Ishihara, K.; Kaino, M.; Naruse, Y.; Yamamoto, H. Stereospecific annulation of hydroxy vinyl ethers. Synthetic application to polyfunctionalized cyclic compounds. *Tetrahedron* **1996,** *52* (21), 7297.

(8) Ishihara, K.; Hanaki, N.; Yamamoto, H. HIGHLY REGIOSELECTIVE AND STEREOSELECTIVE ANNULATION ELIMINATION-REACTIONS OF 1-CYCLOALKENYL 3-HYDROXYPROPYL ETHERS. *Journal of the Chemical Society-Chemical Communications* **1995**, 1117.

(9) Jones, D. N.; Khan, M. A.; Mirza, S. M. The stereospecific synthesis of cis and trans 1-oxabicyclo 4,4,0 decanes and 9-methoxycarbonyl-1-oxabicyclo 4,3,0 nonanes. *Tetrahedron* **1999,** *55* (32), 9933.

(10) Wang, X.; Fang, T.; Tong, X. Enantioselective Amine-Catalyzed [4+2] Annulations of Allenoates and Oxo-dienes: An Asymmetric Synthesis of Dihydropyrans. *Angewandte Chemie International Edition* **2011,** *50* (23), 5361.

(11) Yang, H.-B.; Zhao, Y.-Z.; Sang, R.; Wei, Y.; Shi, M. Asymmetric Synthesis of Bioxindole-Substituted Hexahydrofuro 2,3-b furans via Hydroquinine Anthraquinone-1,4-diyl Diether-Catalyzed Domino Annulation of Acylidenoxindoles/Isatins, Acylidenoxindoles and Allenoates. *Advanced Synthesis & Catalysis* **2014,** *356* (18), 3799.

(12) Yao, W.; Dou, X.; Lu, Y. Highly Enantioselective Synthesis of 3,4-Dihydropyrans through a Phosphine-Catalyzed 4+2 Annulation of Allenones and beta,gamma-Unsaturated alpha-Keto Esters. *Journal of the American Chemical Society* **2015,** *137* (1), 54.

(13) Zhang, S.; Luo, Y.-C.; Hu, X.-Q.; Wang, Z.-Y.; Liang, Y.-M.; Xu, P.-F. Enantioselective Amine-Catalyzed 4+2 Annulations of Allene Ketones and 2,3-Dioxopyrrolidine Derivatives: Synthesis of 4H-Pyran Derivatives. *Journal of Organic Chemistry* **2015,** *80* (14), 7288.

(14) Ashtekar, K. D.; Staples, R. J.; Borhan, B. Development of a Formal Catalytic Asymmetric 4+2 Addition of Ethyl-2,3-butadienoate with Acyclic Enones. *Organic Letters* **2011,** *13* (21), 5732.

(15) Pei, C.-K.; Jiang, Y.; Wei, Y.; Shi, M. Enantioselective Synthesis of Highly Functionalized Phosphonate-Substituted Pyrans or Dihydropyrans Through Asymmetric 4+2 Cycloaddition of beta,gamma-Unsaturated alpha-Ketophosphonates with Allenic Esters. *Angewandte Chemie-International Edition* **2012,** *51* (45), 11328.

(16) Huang, G. T.; Lankau, T.; Yu, C. H. A Computational Study: Reactivity Difference between Phosphine- and Amine-Catalyzed Cycloadditions of Allenoates and Enones. *Journal of Organic Chemistry* **2014,** *79* (4), 1700.

(17) Evans, C. A.; Miller, S. J. Amine-catalyzed coupling of allenic esters to alpha,beta-unsaturated carbonyls. *Journal of the American Chemical Society* **2003,** *125* (41), 12394.

(18) Agopcan, S.; Celebi-Olcum, N.; Ucisik, M. N.; Sanyal, A.; Aviyente, V. Origins of the diastereoselectivity in hydrogen bonding directed Diels-Alder reactions of chiral dienes with achiral dienophiles: a computational study. *Organic & Biomolecular Chemistry* **2011,** *9* (23), 8079.

(19) Atta-ur-Rahman; Shah, Z. *Stereoselective Synthesis in Organic Chemistry*; 1 ed.; Springer-Verlag New York, 1993.

(20) Fisher, M. J.; Hehre, W. J.; Kahn, S. D.; Overman, L. E. FACE SELECTIVITY IN DIELS-ALDER REACTIONS OF CHIRAL DIENES CONTAINING ALLYLIC SUBSTITUENTS. *Journal of the American Chemical Society* **1988,** *110* (14), 4625.

(21) Galley, G.; Patzel, M. Chiral dienes from enantiomerically pure enones. Highly stereoselective intramolecular Diels-Alder reaction involving ethenesulfonates. *Journal of the Chemical Society-Perkin Transactions 1* **1996**, 2297.

(22) Gleiter, R.; Paquette, L. A. SIGMA-PI INTERACTION AS A CONTROLLING FACTOR IN THE STEREOSELECTIVITY OF ADDITION-REACTIONS. *Accounts of Chemical Research* **1983,** *16* (9), 328.

(23) Hamada, T.; Sato, H.; Hikota, M.; Yonemitsu, O. DIELS-ALDER REACTION OF CHIRAL DIENES - REMARKABLE EFFECT OF DIENOPHILE POLARITY UPON DIASTEREO FACE SELECTIVITY. *Tetrahedron Letters* **1989,** *30* (46), 6405.

(24) Nicolaou, K. C.; Snyder, S. A.; Montagnon, T.; Vassilikogiannakis, G. The Diels-Alder reaction in total synthesis. *Angewandte Chemie-International Edition* **2002,** *41* (10), 1668.

(25) Siegel, C.; Thornton, E. R. CONFORMATIONAL MODEL FOR ASYMMETRIC DIELS-ALDER REACTIONS WITH CHIRAL DIENES. *Tetrahedron Letters* **1988,** *29* (41), 5225.

(26) Tripathy, R.; Carroll, P. J.; Thornton, E. R. ASYMMETRIC DIELS-ALDER REACTIONS WITH CHIRAL DIENES - CONTROL OF FACIAL SELECTIVITY THROUGH HYDROGEN-BONDING. *Journal of the American Chemical Society* **1990,** *112* (18), 6743.

(27) Giuliano, R. M.; Jordan, A. D.; Gauthier, A. D.; Hoogsteen, K. DIASTEREOFACIAL SELECTIVITY OF DIELS-ALDER REACTIONS OF CARBOHYDRATE-DERIVED DIENES AND THEIR CARBOCYCLIC ANALOGS. *Journal of Organic Chemistry* **1993,** *58* (18), 4979.

(28) Jin, Z. C.; Yang, R. J.; Du, Y.; Tiwari, B.; Ganguly, R.; Chi, Y. R. Enantioselective Intramolecular Formal 2+4 Annulation of Acrylates and alpha,beta-Unsaturated Imines Catalyzed by Amino Acid Derived Phosphines. *Organic Letters* **2012,** *14* (12), 3226.

(29) Kirillov, N. F.; Gavrilov, A. G.; Slepukhin, P. A.; Vakhrin, M. I. Synthesis and structure of 4,9-diaryl-3a,4,9,9a-tetrahydrospiro- furo 3,4-f chromene-8,1'-cyclopent ane -1,3,7(9bH)-triones. *Russian Journal of Organic Chemistry* **2013,** *49* (5), 717.

(30) Hehre, W. J.; Ditchfield, R.; Pople, J. A. Self—Consistent Molecular Orbital Methods. XII. Further Extensions of Gaussian—Type Basis Sets for Use in Molecular Orbital Studies of Organic Molecules. *The Journal of Chemical Physics* **1972,** *56*, 2257.

(31) Hariharan, P. C.; Pople, J. A. The influence of polarization functions on molecular orbital hydrogenation energies. *Theoretica chimica acta* **1973,** *28* (3), 213.

(32) Becke, A. D. Density‐functional thermochemistry. III. The role of exact exchange. *The Journal of Chemical Physics* **1993,** *98*, 5648.

(33) Becke, A. D. A NEW MIXING OF HARTREE-FOCK AND LOCAL DENSITY-FUNCTIONAL THEORIES. *Journal of Chemical Physics* **1993,** *98* (2), 1372.

(34) Raghavachari, K. Perspective on "Density functional thermochemistry. III. The role of exact exchange" - Becke AD (1993) J Chem Phys 98:5648-52. *Theoretical Chemistry Accounts* **2000,** *103* (3-4), 361.

(35) Corey, E. J. Catalytic enantioselective Diels-Alder reactions: Methods, mechanistic fundamentals, pathways, and applications. *Angewandte Chemie-International Edition* **2002,** *41* (10), 1650.

(36) Lewars, E. G. *Computational Chemistry: Introduction to the Theory and Applications of Molecular and Quantum Mechanics, Second Edition*, 2011.

(37) Wise, K. E.; Wheeler, R. A. Donor-acceptor-assisted Diels-Alder reaction of anthracene and tetracyanoethylene. *Journal of Physical Chemistry A* **1999,** *103* (41), 8279.

(38) Lang, R. W.; Hasen, H. J. α-Allenic esters from α-phosphoranylidene esters and acid chlorides: ethyl 2,3-pentadienoate. *Org. Synth.* **1984,** *62*, 202.

(39) Vogel, A. I. *A Textbook of Organic Chemistry*; 3rd ed., 1957.

(40) Liang, G. A.; Shao, L. L.; Wang, Y.; Zhao, C. G.; Chu, Y. H.; Xiao, J.; Zhao, Y.; Li, X. K.; Yang, S. L. Exploration and synthesis of curcumin analogues with improved structural stability both in vitro and in vivo as cytotoxic agents. *Bioorganic & Medicinal Chemistry* **2009,** *17* (6), 2623.

(41) Weber, W. M.; Hunsaker, L. A.; Abcouwer, S. F.; Deck, L. M.; Vander Jagt, D. L. Anti-oxidant activities of curcumin and related enones. *Bioorganic & Medicinal Chemistry* **2005,** *13* (11), 3811.

(42) Weber, M.; Frey, W.; Peters, R. Catalytic Asymmetric Synthesis of Spirocyclic Azlactones by a Double Michael-Addition Approach. *Chemistry-a European Journal* **2013,** *19* (25), 8342.

(43) Adams, B. K.; Ferstl, E. M.; Davis, M. C.; Herold, M.; Kurtkaya, S.; Camalier, R. F.; Hollingshead, M. G.; Kaur, G.; Sausville, E. A.; Rickles, F. R.et al. Synthesis and biological evaluation of novel curcumin analogs as anti-cancer and anti-angiogenesis agents. *Bioorganic & Medicinal Chemistry* **2004,** *12* (14), 3871.

(44) Liang, G.; Li, X. K.; Chen, L.; Yang, S. L.; Wu, X. D.; Studer, E.; Gurley, E.; Hylemon, P. B.; Ye, F.; Li, Y.et al. Synthesis and anti-inflammatory activities of mono-carbonyl analogues of curcumin. *Bioorganic & Medicinal Chemistry Letters* **2008,** *18* (4), 1525.

(45) Dejongh, H. A. P.; Wynberg, H. SPIRANES .4. LONG RANGE SHIELDING EFFECTS BY BENZENE THOPPHENE AND FURAN RINGS IN PROTON MAGNETIC RESONANCE SPECTRA OF DIARYLSPIROKETONES. *Tetrahedron* **1965,** *21* (3), 515.

(46) Sebesta, R.; Pizzuti, M. G.; Minnaard, A. J.; Feringa, B. L. Copper-catalyzed enantioselective conjugate addition of organometallic reagents to acyclic dienones. *Advanced Synthesis & Catalysis* **2007,** *349* (11-12), 1931.

(47) Ahmed, A.; Dussault, P. H. 1,2,4-Trioxepanes: Redox-cleavable protection for carbonyl groups. *Organic Letters* **2004,** *6* (20), 3609.

(48) Silvanus, A. C.; Groombridge, B. J.; Andrews, B. I.; Kociok-Kohn, G.; Carbery, D. R. Stereoselective Synthesis of Cyclohexanones via Phase Transfer Catalyzed Double Addition of Nucleophiles to Divinyl Ketones. *Journal of Organic Chemistry* **2010,** *75* (21), 7491.

Chapter III: Organocatalytic Asymmetric Synthesis of Cyclohexenone and 4*H*-pyran Derivatives: A Divergent Approach

III-1. Introduction.

In continuing our effort on the applications of dihydropyran products from the formal [4+2] cycloaddition reaction between allenoate and enones, this chapter describes methodologies for the synthesis of both chiral cyclohexenones and chiral 4*H*-pyrans in parallel from the common intermediate—dihydropyrans. These methodologies were developed based on two observations in Chapter I. These are described in detail at the end of section **III-1**. Before that, a highlight of the importance and current methodologies related to chiral cyclohexenones and 4*H*-pyrans will be discussed.

Cyclohexenone is a widely used versatile building block in organic synthesis of a variety of chemical products such as fragrances and pharmaceuticals.[1] As a result, tremendous effort towards the preparation of cyclohexenones through methodologies, such as the Birch reduction and Robinson annulation, have been expanded.[2-4] Examples of the application of these cyclohexenones and their derivatives are the synthesis of

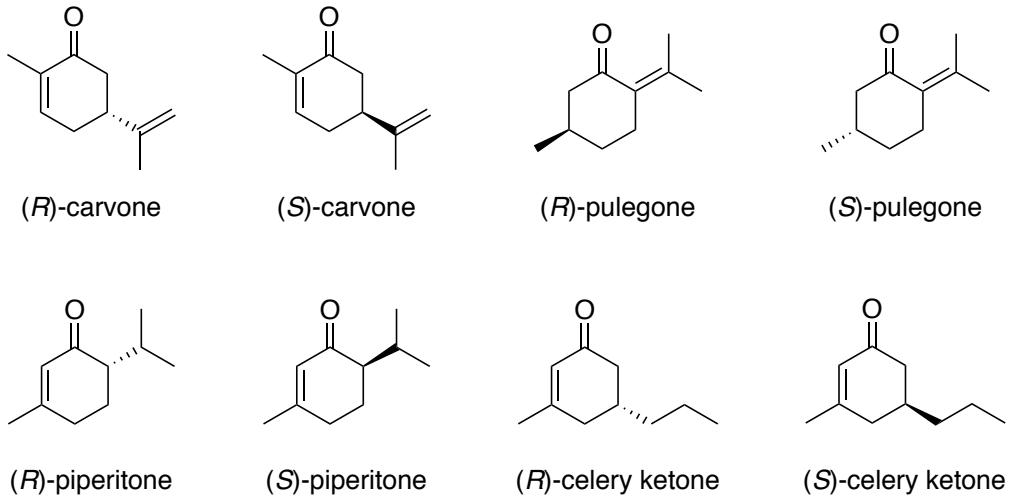

Figure III-1. Examples of readily available compounds from the chiral pool.

biologically active compounds, such as antibiotics and steroids.[5] For instance, the use of the Robinson annulation in preparation of the cyclohexenone core was a key step in the completion of the cortisone synthesis.[6] Due to the readily available chiral pools from nature, the chiral variants of cyclohex-2-enone are prominent building blocks with even more applications for the synthesis of natural product, biologically active compounds,[7-16] and compounds for food, flavor and fragrances manufactoring[17]. As we can see, a well exploited approach is based on the functionalization of those chiral compounds, such as carvone, pulegone, pipertione or celery ketone (see **Figure III-1** for structures).[18] The advantages for this strategy are the optically pure and inexpensive nature of the starting

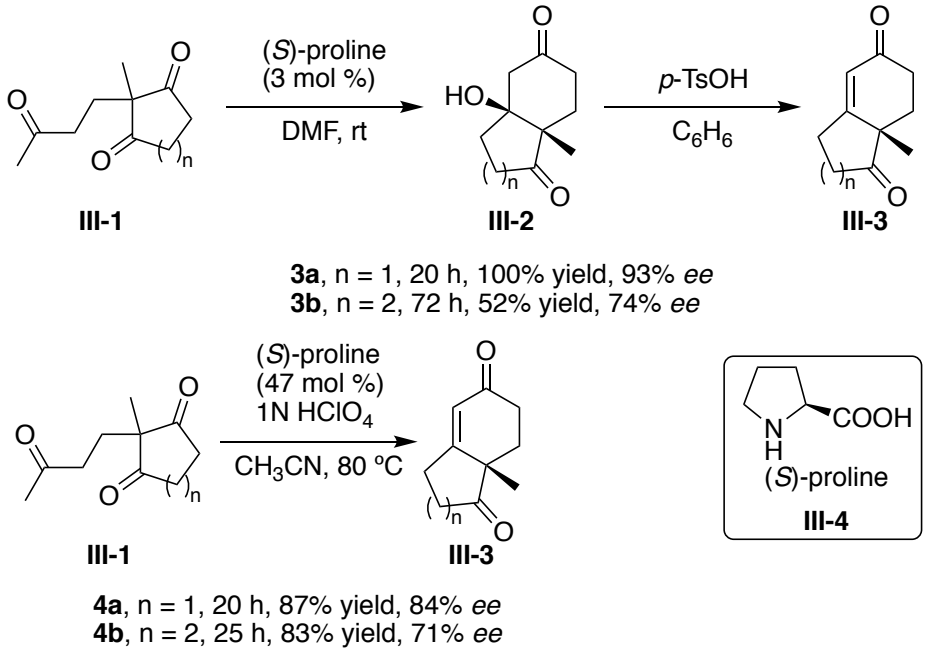

Scheme III-1. Examples of the Hajos-Parrish-Eder-Sauer-Wiechert reaction.

materials. However, the lack of flexibility with the limited number of different starting materials is an obvious limitation to meet the requirements of diversity necessary for specialized products synthesis. Therefore, much attention has been drawn to the development of practical and efficient methods to synthesize these enantio-enriched

a. Kinetic resolution:

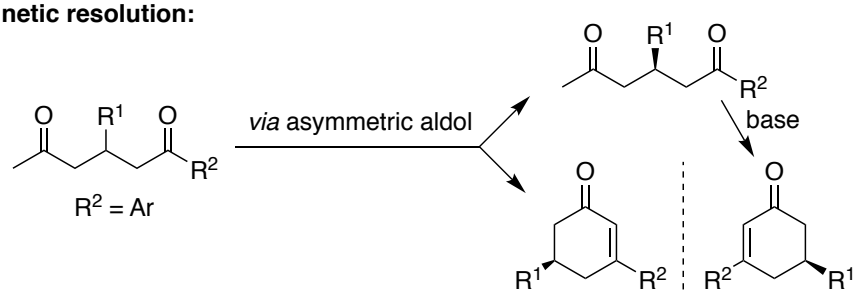

b. Synthesis of cyclohexenones:

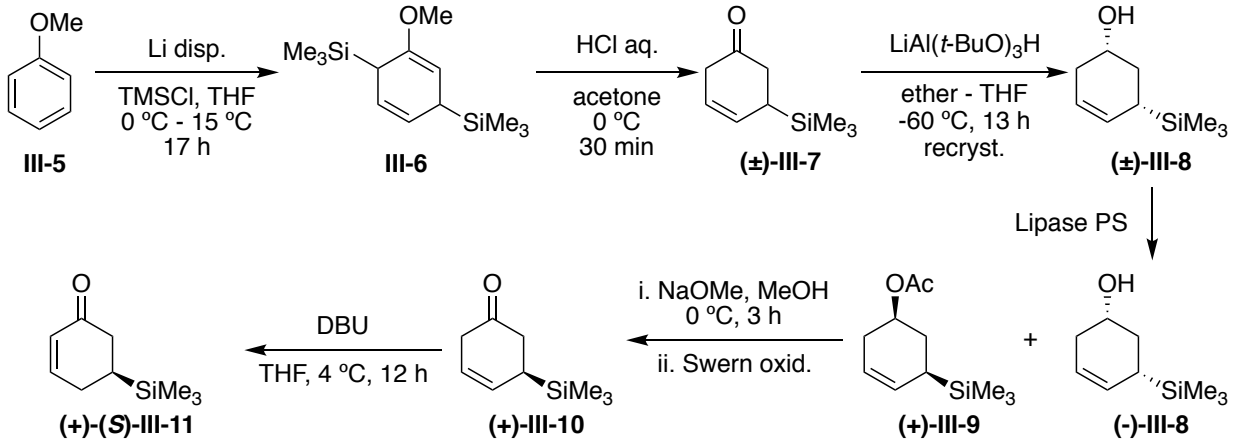

$[\alpha]^{20}_{D}$ = +5.6 (98.4% *ee*)

Scheme III-2. **a.** Organocatalytic kinetic resolution *via* intramolecular aldol reaction; **b.** An example of a multiple step synthesis of enantiomerically pure cyclohexenone.

cyclohex-2-enones.[19] One classical example is the Hajos-Parrish-Eder-Sauer-Wiechert reaction which was discovered in 1970's for the synthesis of chiral Wieland-Miescher ketones (see **Scheme III-1**).[19-23] Also, kinetic resolution[24,25] (**Scheme III-2 a)** and more articulated multiple step synthesis[26-28] (**Scheme III-2 b)** are common protocols to access these optically active cyclohexenones. Over the last decade, organocatalytic asymmetric approaches have enabled efficient and practical routes to chiral cyclohex-2-enones. Many new substrates have been generated using this transformation, together with new approaches developed for the purpose of both target- and diversity-oriented asymmetric synthesis.[19] As an exploration of the Hajos-Parrish-Eder-Sauer-Wiechert cyclization, a plethora of chiral amine catalysts have been employed for the enantioselective variant of

this reaction, such as cinchona derived amines (**Scheme III-3 a**),[29] Jørgensen's proline catalyst[18,30-32] (**Scheme III-3 b** and **c**) and salen-type diamines[33,34] (**Scheme III-3 d**). A few examples of chiral phosphoric acid-catalyzed annulation of chiral cyclohexenone formation have been reported as well.[35,36] Overall, the reaction is either an intramolecular aldolization or intermolecular Robinson annulation. For example, List's group has reported the aldolization of 2,6-heptanediones by utilizing a chiral primary amine as the catalyst.[29] By using diarylprolinol silyl ether, both Jørgensen[18] and Hayashi[32] have demonstrated the Michael-aldol-dehydration cascade reactions between α,β–unsaturated aldehydes and β–keto esters. Zhao et al. has reported this domino reaction

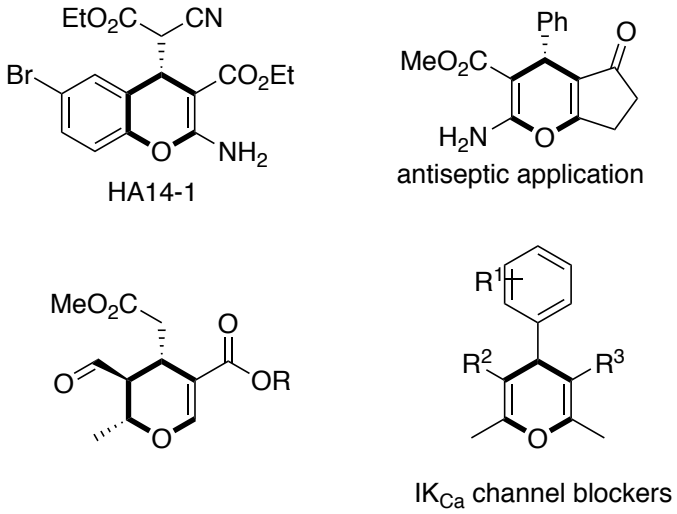

Figure III-2. 4*H*-pyrans in natural products and bioactive molecules.

catalyzed by chiral primary-secondary diamines.[34] A summary of these examples is shown in **Scheme III-3**.

Similar to cyclohexenone, 4*H*-pyran is also an important building block. 4*H*-pyran was first isolated and characterized in 1962 *via* pyrolysis of 2-acetoxy-3,4-dihydro-2*H*-pyran.[37]

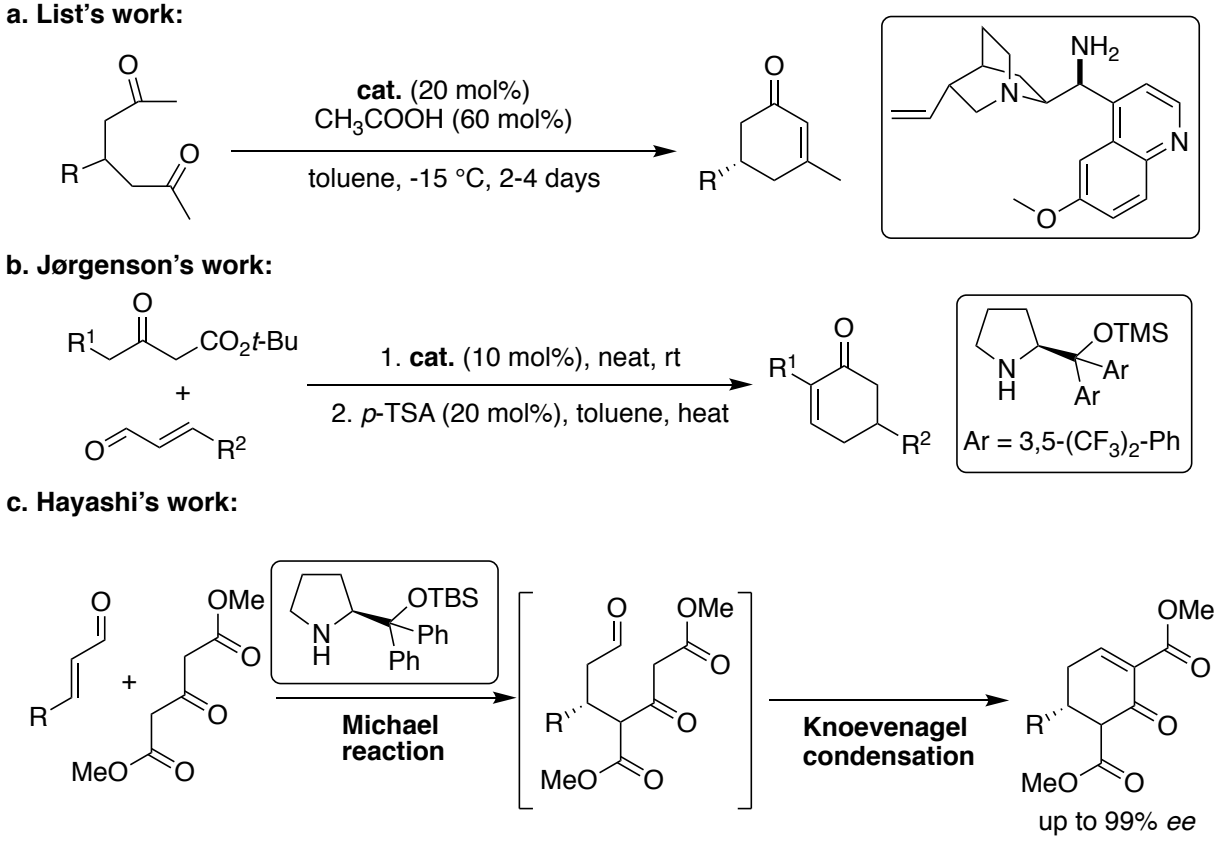

Scheme III-3. **a.** Cinchona derived primary amine catalyzed enantioselective intramolecular aldolization; **b** and **c.** Catalyzed cascade intermolecular cyclohex-2-enone formation; **d.** Diamine mediated cascade reaction of cyclohexenone formation.

It was found to be unstable, particularly in the presence of air. 4*H*-pyran easily disproportionate to the corresponding dihydropyran and the pyrylium ion, which is easily hydrolyzed in aqueous medium. Pyrans themselves have little significance, however, many of their derivatives are important moieties in biological molecules, such as the pyranoflavonoids.[38] Furthermore, chiral 4*H*-pyran scaffolds are widely present in

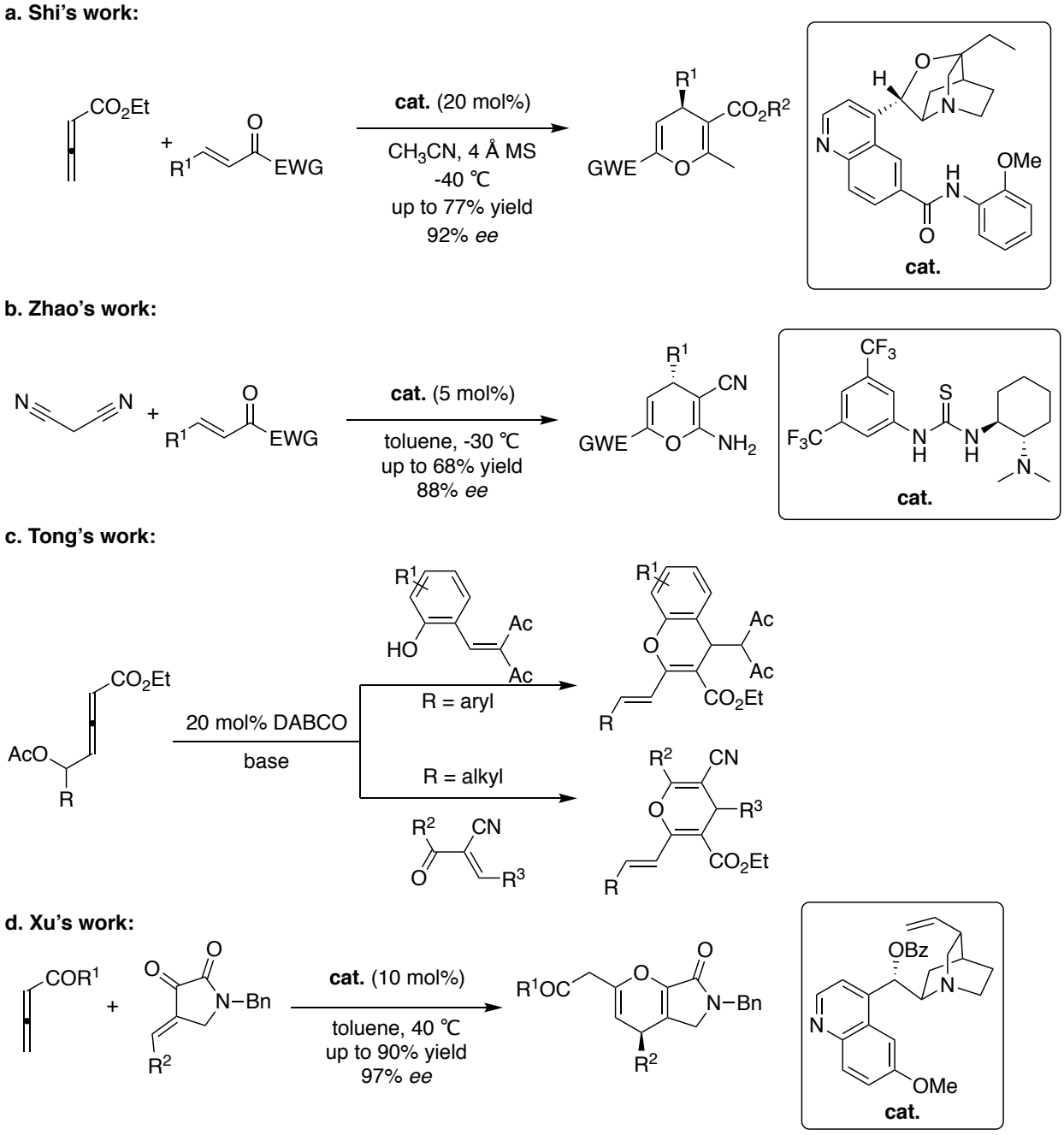

Scheme III-4. Organocatalytic formal [4+2] cycloaddition for the synthesis of 4*H*-pyrans.

biologically and pharmacologically active compounds (see **Figure III-2** for molecules).[39-44] For example, compounds containing 4*H*-pyran motifs are used as anti-cancer agents, anticoagulants, spasmolytics and antianaphylactics, as well as specific IK_{Ca} channel antagonist.[45,46] In addition, some of these compounds are serving as valuable photoactive

a. Zhang's work:

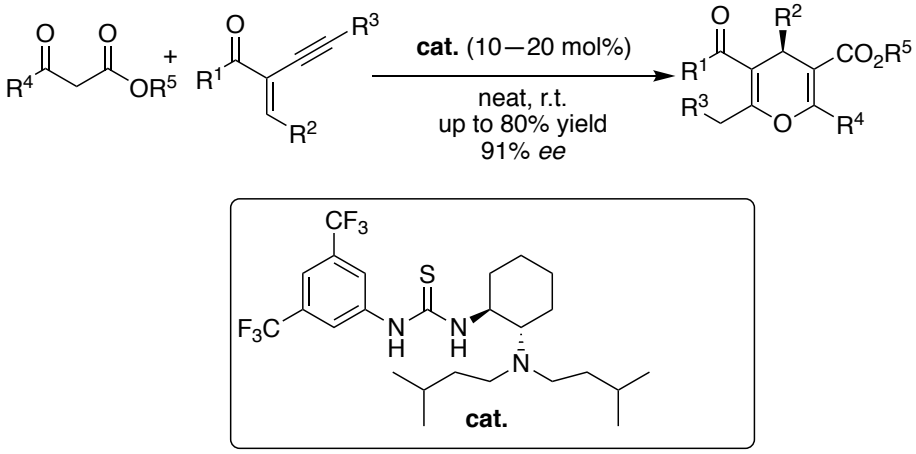

b. Yuan's work:

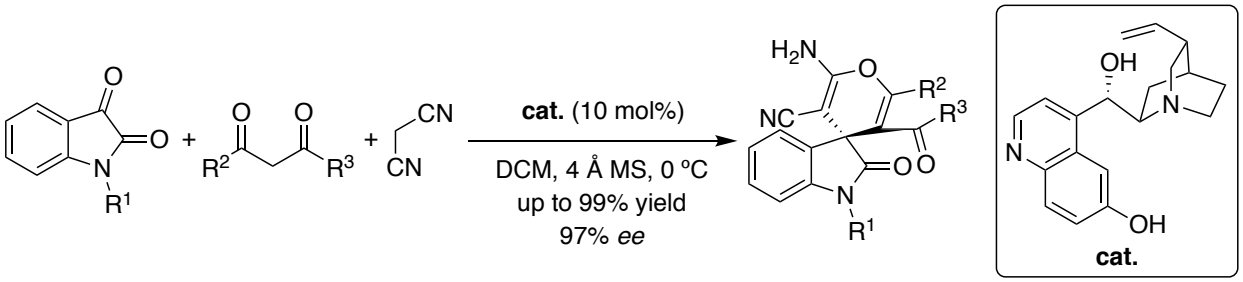

c. Tong's work:

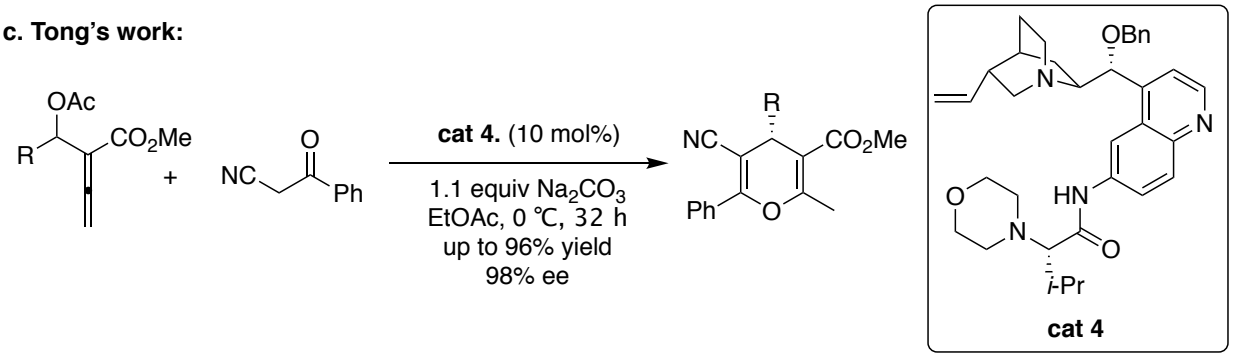

Scheme III-5. Organocatalytic [3+3] cycloaddition for the synthesis of 4*H*-pyrans.

materials. Generally, modification of electron donor-acceptor motifs and extension of the conjugated system will improve 4*H*-pyran derivatives photo-physical behavior. Along with substitution effects, effects of medium can also play a major role in their photo-physical behavior.[47-49] Therefore, with the importance of this scaffold, it is not a surprise that methodologies delivering 4*H*-pyrans have been well developed in the past decades.

Similar to the aforementioned organocatalyzed cyclohexenone formation, organocatalytic cascade reactions are the main contributions to these strategies, which have been intensively investigated for the enantioselective 4*H*-pyran synthesis. Several groups have contributed to this field *via* different cycloaddition protocols. For example, by utilizing

a. Observation of the formation dihydropyran and its regioiosmer

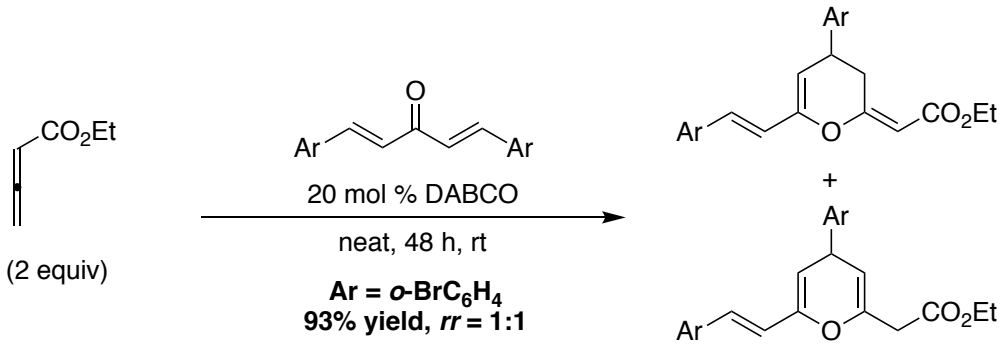

b. Kinya Akiba's work

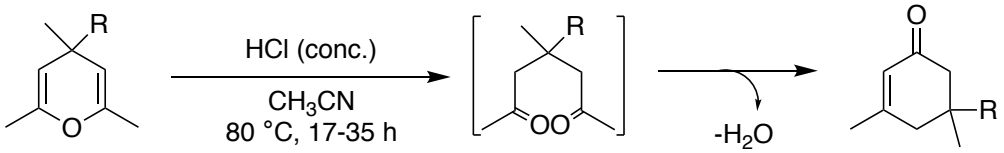

c. Our approach for cyclohexenone and 4*H*-pyran from a common intermediate

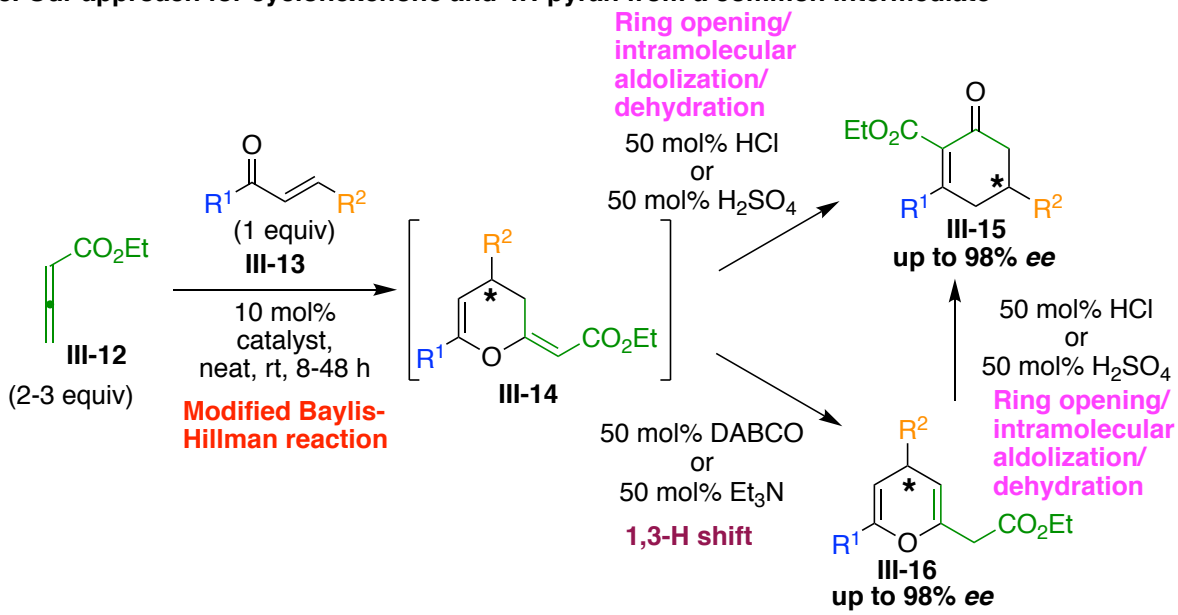

Scheme III-6. **a:** An example of the formation of both dihydropyran and 4*H*-pyran under DABCO catalyzed reaction condition; **b:** Conversion from 4*H*-pyran to cyclohexenone; **c:** One-pot synthesis of cyclohexenone and 4*H*-pyran from a common intermediate.

chiral amine catalysts, asymmetric formal [4+2] cycloaddition reactions were developed by the groups of Shi, Zhao, Tong, Xu and Vo-Thanh (see **Scheme III-4**).[50-54] Meanwhile, the groups of Zhang, Yuan and Tong have independently reported [3+3] cycloaddition reaction to assemble the 4*H*-pyran units catalyzed by different types of chiral amine systems (see **Scheme III-5**).[55-58]

Recently, a number of groups, including ours, have reported on the catalytic asymmetric synthesis of dihydropyran derivatives with good to excellent yields and enantioselectivities, leading to the general structure **III-14** depicted in **Scheme III-6 c**.[52-

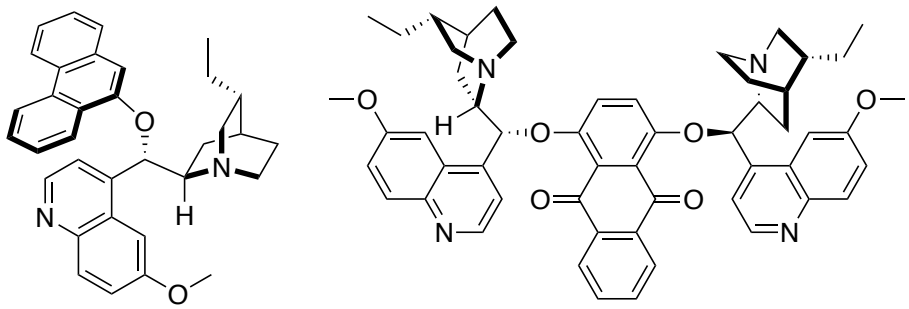

III-17
DHQDPHN

III-18
$(DHQ)_2AQN$

Figure III-3. Catalysts used to synthesize both enantiomers of cyclohexenones and 4*H*-pyrans.

[54,59-62] Parallel to these investigations, we observed that DABCO catalyzes a formal 1,3-H shift, converting dihydropyrans to 4*H*-pyrans (see example in **Scheme III-6 a**). During the period of research for this project, several groups also reported the DABCO mediated 4*H*-pyran synthesis in a racemic format.[51,63,64] Another observation is the formation of cyclohexenone **III-15h** during the optimization of Diels-Alder reaction (in **Chapter II**), where trifluoroacetic acid (TFA) was utilized as a catalyst. Meanwhile, a literature search found a report from Akiba's group that 4*H*-pyrans could be transformed into cyclohexenones with catalytic amounts of HCl (see **Scheme III-6 b**).[65] Considering both

observations, we envisioned the opportunity to access both chiral cyclohexenones and 4*H*-pyrans through a common intermediate—dihydropyran, which can be assembled *via* the modified Morita-Baylis-Hillman reaction of allenoate and enones, developed earlier in our group and discussed in **Chapter II**.[59,66] Furthermore, accessing both enantiomers could be possible by employing either catalyst **III-17** or **III-18** (see **Figure III-3**).

III-2. Preliminary results from model reactions.

Table III-1. Optimization of reaction condition for acid catalyzed synthesis of cyclohexenone **III-15h**

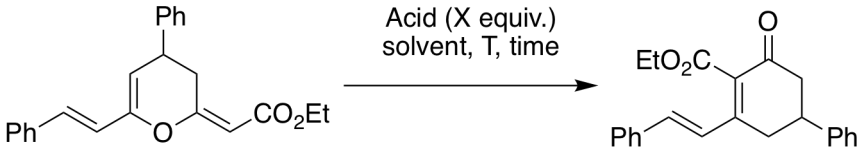

III-14h **III-15h**

Entry	acid	X (equiv.)	solvent	ºC/T	h/t	%/product[a]
1	TFA	1.0	TFE	-40 to rt	3	20
2	TFA	1.0	TFE	-40 to rt	12	50
3	TFA	1.0	DCM	-40 to rt	12	15[b]
4	TFA	1.0	TFE/DCM (1:1)	-40 to rt	12	45[b]
5	$AlCl_3$	1.0	toluene	-40 to rt	12	--[c]
6	$Yb(OTf)_3$	1.0	toluene	-40 to rt	12	--[c]
7	$ZnCl_2$	1.0	toluene	-40 to rt	12	--[c]
8	HCl	1.0	CH_3CN	rt	10	60
9	**HCl**	**0.5**	**CH_3CN**	**60**	**6**	**85**

[a] Isolated yields. [b] Yields were estimated based on the crude ^1H NMR. [c] Partial decomposition of **III-14h** was observed with some recovered **III-14h**.

Our initial investigation utilized dihydropyran **III-14h** as the test substrate for the acid catalyzed rearrangement (see **Table III-1**). Since the cyclohexenone formation was observed under TFA catalyzed condition, several alterations on conditions with TFA were tested (entry 1-4, **Table III-1**), however, none were efficient for delivering the product in high yield. Gratifyingly, based on literature,[65] HCl emerged as a promising choice (entry 8-9, **Table III-1**). Several Lewis acids, such as $AlCl_3$, $ZnCl_2$ and $Yb(OTf)_3$, were tested as well (entry 5-7, **Table III-1**), although, all lead to partial decomposition of the dihydropyran with some starting material recovered.

Table III-2. Optimization of reaction condition for base catalyzed synthesis of 4*H*-pyran **III-16a**

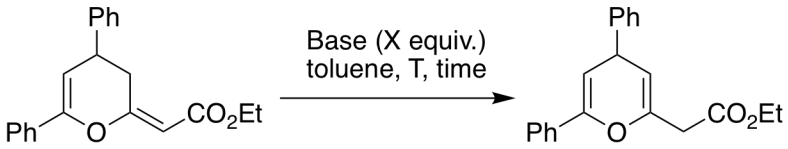

III-14a **III-16a**

Entry	base	X (equiv.)	°C/T	h/t	%/product[a]
1	DABCO	0.5	rt	12	nd
2	**DABCO**	**0.5**	**110**	**12**	**80**
3	DABCO	1.0	110	12	81
4	DBU	0.5	110	4	80
5	Et_3N	0.5	110	12	78
6	pyridine	0.5	110	12	nd

[a] Yields were estimated based on crude ^1H NMR. [b] nd = not determined.

For base catalyzed rearrangement, **III-14a** was selected as the tested substrate (see

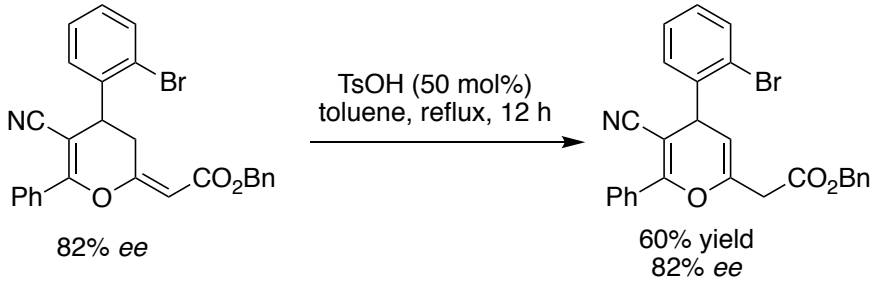

Scheme III-7. Acid catalyzed 4*H*-pyran formation from dihydropyran.

Table III-3. Preliminary results of stepwise *vs.* one-pot synthesis of cyclohexenones and 4*H*-pyrans

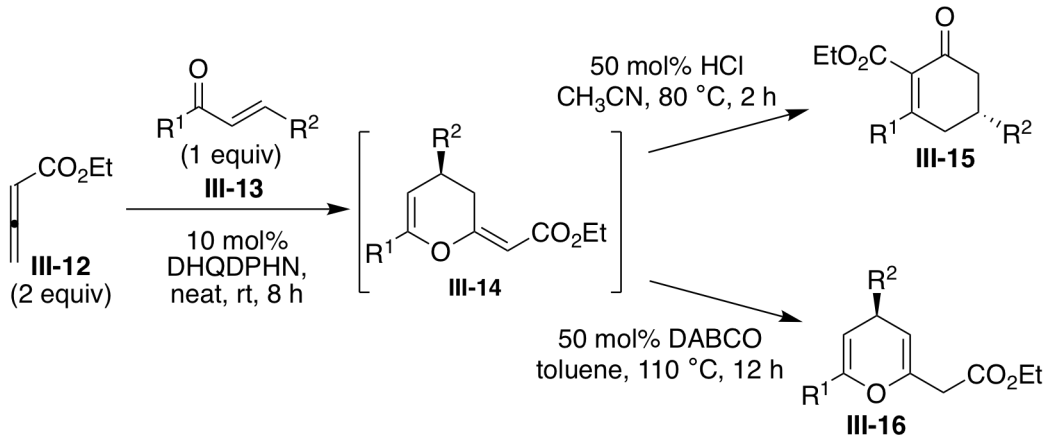

substrate	product	type	overall yields[a] (%)	*ee*[b] (%)
$R^1 = R^2 = Ph$	**III-15a**	stepwise	75	98
		one-pot	86	97
	III-16a	stepwise	75	>99
		one-pot	74	97
R^1 = PhCH=CH	**III-15h**	stepwise	98	94
R^2 = Ph		one-pot	85	95
	III-16h	stepwise	69	97
		one-pot	61	94

[a] Isolated yields. [b] Ratios were determined by chiral HPLC analysis.

Table III-2). When DABCO was used as the catalyst, higher temperature (110 ºC) was necessary for the success of this reaction (entry 1-2, **Table III-2**). Increasing of the catalyst did not improve the yield further (entry 3, **Table III-2**). Both DBU and Et_3N gave similar results as DABCO for this transformation (entry 4-5, **Table III-2**). However, DBU was too basic, potentially epimerizing the chiral center of the substrate, as discussed in **Chapter IV**. Pyridine was not an effective base for this reaction either (entry 6, **Table III-2**). Interestingly, Tong's group reported that TsOH could catalyzed this rearrangement with a similar substrate, as shown in **Scheme III-7**.[60]

To compare the efficiency of stepwise vs one-pot synthesis of both cyclohexenone and 4*H*-pyran, we commenced our investigation with subjecting dihydropyrans **III-14a** and **III-14h** to either catalytic HCl or DABCO reaction condition (see **Table III-3** for details). Gratifyingly, we isolated products **III-15a** and **III-16a** in 75% overall yield, without compromising enantioselectivity, with 98% *ee* and >99% *ee*, respectively. More importantly, similar results, 86% yield with 97% *ee* of **III-15a** and 74% yield with 97% *ee* of **III-16a**, were achieved in a one-pot format. Not surprisingly, product **III-16a** was also successfully converted into cyclohexenone **III-15a** under the same acidic condition. Similarly, the same outcome for stepwise *vs.* one-pot was observed with substrate **III-14h** (see **Table III-3**).

III-3. Results and discussion.

Encouraged by our preliminary results, we analyzed the scope of our methodology with a series substrates. The 1st step, the formal [4+2] cycloaddition reaction, has already

been studied in detail. We focused our study on the 2nd step, which is the acid or base catalyzed rearrangement reaction.

Table III-4. Substrate scope of Brønsted acid catalyzed cyclohexenone synthesis

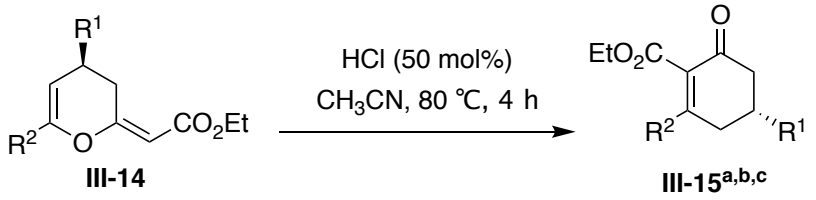

III-14 → **III-15**[a,b,c]

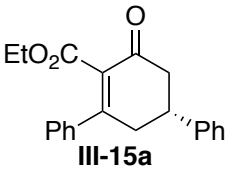

III-15a
81%, 98% *ee* (97% *ee*)

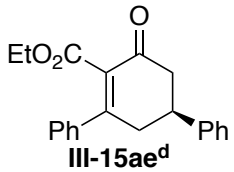

III-15ae[d]
>99%, 90% *ee* (88% *ee*)

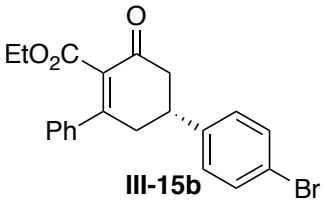

III-15b
89%, 93% *ee* (96% *ee*)

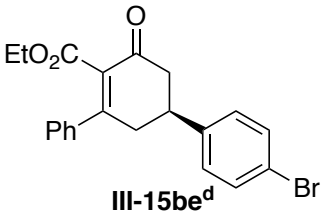

III-15be[d]
70%, 92% *ee* (91% *ee*)

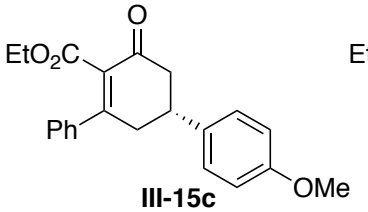

III-15c
62%, 94% *ee* (96% *ee*)

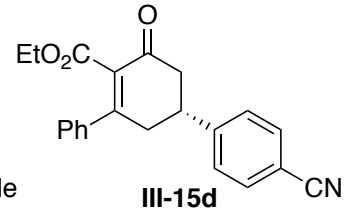

III-15d
74%, 94% *ee* (97% *ee*)

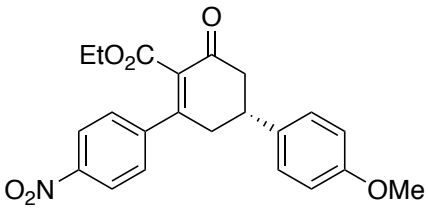

III-15e
74%, 94% *ee* (95% *ee*)

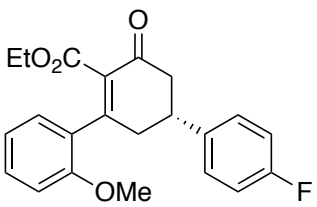

III-15f
>99%, 94% *ee* (97% *ee*)

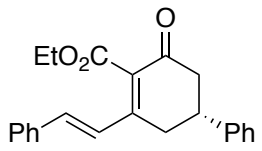

III-15h
85%, 94% *ee* (98% *ee*)

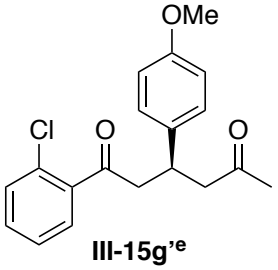

III-15g'[e]
85%, 94% *ee* (97% *ee*)

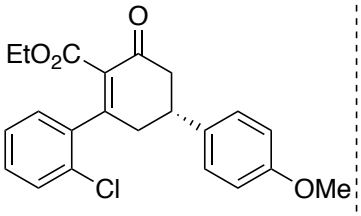

III-15g
(not observed)

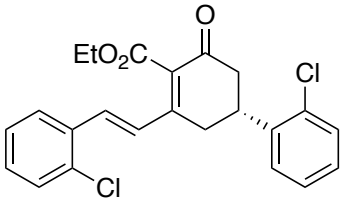

III-15i
>99%, 88% *ee* (87% *ee*)

[a] Isolated yields. [b] Ratios were determined by chiral HPLC analysis. [c] Data in the parenthesis are the *ee* value of **III-14** from formal [4+2] cycloaddition reaction. [d] The enantiomer of **III-14** was used as the substrate. [e] 2.0 equiv. HCl was used at refluxed condition in a sealed tube.

As shown in **Table III-4**, regardless of the electronic properties of the substituents attached, most of the substituted aryl and alkenyl dihydropyrans delivered the cyclohexenones with good to excellent yields (up to quantitative yield) and excellent

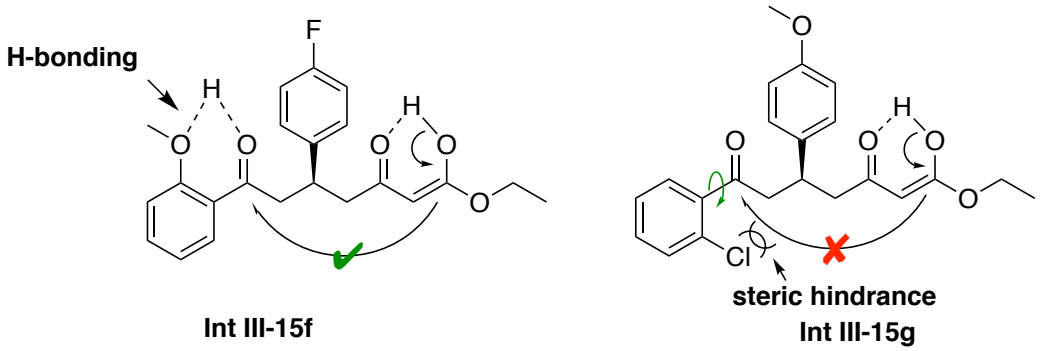

Figure III-4. Proposed cyclization intermediates **Int III-15f** and **Int III-15g**.

retention of enantioselectivity (up to 98% *ee*) (**III-15a** – **III-15f**, **III-15h** – **III-15i**). As expected, both enantiomers **III-14ae** and **III-14be** furnished cyclohexenones **III-15ae** and **III-15be**, correspondingly. Interestingly, substrate **III-14g** with *o*-Cl phenyl substituent did not cyclize to provide the desired cyclohexenone **III-15g**, presumably on account of steric congestion (see **Int III-15g** in **Figure III-4** for explanation). However, it was found that once the reaction was performed under a more forcing condition (2.0 equiv. HCl, at refluxed condition in a sealed tube), decarboxylated product **III-15g'** was formed as the major product. In contrast, *ortho* substituted, but with the ability to form intramolecular H-bonding, such as **III-14f**, can deliver the desired cyclohexenone product. We speculated that the formation of H-bonding between the methoxy group with proximal carbonyl group of **Int III-15f** (see **Figure III-4**), not only locked the rotation of the methoxy phenyl substitution, but also increased the electrophilicity of this carbonyl. The combination of both effects contributes to the success of this transformation (for substrate **III-14f**, quantitative yield and 94% *ee* was achieved). Of note, the X-ray crystal structures of

compounds **III-15b** and **III-15d** (see **III-4 Experimental** section) provided unequivocal evidence for the absolute stereochemistry of the products. With these observations, we speculate the mechanism of this transformation as follows, dihydropyrans undergo hydrolytic cleavage to 1,5-diketone, followed by intramolecular aldol reaction, and dehydration, sequentially, to furnish the desired cyclohexenones (see **Scheme III-8**).

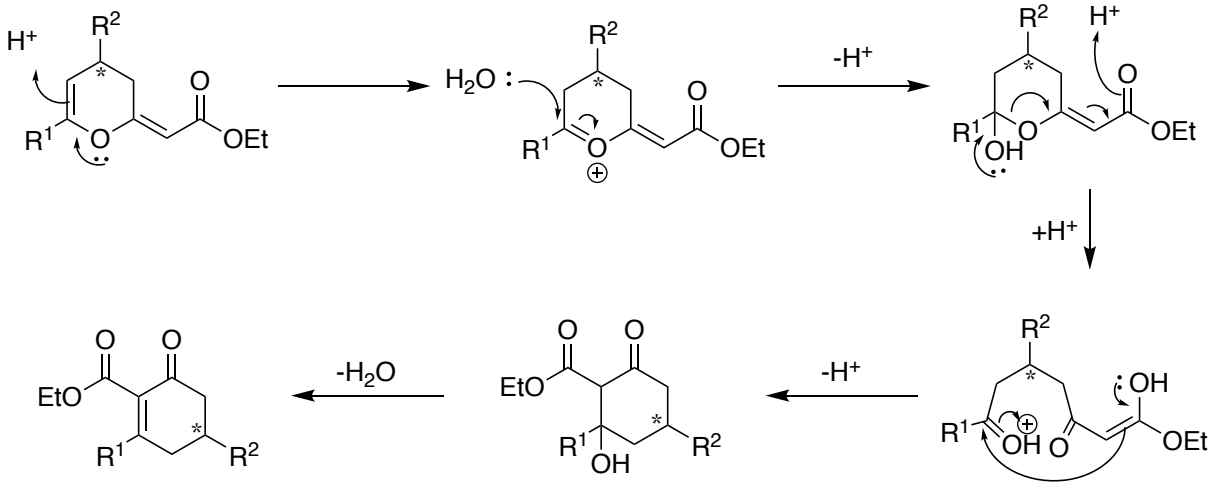

Scheme III-8. Proposed mechanism for the Brønsted acid catalyzed cyclohexenone formation.

Parallel to these experiments, a number of substrates were screened for the synthesis of 4*H*-pyrans, the results of which are indicated in **Table III-5**. Gratifyingly, regardless of the nature of the substituents on the aromatic ring, namely the electronic properties and the substitution patterns, all the aryl, alkenyl and hetero-aryl were compatible with our methodology (**III-16a**–**III-16j**), furnishing the 4*H*-pyrans with moderate to excellent yields (up to 92%) and excellent retention of enantioselectivity (up to >99% *ee*). Enantiomers **III-16ae** and **III-16be** were obtained when **III-14ae** and **III-14be** were used as the starting materials. Noteworthy, for substrate **III-14d**, milder conditions (60 °C) must be applied instead of refluxing to minimize the epimerization of the benzylic center, as the electron withdrawing group makes the benzylic H more acidic. Due to the dual

Table III-5. Substrate scope of DABCO catalyzed 4*H*-pyran synthesis

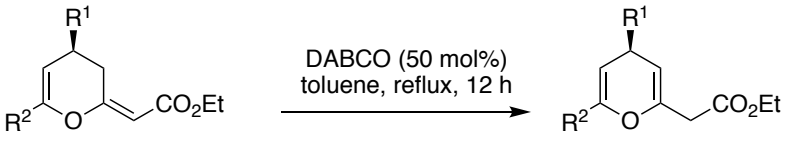

III-14 → **III-16**[a,b,c]

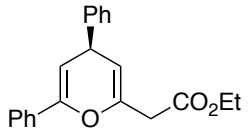

III-16a
81%, >99% *ee* (97% *ee*)

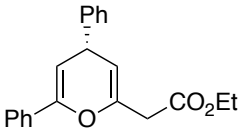

III-16ae[d]
90%, 82% *ee* (88% *ee*)

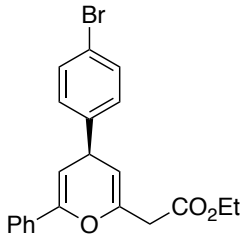

III-16b
63%, 91% *ee* (96% *ee*)

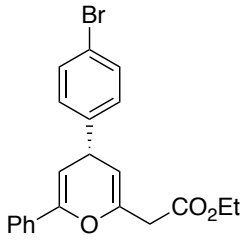

III-16be[d]
43%, 87% *ee* (91% *ee*)

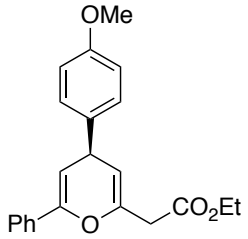

III-16c
70%, 94% *ee* (96% *ee*)

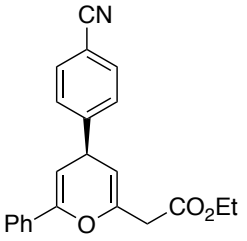

III-16d[e]
92%, 92% *ee* (97% *ee*)

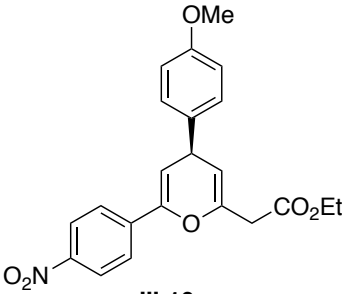

III-16e
28%, 96% *ee* (95% *ee*)

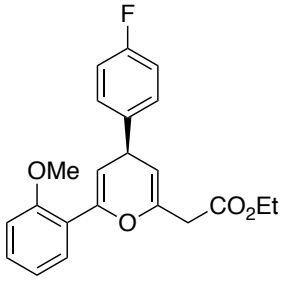

III-16f
70%, 95% *ee* (97% *ee*)

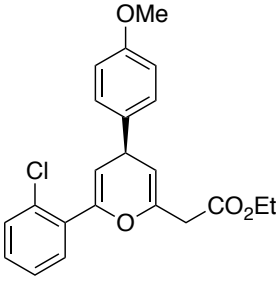

III-16g
66%, 96% *ee* (97% *ee*)

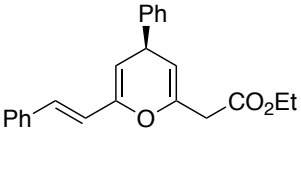

III-16h
90%, 94% *ee* (98% *ee*)

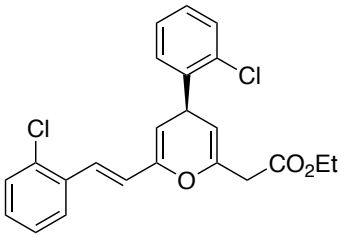

III-16i
80%, 91% *ee* (87% *ee*)

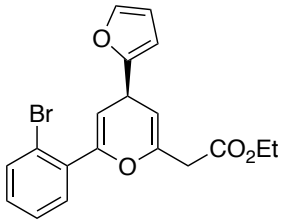

III-16j
63%, 91% *ee* (96% *ee*)

[a] Isolated yields. [b] Ratios were determined by chiral HPLC analysis. [c] Data in the parentheses are the *ee* values of **III-14** from the formal [4+2] cycloaddition reaction. [d] The enantiomer of **III-14** was used as the substrate for this transformation. [e] The reaction temperature was 60 °C.

functions of DABCO, namely the basicity and nucleophilicity, two plausible mechanisms are presented in **Scheme III-9**. In **path a**, DABCO reacts as a Lewis base, which leads to a Michael addition reaction to form enolate **Int a**. After intramolecular deprotonation, enol **Int b** is formed with the DABCO catalyst being ejected. Eventually, **Int b** undergoes

tautomerization to deliver the 4*H*-pyran product.[51] Alternatively, DABCO can react as a Brønsted base, deprotonateing the γ–H of the substrate to form a conjugated enolate intermediate **Int c**, which is protonated at its α–C sequentially to deliver the 4*H*-pryan product **III-16**. The application of the 4*H*-pran was demonstrated by compound **III-16i**, which was subjected to the Diels-Alder reaction to provide the adduct **III-16ia** as a single isomer without compromising enantioinduction (89% *ee* of **III-16ia** *vs* 91% *ee* of the starting material **III-16i**) (see the **III-4. Experimental** for more details).

Path a:

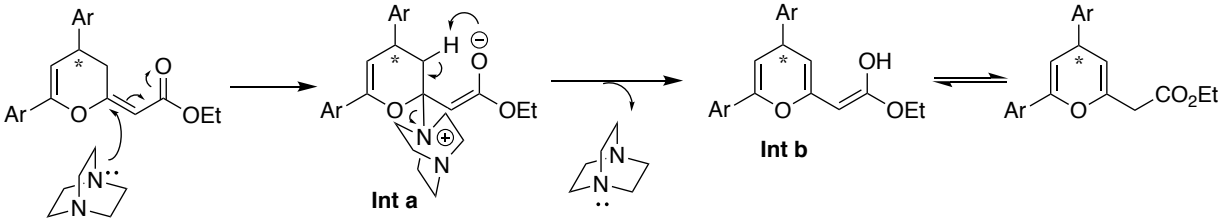

Path b:

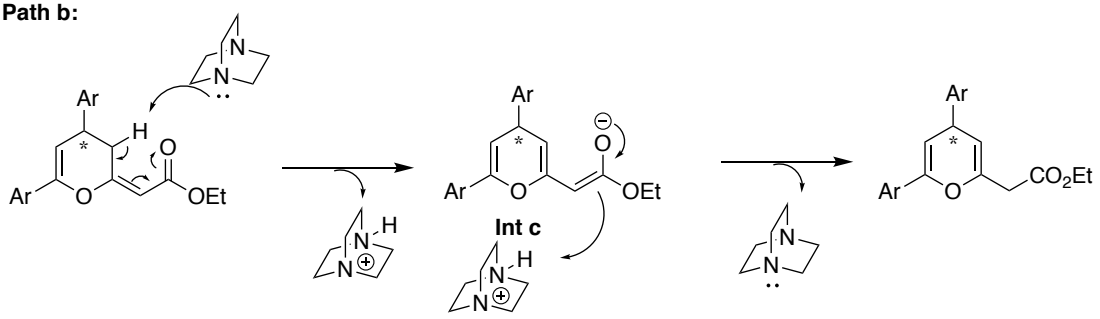

Scheme III-9. Two plausible mechanisms of DABCO catalyzed 4*H*-pyran formation. **Path a**, a Lewis base catalyzed cycle. **Path b**, a Brønsted base catalyzed cycle.

To demonstrate the application of our methodology of cyclohexenone synthesis methodology, one-pot formats to synthesize the derivatives of carvone and celery ketone were investigated (see **Table III-6** for details). Notably, for substrates **III-13k—III-13h**, H_2SO_4 instead of HCl was used for carvone derivatives synthesis, since the isopropenyl group is sensitive towards HCl. In fact, HCl addition of the isopropenyl group was

observed in the reaction. Not surprisingly, some of the carvone or celery ketone derivatives gave lower yields (substrate **III-14k** gave no product), due to the low reactivity of enones **III-13** in the formal [4+2] cycloaddition reaction. To compare the reactivity of the series of enones, ^{1}H NMR analysis was performed. As shown in **Figure III-5**, the more downfield in chemical shift of the β–H in enones **III-13o** to **III-13r** indicates the more electrophilic nature (more reactive) of the β–C towards the formal [4+2] cycloaddition reaction. Therefore, a trend in increasing conversion from **III-15o** to **III-15r** (12.0% to 100.0%) corroborates with the NMR study. However, it is noteworthy that excellent enantioselectivities (80% to 95% *ee*) were obtained for all derivatives. It should be

Table III-6. One-pot synthesis of carvone and celery ketone derivatives

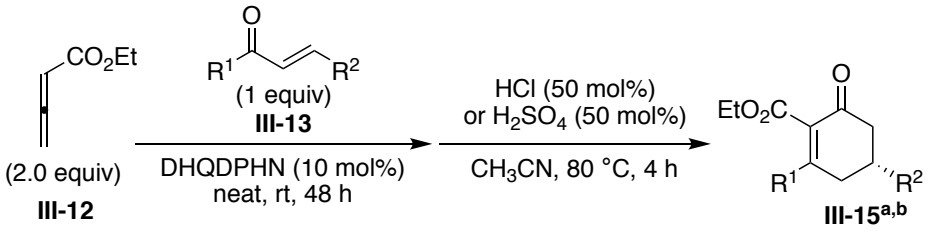

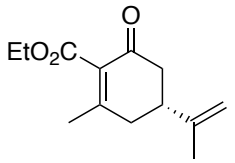

III-15k
reaction fails at 1st step

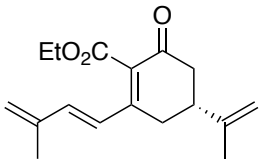

III-15l[d]
19%, 86% *ee*

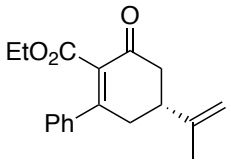

III-15m[d]
17%, 89% *ee*

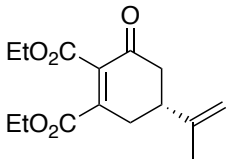

III-15n[d]
36%, ND

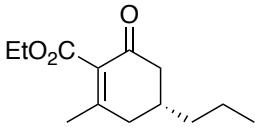

III-15o[c,e]
12% (12.0%), 95% *ee*

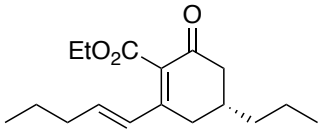

III-15p[c,e]
21% (21.5%), ND

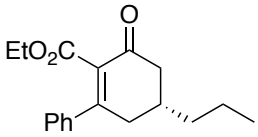

III-15q[c,e]
59% (88.0%), 90% *ee*

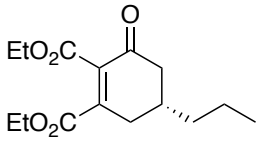

III-15r[c,e]
64% (100.0%), 80% *ee*

[a] Isolated yields over two steps. [b] Ratios were determined by chiral HPLC or GC analysis. [c] HCl was used at the 2nd step. [d] H_2SO_4 was used at the 2nd step. [e] Data in the parentheses were the ^{1}H NMR yields of the formal [4+2] cycloaddition reaction, which was determined by crude ^{1}H NMR with MTBE as the internal standard. ND = not determined.

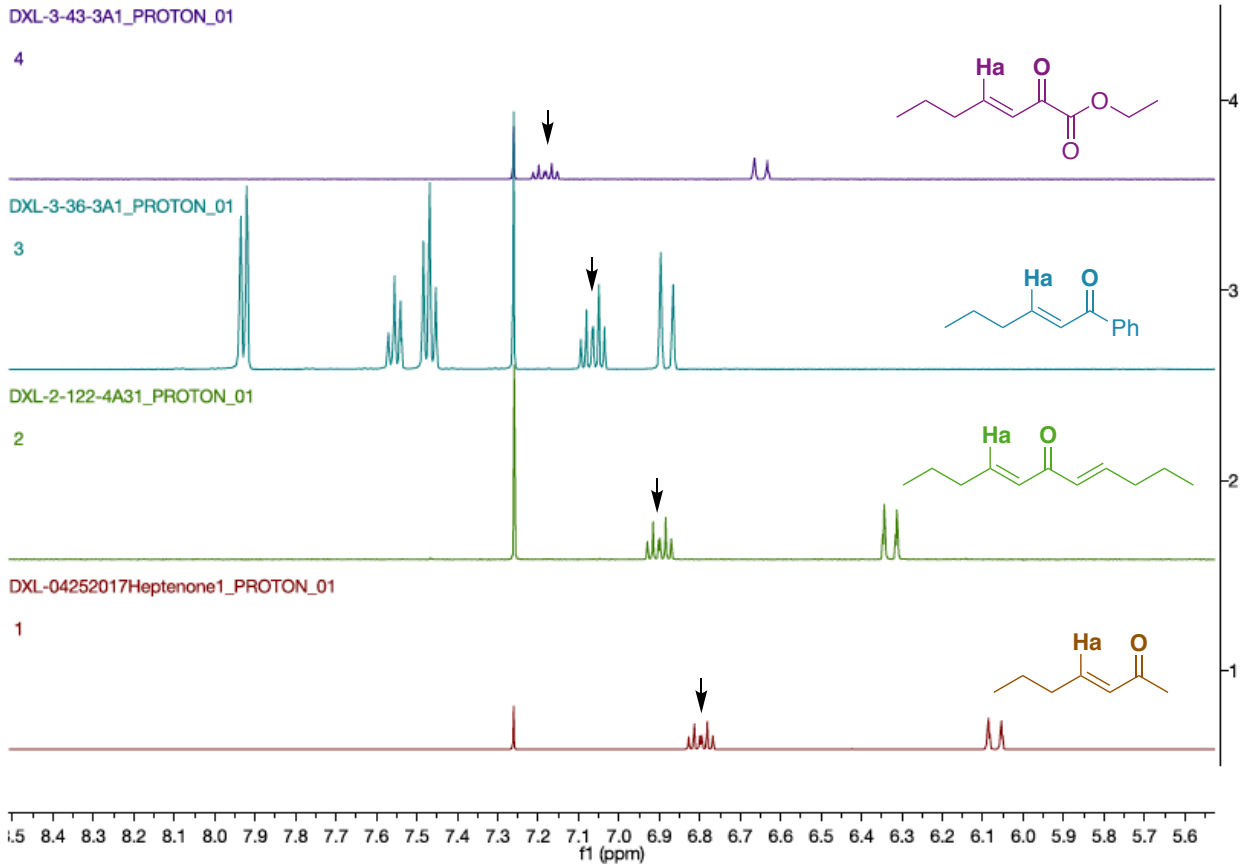

Figure III-5. Investigation of the reactivity of enones **III-13o** to **III-13r** by ^{1}H NMR analysis.

mentioned that several attempts to increase the yields of substrates with low reactivity were infructuous. The attempts included using β-ICD as the catalyst, elongating the reaction time, adding more allenoate or setting up the reaction in mmol scale (it was demonstrated that the formal [4+2] cycloaddition reaction is more efficient when performed in larger scale, as described in **Chapter II**.

In summary, we have elaborated a one-pot protocol to for the divergently synthesis of either chiral cyclohexenone or 4*H*-pyran derivatives with excellent enantioselectivity and good yield by sequential modified Morita-Baylis-Hillman reaction/ Brønsted acids catalyzed rearrangement reaction or modified Morita-Baylis-Hillman reaction/ base

catalyzed rearrangement reaction, respectively. Also, the practicality of this methodology was validated in the synthesis of several chiral carvone and celery ketone synthesis.

III-4. Experimental.

III-4.1. General remarks:

Unless specified, all reagents were purchased from commercial sources and used without purification. THF and diethyl ether were distilled from sodium benzophenone ketyl. Methylene chloride, toluene and triethylamine were dried over CaH_2 and freshly distilled prior to use. Ethyl-2,3-butadienoate was synthesized as reported[67] and stored at -20 ºC. Enones were synthesized as reported[59,66] unless otherwise specified.

Column chromatography was performed using Silicycle 60 Å, 35-75 µm silica gel. Thin layer chromatography was performed using 0.2 mm thickness silica gel 60 F254 plates and visualized using UV light, iodine, potassium permanganate stain, p-anisaldehyde stain or phosphomolybdic acid in EtOH stain.

^{1}H NMR and ^{13}C NMR, as well as all the 2D NMR spectra, were obtained using a 500 MHz Varian NMR spectrometer and referenced using the residual ^{1}H peak from the deuterated solvent. For HRMS (ESI) analysis, a Waters Xevo G2-XS QTOF mass spectrometer (Agilent) instrument was used and referenced against Polyethylene Glycol (PEG-400-600). Optical rotations were obtained on a Jasco P-2000 polarimeter at 20 °C and 589 nm. The specific rotations were calculated according to the equation $[\alpha]^{20}_D = (100\alpha)/(l \times c)$, where l is the path length in decimeters and c is the concentration in g/100mL.

III-4.2. General procedure A for Brønsted acid-catalyzed cyclohexenones synthesis:

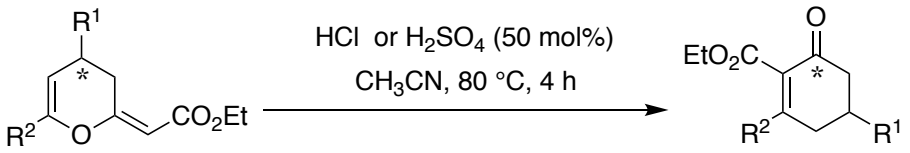

III-14a-i **III-15a-i**

All the dihydropyran derivatives **III-14** were synthesized by reported procedure.[59,66]

To a solution of the corresponding compound **III-14** (1.0 equiv) in CH_3CN, concentrated HCl solution or dilute H_2SO_4 solution (2 N) (50 mol % equiv) was added. The solution was heated up to 80 °C and kept at this temperature for 4 hours. The mixture was concentrated under N_2 flow (or basified by saturated $NaHCO_3$ solution, extracted by DCM and concentrated under reduced pressure if H_2SO_4 was used as the catalyst). The residue was purified by silica gel column chromatography using ethyl acetate in hexane (1.5% to 20%) as the eluent.

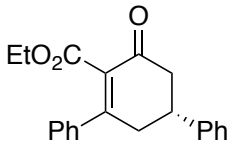

III-15a

III-15a-*R*: Ethyl (*R*)-5'-oxo-1',2',5',6'-tetrahydro-[1,1':3',1''-terphenyl]-4'-carboxylate: Compound **III-14a** (32.0 mg, 0.1 mmol) was subject to general procedure A to provide 25.9 mg (81% yield) of the pure product as a colorless oil; ^1H NMR (500 MHz, $CDCl_3$) δ 7.39-7.34 (7H, m), 7.31-7.25 (3H, m), 4.10 (2H, q, *J* = 7.0 Hz), 3.58-3.50 (1H, m), 3.01-2.97 (2H, m), 2.86 (1H, dd, *J* = 16.0 Hz, 4.0 Hz), 2.78 (1H, dd, *J* = 16.0 Hz, 14.0 Hz), 1.03

(3H, t, J = 7.0 Hz) ppm; ^{13}C NMR (125 MHz, $CDCl_3$) δ 194.9, 166.5, 158.7, 142.4, 138.6, 133.0, 129.7, 128.9, 128.6, 128.1, 127.3, 126.6, 61.3, 43.7, 40.2, 39.3, 13.8 ppm. HRMS (ESI) Calculated Mass for $C_{21}H_{21}O_3$: 321.1491 ($[M+H]^+$), Found 321.1503 ($[M+H]^+$). The enantiomeric excess was determined by HPLC analysis, using DAICEL CHIRALPAK OJ-H column (5% isopropanol in *n*-hexanes at 1.0 mL/min), R_t = 36.0 min (minor) and 52.2 min (major), **III-15a**-*R* (98% *ee*): $[\alpha]^{20}_D$ = -47 (c = 1.90, $CDCl_3$).

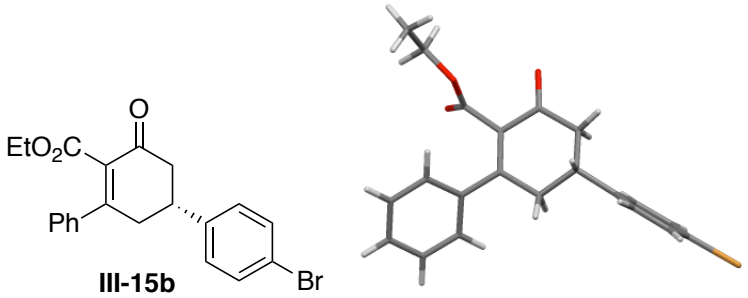

III-15b

III-15b-*R*: **Ethyl (*R*)-4-bromo-5'-oxo-1',2',5',6'-tetrahydro-[1,1':3',1''-terphenyl]-4'-carboxylate:** Compound **III-14b** (39.9 mg, 0.1 mmol) was subject to general procedure A to provide 35.5 mg (89% yield) of the pure product as a colorless crystalline solid, mp 112-114 °C; ^{1}H NMR (500 MHz, $CDCl_3$) δ 7.51-7.46 (2H, m), 7.41-7.34 (5H, m), 7.18-7.13 (2H, m), 4.10 (2H, dd, J = 7.0 Hz, 7.0 Hz), 3.55-3.46 (1H, m), 3.00-2.90 (2H, m), 2.83 (1H, dd, J = 16.0 Hz, 4.0 Hz), 2.74 (1H, dd, J = 16.0 Hz, 14.0 Hz), 1.02 (3H, t, J = 7.0 Hz) ppm; ^{13}C NMR (125 MHz, $CDCl_3$) δ 194.4, 166.4, 158.3, 141.3, 138.4, 133.1, 132.0, 129.7, 128.6, 128.4, 126.6, 121.0, 61.3, 43.5, 39.6, 39.0, 13.7 ppm. HRMS (ESI) Calculated Mass for $C_{21}H_{20}O_3Br$: 399.0596 ($[M+H]^+$), Found 399.0590 ($[M+H]^+$). The enantiomeric excess was determined by HPLC analysis, using DAICEL CHIRALPAK OJ-

H column (20% isopropanol in *n*-hexanes at 1.0 mL/min), R_t = 19.9 min (minor) and 57.8 min (major), **III-15b**-*R* (93% *ee*): $[\alpha]^{20}_D$ = -24 (*c* = 3.08, $CDCl_3$).

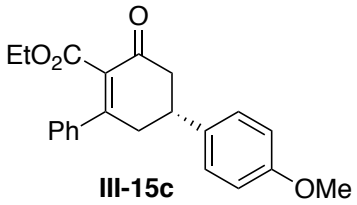

III-15c

III-15c-*R*: **Ethyl (*R*)-4-methoxy-5'-oxo-1',2',5',6'-tetrahydro-[1,1':3',1''-terphenyl]-4'-carboxylate:** Compound **III-14c** (35.0 mg, 0.1 mmol) was subject to general procedure A to provide 21.7 mg (62% yield) of the pure product as a colorless oil; ^{1}H NMR (500 MHz, $CDCl_3$) δ 7.40-7.35 (5H, m), 7.22-7.17 (2H, m), 6.92-6.87 (2H, m), 4.10 (2H, dd, *J* = 7.0 Hz, 7.0 Hz), 3.81 (3H, s), 3.53-3.44 (1H, m), 2.98-2.92 (2H, m), 2.83 (1H, dd, *J* = 16.0 Hz, 4.0 Hz), 2.74 (1H, dd, *J* = 16.0 Hz, 14.0 Hz), 1.02 (3H, t, *J* = 7.0 Hz) ppm; ^{13}C NMR (125 MHz, $CDCl_3$) δ 195.1 166.6, 158.8, 158.7, 138.6, 134.6, 133.0, 129.6, 128.6, 127.6, 126.6, 114.2, 61.2, 55.3, 44.1, 39.6, 39.4, 13.8 ppm. HRMS (ESI) Calculated Mass for $C_{22}H_{23}O_4$: 351.1596 ($[M+H]^+$), Found 351.1599 ($[M+H]^+$). The enantiomeric excess was determined by HPLC analysis, using DAICEL CHIRALPAK OJ-H column (20% isopropanol in *n*-hexanes at 1.0 mL/min), R_t = 30.7 min (major) and 50.2 min (minor), **III-15c**-*R* (94% *ee*): $[\alpha]^{20}_D$ = -28 (*c* = 1.12, $CDCl_3$).

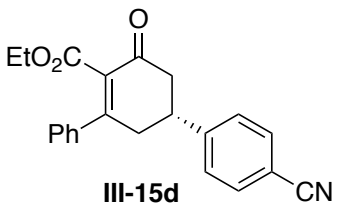

III-15d

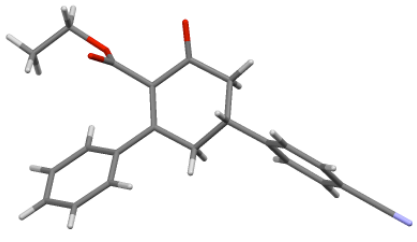

III-15d-*R*: Ethyl (*R*)-4-cyano-5'-oxo-1',2',5',6'-tetrahydro-[1,1':3',1''-terphenyl]-4'-carboxylate: Compound **III-14d** (34.5 mg, 0.1 mmol) was subject to general procedure A to provide 25.5 mg (74% yield) of the pure product as a colorless crystalline solid, mp 120-121 °C; ^{1}H NMR (500 MHz, $CDCl_3$) δ 7.70-7.65 (2H, m), 7.44-7.34 (7H, m), 4.10 (2H, dd, *J* = 7.0 Hz, 7.0 Hz), 3.67-3.56 (1H, m), 3.02-2.93 (2H, m), 2.86 (1H, dd, *J* = 16.0 Hz, 4.0 Hz), 2.77 (1H, dd, *J* = 16.0 Hz, 14.0 Hz), 1.03 (3H, t, *J* = 7.0 Hz) ppm; ^{13}C NMR (125 MHz, $CDCl_3$) δ 193.7, 166.2, 157.9, 147.5, 138.2, 133.2, 132.8, 129.9, 128.7, 127.6, 126.6, 118.5, 111.3, 61.4, 43.1, 40.1, 38.5, 13.7 ppm. HRMS (ESI) Calculated Mass for $C_{22}H_{20}NO_3$: 346.1443 ($[M+H]^+$), Found 346.1444 ($[M+H]^+$). The enantiomeric excess was determined by HPLC analysis, using DAICEL CHIRALPAK OJ-H column (20% isopropanol in *n*-hexanes at 1.0 mL/min), R_t = 56.9 min (minor) and 68.1 min (major), **III-15d-*R*** (94% *ee*): $[\alpha]^{20}_D$ = -27 (*c* = 3.08, $CDCl_3$).

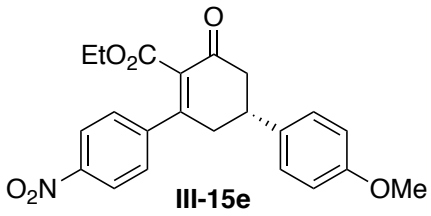

III-15e

III-15e-*R*: Ethyl (*R*)-4-methoxy-4''-nitro-5'-oxo-1',2',5',6'-tetrahydro-[1,1':3',1''-terphenyl]-4'-carboxylate: Compound **III-14e** (39.5 mg, 0.1 mmol) was subject to general procedure A to provide 29.2 mg (74% yield) of the pure product as a colorless oil; ^{1}H NMR (500 MHz, $CDCl_3$) δ 8.27-8.22 (2H, m), 7.58-7.52 (2H, m), 7.22-7.17 (2H, m), 6.94-6.87 (2H, m), 4.11 (2H, dd, *J* = 7.0 Hz, 7.0 Hz), 3.81 (3H, s), 3.56-3.47 (1H, m), 2.97 (1H, dd, *J* = 16.0 Hz, 4.0 Hz), 2.92-2.83 (2H, m), 2.77 (1H, dd, *J* = 16.0 Hz, 14.0 Hz), 1.07

(3H, t, J = 7.0 Hz) ppm; ^{13}C NMR (125 MHz, $CDCl_3$) δ 194.4, 165.7, 158.8, 155.5, 148.1, 144.9, 134.3, 133.9, 127.8, 127.6, 123.8, 114.3, 61.7, 55.3, 43.9, 39.4, 39.3, 13.9 ppm. HRMS (ESI) Calculated Mass for $C_{22}H_{22}NO_6$: 396.1447 ($[M+H]^+$), Found 396.1449 ($[M+H]^+$). The enantiomeric excess was determined by HPLC analysis, using DAICEL CHIRALPAK AD-H column (20% isopropanol in *n*-hexanes at 1.0 mL/min), R_t = 48.4 min (minor) and 75.6 min (major), **III-15e**-*R* (94% *ee*): $[\alpha]^{20}_D$ = -6 (*c* = 0.94, $CDCl_3$).

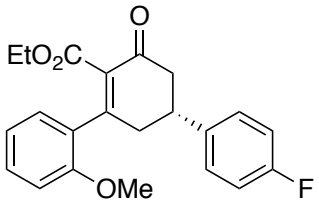

III-15f

III-15f-*R*: **Ethyl (*R*)-4-fluoro-2''-methoxy-5'-oxo-1',2',5',6'-tetrahydro-[1,1':3',1''-terphenyl]-4'-carboxylate:** Compound **III-14f** (36.8 mg, 0.1 mmol) was subject to general procedure A to provide 36.7 mg (quantitative yiled) of the pure product as a colorless oil; ^{1}H NMR (500 MHz, $CDCl_3$) δ 7.35-7.30 (1H, m), 7.26-7.21 (2H, m), 7.16-7.12 (1H, m), 7.06-7.01 (2H, m), 6.96-6.89 (2H, m), 4.11 (2H, ddd, J = 7.0 Hz, 7.0 Hz, 2.0 Hz), 3.83 (3H, s), 3.57-3.47 (1H, m), 3.00-2.88 (2H, m), 2.83 (1H, dd, J = 16.0 Hz, 4.0 Hz), 2.77 (1H, dd, J = 16.0 Hz, 14.0 Hz), 0.93 (3H, t, J = 7.0 Hz) ppm; ^{13}C NMR (125 MHz, $CDCl_3$) δ 194.6, 165.8, 161.7 (d, $^1J_{C,F}$ = 243.9 Hz), 159.3, 155.8, 138.5 (d, $^4J_{C,F}$ = 3.1 Hz), 133.7, 130.6, 128.2 (d, $^3J_{C,F}$ = 7.4 Hz), 128.0, 127.7, 120.5, 115.6 (d, $^2J_{C,F}$ = 21.3 Hz), 111.0, 60.9, 55.7, 44.4, 39.5, 38.8, 13.7 ppm. HRMS (ESI) Calculated Mass for $C_{22}H_{22}O_4F$: 369.1502 ($[M+H]^+$), Found 369.1503 ($[M+H]^+$). The enantiomeric excess was determined by HPLC analysis, using DAICEL CHIRALPAK AD-H column (10%

isopropanol in *n*-hexanes at 1.0 mL/min), R_t = 24.9 min (minor) and 29.3 min (major), **III-15f**-*R* (94% *ee*): $[\alpha]^{20}_D$ = -41 (*c* = 1.16, $CDCl_3$).

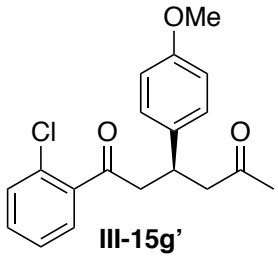

III-15g'

III-15g'-*S*: (*S*)-1-(2-chlorophenyl)-3-(4-methoxyphenyl)hexane-1,5-dione: Compound **III-14g** (38.5 mg, 0.1 mmol) was subject to a modified general procedure A to provide 28.1 mg (85% yield) of the pure product as a colorless oil; ^{1}H NMR (500 MHz, $CDCl_3$) δ 7.38-7.32 (2H, m), 7.27-7.22 (2H, m), 7.14-7.10 (2H, m), 6.83-6.76 (2H, m), 3.81-3.74 (1H, m), 3.77 (3H, s), 3.32 (1H, dd, *J* = 16.0 Hz, 7.0 Hz), 3.23 (1H, dd, *J* = 16.0 Hz, 7.0 Hz), 2.85 (1H, dd, *J* = 16.0 Hz, 7.0 Hz), 2.79 (1H, dd, *J* = 16.0 Hz, 7.0 Hz), 2.06 (3H, s) ppm; ^{13}C NMR (125 MHz, $CDCl_3$) δ 207.3, 201.9, 158.3, 139.3, 135.1, 131.6, 130.7, 130.4, 128.9, 128.4, 126.8, 114.0, 55.2, 49.8, 49.1, 36.2, 30.4 ppm. HRMS (ESI) Calculated Mass for $C_{19}H_{20}O_3Cl$: 331.1101 ($[M+H]^+$), Found 331.1091 ($[M+H]^+$). The enantiomeric excess was determined by HPLC analysis, using DAICEL CHIRALPAK OJ-H column (15% isopropanol in *n*-hexanes at 1.0 mL/min), R_t = 46.7 min (minor) and 62.3 min (major), **III-15g'**-*S* (94% *ee*): $[\alpha]^{20}_D$ = -12 (*c* = 1.66, $CDCl_3$).

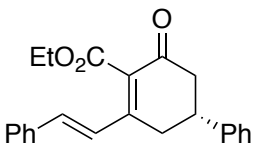

III-15h

III-15h-*R*: Ethyl (*R*,E)-3-oxo-5-styryl-1,2,3,6-tetrahydro-[1,1'-biphenyl]-4-carboxylate: Compound **III-14h** (34.6 mg, 0.1 mmol) was subject to general procedure A to provide 29.4 mg (85% yield) of the pure product as a colorless crystalline solid, mp 124-128 °C; ^{1}H NMR (500 MHz, $CDCl_3$) δ 7.47-7.28 (10H, m), 7.11 (1H, d, *J* = 16.0 Hz), 7.04 (1H, d, *J* = 16.0 Hz), 4.43 (2H, dd, *J* = 7.0 Hz, 7.0 Hz), 3.48-3.35 (1H, m), 3.12 (1H, ddd, *J* = 17.0 Hz, 5.0 Hz, 2.0 Hz), 2.82 (1H, ddd, *J* = 16.0 Hz, 5.0 Hz, 2.0 Hz), 2.80-2.68 (2H, m), 1.41 (3H, t, *J* = 7.0 Hz) ppm; ^{13}C NMR (125 MHz, $CDCl_3$) δ 195.2, 166.8, 152.1, 142.8, 138.3, 135.5, 132.4, 129.8, 129.0, 128.3, 127.6, 127.3, 126.8, 124.9, 61.7, 44.0, 39.8, 33.3, 14.4 ppm. HRMS (ESI) Calculated Mass for $C_{23}H_{23}O_3$: 347.1647 ($[M+H]^+$), Found 347.1655 ($[M+H]^+$). The enantiomeric excess was determined by HPLC analysis, using DAICEL CHIRALPAK OJ-H column (20% isopropanol in *n*-hexanes at 1.0 mL/min), R_t = 31.2 min (minor) and 43.6 min (major), **III-15h-*R*** (94% *ee*): $[\alpha]^{20}_D$ = -64 (*c* = 1.45, $CDCl_3$).

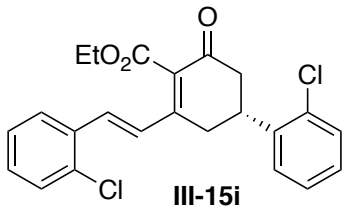

III-15i

III-15i-*R*: Ethyl (*R*,E)-2'-chloro-5-(2-chlorostyryl)-3-oxo-1,2,3,6-tetrahydro-[1,1'-biphenyl]-4-carboxylate: Compound **III-14i** (41.5 mg, 0.1 mmol) was subject to general procedure A to provide 41.3 mg (quantitative yield) of the pure product as a pale yellow crystalline solid, mp 168-169 °C; ^{1}H NMR (500 MHz, $CDCl_3$) δ 7.61-7.56 (1H, m), 7.51 (1H, d, *J* = 16.0 Hz), 7.46-7.42 (1H, m), 7.41-7.37 (1H, m), 7.36-7.31 (2H, m), 7.30-7.23

(3H, m), 7.01 (1H, d, *J* = 16.0 Hz), 4.42 (2H, q, *J* = 7.0 Hz), 4.01-3.90 (1H, m), 3.19 (1H, ddd, *J* = 18.0 Hz, 6.0 Hz, 2.0 Hz), 2.86-2.67 (3H, m), 1.40 (3H, t, *J* = 7.0 Hz) ppm; ^{13}C NMR (125 MHz, $CDCl_3$) δ 194.9, 166.6, 151.8, 139.6, 134.5, 134.1, 133.7, 133.0, 130.5, 130.2, 130.1, 128.5, 127.5, 127.4, 127.2, 127.2, 67.8, 42.7, 35.9 31.4, 14.3 ppm. HRMS (ESI) Calculated Mass for $C_{23}H_{21}O_3Cl_2$: 415.0868 ($[M+H]^+$), Found 415.0868 ($[M+H]^+$). The enantiomeric excess was determined by HPLC analysis, using DAICEL CHIRALPAK AD-H column (3% isopropanol in *n*-hexanes at 0.8 mL/min), R_t = 33.1 min (minor) and 35.7 min (major), **III-15i**-*R* (91% *ee*): $[\alpha]^{20}_D$ = -112 (*c* = 0.66, $CDCl_3$).

III-4.3. General procedure B for one-pot synthesis of cyclohexenones III-15l—III-15r:

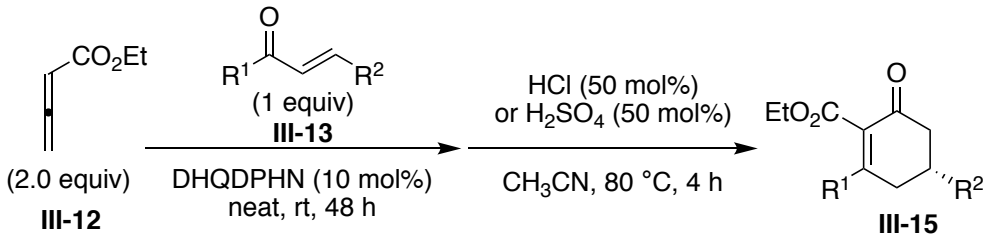

To a mixture of the corresponding enone **III-13** (1.0 equiv) and catalyst (10 mol%) in a vial with stirring bar, allenoate **III-12** (2-4 equiv) was added. The reaction was kept at room temperature for 48 h. The mixture was diluted by CH_3CN, and transferred to a sealed tube by a pipette. To the solution, HCl or H_2SO_4 (50 mol%) was added, followed by heating to 80 ºC. After 4 h, the reaction solution was worked up (when HCl was used as the catalyst, the reaction solution was worked up by removing the solvent under N_2 flow; when H_2SO_4 was used as the catalyst, the reaction was worked up by adding saturated $NaHCO_3$, and extracted with EtOAc and concentrated under rotavap), and the compound was purified following general procedure A.

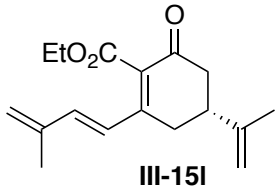

III-15l

III-15l-*R*: Ethyl (*R*,E)-2-(3-methylbuta-1,3-dien-1-yl)-6-oxo-4-(prop-1-en-2-yl)cyclohex-1-ene-1-carboxylate: Compound **III-12l** (32.4 mg, 0.2 mmol) was subject to general procedure B to provide 10.4 mg (19% yield) of the pure product as a colorless oil; ^{1}H NMR (500 MHz, $CDCl_3$) δ 6.86 (1H, d, J = 16.0 Hz), 6.42 (1H, d, J = 16.0 Hz), 5.28-5.32 (2H, m), 4.87-4.90 (1H, m), 4.83-4.85 (1H, m), 4.37 (2H, ddd, J = 7.0 Hz, 7.0 Hz, 1.5 Hz), 2.84 (1H, ddd, J = 17.5 Hz, 4.5 Hz, 1.5 Hz), 2.72-2.79 (1H, m), 2.64 (1H, ddd, J = 16.0 Hz, 3.5 Hz, 1.5 Hz), 2.37-2.48 (2H, m), 1.87-1.91 (3H, m), 1.79-1.82 (3H, m), 1.36 (3H, t, J = 7.0 Hz) ppm; ^{13}C NMR (125 MHz, $CDCl_3$) δ 195.6, 166.8, 152.5, 146.0, 141.5, 140.7, 132.3, 125.5, 123.0, 111.3, 61.5, 42.3, 40.8, 30.3, 20.4, 18.1, 14.3 ppm. HRMS (ESI) Calculated Mass for $C_{17}H_{23}O_3$: 275.1647 ($[M+H]^+$), Found 275.1642 ($[M+H]^+$). The enantiomeric excess was determined by HPLC analysis, using DAICEL CHIRALPAK AD-H column (3% isopropanol in n-hexanes at 0.6 mL/min), R_t = 16.7 min (major) and 18.0 min (minor), **III-15l**-R (86% ee): $[\alpha]^{20}_D$= -28 (c = 0.18, CH_2Cl_2).

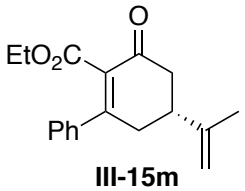

III-15m

III-15m-*R*: Ethyl (*R*)-3-oxo-5-(prop-1-en-2-yl)-3,4,5,6-tetrahydro-[1,1'-biphenyl]-2-carboxylate: Compound **III-12m** (34.4 mg, 0.2 mmol) was subject to general procedure

B to provide 9.6 mg (17% yield) of the pure product as a colorless oil; ^{1}H NMR (500 MHz, $CDCl_3$) δ 7.34-7.43 (5H, m), 4.81-4.92 (2H, m), 4.07 (2H, dd, J = 7.0 Hz, 7.0 Hz), 2.68-2.95 (4H, m), 2.49 (1H, dd, J = 16.0 Hz, 13.5 Hz), 1.80 (3H, s), 1.00 (3H, t, J = 7.0 Hz) ppm; ^{13}C NMR (125 MHz, $CDCl_3$) δ 195.3, 166.5, 159.0, 145.7, 138.8, 132.9, 129.6, 128.6, 126.6, 111.3, 61.2, 42.0, 41.2, 36.6, 20.5, 13.7 ppm. HRMS (ESI) Calculated Mass for $C_{18}H_{21}O_3$: 285.1491 ($[M+H]^+$), Found 285.1490 ($[M+H]^+$). The enantiomeric excess was determined by HPLC analysis, using DAICEL CHIRALPAK AD-H column (5% isopropanol in n-hexanes at 1.0 mL/min), R_t = 13.3 min (minor) and 15.5 min (major), **III-15m**-R (89% ee): $[\alpha]^{20}_D$= -21 (c = 0.58, CH_2Cl_2).

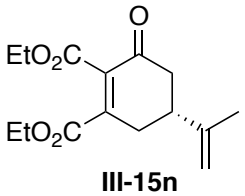

III-15n

III-15n-*R*: Diethyl (*R*)-3-oxo-5-(prop-1-en-2-yl)cyclohex-1-ene-1,2-dicarboxylate: Compound **III-12n** (33.6 mg, 0.2 mmol) was subject to general procedure B to provide 40.0 mg (72% yield) of the pure product as a pale yellow oil; ^{1}H NMR (500 MHz, $CDCl_3$) δ 4.91-4.80 (2H, m), 4.32 (2H, dd, J = 7.0 Hz, 7.0 Hz), 4.28 (2H, dd, J = 7.0 Hz, 7.0 Hz), 2.88 (1H, ddd, J = 18.5 Hz, 4.0 Hz, 1.5 Hz), 2.80-2.72 (1H, m), 2.68 (1H, ddd, J = 16.5 Hz, 4.0 Hz, 2.0 Hz), 2.51 (1H, dd, J = 18.5 Hz, 10.5 Hz), 2.43 (1H, ddd, J = 16.0 Hz, 13.5 Hz), 1.80-1.77 (3H, m), 1.34 (3H, t, J = 7.0 Hz), 1.32 (3H, t, J = 7.0 Hz) ppm. HRMS (ESI) Calculated Mass for $C_{15}H_{21}O_5$: 281.1395 ($[M+H]^+$), Found 281.1389 ($[M+H]^+$). $[\alpha]^{20}_D$= -2 (c = 1.38, $CDCl_3$).

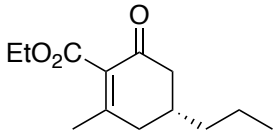

III-15o

III-15o-*R*: Ethyl (*R*)-2-methyl-6-oxo-4-propylcyclohex-1-ene-1-carboxylate: Compound **III-12o** (22.4 mg, 0.2 mmol) was subject to general procedure B to provide 7.6 mg (17% yield) of the pure product as a colorless oil; ^{1}H NMR (500 MHz, $CDCl_3$) δ 4.30 (2H, dd, J = 7.0 Hz, 7.0 Hz), 2.49-2.58 (1H, m), 2.35-2.44 (1H, m), 2.04-2.17 (3H, m), 1.99 (3H, s), 1.32-1.38 (4H, m), 1.32 (3H, t, J = 7.0 Hz), 0.88-0.94 (3H, m) ppm; ^{13}C NMR (125 MHz, $CDCl_3$) δ 195.4, 166.9, 159.5, 133.0, 61.2, 43.3, 38.3, 37.8, 33.7, 22.1, 19.5, 14.2, 14.0 ppm. HRMS (ESI) Calculated Mass for $C_{13}H_{20}O_3Na$: 247.1310 ($[M+Na]^+$), Found 247.1309 ($[M+Na]^+$). The enantiomeric excess was determined by GC analysis, using GAMMA DEX 225 chiral stationary phase (T_1 = 120 °C; rate = 0.1 °C/min; T_2 = 140 °C, hold 10 min, rate = 10 °C/min; T_3 = 200 °C), R_t = 89.7 min (minor) and 89.9 min (major), **III-15o**-R (95% ee): $[\alpha]^{20}_D$= -29 (c = 0.52, $CDCl_3$).

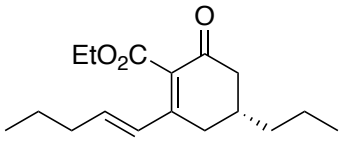

III-15p

III-15p-*R*: Ethyl (*R*,E)-6-oxo-2-(pent-1-en-1-yl)-4-propylcyclohex-1-ene-1-carboxylate: Compound **III-12p** (33.2 mg, 0.2 mmol) was subject to general procedure B to provide 27.8 mg (50% yield) of the pure product as a light yellow oil; ^{1}H NMR (500 MHz, $CDCl_3$) δ 6.25-6.40 (2H, m), 4.34 (2H, dd, J = 7.5 Hz, 7.5 Hz), 2.56-2.77 (2H, m),

2.16-2.24 (2H, m), 2.08-2.15 (3H, m), 1.47 (2H, td, J = 7.0 Hz, 7.0 Hz), 1.35-1.42 (4H, m), 1.34 (3H, t, J = 7.0 Hz), 0.93 (3H, t, J = 7.0 Hz), 0.90-0.94 (3H, m) ppm; ^{13}C NMR (125 MHz, $CDCl_3$) δ 196.3, 167.1, 152.9, 142.2, 131.3, 127.8, 61.4, 43.7, 38.0, 35.6, 33.5, 31.7, 21.9, 19.6, 14.2, 14.0, 13.7 ppm. HRMS (ESI) Calculated Mass for $C_{17}H_{27}O_3$: 279.1960 ($[M+H]^+$), Found 279.1960 ($[M+H]^+$). $[\alpha]^{20}_D$= -34 (c = 0.5, $CDCl_3$).

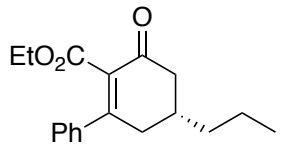

III-15q

III-15q-*R*: Ethyl (*R*)-3-oxo-5-propyl-3,4,5,6-tetrahydro-[1,1'-biphenyl]-2-carboxylate: Compound **III-12q** (34.8 mg, 0.2 mmol) was subject to general procedure B to provide 33.7 mg (59% yield) of the pure product as a light yellow oil; ^{1}H NMR (500 MHz, $CDCl_3$) δ 7.32-7.42 (5H, m), 4.06 (2H, dd, J = 7.0 Hz, 7.0 Hz), 2.74-2.81 (1H, m), 2.64-2.70 (1H, m), 2.46-2.54 (1H, m), 2.19-2.33 (2H, m), 1.35-1.47 (4H, m), 0.99 (3H, t, J = 7.0 Hz), 0.93 (3H, t, J = 7.0 Hz) ppm; ^{13}C NMR (125 MHz, $CDCl_3$) δ 195.7, 166.6, 159.1, 139.0, 133.1, 129.4, 128.5, 126.5, 61.1, 43.4, 38.0, 37.8, 34.1, 19.5, 14.0, 13.7 ppm. HRMS (ESI) Calculated Mass for $C_{18}H_{23}O_3$: 287.1647 ($[M+H]^+$), Found 287.1645 ($[M+H]^+$). The enantiomeric excess was determined by HPLC analysis, using DAICEL CHIRALPAK OJ-H column (1% isopropanol in n-hexane at 1.0 mL/min), Rt = 25.0 min (minor) and 29.6 min (major), **III-15q**-R (90% ee): $[\alpha]^{20}_D$= -56 (c = 4.09, $CDCl_3$).

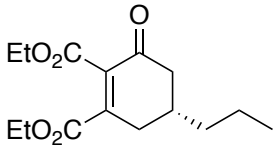

III-15r

III-15r-*R*: Diethyl (*R*)-3-oxo-5-propylcyclohex-1-ene-1,2-dicarboxylate: Compound **III-12r** (34.0 mg, 0.2 mmol) was subject to general procedure B to provide 36.1 mg (64% yield) of the pure product as a light yellow oil; ^{1}H NMR (500 MHz, $CDCl_3$) δ 4.31 (2H, dd, J = 7.0 Hz, 7.0 Hz), 4.26 (2H, dd, J = 7.0 Hz, 7.0 Hz), 2.79-2.86 (1H, m), 2.59-2.66 (1H, m), 2.09-2.29 (3H, m), 1.35-1.44 (4H, m), 1.32 (3H, t, J = 7.0 Hz), 1.30 (3H, t, J = 7.0 Hz), 0.89-0.93 (3H, m) ppm; ^{13}C NMR (125 MHz, $CDCl_3$) δ 196.2, 165.5, 165.4, 145.0, 137.4, 62.2, 61.7, 43.7, 37.6, 33.5, 31.8, 19.4, 14.0, 13.9, 13.9 ppm. HRMS (ESI) Calculated Mass for $C_{15}H_{22}O_5Na$: 305.1365 ($[M+Na]^+$), Found 305.1373 ($[M+Na]^+$). The enantiomeric excess was determined by HPLC analysis, using DAICEL CHIRALPAK AD-H column (2% isopropanol in n-hexane at 0.3 mL/min), Rt = 74.8 min (major) and 81.3 min (minor), **III-15r**-R (80% ee): $[\alpha]^{20}_{D}$= -35 (c = 1.08, $CDCl_3$).

III-4.4. General procedure C for base-catalyzed 4*H*-pyrans synthesis:

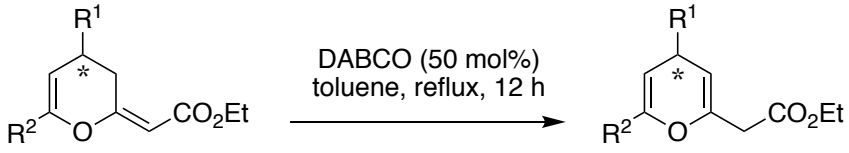

III-14a-j **III-16a-j**

All the dihydropyran derivatives **III-14** were synthesized by reported procedure.[59,66]

To a solution of the corresponding compound **III-14** (1.0 equiv) in toluene, DABCO (50 mol% equiv) was added. The solution was heated to 110 °C and kept at this

temperature for 12 hours. The mixture was concentrated under N_2 flow. The residue was purified by silica gel column chromatography using ethyl acetate in hexanes (0-10%) as the eluent.

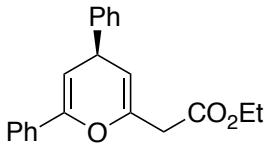

III-16a

III-16a-*S*: Ethyl (*S*)-2-(4,6-diphenyl-4H-pyran-2-yl)acetate: Compound **III-14a** (32.0 mg, 0.1 mmol) was subject to general procedure C to provide 25.9 mg (81% yield) of the pure product as a light orange oil; ^{1}H NMR (500 MHz, $CDCl_3$) δ 7.59-7.55 (2H, m), 7.38-7.27 (7H, m), 7.26-7.22 (1H, m), 5.44-5.39 (1H, m), 4.92-4.87 (1H, m), 4.26-4.23 (1H, m), 4.22 (2H, dd, *J* = 7.0 Hz, 7.0 Hz), 3.27 (1H, d, *J* = 16.0 Hz), 3.23 (1H, d, *J* = 16.0 Hz), 1.30 (3H, t, *J* = 7.0 Hz) ppm; ^{13}C NMR (125 MHz, $CDCl_3$) δ 169.7, 147.9, 146.4, 144.4, 134.0, 128.6, 128.3, 128.2, 127.9, 126.7, 124.5 103.2, 100.3, 61.1, 39.6, 38.3, 14.2 ppm. HRMS (ESI) Calculated Mass for $C_{21}H_{21}O_3$: 321.1491 ($[M+H]^+$), Found 321.1483 ($[M+H]^+$). The enantiomeric excess was determined by HPLC analysis, using DAICEL CHIRALPAK OJ-H column (2% isopropanol in *n*-hexanes at 1.0 mL/min), R_t = 21.2 min (major), **III-16a**-*S* (>99% *ee*): $[\alpha]^{20}_D$ = +41 (*c* = 0.770, $CDCl_3$).

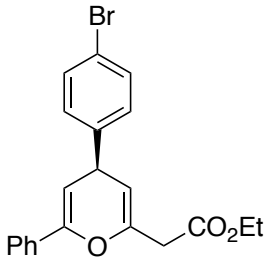

III-16b

III-16b-*S*: Ethyl (S)-2-(4-(4-bromophenyl)-6-phenyl-4H-pyran-2-yl)acetate: Compound **III-14b** (39.9 mg, 0.1 mmol) was subject to general procedure C to provide 25.2 mg (63% yield) of the pure product as a light orange oil; ^{1}H NMR (500 MHz, $CDCl_3$) δ 7.58-7.54 (2H, m), 7.48-7.44 (2H, m), 7.36-7.28 (3H, m), 7.22-7.18 (2H, m), 5.38-5.34 (1H, m), 4.89-4.83 (1H, m), 4.22 (2H, dd, *J* = 7.0 Hz, 7.0 Hz), 4.22-4.18 (1H, m), 3.26 (1H, d, *J* = 16.0 Hz), 3.22 (1H, d, *J* = 16.0 Hz), 1.30 (3H, t, *J* = 7.0 Hz) ppm; ^{13}C NMR (125 MHz, $CDCl_3$) δ 169.5, 148.3, 145.4, 144.8, 133.9, 131.7, 129.7, 128.5, 128.3, 124.5, 120.5, 102.7, 99.8, 61.1, 39.6, 37.9, 14.2 ppm. The enantiomeric excess was determined by HPLC analysis, using DAICEL CHIRALPAK OJ-H column (5% isopropanol in *n*-hexanes at 1.0 mL/min), R_t = 18.0 min (major) and R_t = 55.6 min (minor), **III-16b**-*S* (91% *ee*): $[\alpha]^{20}_{D}$ = +49 (*c* = 1.20, $CDCl_3$).

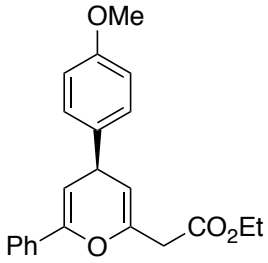

III-16c

III-16c-*S*: Ethyl (S)-2-(4-(4-methoxyphenyl)-6-phenyl-4H-pyran-2-yl)acetate: Compound **III-14c** (35.0 mg, 0.1 mmol) was subject to general procedure C to provide 24.5 mg (70% yield) of the pure product as a light orange oil; ^{1}H NMR (500 MHz, $CDCl_3$) δ 7.59-7.54 (2H, m), 7.36-7.28 (3H, m), 7.26-7.22 (2H, m), 6.90-6.86 (2H, m), 5.42-5.36 (1H, m), 4.90-4.84 (1H, m), 4.21 (2H, dd, *J* = 7.0 Hz, 7.0 Hz), 4.19-4.16 (1H, m), 3.80 (3H,

s), 3.26 (1H, d, *J* = 16.0 Hz), 3.22 (1H, d, *J* = 16.0 Hz), 1.30 (3H, t, *J* = 7.0 Hz) ppm; ^{13}C NMR (125 MHz, $CDCl_3$) δ 169.8, 158.4, 147.7, 144.2, 138.8, 134.1, 128.9, 128.3, 128.2, 124.4, 114.0, 103.5, 100.6, 61.1, 55.3, 39.6, 37.5, 14.2 ppm. HRMS (ESI) Calculated Mass for $C_{22}H_{23}O_4$: 351.1596 ($[M+H]^+$), Found 351.1584 ($[M+H]^+$). The enantiomeric excess was determined by HPLC analysis, using DAICEL CHIRALPAK OJ-H column (20% isopropanol in *n*-hexanes at 1.0 mL/min), R_t = 30.7 min (major) and R_t = 50.2 min (minor), **III-16c**-*S* (94% *ee*): $[\alpha]^{20}_D$ = +38 (*c* = 0.31, $CDCl_3$).

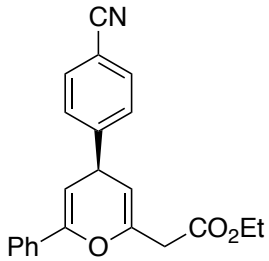

III-16d

III-16d-*S*: Ethyl (S)-2-(4-(4-cyanophenyl)-6-phenyl-4H-pyran-2-yl)acetate: Compound **III-14d** (34.5 mg, 0.1 mmol) was subject to general procedure C to provide 31.7 mg (92% yield) of the pure product as a light orange oil; ^{1}H NMR (500 MHz, $CDCl_3$) δ 7.65-7.62 (2H, m), 7.57-7.53 (2H, m), 7.46-7.43 (2H, m), 7.41-7.32 (3H, m), 5.38-5.33 (1H, m), 4.89-4.84 (1H, m), 4.34-4.28 (1H, m), 4.22 (2H, dd, *J* = 7.0 Hz, 7.0 Hz), 3.28 (1H, d, *J* = 16.0 Hz), 3.24 (1H, d, *J* = 16.0 Hz), 1.30 (3H, t, *J* = 7.0 Hz) ppm; ^{13}C NMR (125 MHz, $CDCl_3$) δ 169.4, 151.5, 148.7, 145.3, 133.5, 132.5, 128.7, 128.5, 128.3, 124.5, 118.9, 110.5, 102.0, 98.9, 61.2, 39.5, 38.5, 14.2 ppm. HRMS (ESI) Calculated Mass for $C_{22}H_{20}NO_3$: 346.1443 ($[M+H]^+$), Found 346.1435 ($[M+H]^+$). The enantiomeric excess was determined by HPLC analysis, using DAICEL CHIRALPAK OD-H column (8% isopropanol in *n*-

hexanes at 1.0 mL/min), R_t = 14.0 min (major) and R_t = 26.0 min (minor), **III-16d**-*S* (92% *ee*): $[\alpha]^{20}_D$ = +49 (*c* = 1.19, $CDCl_3$).

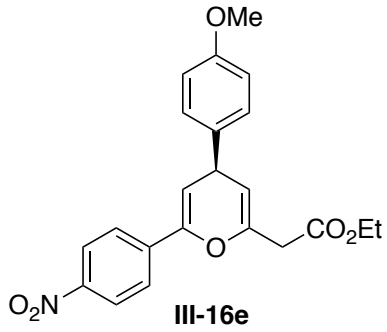

III-16e

III-16e-*S*: Ethyl (S)-2-(4-(4-methoxyphenyl)-6-(4-nitrophenyl)-4H-pyran-2-yl)acetate: Compound **III-14e** (39.5 mg, 0.1 mmol) was subject to general procedure C to provide 11.1 mg (28% yield) of the pure product as a light orange oil; ^{1}H NMR (500 MHz, $CDCl_3$) δ 8.21-8.16 (2H, m), 7.73-7.68 (2H, m), 7.26-7.22 (2H, m), 6.91-6.88 (2H, m), 5.62-5.57 (1H, m), 4.94-4.88 (1H, m), 4.23 (2H, dd, *J* = 7.0 Hz, 7.0 Hz), 4.23-4.19 (1H, m), 3.80 (3H, s), 3.29 (1H, d, *J* = 16.0 Hz), 3.25 (1H, d, *J* = 16.0 Hz), 1.30 (3H, t, *J* = 7.0 Hz) ppm; ^{13}C NMR (125 MHz, $CDCl_3$) δ 169.5, 158.6, 147.4, 145.9, 144.2, 140.0, 137.8, 128.9, 125.0, 123.6, 114.1, 104.7, 103.5, 61.2, 55.3, 39.4, 37.5, 14.2 ppm. HRMS (ESI) Calculated Mass for $C_{22}H_{22}NO_6$: 396.1447 ($[M+H]^+$), Found 396.1423 ($[M+H]^+$). The enantiomeric excess was determined by HPLC analysis, using DAICEL CHIRALPAK OD-H column (3% isopropanol in *n*-hexanes at 0.3 mL/min), R_t = 145.9 min (minor) and R_t = 152.7 min (major), **III-16e**-*S* (96% *ee*): $[\alpha]^{20}_D$ = +33 (*c* = 0.27, $CDCl_3$).

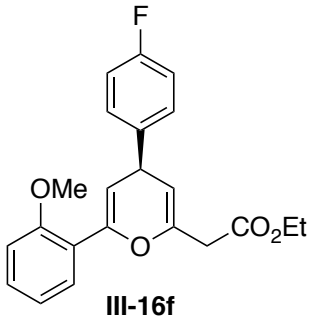

III-16f

III-16f-*S*: Ethyl (S)-2-(4-(4-fluorophenyl)-6-(2-methoxyphenyl)-4H-pyran-2-yl)acetate: Compound **III-14f** (36.8 mg, 0.1 mmol) was subject to general procedure C to provide 25.8 mg (70% yield) of the pure product as a light orange oil; ^{1}H NMR (500 MHz, $CDCl_3$) δ 7.56 (1H, dd, *J* = 8.0 Hz, 2.0 Hz), 7.33-7.29 (2H, m), 7.29-7.25 (1H, m), 7.05-6.99 (2H, m), 6.96 (1H, td, *J* = 7.5 Hz, 1.0 Hz), 6.92-6.89 (1H, m), 5.66-5.56 (1H, m), 4.87-4.77 (1H, m), 4.27-4.24 (1H, m), 4.20 (2H, dd, *J* = 7.0 Hz, 7.0 Hz), 3.82 (3H, s), 3.21 (1H, d, *J* = 16.0 Hz), 3.17 (1H, d, *J* = 16.0 Hz), 1.28 (3H, t, *J* = 7.0 Hz) ppm; ^{13}C NMR (125 MHz, $CDCl_3$) δ 169.7, 161.5 (d, $^{1}J_{C,F}$ = 242.5 Hz), 156.9, 145.0, 144.5, 142.6 (d, $^{3}J_{C,F}$ = 2.5 Hz), 129.4, 129.3, 128.3, 123.1, 120.4, 115.2 (d, $^{2}J_{C,F}$ = 21.3 Hz), 111.3, 104.8, 103.0, 61.0, 55.5, 39.7, 37.8, 14.2 ppm. HRMS (ESI) Calculated Mass for $C_{22}H_{22}O_4F$: 369.1502 ($[M+H]^+$), Found 369.1490 ($[M+H]^+$). The enantiomeric excess was determined by HPLC analysis, using DAICEL CHIRALPAK OD-H column (1% isopropanol in *n*-hexanes at 0.7 mL/min), R_t = 25.3 min (minor) and R_t = 33.1 min (major), **III-16f**-*S* (95% *ee*): $[\alpha]^{20}_D$ = +87 (*c* = 0.71, $CDCl_3$).

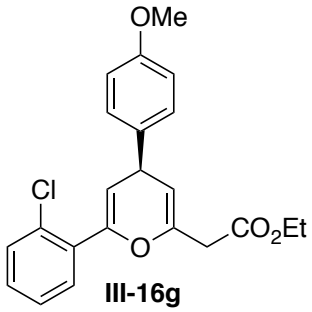

III-16g

III-16g-*S*: Ethyl (S)-2-(6-(2-chlorophenyl)-4-(4-methoxyphenyl)-4H-pyran-2-yl)acetate: Compound **III-14g** (38.5 mg, 0.1 mmol) was subject to general procedure C to provide 25.4 mg (66% yield) of the pure product as a light orange oil; ^{1}H NMR (500 MHz, $CDCl_3$) δ 7.45-7.41 (1H, m), 7.40-7.36 (1H, m), 7.32-7.28 (2H, m), 7.27-7.22 (2H, m), 6.92-6.87 (2H, m), 5.18-5.13 (1H, m), 4.89-4.81 (1H, m), 4.24-4.19 (1H, m), 4.19 (2H, dd, J = 7.0 Hz, 7.0 Hz), 3.80 (3H, s), 3.19 (1H, d, J = 16.0 Hz), 3.15 (1H, d, J = 16.0 Hz), 1.28 (3H, t, J = 7.0 Hz) ppm; ^{13}C NMR (125 MHz, $CDCl_3$) δ 169.7, 158.4, 146.8, 144.3, 138.7, 134.2, 132.8, 130.5, 130.0, 129.6, 128.9, 126.5, 114.0, 105.6, 103.6, 61.0, 55.3, 39.5, 37.6 14.2 ppm. HRMS (ESI) Calculated Mass for $C_{22}H_{22}O_4Cl$: 385.1207 ($[M+H]^+$), Found 385.1183 ($[M+H]^+$). The enantiomeric excess was determined by HPLC analysis, using DAICEL CHIRALPAK OJ-H column (5% isopropanol in n-hexanes at 1.0 mL/min), R_t = 32.8 min (minor) and R_t = 75.4 min (major), **III-16g-*S*** (96% ee): $[\alpha]_{20}^{D}$ = +48 (c = 0.97, $CDCl_3$).

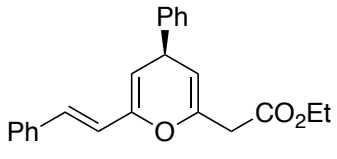

III-16h

III-16h-*S*: Ethyl (S,E)-2-(4-phenyl-6-styryl-4H-pyran-2-yl)acetate: Compound **III-14h**

(34.6 mg, 0.1 mmol) was subject to general procedure C to provide 24.2 mg (70% yield) of the pure product as a light orange oil; ^{1}H NMR (500 MHz, $CDCl_3$) δ 7.42-7.39 (2H, m), 7.37-7.28 (6H, m), 7.26-7.21 (2H, m), 6.89 (1H, d, J = 15.5 Hz), 6.43 (1H, d, J = 15.5 Hz), 5.05-4.97 (1H, m), 4.88-4.83 (1H, m), 4.23 (2H, dd, J = 7.0 Hz, 7.0 Hz), 4.21-4.16 (1H, m), 3.26 (1H, d, J = 16.0 Hz), 3.22 (1H, d, J = 16.0 Hz), 1.31 (3H, t, J = 7.0 Hz) ppm; ^{13}C NMR (125 MHz, $CDCl_3$) δ 169.7,147.2, 146.1, 144.2, 136.7, 128.6, 128.6, 128.2, 127.9, 127.7, 126.7, 126.6, 122.0, 105.9, 103.0, 61.1, 39.6, 38.5, 14.2 ppm. HRMS (ESI) Calculated Mass for $C_{23}H_{23}O_3$: 347.1647 ($[M+H]^+$), Found 347.1625 ($[M+H]^+$). The enantiomeric excess was determined by HPLC analysis, using DAICEL CHIRALPAK OJ-H column (8% isopropanol in n-hexanes at 1.0 mL/min), R_t = 21.4 min (major) and R_t = 27.1 min (minor), **III-16h**-*S* (97% ee): $[\alpha]_{20}^{D}$ = -19 (c = 2.49, $CDCl_3$).

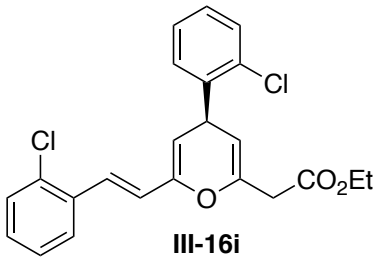

III-16i

III-16i-*S*: Ethyl (S,E)-2-(4-(2-chlorophenyl)-6-(2-chlorostyryl)-4H-pyran-2-yl)acetate: Compound **III-14i** (41.5 mg, 0.1 mmol) was subject to general procedure C to provide 33.2 mg (80% yield) of the pure product as a light orange oil; ^{1}H NMR (500 MHz, $CDCl_3$) δ 7.53 (1H, dd, J = 8.0 Hz, 2.0 Hz), 7.46 (1H, dd, J = 8.0 Hz, 2.0 Hz), 7.36 (2H, ddd, J = 8.0 Hz, 4.5 Hz, 1.0 Hz), 7.29 (1H, td, J = 8.0 Hz, 1.0 Hz), 7.28 (1H, d, J = 15.5 Hz), 7.24-7.15 (3H, m), 6.43 (1H, d, J = 15.5 Hz), 5.13-5.07 (1H, m), 4.92-4.86 (1H, m), 4.75-4.67 (1H, m), 4.24 (2H, dd, J = 7.0 Hz, 7.0 Hz), 3.30 (1H, d, J = 16.0 Hz), 3.26 (1H, d, J = 16.0

Hz), 1.31 (3H, t, J = 7.0 Hz) ppm; ^{13}C NMR (125 MHz, $CDCl_3$) δ 169.6, 147.9, 145.3, 142.4, 134.8, 133.5, 132.3, 130.5, 129.8, 129.3, 128.7, 127.9, 127.4, 126.8, 126.5, 124.4, 124.4, 105.2, 101.3, 61.1, 39.6, 34.7, 14.2 ppm. HRMS (ESI) Calculated Mass for $C_{23}H_{21}O_3Cl_2$: 415.0868 ($[M+H]^+$), Found 415.0865 ($[M+H]^+$). The enantiomeric excess was determined by HPLC analysis, using DAICEL CHIRALPAK OD-H column (1% isopropanol in n-hexanes at 0.8 mL/min), R_t = 23.0 min (minor) and R_t = 26.5 min (major), **III-16i**-*S* (88% ee): $[\alpha]_{20}^{D}$ = -77 (c = 1.55, $CDCl_3$).

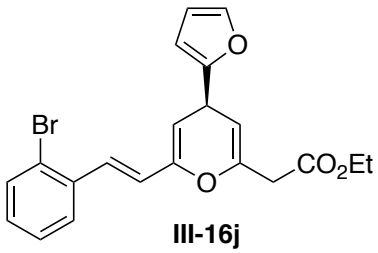

III-16j

III-16j-*S*: Ethyl (S,E)-2-(6-(2-bromostyryl)-4-(furan-2-yl)-4H-pyran-2-yl)acetate: Compound **III-14j** (41.5 mg, 0.1 mmol) was subject to general procedure C to provide 26.1 mg (63% yield) of the pure product as a light orange oil; ^{1}H NMR (500 MHz, $CDCl_3$) δ 7.58 (1H, dd, J = 8.0 Hz, 1.0 Hz), 7.41 (1H, dd, J = 8.0 Hz, 1.5 Hz), 7.36-7.34 (1H, m), 7.29 (1H, td, J = 8.0 Hz, 1.5 Hz), 7.19 (1H, td, J = 8.0 Hz, 2.0 Hz), 6.36-6.32 (1H, m), 6.20-6.15 (1H, m), 5.20-5.16 (1H, m), 5.00-4.95 (1H, m), 4.41-4.37 (1H, m), 4.18 (2H, dd, J = 7.0 Hz, 7.0 Hz), 3.20 (1H, d, J = 16.0 Hz), 3.16 (1H, d, J = 16.0 Hz), 1.27 (3H, t, J = 7.0 Hz) ppm; ^{13}C NMR (125 MHz, $CDCl_3$) δ 169.5, 158.2, 149.2, 145.4, 141.4, 136.0, 133.2, 130.8, 130.1, 127.1, 122.3, 110.4, 105.2, 102.0, 100.3, 61.1, 39.4, 31.8, 14.2 ppm. HRMS (ESI) Calculated Mass for $C_{15}H_{18}O_7Br$: 389.0236 ($[M+H]^+$), Found 389.0251 ($[M+H]^+$). The enantiomeric excess was determined by HPLC analysis, using DAICEL

CHIRALPAK OJ-H column (3% isopropanol in n-hexanes at 0.6 mL/min), R_t = 30.2 min (minor) and R_t = 65.6 min (major), **III-16j**-*S* (90% ee): $[\alpha]_{20}^{D}$ = +23 (c = 0.28, $CDCl_3$).

III-4.5. Synthesis of enone III-13k-III-13l:[68]

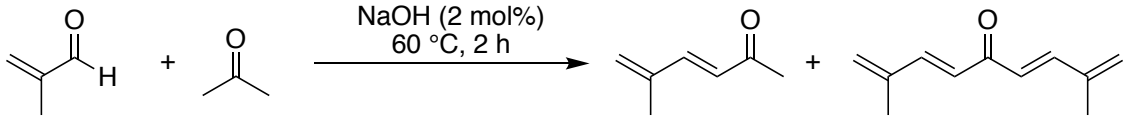

(1 equiv) (5.7 equiv) **III-13k** **III-13l**

To a solution of methacrolein (1.0 g, 1.2 mL, 14.2 mmol) in acetone (6 mL), NaOH (11.4 mg, 0.28 mmol) was added. The reaction mixture was refluxed for 2 h and was then cooled to room temperature. After neutralization with 1 N HCl, the solution was concentrated under vaccum and partitioned with Et_2O (10 mL) and water (10 mL). After separation, the aqueous phase was extracted by Et_2O (2×10 mL). The combined organic phase was dried over anhydrous Na_2SO_4, concentrated, and purified by silica gel column chromatography to provide **III-13k** (500.0 mg, 32% yield) as a light yellow liquid and **III-13l** (38.6 mg, 3% yield) as a light yellow liquid.

III-13k: ^{1}H NMR (500 MHz, $CDCl_3$) δ 7.19 (1H, d, J = 16.0 Hz), 6.13 (1H, d, J = 16.0 Hz), 5.43-5.39 (2H, m), 2.31 (3H, s), 1.90 (3H, d, J = 1.5 Hz) ppm; ^{13}C NMR (125 MHz, $CDCl_3$) δ 199.0, 145.9, 140.9, 127.8, 125.1, 27.3, 18.1 ppm.

III-13l: ^{1}H NMR (500 MHz, $CDCl_3$) δ 7.35 (2H, dd, J = 16.0 Hz, 1.0 Hz), 6.43 (2H, dd, J = 16.0 Hz, 0.5 Hz), 7.46-7.37 (4H, m), 1.94 (6H, dd, J = 1.0 Hz, 0.5 Hz) ppm; ^{13}C NMR (125 MHz, $CDCl_3$) δ 189.8, 145.5, 141.0, 125.9, 125.4, 18.2 ppm.

III-4.6. General procedure D for the synthesis of enone III-13m, III-13q:[69]

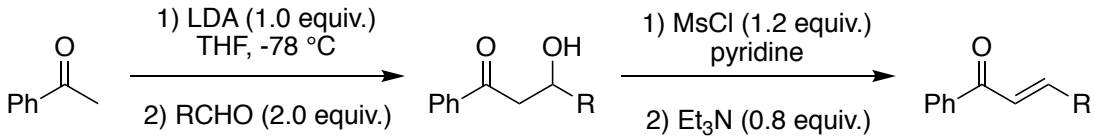

A solution of diisopropylamine (1.01 equiv.) in THF at -78 °C was treated with *n*-BuLi (1.0 equiv.) for 30 min. Enone (1.0 equiv.) was added and after 30 min, aldehyde (2.0 equiv.) (for methacrolein, 1.5 equiv was used). was added at the same temperature. After another 60 min, the reaction was quenched by addition of HOAc-H_2O (1:1 v/v) at -78 °C. The flask was warmed to room temperature, followed by separation of the two phases. The aqueous phase was extracted by Et_2O. The combined organic phase was washed by saturated $NaHCO_3$ and brine, and dried by anhydrous Na_2SO_4. The crude aldol product was used for the next step without further purification.

The aldol production was dissolved in pyridine (12.4 equiv.) at 0 °C and methanesulfonyl chloride (1.22 equiv.) was added. The solution was kept at room temperature overnight and H_2O was added. The mixture was extracted by Et_2O and the combined phase was washed by saturated $CuSO_4$ and brine. The organic layer was dried over anhydrous Na_2SO_4, then concentrated and redissolved in Et_2O, and Et_3N (0.8 equiv.) was added and the mixture was stirred at room temperature for 18 h. Water was added to the reaction, followed by extraction with Et_2O. The combined organic layers were washed by cold 1% HCl, saturated $NaHCO_3$, and then water. The organic phase was dried over $MgSO_4$, then filtrated and concentrated to give a crude oil that was purified by silica gel column chromatography to deliver the enones.

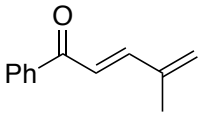

III-13 m

III-13m: Methacrolein (0.87 g, 12.5 mmol) was subject to general procedure D to provide 503.2 mg (35% overall yield) of the pure product as a pale yellow oil; ^{1}H NMR (500 MHz, $CDCl_3$) δ 8.01-7.92 (2H, m), 7.61-7.54 (1H, m), 7.53-7.44 (3H, m), 6.93 (1H, d, J = 15.5 Hz), 5.47 (2H, dd, J = 15.5 Hz, 1.0 Hz), 2.00 (3H, J = 1.5 Hz) ppm; ^{13}C NMR (125 MHz, $CDCl_3$) δ 191.1, 147.2, 141.0, 138.2, 132.7, 128.6, 128.4, 125.8, 122.6, 18.2 ppm.

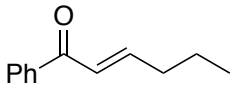

III-13 q

III-13q: Butyraldehyde (1.80 g, 25.0 mmol) was subject to general procedure D to provide 1.76 g (81% overall yield) of the pure product as a pale yellow oil; ^{1}H NMR (500 MHz, $CDCl_3$) δ 7.96-7.90 (2H, m), 7.59-7.53 (1H, m), 7.51-7.44 (2H, m), 7.01 (1H, dt, J = 15.0 Hz, 7.0 Hz), 6.92-6.85 (1H, m), 2.31 (2H, ddd, J = 7.0 Hz, 7.0 Hz, 1.5 Hz), 1.57 (2H, sextet, J = 7.0 Hz), 0.98 (3H, t, J = 7.5 Hz) ppm; ^{13}C NMR (125 MHz, $CDCl_3$) δ 191.0, 149.9, 138.0, 132.6, 128.5, 128.5, 126.0, 34.9, 21.5, 13.8 ppm.

III-4.7. General procedure E for the synthesis of enone III-13n, III-13r:[70]

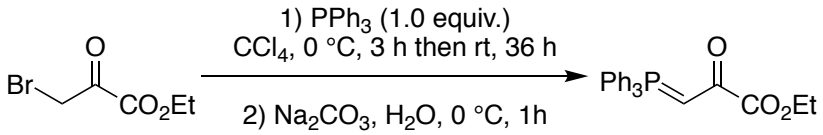

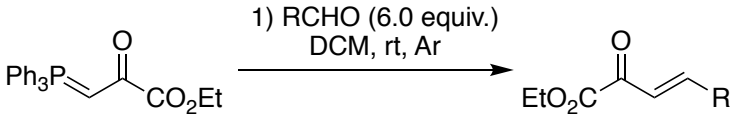

A solution of ethyl bromopyruvate (1.0 equiv.) in dry carbon tetrachloride was added dropwise over 0.5 h to a stirred and cooled (0 °C) solution of triphenyl phosphine (1.0 equiv.) in dry carbon tetrachloride. The reaction was warmed to room temperature and stirred for an additional 24 h. The supernatant was decanted from the yellow hygroscopic crystals, which were then washed with anhydrous ether by trituration and decantation. The resulting dried sticky solid was dissolved in methanol and the solution was cooled to 0 °C. The pH was adjusted to 10 by gradual addition of iced aqueous sodium carbonate (1 N). The solution was diluted with ice water and stirred for 1 h at 0 °C, after which the precipitate was collected and washed with cold water. It was then recrystallized from hot ethanol and water. The resulting ylide crystals separated out as light brown yellow crystals (53% yield).

A solution of aldehyde (6.0 equiv.) and yilde (1.0 equiv.) in dried dichloromethane in sealed tube under Ar protection at room temperature was stirred for 24 h. The mixture was concentrated and separated by silica gel column chromatography to provide **III-13n** and **III-13r**.

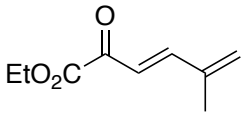

III-13 n

III-13n: Methacrolein (752.8 mg, 2.0 mmol) was subject to general procedure E to provide 63.4 mg (19% yield) of the product as a pale-yellow oil, and it was a mixture with another isomer, however, it would affect the cyclohexanone **III-15n** formation.

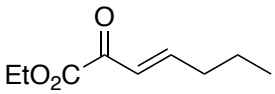

III-13 r

III-13r: Butyraldehyde (752.8g, 2.0 mmol) was subject to general procedure E to provide 162.2 mg (48% yield) of the pure product as a pale yellow oil; ^{1}H NMR (500 MHz, $CDCl_3$) δ 7.19 (1H, dt, J = 16.0 Hz, 7.0 Hz), 6.65 (1H, dt, J = 16.0 Hz, 2.0 Hz), 4.35 (2H, dd, J = 7.0 Hz, 7.0 Hz), 2.29 (2H, qd, J = 7.0 Hz, 1.5 Hz), 1.54 (2H, sextet, J = 7.5 Hz), 1.38 (3H, td, J = 7.5 Hz, 0.5 Hz), 0.96 (3H, t, J = 7.5 Hz) ppm; ^{13}C NMR (125 MHz, $CDCl_3$) δ 183.4, 162.4, 155.0, 125.2, 62.3, 35.1, 21.1, 14.1, 13.7 ppm.

III-4.8. Synthesis of Diels-Alder reaction adduct III-16ia:

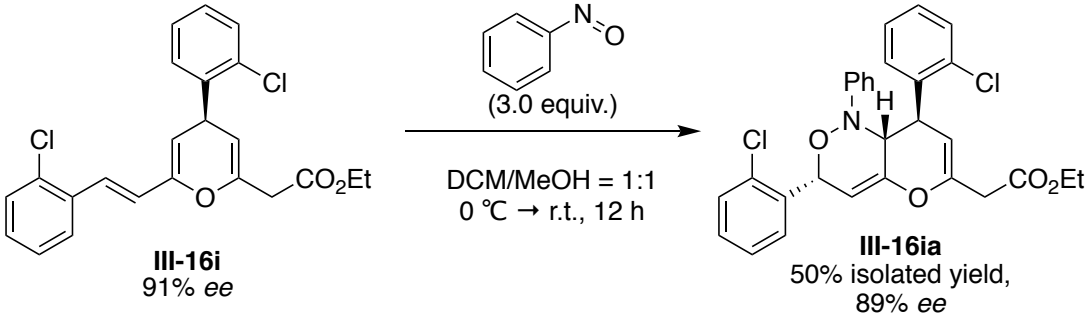

To a solution of nitrosobenzene (3.0 equiv.) in EtOH/DCM (v/v = 1:1), **5i** (1.0 equiv.) was added at 0 °C. The solution was gradually warmed up to room temperature. The reaction was monitored by TLC, and when completed, was quenched with H_2O and extracted with DCM twice. The combined organic layers were dried with anhydrous Na_2SO_4 and concentrated under reduced pressure. The residue was purified by silica gel column chromatography using ethyl acetate in hexanes (1.5%-20%) as eluents to provide **III-16ia** (50% isolated yield) as a light oil.

III-16ia: ^{1}H NMR (500 MHz, $CDCl_3$) δ 7.72 (1H, dd, J = 7.5 Hz, 1.5 Hz), 7.43-7.27 (4H, m), 7.19-7.10 (2H, m), 7.09-7.00 (3H, m), 6.87-6.79 (2H, m), 6.79-6.73 (1H, m), 6.00 (1H, s), 5.55 (1H, s), 4.76 (1H, s), 4.88-4.37 (2H, m), 4.27-4.18 (2H, m), 3.24 (1H, d, J = 16.0 Hz), 3.20 (1H, d, J = 16.0 Hz), 1.31 (3H, t, J = 7.0 Hz) ppm; ^{13}C NMR (125 MHz, $CDCl_3$) δ 169.5, 148.7, 146.8, 135.8, 133.4, 130.5, 129.7, 129.6, 129.3, 128.7, 128.6, 128.0, 127.9, 127.4, 127.1, 126.9, 126.8, 126.5, 121.3, 105.8, 104.5, 71.9, 61.2, 39.6, 39.1, 34.7, 14.2 ppm. HRMS (ESI) Calculated Mass for $C_{29}H_{26}NO_4Cl_2$: 522.1239 ($[M+H]^+$), Found 522.1235 ($[M+H]^+$). The enantiomeric excess was determined by HPLC analysis, using DAICEL CHIRALPAK AD-H column (2% isopropanol in n-hexanes at 1.0 mL/min), R_t = 10.0 min (minor) and R_t = 11.3 min (major), **III-16ia** (89% ee): $[\alpha]_{20}^{D}$ = +43 (c = 1.62, $CDCl_3$).

APPENDIX

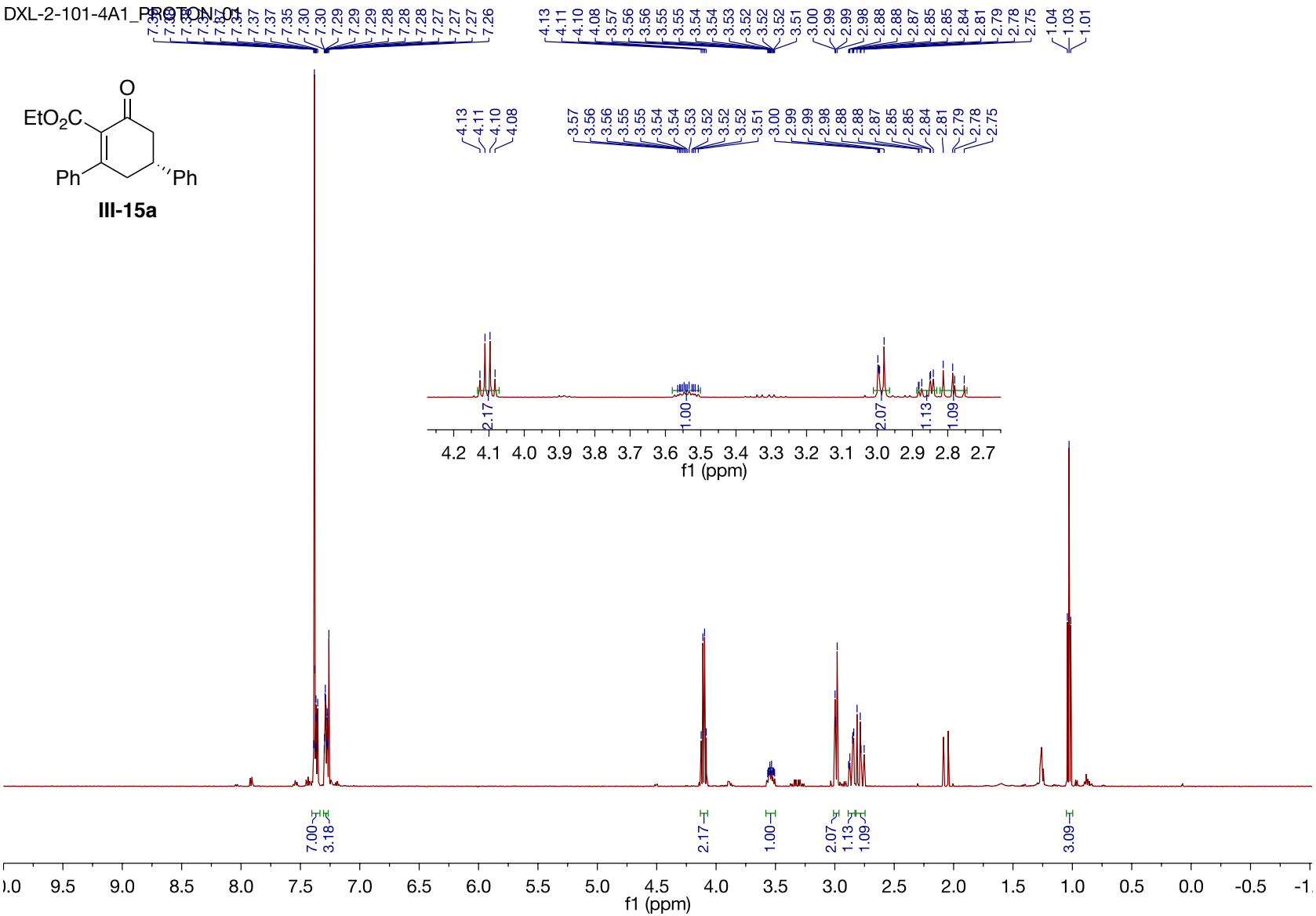
DXL-2-101-4A1_PROTON_01
O
EtO2C
Ph
Ph
III-15a
f1 (ppm)
f1 (ppm)

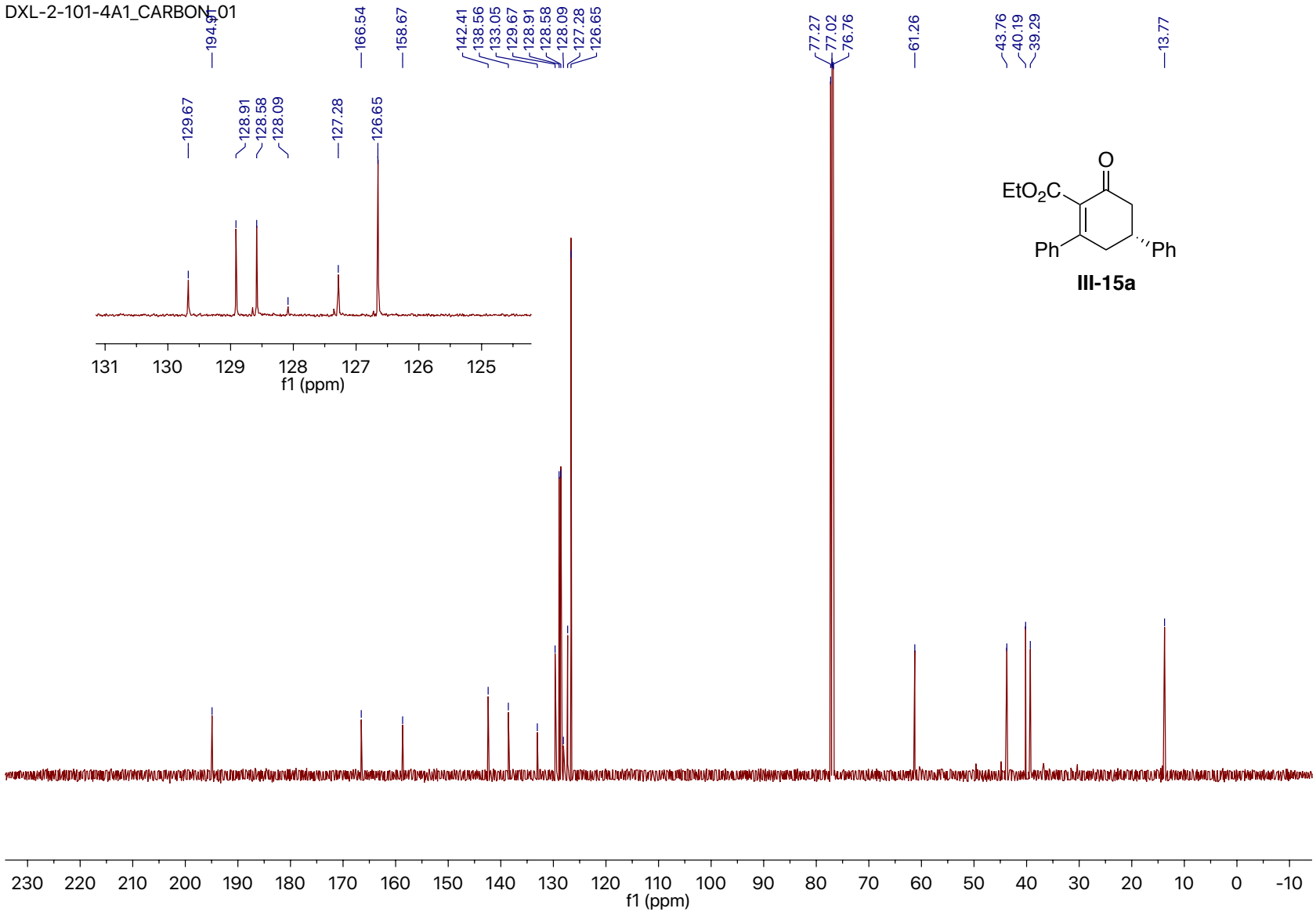
DXL-2-101-4A1_CARBON_01
194.95
166.54
158.67
142.41
138.56
133.05
129.67
128.91
128.58
128.09
127.28
126.65
77.27
77.02
76.76
61.26
43.76
40.19
39.29
13.77
129.67
128.91
128.58
128.09
127.28
126.65
131 130 129 128 127 126 125
f1 (ppm)
O
EtO2C
Ph
Ph
III-15a
230 220 210 200 190 180 170 160 150 140 130 120 110 100 90 80 70 60 50 40 30 20 10 0 -10
f1 (ppm)

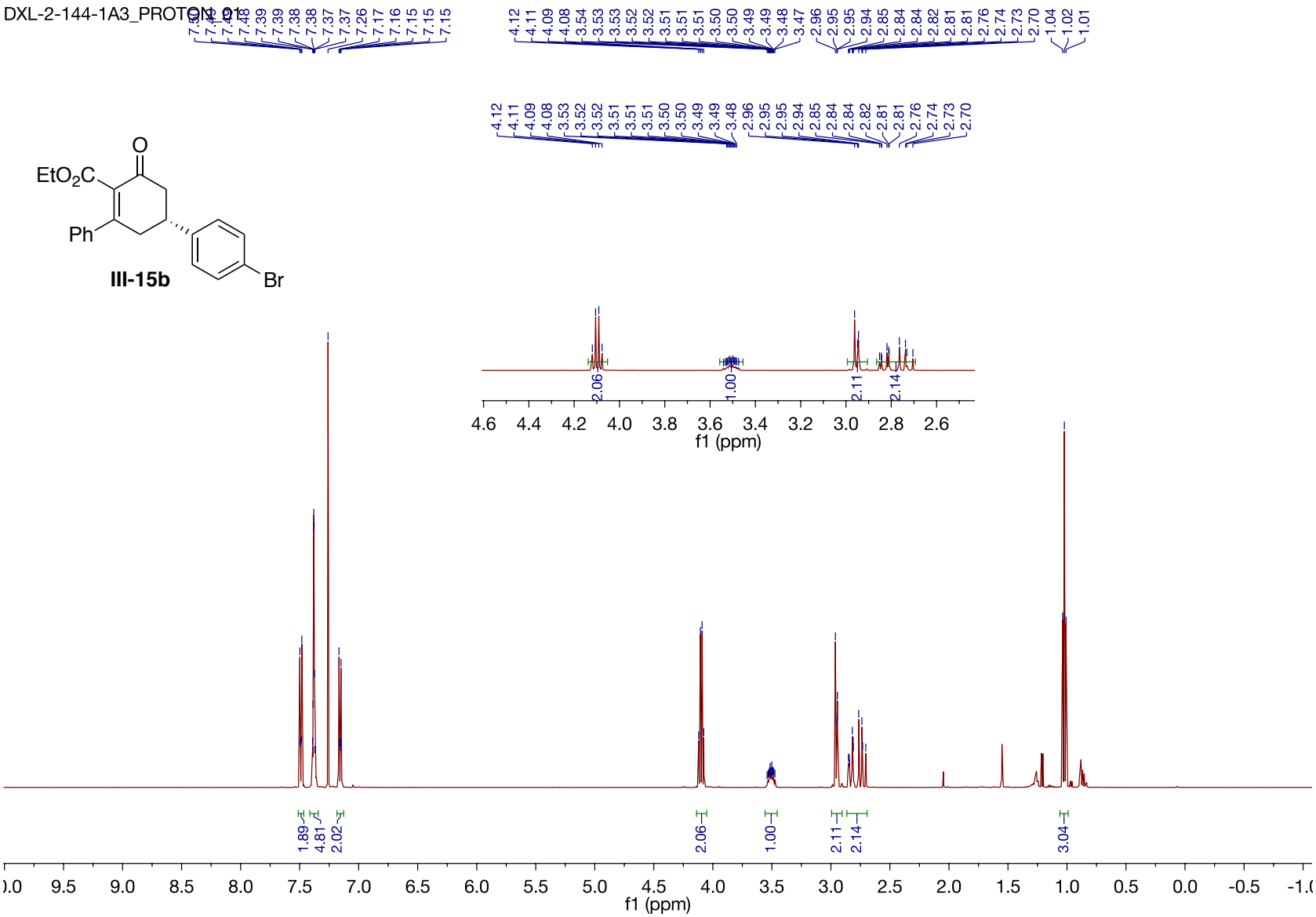
DXL-2-144-1A3_PROTON_01
O
EtO2C
Ph
Br
III-15b
f1 (ppm)

DXL-2-144-1A2_CARBON.001

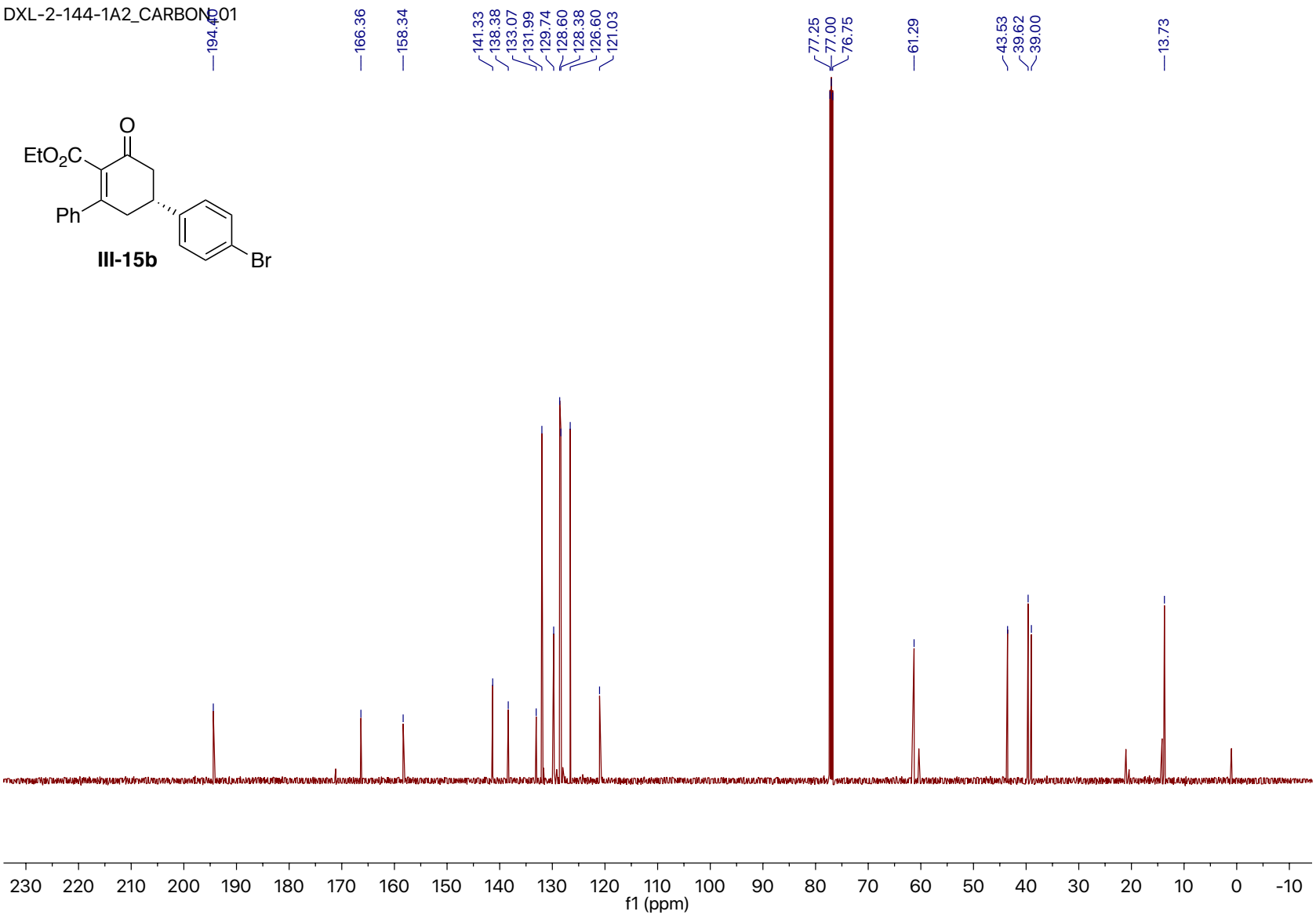

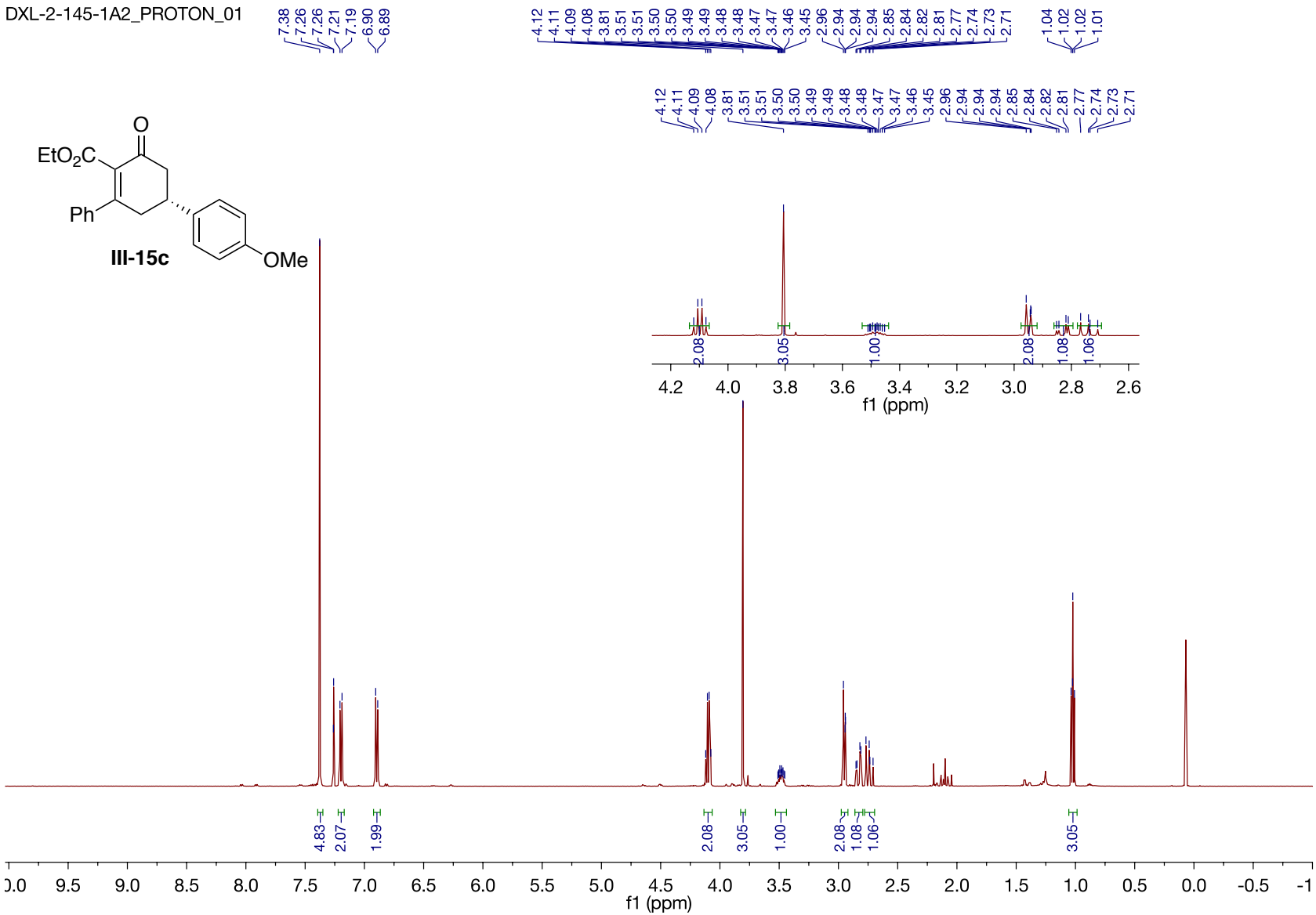
DXL-2-145-1A2_PROTON_01
7.38
7.26
7.26
7.21
7.19
6.90
6.89
4.12
4.11
4.09
4.08
3.81
3.51
3.51
3.50
3.50
3.49
3.49
3.48
3.48
3.47
3.47
3.46
3.45
2.96
2.94
2.94
2.94
2.85
2.84
2.82
2.81
2.77
2.74
2.73
2.71
1.04
1.02
1.02
1.01
O
EtO2C
Ph
OMe
III-15c
2.08
3.05
1.00
2.08
1.08
1.06
f1 (ppm)
4.83
2.07
1.99
2.08
3.05
1.00
2.08
1.08
1.06
3.05
f1 (ppm)

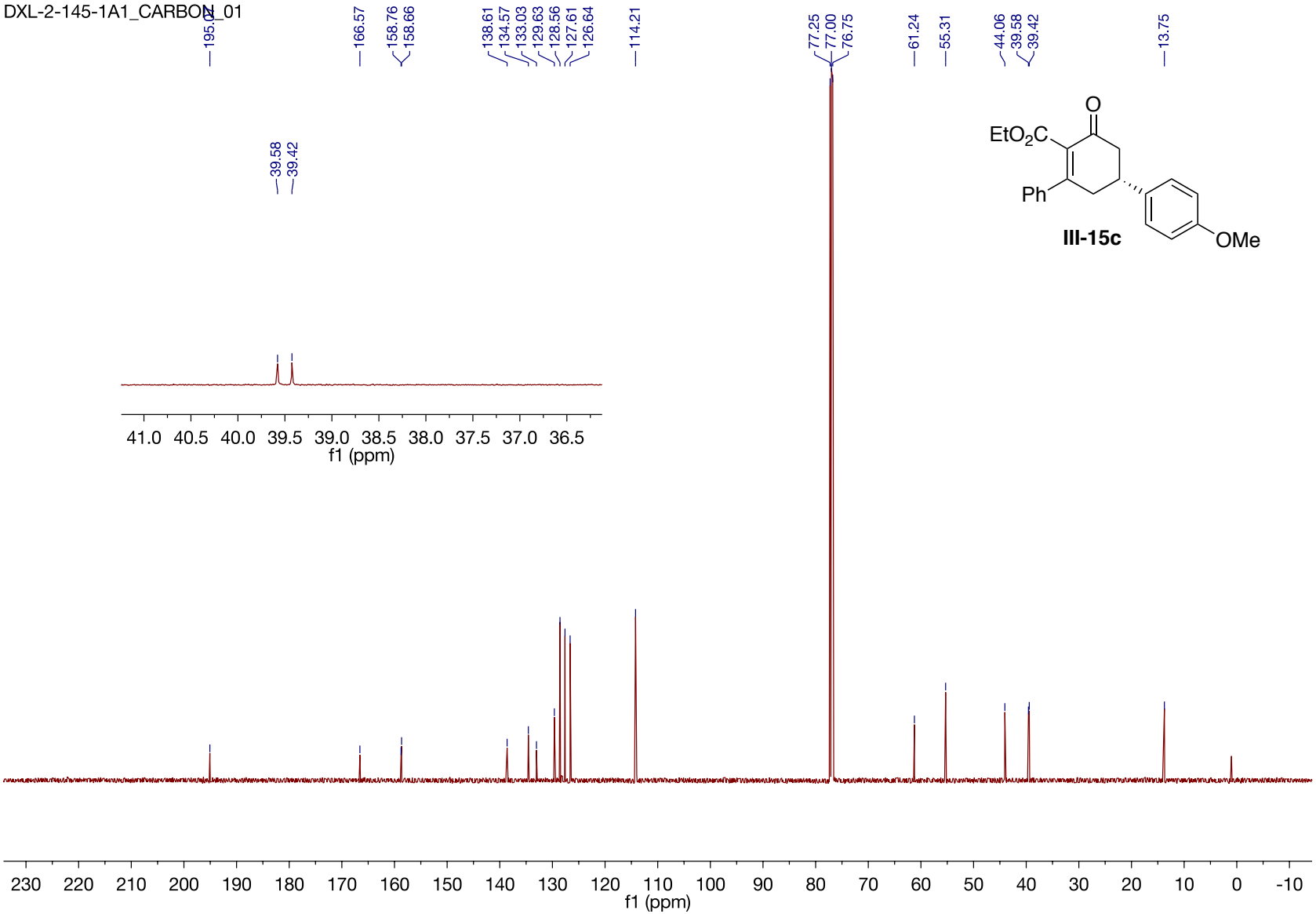
DXL-2-145-1A1_CARBON_01
195.8
166.57
158.76
158.66
138.61
134.57
133.03
129.63
128.56
127.61
126.64
114.21
77.25
77.00
76.75
61.24
55.31
44.06
39.58
39.42
13.75
39.58
39.42
41.0 40.5 40.0 39.5 39.0 38.5 38.0 37.5 37.0 36.5
f1 (ppm)
O
EtO2C
Ph
OMe
III-15c
230 220 210 200 190 180 170 160 150 140 130 120 110 100 90 80 70 60 50 40 30 20 10 0 -10
f1 (ppm)

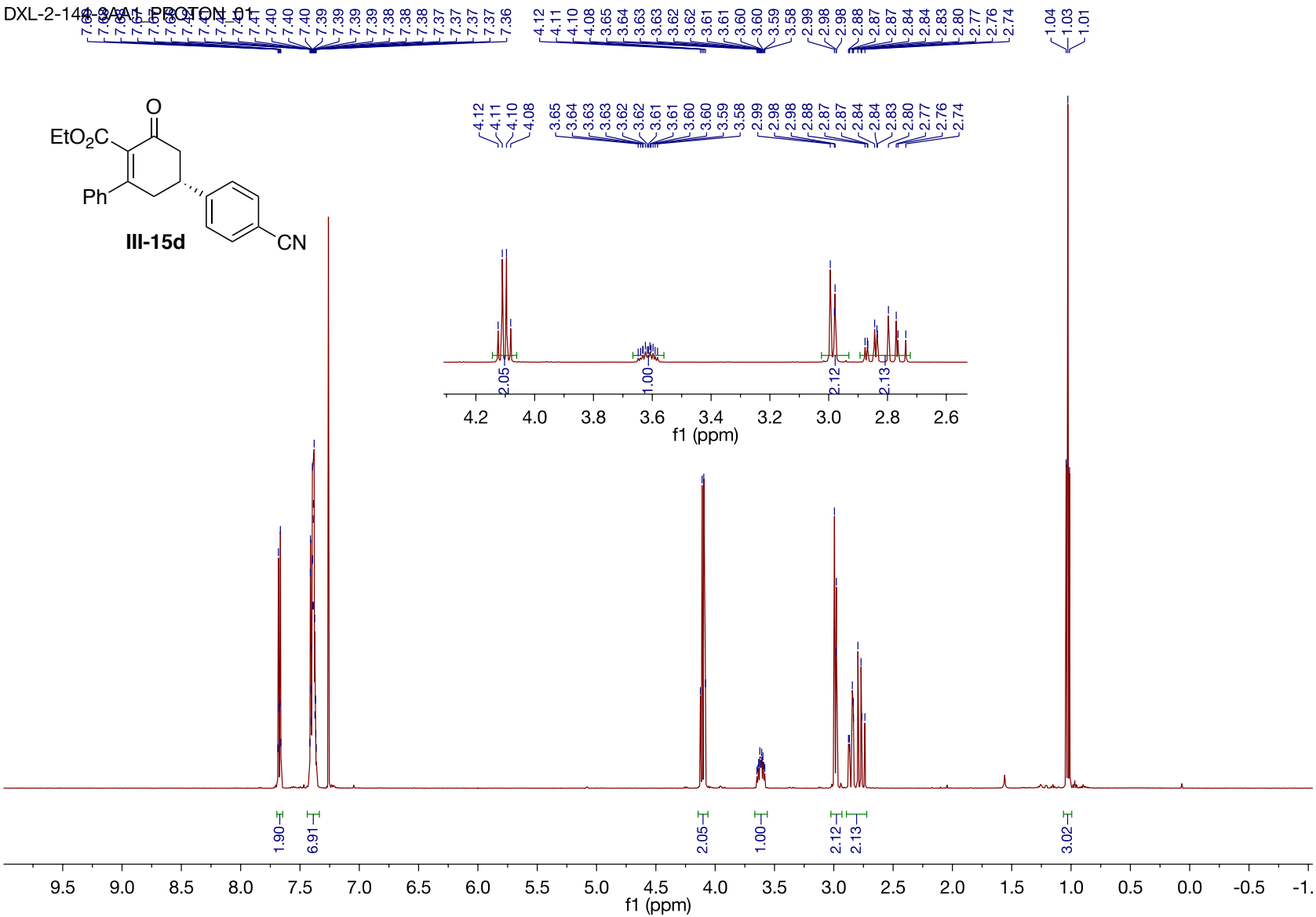
DXL-2-144-3AA1 PROTON 01
O
EtO2C
Ph
CN
III-15d
f1 (ppm)
1.90
6.91
2.05
1.00
2.12
2.13
3.02

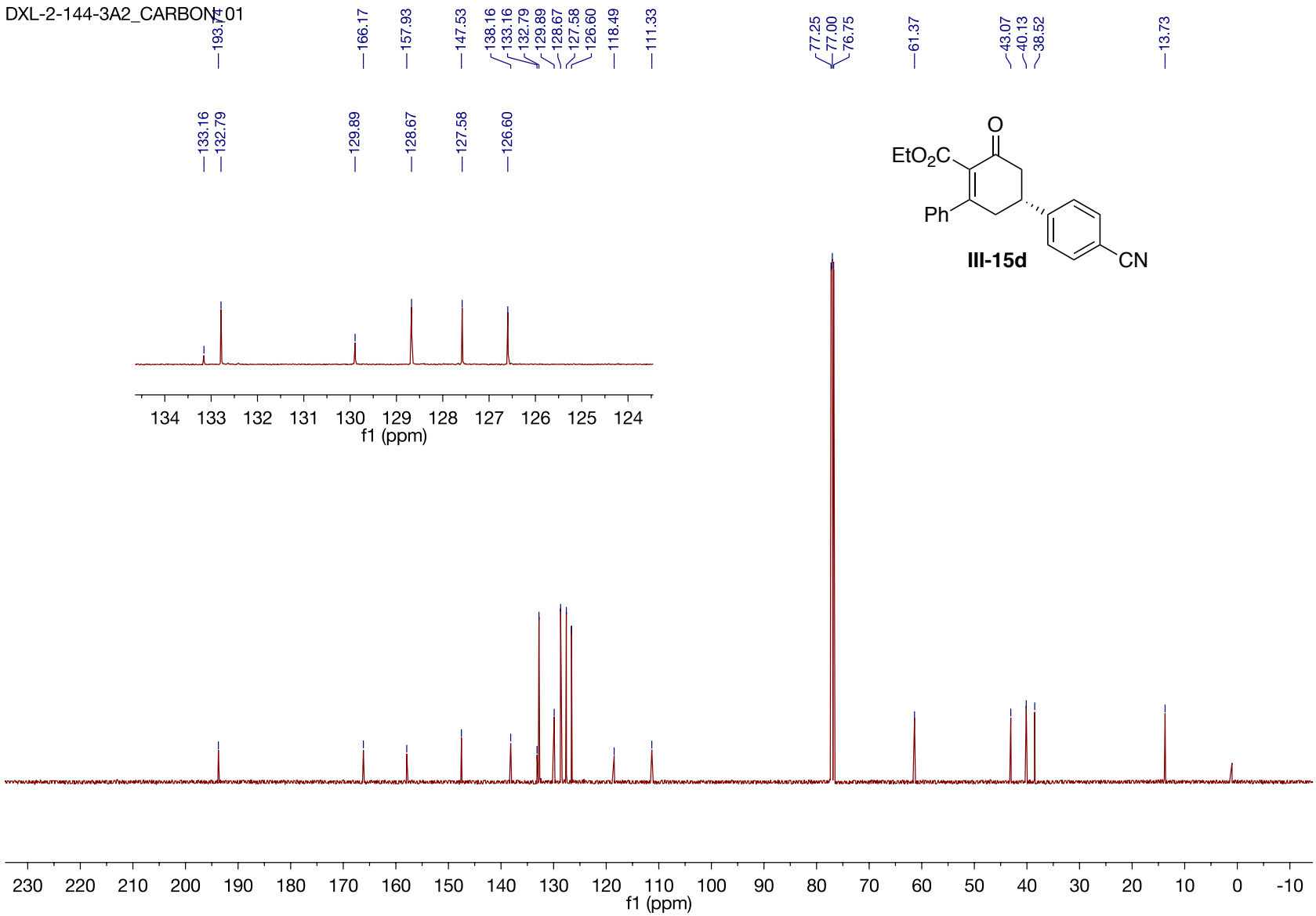
DXL-2-144-3A2_CARBON-01
193.74
166.17
157.93
147.53
138.16
133.16
132.79
129.89
128.67
127.58
126.60
118.49
111.33
77.25
77.00
76.75
61.37
43.07
40.13
38.52
13.73
EtO2C
O
Ph
CN
III-15d
f1 (ppm)
f1 (ppm)

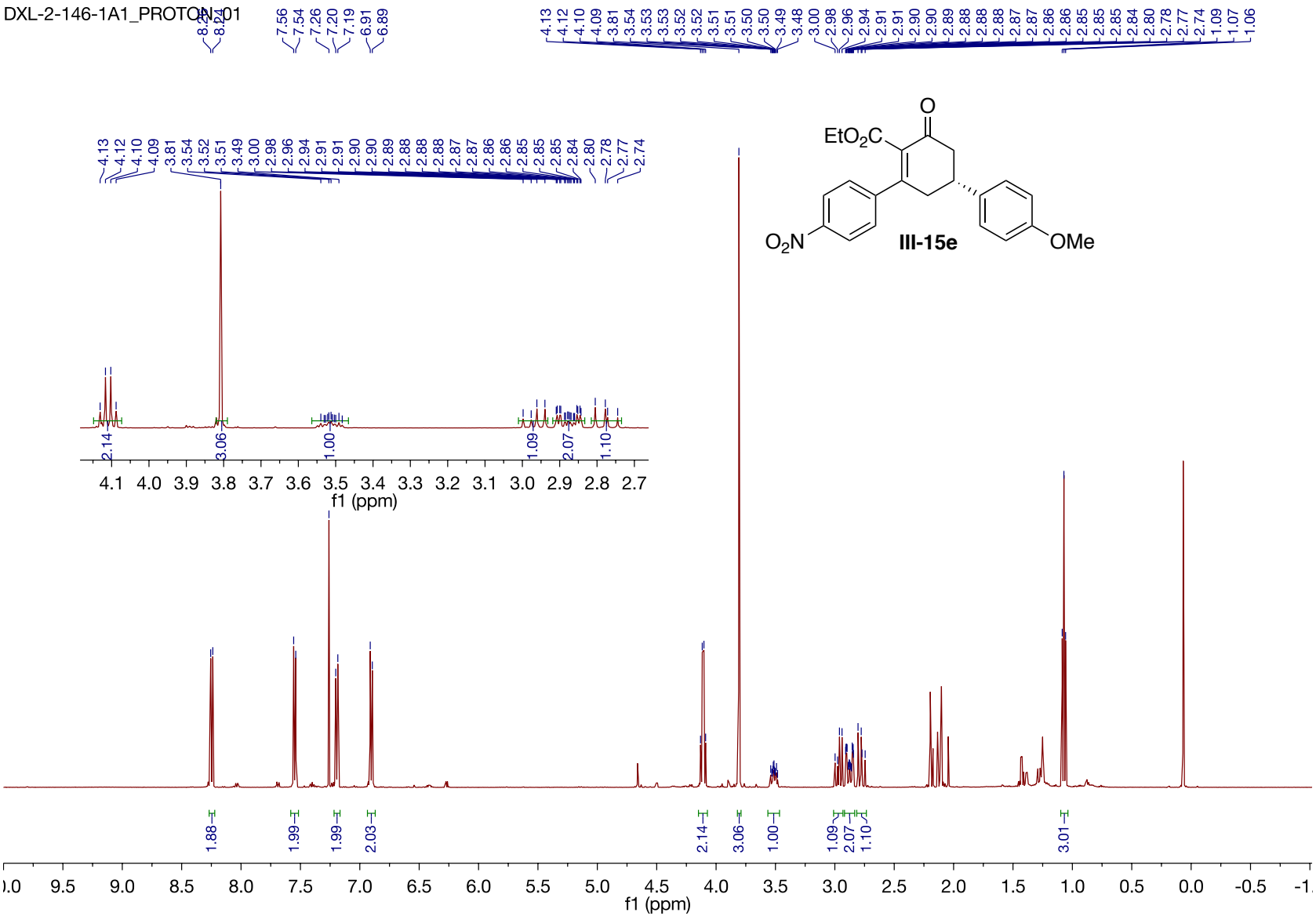
DXL-2-146-1A1_PROTON_01
III-15e
f1 (ppm)

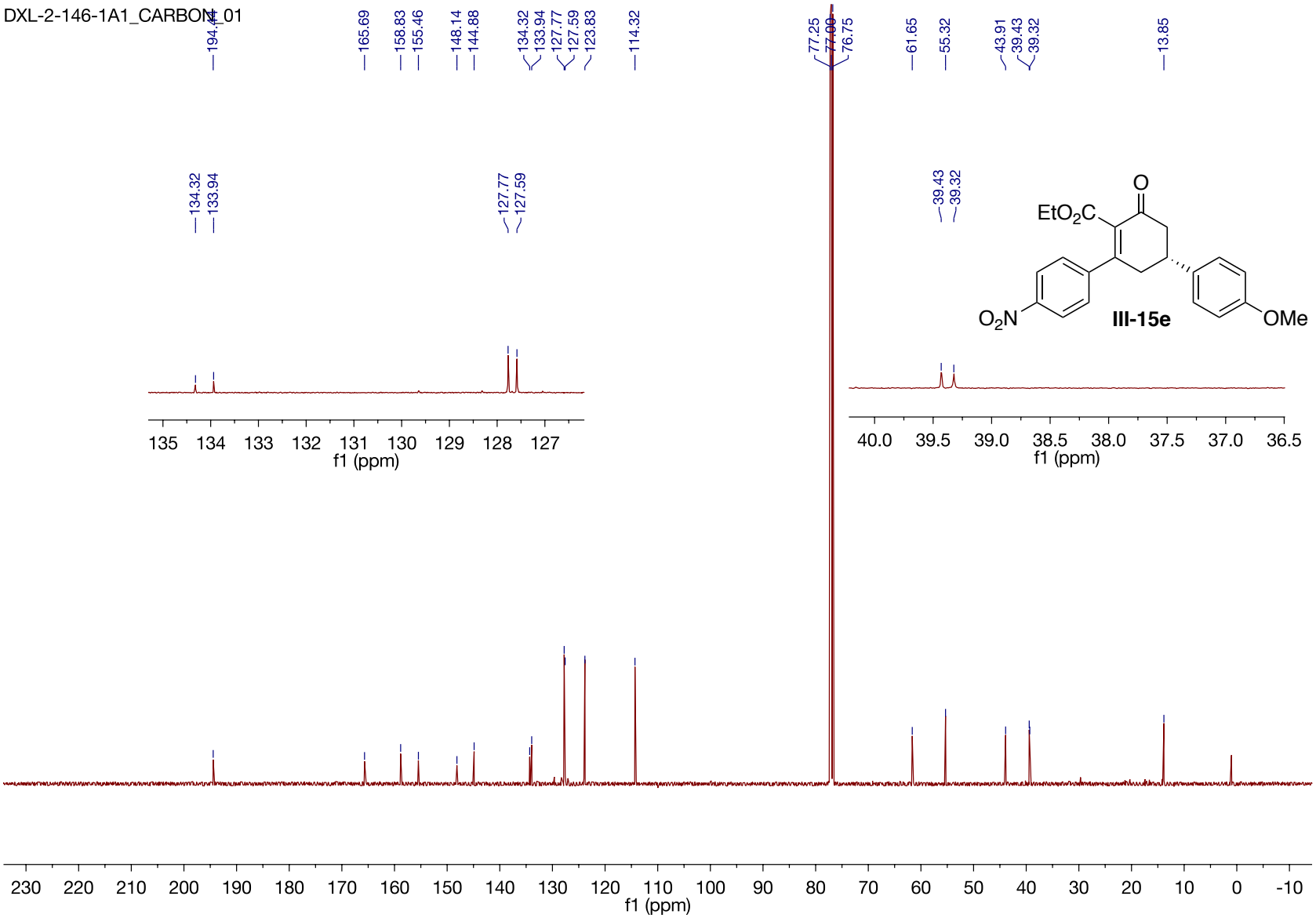
DXL-2-146-1A1_CARBON_01
194.44
165.69
158.83
155.46
148.14
144.88
134.32
133.94
127.77
127.59
123.83
114.32
77.25
77.00
76.75
61.65
55.32
43.91
39.43
39.32
13.85
EtO2C
O
O2N
OMe
III-15e
f1 (ppm)
f1 (ppm)
f1 (ppm)

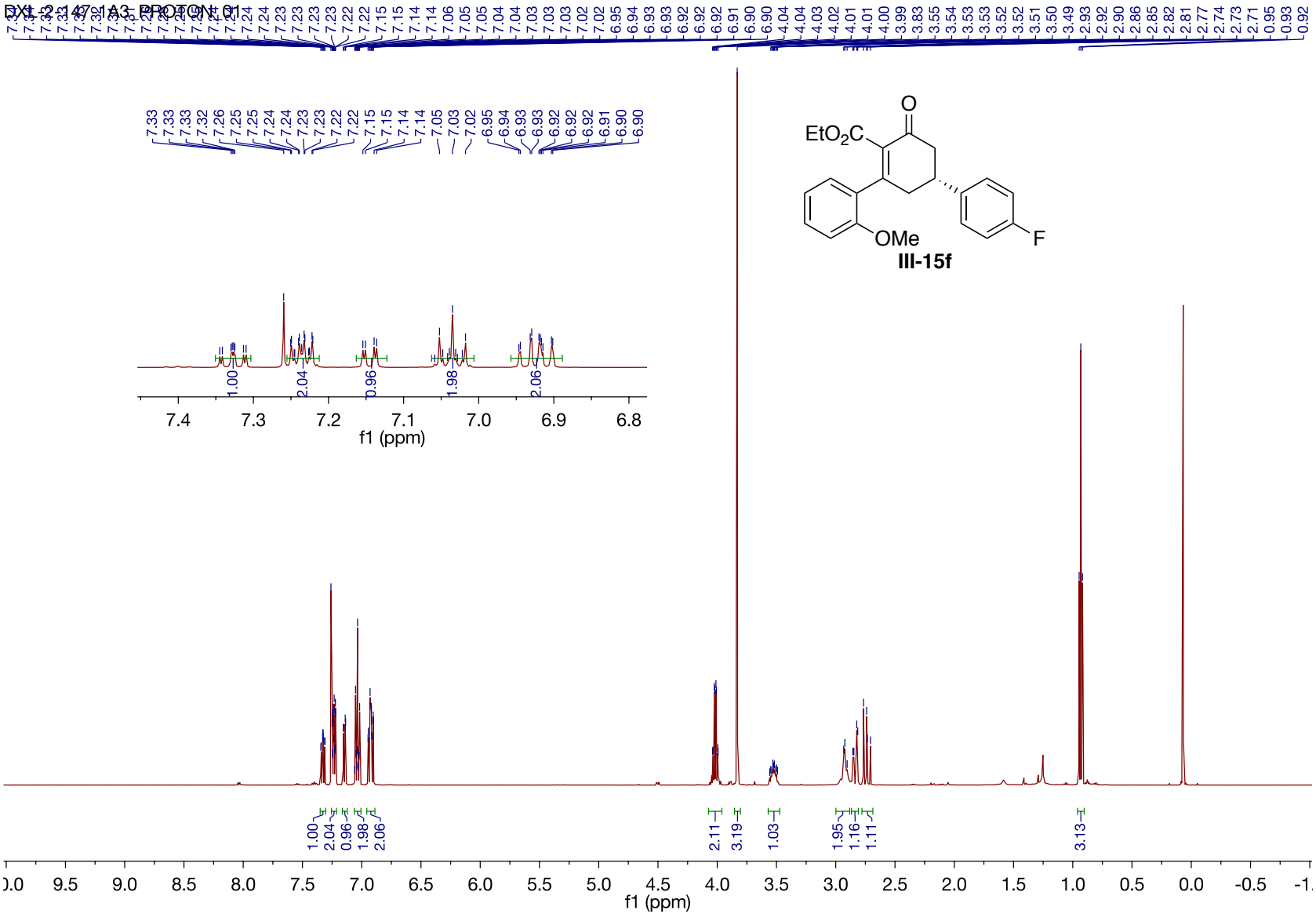
DXL-2-147-1A3-PROTON-01
EtO2C
O
OMe
F
III-15f
f1 (ppm)

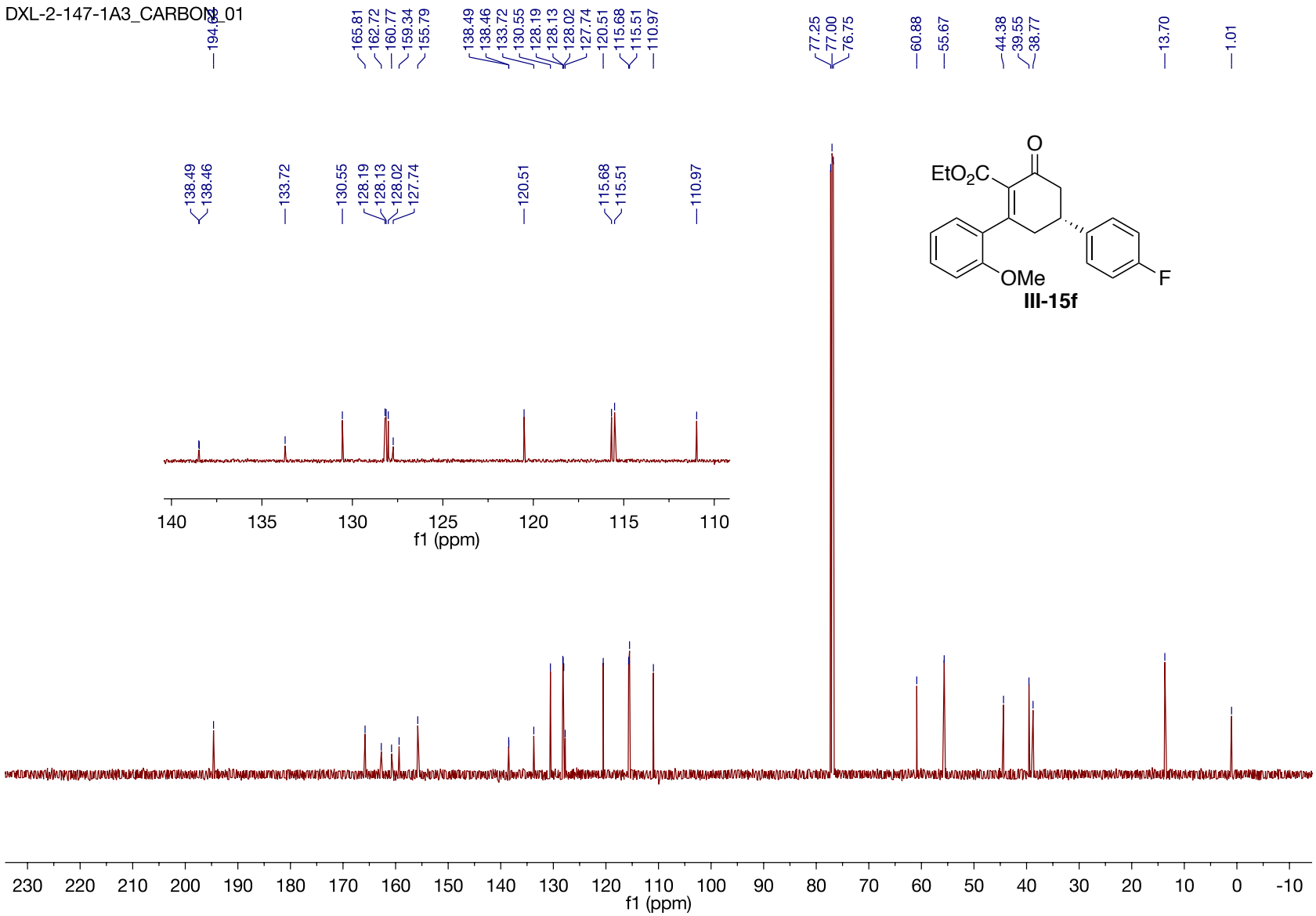
DXL-2-147-1A3_CARBON_01
194.84
165.81
162.72
160.77
159.34
155.79
138.49
138.46
133.72
130.55
128.19
128.13
128.02
127.74
120.51
115.68
115.51
110.97
77.25
77.00
76.75
60.88
55.67
44.38
39.55
38.77
13.70
1.01
O
EtO2C
OMe
F
III-15f
f1 (ppm)
f1 (ppm)

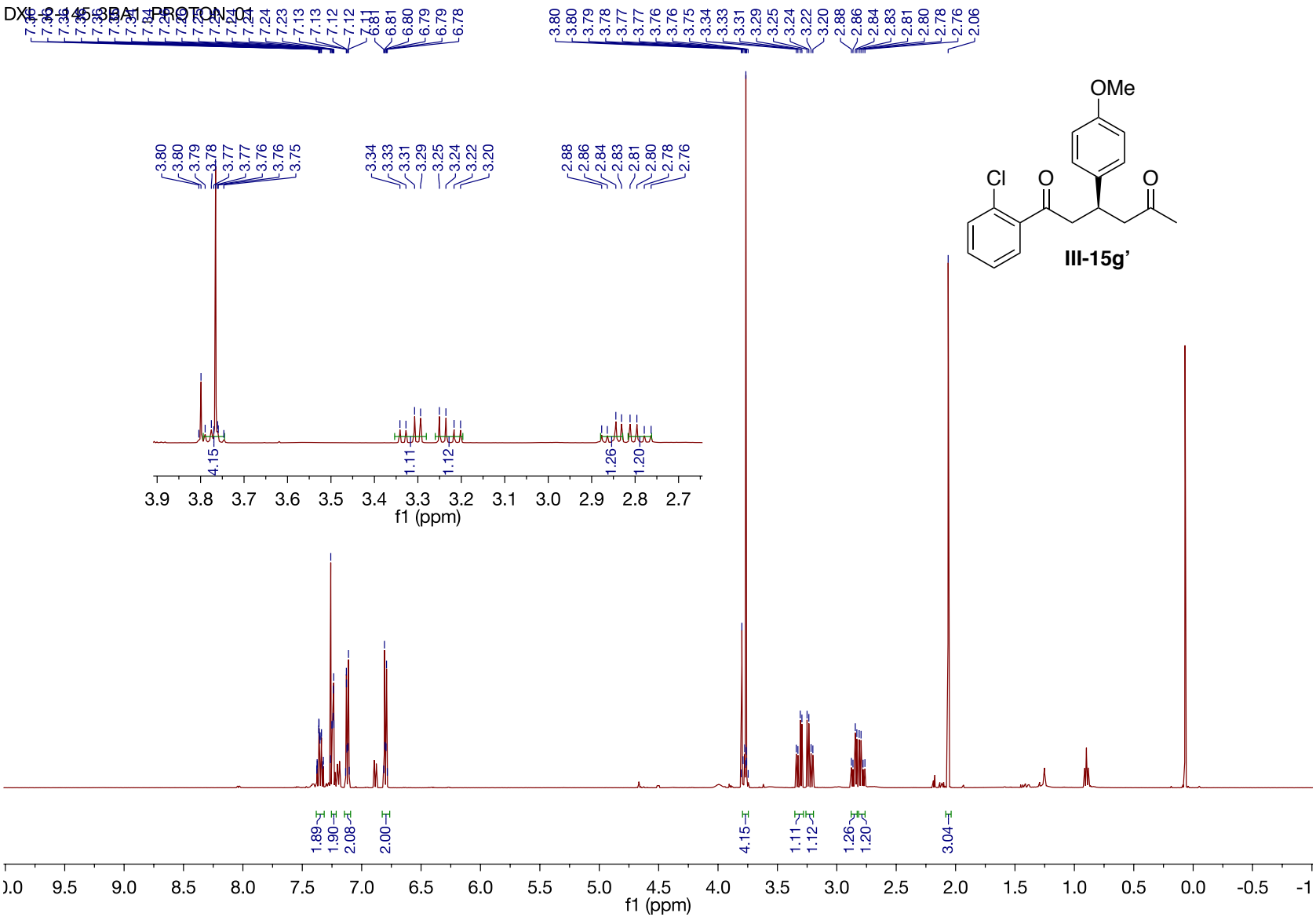
DXP-2-45-3BA1-PROTON-01
OMe
Cl
O
O
III-15g'
f1 (ppm)

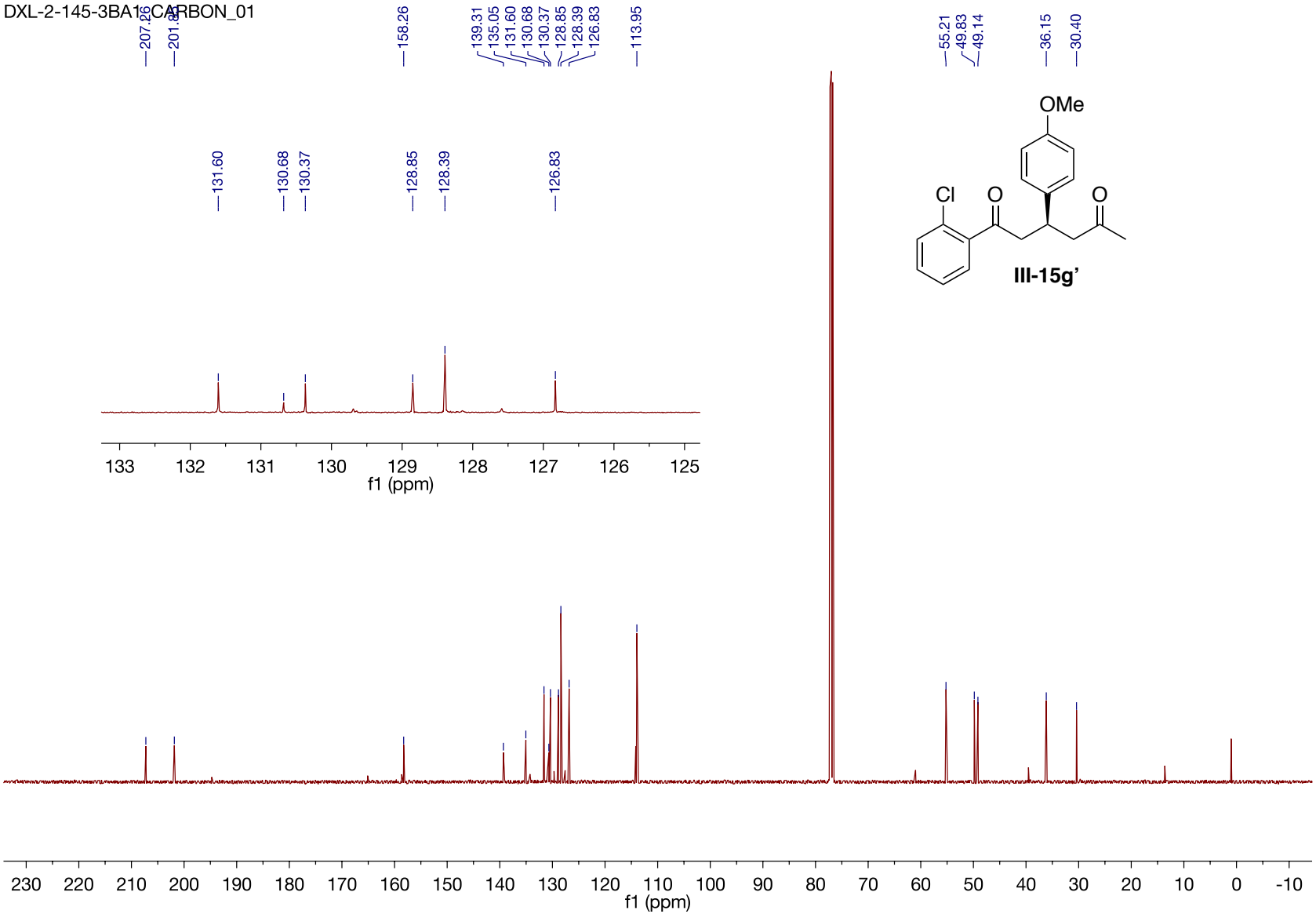
DXL-2-145-3BA1C CARBON_01
207.26
201.38
158.26
139.31
135.05
131.60
130.68
130.37
128.85
128.39
126.83
113.95
55.21
49.83
49.14
36.15
30.40
OMe
Cl
O
O
III-15g'
f1 (ppm)
f1 (ppm)

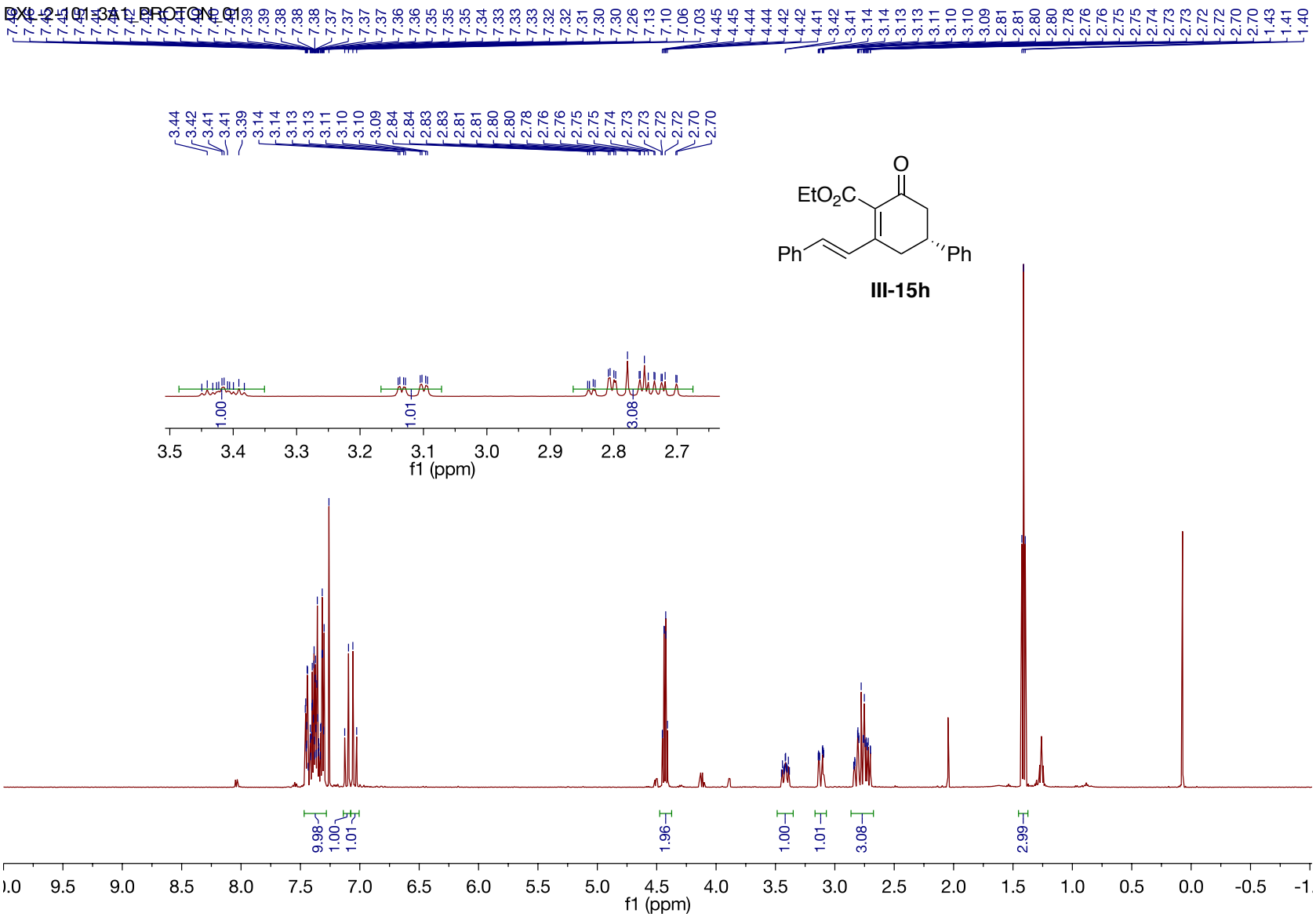
EtO2C
O
Ph
Ph
III-15h
f1 (ppm)

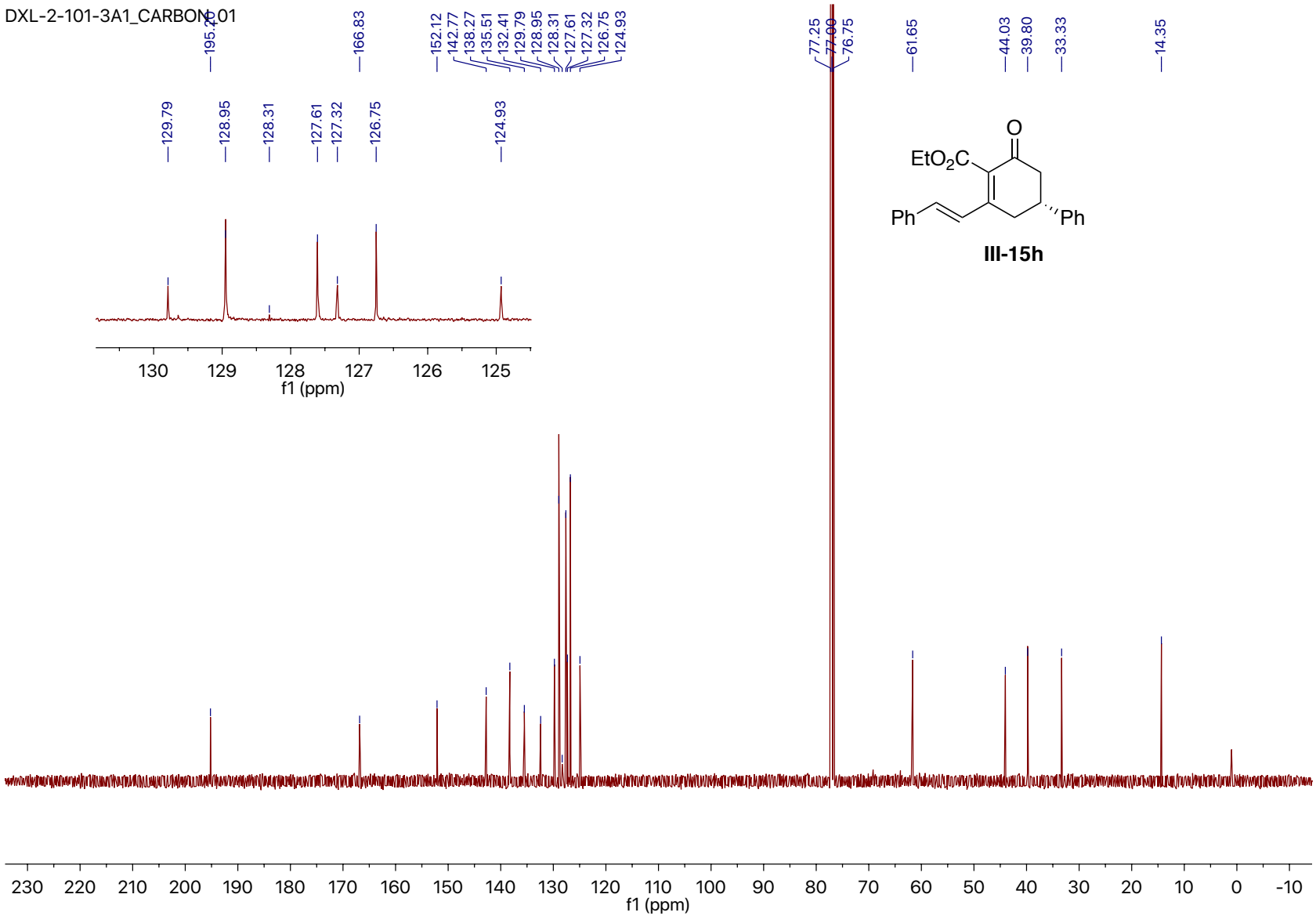
DXL-2-101-3A1_CARBON.01
195.44
166.83
152.12
142.77
138.27
135.51
132.41
129.79
128.95
128.31
127.61
127.32
126.75
124.93
77.25
77.00
76.75
61.65
44.03
39.80
33.33
14.35
129.79
128.95
128.31
127.61
127.32
126.75
124.93
130
129
128
127
126
125
f1 (ppm)
O
EtO2C
Ph
Ph
III-15h
230
220
210
200
190
180
170
160
150
140
130
120
110
100
90
80
70
60
50
40
30
20
10
0
-10
f1 (ppm)

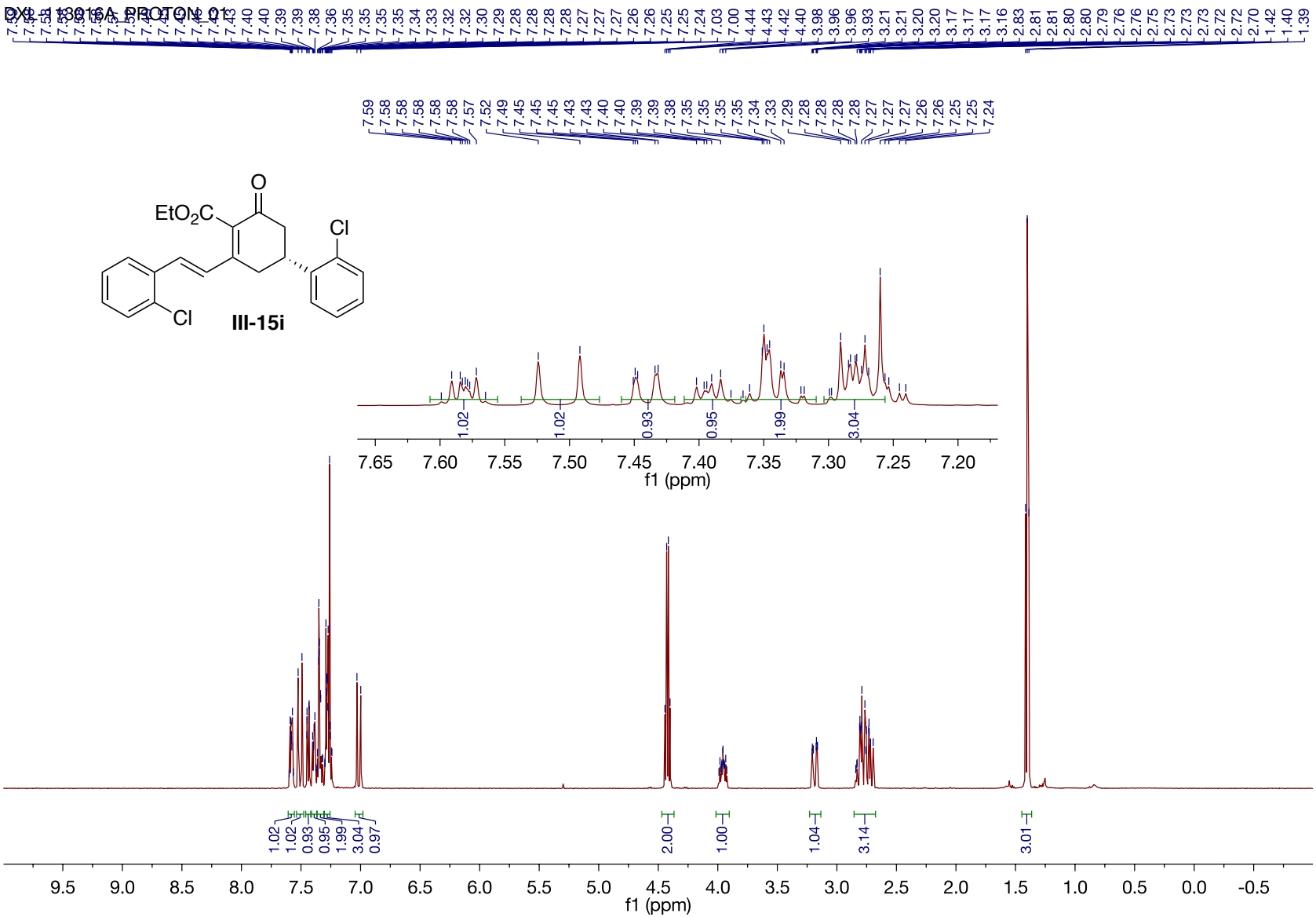
DXB-130164A PROTON 01
O
EtO2C
Cl
Cl
III-15i
f1 (ppm)
f1 (ppm)

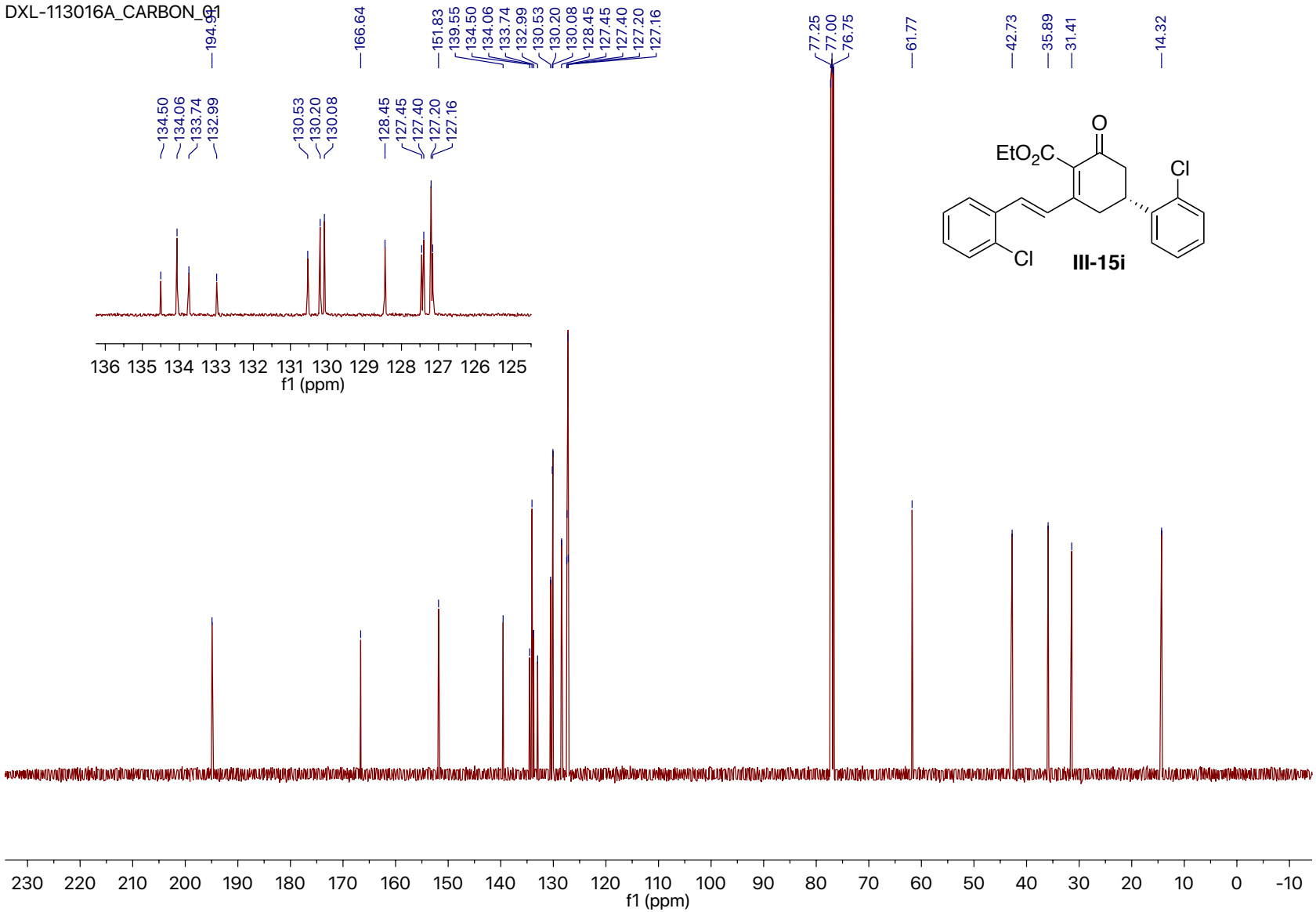
DXL-113016A_CARBON_01
194.91
166.64
151.83
139.55
134.50
134.06
133.74
132.99
130.53
130.20
130.08
128.45
127.45
127.40
127.20
127.16
77.25
77.00
76.75
61.77
42.73
35.89
31.41
14.32
O
EtO2C
Cl
Cl
III-15i
f1 (ppm)
f1 (ppm)

DXL-3-5-4A1_PROTON_01

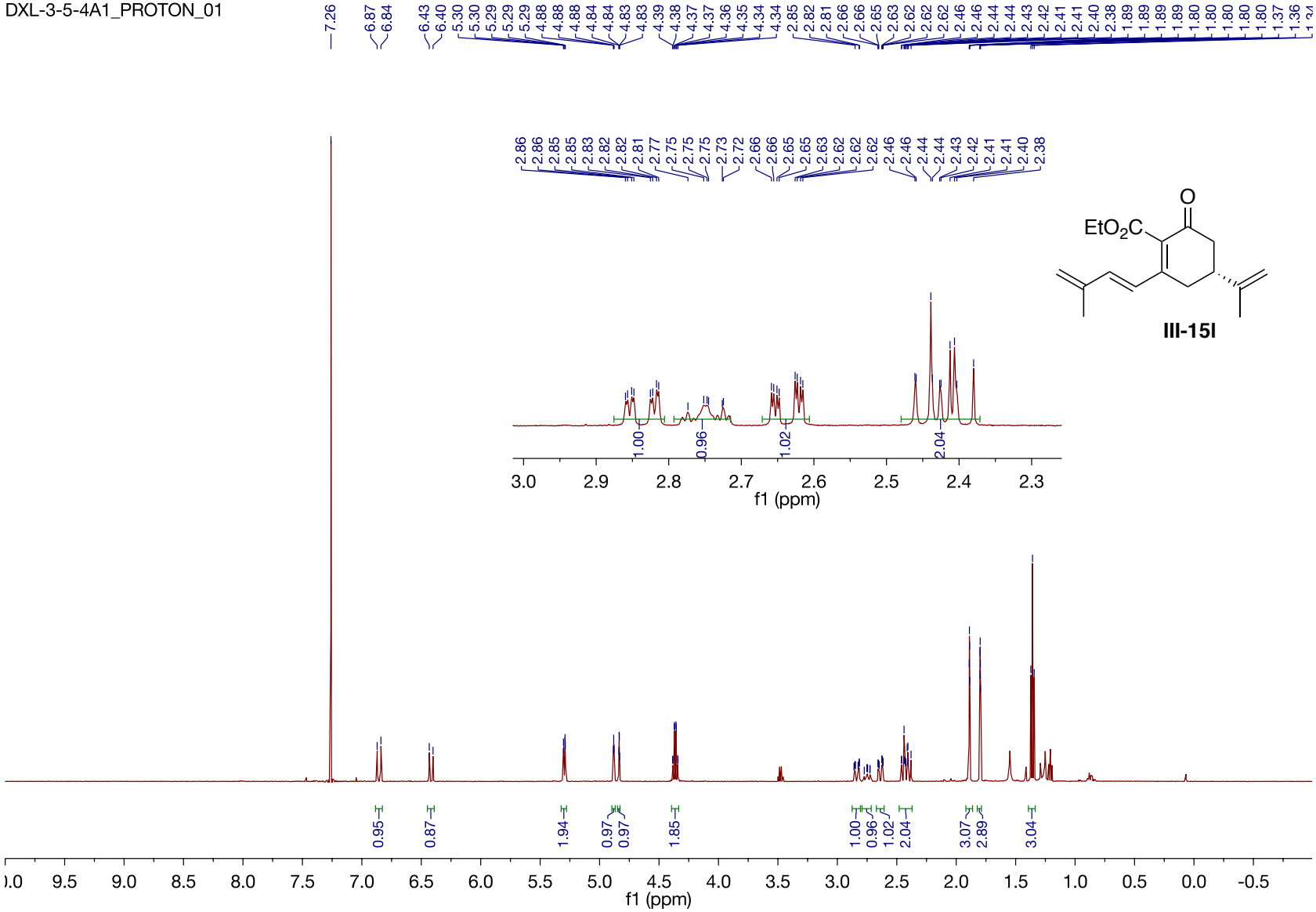

DXL-3-5-4A1_CARBON_01

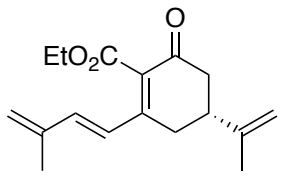

III-15l

DXL-3-39-2AA1_PROTON_01

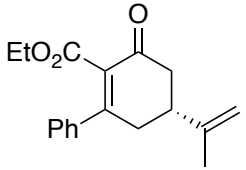

III-15m

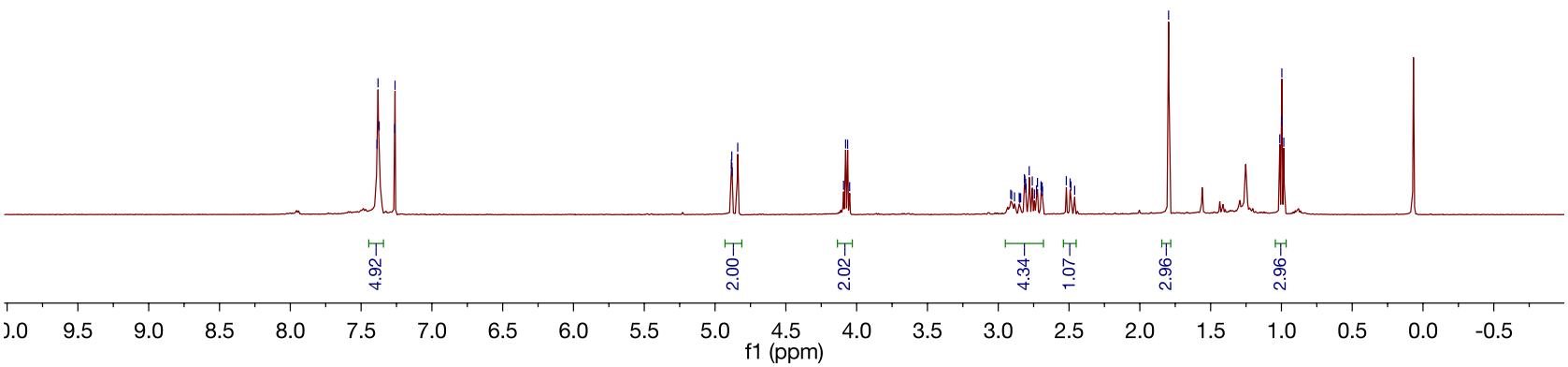

DXL-3-39-2AA1_CARBON_01

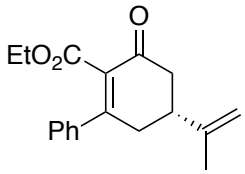

III-15m

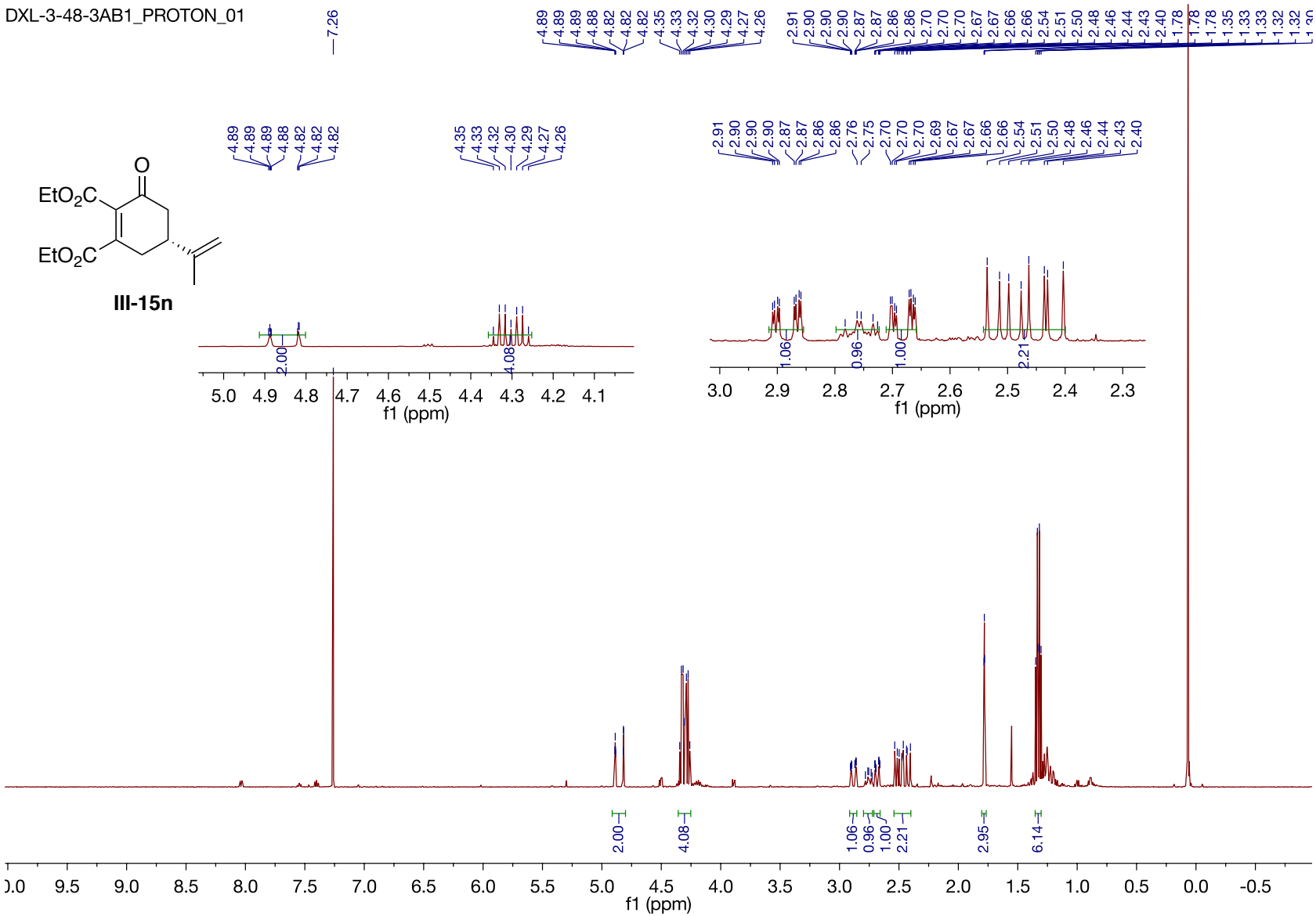
DXL-3-48-3AB1_PROTON_01
EtO2C
EtO2C
O
III-15n
f1 (ppm)

DXL-3-48-3AB1_CARBON_01

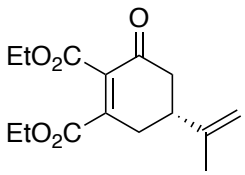

III-15n

DXL-3-23-1A2_PROTON_01

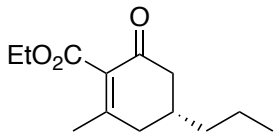

III-15o

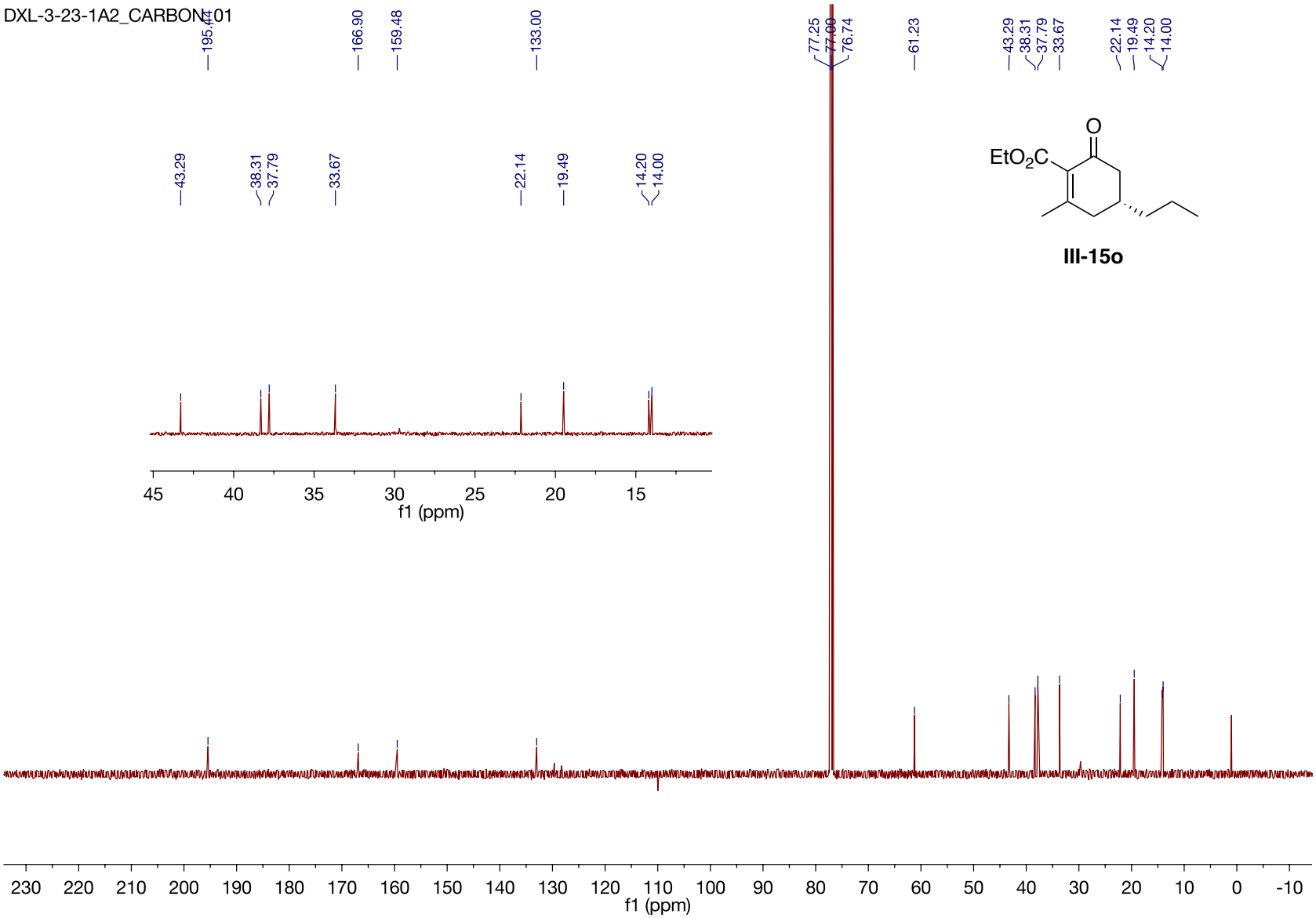
DXL-3-23-1A2_CARBON_01
195.44
166.90
159.48
133.00
77.25
77.00
76.74
61.23
43.29
38.31
37.79
33.67
22.14
19.49
14.20
14.00
EtO2C
O
III-15o
f1 (ppm)
f1 (ppm)

DXL-2-147-3A2_PROTON_01

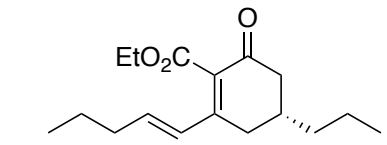

III-15p

DXL-2-147-3A2_CARBON_01

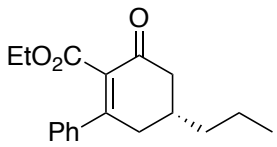

III-15q

DXL-3-47-4AB1_PROTON_01

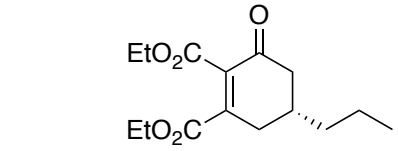

III-15r

DXL-3-47-4AB1_CARBON_01

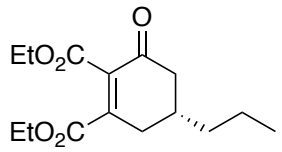

III-15r

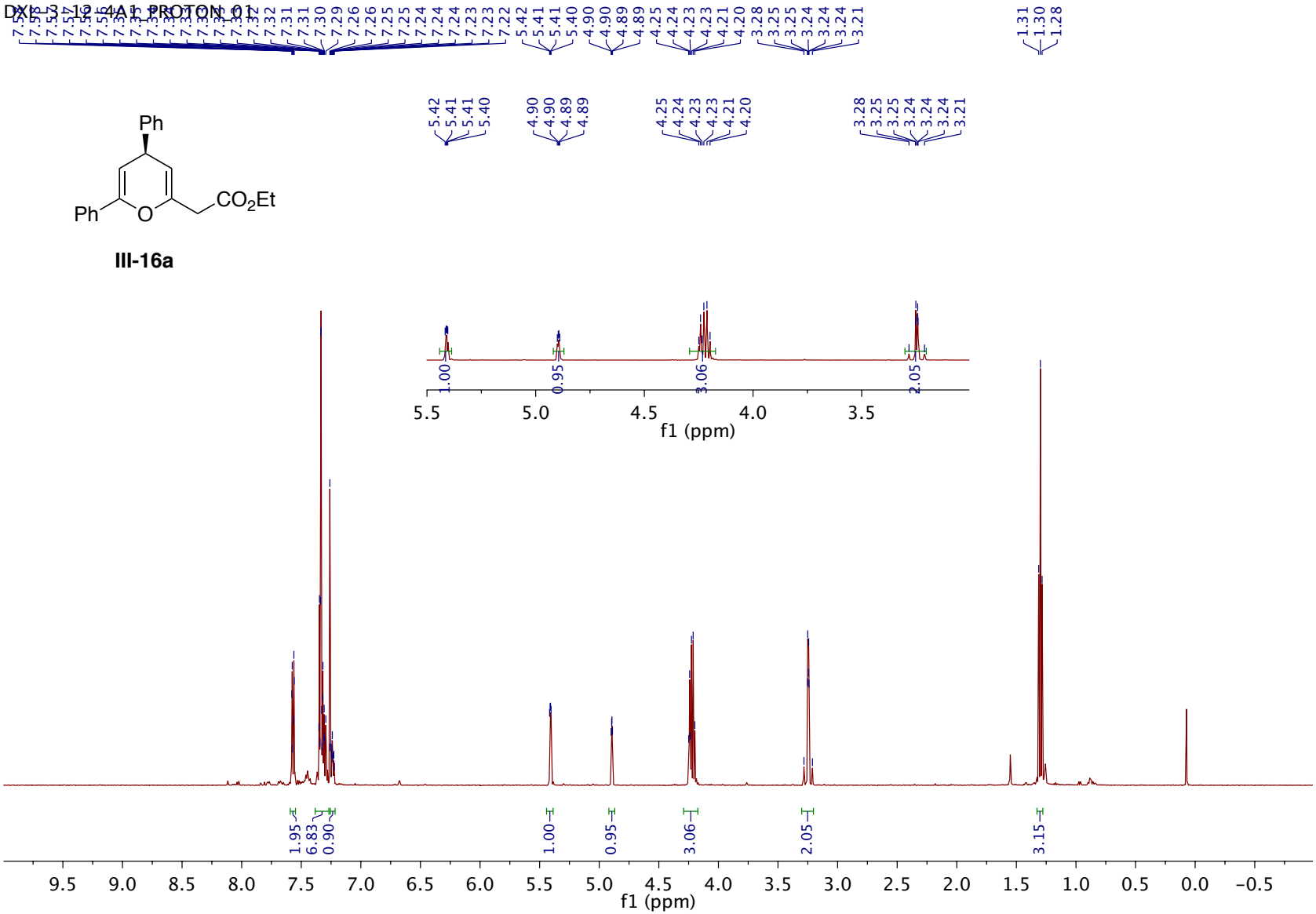
DXL-3-12-4A1-PROTON-01
Ph
Ph
O
CO2Et
III-16a
f1 (ppm)

DXL-3-12-5A1_CARBON_01

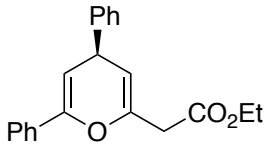

III-16a

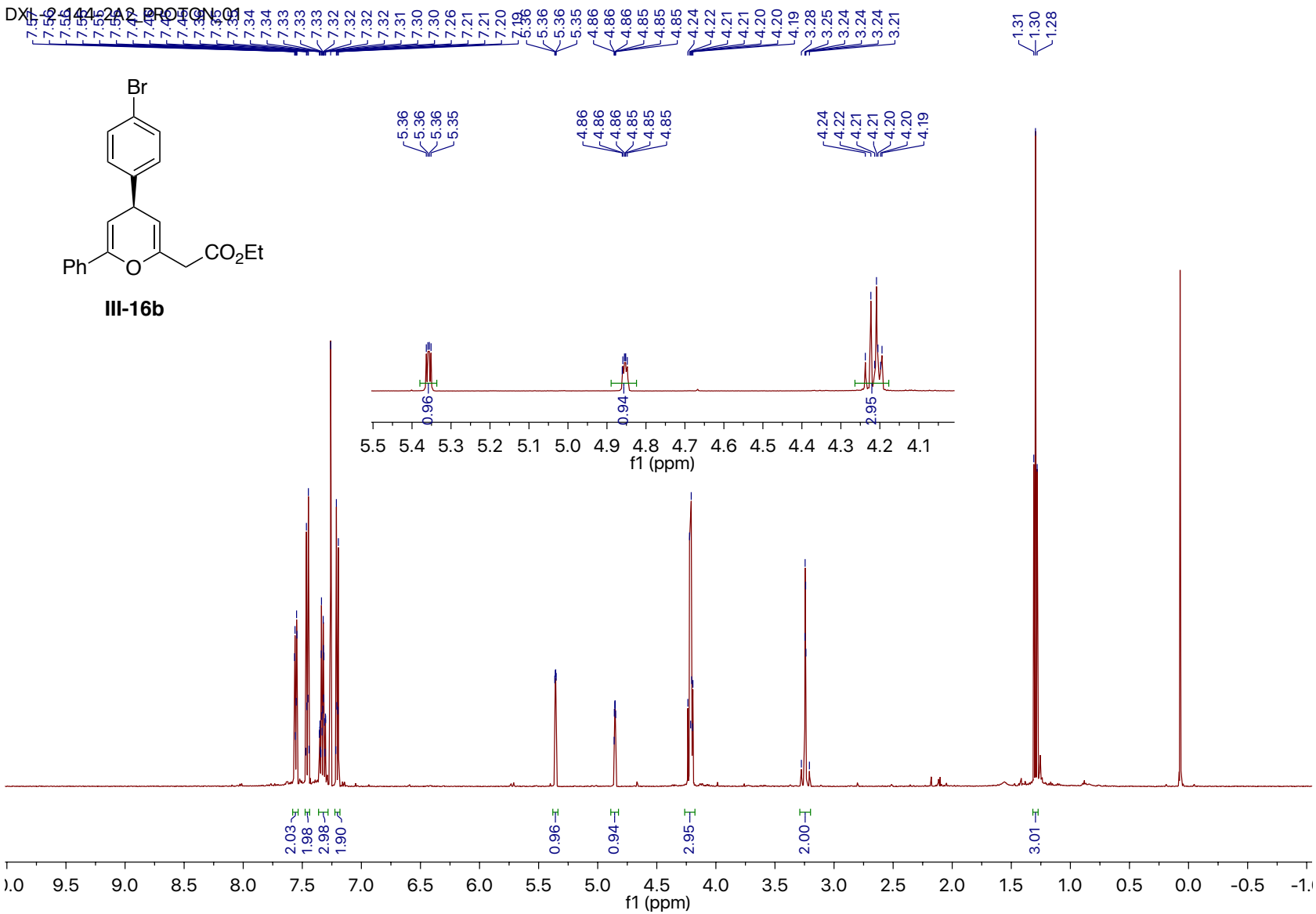
DXL-2-44-2A2-PROTON-01
Br
Ph
O
CO2Et
III-16b
f1 (ppm)

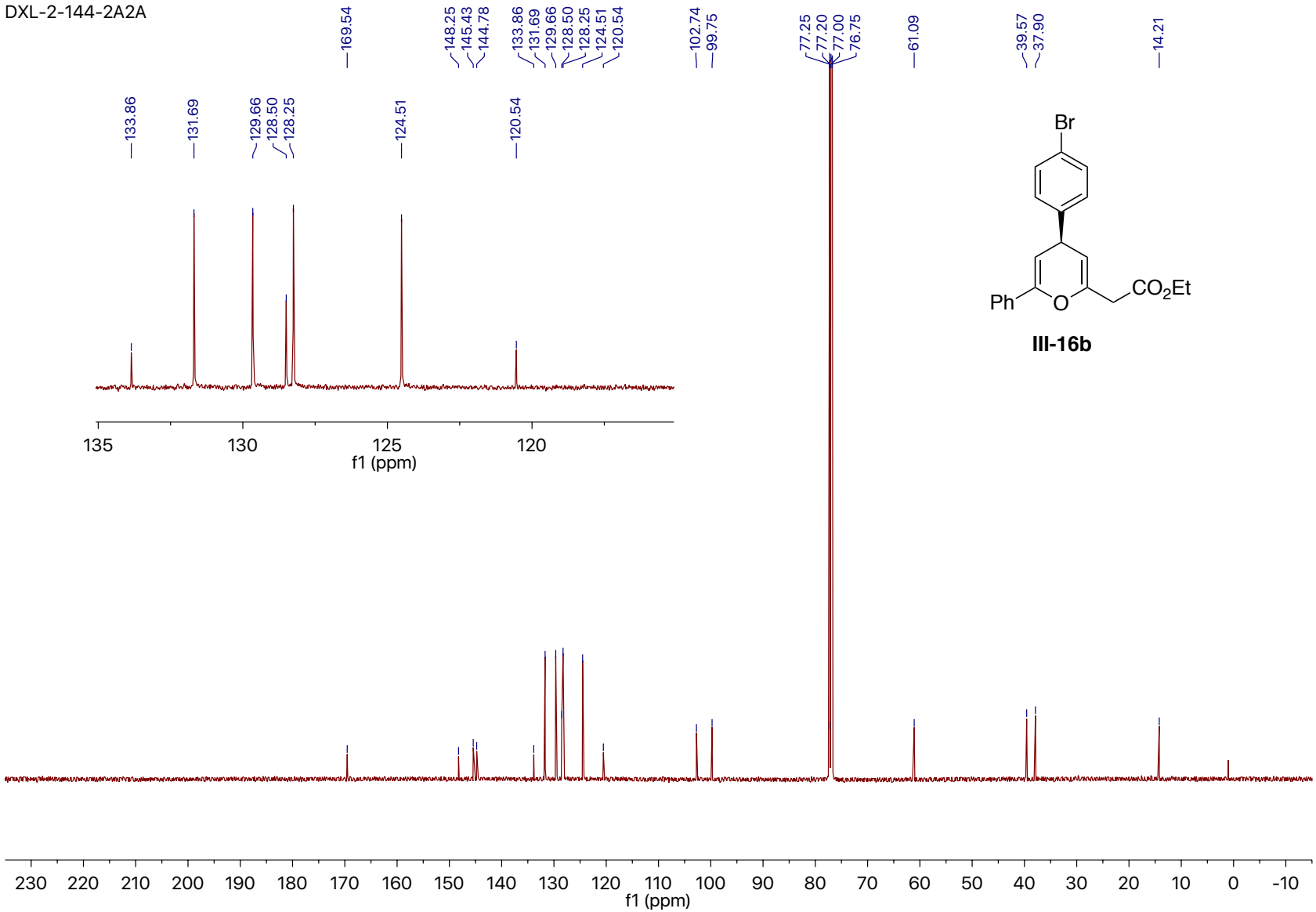
DXL-2-144-2A2A
169.54
148.25
145.43
144.78
133.86
131.69
129.66
128.50
128.25
124.51
120.54
102.74
99.75
77.25
77.20
77.00
76.75
61.09
39.57
37.90
14.21
133.86
131.69
129.66
128.50
128.25
124.51
120.54
135
130
125
120
f1 (ppm)
Br
Ph
O
CO2Et
III-16b
230
220
210
200
190
180
170
160
150
140
130
120
110
100
90
80
70
60
50
40
30
20
10
0
-10
f1 (ppm)

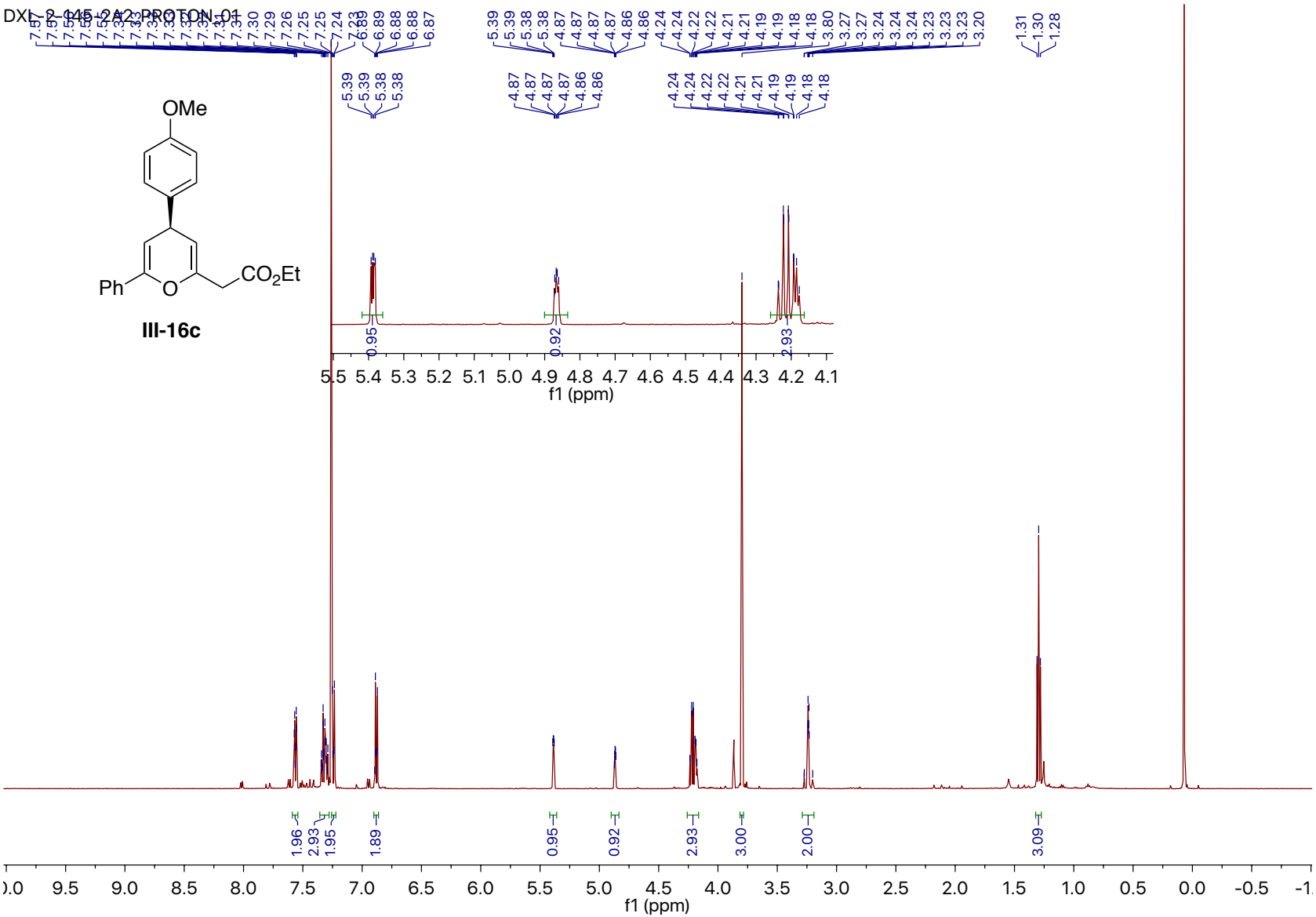
DXL-2-045-2A2-PROTON-01
OMe
Ph
O
CO2Et
III-16c
f1 (ppm)

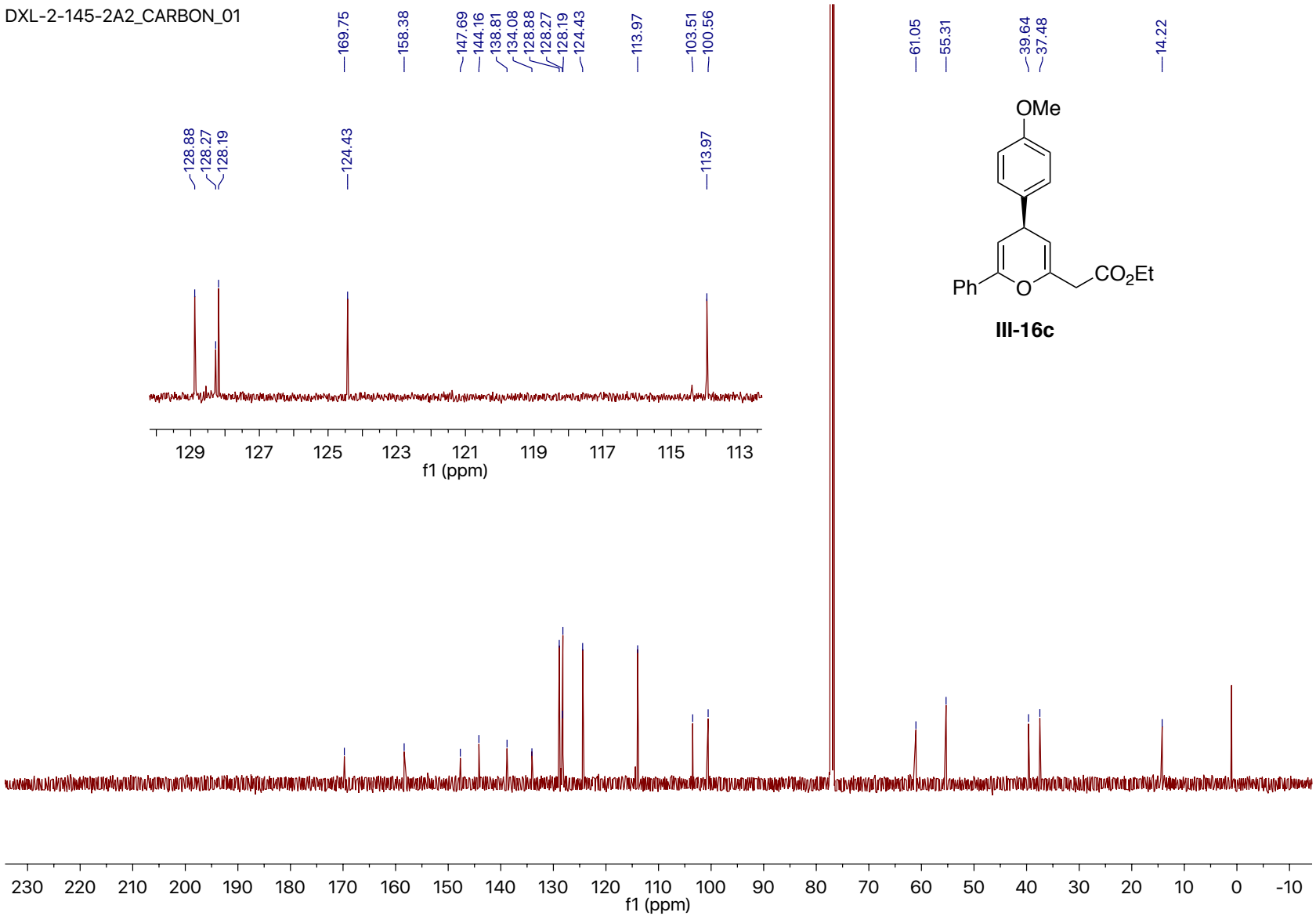
DXL-2-145-2A2_CARBON_01
169.75
158.38
147.69
144.16
138.81
134.08
128.88
128.27
128.19
124.43
113.97
103.51
100.56
61.05
55.31
39.64
37.48
14.22
OMe
Ph
O
CO2Et
III-16c
f1 (ppm)
f1 (ppm)

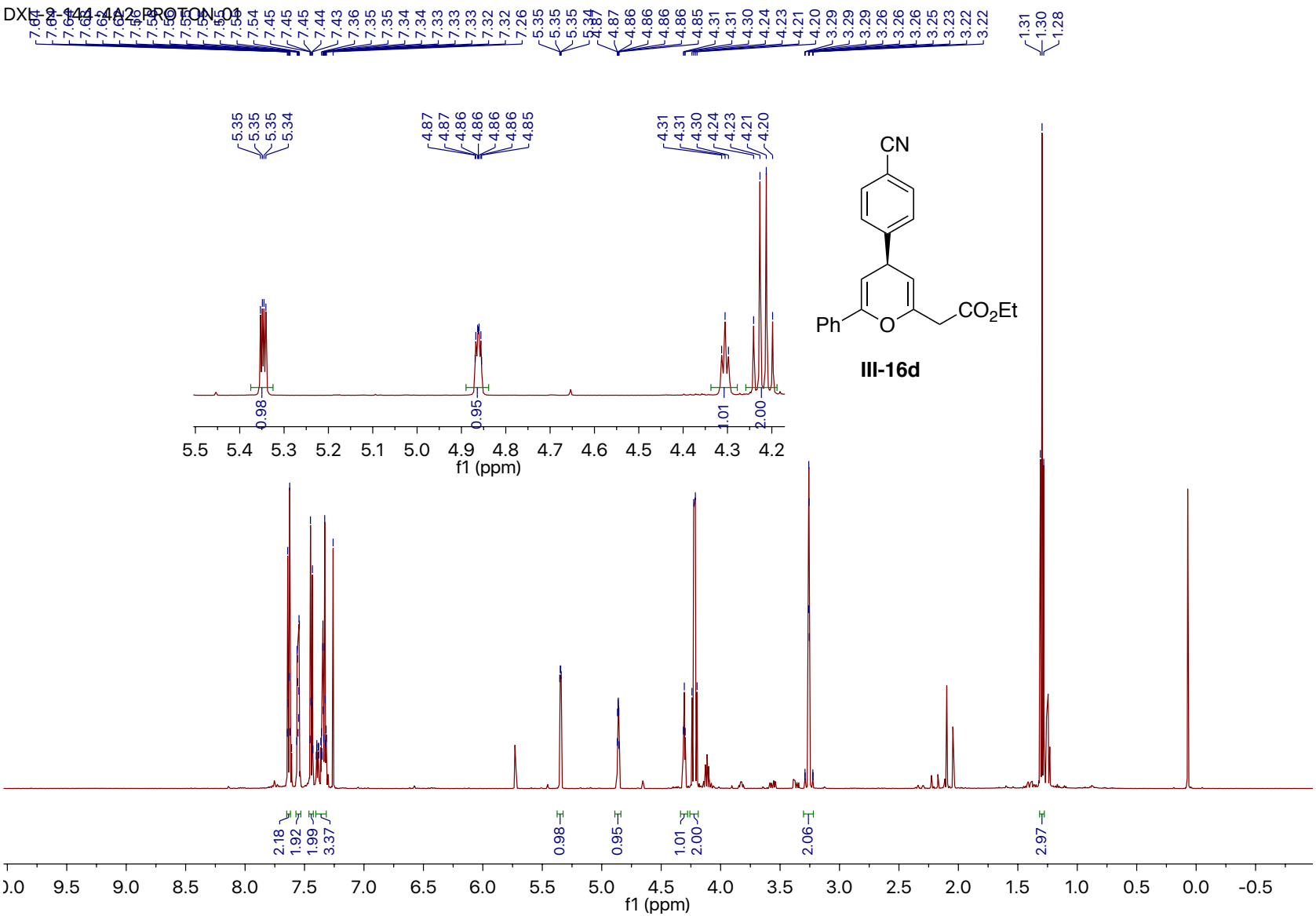
DXL-2-144-4A2-PROTON-01
CN
Ph
O
CO2Et
III-16d
f1 (ppm)

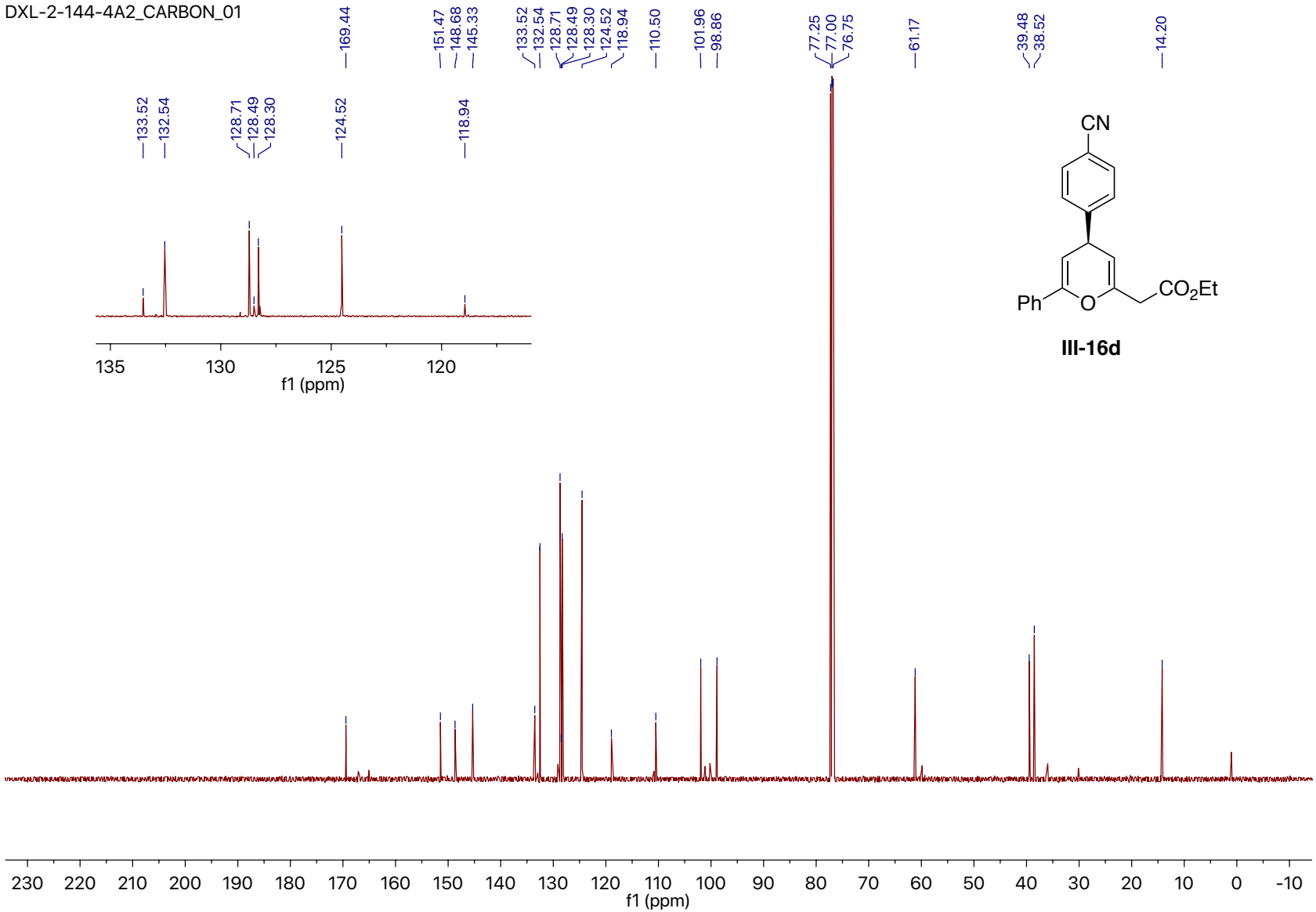
DXL-2-144-4A2_CARBON_01
169.44
151.47
148.68
145.33
133.52
132.54
128.71
128.49
128.30
124.52
118.94
110.50
101.96
98.86
77.25
77.00
76.75
61.17
39.48
38.52
14.20
CN
Ph
O
CO2Et
III-16d
f1 (ppm)
f1 (ppm)

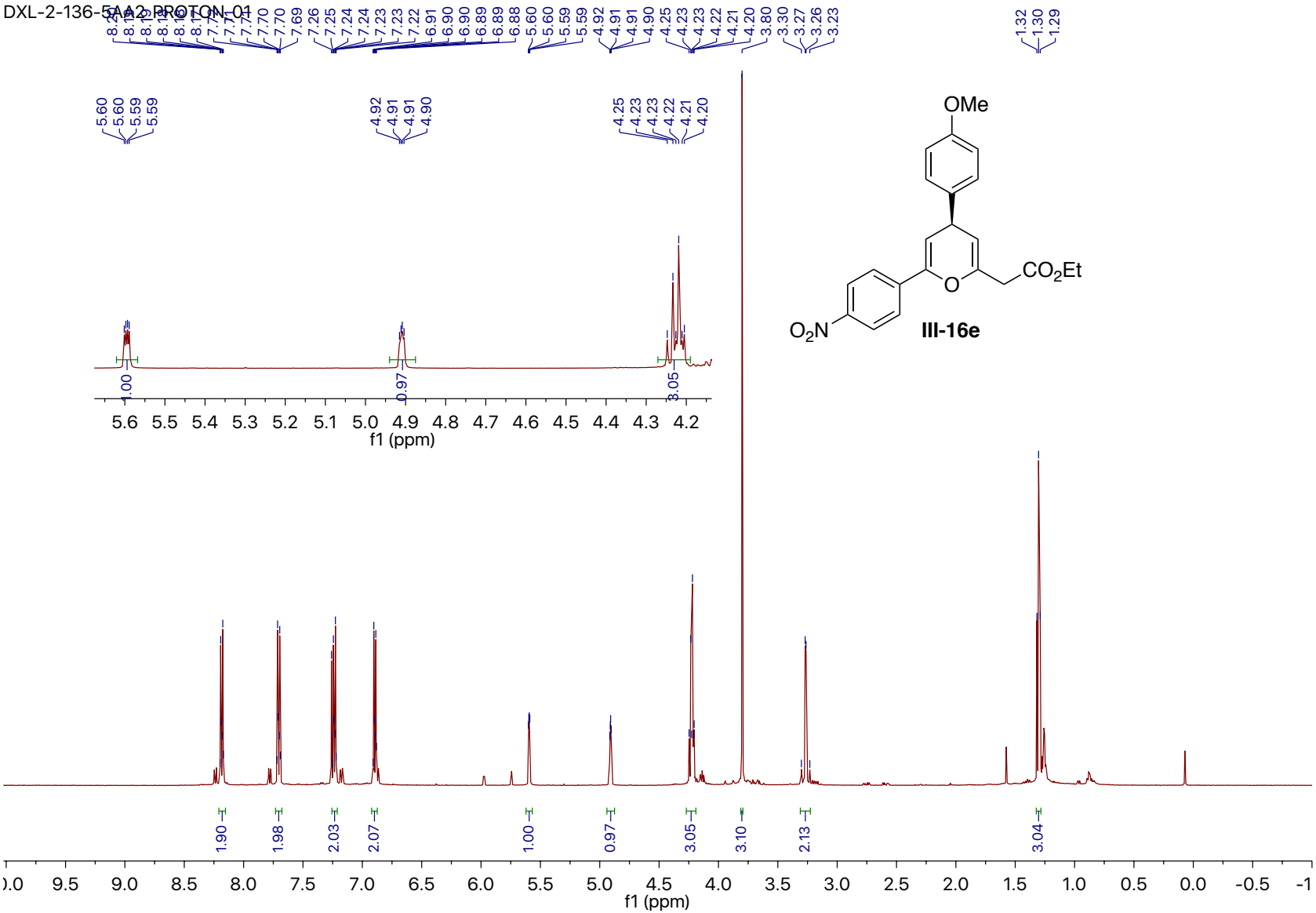
DXL-2-136-5AA2-PROTON-01
OMe
CO_2Et
O
O_2N
III-16e
f1 (ppm)

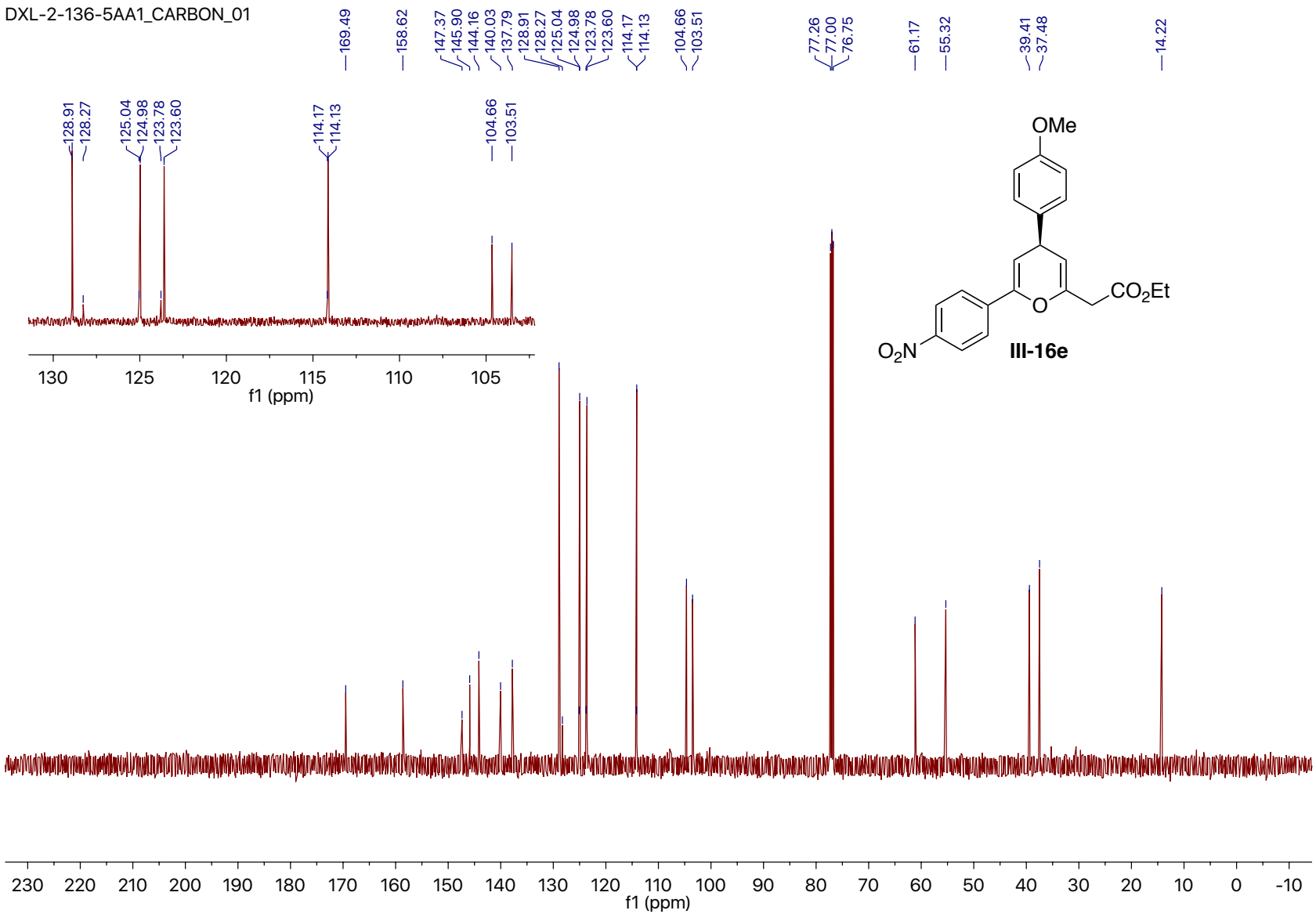
DXL-2-136-5AA1_CARBON_01
169.49
158.62
147.37
145.90
144.16
140.03
137.79
128.91
128.27
125.04
124.98
123.78
123.60
114.17
114.13
104.66
103.51
77.26
77.00
76.75
61.17
55.32
39.41
37.48
14.22
OMe
CO2Et
O
O2N
III-16e
f1 (ppm)

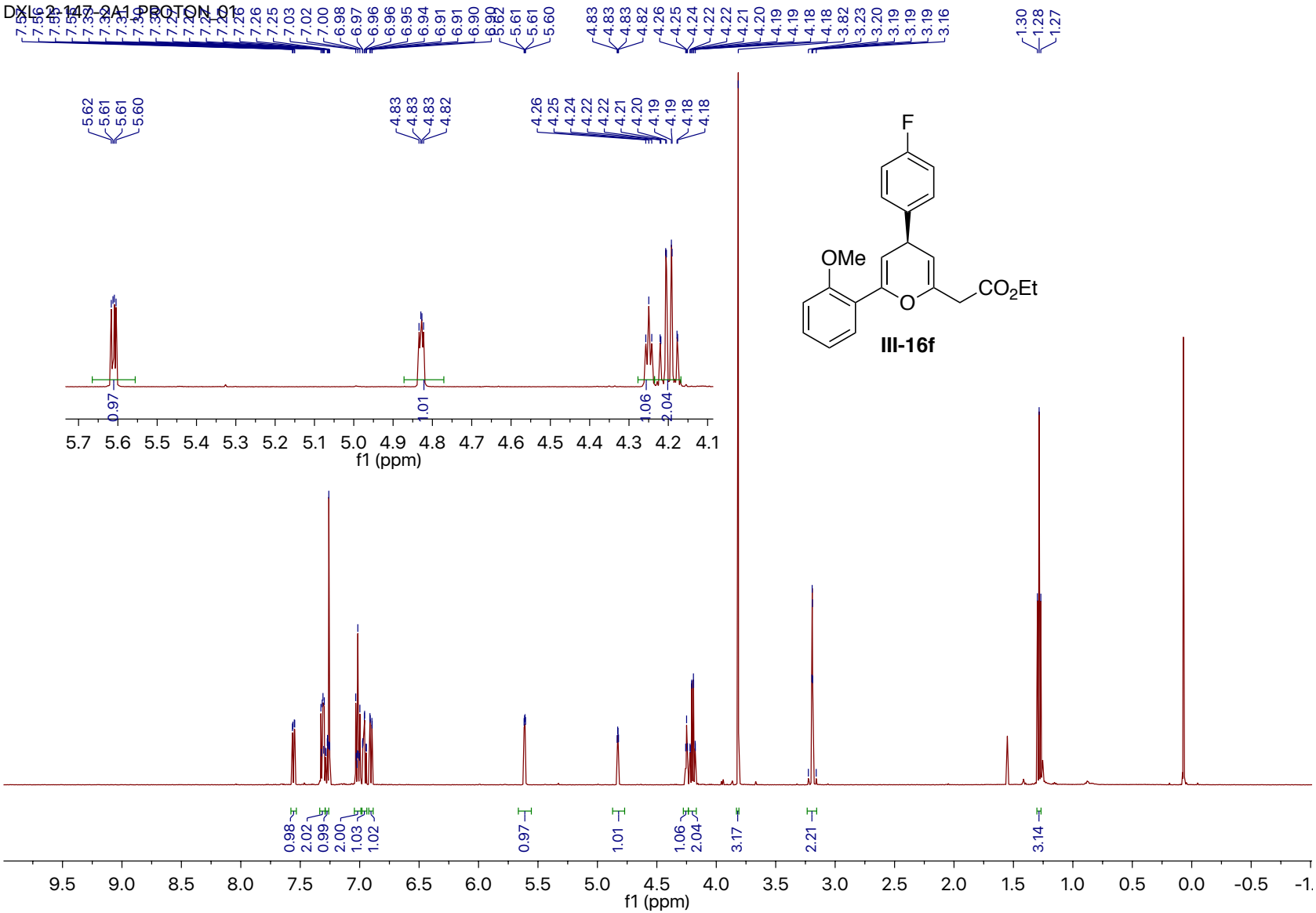
DXL-2-147-2A1-PROTON-01
F
OMe
CO2Et
O
III-16f
f1 (ppm)

DXL-2-147-2A1A_CARBON_01

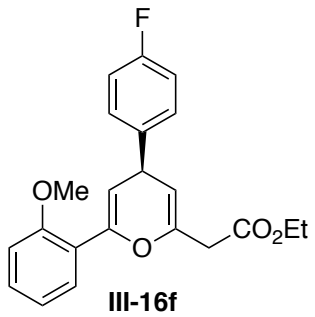

III-16f

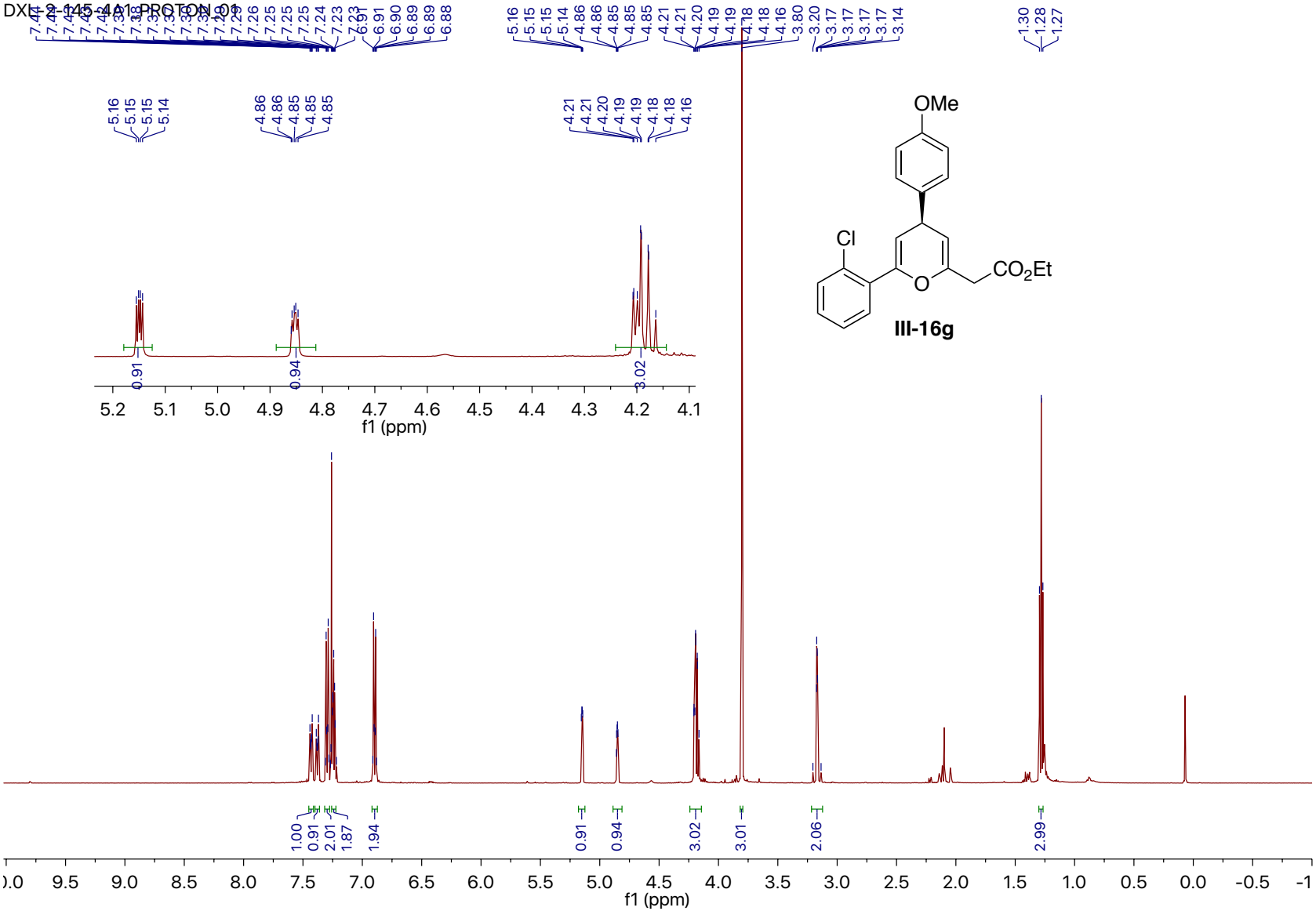
DXL-2-145-4A1-PROTON-01
OMe
Cl
O
CO2Et
III-16g
f1 (ppm)

DXL-2-145-4A1
STANDARD CARBON PARAMETERS

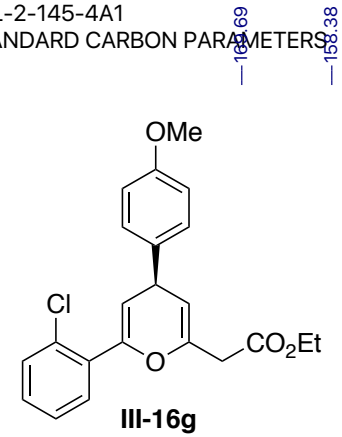

III-16g

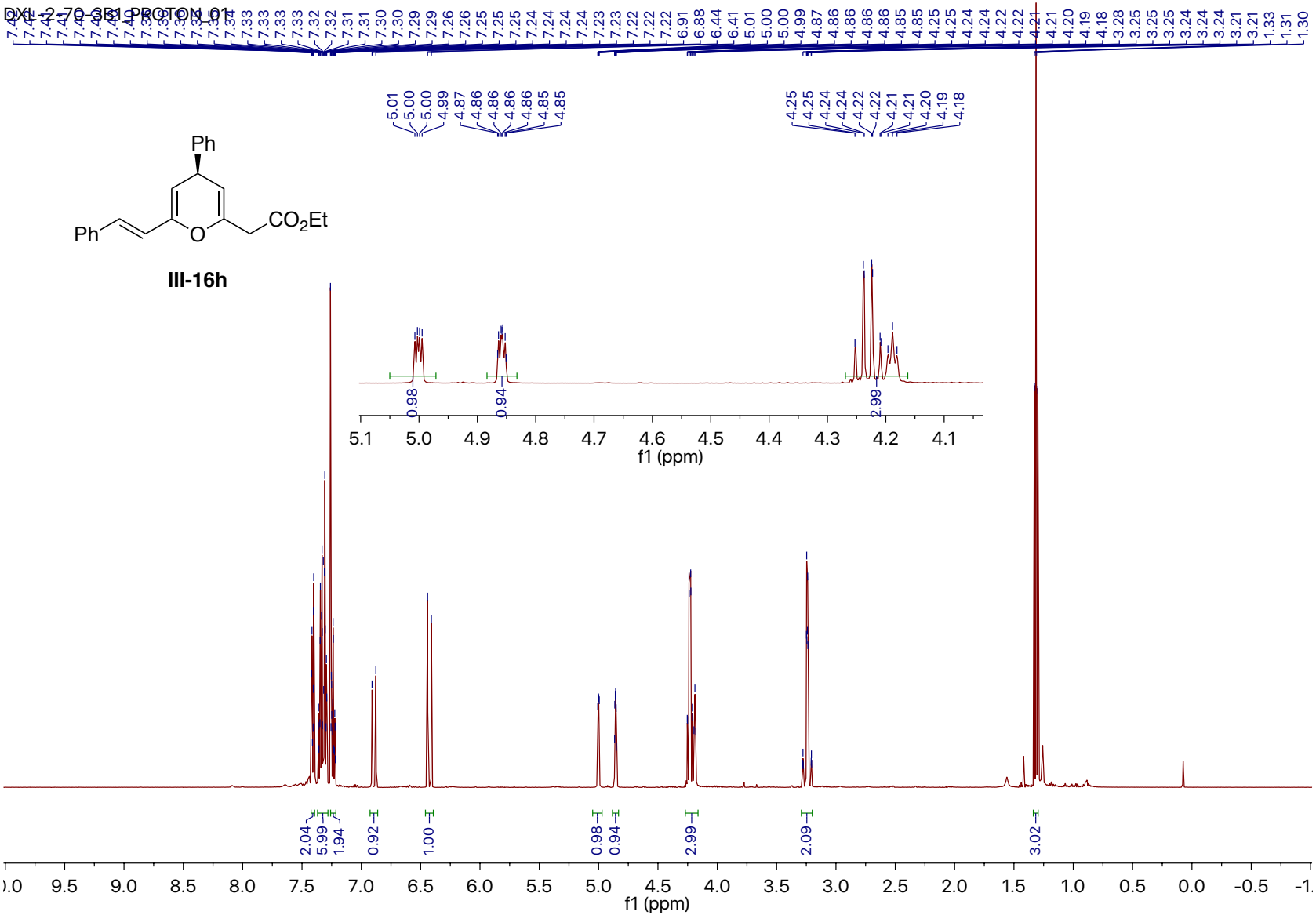
DXL-2-70-3B1 PROTON 01
Ph
Ph
O
CO2Et
III-16h
f1 (ppm)

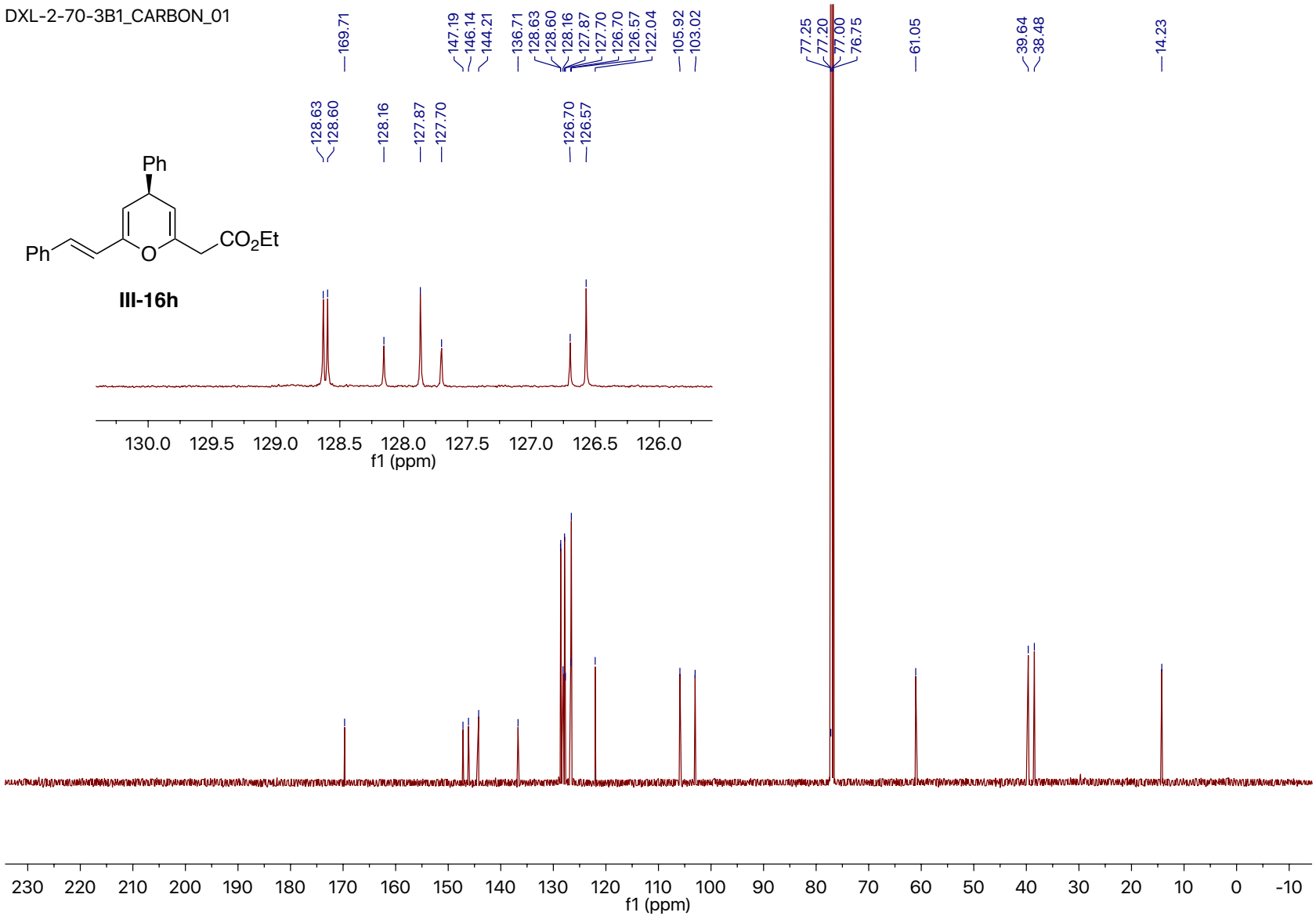
DXL-2-70-3B1_CARBON_01
169.71
147.19
146.14
144.21
136.71
128.63
128.60
128.16
127.87
127.70
126.70
126.57
122.04
105.92
103.02
77.25
77.20
77.00
76.75
61.05
39.64
38.48
14.23
Ph
Ph
O
CO2Et
III-16h
130.0 129.5 129.0 128.5 128.0 127.5 127.0 126.5 126.0
f1 (ppm)
230 220 210 200 190 180 170 160 150 140 130 120 110 100 90 80 70 60 50 40 30 20 10 0 -10
f1 (ppm)

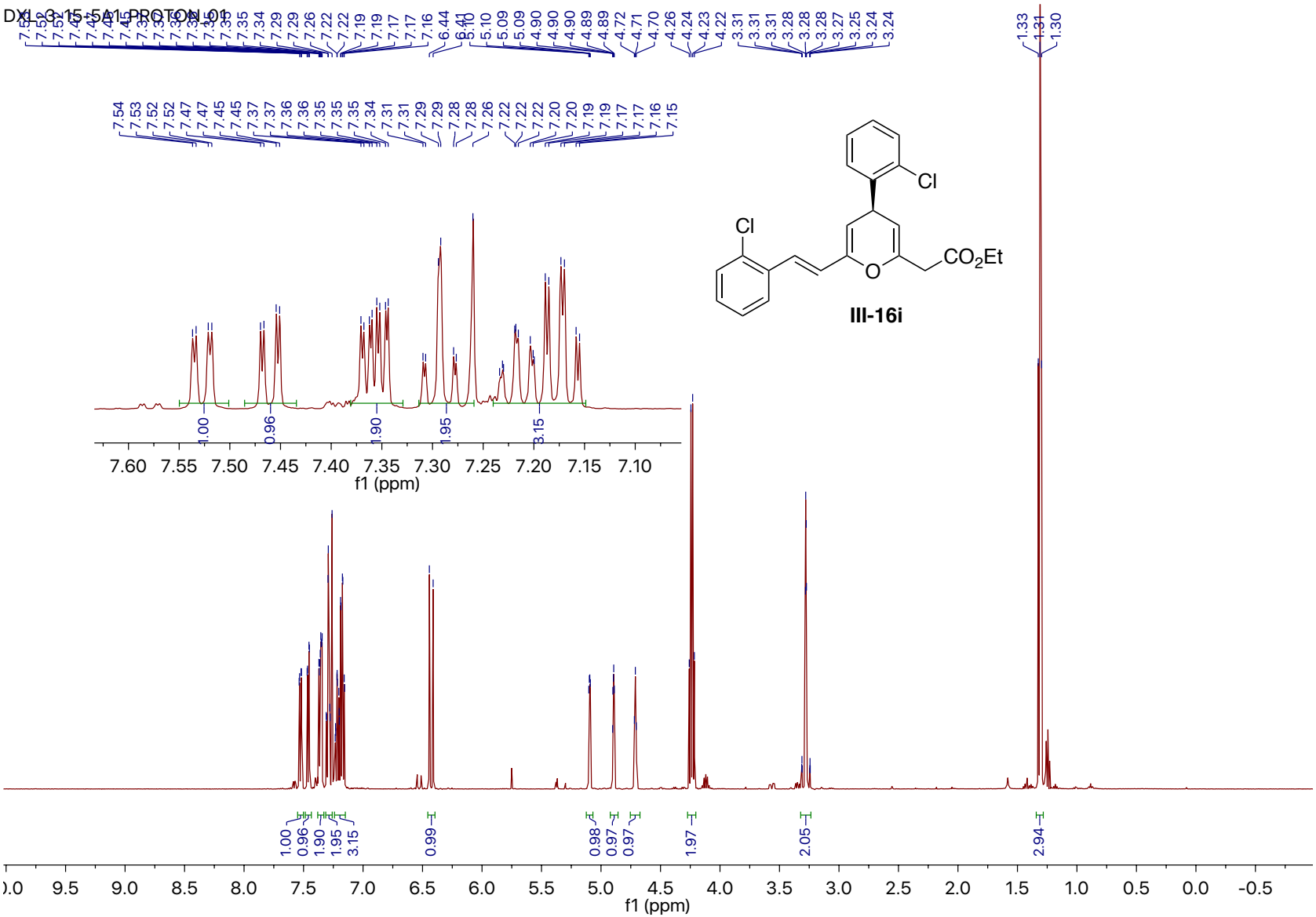
DXL-3-15-5A1-PROTON-01
Cl
Cl
O
CO2Et
III-16i
f1 (ppm)

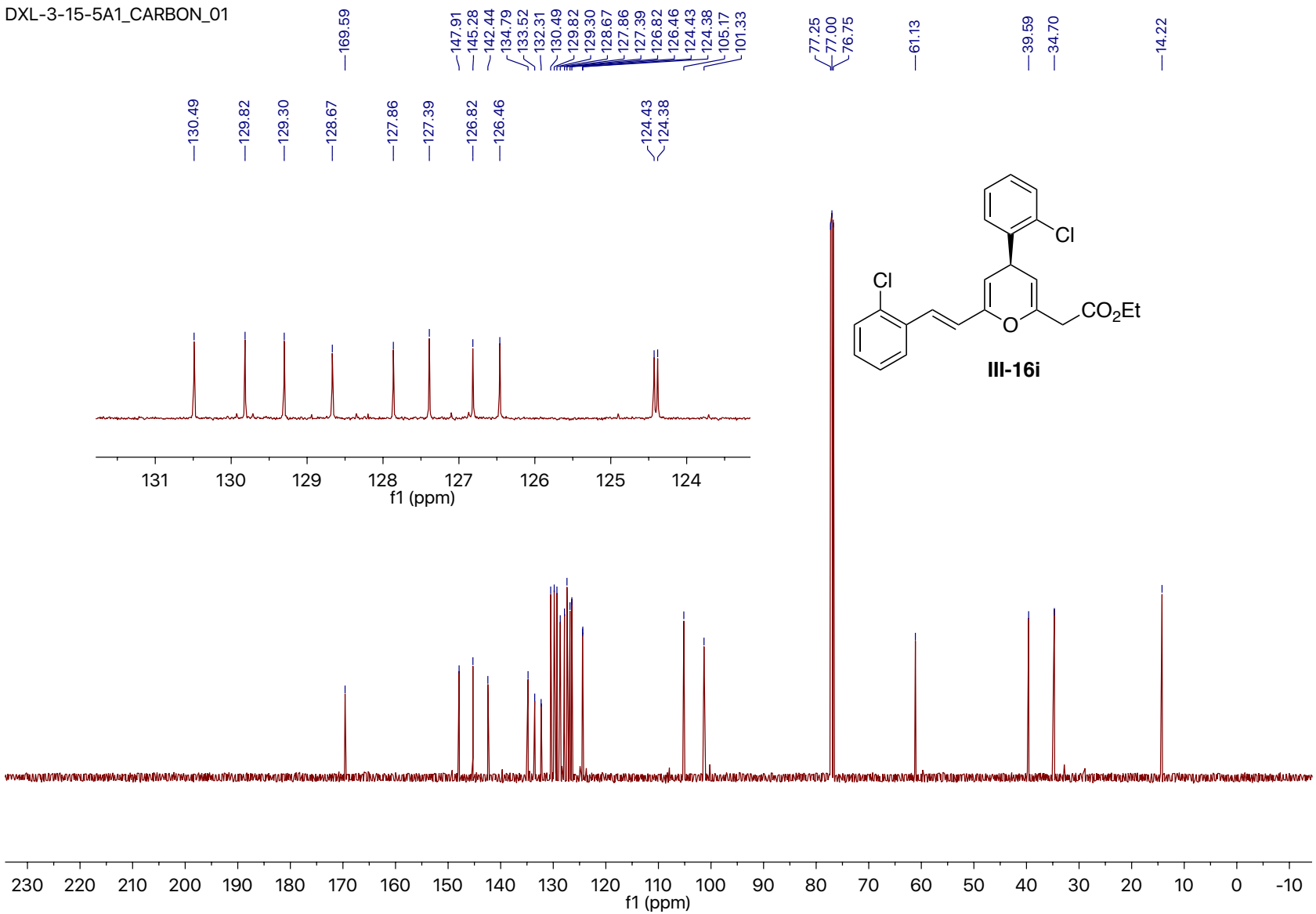
DXL-3-15-5A1_CARBON_01
169.59
147.91
145.28
142.44
134.79
133.52
132.31
130.49
129.82
129.30
128.67
127.86
127.39
126.82
126.46
124.43
124.38
105.17
101.33
77.25
77.00
76.75
61.13
39.59
34.70
14.22
130.49
129.82
129.30
128.67
127.86
127.39
126.82
126.46
124.43
124.38
131
130
129
128
127
126
125
124
f1 (ppm)
Cl
Cl
O
CO2Et
III-16i
230
220
210
200
190
180
170
160
150
140
130
120
110
100
90
80
70
60
50
40
30
20
10
0
-10
f1 (ppm)

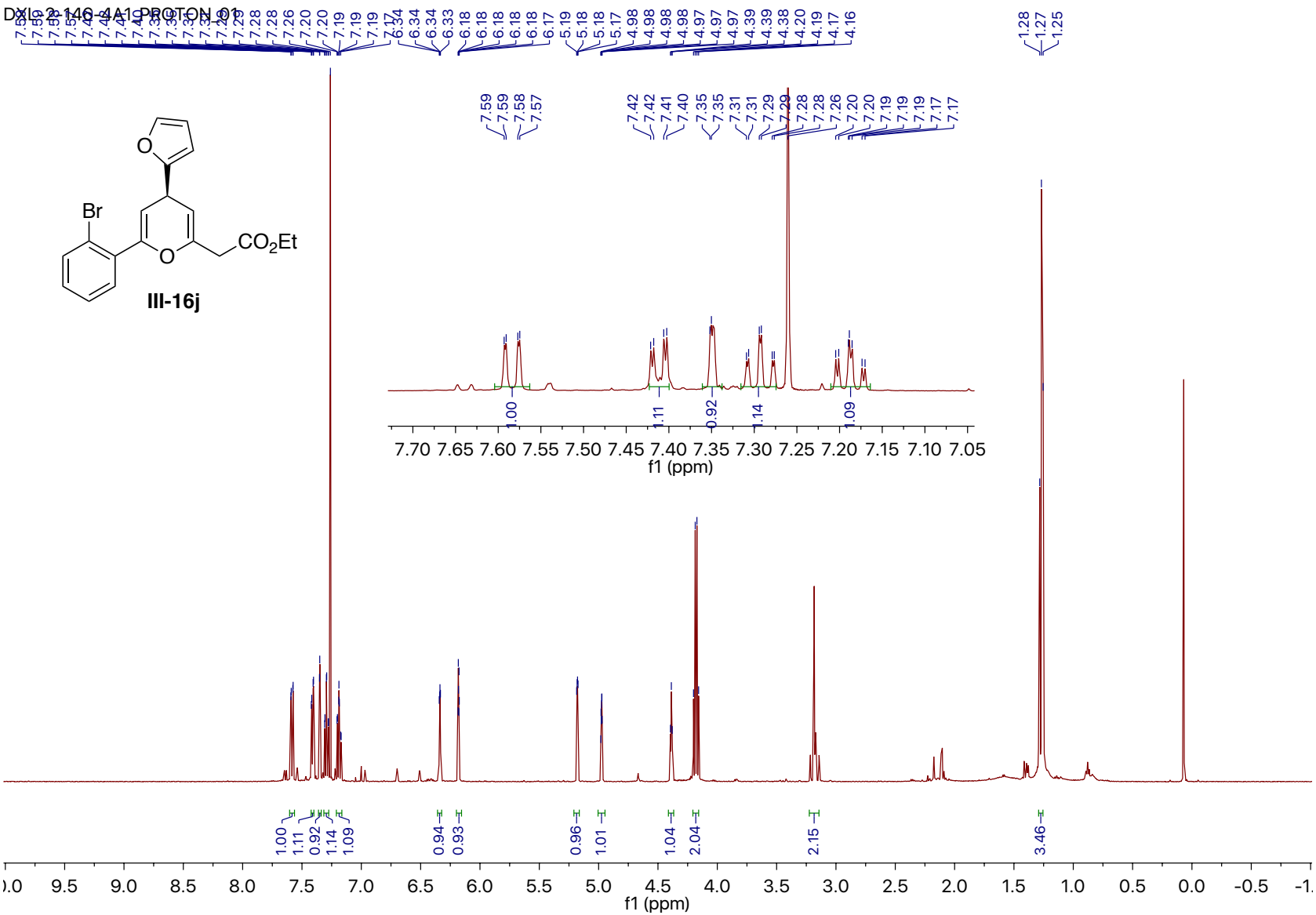
DXlc-2-146-4A1-PROTON-01
Br
O
O
CO2Et
III-16j
f1 (ppm)

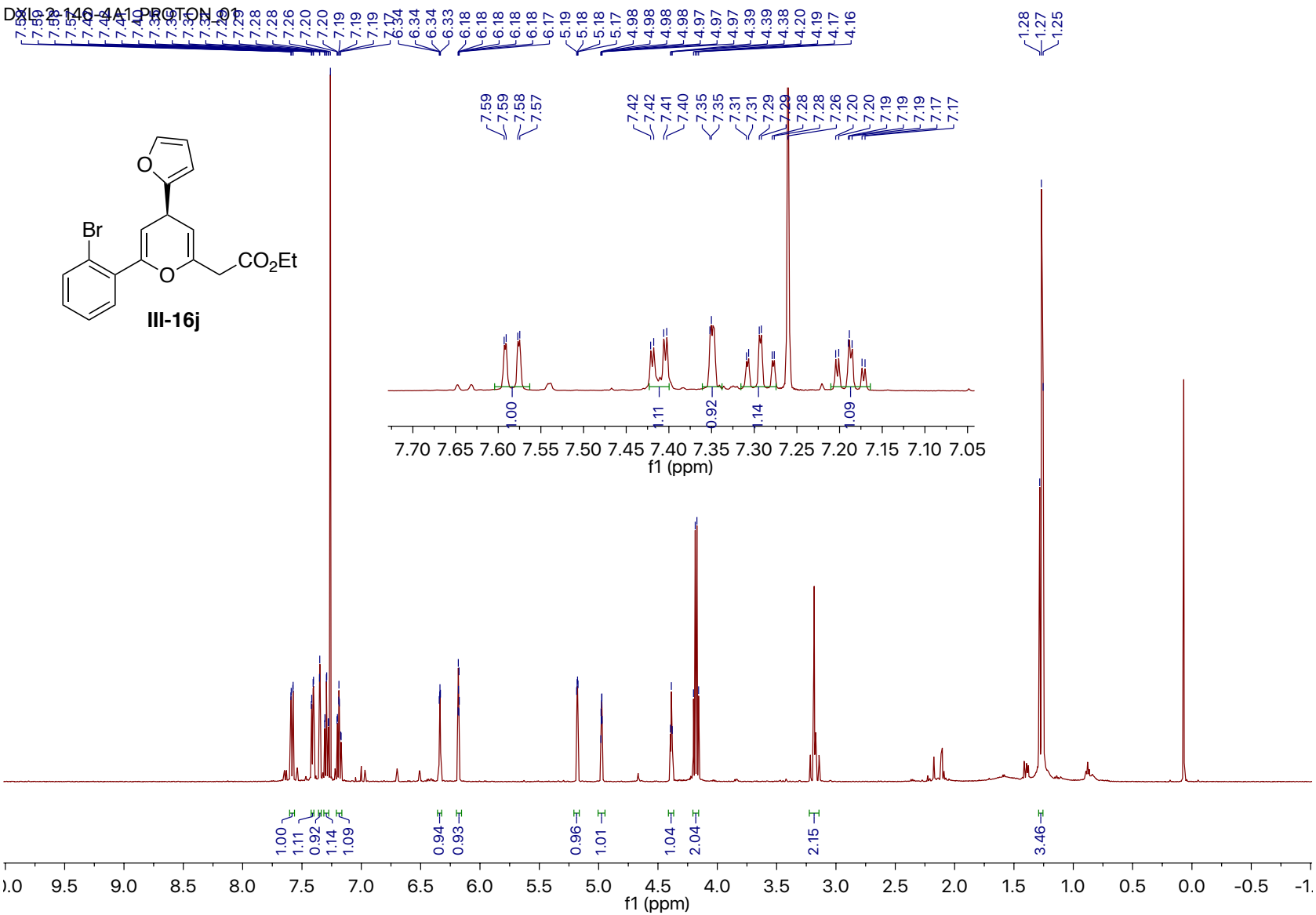
DXIc-2-146-4A1-PROTON-01
Br
O
O
CO2Et
III-16j
f1 (ppm)

DXL-2-146-4A1_CARBON_01

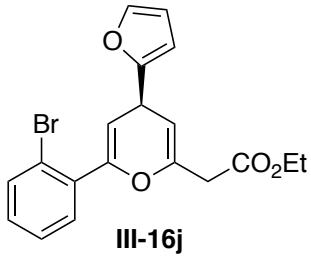

III-16j

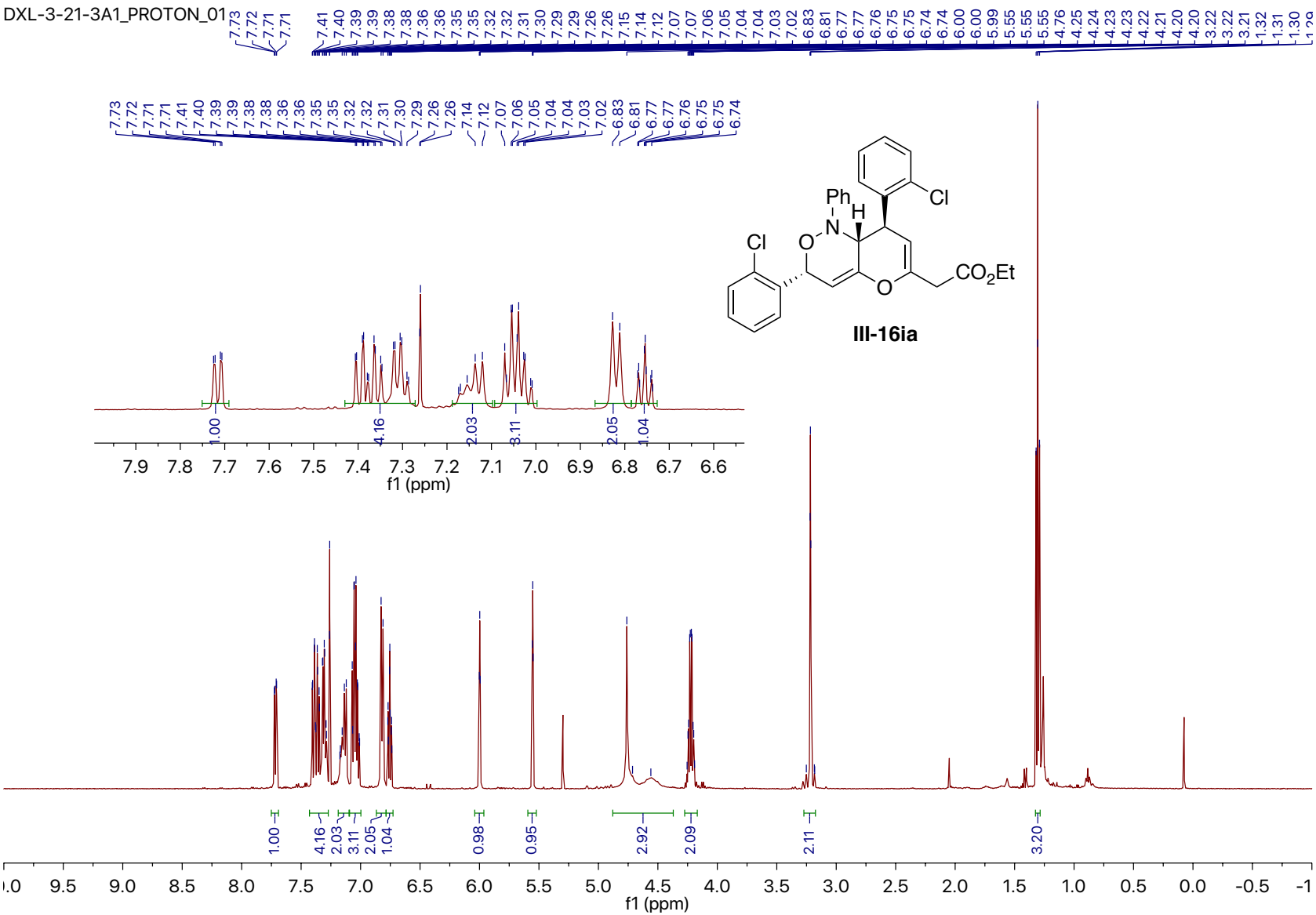
DXL-3-21-3A1_PROTON_01
Ph
H
N
O
Cl
Cl
O
O
CO2Et
III-16ia
f1 (ppm)

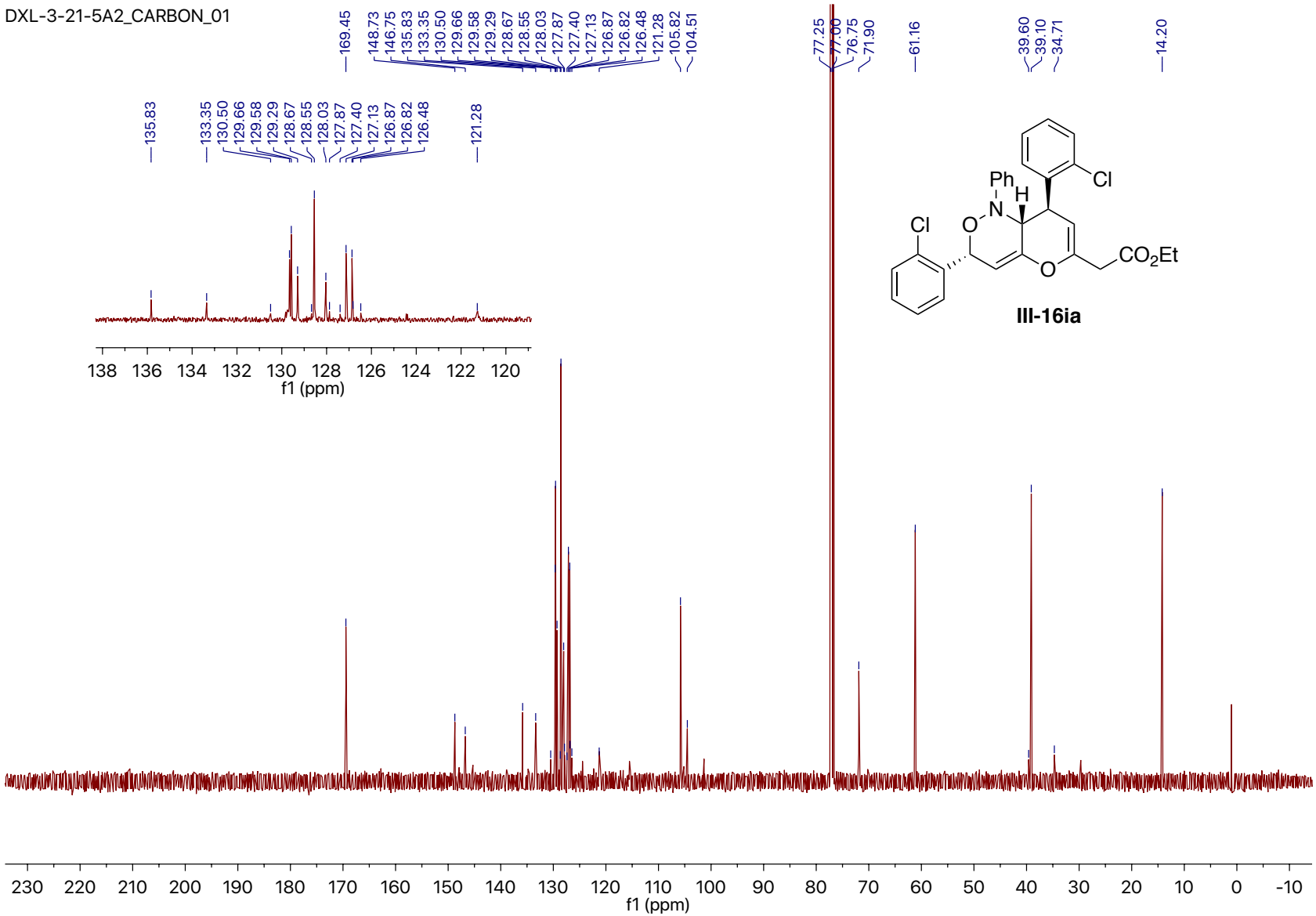
DXL-3-21-5A2_CARBON_01
169.45
148.73
146.75
135.83
133.35
130.50
129.66
129.58
129.29
128.67
128.55
128.03
127.87
127.40
127.13
126.87
126.82
126.48
121.28
105.82
104.51
77.25
77.00
76.75
71.90
61.16
39.60
39.10
34.71
14.20
135.83
133.35
130.50
129.66
129.58
129.29
128.67
128.55
128.03
127.87
127.40
127.13
126.87
126.82
126.48
121.28
138 136 134 132 130 128 126 124 122 120
f1 (ppm)
Ph
N
H
O
Cl
Cl
O
CO2Et
III-16ia
230 220 210 200 190 180 170 160 150 140 130 120 110 100 90 80 70 60 50 40 30 20 10 0 -10
f1 (ppm)

Crystal Structure:

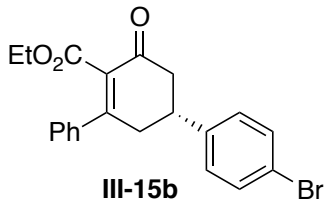

III-15b

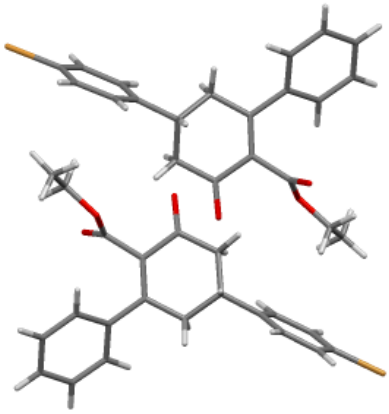

Table 1: Fractional Atomic Coordinates (×10⁴) and Equivalent Isotropic Displacement Parameters (Å²×10³) for **BB216c**. U_{eq} is defined as 1/3 of the trace of the orthogonalised U_{ij}.

Atom	x	y	z	U_{eq}
Br1A	10554.9(8)	2509.8(2)	2129.2(5)	53.1(2)
O1A	820(5)	4838.2(14)	1028(3)	37.0(8)
O2A	859(4)	5990.2(13)	322(3)	27.1(8)
O3A	-250(5)	5635.3(16)	-1788(3)	41.7(10)
C1A	2240(6)	4837(2)	666(4)	24.8(11)
C2A	2529(6)	5269.0(18)	-256(4)	23.8(10)
C3A	4044(7)	5280.1(19)	-736(4)	25.4(11)
C4A	5502(6)	4841.3(18)	-371(5)	26.8(11)
C5A	4722(6)	4315.2(16)	3(4)	21.0(9)
C6A	3706(7)	4414.5(19)	1087(5)	30.5(11)
C7A	903(7)	5653.3(19)	-692(5)	26.0(11)
C8A	-845(7)	6309(2)	74(5)	34.5(12)
C9A	-460(8)	6750(2)	1110(5)	40.5(14)
C10A	4382(6)	5729.0(19)	-1609(4)	24.3(11)
C11A	5151(6)	5629(2)	-2673(4)	26.4(11)
C12A	5458(7)	6037(2)	-3491(5)	30.4(12)
C13A	5004(8)	6564(2)	-3248(5)	34.6(13)
C14A	4272(7)	6673(2)	-2191(5)	35.8(13)
C15A	3967(7)	6259(2)	-1372(5)	32.2(12)
C16A	6214(6)	3885.7(17)	492(4)	21(1)
C17A	5919(6)	3375.6(18)	-54(5)	28.3(11)
C18A	7195(7)	2960(2)	430(4)	31.7(11)
C19A	8813(7)	3073(2)	1454(4)	28.9(11)
C20A	9184(7)	3576(2)	2002(4)	30.9(11)
C21A	7870(6)	3980.9(18)	1518(4)	28.9(11)
Br1B	-5381.3(8)	7388.4(2)	3136.5(5)	49.73(18)
O1B	4410(5)	5046.9(14)	3949(3)	34.8(8)
O2B	5246(5)	4209.2(16)	6617(3)	41.0(9)
O3B	4231(4)	3874.4(13)	4485(3)	29.0(8)
C1B	2934(7)	5037(2)	4250(4)	27.6(11)
C2B	2518(6)	4586.4(19)	5049(4)	24.7(10)
C3B	991(6)	4577.4(19)	5507(4)	23.4(10)
C4B	-396(7)	5034.5(19)	5179(4)	25.8(11)
C5B	-371(7)	5366.1(19)	3920(5)	36.9(12)
C6B	1580(7)	5491(2)	3898(5)	32.4(12)
C7B	4127(7)	4203(2)	5489(5)	27.3(11)
C8B	5951(7)	3565(2)	4742(5)	36.8(12)
C9B	5660(8)	3128(2)	3703(5)	38.9(13)
C10B	656(6)	4139.2(19)	6385(4)	23.6(11)
C11B	-110(6)	4250(2)	7452(4)	27.6(11)
C12B	-381(7)	3845(2)	8299(5)	33.9(13)
C13B	58(8)	3327(2)	8094(5)	37.2(13)
C14B	777(7)	3204(2)	7025(5)	36.3(13)
C15B	1070(7)	3605(2)	6171(5)	29.0(11)
C16B	-1594(7)	5863.5(19)	3779(5)	32.3(11)
C17B	-1006(7)	6317(2)	4592(5)	37.0(13)
C18B	-2118(7)	6778(2)	4419(5)	30.9(11)
C19B	-3821(7)	6764.4(19)	3419(4)	29.0(12)
C20B	-4458(7)	6317(2)	2646(5)	34.4(12)
C21B	-3317(7)	5874(2)	2828(5)	34.4(11)

Table 2: Anisotropic Displacement Parameters (×10^4) **BB216c**. The anisotropic displacement factor exponent takes the form: $-2\pi^2[h^2a^{*2} \times U_{11} + ... + 2hka^* \times b^* \times U_{12}]$

Atom	U_{11}	U_{22}	U_{33}	U_{23}	U_{13}	U_{12}
Br1A	57.5(4)	44.8(4)	48.3(3)	4.5(3)	2.2(3)	24.3(3)
O1A	35(2)	31(2)	52(2)	2.9(16)	24.4(17)	-0.4(17)
O2A	25.7(19)	26.1(19)	29.3(17)	-4.2(13)	7.6(14)	3.1(14)
O3A	39(2)	45(2)	33(2)	-9.3(16)	-0.8(17)	14.0(18)
C1A	28(3)	22(3)	27(2)	-5.5(18)	12(2)	-3(2)
C2A	28(3)	21(3)	22(2)	-1.6(18)	8(2)	1(2)
C3A	28(3)	25(3)	22(2)	-4.5(19)	7(2)	-2(2)
C4A	31(3)	22(3)	30(2)	2(2)	15(2)	1(2)
C5A	24(2)	16(2)	24(2)	-0.3(17)	8.7(19)	-1.6(17)
C6A	39(3)	25(3)	34(3)	6(2)	19(2)	3(2)
C7A	26(3)	26(3)	26(3)	-3(2)	8(2)	-3(2)
C8A	32(3)	25(3)	47(3)	-4(2)	12(2)	3(2)
C9A	47(4)	36(3)	45(3)	-3(2)	24(3)	10(3)
C10A	23(3)	21(3)	28(2)	3.8(19)	6(2)	5(2)
C11A	31(3)	25(3)	23(2)	-2.7(19)	7(2)	3(2)
C12A	35(3)	29(3)	30(3)	0(2)	15(2)	-4(2)
C13A	46(3)	27(3)	33(3)	10(2)	15(3)	-3(3)
C14A	49(4)	20(3)	42(3)	5(2)	19(3)	7(2)
C15A	38(3)	30(3)	33(3)	1(2)	17(2)	2(2)
C16A	25(2)	20(2)	20(2)	1.1(18)	9.6(19)	0(2)
C17A	31(3)	27(3)	27(2)	-2(2)	10(2)	0(2)
C18A	42(3)	23(3)	29(3)	-3.2(19)	9(2)	3(2)
C19A	34(3)	28(3)	26(2)	3(2)	11(2)	4(2)
C20A	27(3)	36(3)	27(2)	4(2)	3(2)	-3(2)
C21A	33(3)	24(2)	29(2)	-1.0(19)	8(2)	-2(2)
Br1B	60.5(4)	37.8(4)	50.3(3)	8.2(2)	15.2(3)	21.3(3)
O1B	34(2)	31(2)	45(2)	0.4(15)	20.5(16)	-3.8(16)
O2B	34(2)	48(2)	37(2)	-12.9(18)	3.5(16)	7.8(18)
O3B	30.6(19)	25.3(19)	32.6(17)	-4.0(14)	11.3(14)	3.7(15)
C1B	32(3)	25(3)	28(3)	-3.7(19)	12(2)	-1(2)
C2B	26(3)	26(3)	25(2)	-5.6(19)	10.4(19)	-3(2)
C3B	27(3)	19(2)	25(2)	-4.9(18)	9(2)	-4(2)
C4B	28(3)	27(3)	24(2)	1.6(19)	10.9(19)	4(2)
C5B	44(3)	30(3)	37(3)	-1(2)	12(2)	2(2)
C6B	39(3)	30(3)	32(3)	2(2)	18(2)	4(2)
C7B	26(3)	26(3)	31(3)	1(2)	11(2)	-4(2)
C8B	30(3)	30(3)	50(3)	-3(2)	12(2)	8(2)
C9B	56(4)	26(3)	41(3)	-6(2)	24(3)	1(2)
C10B	19(2)	27(3)	23(2)	-1(2)	3.6(19)	0(2)
C11B	23(3)	30(3)	30(3)	-2(2)	9(2)	0(2)
C12B	31(3)	44(4)	32(3)	0(2)	16(2)	-1(3)
C13B	40(3)	34(3)	42(3)	11(2)	19(2)	4(3)
C14B	40(3)	25(3)	47(3)	5(2)	18(2)	4(2)
C15B	30(3)	25(3)	36(3)	0(2)	17(2)	4(2)
C16B	44(3)	22(3)	36(3)	3(2)	19(3)	-1(2)
C17B	31(3)	49(3)	30(3)	13(2)	8(2)	10(3)
C18B	38(3)	26(3)	31(3)	-1(2)	14(2)	-1(2)
C19B	41(3)	23(3)	26(2)	7(2)	14(2)	7(2)
C20B	40(3)	33(3)	31(3)	0(2)	11(2)	4(2)
C21B	40(3)	29(3)	41(3)	-6(2)	22(2)	-8(2)

Table 3: Bond Lengths in Å for **BB216c.**

Atom	Atom	Length/Å
Br1A	C19A	1.899(5)
O1A	C1A	1.218(5)
O2A	C7A	1.340(5)
O2A	C8A	1.455(5)
O3A	C7A	1.194(5)
C1A	C2A	1.487(6)
C1A	C6A	1.486(6)
C2A	C3A	1.356(6)
C2A	C7A	1.506(6)
C3A	C4A	1.509(6)
C3A	C10A	1.497(6)
C4A	C5A	1.528(6)
C5A	C6A	1.532(6)
C5A	C16A	1.519(6)
C8A	C9A	1.493(7)
C10A	C11A	1.390(6)
C10A	C15A	1.395(7)
C11A	C12A	1.375(7)
C12A	C13A	1.398(7)
C13A	C14A	1.370(7)
C14A	C15A	1.387(7)
C16A	C17A	1.380(6)
C16A	C21A	1.384(6)
C17A	C18A	1.396(6)
C18A	C19A	1.372(6)
C19A	C20A	1.369(7)
C20A	C21A	1.391(6)
Br1B	C19B	1.913(5)
O1B	C1B	1.226(5)
O2B	C7B	1.206(5)
O3B	C7B	1.332(5)
O3B	C8B	1.452(5)
C1B	C2B	1.473(6)
C1B	C6B	1.489(7)
C2B	C3B	1.351(6)
C2B	C7B	1.496(6)
C3B	C4B	1.508(6)
C3B	C10B	1.479(6)
C4B	C5B	1.532(6)
C5B	C6B	1.493(7)
C5B	C16B	1.521(7)
C8B	C9B	1.490(7)
C10B	C11B	1.396(6)
C10B	C15B	1.399(7)
C11B	C12B	1.382(7)
C12B	C13B	1.364(8)
C13B	C14B	1.384(7)
C14B	C15B	1.383(7)
C16B	C17B	1.394(7)
C16B	C21B	1.363(7)
C17B	C18B	1.399(7)
C18B	C19B	1.375(7)

Atom	Atom	Length/Å
C19B	C20B	1.368(7)
C20B	C21B	1.373(7)

Table 4: Bond Angles in ° for **BB216c**.

Atom	Atom	Atom	Angle/°
C7A	O2A	C8A	115.2(3)
O1A	C1A	C2A	119.3(4)
O1A	C1A	C6A	123.0(4)
C6A	C1A	C2A	117.7(4)
C1A	C2A	C7A	113.2(4)
C3A	C2A	C1A	122.3(4)
C3A	C2A	C7A	124.3(4)
C2A	C3A	C4A	120.7(4)
C2A	C3A	C10A	122.2(4)
C10A	C3A	C4A	117.0(4)
C3A	C4A	C5A	112.6(4)
C4A	C5A	C6A	110.3(3)
C16A	C5A	C4A	113.1(3)
C16A	C5A	C6A	110.3(3)
C1A	C6A	C5A	112.5(3)
O2A	C7A	C2A	111.8(4)
O3A	C7A	O2A	124.9(4)
O3A	C7A	C2A	123.2(4)
O2A	C8A	C9A	107.6(4)
C11A	C10A	C3A	120.7(4)
C11A	C10A	C15A	117.9(4)
C15A	C10A	C3A	121.4(4)
C12A	C11A	C10A	121.4(5)
C11A	C12A	C13A	119.7(5)
C14A	C13A	C12A	119.9(5)
C13A	C14A	C15A	120.0(5)
C14A	C15A	C10A	121.0(4)
C17A	C16A	C5A	120.2(4)
C17A	C16A	C21A	117.7(4)
C21A	C16A	C5A	122.1(4)
C16A	C17A	C18A	122.0(4)
C19A	C18A	C17A	118.1(4)
C18A	C19A	Br1A	118.6(4)
C20A	C19A	Br1A	119.7(4)
C20A	C19A	C18A	121.8(5)
C19A	C20A	C21A	118.9(4)
C16A	C21A	C20A	121.5(4)
C7B	O3B	C8B	115.9(4)
O1B	C1B	C2B	120.3(4)
O1B	C1B	C6B	121.2(4)
C2B	C1B	C6B	118.4(4)
C1B	C2B	C7B	111.9(4)
C3B	C2B	C1B	122.7(5)
C3B	C2B	C7B	124.6(4)
C2B	C3B	C4B	120.2(4)

Atom	Atom	Atom	Angle/°
C2B	C3B	C10B	122.0(4)
C10B	C3B	C4B	117.8(4)
C3B	C4B	C5B	114.6(3)
C6B	C5B	C4B	112.1(4)
C6B	C5B	C16B	112.8(4)
C16B	C5B	C4B	111.4(4)
C1B	C6B	C5B	115.6(4)
O2B	C7B	O3B	124.1(4)
O2B	C7B	C2B	123.2(4)
O3B	C7B	C2B	112.6(4)
O3B	C8B	C9B	108.9(4)
C11B	C10B	C3B	120.3(4)
C11B	C10B	C15B	118.0(4)
C15B	C10B	C3B	121.7(4)
C12B	C11B	C10B	120.7(5)
C13B	C12B	C11B	120.7(5)
C12B	C13B	C14B	119.7(5)
C15B	C14B	C13B	120.4(5)
C14B	C15B	C10B	120.4(4)
C17B	C16B	C5B	122.0(5)
C21B	C16B	C5B	119.7(4)
C21B	C16B	C17B	118.3(5)
C16B	C17B	C18B	121.4(5)
C19B	C18B	C17B	117.2(5)
C18B	C19B	Br1B	118.6(4)
C20B	C19B	Br1B	118.9(4)
C20B	C19B	C18B	122.4(5)
C19B	C20B	C21B	118.8(5)
C16B	C21B	C20B	121.9(5)

Table 5: Torsion Angles in ° for **BB216c**.

Atom	Atom	Atom	Atom	Angle/°
Br1A	C19A	C20A	C21A	-178.4(3)
O1A	C1A	C2A	C3A	-177.6(4)
O1A	C1A	C2A	C7A	-2.9(6)
O1A	C1A	C6A	C5A	149.5(4)
C1A	C2A	C3A	C4A	1.2(7)
C1A	C2A	C3A	C10A	-177.0(4)
C1A	C2A	C7A	O2A	75.0(5)
C1A	C2A	C7A	O3A	-101.3(5)
C2A	C1A	C6A	C5A	-29.6(6)
C2A	C3A	C4A	C5A	24.4(6)
C2A	C3A	C10A	C11A	-143.3(5)
C2A	C3A	C10A	C15A	37.7(7)
C3A	C2A	C7A	O2A	-110.5(5)
C3A	C2A	C7A	O3A	73.2(7)
C3A	C4A	C5A	C6A	-51.0(5)
C3A	C4A	C5A	C16A	-175.0(4)
C3A	C10A	C11A	C12A	179.6(4)
C3A	C10A	C15A	C14A	-179.5(5)

Atom	Atom	Atom	Atom	Angle/°
C4A	C3A	C10A	C11A	38.4(6)
C4A	C3A	C10A	C15A	-140.6(5)
C4A	C5A	C6A	C1A	53.8(5)
C4A	C5A	C16A	C17A	-130.9(4)
C4A	C5A	C16A	C21A	51.4(5)
C5A	C16A	C17A	C18A	-175.6(4)
C5A	C16A	C21A	C20A	176.8(4)
C6A	C1A	C2A	C3A	1.5(6)
C6A	C1A	C2A	C7A	176.2(4)
C6A	C5A	C16A	C17A	105.1(4)
C6A	C5A	C16A	C21A	-72.6(5)
C7A	O2A	C8A	C9A	-165.7(4)
C7A	C2A	C3A	C4A	-172.8(4)
C7A	C2A	C3A	C10A	8.9(7)
C8A	O2A	C7A	O3A	6.9(7)
C8A	O2A	C7A	C2A	-169.4(4)
C10A	C3A	C4A	C5A	-157.3(4)
C10A	C11A	C12A	C13A	0.5(8)
C11A	C10A	C15A	C14A	1.5(7)
C11A	C12A	C13A	C14A	0.6(8)
C12A	C13A	C14A	C15A	-0.5(8)
C13A	C14A	C15A	C10A	-0.5(8)
C15A	C10A	C11A	C12A	-1.4(7)
C16A	C5A	C6A	C1A	179.4(4)
C16A	C17A	C18A	C19A	-2.0(7)
C17A	C16A	C21A	C20A	-1.0(6)
C17A	C18A	C19A	Br1A	179.7(3)
C17A	C18A	C19A	C20A	0.3(7)
C18A	C19A	C20A	C21A	0.9(7)
C19A	C20A	C21A	C16A	-0.6(7)
C21A	C16A	C17A	C18A	2.3(6)
Br1B	C19B	C20B	C21B	178.5(3)
O1B	C1B	C2B	C3B	174.2(4)
O1B	C1B	C2B	C7B	4.4(6)
O1B	C1B	C6B	C5B	161.9(4)
C1B	C2B	C3B	C4B	1.4(7)
C1B	C2B	C3B	C10B	-175.9(4)
C1B	C2B	C7B	O2B	98.5(5)
C1B	C2B	C7B	O3B	-78.6(5)
C2B	C1B	C6B	C5B	-21.9(6)
C2B	C3B	C4B	C5B	22.2(6)
C2B	C3B	C10B	C11B	142.0(5)
C2B	C3B	C10B	C15B	-38.7(7)
C3B	C2B	C7B	O2B	-71.0(7)
C3B	C2B	C7B	O3B	111.8(5)
C3B	C4B	C5B	C6B	-44.3(6)
C3B	C4B	C5B	C16B	-171.8(4)
C3B	C10B	C11B	C12B	-178.3(4)
C3B	C10B	C15B	C14B	178.7(5)
C4B	C3B	C10B	C11B	-35.4(6)
C4B	C3B	C10B	C15B	143.9(4)
C4B	C5B	C6B	C1B	44.1(6)
C4B	C5B	C16B	C17B	77.2(6)

Atom	Atom	Atom	Atom	Angle/˚
C4B	C5B	C16B	C21B	-103.2(5)
C5B	C16B	C17B	C18B	177.7(4)
C5B	C16B	C21B	C20B	-178.8(4)
C6B	C1B	C2B	C3B	-2.0(7)
C6B	C1B	C2B	C7B	-171.8(4)
C6B	C5B	C16B	C17B	-50.0(6)
C6B	C5B	C16B	C21B	129.7(5)
C7B	O3B	C8B	C9B	166.1(4)
C7B	C2B	C3B	C4B	169.9(4)
C7B	C2B	C3B	C10B	-7.4(7)
C8B	O3B	C7B	O2B	-8.9(7)
C8B	O3B	C7B	C2B	168.2(4)
C10B	C3B	C4B	C5B	-160.3(4)
C10B	C11B	C12B	C13B	-1.4(7)
C11B	C10B	C15B	C14B	-2.0(7)
C11B	C12B	C13B	C14B	-0.2(8)
C12B	C13B	C14B	C15B	0.7(8)
C13B	C14B	C15B	C10B	0.5(8)
C15B	C10B	C11B	C12B	2.4(7)
C16B	C5B	C6B	C1B	170.8(4)
C16B	C17B	C18B	C19B	0.5(7)
C17B	C16B	C21B	C20B	0.8(7)
C17B	C18B	C19B	Br1B	-179.6(3)
C17B	C18B	C19B	C20B	2.1(7)
C18B	C19B	C20B	C21B	-3.2(7)
C19B	C20B	C21B	C16B	1.7(7)
C21B	C16B	C17B	C18B	-1.9(7)

Table 6: Hydrogen Fractional Atomic Coordinates ($\times 10^4$) and Equivalent Isotropic Displacement Parameters ($Å^2 \times 10^3$) for **BB216c**. U_{eq} is defined as 1/3 of the trace of the orthogonalised U_{ij}.

Atom	x	y	z	U_{eq}
H4AA	6560	4960	414	32
H4AB	5996	4778	-1159	32
H5A	3775	4177	-841	25
H6AA	3115	4076	1256	37
H6AB	4635	4523	1957	37
H8AA	-1893	6082	167	41
H8AB	-1197	6460	-864	41
H9AA	594	6967	1021	61
H9AB	-144	6596	2034	61
H9AC	-1578	6976	956	61
H11A	5471	5272	-2839	32
H12A	5977	5960	-4217	37
H13A	5203	6847	-3814	42
H14A	3972	7031	-2020	43
H15A	3468	6338	-637	39
H17A	4812	3305	-782	34
H18A	6951	2608	62	38
H20A	10320	3648	2702	37
H21A	8116	4330	1901	35

Atom	x	y	z	U_{eq}
H4BA	-132	5276	5985	31
H4BB	-1674	4887	5029	31
H5B	-947	5138	3098	44
H6BA	1525	5622	2970	39
H6BB	2071	5788	4551	39
H8BA	6283	3409	5676	44
H8BB	6993	3800	4681	44
H9BA	5261	3284	2780	58
H9BB	4690	2882	3814	58
H9BC	6838	2932	3831	58
H11B	-448	4608	7596	33
H12B	-879	3929	9032	41
H13B	-128	3052	8684	45
H14B	1071	2843	6875	44
H15B	1555	3516	5435	35
H17B	175	6312	5279	44
H18B	-1714	7088	4968	37
H20B	-5668	6313	1995	41
H21B	-3740	5566	2275	41

Crystal Structure:

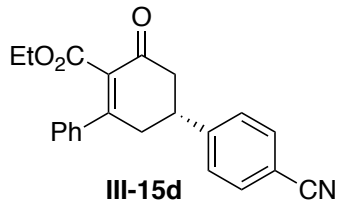

III-15d

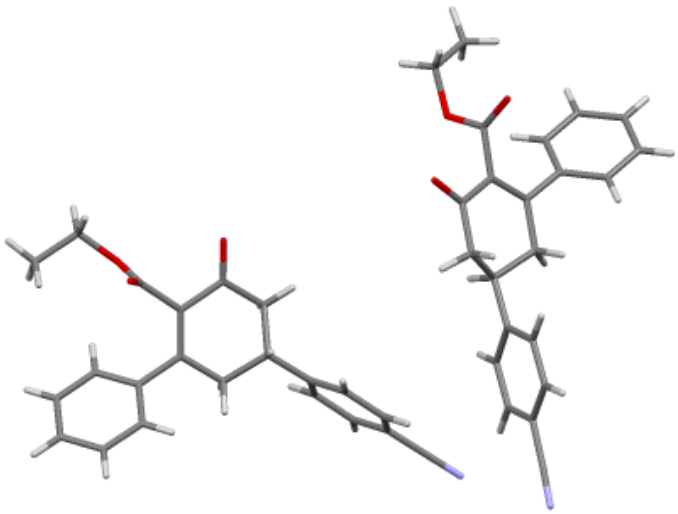

Table 7: Fractional Atomic Coordinates (×10^4) and Equivalent Isotropic Displacement Parameters (Å^2×10^3) for **BB316b**. U_{eq} is defined as 1/3 of the trace of the orthogonalised U_{ij}.

Atom	x	y	z	U_{eq}
O1A	3603.4(10)	9406.9(14)	1459.6(6)	35.1(3)
O2A	3948.9(9)	10889.7(14)	359.1(7)	33.8(3)
O3A	2638.4(9)	10065.7(16)	-55.4(7)	37.9(3)
N1A	5539.0(12)	-216.4(19)	2562.8(9)	39.8(4)
C1A	4027.9(11)	5975.3(19)	1145.8(8)	26.1(4)
C2A	4302.0(12)	7239(2)	1568.6(8)	28.7(4)
C3A	3870.2(12)	8496.9(19)	1221.8(8)	25.9(4)
C4A	3744.2(11)	8588.0(19)	549.3(8)	23.6(3)
C5A	3885.1(11)	7518.4(19)	232.5(8)	24.5(4)
C6A	4221.7(12)	6186.0(19)	557.3(9)	26.4(4)
C7A	4384.0(12)	4644(2)	1471.1(8)	26.0(4)
C8A	3854.0(12)	3685(2)	1574.6(9)	27.5(4)
C9A	4151.0(12)	2434(2)	1850.1(9)	28.6(4)
C10A	4998.8(12)	2123(2)	2033.4(8)	25.9(4)
C11A	5540.4(12)	3072(2)	1934.2(9)	31.2(4)
C12A	5233.5(13)	4321(2)	1659.8(9)	33.0(4)
C13A	5304.8(12)	820(2)	2328.3(9)	29.0(4)
C14A	3370.7(12)	9913(2)	245.1(8)	26.6(4)
C15A	3652.3(18)	12243(2)	99.2(11)	45.2(5)
C16A	3604(2)	12358(3)	-560.9(13)	61.5(8)
C17A	3715.2(11)	7601(2)	-447.4(8)	25.5(4)
C18A	3999.8(13)	8705(2)	-696.9(9)	30.8(4)
C19A	3815.1(15)	8779(3)	-1334.5(10)	41.3(5)
C20A	3354.0(15)	7762(3)	-1727.0(9)	44.3(6)
C21A	3068.1(13)	6658(3)	-1484.9(9)	39.0(5)
C22A	3249.8(12)	6569(2)	-848.4(9)	30.7(4)
O1B	2179.9(11)	6819.3(16)	3580.6(7)	44.9(4)
O2B	3650.8(10)	8264.9(15)	4634.7(7)	37.7(3)
O3B	2825.5(10)	7472.2(18)	5114.6(8)	44.5(4)
N1B	2871.5(15)	-2846(2)	2425.8(11)	53.2(5)
C1B	3331.3(13)	3588(2)	3760.1(9)	33.0(4)
C2B	2559.5(17)	4484(3)	3500.0(11)	47.1(6)
C3B	2634.7(13)	5855(2)	3819.0(9)	33.6(4)
C4B	3238.2(12)	5958(2)	4470.7(9)	27.4(4)
C5B	3671.3(11)	4868(2)	4785.8(8)	26.5(4)
C6B	3641.3(12)	3505(2)	4469.3(9)	28.6(4)
C7B	3208.6(13)	2158(2)	3475.9(8)	31.8(4)
C8B	3807.7(14)	1611(2)	3275.6(10)	37.9(5)
C9B	3731.2(14)	316(2)	3023(1)	37.6(5)
C10B	3034.6(12)	-478(2)	2962.2(8)	28.7(4)
C11B	2427.7(13)	33(2)	3169.4(10)	35.8(4)
C12B	2520.5(14)	1336(2)	3422.9(10)	37.0(5)
C13B	2938.0(14)	-1808(2)	2668.7(10)	35.7(5)
C14B	3210.9(12)	7296(2)	4780.6(9)	31.4(4)
C15B	3626.7(18)	9637(2)	4885.7(13)	50.4(6)
C16B	4240(2)	9768(3)	5544.1(14)	63.7(8)
C17B	4158.7(12)	4944(2)	5466.9(9)	29.8(4)

Atom	x	y	z	U_{eq}
C18B	4705.9(13)	6017(2)	5730.2(10)	36.6(5)
C19B	5106.2(16)	6111(3)	6373.1(11)	49.1(6)
C20B	4960.9(17)	5129(3)	6755.2(10)	54.7(7)
C21B	4429.7(16)	4047(3)	6496.4(10)	47.5(6)
C22B	4032.5(13)	3943(2)	5856.1(10)	35.7(5)

Table 8: Anisotropic Displacement Parameters (×10^4) **BB316b**. The anisotropic displacement factor exponent takes the form: $-2\pi^2[h^2a^{*2} \times U_{11} + \ldots + 2hka^* \times b^* \times U_{12}]$

Atom	U_{11}	U_{22}	U_{33}	U_{23}	U_{13}	U_{12}
O1A	48.5(9)	30.0(7)	28.3(7)	-3.4(6)	16.1(6)	5.3(6)
O2A	40.4(8)	24.6(7)	34.2(7)	1.8(6)	11.4(6)	-0.7(6)
O3A	30.7(7)	39.8(8)	37.6(7)	5.7(7)	6.1(6)	9.3(7)
N1A	36.6(9)	31.8(10)	45.8(10)	6.2(8)	9.3(8)	5.2(8)
C1A	26.3(9)	26.6(9)	24.2(9)	1.9(7)	7.8(7)	-0.3(8)
C2A	33.4(10)	30.3(9)	20.5(8)	-0.2(8)	7.9(7)	1.2(8)
C3A	27.7(9)	25.3(9)	23.9(9)	-3.1(7)	8.6(7)	-2.7(7)
C4A	21.4(8)	25.0(9)	22.3(8)	0.5(7)	5.6(7)	-1.2(7)
C5A	21.7(8)	27.6(9)	23.0(8)	0.2(7)	7.1(7)	-1.4(7)
C6A	31.0(9)	23.4(9)	24.5(8)	-0.6(7)	10.1(7)	1.5(8)
C7A	30.1(9)	27.2(9)	19.3(8)	-1.4(7)	7.4(7)	-1.2(8)
C8A	26.8(9)	28.8(9)	26.5(9)	1.4(8)	9.2(7)	1.9(8)
C9A	30.0(9)	27.9(10)	27.5(9)	0.0(8)	10.3(7)	-3.2(8)
C10A	31.8(9)	25.8(9)	18.7(8)	-1.8(7)	7.8(7)	1.6(8)
C11A	25.7(9)	34.2(10)	31.3(10)	2.3(8)	7.8(8)	1.0(8)
C12A	30.7(10)	33.8(10)	34.2(10)	3.7(8)	11.6(8)	-6.4(8)
C13A	27.1(9)	30.9(10)	27.7(9)	-3.4(8)	8.5(7)	0.0(8)
C14A	30.9(9)	28.9(9)	20.1(8)	-1.8(7)	9.5(7)	2.4(8)
C15A	67.7(16)	22.8(10)	47.1(13)	3.2(10)	23.5(12)	3.9(11)
C16A	105(2)	35.6(13)	50.5(14)	13.9(12)	36.3(16)	13.3(15)
C17A	24.1(9)	29.4(9)	22.5(8)	0.5(7)	8.2(7)	7.4(7)
C18A	34.2(10)	32.5(10)	28.8(9)	2.5(8)	15.3(8)	5.6(9)
C19A	52.6(13)	45.0(13)	33.6(11)	12.2(10)	24.4(10)	13.1(11)
C20A	49.9(13)	62.0(15)	20.5(9)	5.4(10)	12.7(9)	20.9(12)
C21A	31.2(10)	53.9(13)	27.1(10)	-11.1(10)	5.4(8)	6.6(10)
C22A	28.3(9)	35.8(10)	28.9(9)	-4.1(8)	11.6(8)	1.7(8)
O1B	49.4(9)	34.2(8)	36.3(8)	3.6(7)	-1.0(7)	7.0(7)
O2B	43.9(9)	30.2(7)	36.5(8)	-1.8(6)	12.0(7)	-3.2(7)
O3B	41.9(8)	50(1)	47.6(9)	-6.5(8)	23.4(7)	5.0(7)
N1B	56.2(13)	41.0(11)	66.2(14)	-12.7(11)	27.0(11)	-1.8(10)
C1B	36.3(10)	35.3(11)	26.3(9)	0.1(8)	10.3(8)	-4.9(9)
C2B	53.6(14)	36.4(12)	32.1(11)	-2.8(9)	-6.4(10)	5.5(11)
C3B	35.3(10)	31.6(10)	27.7(9)	1.3(8)	4.6(8)	-0.3(9)
C4B	27.0(9)	30.5(9)	25.5(9)	1.2(8)	10.6(7)	-1.8(8)
C5B	23.1(8)	33.7(10)	23.8(9)	-0.4(8)	9.9(7)	-1.7(8)
C6B	27.1(9)	32.7(10)	24.5(9)	1.3(8)	7.8(7)	3.2(8)
C7B	38.4(10)	32.1(10)	19.7(8)	2.7(8)	4.9(7)	-4.2(9)
C8B	35.9(11)	39.4(11)	38.4(11)	1.8(9)	13.7(9)	-9.5(10)
C9B	35.2(11)	41.7(11)	39.6(11)	1.5(9)	18.3(9)	-2.6(9)
C10B	29.3(9)	30.4(10)	23.6(8)	3.2(8)	6.6(7)	1.0(8)
C11B	32.4(10)	35.9(11)	40.7(11)	-4.3(9)	15.3(9)	-5.7(9)
C12B	38.8(11)	37.9(11)	38.1(11)	-5.9(9)	18.7(9)	-0.7(9)
C13B	32.2(10)	36.6(11)	38.3(11)	-0.4(9)	13.0(9)	1.4(9)

Atom	U_{11}	U_{22}	U_{33}	U_{23}	U_{13}	U_{12}
C14B	26.5(9)	35.3(10)	27.5(9)	2.2(8)	4.5(8)	4.7(8)
C15B	58.3(15)	27.9(11)	55.4(15)	-5.5(11)	10.0(12)	0.8(11)
C16B	71.6(19)	42.6(15)	59.8(17)	-16.7(13)	4.6(14)	-0.7(14)
C17B	25.7(9)	38.4(11)	25.2(9)	-1.0(8)	9.2(7)	8.5(8)
C18B	32.7(10)	40.2(11)	31.2(10)	-5.1(9)	5.4(8)	6.8(9)
C19B	44.2(13)	55.0(14)	34.5(12)	-14.8(11)	-1.1(10)	11.8(12)
C20B	56.7(15)	77.8(19)	20.3(10)	-4.9(11)	3.8(10)	29.2(15)
C21B	47.5(13)	67.4(16)	28.6(11)	10.5(11)	15.3(10)	25.3(13)
C22B	33.9(10)	45.9(12)	28.6(10)	7.2(9)	13.0(8)	12.5(9)

Table 9: Bond Lengths in Å for **BB316b**.

Atom	Atom	Length/Å
O1A	C3A	1.219(2)
O2A	C14A	1.331(2)
O2A	C15A	1.460(3)
O3A	C14A	1.203(2)
N1A	C13A	1.146(3)
C1A	C2A	1.533(3)
C1A	C6A	1.531(2)
C1A	C7A	1.510(3)
C2A	C3A	1.501(3)
C3A	C4A	1.490(2)
C4A	C5A	1.347(3)
C4A	C14A	1.496(3)
C5A	C6A	1.503(3)
C5A	C17A	1.490(2)
C7A	C8A	1.388(3)
C7A	C12A	1.399(3)
C8A	C9A	1.382(3)
C9A	C10A	1.395(3)
C10A	C11A	1.392(3)
C10A	C13A	1.445(3)
C11A	C12A	1.383(3)
C15A	C16A	1.501(3)
C17A	C18A	1.393(3)
C17A	C22A	1.400(3)
C18A	C19A	1.390(3)
C19A	C20A	1.379(4)
C20A	C21A	1.384(4)
C21A	C22A	1.389(3)

Atom	Atom	Length/Å
O1B	C3B	1.216(3)
O2B	C14B	1.330(3)
O2B	C15B	1.464(3)
O3B	C14B	1.204(2)
N1B	C13B	1.142(3)
C1B	C2B	1.516(3)
C1B	C6B	1.526(3)
C1B	C7B	1.521(3)
C2B	C3B	1.507(3)
C3B	C4B	1.482(3)
C4B	C5B	1.345(3)
C4B	C14B	1.497(3)
C5B	C6B	1.508(3)
C5B	C17B	1.486(3)
C7B	C8B	1.386(3)
C7B	C12B	1.398(3)
C8B	C9B	1.375(3)
C9B	C10B	1.391(3)
C10B	C11B	1.395(3)
C10B	C13B	1.443(3)
C11B	C12B	1.382(3)
C15B	C16B	1.501(4)
C17B	C18B	1.388(3)
C17B	C22B	1.398(3)
C18B	C19B	1.389(3)
C19B	C20B	1.386(4)
C20B	C21B	1.378(4)
C21B	C22B	1.385(3)

Table 10: Bond Angles in ° for **BB316b**.

Atom	Atom	Atom	Angle/°
C14A	O2A	C15A	116.21(17)
C6A	C1A	C2A	109.98(15)
C7A	C1A	C2A	113.59(15)
C7A	C1A	C6A	112.03(15)
C3A	C2A	C1A	109.91(15)

Atom	Atom	Atom	Angle/°
O1A	C3A	C2A	123.20(16)
O1A	C3A	C4A	119.59(17)
C4A	C3A	C2A	117.17(15)
C3A	C4A	C14A	114.34(15)
C5A	C4A	C3A	122.38(17)

Atom	Atom	Atom	Angle/°
C5A	C4A	C14A	123.01(16)
C4A	C5A	C6A	120.68(15)
C4A	C5A	C17A	121.85(17)
C17A	C5A	C6A	117.47(15)
C5A	C6A	C1A	112.86(15)
C8A	C7A	C1A	119.46(17)
C8A	C7A	C12A	118.34(18)
C12A	C7A	C1A	122.18(17)
C9A	C8A	C7A	121.19(18)
C8A	C9A	C10A	119.85(18)
C9A	C10A	C13A	119.43(18)
C11A	C10A	C9A	119.80(18)
C11A	C10A	C13A	120.77(18)
C12A	C11A	C10A	119.61(18)
C11A	C12A	C7A	121.21(18)
N1A	C13A	C10A	179.2(2)
O2A	C14A	C4A	111.33(15)
O3A	C14A	O2A	125.02(18)
O3A	C14A	C4A	123.65(18)
O2A	C15A	C16A	111.35(19)
C18A	C17A	C5A	121.13(17)
C18A	C17A	C22A	118.89(17)
C22A	C17A	C5A	119.97(17)
C19A	C18A	C17A	120.2(2)
C20A	C19A	C18A	120.6(2)
C19A	C20A	C21A	119.78(18)
C20A	C21A	C22A	120.2(2)
C21A	C22A	C17A	120.3(2)
C14B	O2B	C15B	116.38(19)
C2B	C1B	C6B	111.20(17)
C2B	C1B	C7B	113.30(18)
C7B	C1B	C6B	110.64(16)
C3B	C2B	C1B	114.38(19)

Atom	Atom	Atom	Angle/°
O1B	C3B	C2B	122.59(18)
O1B	C3B	C4B	119.92(19)
C4B	C3B	C2B	117.23(18)
C3B	C4B	C14B	114.23(17)
C5B	C4B	C3B	122.38(18)
C5B	C4B	C14B	122.53(17)
C4B	C5B	C6B	121.33(16)
C4B	C5B	C17B	121.08(18)
C17B	C5B	C6B	117.50(17)
C5B	C6B	C1B	114.20(16)
C8B	C7B	C1B	119.68(19)
C8B	C7B	C12B	117.7(2)
C12B	C7B	C1B	122.63(19)
C9B	C8B	C7B	121.9(2)
C8B	C9B	C10B	119.7(2)
C9B	C10B	C11B	119.8(2)
C9B	C10B	C13B	119.43(19)
C11B	C10B	C13B	120.80(19)
C12B	C11B	C10B	119.36(19)
C11B	C12B	C7B	121.56(19)
N1B	C13B	C10B	178.1(2)
O2B	C14B	C4B	111.98(16)
O3B	C14B	O2B	124.4(2)
O3B	C14B	C4B	123.7(2)
O2B	C15B	C16B	111.5(2)
C18B	C17B	C5B	121.77(19)
C18B	C17B	C22B	119.09(19)
C22B	C17B	C5B	119.07(19)
C17B	C18B	C19B	120.3(2)
C20B	C19B	C18B	120.1(2)
C21B	C20B	C19B	119.9(2)
C20B	C21B	C22B	120.3(2)
C21B	C22B	C17B	120.2(2)

Table 11: Torsion Angles in ° for **BB316b**.

Atom	Atom	Atom	Atom	Angle/°
O1A	C3A	C4A	C5A	-167.73(18)
O1A	C3A	C4A	C14A	6.6(2)
C1A	C2A	C3A	O1A	140.38(19)
C1A	C2A	C3A	C4A	-37.5(2)
C1A	C7A	C8A	C9A	177.61(16)
C1A	C7A	C12A	C11A	-177.36(18)
C2A	C1A	C6A	C5A	-51.7(2)
C2A	C1A	C7A	C8A	112.09(19)
C2A	C1A	C7A	C12A	-69.6(2)
C2A	C3A	C4A	C5A	10.2(3)
C2A	C3A	C4A	C14A	-175.50(16)

Atom	Atom	Atom	Atom	Angle/˚
C3A	C4A	C5A	C6A	-3.1(3)
C3A	C4A	C5A	C17A	176.81(16)
C3A	C4A	C14A	O2A	81.74(19)
C3A	C4A	C14A	O3A	-97.3(2)
C4A	C5A	C6A	C1A	24.5(2)
C4A	C5A	C17A	C18A	48.4(3)
C4A	C5A	C17A	C22A	-130.41(19)
C5A	C4A	C14A	O2A	-104.0(2)
C5A	C4A	C14A	O3A	77.0(2)
C5A	C17A	C18A	C19A	-178.28(18)
C5A	C17A	C22A	C21A	178.14(18)
C6A	C1A	C2A	C3A	57.7(2)
C6A	C1A	C7A	C8A	-122.54(18)
C6A	C1A	C7A	C12A	55.7(2)
C6A	C5A	C17A	C18A	-131.66(18)
C6A	C5A	C17A	C22A	49.5(2)
C7A	C1A	C2A	C3A	-175.81(15)
C7A	C1A	C6A	C5A	-179.00(15)
C7A	C8A	C9A	C10A	0.5(3)
C8A	C7A	C12A	C11A	0.9(3)
C8A	C9A	C10A	C11A	-0.4(3)
C8A	C9A	C10A	C13A	179.20(17)
C9A	C10A	C11A	C12A	0.6(3)
C10A	C11A	C12A	C7A	-0.9(3)
C12A	C7A	C8A	C9A	-0.7(3)
C13A	C10A	C11A	C12A	-179.00(18)
C14A	O2A	C15A	C16A	-85.7(3)
C14A	C4A	C5A	C6A	-176.88(16)
C14A	C4A	C5A	C17A	3.0(3)
C15A	O2A	C14A	O3A	0.7(3)
C15A	O2A	C14A	C4A	-178.35(15)
C17A	C5A	C6A	C1A	-155.40(16)
C17A	C18A	C19A	C20A	-0.4(3)
C18A	C17A	C22A	C21A	-0.7(3)
C18A	C19A	C20A	C21A	0.3(3)
C19A	C20A	C21A	C22A	-0.5(3)
C20A	C21A	C22A	C17A	0.7(3)
C22A	C17A	C18A	C19A	0.6(3)
O1B	C3B	C4B	C5B	170.49(19)
O1B	C3B	C4B	C14B	0.8(3)
C1B	C2B	C3B	O1B	160.8(2)
C1B	C2B	C3B	C4B	-25.0(3)
C1B	C7B	C8B	C9B	179.16(19)

Atom	Atom	Atom	Atom	Angle/°
C1B	C7B	C12B	C11B	-179.24(19)
C2B	C1B	C6B	C5B	-45.5(2)
C2B	C1B	C7B	C8B	133.2(2)
C2B	C1B	C7B	C12B	-48.8(3)
C2B	C3B	C4B	C5B	-3.8(3)
C2B	C3B	C4B	C14B	-173.50(19)
C3B	C4B	C5B	C6B	7.1(3)
C3B	C4B	C5B	C17B	-169.40(17)
C3B	C4B	C14B	O2B	-82.3(2)
C3B	C4B	C14B	O3B	96.7(2)
C4B	C5B	C6B	C1B	18.5(3)
C4B	C5B	C17B	C18B	-48.9(3)
C4B	C5B	C17B	C22B	127.9(2)
C5B	C4B	C14B	O2B	108.0(2)
C5B	C4B	C14B	O3B	-73.0(3)
C5B	C17B	C18B	C19B	175.30(19)
C5B	C17B	C22B	C21B	-174.99(19)
C6B	C1B	C2B	C3B	48.7(3)
C6B	C1B	C7B	C8B	-101.2(2)
C6B	C1B	C7B	C12B	76.8(2)
C6B	C5B	C17B	C18B	134.48(19)
C6B	C5B	C17B	C22B	-48.7(2)
C7B	C1B	C2B	C3B	174.08(19)
C7B	C1B	C6B	C5B	-172.32(17)
C7B	C8B	C9B	C10B	0.2(3)
C8B	C7B	C12B	C11B	-1.2(3)
C8B	C9B	C10B	C11B	-1.3(3)
C8B	C9B	C10B	C13B	177.0(2)
C9B	C10B	C11B	C12B	1.1(3)
C10B	C11B	C12B	C7B	0.1(3)
C12B	C7B	C8B	C9B	1.1(3)
C13B	C10B	C11B	C12B	-177.1(2)
C14B	O2B	C15B	C16B	82.6(3)
C14B	C4B	C5B	C6B	175.89(17)
C14B	C4B	C5B	C17B	-0.6(3)
C15B	O2B	C14B	O3B	-2.3(3)
C15B	O2B	C14B	C4B	176.67(17)
C17B	C5B	C6B	C1B	-164.87(16)
C17B	C18B	C19B	C20B	0.0(3)
C18B	C17B	C22B	C21B	1.9(3)
C18B	C19B	C20B	C21B	1.1(4)
C19B	C20B	C21B	C22B	-0.7(4)
C20B	C21B	C22B	C17B	-0.8(3)
C22B	C17B	C18B	C19B	-1.5(3)

Table 12: Hydrogen Fractional Atomic Coordinates (×10⁴) and Equivalent Isotropic Displacement Parameters (Å²×10³) for **BB316b**. U_{eq} is defined as 1/3 of the trace of the orthogonalised U_{ij}.

Atom	x	y	z	U_{eq}
H1A	3406	5910	1010	31
H2AA	4161	7109	1943	34
H2AB	4915	7356	1707	34
H6AA	4835	6165	671	32
H6AB	3978	5417	266	32
H8A	3277	3893	1454	33
H9A	3779	1787	1915	34
H11A	6117	2863	2054	37
H12A	5606	4971	1598	40
H15A	4036	12955	357	54
H15B	3092	12408	111	54
H16A	4153	12152	-577	92
H16B	3438	13292	-714	92
H16C	3191	11703	-823	92
H18A	4321	9409	-431	37
H19A	4008	9538	-1502	50
H20A	3233	7818	-2162	53
H21A	2747	5959	-1755	47
H22A	3057	5805	-684	37
H1B	3781	4042	3654	40
H2BA	2436	4643	3052	57
H2BB	2079	3982	3535	57
H6BA	3271	2878	4586	34
H6BB	4209	3100	4627	34
H8B	4285	2146	3314	46
H9B	4152	-34	2890	45
H11B	1955	-509	3137	43
H12B	2107	1682	3565	44
H15C	3056	9824	4873	61
H15D	3758	10329	4622	61
H16D	4069	9167	5816	96
H16E	4254	10722	5682	96
H16F	4797	9499	5564	96
H18B	4807	6691	5470	44
H19B	5480	6848	6551	59
H20B	5227	5202	7195	66
H21B	4335	3370	6759	57
H22B	3673	3188	5681	43

REFERENCES

REFERENCES

(1) Podraza, K. F. REGIOSPECIFIC ALKYLATION OF CYCLOHEXENONES - A REVIEW. *Organic Preparations and Procedures International* **1991,** *23* (2), 217.

(2) Organ, M. G.; Anderson, P. Carbonyl and conjugate additions to cyclohexenone - Experiments illustrating reagent selectivity. *Journal of Chemical Education* **1996,** *73* (12), 1193.

(3) Szmant, H. H. *Organic Building Blocks of the Chemical Industry*; Wiley-Interscience: New York, 1989.

(4) Chong, B. D.; Ji, Y. I.; Oh, S. S.; Yang, J. D.; Baik, W.; Koo, S. Highly efficient synthesis of methyl-substituted conjugate cyclohexenones. *Journal of Organic Chemistry* **1997,** *62* (26), 9323.

(5) Heathcock, C. H.; Ellis, J. E.; McMurry, J. E.; Coppolin.A. ACID-CATALYZED ROBINSON ANNELATIONS. *Tetrahedron Letters* **1971,** (52), 4995.

(6) Acheson, R. M.; Robinson, R. EXPERIMENTS BEARING ON THE SYNTHESIS OF CORTISONE .1. SOME CYCLOPENTENONE DERIVATIVES. *Journal of the Chemical Society* **1952**, 1127.

(7) Ho, T. L. *Enantioselective synthesis: natural products synthesis from chiral terpenes*; Wiley: New York, 1992.

(8) Bae, B. H.; Im, K. S.; Choi, W. C.; Hong, J. K.; Lee, C. O.; Choi, J. S.; Son, B. W.; Song, J. I.; Jung, J. H. New acetylenic compounds from the stony coral Montipora sp. *Journal of Natural Products* **2000,** *63* (11), 1511.

(9) Baran, P. S.; Richter, J. M.; Lin, D. W. Direct coupling of pyrroles with carbonyl compounds: Short enantioselective synthesis of (S)-Ketorolac. *Angewandte Chemie-International Edition* **2005,** *44* (4), 609.

(10) Goeke, A.; Mertl, D.; Brunner, G. Alkyl aluminum halide promoted intramolecular cyclization of omega-allyl-cycloalk-2-enones: Access to bridged bi- and tricyclic compounds. *Angewandte Chemie-International Edition* **2005,** *44* (1), 99.

(11) Klunder, A. J. H.; Zhu, J.; Zwanenburg, B. The concept of transient chirality in the stereoselective synthesis of functionalized cycloalkenes applying the retro-Diels-Alder methodology. *Chemical Reviews* **1999,** *99* (5), 1163.

(12) Lakshmi, R.; Bateman, T. D.; McIntosh, M. C. A convenient 3-step synthesis of (R)-7-hydroxycarvone from (S)-alpha-pinene. *Journal of Organic Chemistry* **2005,** *70* (13), 5313.

(13) Miyashita, M.; Sasaki, M.; Hattori, I.; Sakai, M.; Tanino, K. Total synthesis of norzoanthamine. *Science* **2004,** *305* (5683), 495.

(14) Mohr, P. J.; Halcomb, R. L. Total synthesis of (+)-phomactin A using a B-alkyl Suzuki macrocyclization. *Journal of the American Chemical Society* **2003,** *125* (7), 1712.

(15) Varner, M. A.; Grossman, R. B. Annulation routes to trans-decalins. *Tetrahedron* **1999,** *55* (49), 13867.

(16) Yamamoto, H.; Sham, H. L. TOTAL SYNTHESIS OF (+/-)-9-ISOCYANOPUPUKEANANE. *Journal of the American Chemical Society* **1979,** *101* (6), 1609.

(17) Letizia, C. S.; Cocchiara, J.; Wellington, G. A.; Funk, C.; Api, A. M. Monographs on fragrance raw materials. *Food and Chemical Toxicology* **2000,** *38*, S1.

(18) Carlone, A.; Marigo, M.; North, C.; Landa, A.; Jorgensen, K. A. A simple asymmetric organocatalytic approach to optically active cyclohexenones. *Chemical Communications* **2006**, DOI:10.1039/b611366d 10.1039/b611366d(47), 4928.

(19) Yang, X.; Wang, J.; Li, P. F. Recent progress on asymmetric organocatalytic construction of chiral cyclohexenone skeletons. *Organic & Biomolecular Chemistry* **2014,** *12* (16), 2499.

(20) Wieland, P.; Miescher, K. UBER DIE HERSTELLUNG MEHRKERNIGER KETONE. *Helvetica Chimica Acta* **1950,** *33* (7), 2215.

(21) Hajos, Z. G.; Parrish, D. R. ASYMMETRIC SYNTHESIS OF BICYCLIC INTERMEDIATES OF NATURAL PRODUCT CHEMISTRY. *Journal of Organic Chemistry* **1974,** *39* (12), 1615.

(22) Eder, U. S., G. R.; Wiechart, R. In *German Patent* Germany, 1971; Vol. DE 2014757.

(23) Hajos, Z. G. P., D. R. In *German Patent* Germany, 1974; Vol. DE 2102623.

(24) Chen, L. J.; Luo, S. Z.; Li, J. Y.; Li, X.; Cheng, J. P. Organocatalytic kinetic resolution via intramolecular aldol reactions: Enantioselective synthesis of both enantiomers of chiral cyclohexenones. *Organic & Biomolecular Chemistry* **2010,** *8* (11), 2627.

(25) Naasz, R.; Arnold, L. A.; Minnaard, A. J.; Feringa, B. L. Highly enantioselective copper-phosphoramidite catalyzed kinetic resolution of chiral 2-cyclohexenones. *Angewandte Chemie-International Edition* **2001,** *40* (5), 927.

(26) Hanazawa, T.; Koiwa, M.; Hareau, G. P. J.; Sato, F. Optically active trans-4-(tert-butyldimethylsiloxymethyl)-5-(tert-butyldimethylsiloxy)-2- cyclohexenone as a useful chiral building block for preparation of substituted cyclohexane rings: synthesis and its highly stereoselective reaction with RCu(CN)Li. *Tetrahedron Letters* **2000,** *41* (15), 2659.

(27) Hareau, G. P. J.; Koiwa, M.; Hikichi, S.; Sato, F. Synthesis of optically active 5-(tert-butyldimethylsiloxy)-2-cyclohexenone and its 6-substituted derivatives as useful chiral building blocks for the synthesis of cyclohexane rings. Syntheses of carvone, penienone, and penihydrone. *Journal of the American Chemical Society* **1999,** *121* (15), 3640.

(28) Sarakinos, G.; Corey, E. J. Simple and practical routes to enantiomerically pure 5-(trialkylsilyl)-2-cyclohexenones. *Organic Letters* **1999,** *1* (5), 811.

(29) Zhou, J.; Wakchaure, V.; Kraft, P.; List, B. Primary-amine-catalyzed enantioselective intramolecular aldolizations. *Angewandte Chemie-International Edition* **2008,** *47* (40), 7656.

(30) Marigo, M.; Bertelsen, S.; Landa, A.; Jorgensen, K. A. One-pot organocatalytic domino Michael-aldol and intramolecular S(N)2 reactions. Asymmetric synthesis of highly functionalized epoxycyclohexanone derivatives. *Journal of the American Chemical Society* **2006,** *128* (16), 5475.

(31) Liu, Y. K.; Ma, C.; Jiang, K.; Liu, T. Y.; Chen, Y. C. Asymmetric Tandem Michael Addition-Wittig Reaction to Cyclohexenone Annulation. *Organic Letters* **2009,** *11* (13), 2848.

(32) Hayashi, Y.; Toyoshima, M.; Gotoh, H.; Ishikawa, H. Diphenylprolinol Silyl Ether Catalysis in an Asymmetric Formal Carbo 3+3 Cycloaddition Reaction via a Domino Michael/Knoevenagel Condensation. *Organic Letters* **2009,** *11* (1), 45.

(33) Cui, H. F.; Yang, Y. Q.; Chai, Z.; Li, P.; Zheng, C. W.; Zhu, S. Z.; Zhao, G. Enantioselective Synthesis of Functionalized Fluorinated Cyclohexenones via Robinson Annulation Catalyzed by Primary-Secondary Diamines. *Journal of Organic Chemistry* **2010,** *75* (1), 117.

(34) Yang, Y. Q.; Chai, Z.; Wang, H. F.; Chen, X. K.; Cui, H. F.; Zheng, C. W.; Xiao, H.; Li, P.; Zhao, G. Chiral Primary-Secondary Diamines Catalyzed Michael-Aldol-Dehydration Reaction between Benzoylacetates and alpha,beta-Unsaturated Ketones: Highly Enantioselective Synthesis of Functionalized Chiral Cyclohexenones. *Chemistry-a European Journal* **2009,** *15* (48), 13295.

(35) Gu, Q.; Rong, Z. Q.; Zheng, C.; You, S. L. Desymmetrization of Cyclohexadienones via Bronsted Acid-Catalyzed Enantioselective Oxo-Michael Reaction. *Journal of the American Chemical Society* **2010,** *132* (12), 4056.

(36) Mori, K.; Katoh, T.; Suzuki, T.; Noji, T.; Yamanaka, M.; Akiyama, T. Chiral Phosphoric Acid Catalyzed Desymmetrization of meso-1,3-Diones: Asymmetric Synthesis of Chiral Cyclohexenones. *Angewandte Chemie-International Edition* **2009,** *48* (51), 9652.

(37) Masamune, S.; Castellucci, N. T. GAMMA-PYRAN. *Journal of the American Chemical Society* **1962,** *84* (12), 2452.

(38) Yang, B.; Yang, J. L.; Zhao, Y. P.; Liu, H. L.; Jiang, Y. M. The Plant Resources, Structure Characteristics, Biological Activities and Synthesis of Pyranoflavonoids. *Current Medicinal Chemistry* **2016,** *23* (27), 3078.

(39) El-Subbagh, H. I.; Abu-Zaid, S. M.; Mahran, M. A.; Badria, F. A.; Al-Obaid, A. M. Synthesis and biological evaluation of certain alpha,beta-unsaturated ketones and their corresponding fused pyridines as antiviral and cytotoxic agents. *Journal of Medicinal Chemistry* **2000,** *43* (15), 2915.

(40) Goldmann, S.; Stoltefuss, J. 1,4-DIHYDROPYRIDINES - EFFECTS OF CHIRALITY AND CONFORMATION ON THE CALCIUM-ANTAGONIST AND CALCIUM AGONIST ACTIVITIES. *Angewandte Chemie-International Edition in English* **1991,** *30* (12), 1559.

(41) Kang, S. S.; Kim, H. J.; Jin, C.; Lee, Y. S. Synthesis of tyrosinase inhibitory (4-oxo-4H-pyran-2-yl)acrylic acid ester derivatives. *Bioorganic & Medicinal Chemistry Letters* **2009,** *19* (1), 188.

(42) Lee, K. H.; Kim, S. M.; Kim, J. Y.; Kim, Y. K.; Yoon, S. S. Red Fluorescent Organic Light-Emitting Diodes Using Modified Pyran-containing DCJTB Derivatives. *Bulletin of the Korean Chemical Society* **2010,** *31* (10), 2884.

(43) Rostom, S. A. F.; Hassan, G. S.; El-Subbagh, H. I. Synthesis and Biological Evaluation of Some Polymethoxylated Fused Pyridine Ring Systems as Antitumor Agents. *Archiv Der Pharmazie* **2009,** *342* (10), 584.

(44) Wang, J. L.; Liu, D. X.; Zhang, Z. J.; Shan, S. M.; Han, X. B.; Srinivasula, S. M.; Croce, C. M.; Alnemri, E. S.; Huang, Z. W. Structure-based discovery of an organic compound that binds Bcl-2 protein and induces apoptosis of tumor cells. *Proceedings of the National Academy of Sciences of the United States of America* **2000,** *97* (13), 7124.

(45) Bonsignore, L.; Loy, G.; Secci, D.; Calignano, A. SYNTHESIS AND PHARMACOLOGICAL ACTIVITY OF 2-OXO-(2H) 1-BENZOPYRAN-3-CARBOXAMIDE DERIVATIVES. *European Journal of Medicinal Chemistry* **1993,** *28* (6), 517.

(46) Sanchez, A.; Hernandez, F.; Cruz, P. C.; Alcaraz, Y.; Tamariz, J.; Delgado, F.; Vazquez, M. A. Infrared Irradiation-Assisted Multicomponent Synthesis of 2-Amino-3-cyano-4H-pyran Derivatives. *Journal of the Mexican Chemical Society* **2012,** *56* (2), 121.

(47) Kian, R.; Zakerhamidi, M. S.; Shamkhali, A. N.; Teimuri-Mofrad, R.; Rahimpour, K. Media and solute-solvent interaction effects on the photo-physical behavior of some drugs of 4H-Pyran derivatives. *Journal of Molecular Liquids* **2017,** *238*, 508.

(48) Ishibe, N.; Odani, M.; Sunami, M. PHOTOSENSITIZED OXYGENATION OF 4H-PYRAN-4-THIONES AND 4H-THIOPYRAN-4-THIONES. *Journal of the Chemical Society D-Chemical Communications* **1971**, 118.

(49) Guo, Z. Q.; Zhu, W. H.; Tian, H. Hydrophilic Copolymer Bearing Dicyanomethylene-4H-pyran Moiety As Fluorescent Film Sensor for Cu2+ and Pyrophosphate Anion. *Macromolecules* **2010,** *43* (2), 739.

(50) Gu, Y. T.; Li, F. L.; Hu, P. F.; Liao, D. H.; Tong, X. F. Tertiary Amine-Catalyzed (4+2) Annulations of delta-Acetoxy Allenoates: Synthesis of Multisubstituted 4H-Pyran and 4H-Chromene. *Organic Letters* **2015,** *17* (5), 1106.

(51) Ngo, T. T. D.; Kishi, K.; Sako, M.; Shigenobu, M.; Bournaud, C.; Toffano, M.; Guillot, R.; Baltaze, J. P.; Takizawa, S.; Sasai, H.et al. Organocatalyzed 4+2 Annulation of All-Carbon Tetrasubstituted Alkenes with Allenoates:Synthesis of Highly Functionalized 2H- and 4H-Pyran Derivatives. *Chemistryselect* **2016,** *1* (17), 5414.

(52) Pei, C. K.; Jiang, Y.; Wei, Y.; Shi, M. Enantioselective Synthesis of Highly Functionalized Phosphonate-Substituted Pyrans or Dihydropyrans Through Asymmetric 4+2 Cycloaddition of beta,gamma-Unsaturated alpha-Ketophosphonates with Allenic Esters. *Angewandte Chemie-International Edition* **2012,** *51* (45), 11328.

(53) Zhang, S.; Luo, Y. C.; Hu, X. Q.; Wang, Z. Y.; Liang, Y. M.; Xu, P. F. Enantioselective Amine-Catalyzed 4+2 Annulations of Allene Ketones and 2,3-Dioxopyrrolidine Derivatives: Synthesis of 4H-Pyran Derivatives. *Journal of Organic Chemistry* **2015,** *80* (14), 7288.

(54) Zhao, S. L.; Zheng, C. W.; Zhao, G. Enantioselective synthesis of multifunctionalized 4H-pyran derivatives using bifunctional thiourea-tertiary amine catalysts. *Tetrahedron-Asymmetry* **2009,** *20* (9), 1046.

(55) Chen, W. B.; Wu, Z. J.; Pei, Q. L.; Cun, L. F.; Zhang, X. M.; Yuan, W. C. Highly Enantioselective Construction of Spiro 4H-pyran-3,3 '-oxindoles Through a Domino Knoevenagel/Michael/Cyclization Sequence Catalyzed by Cupreine. *Organic Letters* **2010,** *12* (14), 3132.

(56) Ni, C. J.; Tong, X. F. Amine-Catalyzed Asymmetric (3+3) Annulations of beta '-Acetoxy Allenoates: Enantioselective Synthesis of 4H-Pyrans. *Journal of the American Chemical Society* **2016,** *138* (25), 7872.

(57) Yue, Z. T.; Li, W. B.; Liu, L.; Wang, C. H.; Zhang, J. L. Enantioselective Synthesis of 4H-Pyrans Through Organocatalytic Asymmetric Formal 3+3 Cycloadditions of 2-(1-Alkynyl)-2-alken-1-ones with beta-Keto Esters. *Advanced Synthesis & Catalysis* **2016,** *358* (19), 3015.

(58) Zhou, W. P.; Ni, C. J.; Chen, J. F.; Wang, D.; Tong, X. F. Enantioselective Synthesis of 4H-Pyran via Amine-Catalyzed Formal (3+3) Annulation of delta-Acetoxy Allenoate. *Organic Letters* **2017,** *19* (7), 1890.

(59) Ashtekar, K. D.; Staples, R. J.; Borhan, B. Development of a Formal Catalytic Asymmetric 4+2 Addition of Ethyl-2,3-butadienoate with Acyclic Enones. *Organic Letters* **2011,** *13* (21), 5732.

(60) Wang, X. J.; Fang, T.; Tong, X. F. Enantioselective Amine-Catalyzed 4+2 Annulations of Allenoates and Oxo-dienes: An Asymmetric Synthesis of Dihydropyrans. *Angewandte Chemie-International Edition* **2011,** *50* (23), 5361.

(61) Yang, H. B.; Zhao, Y. Z.; Sang, R.; Wei, Y.; Shi, M. Asymmetric Synthesis of Bioxindole-Substituted Hexahydrofuro 2,3-b furans via Hydroquinine Anthraquinone-1,4-diyl Diether-Catalyzed Domino Annulation of Acylidenoxindoles/Isatins, Acylidenoxindoles and Allenoates. *Advanced Synthesis & Catalysis* **2014,** *356* (18), 3799.

(62) Yao, W. J.; Dou, X. W.; Lu, Y. X. Highly Enantioselective Synthesis of 3,4-Dihydropyrans through a Phosphine-Catalyzed 4+2 Annulation of Allenones and beta,gamma-Unsaturated alpha-Keto Esters. *Journal of the American Chemical Society* **2015,** *137* (1), 54.

(63) Liu, Y. F.; Du, Y. L.; Yu, A. M.; Qin, D. B.; Meng, X. T. Diverse synthesis of pyrano 2,3-b indol and dihydropyrano 2,3-b indol via tunable Lewis bases catalyzed domino reactions. *Tetrahedron* **2015,** *71* (40), 7706.

(64) Zhang, X. C.; Cao, S. H.; Wei, Y.; Shi, M. Phosphine- and Nitrogen-Containing Lewis Base Catalyzed Highly Regioselective and Geometric Selective Cyclization of Isatin Derived Electron-Deficient Alkenes with Ethyl 2,3-Butadienoate. *Organic Letters* **2011,** *13* (5), 1142.

(65) Yamamoto, Y.; Kume, T.; Akiba, K. Y. REACTION OF 2,4,6-TRIMETHYLPYRYLIUM SALT WITH ORGANOCOPPER REAGENTS - SELECTIVE SYNTHESIS OF 4H-PYRANS. *Heterocycles* **1987,** *26* (6), 1495.

(66) Ashtekar, K. D.; Ding, X. L.; Toma, E.; Sheng, W.; Gholami, H.; Rahn, C.; Reed, P.; Borhan, B. Mechanistically Inspired Route toward Hexahydro-2H-chromenes via Consecutive 4+2 Cycloadditions. *Organic Letters* **2016,** *18* (16), 3976.

(67) Lang, R. W. H., H. J. α-Allenic esters from α-phosphoranylidene esters and acid chlorides: ethyl 2,3-pentadienoate. *Org. Synth.* **1984,** *62*, 202.

(68) Zou, Y.; Garayalde, D.; Wang, Q. R.; Nevado, C.; Goeke, A. Gold-Catalyzed Cycloisomerization of Cyclopropyl Alkynyl Acetates: A Versatile Approach to 5-, 6-, and 7-Membered Carbocycles. *Angewandte Chemie-International Edition* **2008,** *47* (52), 10110.

(69) Oare, D. A.; Henderson, M. A.; Sanner, M. A.; Heathcock, C. H. ACYCLIC STEREOSELECTION .46. STEREOCHEMISTRY OF THE MICHAEL ADDITION OF N,N-DISUBSTITUTED AMIDE AND THIOAMIDE ENOLATES TO ALPHA,BETA-UNSATURATED KETONES. *Journal of Organic Chemistry* **1990,** *55* (1), 132.

(70) Allais, C.; Lieby-Muller, F.; Rodriguez, J.; Constantieux, T. Metal-Free Michael-Addition-Initiated Three-Component Reaction for the Regioselective Synthesis of Highly Functionalized Pyridines: Scope, Mechanistic Investigations and Applications. *European Journal of Organic Chemistry* **2013**, 4131.

Chapter IV: Amine-mediated Dihydropyran Rearrangements Toward Pyran and Carbocyclic *β*–Amino Ester Synthesis

IV-1. Introduction

Optimization of base catalyzed double bond migration from *exo*- to *endo*-dihydropyran was described in **Chapter III**. During these studies, we observed the formation of pyran, instead of 4*H*-pyran, when vinyl dihydropyran (**III-14h**) was used as the substrate and DBU was used as the catalyst. Further, this pyran derivative partially rearranged under silica gel column conditions to phenolic side products. These observations, which will be discussed in detail in section **IV-2**, attracted our attention to further investigate and explore these transformations, because both pyran and phenolic compounds are important building blocks. Since amidines are critical bases for the success of this transformation, the chapter will begin with an introduction of amidine family of bases.

IV-1.1. Amidines, isothioureas and guanidines as nucleophilic catalysts

In the past decade, there has been a dramatic increase in the advancement of organocatalysis. Generally, organocatalysts can be classified into Lewis bases, Lewis acids, Brønsted bases and Brønsted acids.[1] Among these, Lewis base catalysts as nucleophilic organocatalysts are the most popular in this field. One of the reasons is that these catalysts are readily available and easily re-designable. At least, three families, including tertiary amines, phosphines and *N*-heterocyclic carbenes (NHCs), are common options for a variety of reactions. The principle of this categorization in organocatalysis is based on the proposed mechanism and the activation mode of the catalyst in the catalytic

cycle. As a result, it is possible that a catalyst plays an ambiguous role or dual/multiple roles in a reaction process. Another reason attributed to the puzzle of this categorization is the dual functions of these catalysts, namely its basicity and nucleophilicity. Amidines and guanidines are such compounds, often thought of as strong non-nucleophilic organic bases. However, recently, a number of examples show that these small molecules react as efficient nucleophilic catalysts as well.[2] The evidence for the nucleophilic nature of these catalysts is their increasing applications on a wide range of reactions, such as acyl transfers,[3,4] aldols,[5,6] the Morita-Baylis-Hillman (MBH) reaction,[7,8] conjugate additions,[9] and carbonylations,[10] to name a few. Along with the acyl transfer reaction (such as esterification[11,12] and kinetic resolution[13,14]), which is the most common application of these catalysts, the rest of the nucleophilic based reactions are also becoming areas of interest.

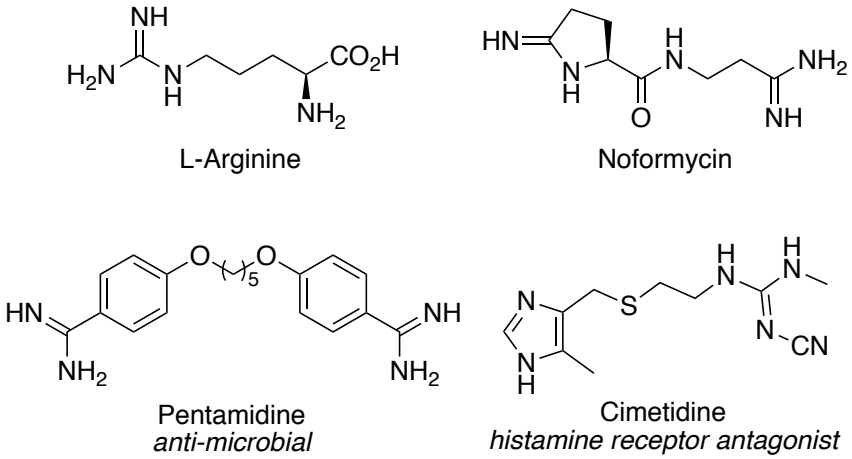

Figure IV-1. Examples of amidine and guanidine containing natural products and drug molecules.

Amidines and guanidines based molecules are found throughout natural products and drugs (see **Figure IV-1**),[2] having been widely used in organic chemistry. With their ability of delocalizing the charge over two/three nitrogen atoms after protonation, they are

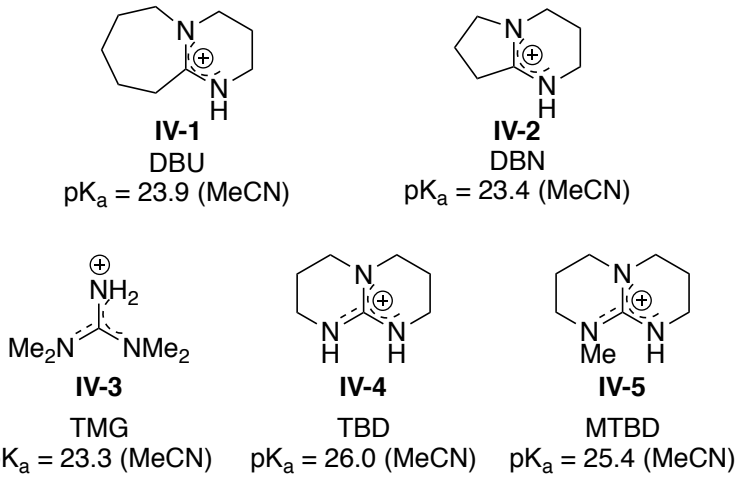

Figure IV-2. Structures and pK_as of some representative amidine and guanidine bases.

traditionally recognized as strong neutral organic bases. The structures and pK_as of several of the most commonly used amidines and guanidines are shown in **Figure IV-2**.[15,16] Among them, the bicyclic amidines 1,8-diazabicyclo[5.4.0]undec-7-ene (DBU) **IV-1** and 1,5-diazabicyclo[4.3.0]non-5-ene (DBN) **IV-2** are representative examples of organocatalysts for base-mediated organic transformations, such as elimination and isomerization, under milder conditions as compared to other types of nitrogen bases.[17] For example, DBU has been employed to convert β,γ–unsaturated nitriles into the corresponding α,β–unsaturated isomers, which are thermodynamically more favored.[18] (see **Scheme IV-1**)

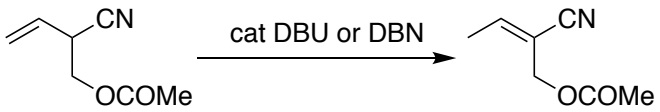

Scheme IV-1. An example of DBU/ DBN mediated isomerization reaction.

However, in some of these reactions, unexpected side-products were obtained. For instance, in 1981, McCoy reported an unusual tetracyclic dihydropyridin-4-one compound **IV-10** was isolated and characterized from the dehydrohalogenation reaction of

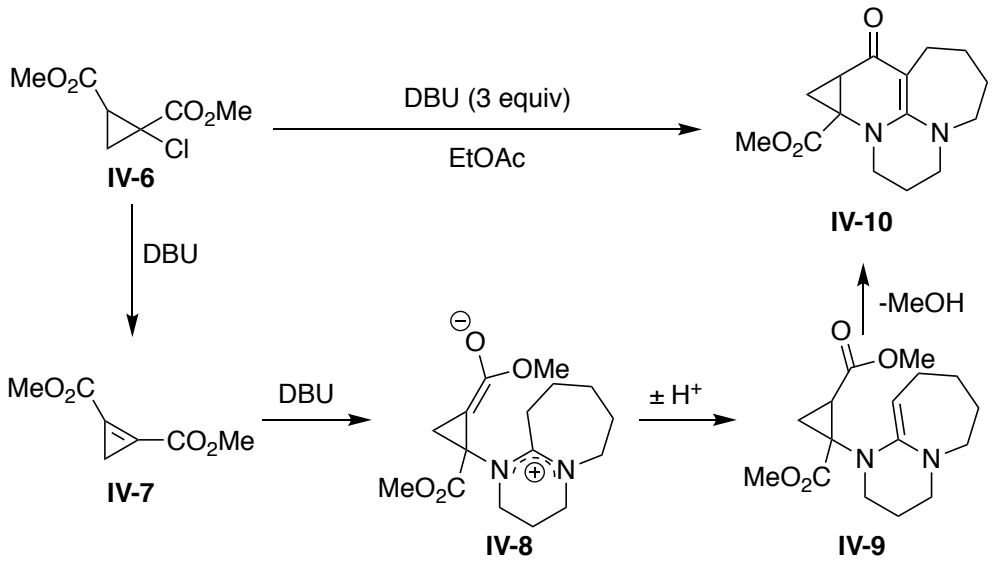

Scheme IV-2. Formation of unexpected byproduct **IV-10** during a DBU involved nucleophilic attack.

cyclopropane diester **IV-6** when excess DBU was used, as described in **Scheme IV-2**. It was proposed that incorporation of DBU fragment into the final product **IV-10** occurred through nucleophilic attack of intermediate **IV-7**.[19] Later on, in 1993 Bertrand's group provided direct evidence that DBU and DBN can react as strong nucleophiles through

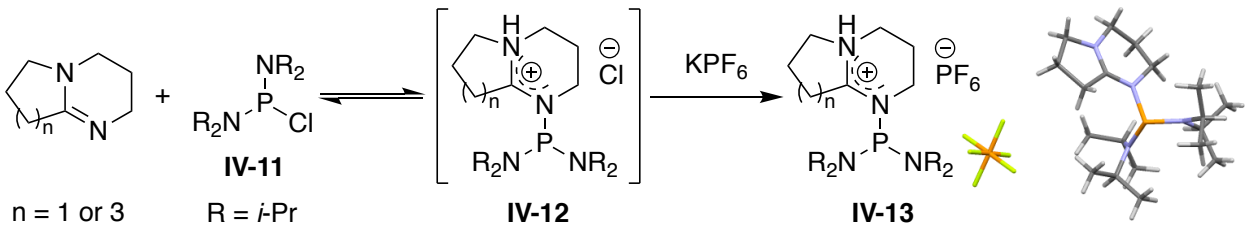

Scheme IV-3. The first direct evidence that DBU/ DBN reacts as nucleophile *via* reaction with chloro-phosphanes **IV-11**.

crystallographic studies.[20] First they isolated and characterized cationic phosphane **IV-13**, which is the product from DBU/ DBN reacting with chloro-phosphane **IV-11**, followed by the chloride counter-ion exchange with hexafluorophosphate (see **Scheme IV-3**). From the X-ray crystal structure (**Scheme IV-3**, DBN as an example), it was also

suggested that the positive charge is delocalized over both N atoms as both amidine C-N bonds are of similar length.

Not only qualitatively (from the observation of experiments), but also quantitatively (from calculation based on the results of experiments), researchers have demonstrated that DBU and DBN can act as nucleophiles. More recently, to compare the nucleophilicity of DBU and DBN, as well as isothiourea derivatives, with well-known nucleophilic catalysts, Mayr and co-workers have performed a number of kinetic experiments.[21,22] They investigated the equilibrium between a variety of nucleophilic catalysts and a range of benzhydrylium tetrafluoroborate anions by photometrical methods. Consequently, the

$$\log k = s(E + N)$$

Equation IV-1. Nucleophilicity parameter (*N*) used to compare the nucleophilic nature of Lewis basic catalysts.

results of these kinetic experiments were analyzed by using **Equation IV-1**, where *k* is the second order rate constant, *s* is the nucleophile-specific slope parameter, *N* is the nucleophilicity parameter, and *E* is the electrophilicity parameter. This analysis enabled to directly compare the nucleophilicity parameter (*N*) of a number of Lewis basic catalysts, as presented in **Scheme IV-4**.[22] Interestingly, DBN has a superior nucleophilicity over 4-(dimethylamino)pyridine (DMAP), which is considered to be one of the most powerful nucleophilic catalysts. Overall, DBN is more nucleophilic than most of the catalysts studied in **Scheme IV**, with the exception of 1,4-diazabicylco[2.2.2]octane (DABCO). Besides, this study also revealed that DBU, as well as some isothiourea derivatives, exhibit comparable nucleophilicity to DMAP. Zipse's group also performed a study, by calculating the methyl cation affinities of over 40 common organocatalysts, which

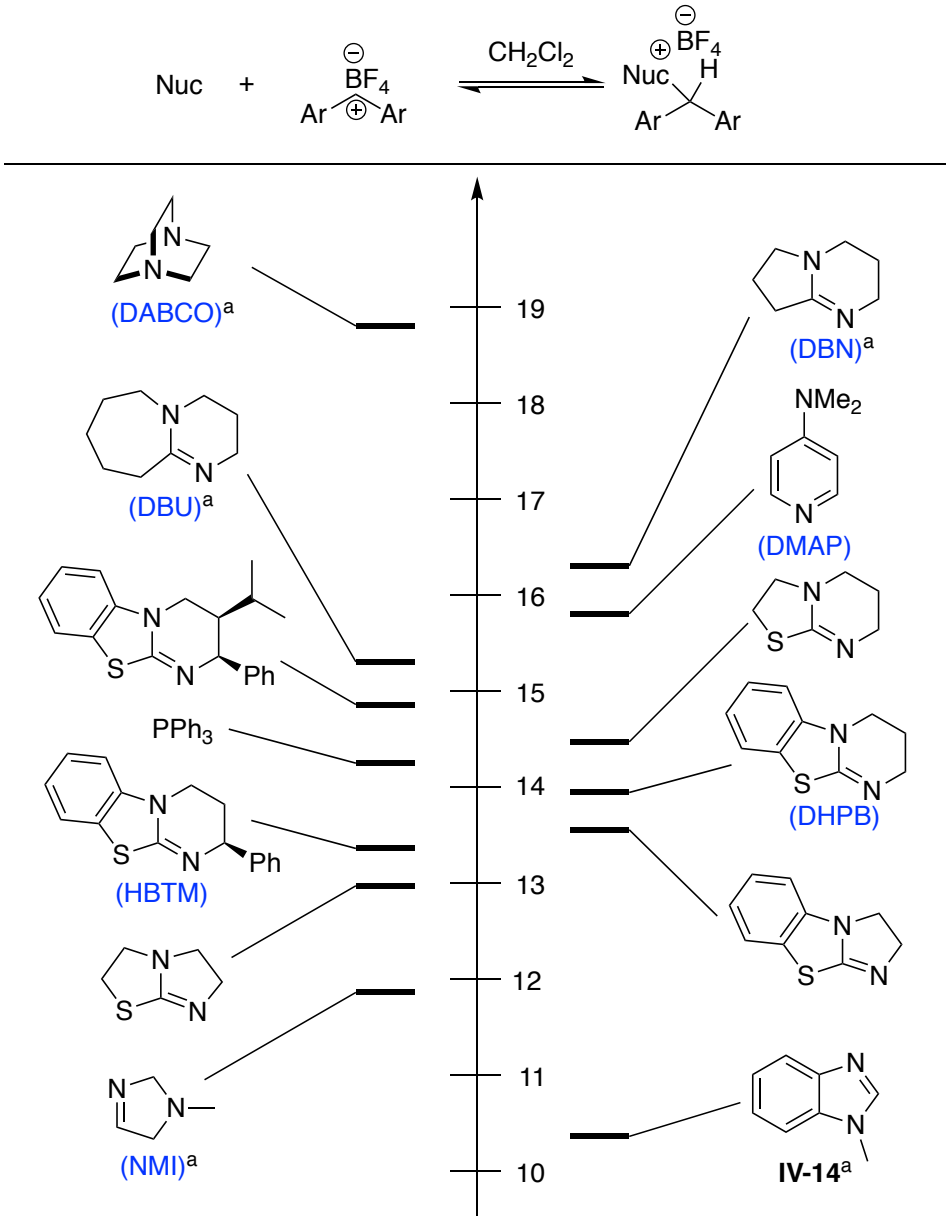

Scheme IV-4. Relative nucleophilicities of selected catalysts. [a] Measurements made in MeCN. Modified scheme from reference 22.

coincidently showed DBU and DBN have greater methyl cation affinities than many DMAP and cinchona alkaloid derivatives.[23] From both studies, it was revealed that bicyclic amidines are considerably more basic than many other Lewis bases. However, the relatively high basicity of these amines has limited their potential application as

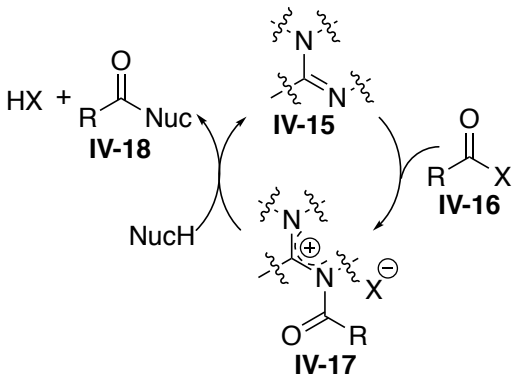

Scheme IV-5. General mechanism for amidine and guanidine catalyzed acylation reactions.

nucleophilic catalysts, because they may lead to the deactivation by competing protonation reaction.

Amidine, guanidine and isothiourea derivatives have become popular catalysts as a result of their highly nucleophilic nature. In this field, A number of these catalysts have been successfully applied as acyl transfer agents for several types of acyl donors, including acyl chlorides, acid anhydrides and esters. A generalized mechanism for these base catalyzed acyl transfer processes is given in **Scheme IV-5**. Briefly, the catalyst **IV-15** activates the acyl donor **IV-16** by nucleophilic attack to generate intermediate **IV-17**, followed by the addition of a nucleophile, the formation of the acylated product **IV-18** and

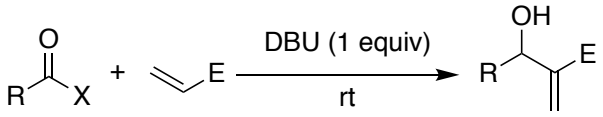

E = CO_2Me, CN, COR^2 17-95% yield

Scheme IV-6. Examples of DBU mediated MBH reaction discovered by Aggarwal's group.

regeneration of the catalyst.[2] A less common, but attractive application is that some of these bases can be used as catalysts for the Morita-Baylis-Hillman (MBH) reaction. It was first discovered by Aggarwal and co-workers in 1999 that DBU was an efficient catalyst for the MBH reaction, with a faster reaction rate as compared to DABCO initiated

Scheme IV-7. DBU catalyzed cycloaddition reaction of salicylic aldehydes with allenes to form 2*H*-1-chromenes.

reactions (see **Scheme IV-6**).[7] Since then, more examples have been reported by different groups, both experimentally and computationally.[7,8,24-26] One of them is from Shi's group, in which they found that 10 mol% DBU can be used to catalyze the reaction between salicylic aldehydes and activated allenes to form 2*H*-1-chromenes (**Scheme IV-7**).[8] The authors proposed three pathways to explain the formation of both the product and side-product as described in **Scheme IV-8**. Both pathway A and B show DBU acts as a Lewis base. In pathway A, DBU is believed to activate the allenoate **IV-19** to produce γ–enolate, which deprotonates the salicylic aldehyde **IV-22** to form intermediate **IV-23** and **IV-24**. After a Michael addition between these two intermediates, a zwitterionic intermediate **IV-26** is formed. By an intramolecular aldol cyclization, proton transfer and DBU elimination, the final product **IV-28** is achieved. In pathway B, the resonance structure **IV-21** undergoes an intermolecular MBH reaction, followed by cyclization and DBU elimination to give the final product. However, in pathway C, DBU is believed to react as a Brønsted base to deprotonate the salicylic aldehyde, which then attacks the allene, followed by γ–cyclization to produce the side-product **IV-31**. Nonetheless, a possible α–cyclization pathway D or intramolecular MBH reaction (see dash box in **Scheme IV-8**) was not considered, which can also furnish the major product **IV-28**. From this viewpoint, the role that DBU in the process is still unclear.

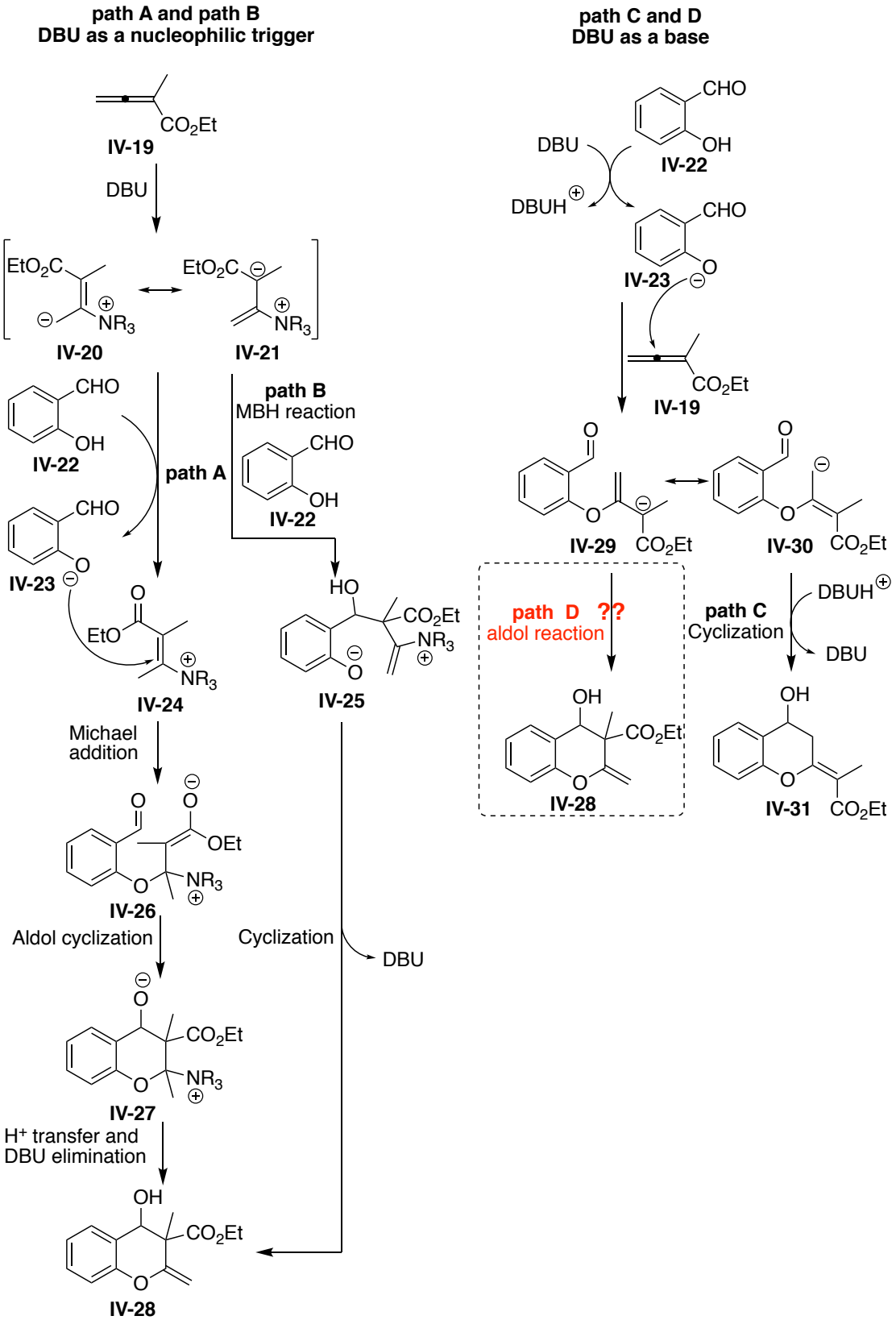

Scheme IV-8. Plausible mechanisms for DBU catalyzed cycloaddition reaction of salicylic aldehydes with allenes to form 2*H*-1-chromenes. Modified scheme from reference 8.

IV-1.2. A brief introduction of pyran and phenol derivatives

As described in **Chapter III**, many pyrans and fused pyrans derivatives, such as benzopyran derivatives, are biologically active compounds with antimicrobial, antitumor, antifungal, anticoagulant, antianaphylactic, diuretic and spasmolytic activities.[27-30] They are also important motifs that exist in many of natural products, *e.g.* coumarins, sugars, flavonoids and so on.[31-33] Besides, some benzopyran derivatives possess photochemical activities and a number of 2-amino-4*H*-pyrans are utilized as photoactive materials, biodegradable agrochemicals and pigments.[34-36] As a matter of fact, many methodologies have been developed for the synthesis of pyran and fused pyran derivatives. For example, the Knoevenagel-hetero-Diels-Alder (DKHDA) cascade reaction is a trusted protocol for the synthesis of pyran scaffolds by reaction of barbituric acid with aromatic aldehydes followed by condensation with ethyl vinyl ether or resorcinol with $\boldsymbol{\alpha,\beta}$–unsaturated aldehydes.[37,38] Recently, one-pot three components reactions of arylaldehydes, active methylene compounds and electron rich agents are becoming one of the most efficient and simplest methods to approach pyran derivatives.[39-41]

Although not well reported, our observation that indicates conversion of the pyrans to phenolic compounds, should be further explored, since it could lead to a novel approach for obtaining hard to access phenols.

Phenol and its derivatives, most commonly known as phenolic compounds, ubiquitous in plants, are secondary metabolites and essential part of the human diet. Beside contributing to the color and sensory characteristics of fruits and vegetables, they also play a critical role in growth and reproduction, providing protection against pathogens

Table IV-1 Classes of phenolic compounds in plants

Class	Structure
Simple phenolics, benzoquinones	C_6
Hydroxybenzoic acids	$C_6{-}C_1$
Acetohophenones, phenylacetic acids	$C_6{-}C_2$
Hydroxycinnamic acids, phenypropanoids (coumarins, isocoumarins, chromones, chromenes)	$C_6{-}C_3$
Napthoquinones	$C_6{-}C_4$
Xanthones	$C_6{-}C_1{-}C_6$
Stilbenes, anthraquinones	$C_6{-}C_2{-}C_6$
Flavonoids, isoflavonoids	$C_6{-}C_3{-}C_6$
Lignans, neolignans	$(C_6{-}C_3)_2$
Biflavonoids	$(C_6{-}C_3{-}C_6)_2$
Lignins	$(C_6{-}C_3)_n$
Condensed tannins (proanthocyanidins or flavolans)	$(C_6{-}C_3{-}C_6)_n$

and predators.[42] The antioxidant activity of food phenolic compounds is of nutritional interest as they are associated to the human health through the prevention of several diseases.[43] In addition, phenolic compounds exhibit a wide range of pharmacological and physiological properties, such as anti-cancer, antioxidant, anti-microbial, anti-allergenic, anti-artherogenic, anti-inflammatory, anti-thrombotic, cardioprotective and vasodilatory effects.[44-49] Structurally, these compounds comprise one or more aromatic rings, bearing one or more hydroxyl substituents, ranging from a simple phenolic molecule (e.g. gallic

acid) to a complex high-molecular weight polymer (e.g. tannins).[42,50] The diversity in structure leads to a wide range of phenolic compounds with over 8,000 variants in nature, however, they are generally categorized as phenolic acids, flavonoids, tannins, stilbenes, curcuminoids, coumarins, lignans, quinones and so on, as shown in **Table IV-1**.[50,51] Among these, phenolic acids, flavonoids and tannins are regarded as the main dietary phenolic compounds.[52]

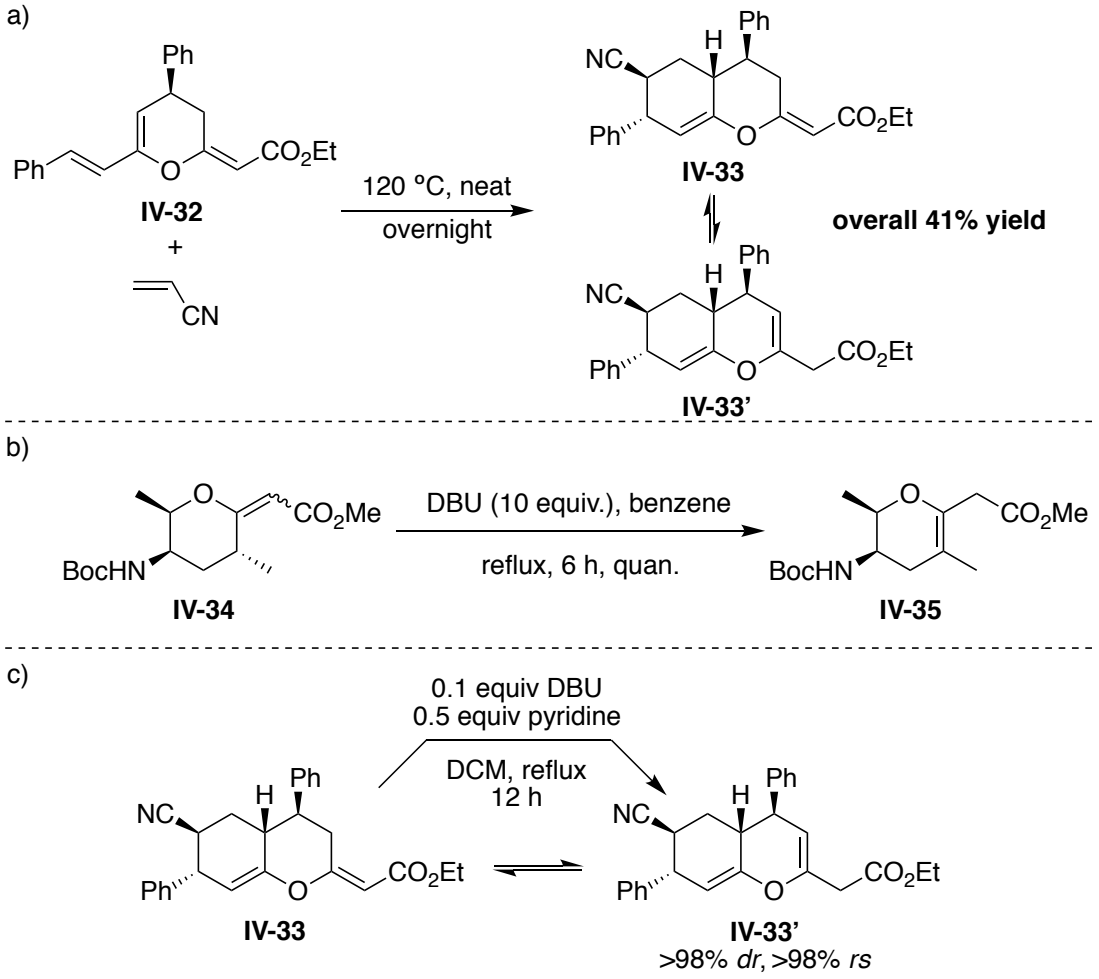

Scheme IV-9. (a) A mixture of regio-isomers formation under Diels-Alder reaction of substrate **IV-32** and acrylonitrile. (b) DBU catalyzed deconjugation of α,β–unsaturated ester **IV-34** to form β,γ–unsaturated ester **IV-35**. (c) Complete conversion of a mixture of **IV-33** and **IV-33'** to a single isomer **IV-33'** under DBU catalyzed reaction conditions.

IV-2. Amidine-mediated formal [1,5]-H rearrangement towards pyran synthesis from dihydropyran

In our effort to develop a concise assembly towards hexahydro-2*H*-chromenes *via* consecutive [4+2]/[4+2] cycloadditions in **Chapter II**, it was found that substrate **IV-32** reacts with acrylonitrile to furnish a mixture of **IV-33** and **IV-33'**, as shown in **Scheme IV-9a**.[53] According to the literature, DBU is able to initiate de-conjugation of α,β–unsaturated ester **IV-34** to β,γ–unsaturated ester **IV-35** (**Scheme IV-9b**).[54] Based on this, a mixture

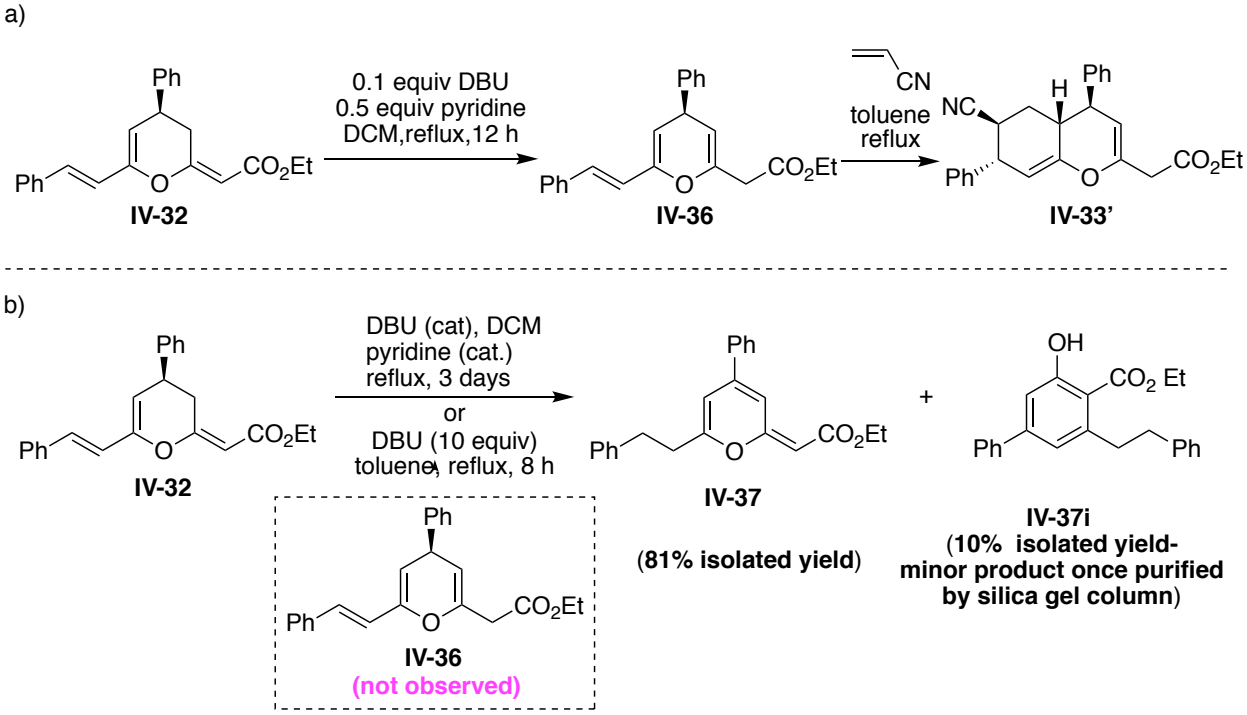

Scheme IV-10. a). An attempt to synthesize 4*H*-pyran **IV-36** from dihydropyran **IV-32**, followed by the Diels-Alder reaction to deliver the adduct **IV-33'**. b). DBU catalyzed formal [1,5]-H rearrangement towards the synthesis of pyran **IV-36**, which partially rearranged to salicylate derivative when purified with silica gel.

of compounds **IV-33** and **IV-33'** was subjected to the DBU dictated isomerization reaction condition, which led a single isomer **IV-33'** (**Scheme IV-9c**). Therefore, it is possible that dihydropyran **IV-32** might be converted to 4*H*-pyran **IV-36**, which could potentially react

as a dienophile with acrylonitrile to deliver adduct **IV-33'** as a single isomer (**Scheme 10a**).

Table IV-2. A series of bases were tested for the rearrangement reaction.

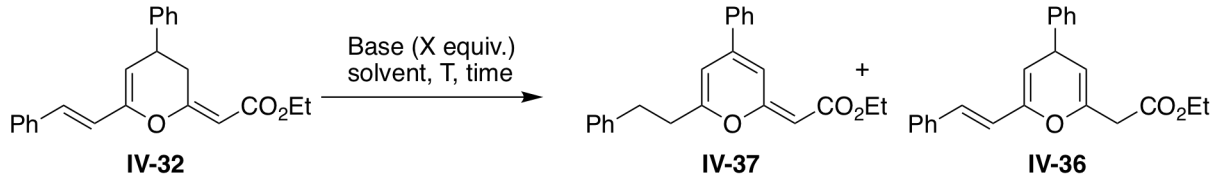

IV-32 **IV-37** **IV-36**

Entry	base	X	solvent	°C/T	h/t	pK_a[a,f]	%/conv. (IV-37/36)[b,c,d]
1	DBU	0.1	DCM	60	12	11.9[55]	80/trace
2	DBU	0.1	toluene	110	5	11.9	94/trace
3	DBU	1.0	toluene	110	3	11.9	95/trace
4	DBU	10.0	toluene	110	1.5	11.9	>98/n.o.
5	DBU	10.0	toluene	rt	4	11.9	>98/n.o.
6	DBN	10.0	toluene	110	2	12.7[e]	>98/n.o.
7	pyridine	10.0	toluene	110	12	5.21[56]	No reaction
8	Et_3N	10.0	toluene	110	12	10.75	n.o./55
9	quinuclidine	10.0	toluene	110	12	11.0	n.o./28
10	DMAP	10.0	toluene	110	12	9.2	n.o./40
11	TMG	10.0	toluene	110	12	13.6[57]	30/60
12	DABCO	10.0	toluene	110	12	8.82	n.o./90
13	Ph_3P	10.0	toluene	110	12	20.9[58]	n.o./23

Reaction conditions: substrate (0.03 mmol) was dissolved in 0.5 mL solvent. [a] pK_a of conjugated acid in water. The aqueous pK_a values are from Evan's pK_a table, otherwise specified. [b] conversion estimated from ^{1}H NMR analysis of the crude reaction mixture. [c] n.o. = not observed. [d] except for product, starting material was observed with trace impurities from ^{1}H NMR of the crude mixture. [e] pK_a from San-Apro Ltd. [f] Calculated pK_a value of Ph_3P from reference 58.

However, when a reaction was set up under the same reaction condition, surprisingly, compound pyran **IV-37** was isolated, instead of the de-conjugated compound **IV-36,** in 91% yield, as shown in **Scheme IV-10b**. Moreover, it was also discovered that pyran **IV-37** could partially (~ 10%) decompose to salicylate **IV-38** when purified by silica gel column. These results are different from those observed in DABCO catalyzed reactions, in which 4*H*-pyran derivatives were formed through a formal [1,3]-*H* rearrangement. Sequentially, these 4*H*-pyrans could be converted into cyclohexenones under acidic conditions. The different results could be on account of their different basicity. As a result, a series of bases with different basicity and nucleophilicity were tested.

IV-3. Results and discussion

To investigate the underpinnings of the basicity and nucleopilicity in the formal [1,5]-*H* rearrangement reaction, a series of N-based catalysts, as well as Ph_3P, were tested by using racemic **IV-32** as a model substrate. As shown in **Table IV-2**, both DBU and DBN can efficiently catalyze the formal [1,5]-*H* rearrangement reaction (entry 1-6), even under room temperature (entry 5), or with 10 mol% of catalyst loading (entry 1 and 2) in different solvents. As noticed, these two have the highest pK_a aside from tetramethylguanidine (TMG). However, TMG promoted a sluggish process, giving only 30% of **IV-37** with 60% of **IV-36** (entry 11, **Table IV-2**). It suggests that this transformation is presumably the outcome of a combination effect of both basicity and nucleopilicity of the bases. No **IV-37** formation was observed for the rest of the bases (entry 7-10 and 12-13, **Table IV-2**), which have relatively low pK_a values, even though Et_3N and quinuclidine have closer pK_a values to DBU (entry 8-9, **Table IV-2**). Not surprisingly, no reaction was detected for

pyridine as it has the lowest pK_a value (entry 7, **Table IV-2**). Even Ph_3P with the highest

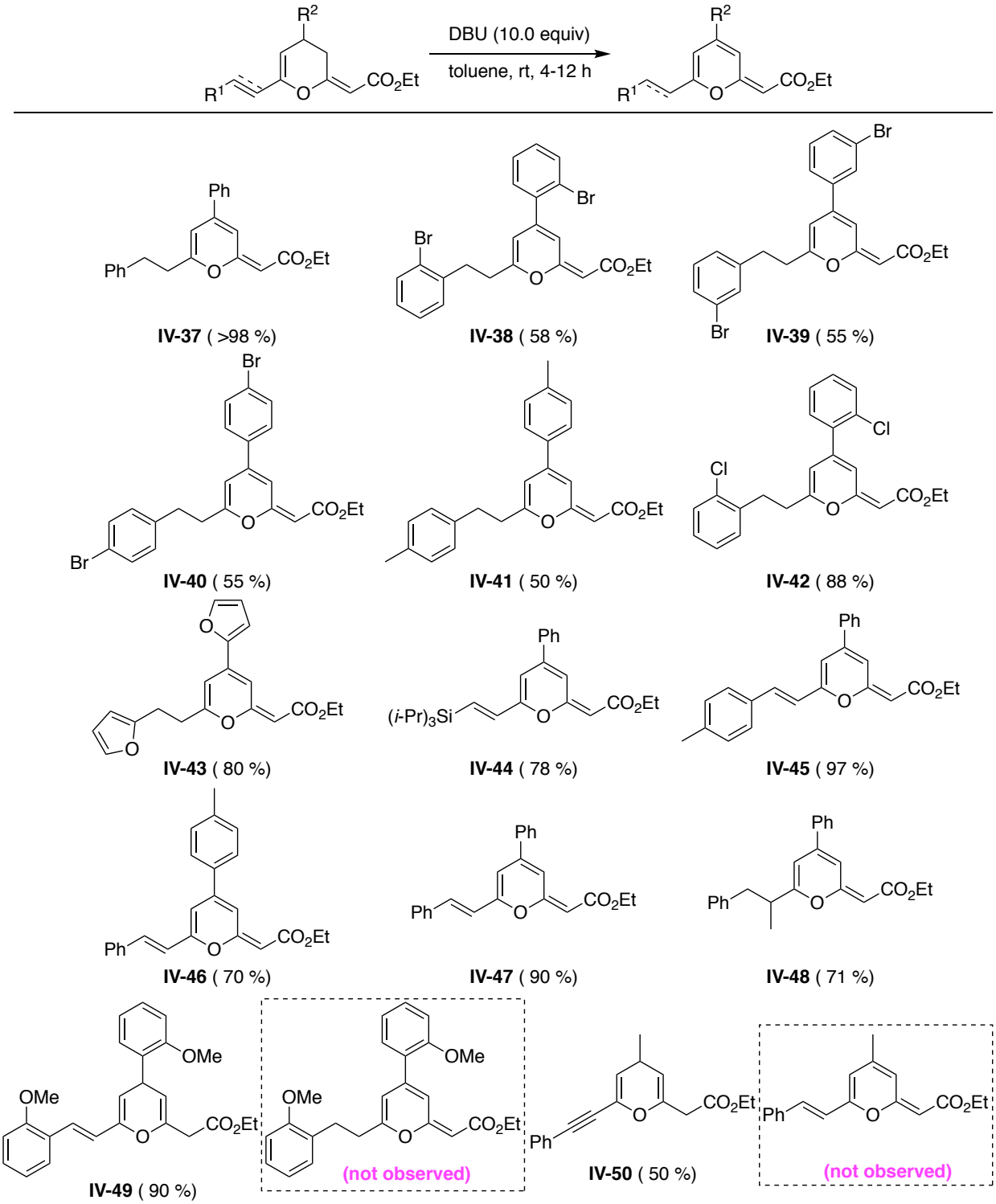

Scheme IV-11. [a] Reaction conditions: substrate (0.2 mmol) was dissolved in toluene (0.1 mL) with DBU (10 equiv.). [b] Isolated yield (combined yield of pyran and its rearranged phenol side products).

pK_a value, it was unable to deliver the pyran product, but instead provided 4*H*-pyran with only 23% conversion (entry 13, **Table IV-2**). Based on the observation, optimized conditions for our formal [1,5]-*H* rearrangement were to use DBU (10.0 equiv) in toluene at room temperature (entry 5, **Table IV-2**).

In order to probe the substrate scope for this reaction, a range of dihydropyrans have been prepared and subjected to the optimized reaction conditions (**Scheme IV-11**). As can be seen from the results in general, both vinyl and propargyl dihydropyrans were compatible with the reaction. The substrate scope also revealed that the nature of the fragment R^1 did not have a substantial influence on the reaction outcome. In other words, R^1 could be aryl regardless of its substitution patterns and/or electronic properties (product **IV-37**—**IV-42** and **IV-45**—**IV-47**, **Scheme IV-11**), heteroaryl and silyl (product **IV-43**—**IV-44**, **Scheme IV-11**) (and presumably alkyl, although none was studied in this case). In contrast, the electronic nature (relatively electron-rich substitution) of aryl and alkyl as R^2 moieties deteriorated the formal [1,5]-*H* rearrangement, but generate 4*H*-pyrans through [1,3]-*H* rearrangement (product **IV-49**—**IV-50**, **Scheme IV-11**). Nonetheless, the H of C4 in the dihydropyran should be acidic enough for these amidines to deprotonate. However, either electron-rich aryl (-OMe, **IV-49**) or alkyl (**IV-50**) as R^2, would more or less decrease the acidity of this H. Fortunately, when R^2 was electron-deficient aryl (product **IV-38**—**IV-40**, **IV-42**, **Scheme IV-11**), slightly electron rich aryl (product **IV-41** and **IV-46**, **Scheme IV-11**), heteroaryl (product **IV-43**, **Scheme IV-11**), or just phenyl (product **IV-37, IV-44**—**IV-45** and **IV-47**—**IV-48**, **Scheme IV-11**), moderate to excellent yields were obtained (50 - >98%, **Scheme IV-11**). It was found that some of

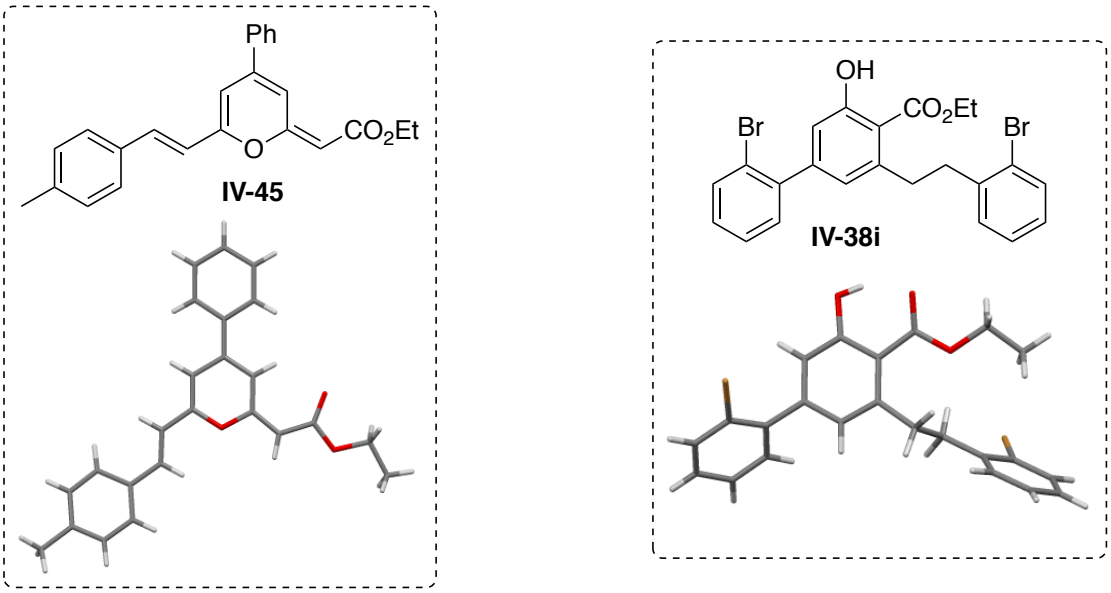

Figure IV-3. X-ray crystal structures for **IV-45** and **IV-38i**.

these pyrans (see **IV-5 Experimental** for details) would rearrange to give the corresponding salicylate derivatives when purified by silica gel column (see **IV-37i** in

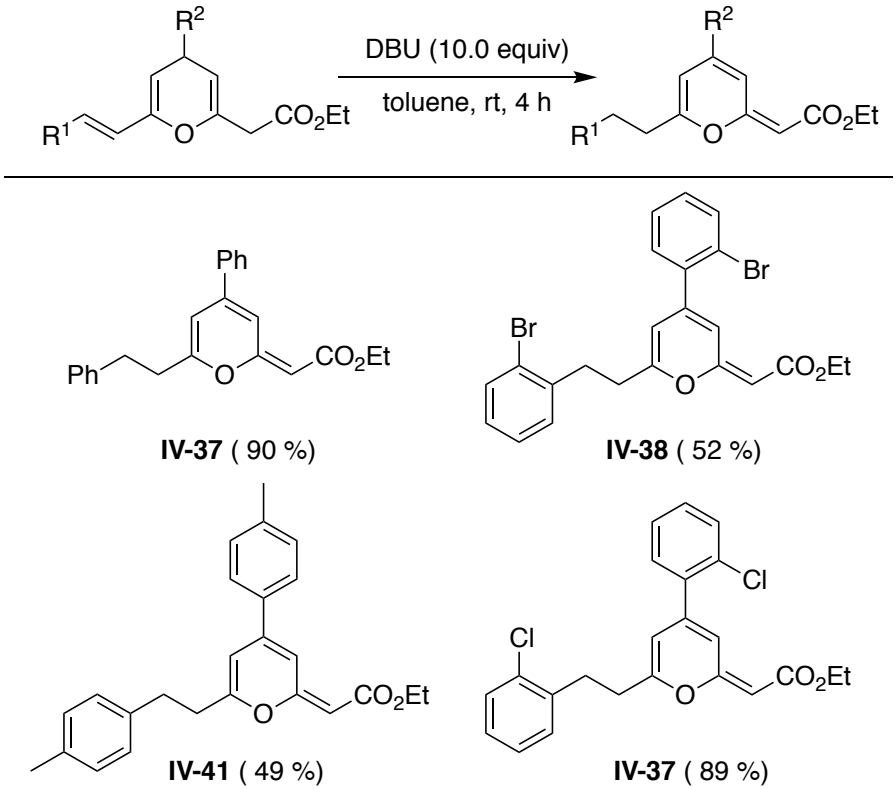

Scheme IV-12. DBU catalyzed double bond isomerization from 4*H*-pyrans to pyrans.

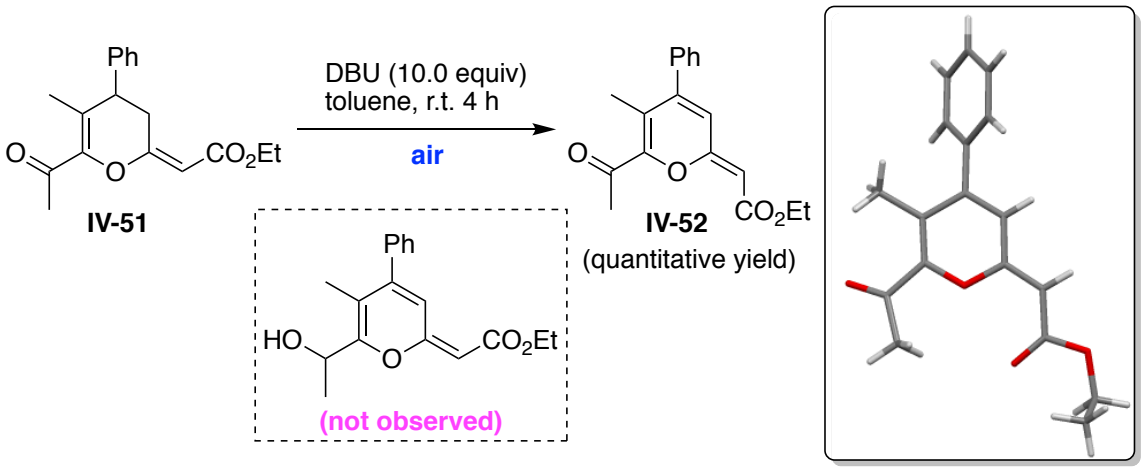

Scheme IV-13. DBU catalyzed oxidation reaction of acetyl dihydropyran **IV-51** to pyran **IV-52** with air as the oxidant.

Scheme **IV-10b** as an example). To simplify the yield calculation, a combination yield of isolate pyrans and their silylates was reported as the silylates were from the pyran rearrangement in the column. Interestingly, even a tri-substituted vinyl dihydropyran could afford the pyran product **IV-48** through our methodology (**Scheme IV-11**). Of note, the configurations of the product **IV-38i** and **IV-45** were unambiguously assigned by the X-ray crystal structure, as shown in **Figure IV-3**.

To demonstrate the 4*H*-pyran was formed as a potential intermediate, a number of 4*H*-pyrans were subjected to the same reaction condition. As expected, all of the tested substrates were able to furnish the pyran products with similar yields (see **Scheme IV-12**).

Surprisingly, when an acetyl dihydropyran **IV-51** was used as substrate for this transformation, it was oxidized to the pyran **IV-52** with isomerization of the α,β–unsaturated ester moiety from ***E*** to ***Z***, as presented in **Scheme IV-13**. However, no double

bond reduction was observed in this reaction; presumably the air reacted as the oxidant. The structure of **IV-52** was assigned by X-ray crystallography.

Table IV-3. Optimization of reaction conditions for the conversion of pyran to salicylate

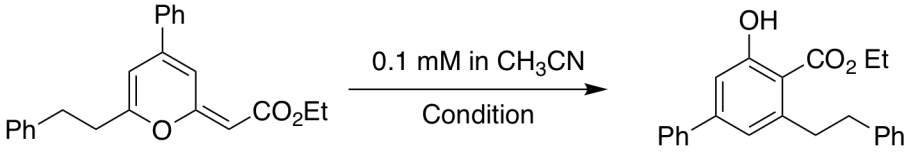

IV-37 **IV-37i**

Condition	Observation
(1.5 N) LiOH (10.0 equiv)	N.R
(4.0 N) LiOH, then HCl (10.0 equiv)	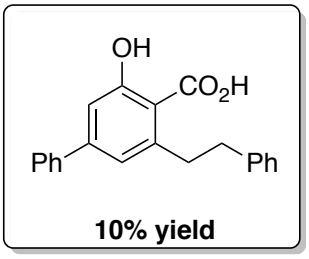 **10% yield**
conc. HCl (10.0 equiv)	trace
conc. TFA (10.0 equiv)	trace
silica, (1.0 N) HCl (10.0 equiv)	15% yield

Reaction conditions: 0.1 mmol substrate was used in 1 mL CH_3CN at room temperature.

The propensity for pyrans to rearrange to salicylates on silica gel piqued our interest to develop a method, in which salicylate derivatives could be obtained in high yield. However, either acid or base employed to accelerate this transformation failed in giving a decent outcome, as shown in **Table IV-3**. Interestingly, as can be seen from **Scheme IV-14**, when pyran **IV-38** was treated with silica (20 g/mmol) in EtOAc with water (v:v = 1:1) at room temperature, **IV-38i** was obtained in quantitative yield. Unfortunately, the

efficiency of this method was substrate dependent and limited (substrate **IV-41** and **IV-37**, Scheme **IV-14**). Apparently, more optimization is required to generalize this transformation.

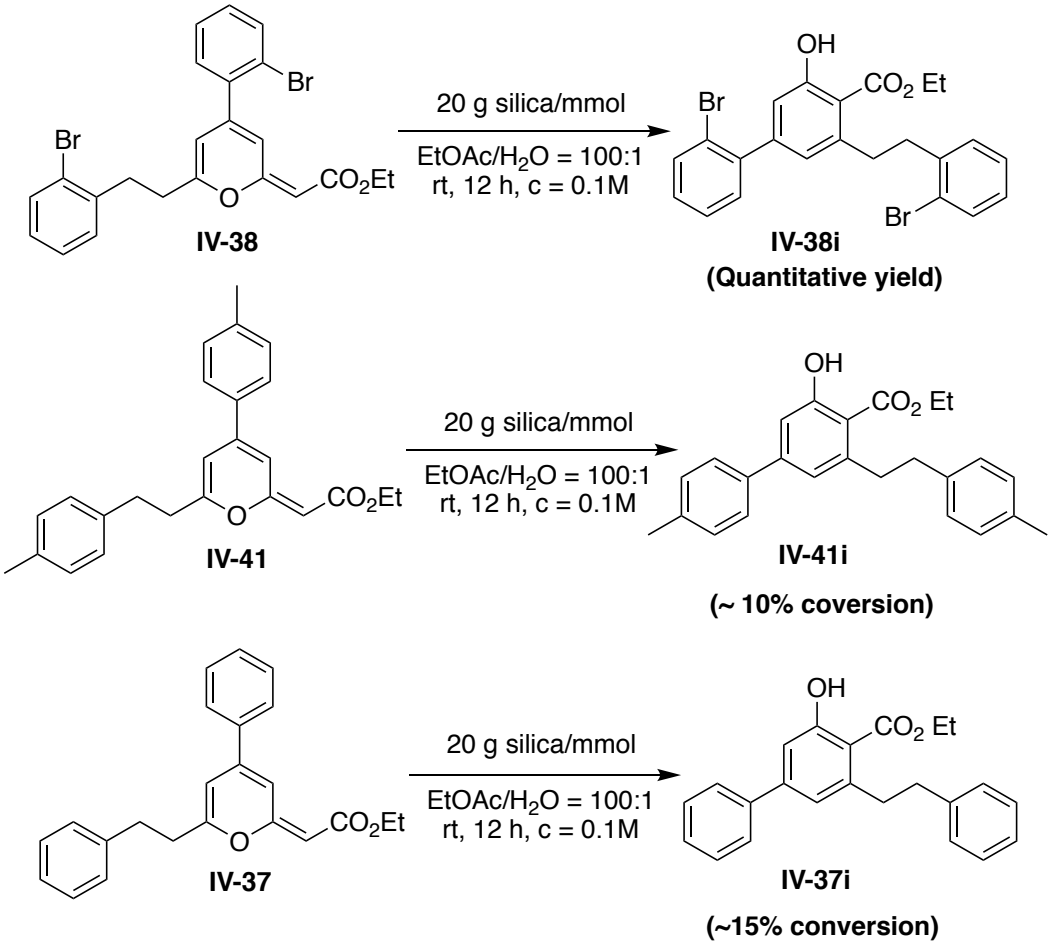

Scheme IV-14. Silica catalyzed rearrangement of pyran to salicylate.

Further manipulation was also performed to demonstrate the application of the vinyl pyrans, the products of formal [1,5]-H rearrangement, by Diels-Alder reaction to give chromene derivatives as shown in **Scheme IV-15**. The adducts were successfully obtained, although with low isolated yields. Unfortunately, acrylonitrile and ethyl vinyl ether did not provide conclusive results.

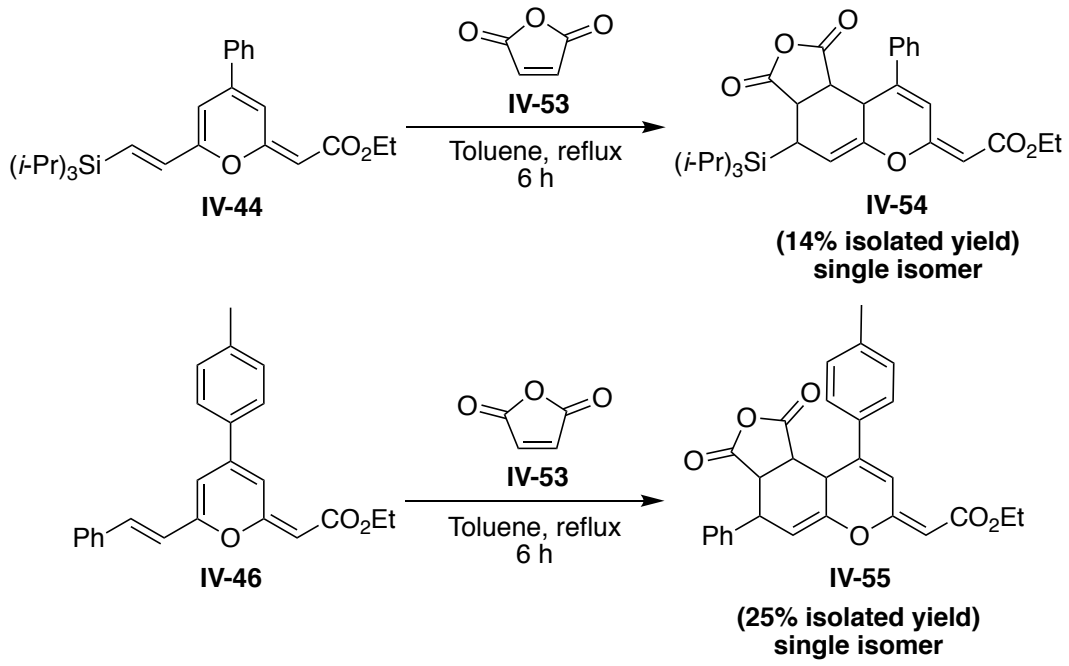

Scheme IV-15. Diels-Alder reaction of vinyl-pyrans with maleic anhydride to give chromene derivatives.

Based on base and substrate scope screening, as well as the rearranged salicylates formation, a proposed mechanism is presented in **Scheme IV-16**. DBU reacts as a Brønsted base, deprotonating the γ–H of substrate **IV-32** to furnish enolate intermediate, followed by α–protonation to give 4*H*-pyran **IV-36**. As a strong base, DBU will further deprotonate the C4 H to provide a pyran intermediate, which can tautomerize to pyran **IV-37** with the assistance from DBU. Pyran ring of **IV-37** can be hydrolyzed under acidic condition to a diketone ester, which will cyclize to afford cyclohexa-2,4-dien-1-one intermediate, and eventually tautomerize to salicylate **IV-37i** as the product. However, we cannot exclude the possibility that DBU reacts as a nucleophile, initiating the reaction in the same way as DABCO, as described in **Chapter III**.

As reported, DBU can be used as a nucleophilic catalyst. Therefore, we tried to develop a one-pot synthesis of pyran **IV-37** directly from allenoate **IV-56** and dibenzylideneacetone **IV-57**. Interestingly, an adduct with MS of [**IV-56**+**IV-57**+**DBU**+H]$^+$

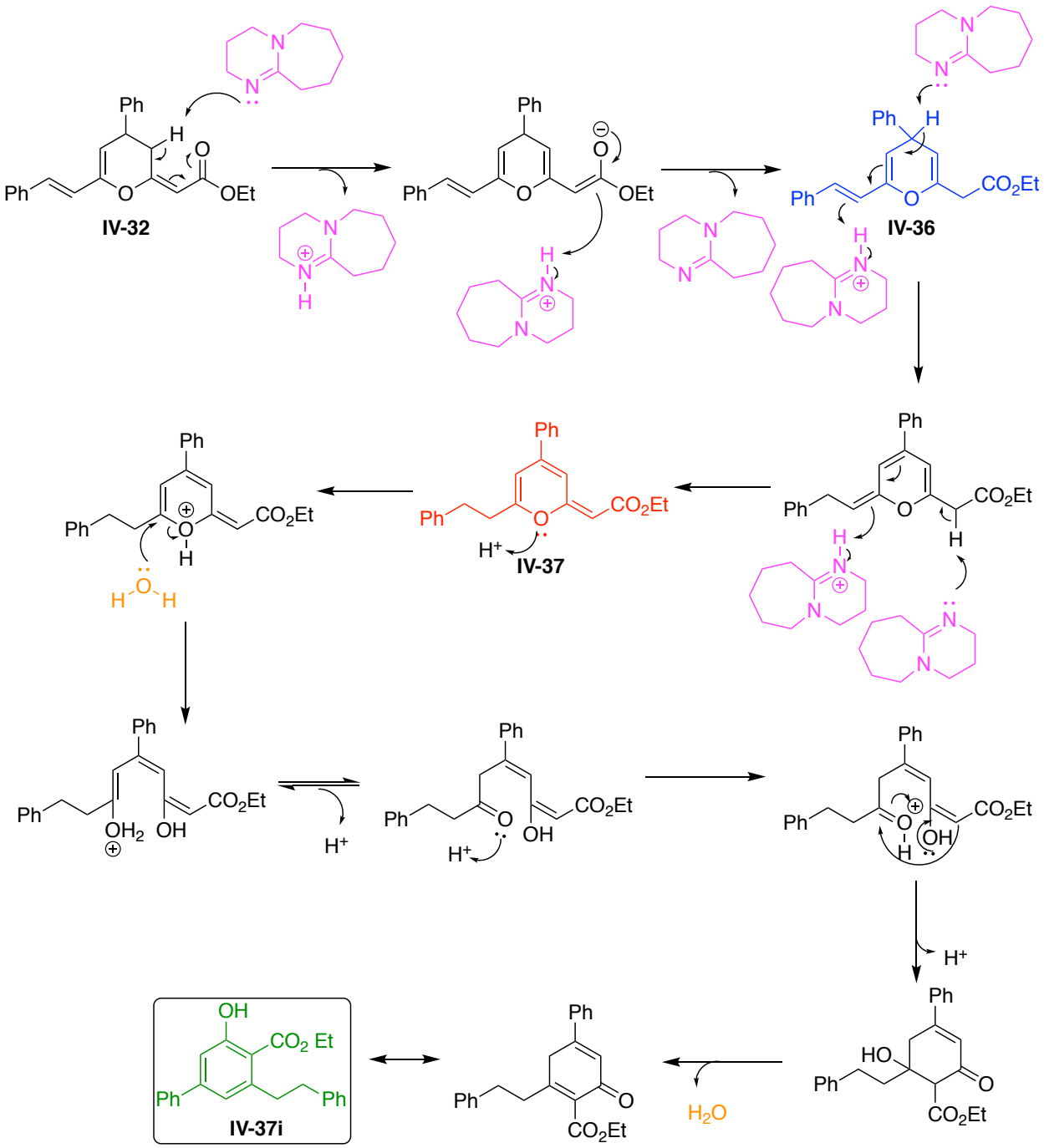

Scheme IV-16. Plausible mechanism for DBU mediates formal [1,5]-H shift and acid catalyzed rearrangement yielding phenol product.

was detected, as depicted in **Scheme IV-17**. However, an attempt to isolate the adduct was unsuccessful.

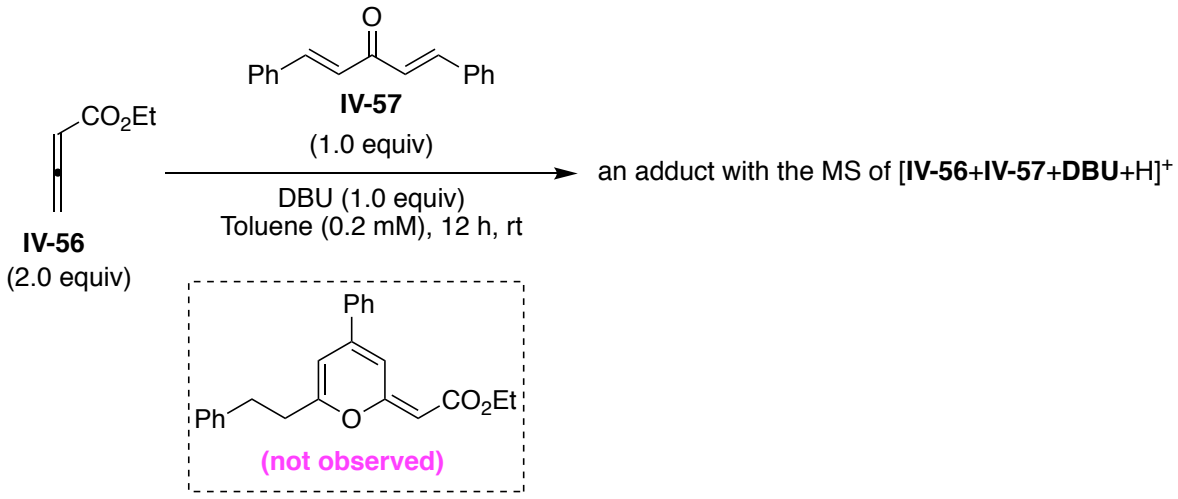

Scheme IV-17. Attempt to develop one-pot synthesis of pyran **IV-37**, while an adduct with the MS of [**IV-56**+**IV-57**+**DBU**+H]$^+$ was observed.

IV-4. Primary amine mediated multi-substituted carbocyclic *β*–amino ester synthesis

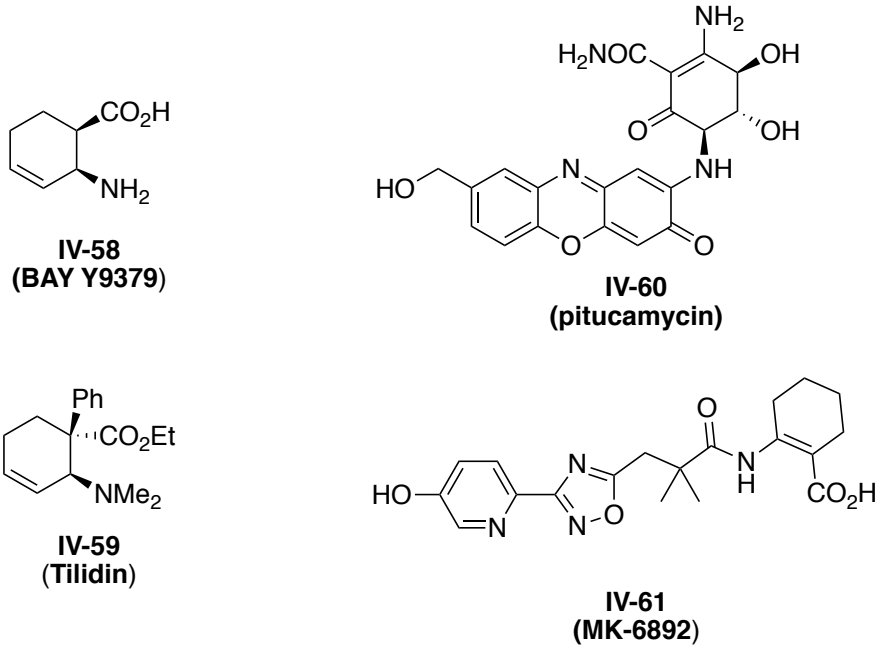

Figure IV-4. Representative examples of *β*–amino acid drugs and pharmacologically active *β*–amino acid derivatives.

Comparing to their *α*–analogues, although of less importance, conformationally constrained carbocyclic *β*–amino acids have also attracted great attention from both

synthetic and medicinal chemists in the past decades due to their critical biological effects.[59-63] Examples of these compounds are found in nature or antibiotics (**IV-58** and **IV-59**, Figure **IV-4**). Also, they are considered as key precursors for pharmacologically interesting ***β***–lactams and other bioactive compounds (**IV-60** and **IV-61**, Figure **IV-4**).[60,64] Besides, these compounds are important building blocks for biologically active small molecules and peptide synthesis with potential pharmacological applications. In peptide synthesis, incorporation of novel conformationally restricted ***β***–amino acids as subunits, especially into foldamers, is attractive from the aspect of design and synthesis of peptide-based drug molecules with high biological potential.[65,66] Consequently, a great deal of progress has been made in the past 10 years, leading to a large number of original papers

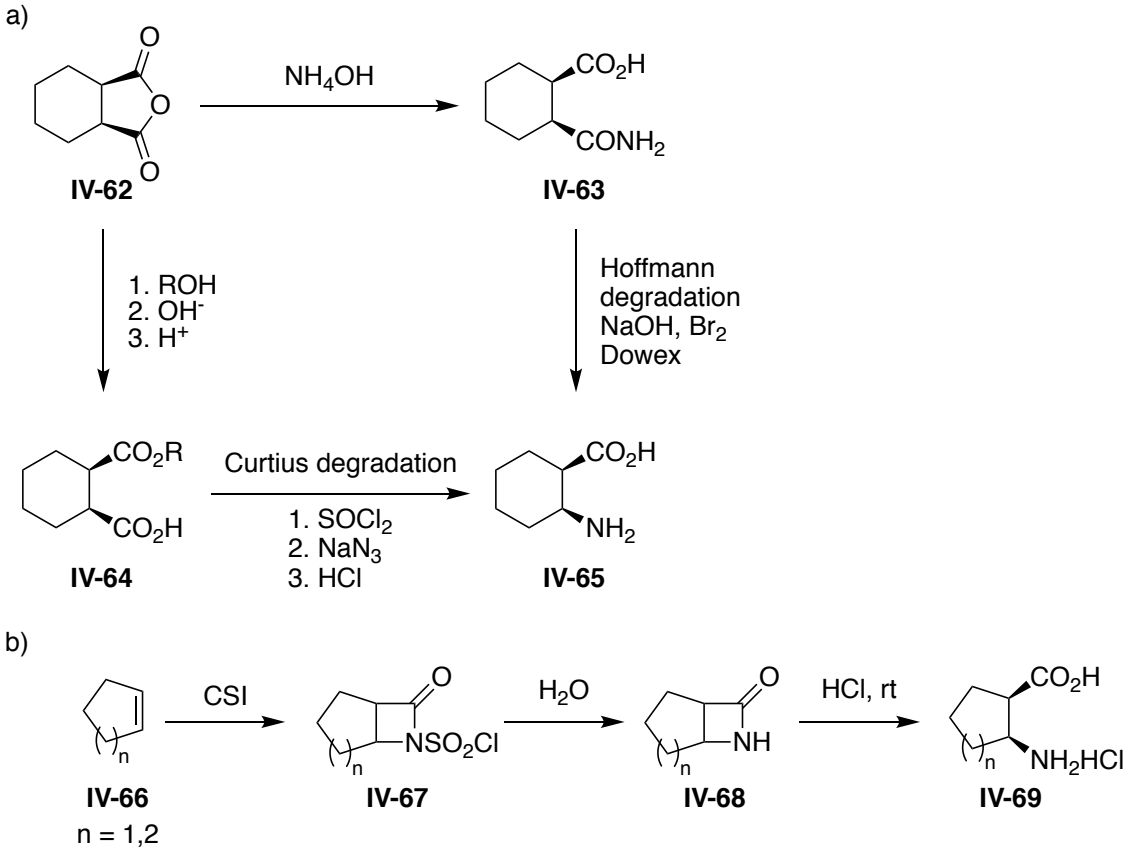

Scheme IV-18. Two commonly used routes to approach ***β***–amino acids synthesis.

and reviews published in this field.[60,64,67-71] Among these reports, a considerable number of them are about carbocyclic and heterocyclic ***β***–amino acid derivative synthesis, both in racemic forms and enantiomerically pure forms. In addition, further manipulation of these ***β***–amino acids to heterocycles, peptides, as well as other bioactive derivatives has also been reported.[68] There are two general modes commonly used to access to ***β***–aminocyclohexanecarboxylic acid.[60,64] One is based on the transformation of hexahydrophthalic by amindation and Hoffman degradation of the resulting amide to the corresponding ***β***–aminocyclohexanecarboxylic acid, or an alternative route, in which Curtius degradation is used (see **Scheme IV-18a** for details). An alternative route consists

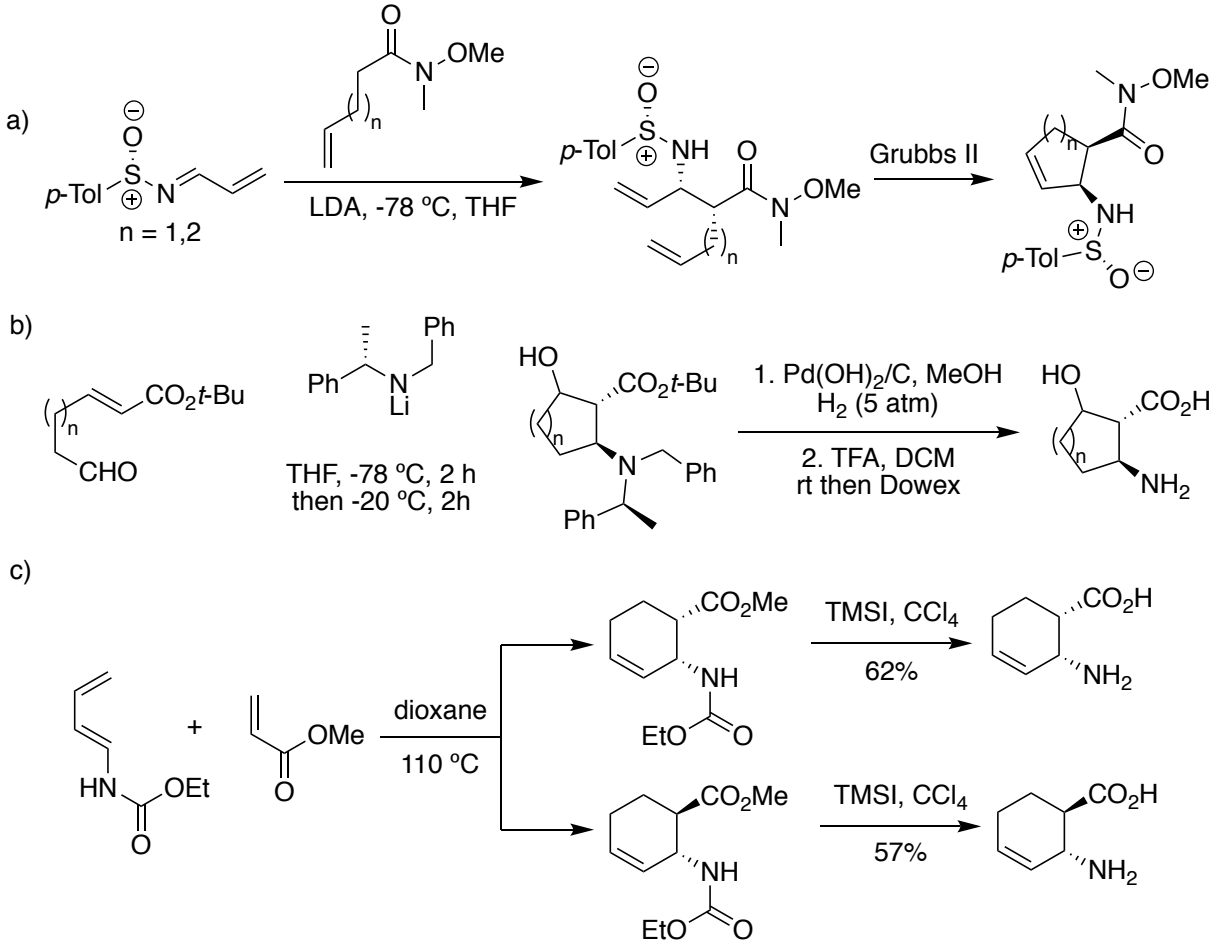

Scheme IV-19. Representative examples of other methods for ***β***–amino acids synthesis. a) Metathesis pathway; b) Amino group conjugation addition pathway; c) Cycloaddition pathway.

of the ring-opening transformation of bicyclic ***β***–lactams derived from cycloalkenes by the cycloaddition of chlorosulfonylisocyanate (CSI), as shown in **Scheme IV-18b**.[64] However, other methodologies that utilize other transformations, such as metathesis, amino group conjugate addition, cycloaddition, desymmetrization of *meso*-anhydrides, have also been developed to overcome certain limitations of the two general approaches (representative examples shown in **Scheme IV-19**[72-74]). Furthermore, routes of modification of ***β***–keto esters or natural sources are also investigated for the synthesis of ***β***–amino acids.[64]

During our investigation in cyclohexenone synthesis described in **Chapter III**, we highlighted that the reaction produces a 1,5-dicarbonyl intermediate from dihydropyran under acidic ring opening reaction condition. Actually, this intermediate is common for

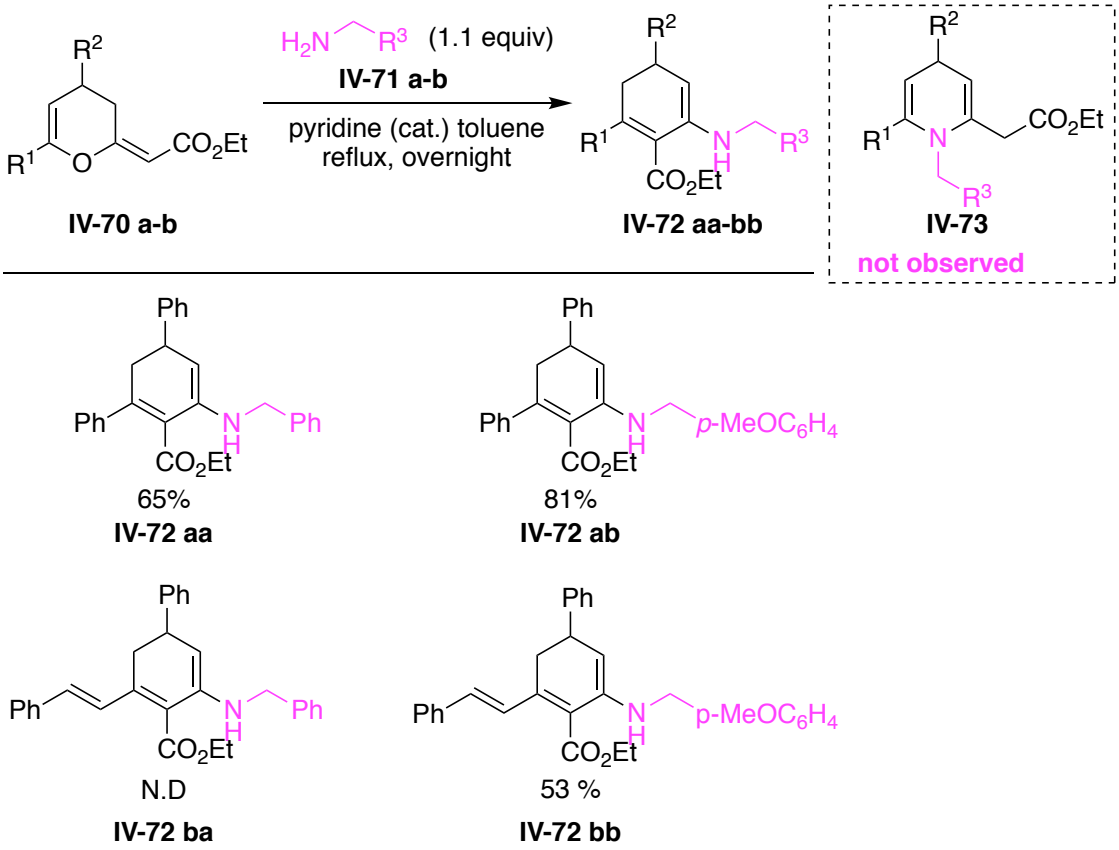

Scheme IV-20. Substrate scope of primary amine mediated ***β***–amino ester synthesis from dihydropyrans. N.D = not determined.

several routes toward pyridine synthesis, such as the Kröhnke[75] and the Hantzsch[76] dihydropyridine (pyridine) synthesis. This piqued our interest to develop a synthesis for dihydropyridine (pyridine) derivatives from our ready available dihydropyrans. We postulated that the benzylic amine attacks the dihydropyran to open the ring, followed by two tautomerizations to furnish the enamine intermediate. An intramolecular ring closing "N-attack" and an $E1_{cb}$ elimination would provide the dihydropyridine **IV-73** as the product (see **Scheme IV-21**, pathway A). However, it turns out that an unexpected carbocyclic $\boldsymbol{\beta}$–amino ester **IV-72 aa** was formed. For the initial study of this transformation, two of the benzylic amines, together with two dihydropyran substrates, have been employed to test the substrate scope. Gratifyingly, good results were obtained for the tested substrates (up to 81% isolated yield, need to be optimized) (see **Scheme IV-20**). The structures of **IV-72ab** was assigned by 2D NMR techniques. A proposed mechanism is depicted in **Scheme IV-21b**. It is believed that the benzylic amine initiates a ring opening reaction of the dihydropyran to furnish an enolate intermediate, which then undergoes an intramolecular ring closing reaction by "C-attack" instead of "N-attack", followed by dehydration and tautomerization to deliver the $\boldsymbol{\beta}$–amino ester as the product. We speculate that $\boldsymbol{\alpha}$–C of the $\boldsymbol{\beta}$–inmino ester intermediate is more nucleophilic as compared to the secondary amine under this reaction condition. Further exploration and mechanistic studies of this transformation are needed.

In summary, continuous development of the applications of our dihydropyran, an amidine-mediated formal [1,5]-*H* rearrangement toward pyran synthesis in moderate to

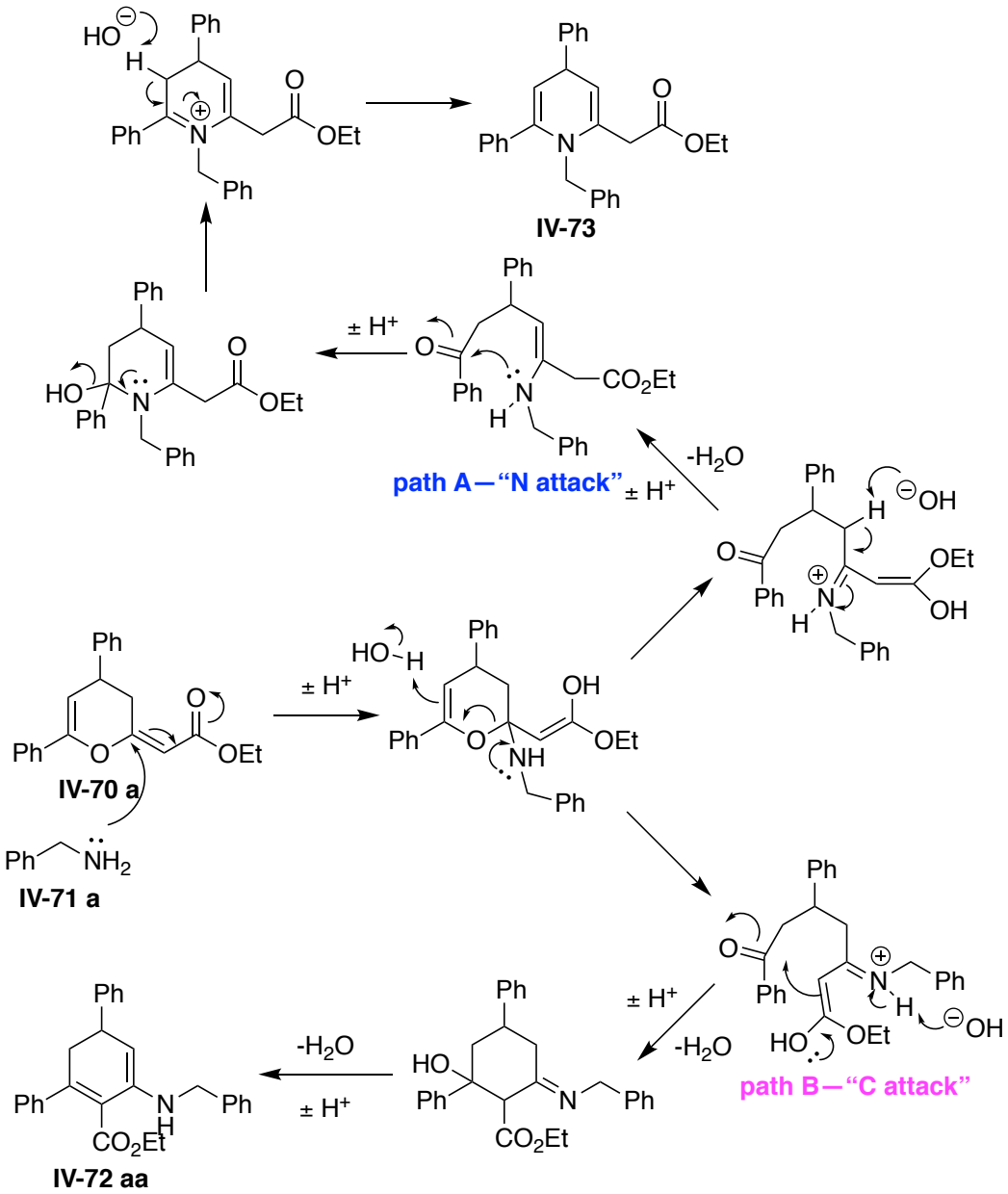

Scheme IV-21. a). An assumption of dihydropyridine synthesis from dihydropyran and benzylic amine through an intramolecular "N-attack" in the process. b). Proposed mechanism for primary amine mediated ***β***–amino ester synthesis from dihydropyrans through an intramolecular "C-attack" in the process.

high yield has been discovered, and some of these pyrans can undergo further rearrangement to salicylate derivatives under acidic condition. Also, we disclosure a primary amine initiated ***β***–amino ester synthesis from our dihydropyrans in good yield.

IV-5. Experimental.

IV-5.1. General remarks:

Molecular sieves (4 Å) were dried at 160 ºC under 0.25 mtorr vacuum prior to use. Unless specified, solvents were purified as follows. Toluene and DCM were dried over CaH_2. THF and Et_2O were dried over sodium (dryness was monitored by colorization of benzophenone ketyl radical); they were freshly distilled prior to use. All the dihydropyrans were prepared as reported.[53,77] Ethyl-2,3-butadienoate was synthesized according reported literature and stored at -20 ºC.[78]

1D and 2D NMR spectra were obtained from a 500 MHz Varian NMR spectrometers and referenced using the residual ^1H peak from the deuterated solvent. Melting point was detected by MelTem 019. Waters 2795 (Alliance HT) instrument was used for HRMS (ESI) analysis with polyethylene glycol (PEG-400-600) as a reference.

Column chromatography was performed using Silicycle 60 Å, 35-75 μm silica gel. Pre-coated 0.25 mm thick silica gel 60 F254 plates were used for analytical TLC and visualized using UV light, iodine, potassium permanganate stain or phosphomolybdic acid in EtOH stain.

IV-5.2. General procedure A for DBU-mediated formal [1,5]-H shift toward pyran synthesis:

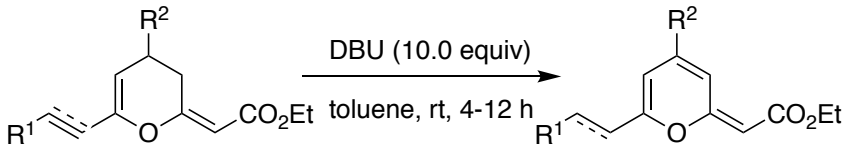

To a solution of the corresponding compound (1.0 equiv) in toluene, DBU (10.0 equiv) was added. Then the solution was stirred at room temperature for 4-12 hours. The mixture was concentrated under N_2 flow. The residue was purified by silica gel column chromatography using ethyl acetate in hexanes (1.5-10%) as the eluent.

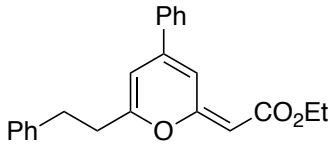

IV-37

IV-37: Ethyl (E)-2-(6-phenethyl-4-phenyl-2H-pyran-2-ylidene)acetate: Compound **IV-37**s (69.3 mg, 0.2 mmol) was subject to general procedure A to provide 63.0 mg (90% yield) of the pure product as a light yellow oil; ^{1}H NMR (500 MHz, $CDCl_3$) δ 8.04-7.95 (1H, m), 7.57-7.54 (2H, m), 7.41-7.38 (3H, m), 7.33-7.29 (2H, m), 7.25-7.19 (3H, m), 5.95-5.89 (1H, m), 5.25 (1H, s), 4.18 (2H, dd, J = 7.0 Hz, 7.0 Hz), 2.96 (2H, t, J = 7.0 Hz), 2.71 (2H, t, J = 7.0 Hz), 1.30 (3H, t, J = 7.0 Hz) ppm; ^{13}C NMR (125 MHz, $CDCl_3$) δ 168.1, 166.2, 160.1, 143.2, 140.1, 136.4, 129.5, 128.8, 128.5, 128.3, 126.3, 126.2, 112.5, 102.4, 88.5, 59.0, 35.5, 33.2, 14.6 ppm. HRMS (ESI) Calculated Mass for $C_{23}H_{23}O_3$: 347.1647 ($[M+H]^+$), Found 347.1659 ($[M+H]^+$).

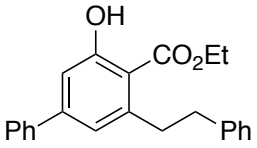

IV-37i

IV-37i: Ethyl 3-hydroxy-5-phenethyl-[1,1'-biphenyl]-4-carboxylate: 6.9 mg (10% yield) of the pure product was isolated as a colorless oil; ^{1}H NMR (500 MHz, $CDCl_3$) δ 11.43 (1H, s), 7.58-7.51 (2H, m), 7.48-7.35 (3H, m), 7.33-7.27 (2H, m), 7.25-7.17 (3H, m), 7.11 (1H, d, J = 2.0 Hz), 6.89 (1H, d, J = 2.0 Hz), 4.50 (2H, dd, J = 7.0 Hz, 7.0 Hz), 3.32 (2H, t, J = 8.0 Hz), 2.94 (2H, t, J = 8.0 Hz), 1.44 (3H, t, J = 7.0 Hz) ppm; ^{13}C NMR (125 MHz, $CDCl_3$) δ 171.4, 163.1, 146.7, 145.1, 141.7, 139.5, 128.8, 128.4, 128.4, 128.3, 127.1, 126.0, 121.8, 114.2, 110.7, 61.8, 38.4, 38.3, 14.3 ppm. HRMS (ESI) Calculated Mass for $C_{23}H_{23}O_3$: 347.1647 ($[M+H]^+$), Found 347.1653 ($[M+H]^+$).

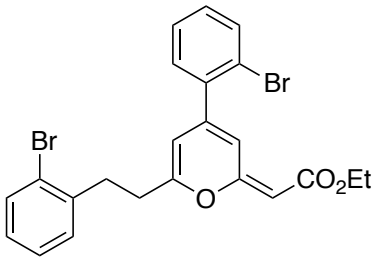

IV-38

IV-38: Ethyl (E)-2-(6-(2-bromophenethyl)-4-(2-bromophenyl)-2H-pyran-2-ylidene)acetate: Compound **IV-38**s (50.4 mg, 0.1 mmol) was subject to general procedure A to provide 29.2 mg (58% yield) of the pure product as a light yellow crystal; ^{1}H NMR (500 MHz, $CDCl_3$) δ 7.72-7.65 (1H, m), 7.59-7.51 (2H, m), 7.33-7.29 (1H, m), 7.28-7.24 (1H, m), 7.24-7.17 (3H, m), 7.10-7.04 (1H, m), 5.78-5.65 (1H, m), 5.27 (1H, s), 4.14 (2H, dd, J = 7.0 Hz, 7.0 Hz), 3.07 (2H, t, J = 7.0 Hz), 2.70 (2H, t, J = 7.0 Hz), 1.27

(3H, t, J = 7.0 Hz) ppm; ^{13}C NMR (125 MHz, $CDCl_3$) δ 167.8, 165.6, 158.3, 144.5, 139.3, 139.0, 133.3, 132.9, 130.6, 130.0, 130.0, 128.1, 127.6, 127.6, 124.3, 121.3, 116.1, 105.3, 89.3, 59.0, 33.6, 33.5, 14.5 ppm. HRMS (ESI) Calculated Mass for $C_{23}H_{21}O_3Br_2$: 502.9857 ($[M+H]^+$), Found 502.9879 ($[M+H]^+$).

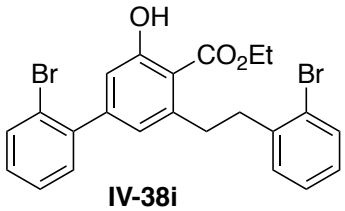

IV-38i

IV-38i: Ethyl 2'-bromo-3-(2-bromophenethyl)-5-hydroxy-[1,1'-biphenyl]-4-carboxylate: 3.0 mg (3% yield) of the pure product was isolated as a light yellow crystal; mp: 86-88 ºC. ^{1}H NMR (500 MHz, $CDCl_3$) δ 11.37 (1H, s), 7.67-7.62 (1H, m), 7.56-7.52 (1H, m), 7.36-7.31 (1H, m), 7.23-7.18 (3H, m), 7.11-7.04 (2H, m), 6.93 (1H, d, J = 2.0 Hz), 6.72 (1H, d, J = 2.0 Hz), 4.50 (2H, dd, J = 7.0 Hz, 7.0 Hz), 3.34 (2H, t, J = 7.0 Hz), 3.08 (2H, t, J = 7.0 Hz), 1.44 (3H, t, J = 7.0 Hz) ppm; ^{13}C NMR (125 MHz, $CDCl_3$) δ 171.2, 162.3, 146.7, 143.7, 141.1, 140.7, 133.2, 132.8, 130.7, 130.3, 129.2, 127.7, 127.3, 124.6, 124.3, 124.2, 121.9, 116.9, 111.3, 61.9, 38.0, 36.1, 14.2 ppm. HRMS (ESI) Calculated Mass for $C_{23}H_{21}O_3Br_2$: 502.9857 ($[M+H]^+$), Found 502.9860 ($[M+H]^+$).

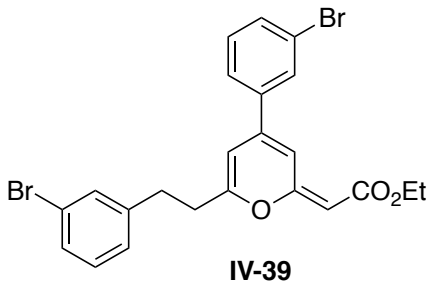

IV-39

IV-39: Ethyl (E)-2-(6-(3-bromophenethyl)-4-(3-bromophenyl)-2H-pyran-2-ylidene)acetate: Compound **IV-39**s (50.4 mg, 0.1 mmol) was subject to general procedure A to provide 27.7 mg (55% yield) of the pure product as a yellow oil; ^{1}H NMR (500 MHz, $CDCl_3$) δ 7.98-7.92 (1H, m), 7.66-7.64 (1H, m), 7.54-7.45 (2H, m), 7.38-7.34 (2H, m), 7.29-7.25 (1H, m), 7.20-7.14 (1H, m), 7.13-7.09 (1H, m), 5.86-5.80 (1H, m), 5.25 (1H, s), 4.17 (2H, dd, J = 7.0 Hz, 7.0 Hz), 2.92 (2H, t, J = 7.0 Hz), 2.69 (2H, t, J = 7.0 Hz), 1.30 (3H, t, J = 7.0 Hz) ppm; ^{13}C NMR (125 MHz, $CDCl_3$) δ 167.9, 165.5, 159.8, 142.3, 141.5, 138.6, 12.5, 131.4, 130.3, 130.1, 129.6, 129.1, 127.1, 124.8, 123.1, 122.6, 113.3, 102.2, 89.6, 59.2, 35.2, 32.8, 14.6 ppm. HRMS (ESI) Calculated Mass for $C_{23}H_{21}O_3Br_2$: 502.9857 ($[M+H]^+$), Found 502.9860 ($[M+H]^+$).

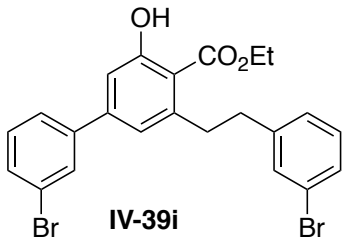

IV-39i

IV-39i: Ethyl 3'-bromo-3-(3-bromophenethyl)-5-hydroxy-[1,1'-biphenyl]-4-carboxylate: 2.0 mg (2% yield) of the pure product was isolated as a light yellow oil; ^{1}H NMR (500 MHz, $CDCl_3$) δ 11.40 (1H,s), 7.66-7.61 (1H, m), 7.54-7.43 (2H, m), 7.38-7.33 (2H, m), 7.32-7.29 (1H, m), 7.20-7.14 (1H, m), 7.09-7.05 (2H, m), 6.81-6.71 (1H, m), 4.50 (2H, dd, J = 7.0 Hz, 7.0 Hz), 3.30 (2H, t, J = 7.0 Hz), 2.90 (2H, t, J = 7.0 Hz), 1.44 (3H, t, J = 7.0 Hz) ppm.

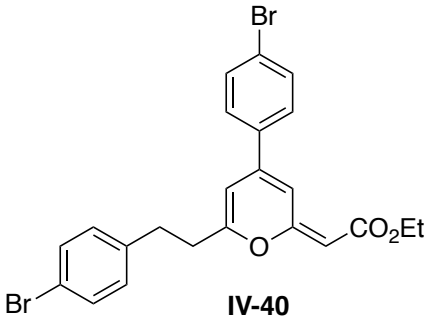

IV-40

IV-40: Ethyl (E)-2-(6-(4-bromophenethyl)-4-(4-bromophenyl)-2H-pyran-2-ylidene)acetate: Compound **IV-40**s (50.4 mg, 0.1 mmol) was subject to general procedure A to provide 27.7 mg (55% yield) of the not pure product as a yellow oil.

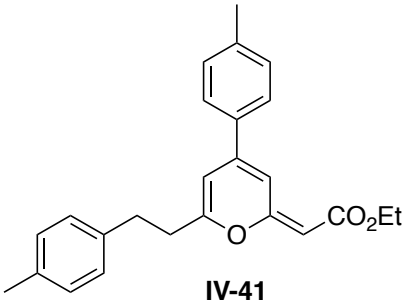

IV-41

IV-41: Ethyl (E)-2-(6-(4-methylphenethyl)-4-(p-tolyl)-2H-pyran-2-ylidene)acetate: Compound **IV-41**s (37.4 mg, 0.1 mmol) was subject to general procedure A to provide 18.7 mg (50% yield) of the pure product as a yellow oil; ^{1}H NMR (500 MHz, $CDCl_3$) δ 7.98 (1H, d, J = 1.5 Hz), 7.50-7.44 (2H, m), 7.22-7.19 (2H, m), 7.12-7.07 (4H, m), 5.97-5.90 (1H, m), 5.22 (1H, s), 4.17 (2H, dd, J = 7.0 Hz, 7.0 Hz), 2.92 (2H, t, J = 7.0 Hz), 2.68 (2H, t, J = 7.0 Hz), 2.38 (3H, s), 2.32 (3H, s), 1.30 (3H, t, J = 7.0 Hz) ppm; ^{13}C NMR (125 MHz, $CDCl_3$) δ 168.2, 166.4, 160.2, 143.1, 139.9, 137.1, 135.8, 133.4, 129.5, 129.2, 128.2, 126.1, 111.7, 102.3, 88.0, 58.9, 35.6, 32.8, 21.3, 21.0, 14.6 ppm. HRMS (ESI) Calculated Mass for $C_{25}H_{27}O_3$: 375.1960 ($[M+H]^+$), Found 375.1967 ($[M+H]^+$).

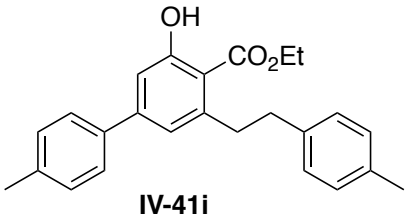

IV-41i

IV-41i: Ethyl 3-hydroxy-4'-methyl-5-(4-methylphenethyl)-[1,1'-biphenyl]-4-carboxylate: 3.7 mg (5% yield) of the pure product was isolated as a light yellow oil; ^{1}H NMR (500 MHz, $CDCl_3$) δ 11.40 (1H, s), 7.46-7.42 (2H, m), 7.26-7.22 (2H, m), 7.12-7.08 (5H, m), 6.87 (1H, d, J = 1.5 Hz), 4.49 (2H, dd, J = 7.0 Hz, 7.0 Hz), 3.29 (2H, t, J = 7.0 Hz), 2.89 (2H, t, J = 7.0 Hz), 2.40 (3H, s), 2.34 (3H, s), 1.44 (3H, t, J = 7.0 Hz) ppm; ^{13}C NMR (125 MHz, $CDCl_3$) δ 171.4, 163.1,146.6, 145.2, 138.7, 138.3, 136.6, 135.4, 129.5, 129.0, 128.2, 127.0, 121.6, 113.8, 110.4, 61.8, 38.6, 37.9, 29.7, 21.2, 14.3 ppm. HRMS (ESI) Calculated Mass for $C_{25}H_{27}O_3$: 375.1960 ($[M+H]^+$), Found 375.1973 ($[M+H]^+$).

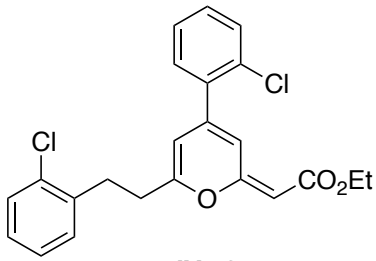

IV-42

IV-42: Ethyl (E)-2-(6-(2-chlorophenethyl)-4-(2-chlorophenyl)-2H-pyran-2-ylidene)acetate: Compound **IV-42**s (41.5 mg, 0.1 mmol) was subject to general procedure A to provide 32.0 mg (77% yield) of the pure product as a yellow oil; ^{1}H NMR (500 MHz, $CDCl_3$) δ 7.73 (1H, d, J = 1.5 Hz), 7.41-7.34 (2H, m), 7.32-7.26 (3H, m), 7.22-7.14 (3H, m), 5.76-5.71 (1H, m), 5.27 (1H, s), 4.15 (2H, dd, J = 7.0 Hz, 7.0 Hz), 3.07 (2H,

t, J = 7.0 Hz), 2.71 (2H, t, J = 7.0 Hz), 1.28 (3H, t, J = 7.0 Hz) ppm; ^{13}C NMR (125 MHz, $CDCl_3$) δ 167.8, 165.6, 158.4, 143.1, 137.6, 137.0, 133.8, 132.0, 130.6, 130.0, 130.0, 129.9, 129.5, 127.9, 127.0, 126.9, 116.2, 105.1, 89.3, 59.0, 33.4, 31.1, 14.5 ppm. HRMS (ESI) Calculated Mass for $C_{23}H_{21}O_3Cl_2$: 415.0868 ($[M+H]^+$), Found 415.0874 ($[M+H]^+$).

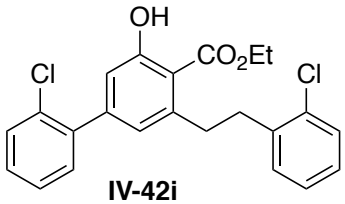

IV-42i

IV-42i: Ethyl 2'-chloro-3-(2-chlorophenethyl)-5-hydroxy-[1,1'-biphenyl]-4-carboxylate: 9.1 mg (11% yield) of the pure product was isolated as a light yellow oil; ^{1}H NMR (500 MHz, $CDCl_3$) δ 11.35 (1H, s), 7.48-7.42 (1H, m), 7.38-7.32 (1H, m), 7.32-7.27 (2H, m), 7.24-7.20 (1H, m), 7.18-7.12 (2H, m), 7.12-7.06 (1H, m), 6.96 (1H, d, J = 1.5 Hz), 6.72 (1H, d, J = 1.5 Hz), 4.50 (2H, dd, J = 7.0 Hz, 7.0 Hz), 3.33 (2H, t, J = 7.0 Hz), 3.06 (2H, t, J = 7.0 Hz), 1.43 (3H, t, J = 7.0 Hz) ppm; ^{13}C NMR (125 MHz, $CDCl_3$) δ 171.2, 162.4, 145.1, 143.9, 139.1, 139.0, 130.8, 130.4, 130.0, 129.5, 129.1, 127.5, 126.8, 126.7, 124.2, 117.0, 111.2, 61.9, 36.0, 35.6, 14.2 ppm. HRMS (ESI) Calculated Mass for $C_{21}H_{21}O_3Cl_2$: 415.0868 ($[M+H]^+$), Found 415.0878 ($[M+H]^+$).

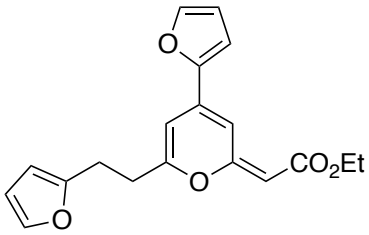

IV-43

IV-43: Ethyl (E)-2-(4-(furan-2-yl)-6-(2-(furan-2-yl)ethyl)-2H-pyran-2-ylidene)acetate: Compound **IV-43**s (32.6 mg, 0.1 mmol) was subject to general procedure A to provide 26.1 mg (80% yield) of the pure product as a yellow oil; ^{1}H NMR (500 MHz, $CDCl_3$) δ 8.03-7.92 (1H, m), 7.54-7.42 (1H, m), 7.35-7.29 (1H, m), 6.78-6.70 (1H, m), 6.53-6.44 (1H, m), 6.32-6.25 (1H, m), 6.08-6.02 (1H, m), 5.93-5.86 (1H, m), 5.18 (1H, s), 4.16 (2H, dd, J = 7.0 Hz, 7.0 Hz), 2.96 (2H, t, J = 7.0 Hz), 2.72 (2H, t, J = 7.0 Hz), 1.29 (3H, t, J = 7.0 Hz) ppm; ^{13}C NMR (125 MHz, $CDCl_3$) δ 168.0, 165.7, 159.5, 153.7, 150.4, 144.4, 141.3, 132.1, 112.2, 110.3, 110.2, 108.7, 105.7, 99.4, 88.8, 59.0, 32.2, 25.5, 14.6 ppm. HRMS (ESI) Calculated Mass for $C_{19}H_{19}O_5$: 327.1232 ($[M+H]^+$), Found 327.1245 ($[M+H]^+$).

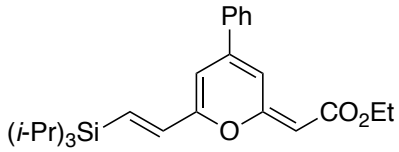

IV-44

IV-44: Ethyl (E)-2-(4-phenyl-6-((E)-2-(triisopropylsilyl)vinyl)-2H-pyran-2-ylidene)acetate: Compound **IV-44**s (33.2 mg, 0.1 mmol) was subject to general procedure A to provide mg (78% yield) of the pure product as a yellow oil; ^{1}H NMR (500 MHz, $CDCl_3$) δ 8.07 (1H, d, J = 1.5 Hz), 7.66-7.59 (2H, m), 7.44-7.39 (3H, m), 6.64 (1H, d, J = 19.0 Hz), 6.45 (1H, d, J = 19.0 Hz), 6.12 (1H, d, J = 1.5 Hz), 5.35 (1H, s), 4.17 (2H, dd, J = 7.0 Hz, 7.0 Hz), 1.28 (3H, t, J = 7.0 Hz), 1.19-1.14 (3H, m), 1.08 (18H, d, J = 7.0 Hz) ppm; ^{13}C NMR (125 MHz, $CDCl_3$) δ 168.1, 165.2, 154.4, 143.3, 136.4, 136.3, 130.9, 129.6, 128.9, 126.2, 114.3, 105.1, 89.4, 59.0, 29.7, 18.7, 18.6, 18.6, 14.6, 10.9 ppm.

HRMS (ESI) Calculated Mass for $C_{26}H_{37}O_3Si$: 425.2512 ($[M+H]^+$), Found 425.2515 ($[M+H]^+$).

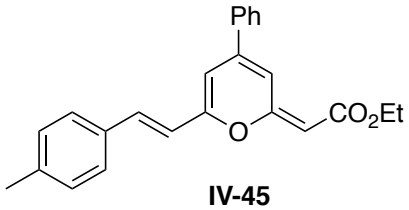

IV-45

IV-45: Ethyl (E)-2-(6-((E)-4-methylstyryl)-4-phenyl-2H-pyran-2-ylidene)acetate: Compound **IV-45**s (35.8 mg, 0.1 mmol) was subject to general procedure A to provide 34.7 mg (97% yield) of the pure product was as a dark purple needle crystal; mp: 120-122 ºC. ^{1}H NMR (500 MHz, $CDCl_3$) δ 8.06 (1H, d, J = 2.0 Hz), 7.65-7.60 (2H, m), 7.45-7.39 (5H, m), 7.24 (1H, d, J = 17.0 Hz), 7.21-7.18 (2H, m), 6.58 (1H, d, J = 17.0 Hz), 6.21-6.16 (1H, m), 5.37 (1H, s), 4.18 (2H, dd, J = 7.0 Hz, 7.0 Hz), 2.37 (3H, s), 1.31 (3H, t, J = 7.0 Hz) ppm; ^{13}C NMR (125 MHz, $CDCl_3$) δ 168.1, 165.2, 155.3, 143.2, 139.2, 136.4, 132.9, 132.7, 129.6, 128.9, 127.1, 126.1, 118.7, 113.7, 105.2, 89.3, 59.1, 29.7, 14.6 ppm. HRMS (ESI) Calculated Mass for $C_{24}H_{23}O_3$: 359.1647 ($[M+H]^+$), Found 359.1660 ($[M+H]^+$).

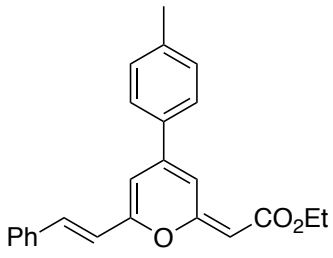

IV-46

IV-46: Ethyl (E)-2-(6-((E)-styryl)-4-(p-tolyl)-2H-pyran-2-ylidene)acetate: Compound **IV-46**s (35.8 mg, 0.1 mmol) was subject to general procedure A to provide 25.1 mg (70% yield) of the pure product was as a yellow oil; ^{1}H NMR (500 MHz, $CDCl_3$) δ 8.07 (1H, d, J = 2.0 Hz), 7.55-7.48 (4H, m), 7.40-7.36 (2H, m), 7.34-7.30 (1H, m), 7.27 (1H, d, J = 17.0 Hz), 7.25-7.22 (2H, m), 6.62 (1H, d, J = 16.0 Hz), 6.20 (1H, d, J = 2.0 Hz), 5.36 (1H, s), 4.19 (2H, dd, J = 7.0 Hz, 7.0 Hz), 2.40 (3H, s), 1.31 (3H, t, J = 7.0 Hz) ppm; ^{13}C NMR (125 MHz, $CDCl_3$) δ 168.1, 165.3, 155.0, 143.0, 140.0, 135.7, 132.6, 129.6, 128.9, 128.8, 127.2, 126.1, 125.7, 119.8, 113.3, 105.6, 89.1, 59.1, 29.7, 14.6 ppm. HRMS (ESI) Calculated Mass for $C_{24}H_{23}O_3$: 359.1647 ($[M+H]^+$), Found 359.1659 ($[M+H]^+$).

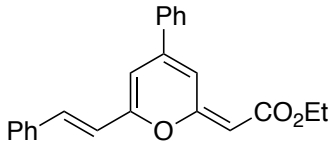

IV-47

IV-47: Ethyl (E)-2-(4-phenyl-6-((E)-styryl)-2H-pyran-2-ylidene)acetate: Compound **IV-47**s (34.4 mg, 0.1 mmol) was subject to general procedure A to provide 31.0 mg (90% yield) of the pure product as a yellow oil; ^{1}H NMR (500 MHz, $CDCl_3$) δ 8.08 (1H, d, J = 2.0 Hz), 7.65-7.61 (2H, m), 7.52-7.49 (2H, m), 7.45-7.42 (3H, m), 7.40-7.37 (2H, m), 7.34-7.31 (1H, m), 7.27 (1H, d, J = 16.0 Hz), 6.62 (1H, d, J = 16.0 Hz), 6.20 (1H, d, J = 2.0 Hz), 5.39 (1H, s), 4.18 (2H, dd, J = 7.0 Hz, 7.0 Hz), 1.31 (3H, t, J = 7.0 Hz) ppm; ^{13}C NMR (125 MHz, $CDCl_3$) δ 168.0, 165.1, 155.1, 143.1, 136.3, 135.7, 132.7, 129.7, 129.0, 129.0, 128.9, 128.9, 128.7, 127.5, 127.2, 126.2, 125.8, 119.7, 114.0, 105.6, 89.5, 59.1, 53.4, 29.7, 14.6 ppm.

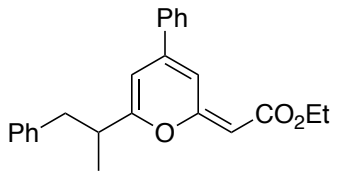

IV-48

IV-48: Ethyl (E)-2-(4-phenyl-6-(1-phenylpropan-2-yl)-2H-pyran-2-ylidene)acetate: Compound **IV-48**s (36.0 mg, 0.1 mmol) was subject to general procedure A to provide 25.6 mg (71% yield) of the pure product as a yellow oil; ^{1}H NMR (500 MHz, $CDCl_3$) δ 7.97 (1H, d, J = 2.0 Hz), 7.55-7.50 (2H, m), 7.41-7.36 (4H, m), 7.29-7.27 (1H, m), 7.22-7.17 (1H, m), 7.15-7.11 (2H, m), 5.83 (1H, d, J = 2.0 Hz), 5.26 (1H, s), 4.17 (2H, dd, J = 7.0 Hz, 7.0 Hz), 3.03-2.97 (1H, m), 2.81-2.70 (2H, m), 1.30 (3H, t, J = 7.0 Hz), 1.21 (3H, d, J = 1.5 Hz) ppm; ^{13}C NMR (125 MHz, $CDCl_3$) δ 168.1, 166.2, 163.9, 143.3, 139.2, 136.6, 129.5, 129.0, 128.8, 128.4, 126.3, 126.2, 112.5, 101.4, 88.3, 59.0, 41.0, 40.3, 17.7, 14.6 ppm. HRMS (ESI) Calculated Mass for $C_{24}H_{25}O_3$: 361.1804 ($[M+H]^+$), Found 361.1821 ($[M+H]^+$).

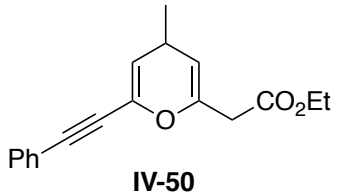

IV-50

IV-50: Ethyl 2-(4-methyl-6-(phenylethynyl)-4*H*-pyran-2-yl)acetate: Compound **IV-50**s (28.2 mg, 0.1 mmol) was subject to general procedure A to provide 14.1 mg (50% yield) of the pure product as a yellow oil; ^{1}H NMR (500 MHz, $CDCl_3$) δ 7.50-7.44 (2H, m), 7.37-7.29 (3H, m), 5.26-5.22 (1H, m), 4.69-4.63 (1H, m), 4.19 (2H, dd, J = 6.5 Hz, 6.5 Hz), 3.10

(2H, d, J = 16.0 Hz), 3.07-3.00 (1H, m), 1.28 (3H, t, J = 7.5 Hz), 1.14 (3H, d, J = 7.0 Hz) ppm; ^{13}C NMR (125 MHz, $CDCl_3$) δ 169.6, 144.3, 133.9, 131.7, 128.7, 128.3, 122.1, 113.5, 104.5, 88.4, 83.3, 77.3, 61.0, 39.3, 26.9, 24.4, 14.2 ppm.

IV-5.3. Analytical data for propargyl dihydropyran IV-44s to IV-47s and dihydropyran IV-48s:

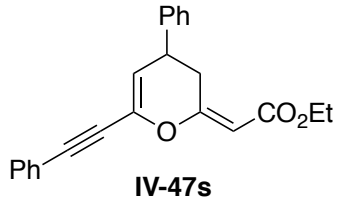

IV-47s

IV-47s: Ethyl (*E*)-2-(4-phenyl-6-(phenylethynyl)-3,4-dihydro-2*H*-pyran-2-ylidene)acetate: Compound **IV-47**ss (23.4 mg, 0.1 mmol) was subject to general procedure of dihydropyran synthesis to provide 27.2 mg (79% yield) of the pure product as a yellow oil; ^{1}H NMR (500 MHz, $CDCl_3$) δ 7.55-7.48 (2H, m), 7.39-7.29 (5H, m), 7.28-7.24 (3H, m), 5.78-5.72 (1H, m), 5.66-5.61 (1H, m), 4.15-4.07 (2H, m), 3.73-3.64 (2H, m), 3.17-3.08 (1H, m), 1.24 (3H, t, J = 7.0 Hz) ppm; ^{13}C NMR (125 MHz, $CDCl_3$) δ 167.0, 165.5, 142.1, 135.0, 131.8, 129.1, 128.7, 128.4, 127.3, 127.1, 121.6, 114.4, 99.9, 89.3, 82.6, 59.8, 36.2, 30.3, 14.3 ppm.

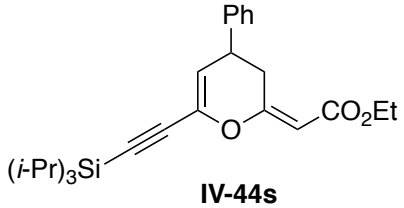

IV-44s

IV-44s: Ethyl (*E*)-2-(4-phenyl-6-((triisopropylsilyl)ethynyl)-3,4-dihydro-2*H*-pyran-2-ylidene)acetate: Compound **IV-44**ss (31.3 mg, 0.1 mmol) was subject to general procedure of dihydropyran synthesis to provide 32.2 mg (76% yield) of the pure product as a yellow oil; ^{1}H NMR (500 MHz, $CDCl_3$) δ 7.35-7.30 (2H, m), 7.26-7.19 (3H, m), 5.70-5.64 (1H, m), 5.64-5.55 (1H, m), 4.13-4.06 (2H, m), 3.71-3.59 (2H, m), 3.07 (1H, qd, J = 8.0 Hz, 1.5 Hz), 1.24 (3H, t, J = 7.0 Hz) ppm; ^{13}C NMR (125 MHz, $CDCl_3$) δ 167.1, 165.5, 142.2, 134.9, 128.7, 128.7, 127.3, 127.1, 114.6, 99.8, 99.6, 92.1, 59.7, 36.1, 30.1, 18.6, 14.3, 11.2 ppm.

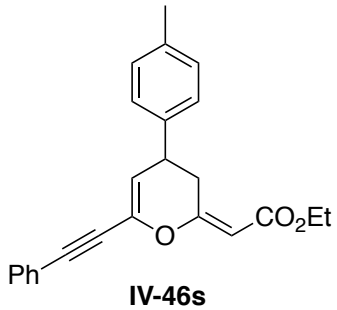

IV-46s

IV-46s: Ethyl (*E*)-2-(6-(phenylethynyl)-4-(*p*-tolyl)-3,4-dihydro-2*H*-pyran-2-ylidene)acetate: Compound **IV-46**ss (24.6 mg, 0.1 mmol) was subject to general procedure of dihydropyran synthesis to provide 22.2 mg (62% yield) of the pure product as a yellow oil; ^{1}H NMR (500 MHz, $CDCl_3$) δ 7.56-7.49 (2H, m), 7.38-7.32 (3H, m), 7.16-7.12 (4H, m), 5.83-5.68 (1H, m), 5.63 (1H, s), 4.16-4.07 (2H, m), 3.70-3.62 (2H, m), 3.17-3.04 (1H, m), 2.34 (3H, s), 1.25 (3H, t, J = 7.0 Hz) ppm; ^{13}C NMR (125 MHz, $CDCl_3$) δ 167.1, 165.6, 139.1, 136.6, 134.9, 131.7, 131.7, 129.4, 129.1, 129.0, 128.4, 128.3, 127.9, 127.1, 121.7, 114.7, 99.8, 89.2, 82.6, 59.7, 35.8, 30.3, 29.7, 21.0, 14.3 ppm.

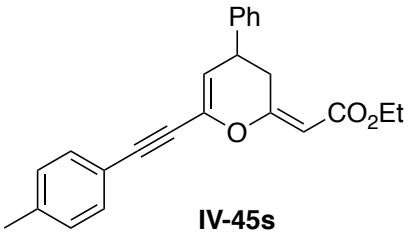

IV-45s

IV-45s: Ethyl (*E*)-2-(4-phenyl-6-(*p*-tolylethynyl)-3,4-dihydro-2*H*-pyran-2-ylidene)acetate: Compound **IV-45**ss (24.6 mg, 0.1 mmol) was subject to general procedure of dihydropyran synthesis to provide 33.7 mg (94% yield) of the pure product as a yellow oil; ^{1}H NMR (500 MHz, $CDCl_3$) δ 7.45-7.39 (2H, m), 7.37-7.30 (2H, m), 7.28-7.23 (3H, m), 7.18-7.13 (2H, m), 5.72 (1H, d, J = 3.5 Hz), 5.63 (1H, s), 4.16-4.05 (2H, m), 3.73-3.64 (2H, m), 3.17-3.07 (1H, m), 2.37 (3H, s), 1.24 (3H, t, J = 7.0 Hz) ppm; ^{13}C NMR (125 MHz, $CDCl_3$) δ 167.1, 165.5, 142.2, 139.3, 135.1, 131.7, 129.2, 128.7, 127.3, 127.0, 118.5, 114.0, 99.8, 89.5, 82.0, 59.7, 36.2, 30.3, 21.6, 14.3 ppm.

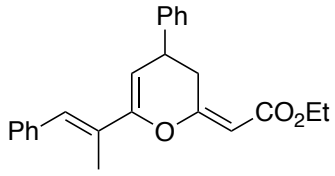

IV-48s

IV-48s: Ethyl (*E*)-2-(4-phenyl-6-((*E*)-1-phenylprop-1-en-2-yl)-3,4-dihydro-2*H*-pyran-2-ylidene)acetate: Compound **IV-48**ss (24.8 mg, 0.1 mmol) was subject to general procedure of dihydropyran synthesis to provide 11.2 mg (31% yield) of the pure product as a yellow oil; ^{1}H NMR (500 MHz, $CDCl_3$) δ 7.40-7.31 (6H, m), 7.29-7.26 (4H, m), 7.15 (1H, s), 5.69 (1H, s), 5.50 (1H, d, J = 3.5 Hz), 4.16-4.08 (2H, m), 3.77-3.69 (2H, m), 3.16-3.05 (1H, m), 2.03 (3H, d, J = 1.0 Hz) 1.26 (3H, t, J = 7.0 Hz) ppm; ^{13}C NMR (125 MHz,

$CDCl_3$) δ 167.4, 166.6, 150.5, 143.2, 137.4, 129.4, 128.7, 128.7, 128.2, 127.3, 126.9, 126.8, 126.8, 105.3, 98.8, 59.6, 36.1, 30.9, 14.3, 14.0 ppm.

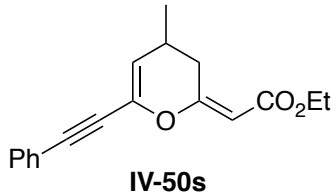

IV-50s

IV-50s: Ethyl (*E*)-2-(4-methyl-6-(phenylethynyl)-3,4-dihydro-2*H*-pyran-2-ylidene)acetate: Compound **IV-50**ss (34.0 mg, 0.2 mmol) was subject to general procedure of dihydropyran synthesis to provide 21.1 mg (37% yield) of the pure product was isolated as a yellow oil; ^{1}H NMR (500 MHz, $CDCl_3$) δ 7.50-7.47 (2H, m), 7.36-7.31 (3H, m), 5.60 (1H, d, J = 1.0 Hz), 5.53 (1H, d, J = 4.0 Hz), 4.16 (2H, ddd, J = 1.0, 7.0, 7.0 Hz), 3.46 (1H, ddd, J = 0.5, 1.5, 15 Hz), 2.70 (1H, ddd, J = 1.0, 8.5, 15 Hz), 2.55-2.46 (1H, m), 1.28 (3H, t, J = 7.5 Hz) 1.11 (3H, d, J = 7.0 Hz) ppm; ^{13}C NMR (125 MHz, $CDCl_3$) δ 167.4, 166.5, 133.9, 131.7, 128.9, 128.3, 121.8, 117.3, 99.3, 88.8, 82.7, 77.3, 77.0, 76.8, 59.7, 29.6, 25.2, 20.2, 14.3 ppm.

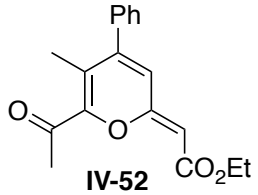

IV-52

IV-52: Ethyl (*Z*)-2-(6-acetyl-5-methyl-4-phenyl-2*H*-pyran-2-ylidene)acetate: Quantitative yield of the pure product was isolated as a dark red crystal. m.p: 75 ºC;

HRMS (ESI) Calculated Mass for $C_{18}H_{18}O_4$: 299.1283 ($[M+H]^+$), Found 299.1283 ($[M+H]^+$).

IV-5.4. General procedure B for the synthesis of enones IV-44ss to IV-47ss and IV-50ss:[79]

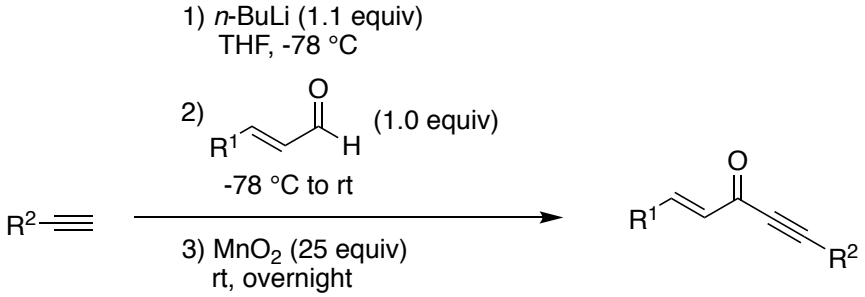

To a solution of alkyne (1.0 equiv) in THF, *n*-BuLi (1.1 equiv) was added dropwise at -78 ºC. The solution was left to stir for 10 min, allowed to warm up to room temperature and kept for another 30 min. It was then cooled down to -78 ºC, and enal (1.0 equiv) in THF was added. The reaction was warmed to room temperature and kept for another 4 hours. After the reaction was completed (followed by TLC detection), saturated NH_4Cl was added and the product was extracted with EtOAc. The combined organic layers were washed by brine and dried over Na_2SO_4, filtered, and concentrated under reduced pressure. The crude product was used for the next step without further purification.

The crude enol from the last step was dissolved in DCM, and MnO_2 (25.0 equiv) was added, and the mixture was stirred at room temperature for 24 hours. The solution was filtered and concentrated, followed by purification by silica gel column chromatography to provide the enones using ethyl acetate and hexanes as the eluent.

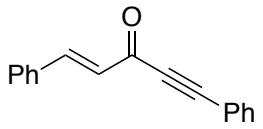

IV-47ss

IV-47ss: Phenylacetylene (102.1 mg, 1.0 mmol) and cinnamaldehyde (132.2 mg, 1.0 mmol) were subject to general procedure B to provide 178.9 mg (71% yield) of the pure product as a yellow crystal. m.p: 56 ºC; ^{1}H NMR (500 MHz, $CDCl_3$) δ 7.92 (1H, d, J = 16.5 Hz), 7.68-7.64 (2H, m), 7.64-7.60 (2H, m), 7.51-7.41 (6H, m), 6.88 (1H, d, J = 16.5 Hz) ppm; ^{13}C NMR (125 MHz, $CDCl_3$) δ 178.2, 148.3, 134.0, 132.9, 131.2, 130.6, 129.1, 128.7, 128.7, 128.5, 120.2, 91.5, 86.6 ppm.

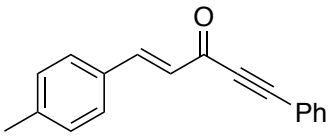

IV-46ss

IV-46ss: Phenylacetylene (102.1 mg, 1.0 mmol) and *p*-methyl cinnamaldehyde (146.2 mg, 1.0 mmol) were subject to general procedure B to provide 160.1 mg (65% yield) of the pure product as a brown solid. m.p: 50 ºC; ^{1}H NMR (500 MHz, $CDCl_3$) δ 7.90 (1H, d, J = 16.0 Hz), 7.68-7.64 (2H, m), 7.52-7.49 (2H, m), 7.48-7.45 (1H, m), 7.45-7.39 (2H, m), 7.26-7.22 (2H, m), 6.84 (1H, d, J = 16.5 Hz), 2.40 (3H, s) ppm; ^{13}C NMR (125 MHz, $CDCl_3$) δ 178.3, 148.5, 141.9, 132.9, 132.1, 131.3, 130.5, 129.8, 128.7, 128.6, 128.3, 127.6, 120.3, 91.3, 86.6, 21.6 ppm.

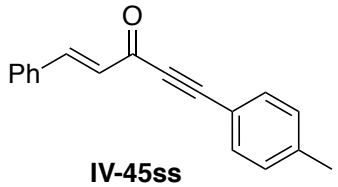

IV-45ss

IV-45ss: 4-Ethynyltoluene (116.2 mg, 1.0 mmol) and cinnamaldehyde (132.2 mg, 1.0 mmol) were subject to general procedure B to provide 209.4 mg (85% yield) of the pure product as a yellow crystal. m.p: 67 ºC; ^{1}H NMR (500 MHz, $CDCl_3$) δ 7.91 (1H, d, J = 16.0 Hz), 7.64-7.59 (2H, m), 7.57-7.54 (2H, m), 7.47-7.41 (3H, m), 7.25-7.20 (2H, m), 6.87 (1H, d, J = 16.5 Hz), 2.41 (3H, s) ppm; ^{13}C NMR (125 MHz, $CDCl_3$) δ 178.3, 148.1, 141.3, 134.1, 130.0, 129.1, 128.7, 128.6, 117.0, 92.2, 86.4, 21.8 ppm.

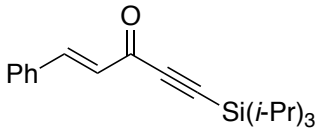

IV-44ss

IV-44ss: (Triisopropylsilyl)acetylene (182.4 mg, 1.0 mmol) and cinnamaldehyde (132.2 mg, 1.0 mmol) were subject to general procedure B to provide 240.5 mg (77% yield) of the pure product as a yellow oil; ^{1}H NMR (500 MHz, $CDCl_3$) δ 7.93 (1H, d, J = 16.5 Hz), 7.56-7.53 (2H, m), 7.45-7.40 (3H, m), 6.79 (1H, d, J = 16.5 Hz), 1.16 (18H, d, J = 5.0 Hz), 1.22-1.15 (3H, m) ppm; ^{13}C NMR (125 MHz, $CDCl_3$) δ 178.1, 149.0, 134.1, 131.2, 129.1, 128.7, 128.6, 128.6, 102.6, 96.2, 18.6,18.6, 11.1 ppm.

IV-5.5. General procedure C for the synthesis of enones IV-48ss, IV-74ss and IV-75ss:[80,81]

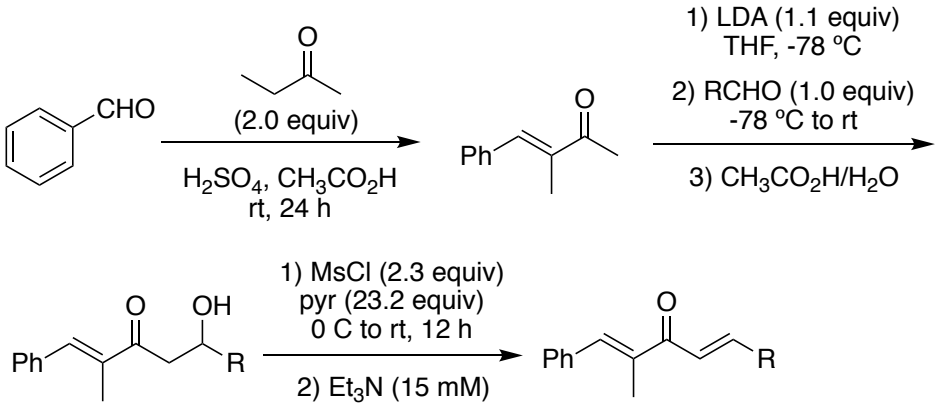

To a stirred solution of benzaldehyde (1.0 equiv) and 2-butanone (2.0 equiv) in acetic acid (1.25 mM), concentrated H_2SO_4 (0.95 equiv) was added slowly at room temperature. The reaction was allowed to stir for 20 h. The mixture was neutralized with 25% aqueous NaOH solution. The residue was extracted with EtOAc and the combined organic layers were separated and dried over Na_2SO_4, and concentrated under reduced pressure. The crude was purified by silica gel column chromatography to provide the enones using ethyl acetate and hexanes as the eluent.

A solution of diisopropylamine (1.01 equiv.) in THF at -78 °C was treated with *n*-BuLi (1.0 equiv.) for 30 min, and the enone (1.0 equiv.) was added. After 30 min, aldehyde (2.0 equiv.) was added at the same temperature. After another 60 min, the reaction was quenched by addition of HOAc-H_2O (1:1 v/v) at -78 °C. The flask was warmed up to room temperature, followed by separation of the two phases. The aqueous phase was extracted with Et_2O. The combined organic phases were washed with saturated $NaHCO_3$ and brine, and dried with anhydrous Na_2SO_4. The crude aldol product was used for the next step without further purification.

The aldol production was dissolved in pyridine (12.4 equiv.) at 0 °C and methanesulfonyl chloride (1.22 equiv.) was added. The solution was kept at room

temperature overnight and H_2O was added. The mixture was extracted with Et_2O and the combined phase was washed by saturated $CuSO_4$ and brine. The organic layer was dried over anhydrous Na_2SO_4, concentrated under reduced pressure, and redisposed in Et_2O. Et_3N (15 mM) was added and the mixture was stirred at room temperature for 18 h. The reaction was quenched by addition of water, followed by extraction with Et_2O. The combined organic layers were washed with cold 1% HCl, saturated $NaHCO_3$, and then water. The organic phase was dried over $MgSO_4$, then filtrated and concentrated under reduced pressure to a crude oil, which was purified by silica gel column chromatography to deliver the asymmetric dienone using ethyl acetate and hexanes as the eluent.

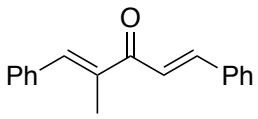

IV-48ss

IV-48ss: Benzaldehyde (106.1 mg, 1.0 mmol) was subject to general procedure C to provide 119.2 mg (48% yield) of the pure product as a light yellow oil; ^1H NMR (500 MHz, $CDCl_3$) 7.71 (1H, d, J = 16.0 Hz), 7.66-7.57 (3H, m), 7.50-7.34 (9H, m), 2.20 (3H, d, J = 1.0 Hz) ppm; ^{13}C NMR (125 MHz, $CDCl_3$) δ 192.7, 143.4, 138.7, 138.5, 136.0, 135.1, 130.2, 129.7, 128.9, 128.5, 128.5, 128.2, 121.9, 13.8 ppm.

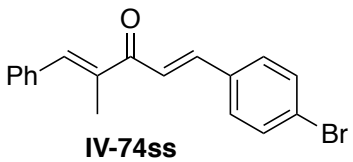

IV-74ss

IV-74ss: 4-Bromobenzaldehyde (185.2 mg, 1.0 mmol) was subject to general procedure C to provide 147.2 mg (45% yield) of the pure product as a light yellow solid. m.p: 85 ºC;

^{1}H NMR (500 MHz, $CDCl_3$) 7.63 (1H, d, J = 16.0 Hz), 7.59-7.34 (11H, m), 2.19 (3H, d, J = 1.5 Hz) ppm; ^{13}C NMR (125 MHz, $CDCl_3$) δ 192.4, 142.0, 138.9, 138.5, 135.8, 134.0, 132.1, 129.8, 129.7, 129.6, 128.6, 128.5, 124.4, 122.4, 13.8 ppm.

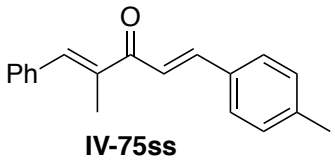

IV-75ss

IV-75ss: *p*-tolualdehyde (120.2 mg, 1.0 mmol) was subject to general procedure C to provide 65.6 mg (25% yield) of the pure product as a light yellow oil; ^{1}H NMR (500 MHz, $CDCl_3$) 7.74-7.32 (9H, m), 7.25-7.16 (2H, m), 2.38 (3H, s), 2.19 (3H, d, J = 1.5 Hz) ppm; ^{13}C NMR (125 MHz, $CDCl_3$) δ 192.8, 143.6, 143.5, 140.7, 138.6, 138.4, 138.4, 136.0, 132.3, 129.7, 129.7, 129.6, 128.5, 128.4, 128.3, 128.3, 120.9, 120.9, 21.5, 13.9 ppm.

IV-5.6. General procedure D for the synthesis of adducts IV-54 and IV-55:

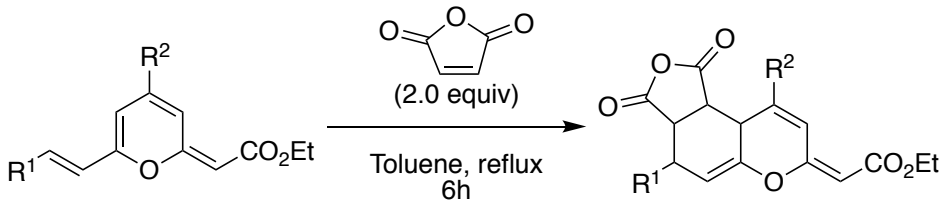

To a solution of pyran (1.0 equiv) in toluene (0.12 mM), maleic anhydride (2.0 equiv) was added. The solution was heated and kept refluxing for 6 h. The solvent was removed by a stream of N_2 gas. The crude was purified by silica gel column chromatography to deliver the adduct using ethyl acetate in hexanes (5-20%) as the eluent.

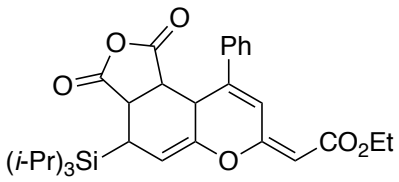

IV-54

IV-54: IV-44 (25.0 mg, 0.06 mmol) was subject to general procedure D to provide 4.2 mg (14% yield) of the pure product as a light yellow oil; ^{1}H NMR (500 MHz, $CDCl_3$) 8.31 (1H, d, J = 2.0 Hz), 7.67-7.58 (2H, m), 7.49-7.43 (3H, m), 6.52 (2H, s), 6.31 (1H, d, J = 2.0 Hz), 4.70-4.61 (1H, m), 4.23 (2H, ddd, J = 7.5, 7.5, 3.0 Hz),3.23 (1H, dd, J = 10.5, 19.0 Hz), 2.93 (1H, dd, J = 6.5, 19.0 Hz), 1.31 (3H, t, J = 7.5 Hz), 1.12-1.06 (21H, m) ppm; ^{13}C NMR (125 MHz, $CDCl_3$) δ 170.8, 163.0, 154.6, 144.8, 136.1, 136.0, 132.0, 130.1, 129.1, 126.3, 114.6, 105.9, 96.2, 60.7, 36.6, 24.7, 18.6, 18.6, 14.0, 10.9, 1.02 ppm; HRMS (ESI) Calculated Mass for $C_{30}H_{39}O_6Si$: 523.2516 ($[M+H]^+$), Found 523.2529 ($[M+H]^+$).

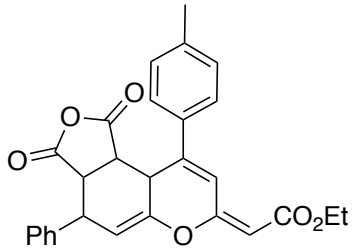

IV-55

IV-55: IV-46 (16.0 mg, 0.045 mmol) was subject to general procedure D to provide 5.2 mg (25% yield) of the pure product was isolated as a light yellow oil; ^{1}H NMR (500 MHz, $CDCl_3$) 8.31 (1H, d, J = 1.5 Hz), 7.56-7.50 (4H, m), 7.44-7.38 (2H, m), 7.38-7.33 (1H, m), 7.29-7.27 (1H, m), 7.11 (1H, d, J = 16.0 Hz), 6.69 (1H, d, J = 16.0 Hz), 6.38 (1H, d, J = 1.5 Hz), 4.79-4.70 (1H, m), 4.24 (2H, ddd, J = 7.0, 7.0, 1.5 Hz), 3.32 (1H, dd, J = 10.5, 19.0 Hz), 2.98 (1H, dd, J = 7.0, 19.0 Hz), 2.41 (3H, s), 1.32 (3H, t, J = 7.0 Hz) ppm; ^{13}C

NMR (125 MHz, $CDCl_3$) δ 170.9, 163.2, 144.6, 140.6, 135.2, 133.0, 129.8, 129.4, 129.0, 127.3, 126.2, 119.5, 113.6, 106.4, 95.9, 60.6, 21.4, 14.1, 1.0 ppm; HRMS (ESI) Calculated Mass for $C_{28}H_{25}O_6$: 457.1651 ($[M+H]^+$), Found 457.1688 ($[M+H]^+$).

IV-5.7. General procedure E for the synthesis of carbocyclic *β*–amino ester:

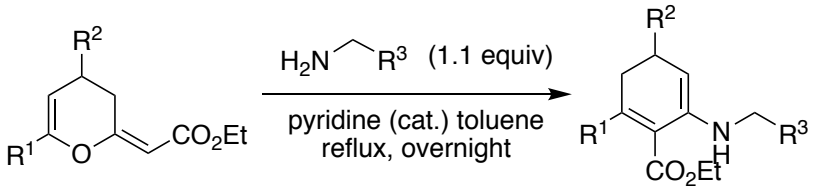

To a solution of dihydropyran (1.0 equiv) and amine (1.1 equiv) in toluene, pyridine (cat.) was added. The solution was kept refluxing overnight. The solvent was removed under N_2 flow. The crude was purified by silica gel column chromatography to deliver the adduct using ethyl acetate and hexanes as the eluent.

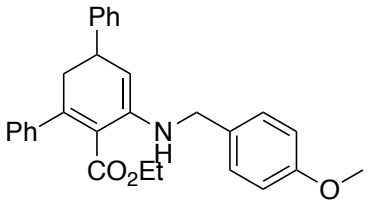

IV-72 ab

IV-55: **IV-32** (32.0 mg, 0.1 mmol) and 4-methoxybenzylamine (27.4 mg, 0.2 mmol) were subject to general procedure E to provide 35.6 mg (81% yield) of the pure product as a light yellow oil; ^1H NMR (500 MHz, $CDCl_3$) 9.73 (1H, t, J = 6.0 Hz), 7.32-7.22 (11H, m), 7.17-7.13 (2H, m), 6.89-6.84 (2H, m), 5.56 (1H, d, J = 3.5 Hz), 4.42 (2H, ddd, J = 15.5, 15.5, 6.0 Hz), 3.84-3.73 (2H, m), 3.80 (3H, s), 3.63 (1H, dt, J = 4.5, 13.0 Hz), 2.80 (1H, dd, J = 5.5, 16.0 Hz), 2.55 (1H, dd, J = 14.0, 16.0 Hz), 0.62 (3H, t, J = 7.0 Hz) ppm; ^{13}C NMR (125 MHz, $CDCl_3$) δ 169.4, 163.0, 158.9, 144.2, 144.0, 140.0, 130.0, 128.6, 128.1,

127.7, 127.6, 126.6, 126.2, 126.0, 121.0, 114.2, 93.4, 58.6, 55.3, 46.7, 40.2, 34.7, 29.7, 13.3 ppm.

APPENDIX

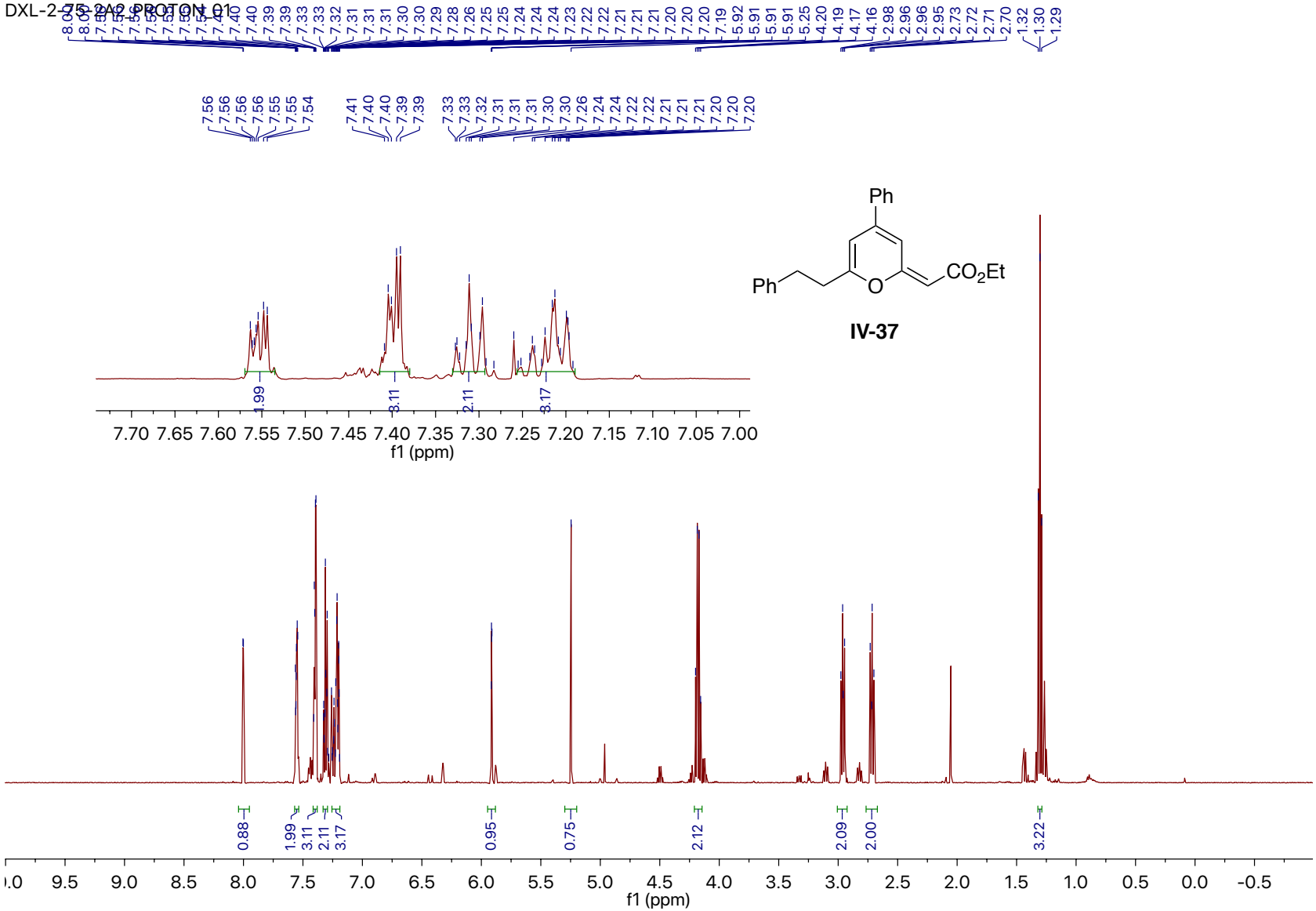
DXL-2-75-2A2 PROTON 01
Ph
Ph
O
CO2Et
IV-37
1.99
3.11
2.11
3.17
7.70 7.65 7.60 7.55 7.50 7.45 7.40 7.35 7.30 7.25 7.20 7.15 7.10 7.05 7.00
f1 (ppm)
0.88
1.99
3.11
2.11
3.17
0.95
0.75
2.12
2.09
2.00
3.22
9.5 9.0 8.5 8.0 7.5 7.0 6.5 6.0 5.5 5.0 4.5 4.0 3.5 3.0 2.5 2.0 1.5 1.0 0.5 0.0 -0.5
f1 (ppm)

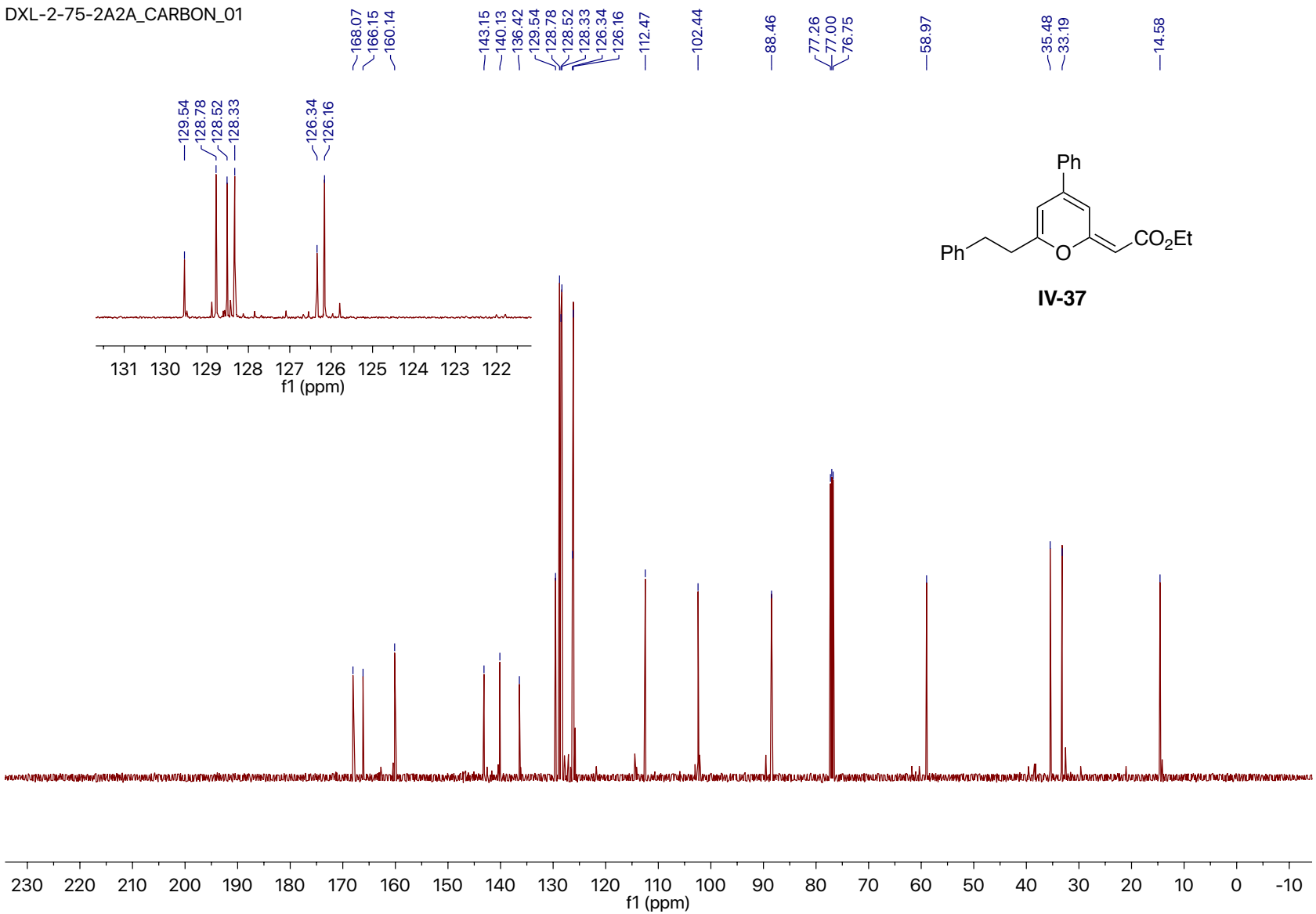
DXL-2-75-2A2A_CARBON_01
168.07
166.15
160.14
143.15
140.13
136.42
129.54
128.78
128.52
128.33
126.34
126.16
112.47
102.44
88.46
77.26
77.00
76.75
58.97
35.48
33.19
14.58
Ph
Ph
O
CO2Et
IV-37
f1 (ppm)
f1 (ppm)

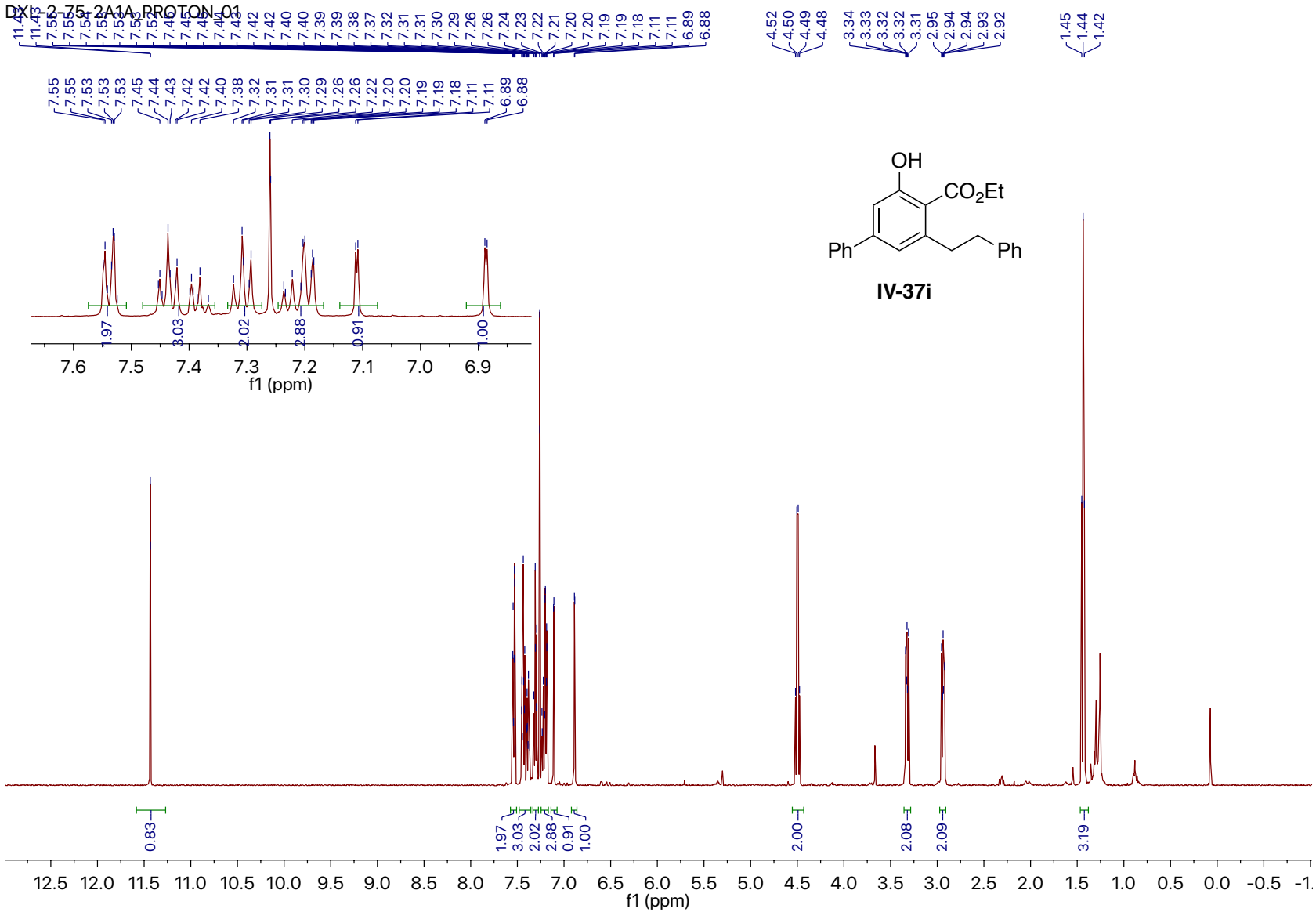
DXL-2-75-2A1A-PROTON-01
OH
CO2Et
Ph
Ph
IV-37i
f1 (ppm)
f1 (ppm)

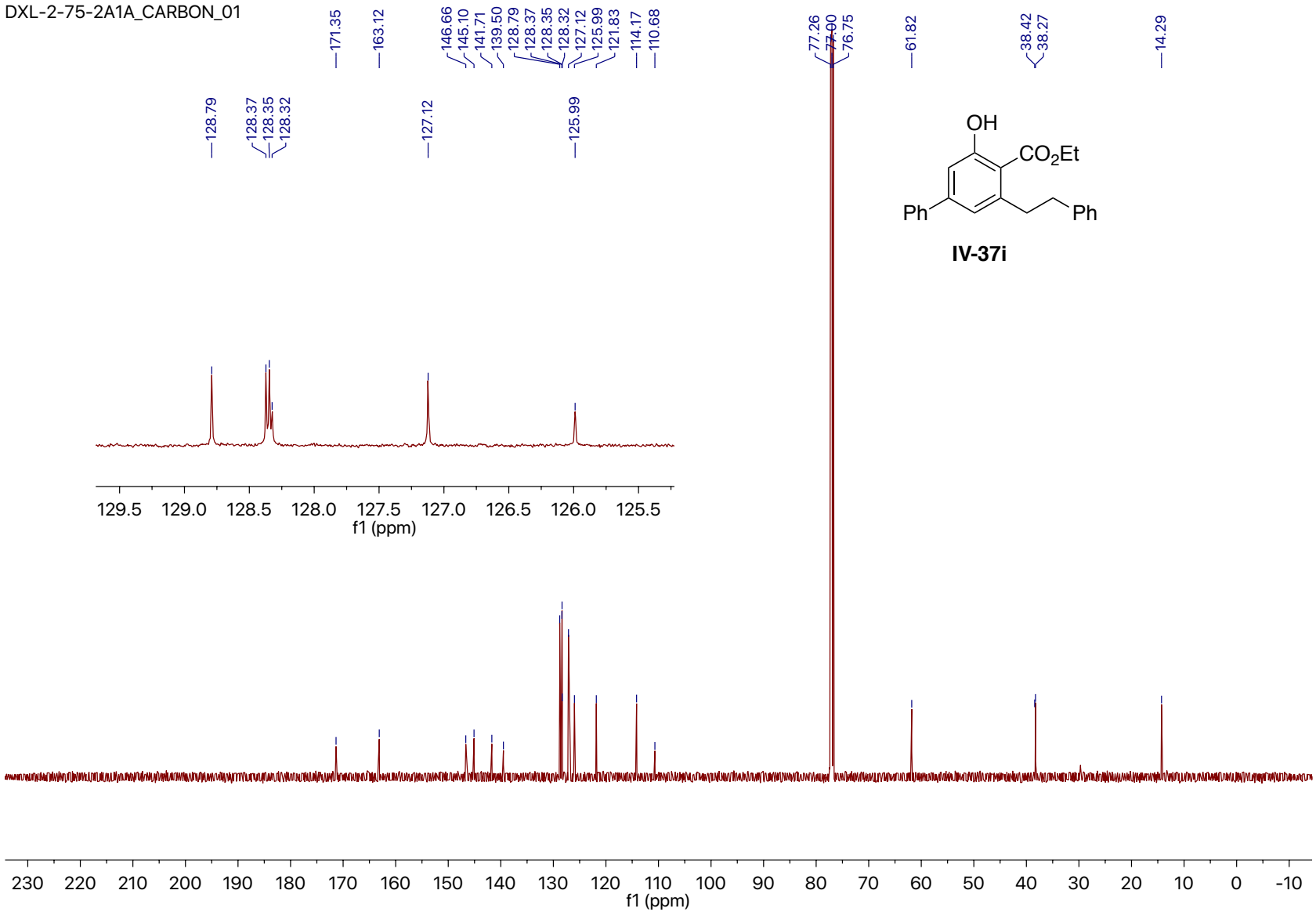
DXL-2-75-2A1A_CARBON_01
171.35
163.12
146.66
145.10
141.71
139.50
128.79
128.37
128.35
128.32
127.12
125.99
121.83
114.17
110.68
77.26
77.00
76.75
61.82
38.42
38.27
14.29
OH
CO2Et
Ph
Ph
IV-37i
f1 (ppm)
f1 (ppm)

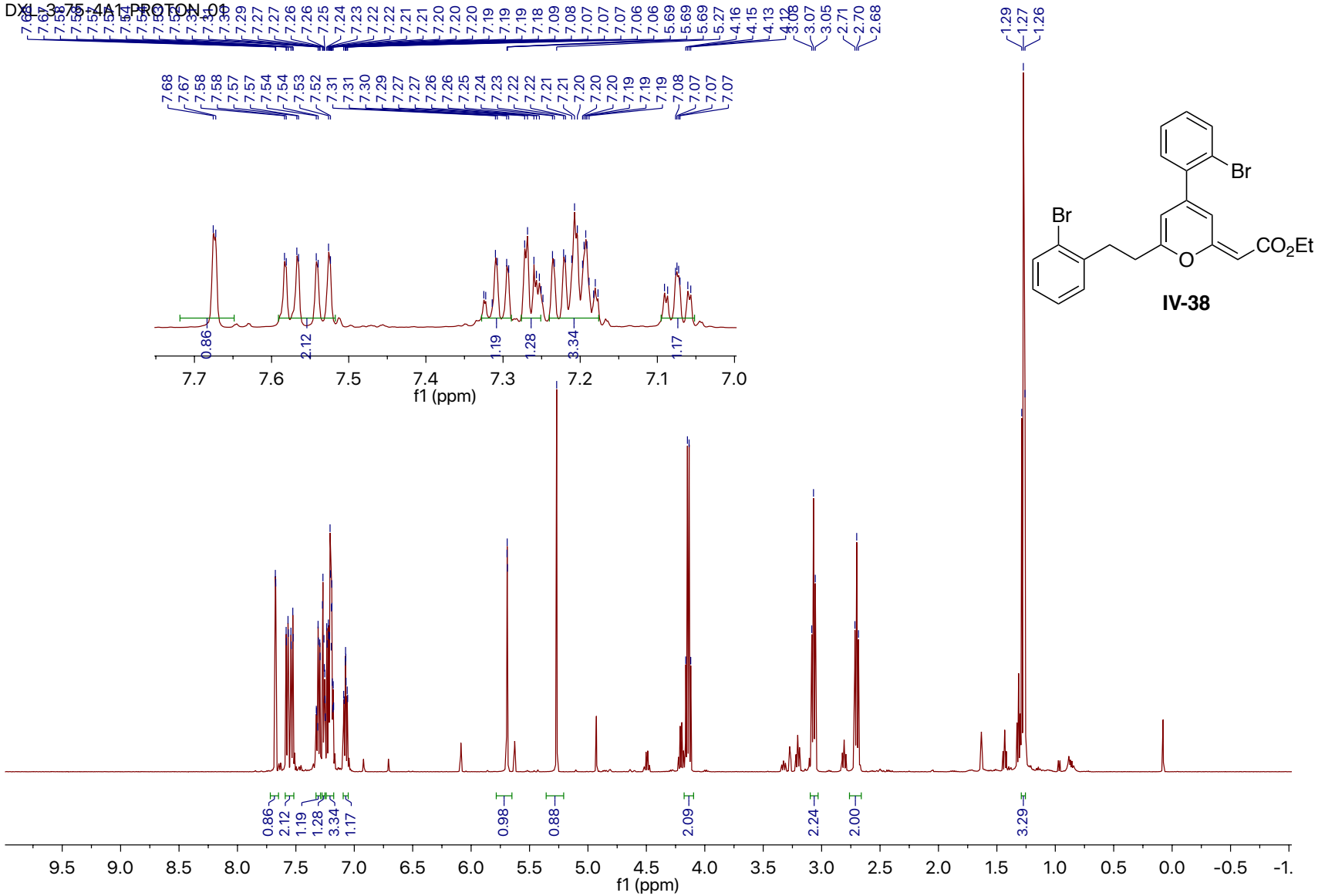
DXL-3-75-4A1-PROTON-01
Br
Br
O
CO2Et
IV-38
f1 (ppm)

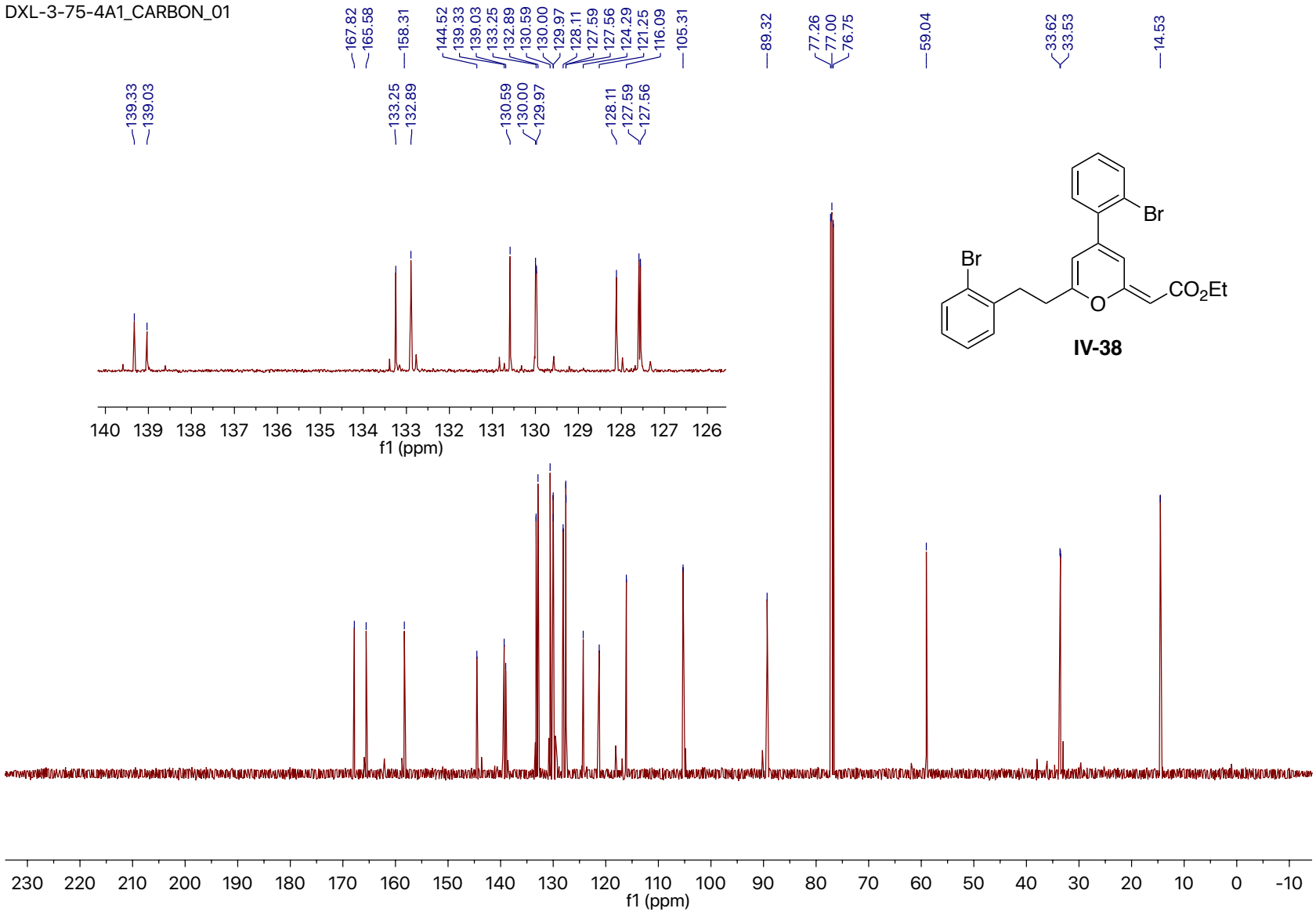
DXL-3-75-4A1_CARBON_01
167.82
165.58
158.31
144.52
139.33
139.03
133.25
132.89
130.59
130.00
129.97
128.11
127.59
127.56
124.29
121.25
116.09
105.31
89.32
77.26
77.00
76.75
59.04
33.62
33.53
14.53
Br
Br
O
CO2Et
IV-38
f1 (ppm)
f1 (ppm)

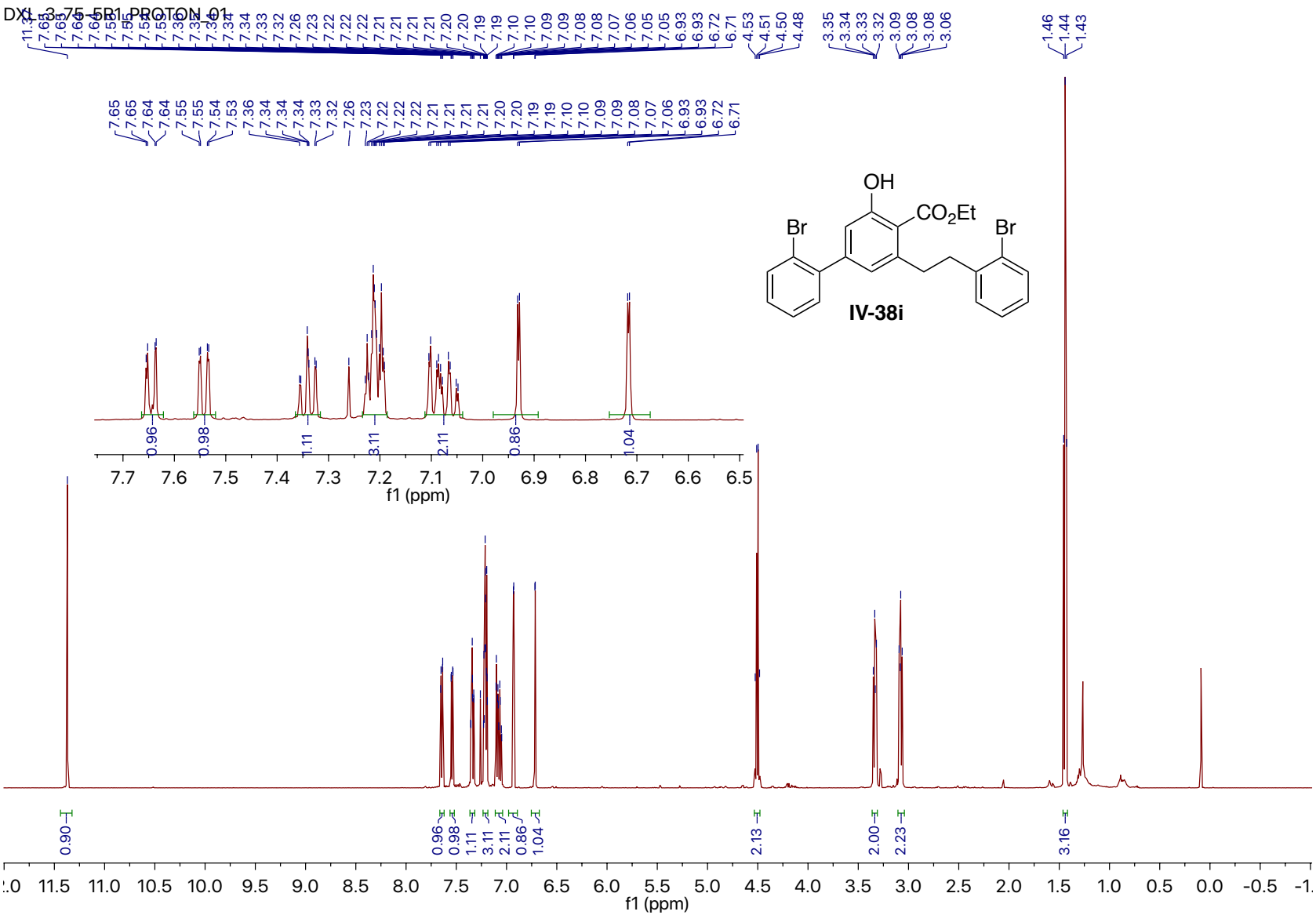
DXL-3-75-5R1-PROTON-01
OH
CO2Et
Br
Br
IV-38i
f1 (ppm)

DXL-3-75-5R1_CARBON_01

171.16
162.33
146.66
143.73
141.11
140.65
133.16
132.77
130.73
130.33
129.22
127.69
127.33
124.55
124.25
124.23
121.94
116.89
111.25
77.25
77.00
76.75
61.90
38.02
36.09
14.24

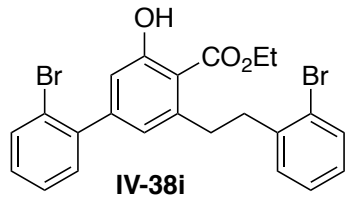

IV-38i

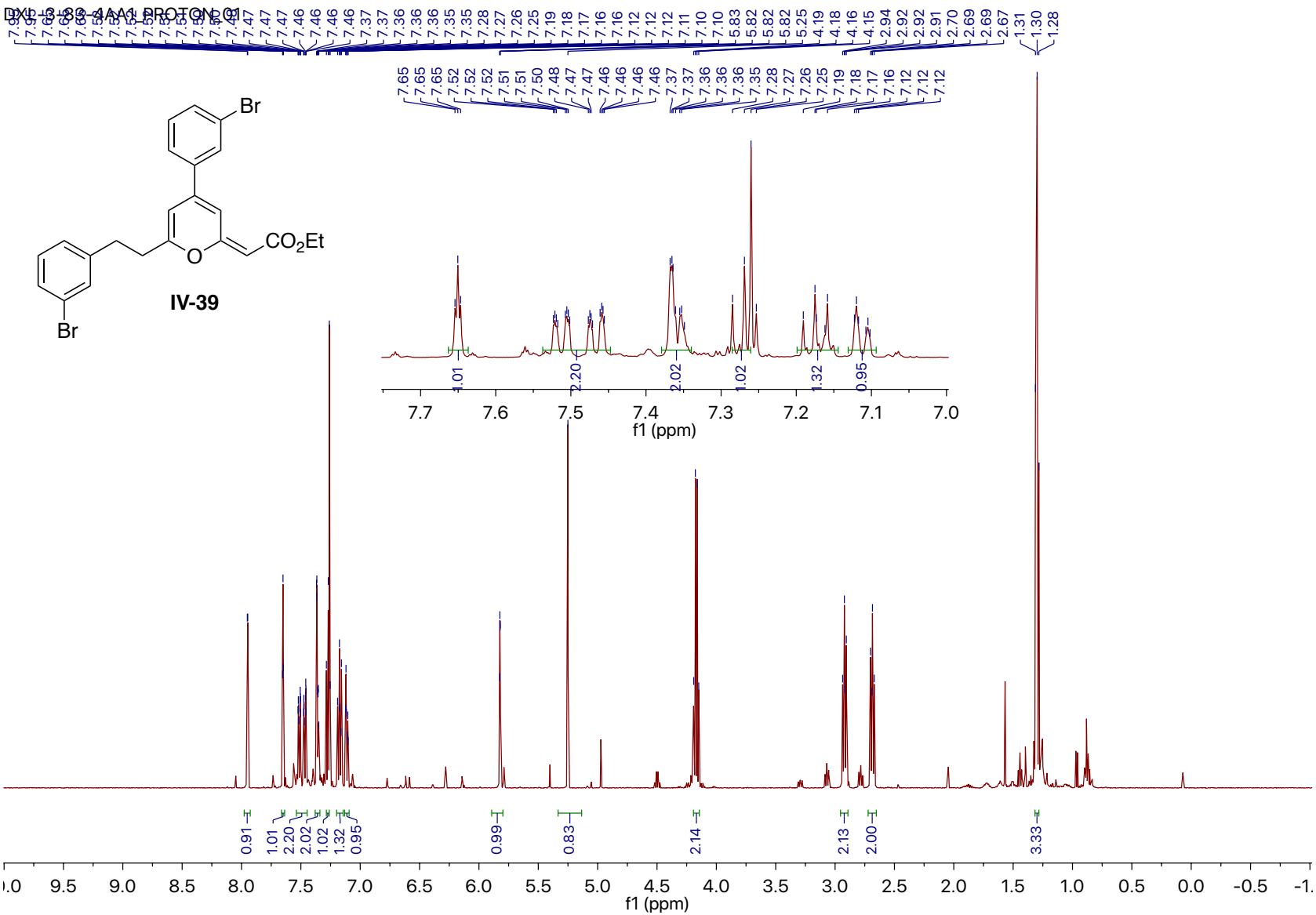
DXL-3-88-4AA1 PROTON-01
Br
CO2Et
O
Br
IV-39
f1 (ppm)

DXL-3-83-4AA1_CARBON_01

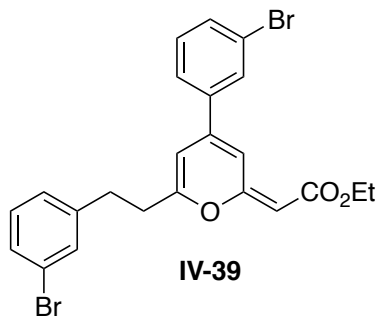

IV-39

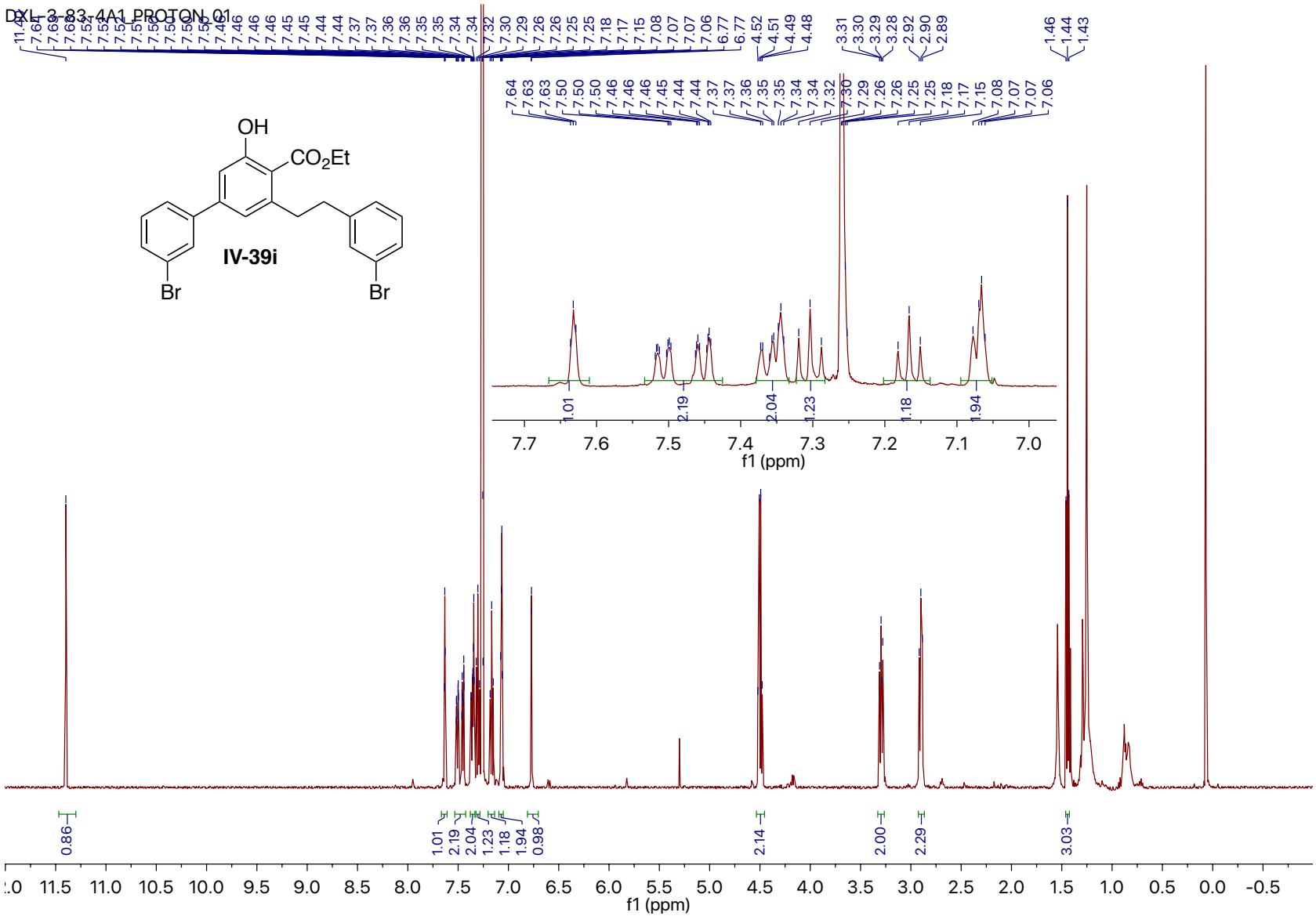
DXL-3-83-4A1 PROTON 01
OH
CO2Et
IV-39i
Br
Br
f1 (ppm)

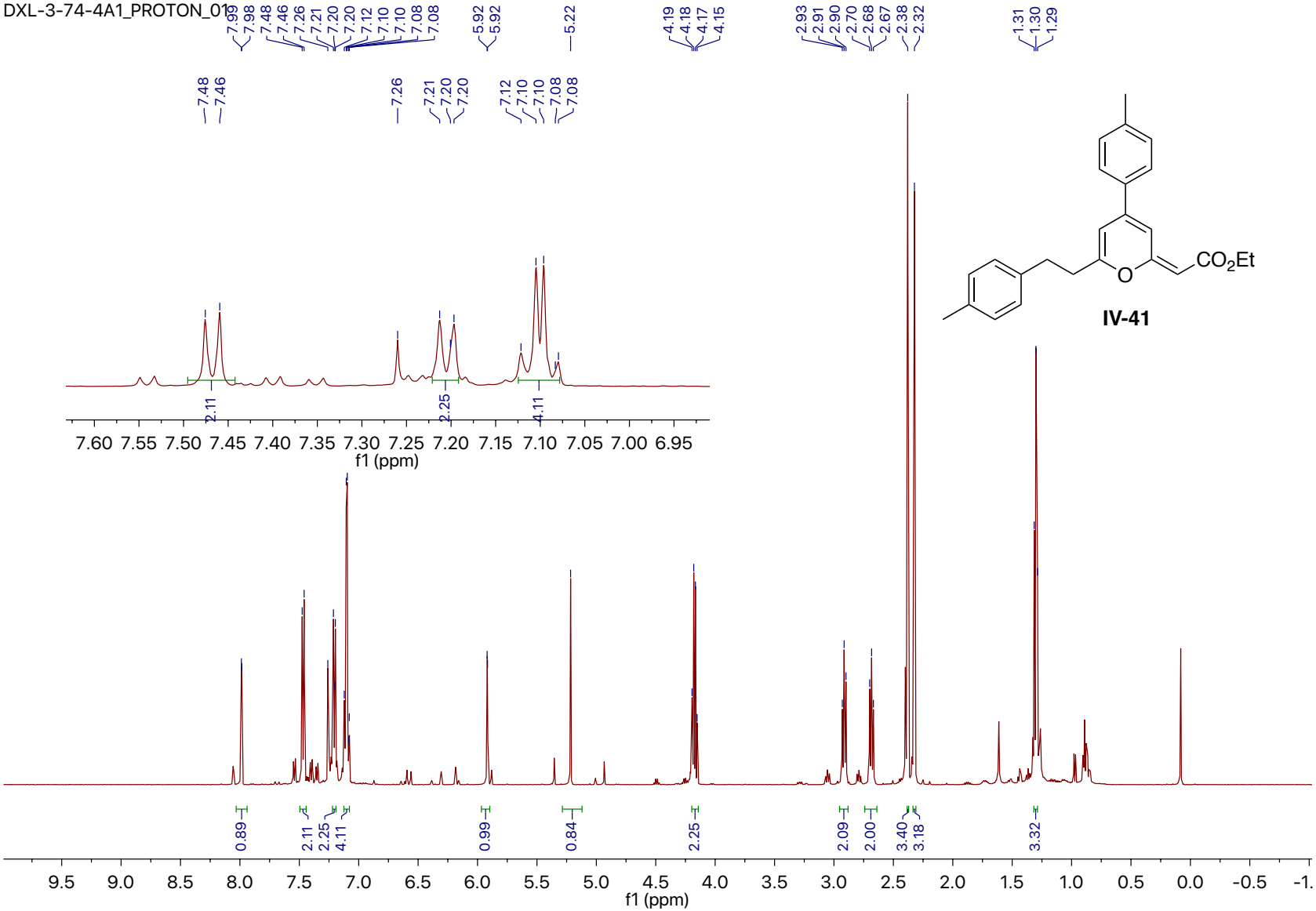
DXL-3-74-4A1_PROTON_01
7.99
7.98
7.48
7.46
7.26
7.21
7.20
7.20
7.12
7.10
7.10
7.08
7.08
5.92
5.92
5.22
4.19
4.18
4.17
4.15
2.93
2.91
2.90
2.70
2.68
2.67
2.38
2.32
1.31
1.30
1.29
CO2Et
O
IV-41
2.11
2.25
4.11
f1 (ppm)
0.89
2.11
2.25
4.11
0.99
0.84
2.25
2.09
2.00
3.40
3.18
3.32
f1 (ppm)

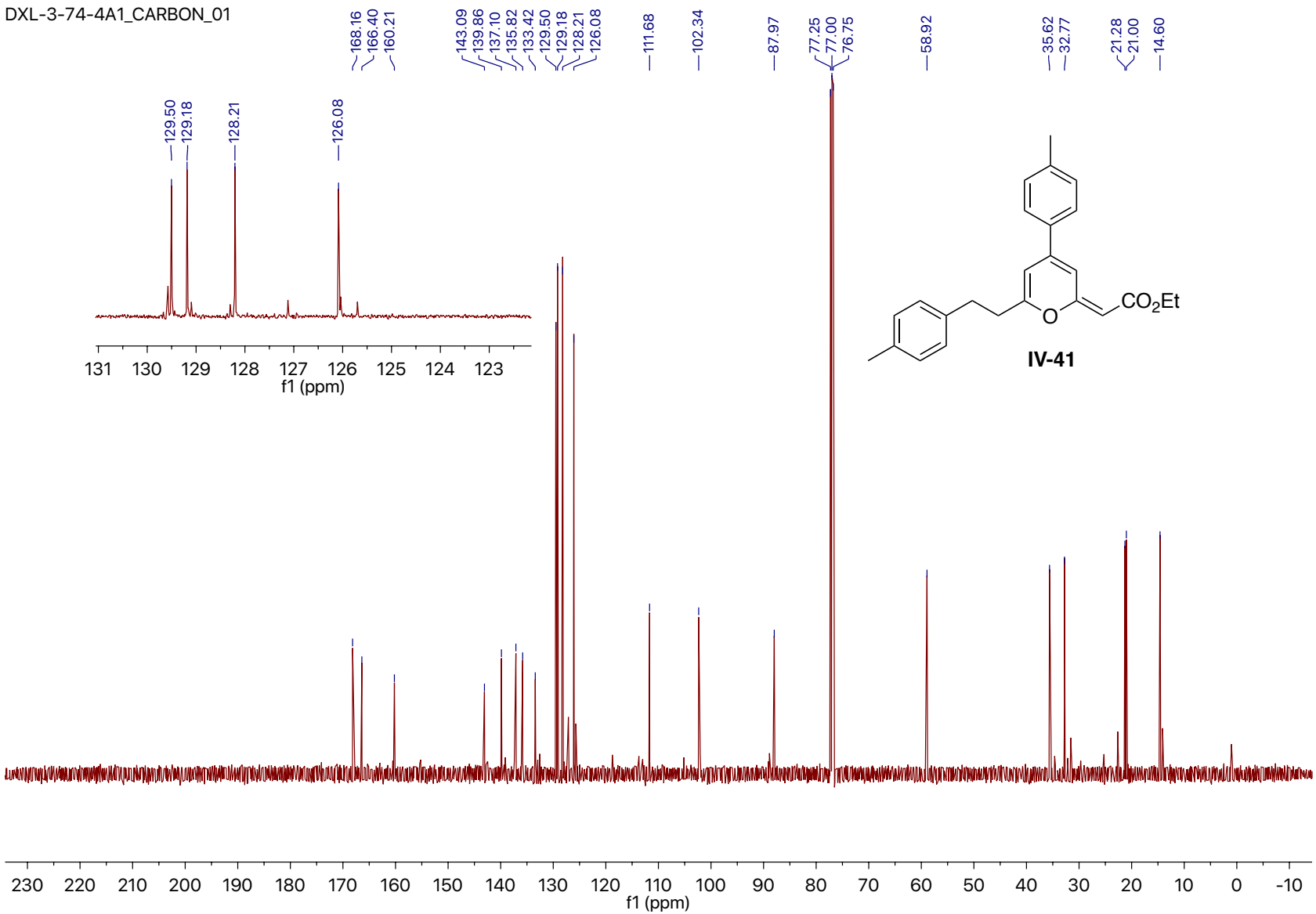
DXL-3-74-4A1_CARBON_01
168.16
166.40
160.21
143.09
139.86
137.10
135.82
133.42
129.50
129.18
128.21
126.08
111.68
102.34
87.97
77.25
77.00
76.75
58.92
35.62
32.77
21.28
21.00
14.60
129.50
129.18
128.21
126.08
131 130 129 128 127 126 125 124 123
f1 (ppm)
CO2Et
O
IV-41
230 220 210 200 190 180 170 160 150 140 130 120 110 100 90 80 70 60 50 40 30 20 10 0 -10
f1 (ppm)

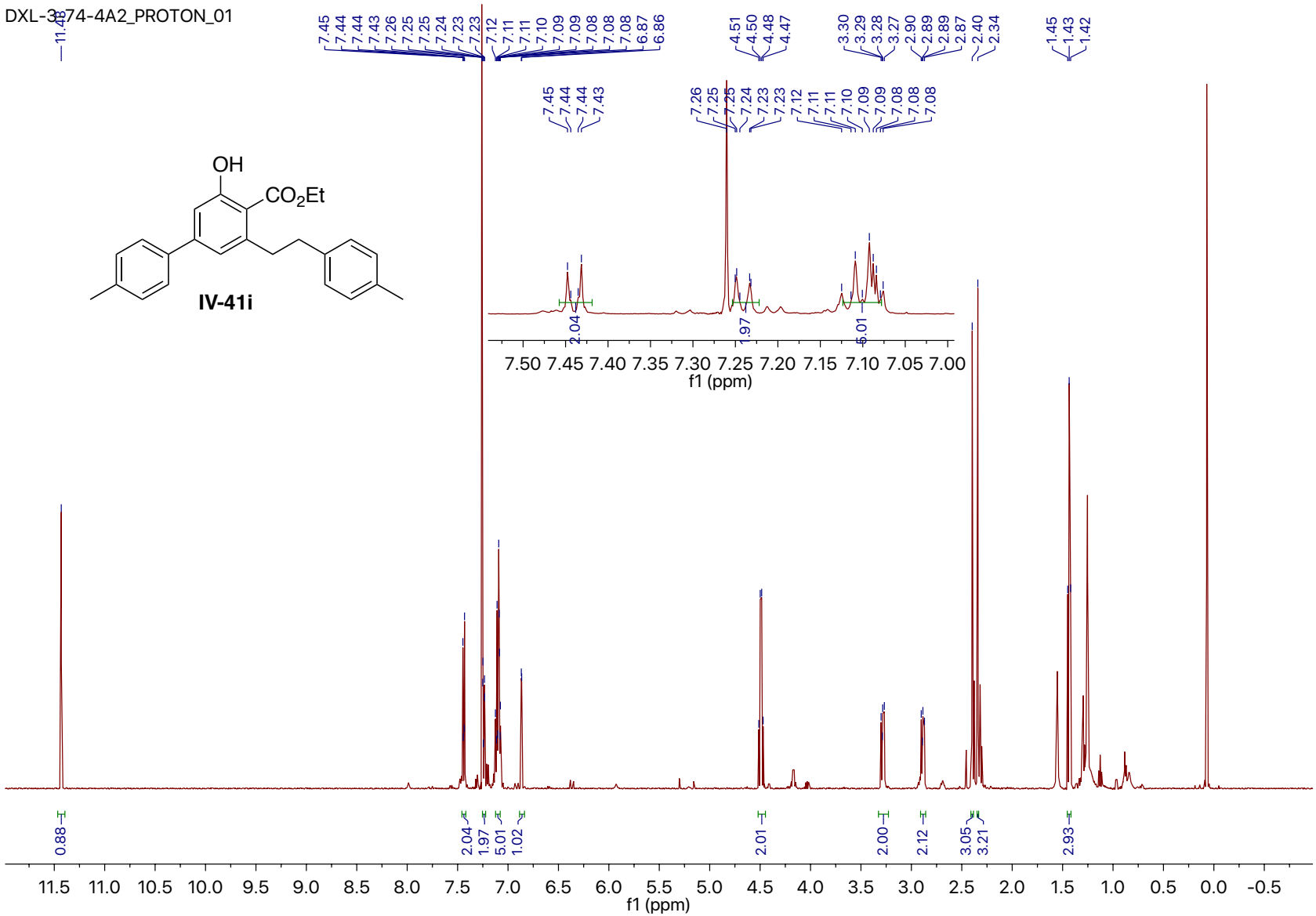
DXL-3874-4A2_PROTON_01
OH
CO2Et
IV-41i
f1 (ppm)
f1 (ppm)

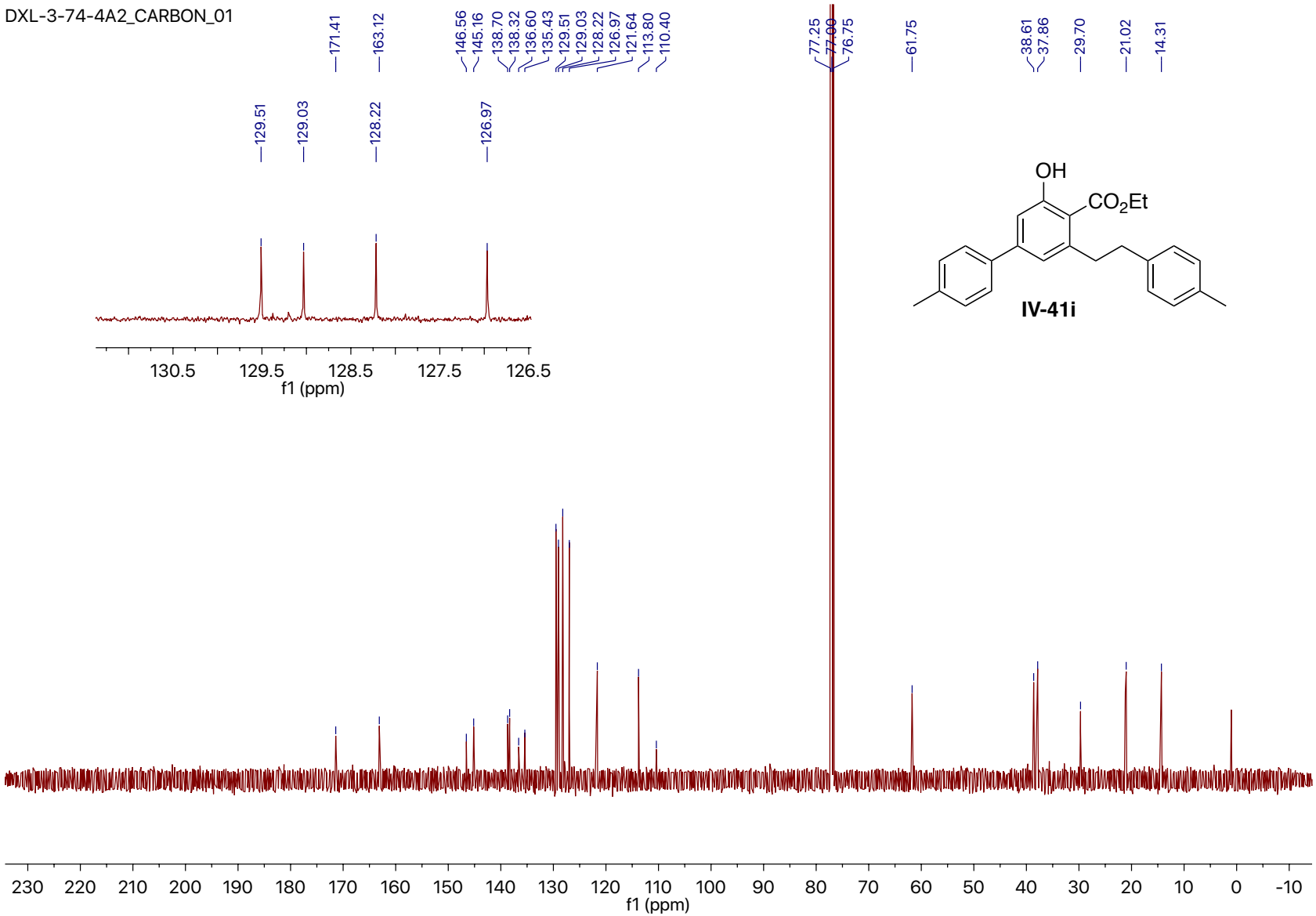
DXL-3-74-4A2_CARBON_01
171.41
163.12
146.56
145.16
138.70
138.32
136.60
135.43
129.51
129.03
128.22
126.97
121.64
113.80
110.40
77.25
77.00
76.75
61.75
38.61
37.86
29.70
21.02
14.31
129.51
129.03
128.22
126.97
130.5
129.5
128.5
127.5
126.5
f1 (ppm)
OH
CO2Et
IV-41i
230
220
210
200
190
180
170
160
150
140
130
120
110
100
90
80
70
60
50
40
30
20
10
0
-10
f1 (ppm)

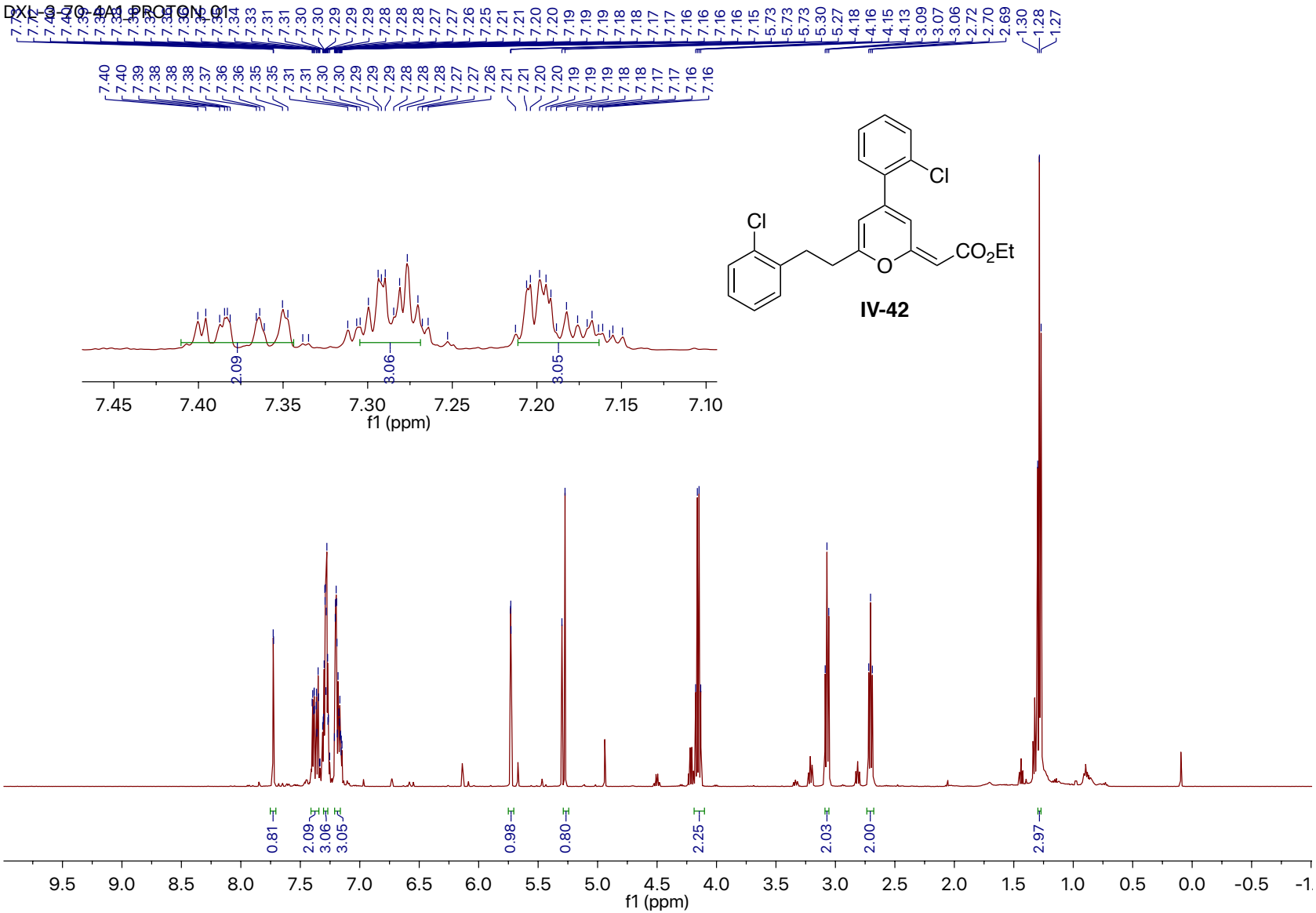
DXL-3-70-4A1 PROTON 01
Cl
Cl
O
CO2Et
IV-42
f1 (ppm)
f1 (ppm)

DXL-3-70-4A1_CARBON_01

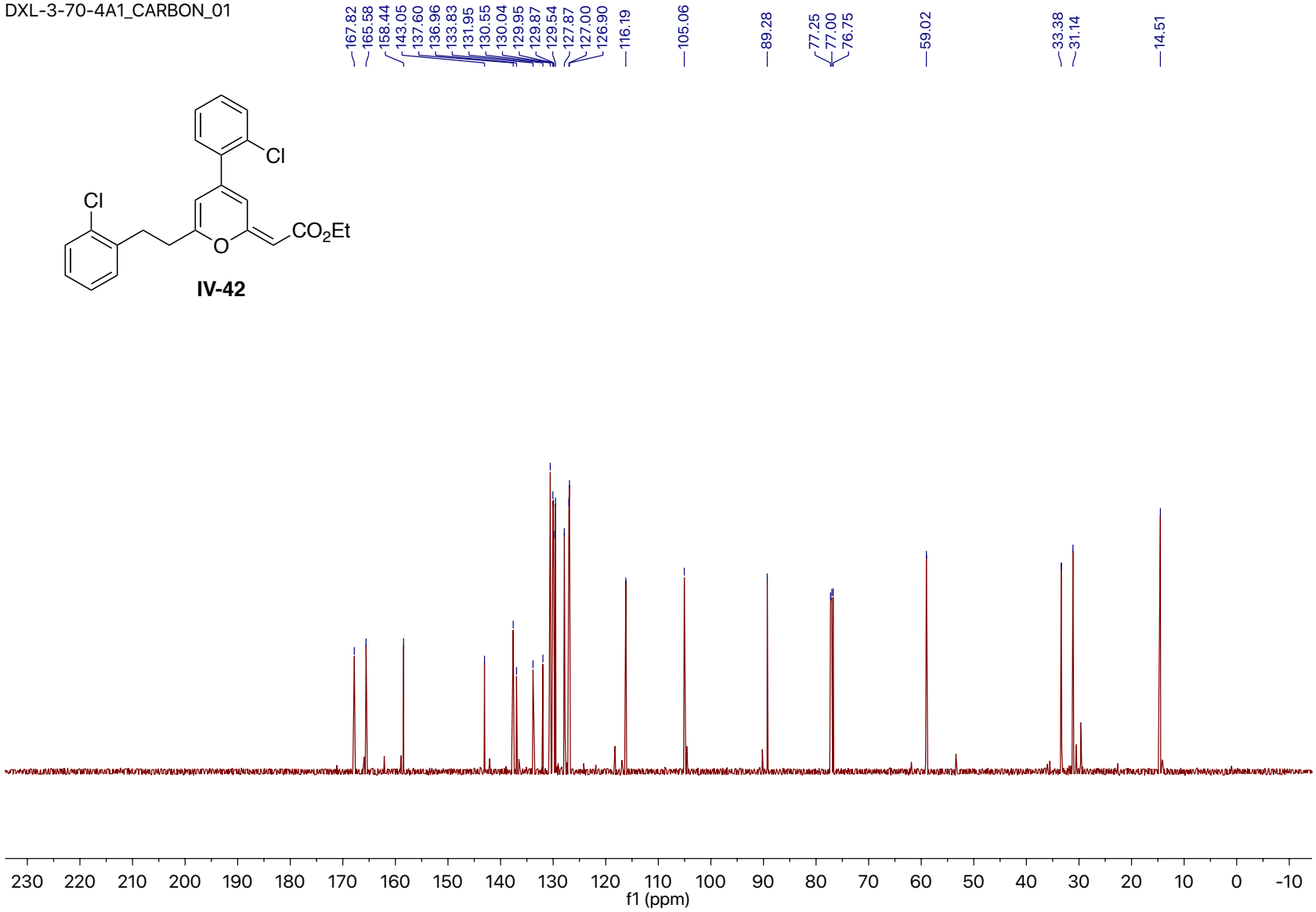

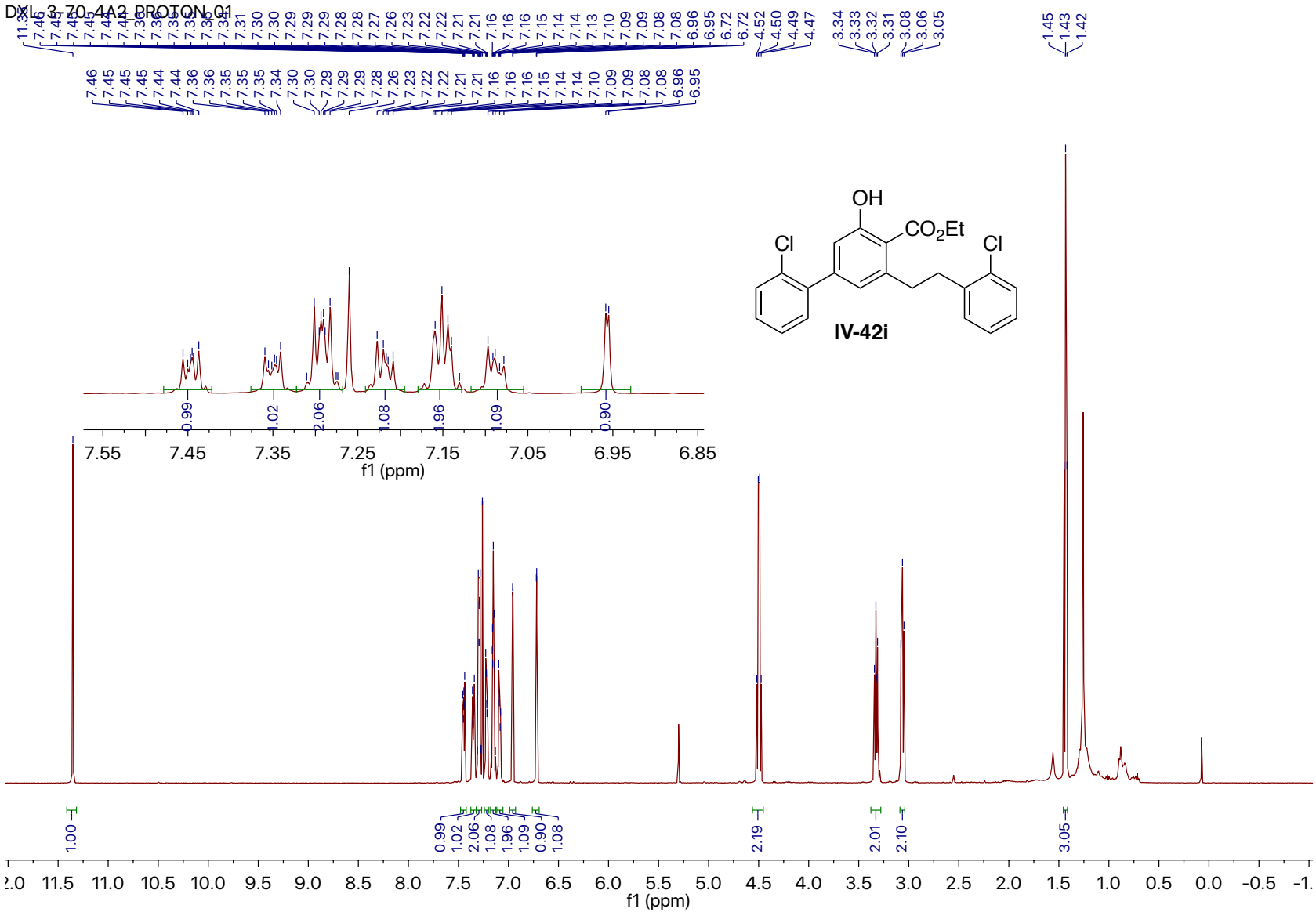
DXL-3-70-4A2 PROTON-01
OH
CO2Et
Cl
Cl
IV-42i
f1 (ppm)

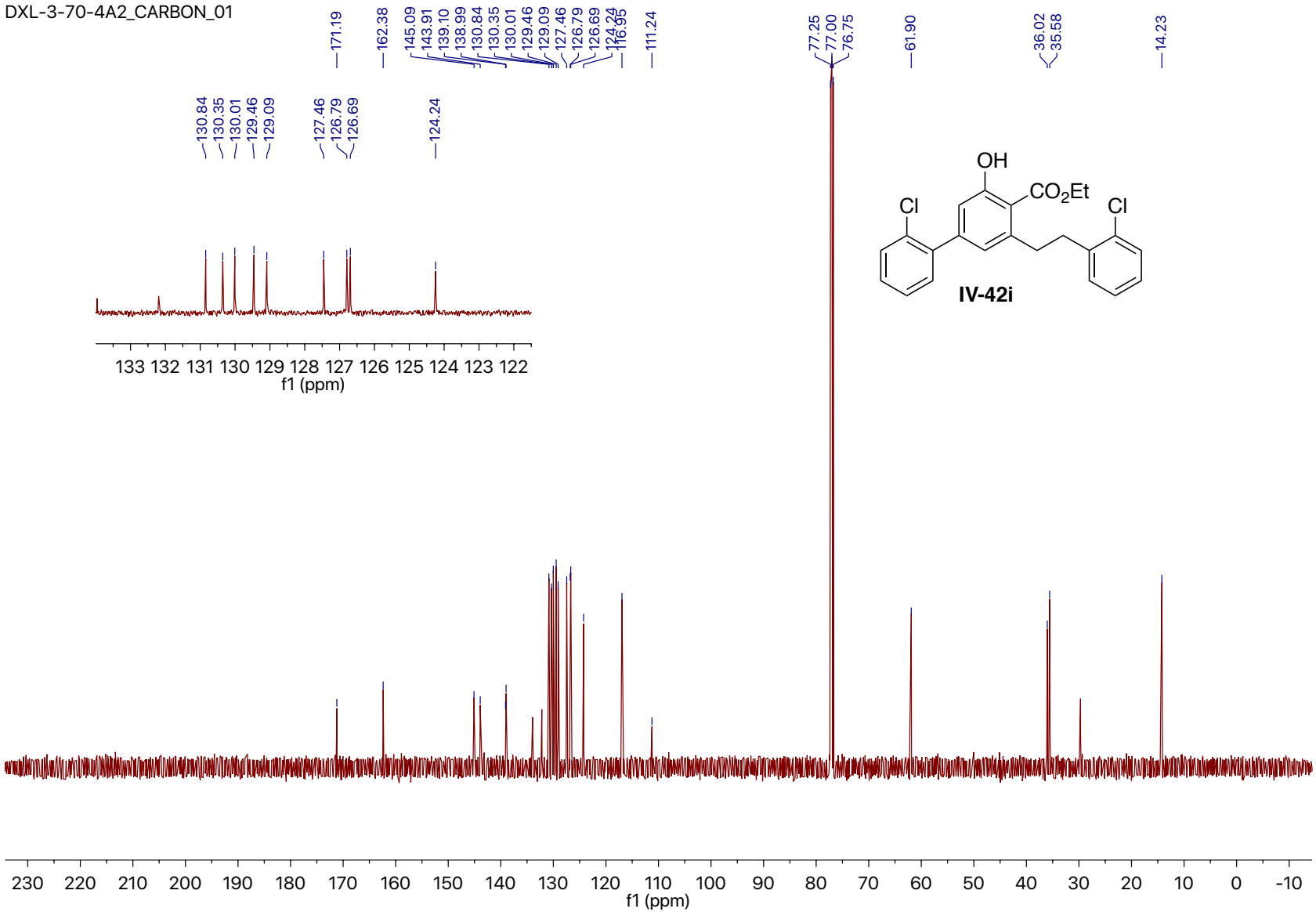
DXL-3-70-4A2_CARBON_01
171.19
162.38
145.09
143.91
139.10
138.99
130.84
130.35
130.01
129.46
129.09
127.46
126.79
126.69
124.24
116.95
111.24
77.25
77.00
76.75
61.90
36.02
35.58
14.23
OH
CO2Et
Cl
Cl
IV-42i
f1 (ppm)
f1 (ppm)

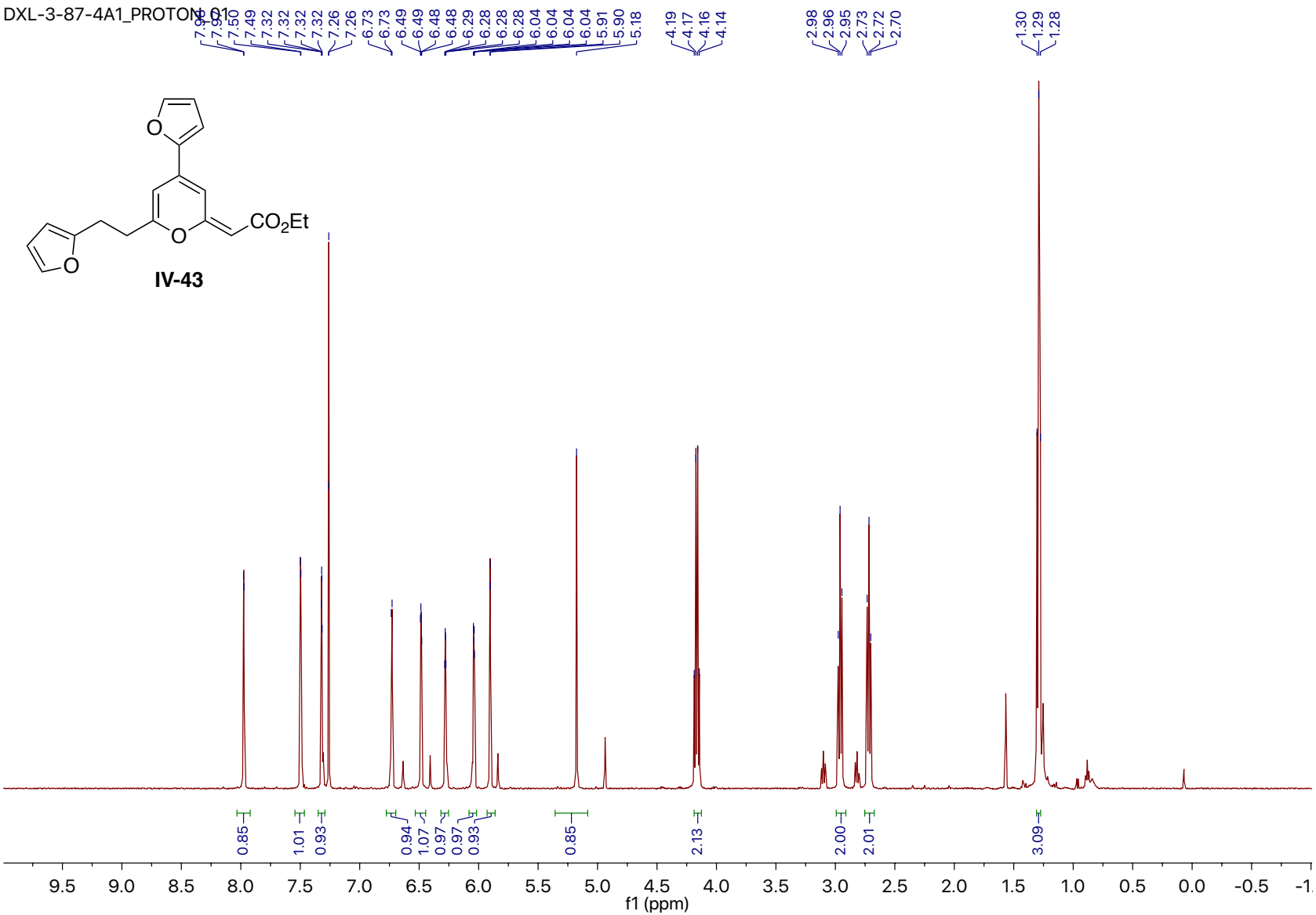
DXL-3-87-4A1_PROTON_01
7.99
7.97
7.50
7.49
7.32
7.32
7.32
7.32
7.26
7.26
6.73
6.73
6.49
6.49
6.48
6.48
6.29
6.28
6.28
6.28
6.04
6.04
6.04
6.04
5.91
5.90
5.18
4.19
4.17
4.16
4.14
2.98
2.96
2.95
2.73
2.72
2.70
1.30
1.29
1.28
O
O
O
CO2Et
IV-43
0.85
1.01
0.93
0.94
1.07
0.97
0.97
0.93
0.85
2.13
2.00
2.01
3.09
9.5
9.0
8.5
8.0
7.5
7.0
6.5
6.0
5.5
5.0
4.5
4.0
3.5
3.0
2.5
2.0
1.5
1.0
0.5
0.0
-0.5
f1 (ppm)

DXL-3-87-4A1_CARBON_01

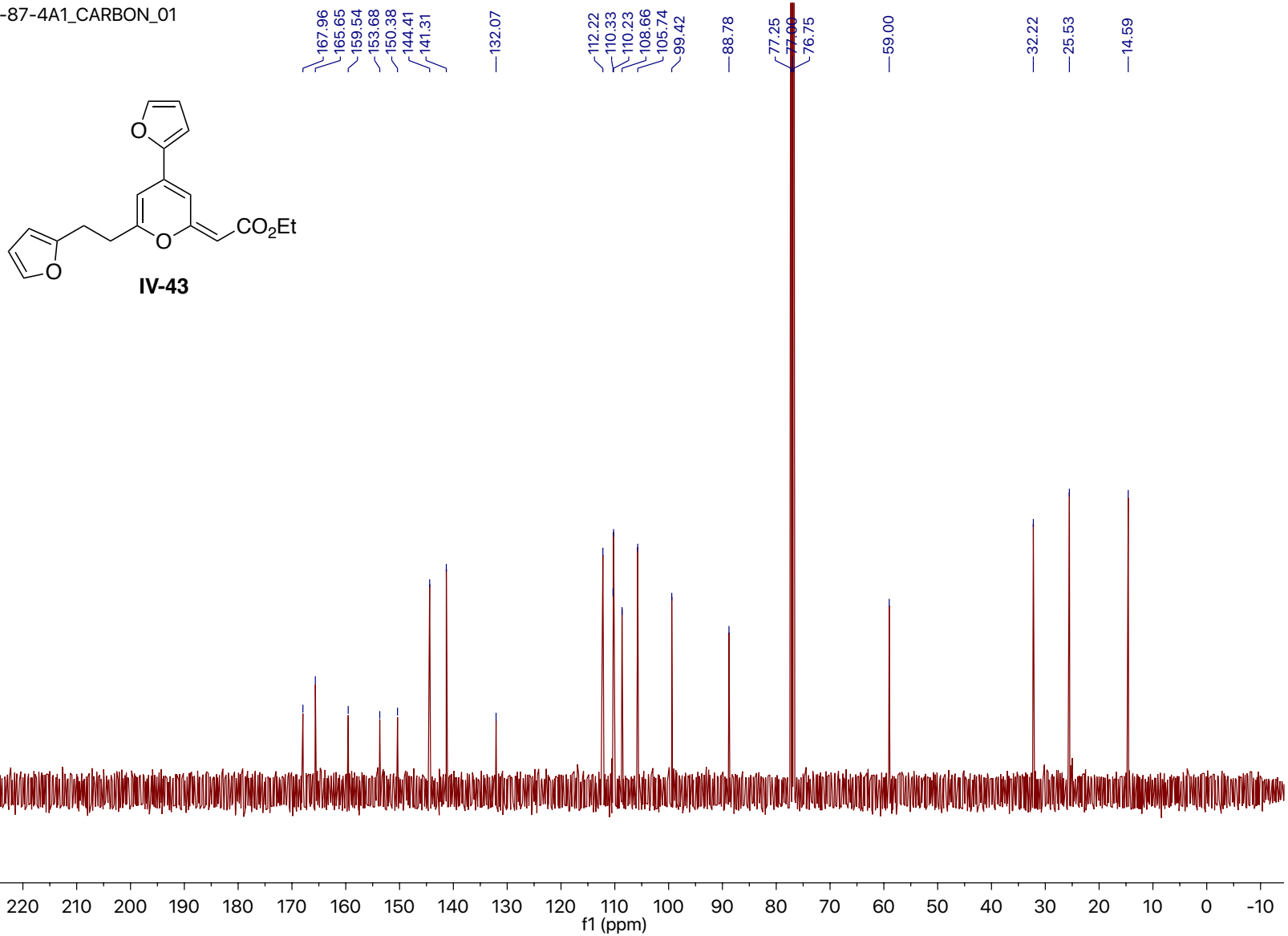

IV-43

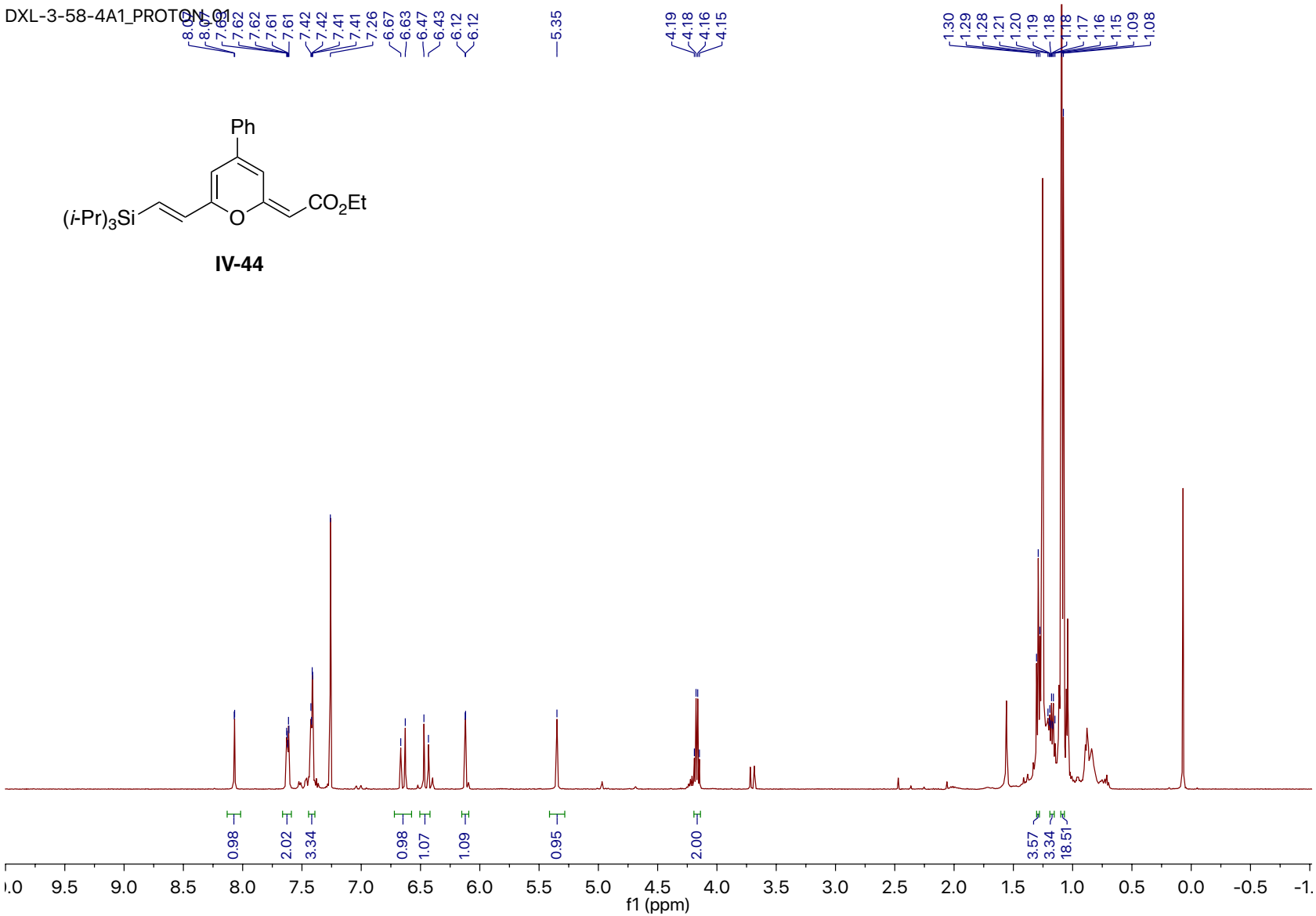
DXL-3-58-4A1_PROTON_01
8.07
8.06
7.63
7.62
7.62
7.61
7.61
7.42
7.42
7.41
7.41
7.26
6.67
6.63
6.47
6.43
6.12
6.12
5.35
4.19
4.18
4.16
4.15
1.30
1.29
1.28
1.21
1.20
1.19
1.18
1.18
1.17
1.16
1.15
1.09
1.08
Ph
(i-Pr)3Si
O
CO2Et
IV-44
0.98
2.02
3.34
0.98
1.07
1.09
0.95
2.00
3.57
3.34
18.51
f1 (ppm)

DXL-3-58-4A1_CARBON_01

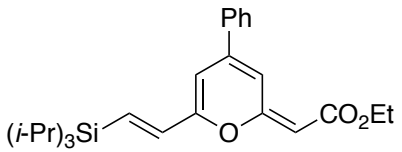

IV-44

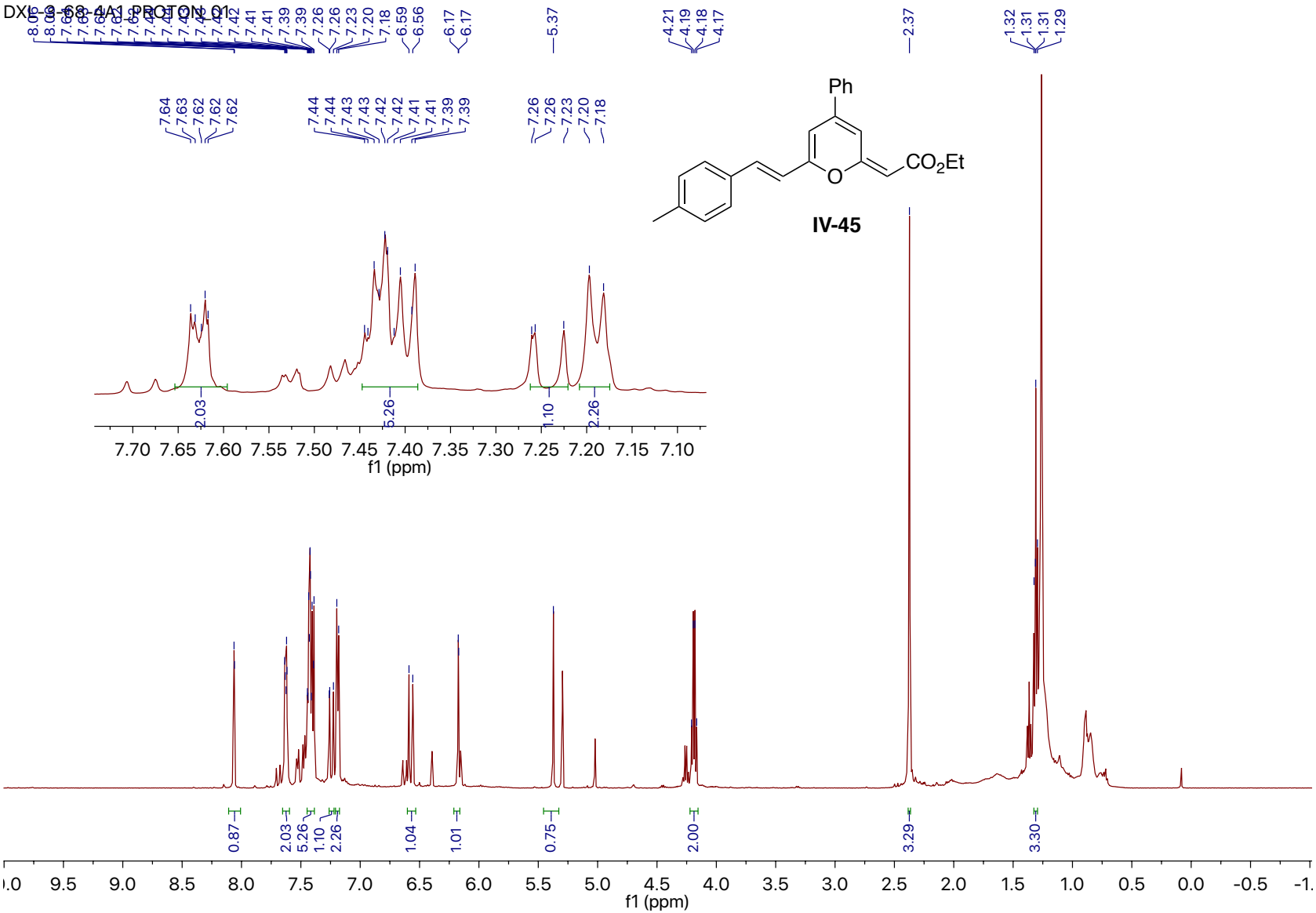
DXL-3-68-4A1 PROTON 01
Ph
CO2Et
O
IV-45
f1 (ppm)

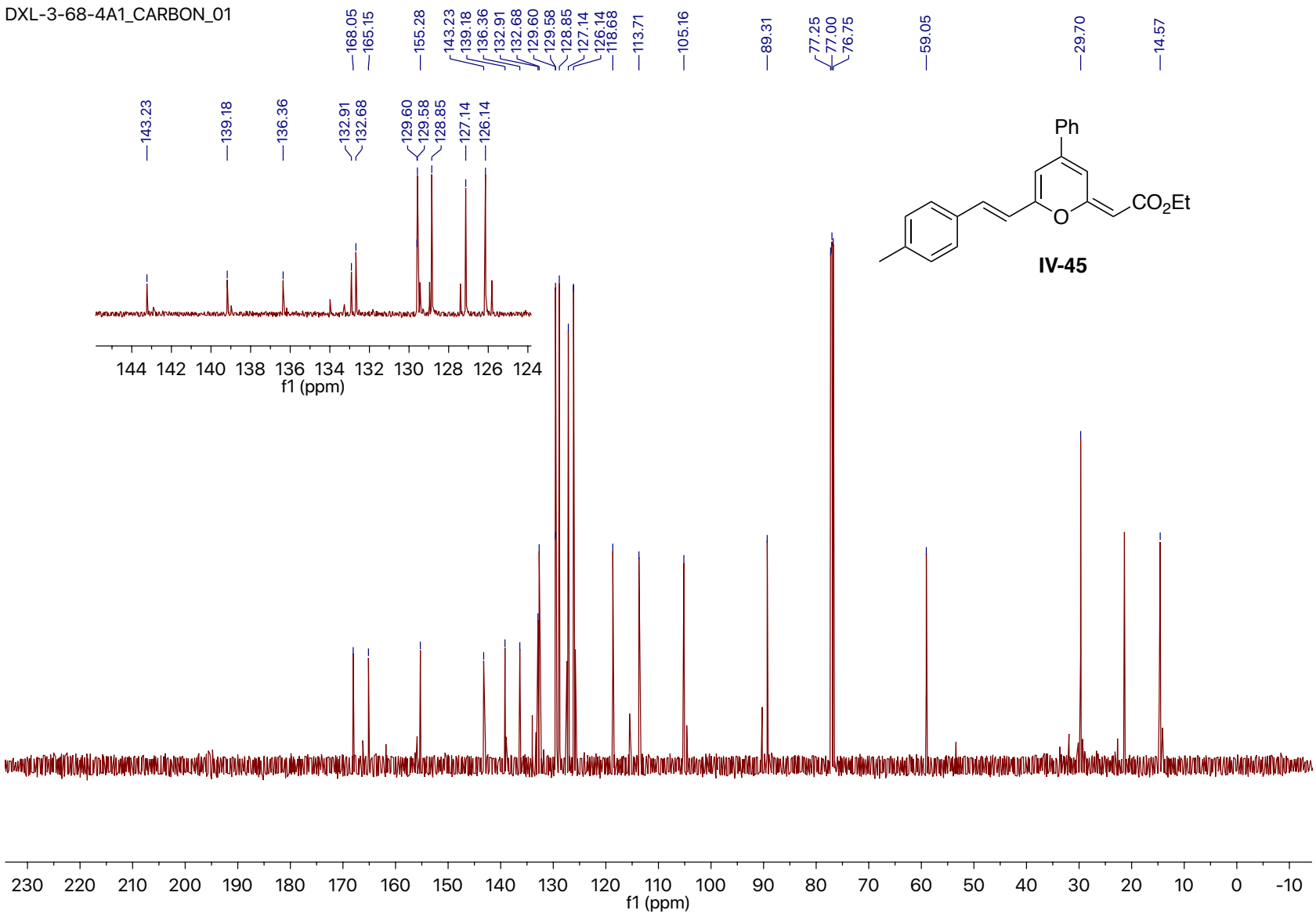
DXL-3-68-4A1_CARBON_01
168.05
165.15
155.28
143.23
139.18
136.36
132.91
132.68
129.60
129.58
128.85
127.14
126.14
118.68
113.71
105.16
89.31
77.25
77.00
76.75
59.05
29.70
14.57
Ph
CO2Et
O
IV-45
144 142 140 138 136 134 132 130 128 126 124
f1 (ppm)
230 220 210 200 190 180 170 160 150 140 130 120 110 100 90 80 70 60 50 40 30 20 10 0 -10
f1 (ppm)

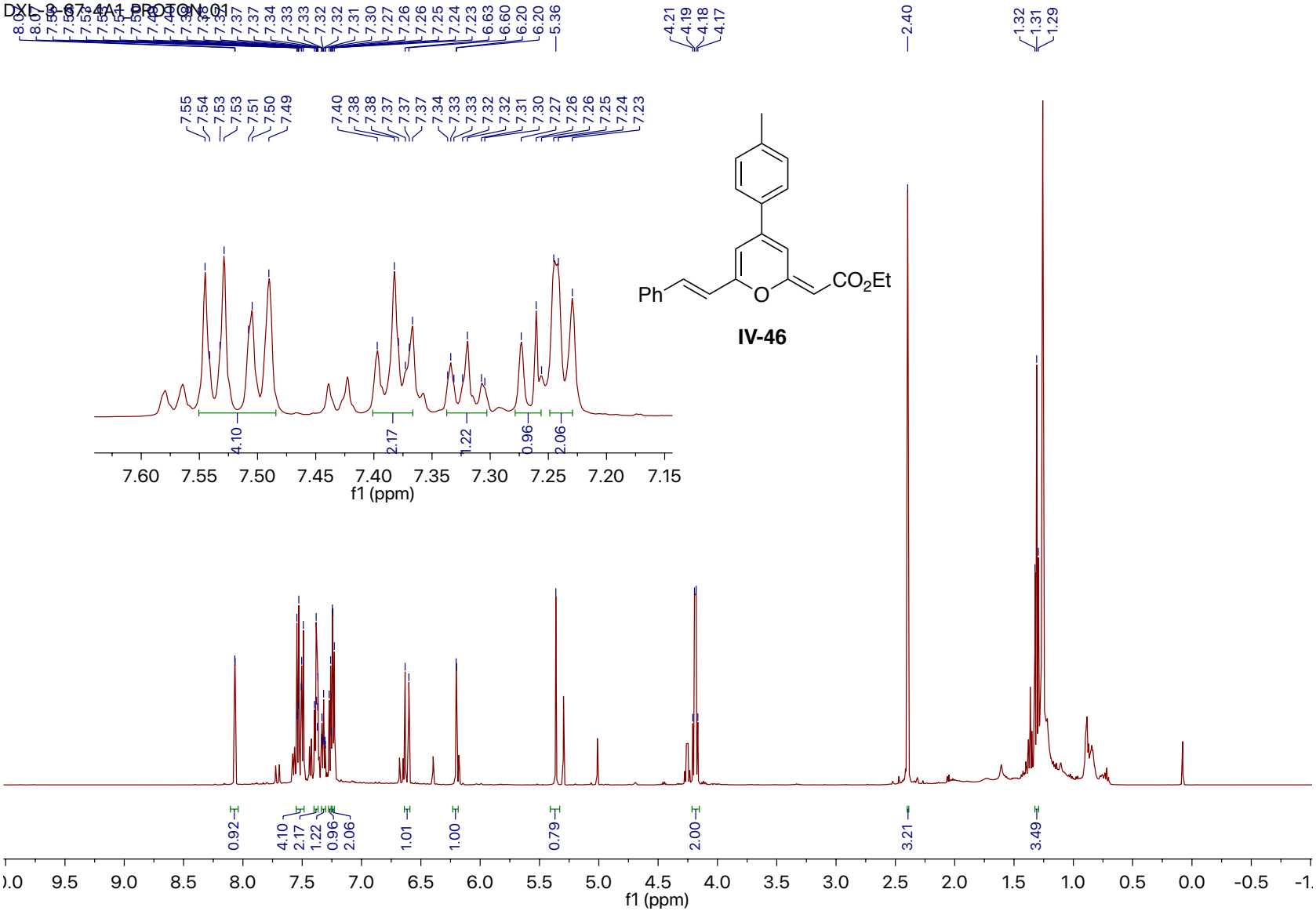
DXL-3-67-4A1 PROTON-01
Ph
O
CO2Et
IV-46
f1 (ppm)

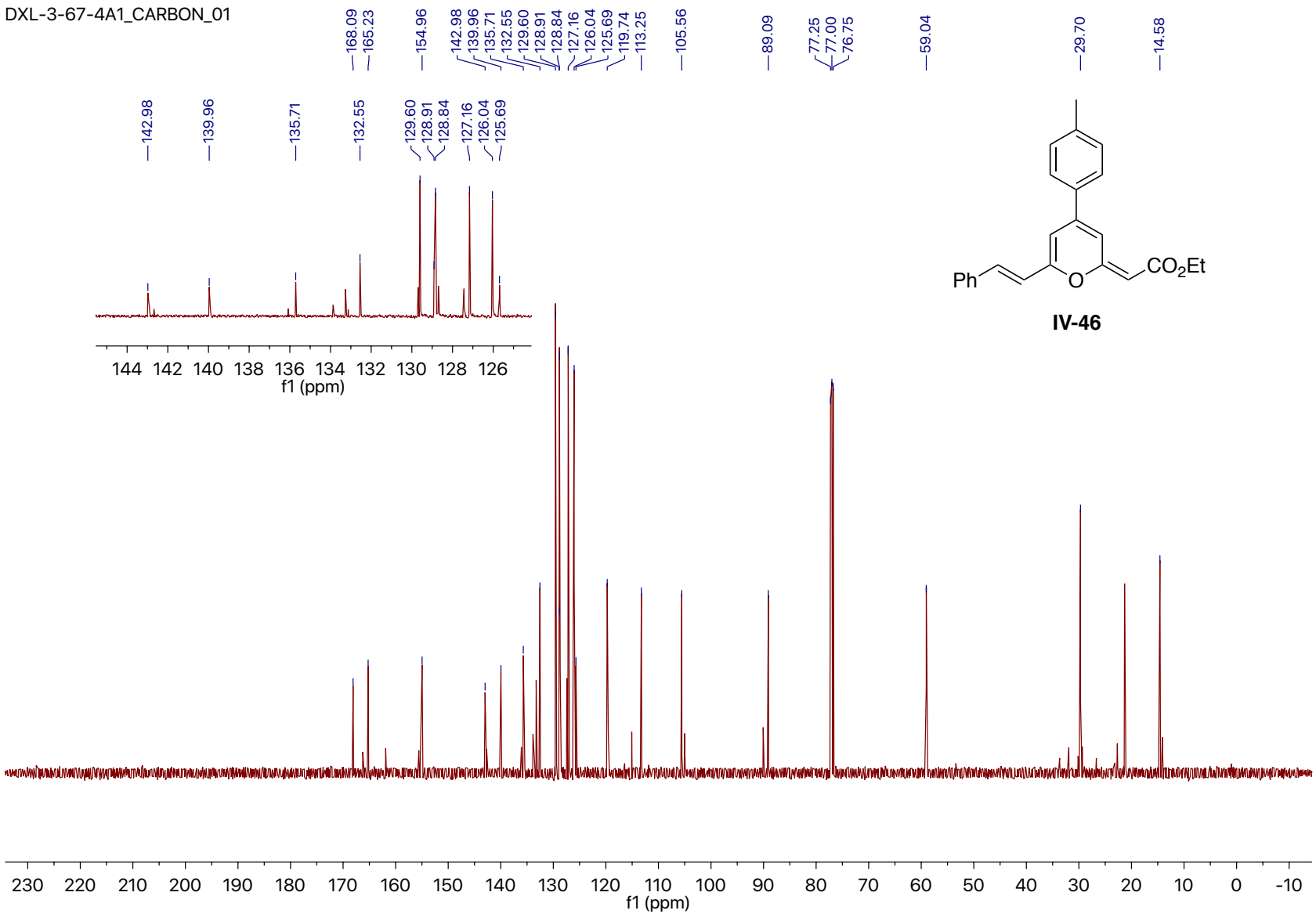
DXL-3-67-4A1_CARBON_01
168.09
165.23
154.96
142.98
139.96
135.71
132.55
129.60
128.91
128.84
127.16
126.04
125.69
119.74
113.25
105.56
89.09
77.25
77.00
76.75
59.04
29.70
14.58
142.98
139.96
135.71
132.55
129.60
128.91
128.84
127.16
126.04
125.69
144 142 140 138 136 134 132 130 128 126
f1 (ppm)
Ph
O
CO2Et
IV-46
230 220 210 200 190 180 170 160 150 140 130 120 110 100 90 80 70 60 50 40 30 20 10 0 -10
f1 (ppm)

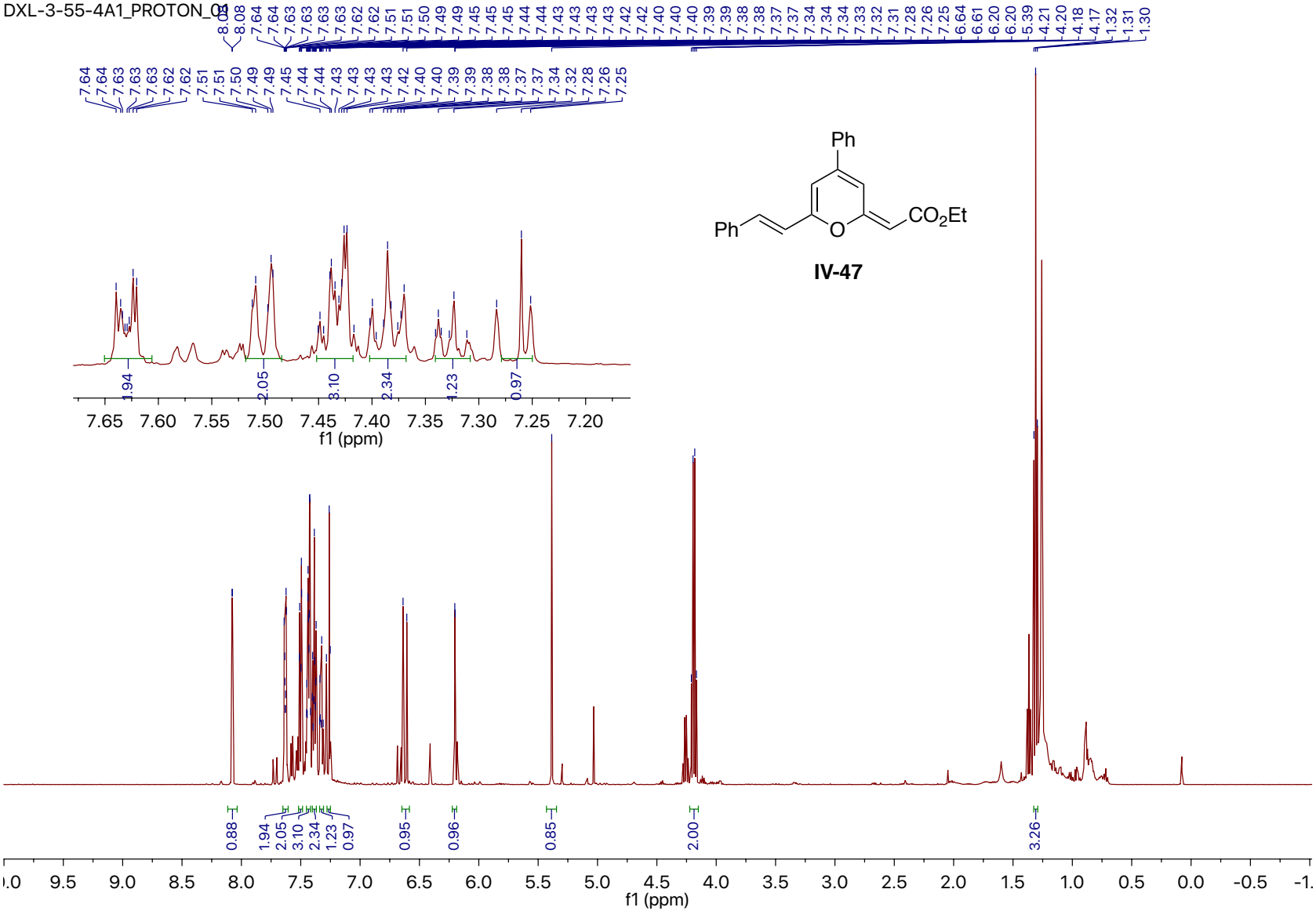
DXL-3-55-4A1_PROTON_01
Ph
Ph
O
CO2Et
IV-47
f1 (ppm)

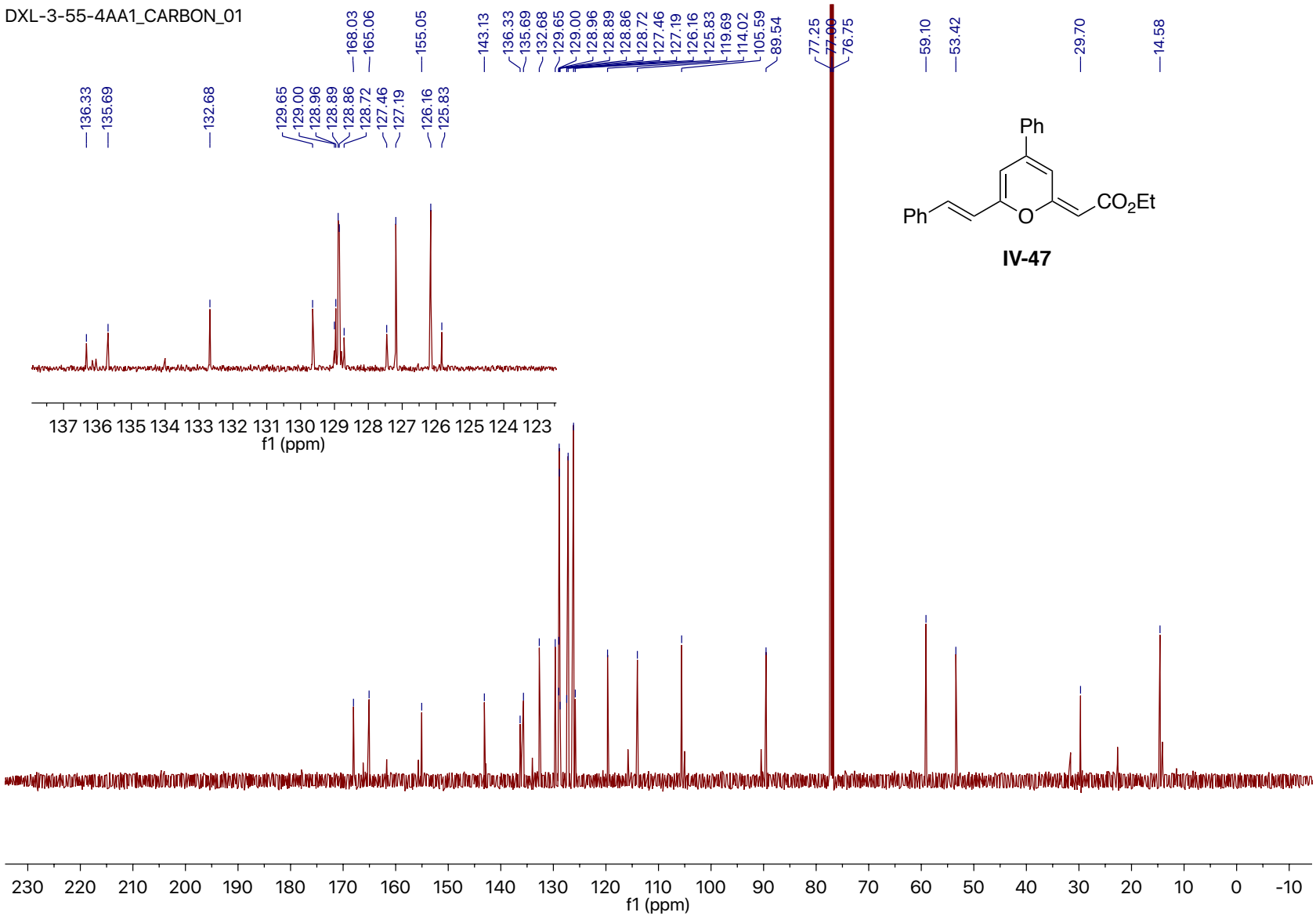
DXL-3-55-4AA1_CARBON_01
168.03
165.06
155.05
143.13
136.33
135.69
132.68
129.65
129.00
128.96
128.89
128.86
128.72
127.46
127.19
126.16
125.83
119.69
114.02
105.59
89.54
77.25
77.00
76.75
59.10
53.42
29.70
14.58
Ph
Ph
O
CO2Et
IV-47
137 136 135 134 133 132 131 130 129 128 127 126 125 124 123
f1 (ppm)
230 220 210 200 190 180 170 160 150 140 130 120 110 100 90 80 70 60 50 40 30 20 10 0 -10
f1 (ppm)

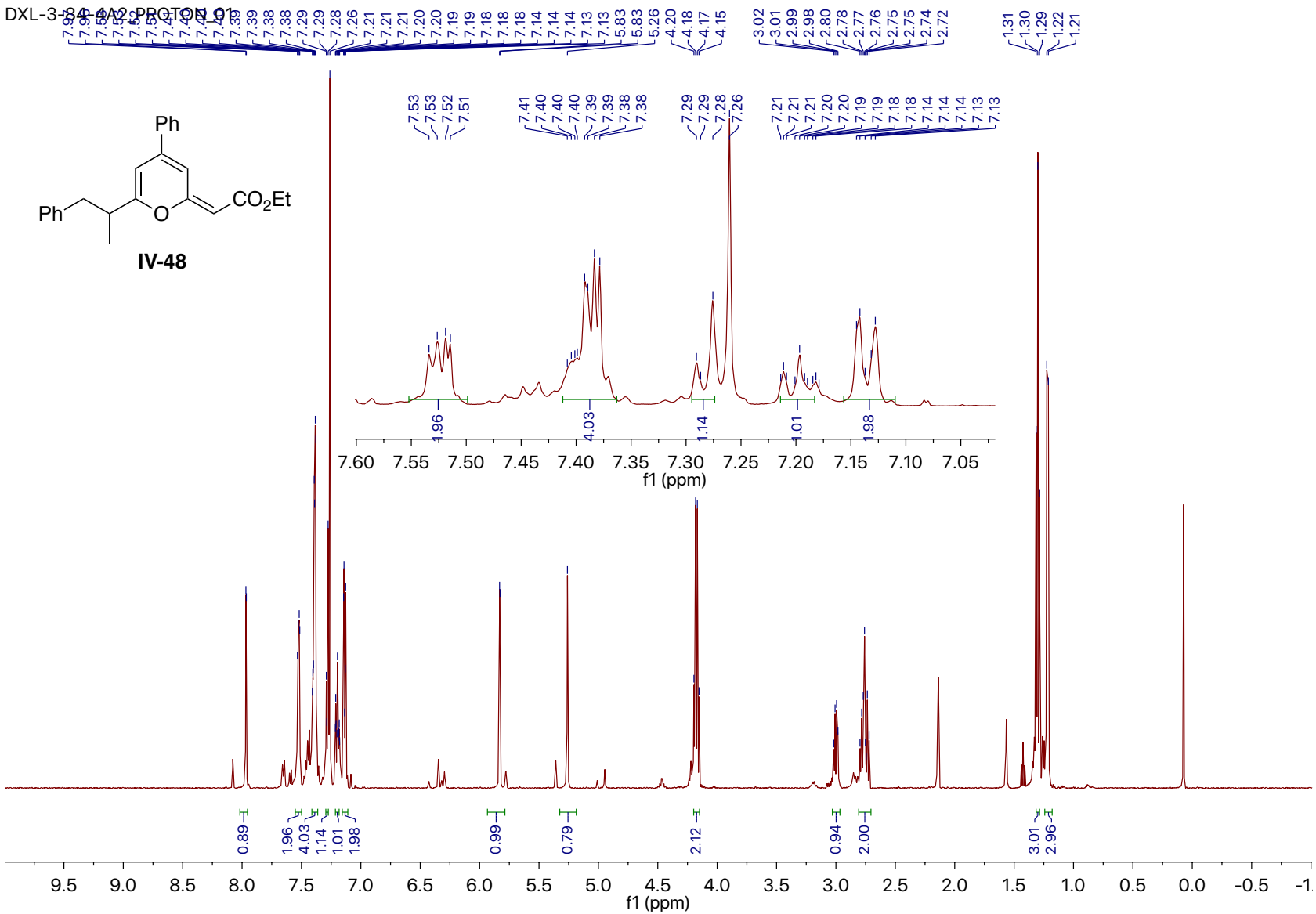
DXL-3-84-4A2 PROTON 01
Ph
Ph
O
CO2Et
IV-48
f1 (ppm)

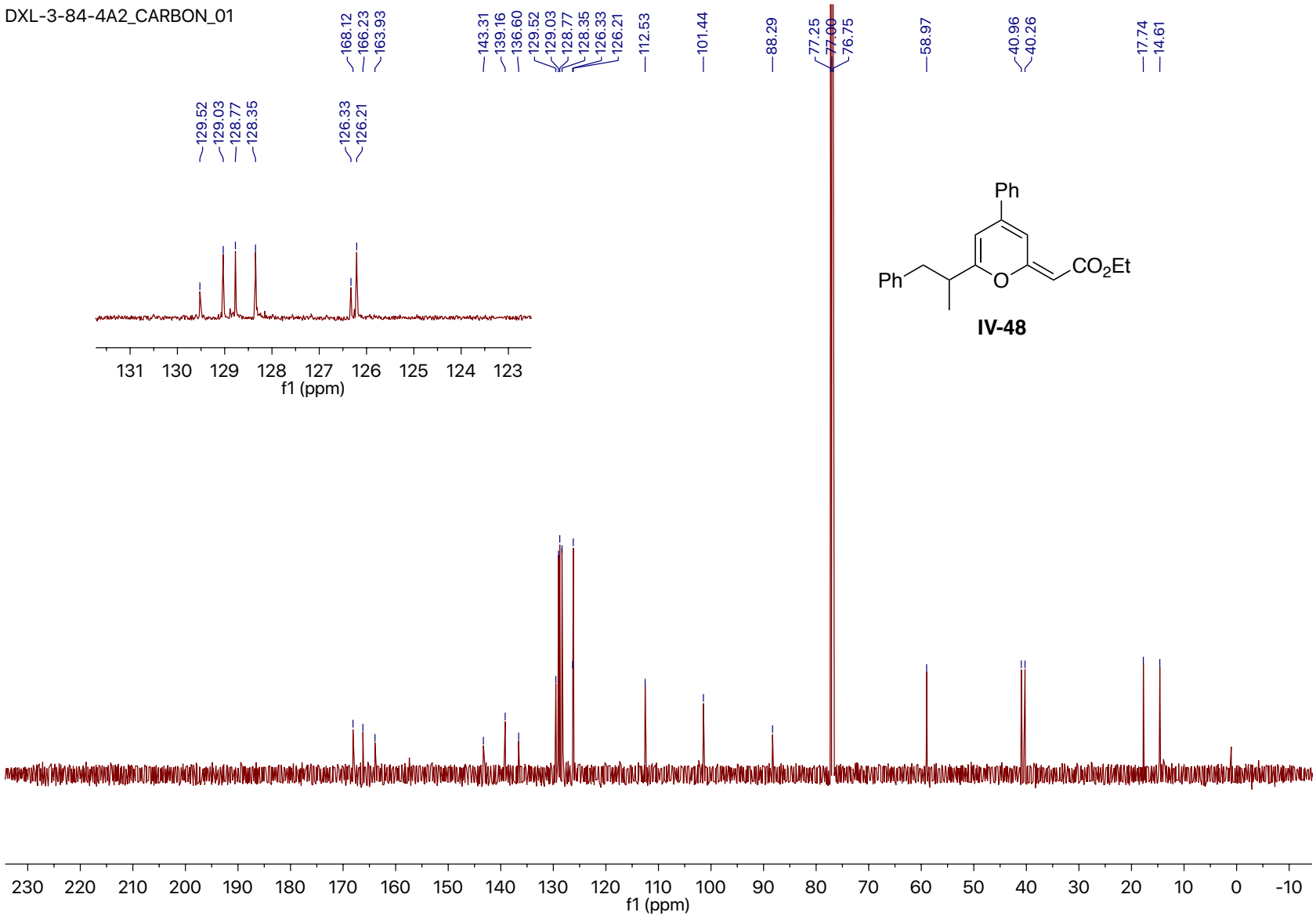
DXL-3-84-4A2_CARBON_01
168.12
166.23
163.93
143.31
139.16
136.60
129.52
129.03
128.77
128.35
126.33
126.21
112.53
101.44
88.29
77.25
77.00
76.75
58.97
40.96
40.26
17.74
14.61
129.52
129.03
128.77
128.35
126.33
126.21
131 130 129 128 127 126 125 124 123
f1 (ppm)
Ph
Ph
O
CO2Et
IV-48
230 220 210 200 190 180 170 160 150 140 130 120 110 100 90 80 70 60 50 40 30 20 10 0 -10
f1 (ppm)

Crystal Structure:

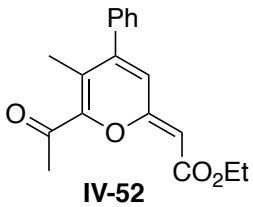

IV-52

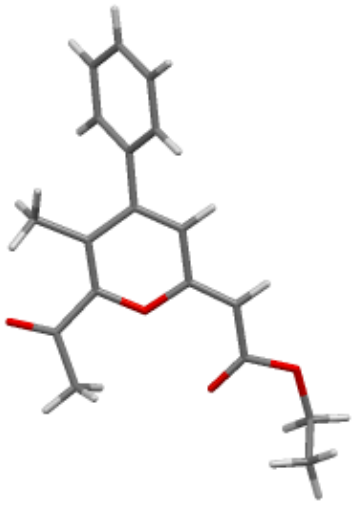

Table 1: Fractional Atomic Coordinates (×10⁴) and Equivalent Isotropic Displacement Parameters (Å²×10³) for **BB917C**. U_{eq} is defined as 1/3 of the trace of the orthogonalised U_{ij}.

Atom	x	y	z	U_{eq}
O1	8121.0(5)	3625.6(9)	5716(3)	34.5(3)
O2	8334.1(7)	1580.3(11)	9492(5)	58.1(5)
O3	8628.8(6)	5687.3(9)	-118(3)	37.9(3)
O4	8884.3(6)	4281.8(9)	1575(4)	40.1(3)
C1	7941.9(8)	2979.6(12)	7725(5)	31.6(4)
C2	7412.8(8)	3006.6(12)	9019(4)	30.3(4)
C3	7023.3(8)	3765.4(12)	8206(5)	30.8(4)
C4	7219.7(7)	4421.6(12)	6366(5)	31.6(4)
C5	7781.0(8)	4364.8(12)	5010(5)	31.0(4)
C6	8421.1(9)	2284.2(13)	8125(5)	37.3(5)
C7	8998.3(9)	2492.6(15)	6767(7)	48.6(6)
C8	7231.8(8)	2331.9(13)	11344(5)	35.7(4)
C9	6421.2(8)	3826.6(13)	9407(5)	33.0(4)
C10	6034.0(9)	3085.6(15)	9168(5)	39.8(5)
C11	5475.3(9)	3143.6(16)	10306(6)	46.4(6)
C12	5294.9(9)	3936.4(16)	11717(6)	49.7(6)
C13	5670.5(10)	4675.9(16)	11921(6)	48.9(6)
C14	6230.1(9)	4627.9(15)	10759(5)	40.1(5)
C15	7984.1(8)	4980.9(13)	3031(5)	32.1(4)
C16	8537.9(8)	4916.5(12)	1505(5)	31.1(4)
C17	9147.4(9)	5684.1(15)	-1917(5)	40.2(5)
C18	9674.5(8)	6031.5(16)	-285(6)	44.8(5)

Table 2: Anisotropic Displacement Parameters (×10⁴) **BB917C**. The anisotropic displacement factor exponent takes the form: $-2\pi^2[h^2a^{*2} \times U_{11} + \ldots + 2hka^* \times b^* \times U_{12}]$

Atom	U_{11}	U_{22}	U_{33}	U_{23}	U_{13}	U_{12}
O1	30.7(6)	29.8(7)	43.0(9)	3.7(6)	-1.8(6)	3.0(5)
O2	54.9(9)	35.6(8)	83.7(14)	15.6(9)	9.4(10)	12.2(7)
O3	35.1(6)	36.6(7)	42.0(8)	6.2(7)	0.1(6)	2.8(5)
O4	38.8(7)	33.9(7)	47.6(8)	0.1(7)	-0.8(7)	5.9(6)
C1	33.7(9)	24.5(9)	36.5(11)	-0.8(9)	-7.1(9)	-1.1(7)
C2	33.1(9)	25.1(9)	32.8(10)	-4.6(8)	-7.8(8)	-1.2(7)
C3	32.7(9)	26.6(9)	33.1(10)	-5.6(9)	-7.8(8)	-1.1(7)
C4	31.9(9)	26.2(9)	36.7(10)	-2.9(9)	-8.4(9)	2.2(7)
C5	32.0(9)	24.9(9)	36.2(11)	-4.5(8)	-8.4(9)	0.2(7)
C6	38.1(10)	26.6(10)	47.4(12)	-2.6(10)	-6(1)	3.6(8)
C7	38.0(11)	41.8(12)	66.1(16)	5.4(12)	-1.0(12)	10.7(9)
C8	39.7(10)	30.3(10)	37.0(11)	-2.2(9)	-3(1)	1.2(7)
C9	32.8(9)	34.4(10)	31.7(10)	-1.1(9)	-5.6(9)	2.4(7)
C10	36.4(10)	37.6(11)	45.4(12)	-2(1)	-5(1)	0.5(8)
C11	35(1)	49.4(12)	54.7(14)	8.5(12)	-4.8(11)	-2.4(9)
C12	36(1)	61.2(14)	51.8(14)	13.3(13)	6.9(11)	11.6(10)
C13	48.0(12)	47.8(13)	50.9(14)	-2.2(12)	4.3(11)	16.5(10)
C14	41.9(10)	35.0(11)	43.4(13)	-1.0(9)	-2.8(10)	4.1(8)
C15	33.0(9)	26.7(9)	36.6(10)	-2.9(9)	-9.0(9)	0.5(7)
C16	34.0(9)	27.7(9)	31.6(10)	-2.2(9)	-6.8(9)	-2.0(7)
C17	40.4(11)	43.2(12)	36.8(11)	3.6(10)	1.7(10)	2.0(9)
C18	35.7(10)	45.6(12)	53.0(14)	-2.0(11)	3.4(11)	1.6(9)

Table 3: Bond Lengths in Å for **BB917C**.

Atom	Atom	Length/Å
O1	C1	1.378(2)
O1	C5	1.362(2)
O2	C6	1.215(3)
O3	C16	1.360(2)
O3	C17	1.445(2)
O4	C16	1.213(2)
C1	C2	1.347(3)
C1	C6	1.499(3)
C2	C3	1.463(3)
C2	C8	1.507(3)
C3	C4	1.350(3)
C3	C9	1.484(3)
C4	C5	1.428(3)
C5	C15	1.357(3)
C6	C7	1.489(3)
C9	C10	1.395(3)
C9	C14	1.388(3)
C10	C11	1.382(3)
C11	C12	1.382(3)
C12	C13	1.376(3)
C13	C14	1.387(3)
C15	C16	1.449(3)
C17	C18	1.505(3)

Table 4: Bond Angles in ° for **BB917C**.

Atom	Atom	Atom	Angle/°
C5	O1	C1	121.68(15)
C16	O3	C17	115.92(15)
O1	C1	C6	108.83(17)
C2	C1	O1	122.89(17)
C2	C1	C6	128.28(19)
C1	C2	C3	116.97(18)
C1	C2	C8	122.74(17)
C3	C2	C8	120.17(17)
C2	C3	C9	120.83(18)
C4	C3	C2	119.21(18)
C4	C3	C9	119.96(17)
C3	C4	C5	122.13(17)
O1	C5	C4	116.91(17)
C15	C5	O1	118.86(17)
C15	C5	C4	124.20(17)
O2	C6	C1	120.60(19)
O2	C6	C7	122.16(19)
C7	C6	C1	117.24(18)
C10	C9	C3	120.75(18)
C14	C9	C3	120.54(17)
C14	C9	C10	118.70(19)
C11	C10	C9	120.5(2)

Atom	Atom	Atom	Angle/°
C10	C11	C12	120.3(2)
C13	C12	C11	119.6(2)
C12	C13	C14	120.6(2)
C13	C14	C9	120.3(2)
C5	C15	C16	125.51(17)
O3	C16	C15	110.26(15)
O4	C16	O3	122.54(18)
O4	C16	C15	127.20(18)
O3	C17	C18	111.60(18)

Table 5: Hydrogen Fractional Atomic Coordinates ($\times 10^4$) and Equivalent Isotropic Displacement Parameters ($Å^2 \times 10^3$) for **BB917C**. U_{eq} is defined as 1/3 of the trace of the orthogonalised U_{ij}.

Atom	x	y	z	U_{eq}
H4	6977	4938	5960	38
H7A	9158	3061	7608	73
H7B	8947	2573	4668	73
H7C	9269	1981	7131	73
H8A	6966	2637	12711	53
H8B	7580	2115	12386	53
H8C	7032	1805	10446	53
H10	6156	2537	8214	48
H11	5214	2637	10118	56
H12	4914	3970	12540	60
H13	5545	5224	12866	59
H14	6484	5146	10890	48
H15	7743	5498	2610	39
H17A	9080	6079	-3641	48
H17B	9224	5048	-2605	48
H18A	10017	6022	-1567	67
H18B	9747	5634	1400	67
H18C	9602	6665	374	67

Crystal Structure:

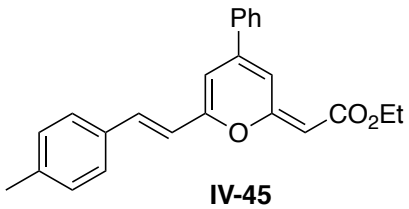

IV-45

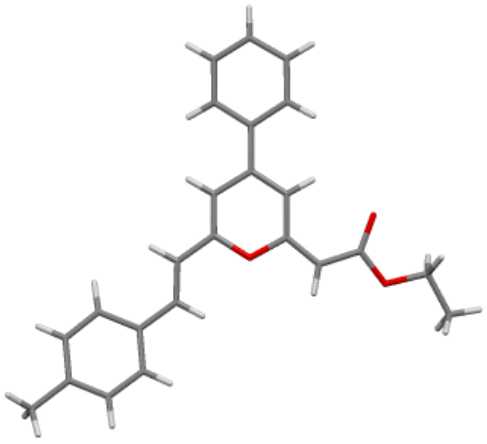

Table 6: Fractional Atomic Coordinates (×10⁴) and Equivalent Isotropic Displacement Parameters (Å²×10³) for **BB917D**. U_{eq} is defined as 1/3 of the trace of the orthogonalised U_{ij}.

Atom	x	y	z	U_{eq}
O1	6474.8(17)	2818.0(11)	5430(8)	64.5(13)
O2	5574.6(18)	2870.8(11)	-655(9)	66.6(13)
O3	5731.7(19)	3350.2(11)	624(10)	72.7(14)
C00O	5098(3)	2762.0(19)	-3694(14)	81(2)
C1	6698(2)	2917.3(17)	7281(13)	63.4(18)
C2	6735(2)	3218.4(17)	7791(12)	61.4(18)
C3	6533(2)	3453.3(17)	6416(13)	61.7(18)
C4	6306(2)	3349.2(17)	4591(13)	65.0(19)
C5	6267(2)	3030.9(16)	4083(13)	61.6(17)
C6	6864(2)	2662.0(17)	8634(12)	63.0(18)
C7	6818(2)	2362.2(17)	8224(13)	61.2(17)
C8	6967(2)	2102.4(17)	9606(12)	62.3(18)
C9	7133(2)	2151.0(17)	11790(13)	65.9(19)
C10	7277(3)	1900.0(18)	12985(13)	66.8(19)
C11	7260(2)	1597.6(18)	12226(13)	66.1(19)
C12	7093(2)	1551.4(17)	10147(14)	66.6(19)
C13	6949(2)	1799.6(16)	8860(12)	62.0(18)
C14	7383(3)	1321.7(19)	13676(16)	85(2)
C15	6572(2)	3786.6(17)	6994(13)	61.2(17)
C16	6461(3)	4023.8(18)	5518(16)	76(2)
C17	6501(3)	4335.2(19)	6059(17)	79(2)
C18	6655(3)	4423.4(19)	8105(19)	83(3)
C19	6762(3)	4198(2)	9576(18)	93(3)
C20	6715(3)	3887(2)	9058(16)	88(3)
C21	6037(3)	2894.3(16)	2364(13)	62.4(17)
C22	5775(3)	3065.2(17)	775(14)	63.8(18)
C23	5292(3)	3021.2(17)	-2310(13)	69(2)

Table 7: Anisotropic Displacement Parameters (×10⁴) **BB917D**. The anisotropic displacement factor exponent takes the form: $-2\pi^2[h^2a^{*2} \times U_{11} + \ldots + 2hka^* \times b^* \times U_{12}]$

Atom	U_{11}	U_{22}	U_{33}	U_{23}	U_{13}	U_{12}
O1	65(3)	57(3)	72(3)	2(2)	-5(3)	-1(2)
O2	72(3)	55(3)	73(3)	1(2)	-8(3)	-6(2)
O3	78(4)	58(3)	83(3)	-6(3)	-9(3)	4(3)
C00O	92(6)	70(5)	81(5)	5(4)	-12(5)	-8(5)
C1	47(4)	64(5)	80(4)	-8(4)	5(4)	-6(3)
C2	50(4)	62(4)	73(4)	4(4)	-2(3)	-4(3)
C3	44(4)	58(4)	83(5)	5(4)	7(3)	0(3)
C4	51(4)	68(5)	76(4)	11(4)	4(4)	-1(3)
C5	54(4)	52(4)	79(4)	3(3)	8(4)	-1(3)
C6	58(4)	64(5)	67(4)	5(3)	-1(4)	-8(3)
C7	48(4)	64(4)	72(4)	4(4)	7(3)	1(3)
C8	48(4)	64(4)	75(4)	3(4)	1(4)	-8(3)
C9	57(4)	59(4)	82(5)	2(4)	6(4)	-10(3)
C10	61(4)	70(5)	70(4)	9(4)	3(4)	-14(4)
C11	50(4)	65(5)	83(5)	12(4)	-1(4)	-1(3)
C12	59(4)	50(4)	91(5)	-1(4)	15(4)	-5(3)
C13	58(4)	56(4)	72(4)	-1(4)	8(4)	-8(3)
C14	72(6)	78(5)	105(6)	10(5)	-9(5)	-4(4)

Atom	U_{11}	U_{22}	U_{33}	U_{23}	U_{13}	U_{12}
C15	42(4)	61(4)	81(4)	0(4)	3(4)	-6(3)
C16	57(4)	67(5)	104(6)	1(5)	-10(5)	5(4)
C17	59(5)	62(5)	116(7)	1(5)	-7(5)	4(4)
C18	61(5)	52(4)	135(8)	-7(5)	15(5)	-3(4)
C19	112(8)	68(6)	99(6)	-2(5)	2(6)	-14(5)
C20	101(7)	69(5)	94(6)	-4(5)	1(6)	-12(5)
C21	60(4)	54(4)	73(4)	0(4)	6(4)	3(3)
C22	50(4)	57(4)	84(5)	-3(4)	2(4)	-3(3)
C23	64(5)	63(5)	81(5)	7(4)	-10(4)	3(4)

Table 8: Bond Lengths in Å for **BB917D**.

Atom	Atom	Length/Å
O1	C1	1.372(9)
O1	C5	1.370(8)
O2	C22	1.341(9)
O2	C23	1.456(9)
O3	C22	1.231(8)
C00O	C23	1.507(10)
C1	C2	1.332(9)
C1	C6	1.453(10)
C2	C3	1.439(10)
C3	C4	1.370(10)
C3	C15	1.475(10)
C4	C5	1.403(9)
C5	C21	1.376(10)
C6	C7	1.316(9)
C7	C8	1.462(10)
C8	C9	1.431(10)
C8	C13	1.376(9)
C9	C10	1.366(10)
C10	C11	1.377(10)
C11	C12	1.371(11)
C11	C14	1.519(10)
C12	C13	1.387(10)
C15	C16	1.395(11)
C15	C20	1.393(11)
C16	C17	1.380(11)
C17	C18	1.377(14)
C18	C19	1.354(13)
C19	C20	1.377(11)
C21	C22	1.437(10)

Table 9: Bond Angles in ° for **BB917D**.

Atom	Atom	Atom	Angle/°
C5	O1	C1	119.9(6)
C22	O2	C23	115.1(6)
O1	C1	C6	113.1(6)
C2	C1	O1	122.1(7)

Atom	Atom	Atom	Angle/˚
C2	C1	C6	124.8(7)
C1	C2	C3	120.6(7)
C2	C3	C15	120.4(7)
C4	C3	C2	116.4(7)
C4	C3	C15	123.1(7)
C3	C4	C5	122.3(7)
O1	C5	C4	118.6(7)
O1	C5	C21	113.0(6)
C21	C5	C4	128.4(7)
C7	C6	C1	126.4(7)
C6	C7	C8	127.1(7)
C9	C8	C7	121.7(7)
C13	C8	C7	121.1(7)
C13	C8	C9	117.2(7)
C10	C9	C8	119.1(7)
C9	C10	C11	123.5(8)
C10	C11	C14	122.0(8)
C12	C11	C10	117.3(7)
C12	C11	C14	120.6(7)
C11	C12	C13	121.3(7)
C8	C13	C12	121.7(7)
C16	C15	C3	122.3(7)
C20	C15	C3	122.6(7)
C20	C15	C16	115.2(7)
C17	C16	C15	122.1(9)
C18	C17	C16	120.6(9)
C19	C18	C17	118.6(8)
C18	C19	C20	121.0(10)
C19	C20	C15	122.5(9)
C5	C21	C22	123.9(7)
O2	C22	C21	110.8(6)
O3	C22	O2	121.5(8)
O3	C22	C21	127.7(7)
O2	C23	C00O	106.1(6)

Table 10: Hydrogen Fractional Atomic Coordinates (×10^4) and Equivalent Isotropic Displacement Parameters (Å^2×10^3) for **BB917D**. U_{eq} is defined as 1/3 of the trace of the orthogonalised U_{ij}.

Atom	x	y	z	U_{eq}
H00A	4935	2851	-4952	122
H00B	4887	2638	-2806	122
H00C	5345	2628	-4223	122
H2	6897	3279	9074	74
H4	6170	3498	3635	78
H6	7021	2717	9943	76
H7	6673	2309	6882	73
H9	7143	2355	12400	79
H10	7395	1936	14417	80
H12	7076	1345	9577	80
H13	6834	1759	7427	74
H14A	7625	1382	14694	127

Atom	x	y	z	U_{eq}
H14B	7487	1148	12756	127
H14C	7115	1256	14515	127
H16	6355	3969	4094	91
H17	6421	4490	5012	94
H18	6685	4638	8476	99
H19	6873	4256	10987	111
H20	6781	3736	10151	105
H21	6052	2674	2220	75
H23A	5476	3164	-3226	83
H23B	5046	3142	-1605	83

Crystal Structure:

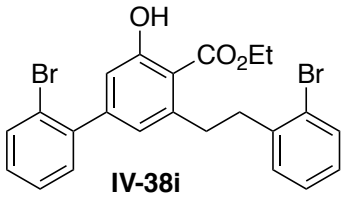

IV-38i

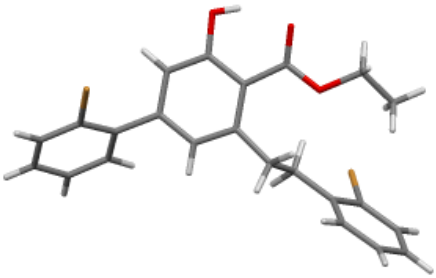

Table 11: Fractional Atomic Coordinates (×10⁴) and Equivalent Isotropic Displacement Parameters (Å²×10³) for **BB1017B**. U_{eq} is defined as 1/3 of the trace of the orthogonalised U_{ij}.

Atom	x	y	z	U_{eq}
Br1	1742.7(5)	542.2(5)	8712.4(3)	36.16(13)
Br2	6368.1(6)	3201.1(5)	1130.9(3)	47.66(15)
O1	8935(3)	1237(4)	4334(2)	38.8(7)
O2	6151(3)	3094(3)	6460.7(19)	32.4(6)
O3	8714(3)	2516(3)	5669(2)	39.3(7)
C1	7239(4)	1717(4)	4298(3)	27.5(8)
C2	6233(4)	2419(4)	4990(3)	25.5(7)
C3	4459(4)	2865(4)	4889(2)	24.5(7)
C4	3797(4)	2585(4)	4139(3)	27.2(7)
C5	4803(4)	1894(4)	3465(2)	25.5(7)
C6	6529(4)	1464(4)	3563(3)	30.1(8)
C7	7149(4)	2679(4)	5724(3)	29.1(8)
C8	6984(5)	3343(5)	7216(3)	36.7(9)
C9	5666(6)	3385(8)	8083(4)	75(2)
C10	3232(4)	3667(4)	5540(2)	25.5(7)
C11	2542(4)	2629(4)	6538(2)	24.8(7)
C12	1538(4)	3386(4)	7282(3)	25.9(7)
C13	1077(4)	2600(4)	8274(3)	28.4(8)
C14	149(5)	3240(5)	8989(3)	36.9(9)
C15	-332(5)	4736(5)	8699(3)	43.4(10)
C16	123(5)	5550(5)	7731(3)	40.7(10)
C17	1025(4)	4880(4)	7031(3)	31.7(8)
C18	4002(5)	1611(4)	2685(3)	28.4(8)
C19	4535(5)	2076(5)	1654(3)	34.5(9)
C20	3740(6)	1764(5)	973(3)	45.7(11)
C21	2371(6)	992(6)	1306(3)	47.7(11)
C22	1785(5)	541(5)	2322(3)	37.0(9)
C23	2600(5)	866(4)	2994(3)	31.2(8)

Table 12: Anisotropic Displacement Parameters (×10⁴) **BB1017B**. The anisotropic displacement factor exponent takes the form: $-2\pi^2[h^2a^{*2} \times U_{11} + \ldots + 2hka^* \times b^* \times U_{12}]$

Atom	U_{11}	U_{22}	U_{33}	U_{23}	U_{13}	U_{12}
Br1	44.2(2)	35.1(2)	25.5(2)	-6.72(16)	2.00(16)	-6.38(17)
Br2	50.3(3)	53.4(3)	30.6(2)	-4.79(19)	7.76(19)	-11.4(2)
O1	21.4(13)	59(2)	33.8(15)	-18.6(14)	-2.6(11)	6.4(12)
O2	25.4(12)	49.0(17)	28.2(13)	-18.1(12)	-3.2(10)	-6.7(11)
O3	25.2(13)	55.7(19)	38.5(15)	-16.3(13)	-3.1(11)	-5.9(12)
C1	21.1(16)	32(2)	23.1(17)	-4.6(14)	2.6(13)	0.4(14)
C2	22.1(16)	30(2)	22.2(17)	-6.2(14)	-0.1(13)	-4.5(14)
C3	24.6(16)	24.4(18)	20.7(16)	-3.9(13)	0.9(13)	-2.9(13)
C4	20.6(16)	34(2)	24.9(17)	-8.4(14)	0.7(13)	-1.4(14)
C5	25.2(17)	27.0(19)	21.0(17)	-5.9(13)	-1.6(13)	0.8(14)
C6	28.4(18)	34(2)	21.5(17)	-9.0(14)	2.6(14)	5.9(15)
C7	26.8(18)	32(2)	25.0(18)	-4.3(14)	-2.9(14)	-3.7(15)
C8	37(2)	46(3)	34(2)	-16.5(18)	-10.1(16)	-8.9(18)
C9	50(3)	148(7)	56(3)	-70(4)	1(2)	-19(3)
C10	23.3(16)	27.7(19)	23.2(17)	-9.1(14)	1.5(13)	0.5(14)
C11	24.5(16)	25.1(18)	24.4(17)	-9.5(14)	1.0(13)	-2.7(14)
C12	17.6(15)	37(2)	25.0(17)	-13.9(15)	0.3(13)	-2.4(14)

Atom	U_{11}	U_{22}	U_{33}	U_{23}	U_{13}	U_{12}
C13	22.4(16)	32(2)	29.6(19)	-9.8(15)	-2.5(14)	-1.5(14)
C14	37(2)	47(3)	23.0(19)	-12.6(17)	2.2(15)	0.4(18)
C15	42(2)	55(3)	33(2)	-25(2)	1.9(17)	7(2)
C16	33(2)	41(2)	46(2)	-20.8(19)	-4.4(17)	11.6(17)
C17	28.5(18)	37(2)	27.7(19)	-11.8(16)	0.4(14)	-0.2(15)
C18	31.7(18)	28.2(19)	22.6(17)	-11.6(14)	-1.2(14)	7.1(15)
C19	32.9(19)	42(2)	26.0(19)	-12.8(16)	-0.8(15)	1.8(16)
C20	51(3)	59(3)	24(2)	-15.7(19)	-2.1(18)	3(2)
C21	48(2)	63(3)	40(2)	-29(2)	-16.9(19)	6(2)
C22	36(2)	38(2)	39(2)	-17.3(18)	-6.3(17)	-1.3(17)
C23	30.6(19)	35(2)	26.8(19)	-12.5(15)	-2.6(14)	3.5(16)

Table 13: Bond Lengths in Å for **BB1017B**.

Atom	Atom	Length/Å
Br1	C13	1.911(4)
Br2	C19	1.906(4)
O1	C1	1.355(4)
O2	C7	1.324(4)
O2	C8	1.456(4)
O3	C7	1.225(4)
C1	C2	1.425(5)
C1	C6	1.374(5)
C2	C3	1.423(5)
C2	C7	1.477(5)
C3	C4	1.383(5)
C3	C10	1.515(4)
C4	C5	1.402(5)
C5	C6	1.384(5)
C5	C18	1.486(5)
C8	C9	1.480(6)
C10	C11	1.536(4)
C11	C12	1.513(4)
C12	C13	1.391(5)
C12	C17	1.391(5)
C13	C14	1.394(5)
C14	C15	1.388(6)
C15	C16	1.371(6)
C16	C17	1.388(5)
C18	C19	1.396(5)
C18	C23	1.385(5)
C19	C20	1.378(6)
C20	C21	1.379(7)
C21	C22	1.386(6)
C22	C23	1.383(5)

Table 14: Bond Angles in ° for **BB1017B**.

Atom	Atom	Atom	Angle/°
C7	O2	C8	117.4(3)
O1	C1	C2	122.5(3)
O1	C1	C6	115.9(3)
C6	C1	C2	121.5(3)
C1	C2	C7	116.6(3)
C3	C2	C1	117.7(3)
C3	C2	C7	125.6(3)
C2	C3	C10	124.2(3)
C4	C3	C2	118.8(3)
C4	C3	C10	117.0(3)
C3	C4	C5	122.8(3)
C4	C5	C18	119.9(3)
C6	C5	C4	118.3(3)
C6	C5	C18	121.7(3)
C1	C6	C5	120.8(3)
O2	C7	C2	115.0(3)
O3	C7	O2	121.9(3)
O3	C7	C2	123.1(3)
O2	C8	C9	107.0(3)
C3	C10	C11	112.2(3)
C12	C11	C10	114.1(3)
C13	C12	C11	120.8(3)
C17	C12	C11	123.2(3)
C17	C12	C13	116.0(3)
C12	C13	Br1	119.8(3)
C12	C13	C14	123.3(4)
C14	C13	Br1	116.9(3)
C15	C14	C13	118.4(4)
C16	C15	C14	120.0(4)
C15	C16	C17	120.3(4)
C16	C17	C12	122.0(4)
C19	C18	C5	124.6(4)

Atom	Atom	Atom	Angle/°
C23	C18	C5	118.1(3)
C23	C18	C19	117.3(3)
C18	C19	Br2	121.2(3)
C20	C19	Br2	117.3(3)
C20	C19	C18	121.5(4)

Atom	Atom	Atom	Angle/°
C19	C20	C21	119.9(4)
C20	C21	C22	120.1(4)
C23	C22	C21	119.1(4)
C22	C23	C18	122.1(4)

Table 15: Hydrogen Fractional Atomic Coordinates ($\times 10^4$) and Equivalent Isotropic Displacement Parameters ($Å^2 \times 10^3$) for **BB1017B**. U_{eq} is defined as 1/3 of the trace of the orthogonalised U_{ij}.

Atom	x	y	z	U_{eq}
H1	9190(60)	1510(50)	4770(40)	42(13)
H4	2610	2874	4079	33
H6	7231	988	3116	36
H8A	7454	4275	6943	44
H8B	7935	2550	7425	44
H9A	4780	4222	7880	112
H9B	6199	3472	8632	112
H9C	5146	2488	8312	112
H10A	2259	4228	5168	31
H10B	3828	4365	5682	31
H11A	1795	2038	6395	30
H11B	3518	1956	6851	30
H14	-147	2666	9660	44
H15	-976	5197	9170	52
H16	-181	6577	7539	49
H17	1300	5461	6360	38
H20	4134	2080	276	55
H21	1828	769	837	57
H22	837	16	2554	44
H23	2185	570	3689	37

Table 16: Hydrogen Bond information for **BB1017B**.

D	H	A	d(D-H)/Å	d(H-A)/Å	d(D-A)/Å	D-H-A/deg
O1	H1	O3	0.82(5)	1.79(5)	2.548(4)	152(5)

REFERENCES

REFERENCES

(1) Seayad, J.; List, B. Asymmetric organocatalysis. *Organic & Biomolecular Chemistry* **2005,** *3* (5), 719.

(2) Taylor, J. E.; Bull, S. D.; Williams, J. M. J. Amidines, isothioureas, and guanidines as nucleophilic catalysts. *Chemical Society Reviews* **2012,** *41* (6), 2109.

(3) Joannesse, C.; Simal, C.; Concellon, C.; Thomson, J. E.; Campbell, C. D.; Slawin, A. M. Z.; Smith, A. D. Amidine catalysed O- to C-carboxyl transfer of heterocyclic carbonate derivatives. *Organic & Biomolecular Chemistry* **2008,** *6* (16), 2900.

(4) Taylor, J. E.; Jones, M. D.; Williams, J. M. J.; Bull, S. D. Friedel-Crafts Acylation of Pyrroles and Indoles using 1,5-Diazabicyclo 4.3.0 non-5-ene (DBN) as a Nucleophilic Catalyst. *Organic Letters* **2010,** *12* (24), 5740.

(5) Ghobril, C.; Sabot, C.; Mioskowski, C.; Baati, R. TBD-catalyzed direct 5- and 6-enolexo aldolization of ketoaldehydes. *European Journal of Organic Chemistry* **2008**, 4104.

(6) Leverett, C. A.; Purohit, V. C.; Romo, D. Enantioselective, Organocatalyzed, Intramolecular Aldol Lactonizations with Keto Acids Leading to Bi- and Tricyclic beta-Lactones and Topology-Morphing Transformations. *Angewandte Chemie-International Edition* **2010,** *49* (49), 9479.

(7) Aggarwal, V. K.; Mereu, A. Superior amine catalysts for the Baylis-Hillman reaction: the use of DBU and its implications. *Chemical Communications* **1999**, DOI:10.1039/a907754e 10.1039/a907754e(22), 2311.

(8) Zhao, G. L.; Shi, Y. L.; Shi, M. Synthesis of functionalized 2H-1-benzopyrans by DBU-catalyzed reactions of salicylic aldehydes with allenic ketones and esters. *Organic Letters* **2005,** *7* (20), 4527.

(9) Murtagh, J. E.; McCooey, S. H.; Connon, S. J. Novel amine-catalysed hydroalkoxylation reactions of activated alkenes and alkynes. *Chemical Communications* **2005**, 227.

(10) Perez, E. R.; Santos, R. H. A.; Gambardella, M. T. P.; de Macedo, L. G. M.; Rodrigues, U. P.; Launay, J. C.; Franco, D. W. Activation of carbon dioxide by bicyclic amidines. *Journal of Organic Chemistry* **2004,** *69* (23), 8005.

(11) Birman, V. B.; Li, X. M.; Han, Z. F. Nonaromatic amidine derivatives as acylation catalysts. *Organic Letters* **2007,** *9* (1), 37.

(12) Kobayashi, M.; Okamoto, S. Unexpected reactivity of annulated 3H-benzothiazol-2-ylideneamines as an acyl transfer catalyst. *Tetrahedron Letters* **2006,** *47* (26), 4347.

(13) Muller, C. E.; Schreiner, P. R. Organocatalytic Enantioselective Acyl Transfer onto Racemic as well as meso Alcohols, Amines, and Thiols. *Angewandte Chemie-International Edition* **2011,** *50* (27), 6012.

(14) Pellissier, H. Catalytic Non-Enzymatic Kinetic Resolution. *Advanced Synthesis & Catalysis* **2011,** *353* (10), 1613.

(15) Ishikawa, T. *Superbases for organic synthesis: guanidines, amidines, phosphazenes and related organocatalysts*; Wiley: Chippenham, 2009.

(16) Leffek, K. T.; Pruszynski, P.; Thanapaalasingham, K. BASICITY OF SUBSTITUTED 2-PHENYL-1,1,3,3-TETRAMETHYLGUANIDINES AND OTHER BASES IN ACETONITRILE SOLVENT. *Canadian Journal of Chemistry-Revue Canadienne De Chimie* **1989,** *67* (4), 590.

(17) Oediger, H.; Eiter, K.; Moller, F. BICYCLIC AMIDINES AS REAGENTS IN ORGANIC SYNTHESES. *Synthesis-International Journal of Methods in Synthetic Organic Chemistry* **1972,** (11), 591.

(18) Disselnkotter, H. K., P.; Patent, G., Ed., 1971.

(19) McCoy, L. L.; Mal, D. 3-MEMBERED RINGS .8. REACTION OF 1-HALOCYCLOPROPANE 1,2-DIESTERS WITH 1,8-DIAZABICYCLO 5.4.0 UNDEC-7-ENE - UNEXPECTED PRODUCTS. *Journal of Organic Chemistry* **1981,** *46* (5), 1016.

(20) Reed, R.; Reau, R.; Dahan, F.; Bertrand, G. DBU AND DBN ARE STRONG NUCLEOPHILES - X-RAY CRYSTAL-STRUCTURES OF ONIO-SUBSTITUTED AND DIONIO-SUBSTITUTED PHOSPHANES. *Angewandte Chemie-International Edition in English* **1993,** *32* (3), 399.

(21) Baidya, M.; Mayr, H. Nucleophilicities and carbon basicities of DBU and DBN. *Chemical Communications* **2008**, 1792.

(22) Maji, B.; Joannesse, C.; Nigst, T. A.; Smith, A. D.; Mayr, H. Nucleophilicities and Lewis Basicities of Isothiourea Derivatives. *Journal of Organic Chemistry* **2011,** *76* (12), 5104.

(23) Wei, Y.; Sastry, G. N.; Zipse, H. Methyl cation affinities of commonly used organocatalysts. *Journal of the American Chemical Society* **2008,** *130* (11), 3473.

(24) Grainger, R. S.; Leadbeater, N. E.; Pamies, A. M. The tetramethylguanidine catalyzed Baylis-Hillman reaction: Effects of co-catalysts and alcohol solvents on reaction rate. *Catalysis Communications* **2002,** *3* (10), 449.

(25) Luo, S. Z.; Mi, X. L.; Xu, H.; Wang, P. G.; Cheng, J. P. Efficient Baylis-Hillman reactions of cyclic enones in methanol as catalyzed by methoxide anion. *Journal of Organic Chemistry* **2004,** *69* (24), 8413.

(26) Robiette, R.; Aggarwal, V. K.; Harvey, J. N. Mechanism of the Morita-Baylis-Hillman reaction: A computational investigation. *Journal of the American Chemical Society* **2007,** *129* (50), 15513.

(27) Chattapadhyay, T. K.; Dureja, P. Antifungal activity of 4-methyl-6-alkyl-2H-pyran-2-ones. *Journal of Agricultural and Food Chemistry* **2006,** *54* (6), 2129.

(28) DeSimone, R. W.; Currie, K. S.; Mitchell, S. A.; Darrow, J. W.; Pippin, D. A. Privileged structures: Applications in drug discovery. *Combinatorial Chemistry & High Throughput Screening* **2004,** *7* (5), 473.

(29) Heravi, M. M.; Baghernejad, B.; Oskooie, H. A. A novel and efficient catalyst to one-pot synthesis of 2-amino-4H-chromenes by methanesulfonic acid. *Journal of the Chinese Chemical Society* **2008,** *55* (3), 659.

(30) Wang, T. T.; Liu, J.; Zhong, H. Y.; Chen, H.; Lv, Z. L.; Zhang, Y. K.; Zhang, M. F.; Geng, D. P.; Niu, C. J.; Li, Y. M.et al. Synthesis and anti-tumor activity of novel ethyl 3-aryl-4-oxo-3,3a,4,6-tetrahydro-1H- furo 3,4-c pyran-3a-carboxylates. *Bioorganic & Medicinal Chemistry Letters* **2011,** *21* (11), 3381.

(31) Xu, R. S. Y., Y.; Zhao, W. M. *Introduction to Natural Products Chemistry*; CRC Press, Taylor & Francis Group: Boca Raton, 2012.

(32) Yang, B.; Yang, J. L.; Zhao, Y. P.; Liu, H. L.; Jiang, Y. M. The Plant Resources, Structure Characteristics, Biological Activities and Synthesis of Pyranoflavonoids. *Current Medicinal Chemistry* **2016,** *23* (27), 3078.

(33) Zaha, A. A.; Hazem, A. Antimicrobial activity of two novel coumarin derivatives: 3-cyanonaphtho 1,2-(e) pyran-2-one and 3-cyanocoumarin. *Microbiologica* **2002,** *25* (2), 213.

(34) Armesto, D.; Horspool, W. M.; Martin, N.; Ramos, A.; Seoane, C. SYNTHESIS OF CYCLOBUTENES BY THE NOVEL PHOTOCHEMICAL RING CONTRACTION OF 4-SUBSTITUTED 2-AMINO-3,5-DICYANO-6-PHENYL-4H-PYRANS. *Journal of Organic Chemistry* **1989,** *54* (13), 3069.

(35) Kumar, D.; Reddy, V. B.; Sharad, S.; Dube, U.; Kapur, S. A facile one-pot green synthesis and antibacterial activity of 2-amino-4H-pyrans and 2-amino-5-oxo-5,6,7,8-tetrahydro-4H-chromenes. *European Journal of Medicinal Chemistry* **2009,** *44* (9), 3805.

(36) Rideout, J. A.; Smith, I. R.; Sutherland, M. D. PIGMENTS OF MARINE ANIMALS .12. SYNTHESIS OF CERTAIN SUBSTITUTED NAPHTHOPYRONES RELATED TO CRINOID PIGMENTS. *Australian Journal of Chemistry* **1976,** *29* (5), 1087.

(37) Lee, Y. R.; Xia, L. K. Efficient one-pot synthetic approaches for cannabinoid analogues and their application to biologically interesting (-)-hexahydrocannabinol and (+)-hexahydrocannabinol. *Tetrahedron Letters* **2008,** *49* (20), 3283.

(38) Palasz, A. Synthesis of fused uracils: pyrano 2,3-d pyrimidines and 1,4-bis(pyrano 2,3-d pyrimidinyl)benzenes by domino Knoevenagel/Diels-Alder reactions. *Monatshefte Fur Chemie* **2012,** *143* (8), 1175.

(39) Banothu, J.; Bavanthula, R. Bronsted acidic ionic liquid catalyzed highly efficient synthesis of chromeno pyrimidinone derivatives and their antimicrobial activity. *Chinese Chemical Letters* **2012,** *23* (9), 1015.

(40) Sangani, C. B.; Mungra, D. C.; Patel, M. P.; Patel, R. G. Synthesis and in vitro antimicrobial screening of new pyrano 4,3-b pyrane derivatives of 1H-pyrazole. *Chinese Chemical Letters* **2012,** *23* (1), 57.

(41) Shestopalov, A. A.; Rodinovskaya, L. A.; Shestopalov, A. M.; Litvinov, V. P. Single-step synthesis of substituted 7-aminopyrano 2,3-d pyrimidines. *Russian Chemical Bulletin* **2004,** *53* (10), 2342.

(42) Bravo, L. Polyphenols: Chemistry, dietary sources, metabolism, and nutritional significance. *Nutrition Reviews* **1998,** *56* (11), 317.

(43) Lampe, J. W. Health effects of vegetables and fruit: assessing mechanisms of action in human experimental studies. *American Journal of Clinical Nutrition* **1999,** *70* (3), 475S.

(44) Benavente-Garcia, O.; Castillo, J.; Marin, F. R.; Ortuno, A.; Del Rio, J. A. Uses and properties of Citrus flavonoids. *Journal of Agricultural and Food Chemistry* **1997,** *45* (12), 4505.

(45) Cook, N. C.; Samman, S. Flavonoids - Chemistry, metabolism, cardioprotective effects, and dietary sources. *Journal of Nutritional Biochemistry* **1996,** *7* (2), 66.

(46) Huang, W. Y.; Cai, Y. Z.; Zhang, Y. B. Natural Phenolic Compounds From Medicinal Herbs and Dietary Plants: Potential Use for Cancer Prevention. *Nutrition and Cancer-an International Journal* **2010,** *62* (1), 1.

(47) Manach, C.; Williamson, G.; Morand, C.; Scalbert, A.; Remesy, C. Bioavailability and bioefficacy of polyphenols in humans. I. Review of 97 bioavailability studies. *American Journal of Clinical Nutrition* **2005,** *81* (1), 230S.

(48) Middleton, E.; Kandaswami, C.; Theoharides, T. C. The effects of plant flavonoids on mammalian cells: Implications for inflammation, heart disease, and cancer. *Pharmacological Reviews* **2000,** *52* (4), 673.

(49) Puupponen-Pimia, R.; Nohynek, L.; Meier, C.; Kahkonen, M.; Heinonen, M.; Hopia, A.; Oksman-Caldentey, K. M. Antimicrobial properties of phenolic compounds from berries. *Journal of Applied Microbiology* **2001,** *90* (4), 494.

(50) Balasundram, N.; Sundram, K.; Samman, S. Phenolic compounds in plants and agri-industrial by-products: Antioxidant activity, occurrence, and potential uses. *Food Chemistry* **2006,** *99* (1), 191.

(51) Harborne, J. B. B., H.; Moss, G. P. *Phytochemical dictionary: handbook of bioactive compounds from plants*; Taylor & Francis: London, 1999.

(52) King, A.; Young, G. Characteristics and occurrence of phenolic phytochemicals. *Journal of the American Dietetic Association* **1999,** *99* (2), 213.

(53) Ashtekar, K. D.; Ding, X. L.; Toma, E.; Sheng, W.; Gholami, H.; Rahn, C.; Reed, P.; Borhan, B. Mechanistically Inspired Route toward Hexahydro-2H-chromenes via Consecutive 4+2 Cycloadditions. *Organic Letters* **2016,** *18* (16), 3976.

(54) Motoyoshi, H.; Horigome, M.; Watanabe, H.; Kitahara, T. Total synthesis of FR901464: second generation. *Tetrahedron* **2006,** *62* (7), 1378.

(55) Srivastava, R. An efficient, eco-friendly process for aldol and Michael reactions of trimethylsilyl enolate over organic base-functionalized SBA-15 catalysts. *Journal of Molecular Catalysis a-Chemical* **2007,** *264* (1-2), 146.

(56) Linnell, R. H. DISSOCIATION CONSTANTS OF 2-SUBSTITUTED PYRIDINES. *Journal of Organic Chemistry* **1960,** *25* (2), 290.

(57) Perrin, D. D. *Dissociation constants of organic bases in aqueous solution: Published as a supplement to Pure and Applied Chemistry*; Butterworth: London, 1965.

(58) Kaupmees, K.; Trummal, A.; Leito, I. Basicities of Strong Bases in Water: A Computational Study. *Croatica Chemica Acta* **2014,** *87* (4), 385.

(59) Coursindel, T.; Martinez, J.; Parrot, I. Concise Pathway to New Multifunctionalized Constrained Pentacin Derivatives by Means of Two Stereospecific Tandem Reactions. *European Journal of Organic Chemistry* **2011**, 4519.

(60) Fulop, F. The chemistry of 2-aminocycloalkanecarboxylic acids. *Chemical Reviews* **2001,** *101* (7), 2181.

(61) Liljeblad, A.; Kanerva, L. T. Biocatalysis as a profound tool in the preparation of highly enantiopure beta-amino acids. *Tetrahedron* **2006,** *62* (25), 5831.

(62) Liu, M.; Sibi, M. P. Recent advances in the stereoselective synthesis of beta-amino acids. *Tetrahedron* **2002,** *58* (40), 7991.

(63) Mittendorf, J.; Kunisch, F.; Matzke, M.; Militzer, H. C.; Schmidt, A.; Schonfeld, W. Novel antifungal beta-amino acids: Synthesis and activity against Candida albicans. *Bioorganic & Medicinal Chemistry Letters* **2003,** *13* (3), 433.

(64) Kiss, L.; Fulop, F. Synthesis of Carbocyclic and Heterocyclic beta-Aminocarboxylic Acids. *Chemical Reviews* **2014,** *114* (2), 1116.

(65) Martinek, T. A.; Fulop, F. Peptidic foldamers: ramping up diversity. *Chemical Society Reviews* **2012,** *41* (2), 687.

(66) Mowery, B. P.; Lee, S. E.; Kissounko, D. A.; Epand, R. F.; Epand, R. M.; Weisblum, B.; Stahl, S. S.; Gellman, S. H. Mimicry of antimicrobial host-defense peptides by random copolymers. *Journal of the American Chemical Society* **2007,** *129* (50), 15474.

(67) Elaridi, J.; Thaqi, A.; Prosser, A.; Jackson, W. R.; Robinson, A. J. An enantioselective synthesis of beta(2)-amino acid derivatives. *Tetrahedron-Asymmetry* **2005,** *16* (7), 1309.

(68) Forro, E.; Fulop, F. The first direct enzymatic hydrolysis of alicyclic beta-amino esters: A route to enantiopure cis and trans beta-amino acids. *Chemistry-a European Journal* **2007,** *13* (22), 6397.

(69) Kritzer, J. A.; Stephens, O. M.; Guarracino, D. A.; Reznik, S. K.; Schepartz, A. beta-Peptides as inhibitors of protein-protein interactions. *Bioorganic & Medicinal Chemistry* **2005,** *13* (1), 11.

(70) Miller, J. A.; Nguyen, S. B. T. The enantioselective synthesis of conformationally constrained cyclic beta-amino acids. *Mini-Reviews in Organic Chemistry* **2005,** *2* (1), 39.

(71) Tang, W. J.; Wu, S. L.; Zhang, X. M. Enantioselective hydrogenation of tetrasubstituted olefins of cyclic beta-(acylamino)acrylates. *Journal of the American Chemical Society* **2003,** *125* (32), 9570.

(72) Choi, S.; Silverman, R. B. Inactivation and inhibition of gamma-aminobutyric acid aminotransferase by conformationally restricted vigabatrin analogues. *Journal of Medicinal Chemistry* **2002,** *45* (20), 4531.

(73) Davies, S. G.; Diez, D.; Dominguez, S. H.; Garrido, N. M.; Kruchinin, D.; Price, P. D.; Smith, A. D. Cyclic beta-amino acid derivatives: synthesis via lithium amide promoted tandem asymmetric conjugate addition-cyclisation reactions. *Organic & Biomolecular Chemistry* **2005,** *3* (7), 1284.

(74) Davis, F. A.; Theddu, N. Asymmetric Synthesis of Cyclic cis-beta-Amino Acid Derivatives Using Sulfinimines and Prochiral Weinreb Amide Enolates. *Journal of Organic Chemistry* **2010,** *75* (11), 3814.

(75) Krohnke, F.; Zecher, W. SYNTHESES USING MICHAEL ADDITION OF PYRIDINIUM SALTS .1. *Angewandte Chemie-International Edition* **1962,** *74* (12), 626.

(76) Hantzsch, A. Condensationprodukte aus Aldehydammoniak und Ketonartigen Verbindungen. *Chemische Berichte* **1881,** *14* (4), 1637.

(77) Ashtekar, K. D.; Staples, R. J.; Borhan, B. Development of a Formal Catalytic Asymmetric 4+2 Addition of Ethyl-2,3-butadienoate with Acyclic Enones. *Organic Letters* **2011,** *13* (21), 5732.

(78) Lang, R. W. H. H. J. α-Allenic esters from α-phosphoranylidene esters and acid chlorides: ethyl 2,3-pentadienoate. *Org. Synth.* **1984,** *62*, 202.

(79) Rosiak, A.; Christoffers, J. Synthesis of unsymmetrically 2,6-disubstituted 2,3-dihydrothiopyran-4-ones. *Tetrahedron Letters* **2006,** *47* (29), 5095.

(80) Oare, D. A.; Henderson, M. A.; Sanner, M. A.; Heathcock, C. H. ACYCLIC STEREOSELECTION .46. STEREOCHEMISTRY OF THE MICHAEL ADDITION OF N,N-DISUBSTITUTED AMIDE AND THIOAMIDE ENOLATES TO ALPHA,BETA-UNSATURATED KETONES. *Journal of Organic Chemistry* **1990,** *55* (1), 132.

(81) Too, P. C.; Noji, T.; Lim, Y. J.; Li, X. W.; Chiba, S. Rhodium(III)-Catalyzed Synthesis of Pyridines from alpha,beta-Unsaturated Ketoximes and Internal Alkynes. *Synlett* **2011**, 2789.